

UNIVERSITÉ DU QUÉBEC A MONTRÉAL

LES KYSTES DE DINOFLAGELLÉS DANS LES SÉDIMENTS DE SURFACE
DU PACIFIQUE DU NORD-EST : DISTRIBUTION ET POTENTIEL COMME
PROXY DE PALÉOPRODUCTIVITÉ

THÈSE
PRÉSENTÉE
COMME EXIGENCE PARTIELLE
DU DOCTORAT EN SCIENCES DE L'ENVIRONNEMENT

PAR

TAOUFIK RADI

JANVIER 2008

UNIVERSITÉ DU QUÉBEC À MONTRÉAL
Service des bibliothèques

Avertissement

La diffusion de cette thèse se fait dans le respect des droits de son auteur, qui a signé le formulaire *Autorisation de reproduire et de diffuser un travail de recherche de cycles supérieurs* (SDU-522 – Rév.01-2006). Cette autorisation stipule que «conformément à l'article 11 du Règlement no 8 des études de cycles supérieurs, [l'auteur] concède à l'Université du Québec à Montréal une licence non exclusive d'utilisation et de publication de la totalité ou d'une partie importante de [son] travail de recherche pour des fins pédagogiques et non commerciales. Plus précisément, [l'auteur] autorise l'Université du Québec à Montréal à reproduire, diffuser, prêter, distribuer ou vendre des copies de [son] travail de recherche à des fins non commerciales sur quelque support que ce soit, y compris l'Internet. Cette licence et cette autorisation n'entraînent pas une renonciation de [la] part [de l'auteur] à [ses] droits moraux ni à [ses] droits de propriété intellectuelle. Sauf entente contraire, [l'auteur] conserve la liberté de diffuser et de commercialiser ou non ce travail dont [il] possède un exemplaire.»

À Maïssame, mon rayon de soleil...

REMERCIEMENTS

Au terme de ce travail, il m'est extrêmement agréable de remercier tous ceux qui m'ont aidé, d'une manière ou d'une autre. Tout d'abord, j'exprime ma gratitude à ma directrice de thèse, Madame Anne de Vernal, Professeur au département des Sciences de la Terre de l'UQAM et chercheur au GEOTOP, qui m'a accueilli dans son laboratoire et a suivi mon travail avec un vif intérêt. Merci pour sa rigueur scientifique ainsi que ses encouragements dans les moments difficiles. Elle a toujours fait preuve d'une grande disponibilité malgré ses diverses occupations. Qu'elle trouve ici le témoignage de ma grande admiration et de ma sincère reconnaissance. Merci à Vera Pospelova, professeur à l'Université de Victoria, pour sa collaboration et son amitié. Je remercie également Fabienne Marret, de l'Université de Liverpool, Paul Del Giorgio de l'UQAM et Kim Juniper de l'Université de Victoria, d'avoir accepté de faire partie de mon comité d'encadrement. Merci pour leurs nombreux conseils. Je remercie également les membres de mon jury d'avoir accepté de juger ce travail.

Je remercie B. Conard du centre de géologie marine de l'Oregon State University, A. Dallimore et K. Conway de la Commission Géologique du Canada et A.-C. Ruiz-Fernandez de l'Universidad Nacional Autónoma de México à Mazatlan, de m'avoir donné accès aux échantillons de sédiments de surface du Pacifique. Merci au service des archives de la Goddard Space Flight Center de la NASA pour les données de productivité.

Les ateliers de travail qui ont été organisés à Montréal, Dartmouth, Liverpool ou Copenhague ont toujours été sources de progrès, notamment dans la résolution des problèmes taxinomiques. Merci à Martin Head de Brock University, André Rochon de l'UQAR et Karin Zonneveld de l'Université de Bremen.

Je ne saurais suffisamment remercier Maryse Henry pour son aide en laboratoire. Je pense particulièrement à tous les assistants du laboratoire de micropaléontologie qui ont passé beaucoup de temps à préparer mes échantillons. Merci à Linda Genovesi, Audrey Limoges et Stéphanie Ladouceur de m'avoir simplifié le travail durant mes activités d'enseignement cet hiver.

Les collègues de bureau sont très importants. Je remercie tous les étudiants et le personnel du GEOTOP que j'ai côtoyés pendant ces années de thèse. Je remercie particulièrement Josée Savard et Denisa Mirica-Parveté pour les tâches administratives, Bianca Fréchette pour les discussions, souvent fructueuses, concernant les analyses statistiques. Enfin, grâce aux nombreuses discussions à huis clos avec mon colocataire de bureau, le "super haricot vert", j'ai appris beaucoup sur la géochimie organique et je suis sûr qu'il en a appris autant sur les kystes de dinoflagellés. Merci également à Sandrine Solignac, J-F Kielt et Chantal Gosselin. Merci à Bass et Greg pour les pauses "nicotine" qui faisaient du bien au moral.

Il m'est agréable de marquer mon affectueuse reconnaissance à mes parents qui m'ont encouragé pendant de (trop!) nombreuses années. Leur soutien et leur attention ont été très importants pour me permettre d'aller au bout de cette thèse. Je ne pourrais jamais assez les remercier.

Merci au Conseil de Recherche en Sciences Naturelles et en Génie du Canada (CRSNG) qui a financé cette thèse pendant deux années. Pour le reste, je remercie le soutien financier de ma directrice, à même ses fonds de recherche et les bourses FARE de l'UQAM.

Enfin, Je remercie Emeline d'avoir supporté mes sautes d'humeur, merci pour son écoute, ses attentions et son aide de chaque instant.

AVANT – PROPOS

Cette thèse est présentée sous forme d'articles rédigés en anglais. Elle inclut trois chapitres principaux : Deux d'entre eux sont déjà publiés dans des revues scientifiques à comité de lecture, et le troisième a été soumis pour publication. La thèse inclut également des annexes qui sont des articles auxquels j'ai participé. La mise en forme des chapitres et annexes est conforme à celle exigée par les revues. Pour l'ensemble de ces chapitres, j'étais responsable de la compilation de données environnementales, des analyses palynologiques (sauf pour le chapitre 3) et statistiques, de l'interprétation des résultats ainsi que de la première rédaction des manuscrits. Ma directrice de recherche Anne de Vernal m'a supervisé tout au long de ces activités. Les autres co-auteurs ont contribué par leur expertise, en fournissant des échantillons ou des données et en me prodiguant conseils ou critiques.

Le premier chapitre est un article publié en 2004 dans *Review of Palaeobotany and Palynology* (vol. 128, 169-193). Il est intitulé *Dinocyst distribution in surface sediments from the northeastern Pacific margin (40-60 °N) in relation to hydrographic conditions, productivity and upwelling*. Cet article, écrit en collaboration avec Anne de Vernal, montre le potentiel des kystes de dinoflagellés préservés dans le sédiment comme traceurs de productivité primaire dans le Pacifique du nord-est.

Le deuxième chapitre a été publié en 2007 dans *Marine Micropaleontology* (vol. 62, 269-297) intitulé *Dinoflagellate cysts as indicators of water quality and productivity in British Columbia estuarine environments*. Cet article est écrit en collaboration avec Vera Pospelova, Anne de Vernal et J. Vaughn Barrie. Il met en lumière la relation entre la distribution des dinokystes dans le sédiment et certains paramètres environnementaux incluant la température, la salinité, la concentration en nutriments

et la productivité primaire dans les milieux estuariens de la Colombie Britannique. Cette étude traite de l'impact de la pollution marine et de la variabilité naturelle de l'environnement sur les assemblages de dinokystes.

Le troisième et dernier chapitre, intitulé *Dinocysts as proxy of primary productivity in mid-high latitudes of the Northern Hemisphere*, constitue une compilation de données palynologique de 1171 échantillons de sédiments de surface et de données de productivité primaire océanique calculées à partir de deux types d'imagerie satellite. Cette base de données est représentative de l'hémisphère nord, incluant les océans Atlantique, Arctique et Pacifique. Ce chapitre vise à explorer les liens entre la distribution des dinokystes et la productivité primaire à l'échelle hémisphérique et à évaluer le degré de fiabilité de fonctions de transfert se basant sur la méthode des meilleurs analogues pour reconstituer la productivité primaire en utilisant les assemblages de dinokystes fossiles. Le manuscrit, écrit en collaboration avec ma directrice Anne de Vernal, est soumis pour publication à la revue *Marine Micropaleontology*. Les données de dinokystes incluent celles des chapitres 1 et 2 ainsi que des données provenant de plusieurs travaux publiés ou non (cf. annexe 2, de Vernal et al., 2001, 2005).

L'annexe 1 (Guilbault et al., 2003; *Paleoenvironments associated with the deglaciation process in the Strait of Georgia, off British Columbia: microfaunal and microfloral evidence. Quaternary Science Reviews* 22, 839-857) constitue un travail de collaboration avec J. P. Guilbault, J.V. Barrie, K. Conway, et M. Lapointe. Dans ce travail, qui vise à reconstituer l'histoire de la dernière déglaciation dans le détroit de Géorgie, j'étais responsable des analyses palynologiques, de l'interprétation des résultats de dinokystes et d'une partie de la première rédaction du manuscrit.

L'annexe 2 (de Vernal et al., 2005; *Reconstruction of sea-surface conditions at middle to high latitudes of the Northern Hemisphere during the Last Glacial*

Maximum (LGM) based on dinoflagellate cyst assemblages. Quaternary Science Reviews 24, 897-924) constitue le fruit d'une étroite collaboration entre plusieurs auteurs. J'y ai contribué par l'analyse palynologique de plusieurs dizaines d'échantillons de sédiments de surface ainsi que par les traitements statistiques et les analyses multivariées.

L'annexe 3 (de Vernal, A., Rochon, A., et Radi, T., 2007) constitue un chapitre publié dans *L'Encyclopedia of Quaternary Science* par Elsevier et intitulé *Dinoflagellates*. J'y ai contribué par la compilation de données, la revue d'une partie de littérature concernant les affinités écologiques de certains taxons et la préparation de figures.

TABLE DES MATIÈRES

AVANT-PROPOS.....	v
LISTE DES FIGURES.....	xiii
LISTE DES TABLEAUX.....	xviii
LISTE DES PLANCHES PHOTOGRAPHIQUES.....	xx
RÉSUMÉ GÉNÉRAL.....	xxi
INTRODUCTION GÉNÉRALE.....	1
CHAPITRE 1	
DINOCYST DISTRIBUTION IN SURFACE SEDIMENTS FROM THE NORTHEASTERN PACIFIC MARGIN (40-60 °N) IN RELATION TO HYDROGRAPHIC CONDITIONS, PRODUCTIVITY AND UPWELLING.....	11
Résumé.....	12
Abstract.....	13
1.1 Introduction.....	14
1.2 Method.....	15
1.2.1 Sampling and laboratory procedure.....	15
1.2.2 Nomenclature of dinoflagellate cysts.....	16
1.2.3 Statistical methods.....	17
1.2.4 Hydrographical data.....	17

1.3 Oceanographical settings.....	18
1.3.1 Atmospheric circulation.....	18
1.3.2 Surface water circulation.....	18
1.3.3 Productivity.....	19
1.3.4 Temperature and salinity.....	19
1.4 Dinoflagellate cyst distribution.....	20
1.5 Discussion.....	23
1.5.1 Relationship between dinocyst assemblages and environmental conditions.....	23
1.5.2 Dinocyst taxa and assemblages <i>versus</i> upwelling.....	24
1.6 Conclusion.....	26
1.7 Acknowledgements.....	26
1.8 References.....	28
1.9. Figure captions.....	33
1.10 Table captions.....	35
1.11 Plate captions.....	35

CHAPITRE 2

DINOFLAGELLATE CYSTS AS INDICATORS OF WATER QUALITY AND PRODUCTIVITY IN BRITISH COLUMBIA ESTUARINE

ENVIRONMENTS.....	59
Résumé.....	60
Abstract.....	61
2.1 Introduction.....	62
2.2 Regional setting.....	64
2.2.1 Seymour-Belize and Effingham Inlets.....	64
2.2.2 Georgia strait.....	65
2.3 Materials and methods.....	67
2.3.1 Sampling and laboratory treatments.....	67

2.3.2	Dinoflagellate cysts nomenclature.....	68
2.3.3	Sources of environmental data.....	68
2.3.4	Multivariate analyses.....	69
2.3.5	Transfer functions and validation exercises.....	71
2.4	Results.....	71
2.4.1	Dinocyst concentration and assemblages.....	71
2.4.2	Multivariate analyses.....	72
2.4.3	Evaluation of transfer function for estimating SST, SSS and productivity.....	74
2.5	Discussion.....	75
2.5.1	Composition of assemblages.....	75
2.5.2	Dinocyst concentrations and distribution <i>versus</i> environmental parameters.....	76
2.5.3	Quantitative approaches for the reconstruction of sea-surface parameters.....	80
2.6	Conclusion.....	81
2.7	Acknowledgements.....	82
2.8	References.....	83
2.9	Figure captions.....	93
2.10	Table captions.....	96

CHAPITRE 3

DINOCYSTS AS PROXY OF PRIMARY PRODUCTIVITY IN MID-HIGH LATITUDES OF THE NORTHERN HEMISPHERE.....		122
Résumé.....		123
Abstract.....		124
3.1	Introduction.....	125
3.2	Methodology.....	128
3.2.1	Dinocyst data bases.....	128

3.2.2 Hydrographic and Productivity data.....	130
3.2.2.1 Hydrographic data.....	130
3.2.2.2 Productivity data.....	130
3.2.3 Statistical treatment and transfer function.....	133
3.3 Results of CCA analyses-relationship between assemblages and productivity.....	136
3.3.1 Arctic Ocean.....	136
3.3.2 North Atlantic Ocean.....	137
3.3.3 North Pacific Ocean.....	138
3.3.4 Northern Hemisphere.....	139
3.4 Discussion.....	139
3.4.1 Significance and co-variability of hydrographic parameters and productivity.....	139
3.4.2 The use of dinocysts for quantitative reconstructions of paleoproductivity.....	141
3.4.3 Accuracy of reconstructions based on MAT.....	142
3.5 Example of application: core HU 91-045-094.....	144
3.6 Conclusion.....	147
3.7 Acknowledgments.....	148
3.8 References.....	149
3.9 Figure captions.....	162
3.10 Table captions.....	165
 CONCLUSION GÉNÉRALE.....	 187
 BIBLIOGRAPHIE GÉNÉRALE.....	 195

ANNEXE 1

Guilbault, J.P., Barrie, J.V., Conway, K, Lapointe, M., Radi, T. 2003. Paleoenvironments associated with the deglaciation process in the Strait of Georgia, off British Columbia: microfaunal and microfloral evidence. *Quaternary Science Reviews* 22, 839-857.....210

ANNEXE 2

de Vernal, A., Eynaud, F., Henry, M., Hillaire-Marcel, C., Londeix, L., Mangin, S., Matthiessen, J., Marret, F., Radi, T., Rochon, A., Solignac, S., Turon, J.-L. 2005. Reconstruction of sea-surface conditions at middle to high latitudes of the Northern Hemisphere during the Last Glacial Maximum (LGM) based on dinoflagellate cyst assemblages. *Quaternary Science Reviews* 24, 897-924.....230

ANNEXE 3

de Vernal, A., Rochon, A., Radi, T. et al., 2007. Dinoflagellates. *Encyclopedia of Quaternary Science*, Elsevier, 1652-1667.....259

LISTE DES FIGURES

CHAPITRE 1

- Figure 1. Location map of study sites (dots). The arrows indicate the mean pathway of the surface currents. Isobaths indicate water depth at 200 and 1000 meters.....37
- Figure 2. Seasonal change in productivity and upwelling index (UI) at selected coastal sites. Productivity data are from Antoine et al. (1996). The UI data are from the PFEL data set of NOAA (<http://www.pfeg.noaa.gov/index.html>). UI data represent mean values calculated from 1967 to 2001. UI is expressed in term of $\text{m}^3 \text{s}^{-1}$ per 100 m of coastline.....38
- Figure 3. Sea-surface temperature in August plotted against annual primary productivity. Black dots indicate sites with low temperature and high productivity, which corresponds to upwelling situation.....39
- Figure 4. Seasonal variation in primary productivity (Antoine et al., 1996) and temperature (NODC, 1994) at selected sites. Black arrows indicate the spring bloom and white arrows indicate the summer to late summer bloom. AP = Annual primary productivity in term of $\text{gC m}^{-2} \text{yr}^{-1}$40
- Figure 5. Relationship between sea-surface temperature in August, sea-surface temperature in February and sea-surface salinity in August. Black dots indicate sites characterized by fresh water input and thus by particularly low salinity.....41
- Figure 6. Diagram illustrating the percentages of all dinocyst taxa except *Bitectatodinium tepikiense* and *Echinidinium* spp., which occur only occasionally. On the right of the diagram are indicated the total cyst concentration, the two first principal components (PC1 and PC2) which respectively represent 80.4% and 7.1% of the variance, the sea-surface temperature and the primary productivity.....42
- Figure 7. Maps showing the percentages of dinocyst taxa in the northeastern Pacific.....43
- Figure 8. Ordination of each taxon based on the two first principal component axes. The white diamonds represent cysts of autotrophic taxa and the black diamonds, cysts of heterotrophic taxa.....48
- Figure 9. Maps showing the geographical distribution of PC1 and PC2 values.....49

Figure 10. Definition of dinocyst assemblages according to PC1 and PC2. PC1 permits the separation of neritic and oceanic areas, whereas PC2 exhibits a latitudinal gradient.....50

Figure 11. Relationship between the percentages of heterotrophic taxa and productivity and mean UI in summer (average over June, July, August and September). Only coastal sites, where a UI can be generated, are represented. The coefficients of correlations were calculated based on a logarithmic relationship.....51

Figure 12. Relationship between PC1 and the annual primary productivity and the percentages of heterotrophic taxa. The coefficient of correlation was calculated based on a logarithmic curve (PC1 versus Productivity) and a linear relationship (PC1 versus heterotrophic taxa percentages).....52

Figure 13. Relationship between the summer UI and PC1. Only coastal sites, where a UI can be generated, are represented. The coefficient of correlation was calculated based on a linear relationship.....53

Figure 14. Relationship between PC2 and productivity. The coefficient of correlation is calculated after a linear regression.....53

CHAPITRE 2

Figure 1. Map of study area showing sampling site locations (dots) within EFF, SB and GS (A). Arrows indicate main summer surface circulation pattern. Regional surface circulation pattern for the GS is shown in (B) where grey arrows indicate circulation of brackish Fraser River water, mixing with saline oceanic water from Juan de Fuca Strait and Discovery Pass. Isolines of equal mean tidal range are indicated in (C) (compiled from Barker, 1974; Thomson, 1981 and Thomson et al., 1989).....98

Figure 2. SST, SSS and productivity distributions in the coastal waters of BC. February and August SST and SSS data are from The World Ocean Atlas (2001). Productivity data are from Antoine et al. (1996) based on satellite observation of the chlorophyll yielded by the CZCS program.....99

Figure 3. Summer SSS plotted against summer SST, winter SST and summer productivity in the GS (diamonds), SB Inlets (squares) and EFF Inlet (circles).....100

Figure 4. Winter and summer distribution maps of nitrate, phosphate and silica concentrations in the surface water of the GS. Data are from STRATOGEM (Strait of

- Georgia Ecosystem Modeling project; <http://www.stratogem.ubc.ca/data.html>) and the World Ocean Atlas (2001).....101
- Figure 5. Average distribution of temperature (a) and dissolved oxygen (b) in the water column along the Georgia Strait and Juan de Fuca Strait. Data are from Masson (2006) and represent average of measurements made between 1999 and 2003 at 20 stations.....102
- Figure 6. Satellite images of suspended sediment in the Georgia Strait, from the AVHRR (Very High Resolution Radiometer) aboard a NOAA weather satellite, showing the extent of the Fraser River plume in February, May and August 2002.....103
- Figure 7. Diagram showing the basic physical mechanisms of water circulation in the Georgia Strait and Juan de Fuca Strait. Grey arrows represent upwelled water coming from Juan de Fuca Strait and mixing with brackish Fraser River water in the central and southern parts of the Georgia Strait (adapted from Thomson, 1981).....104
- Figure 8. Percentages diagram of dinocyst taxa (except *Operculodinium janduchenei*, *Impagidinium paradoxum* and *Islandinium brevispinosum*, which only occur in very low numbers).....105
- Figure 9. Percentage distributions of the most important taxa in the GS, according to their ordination upon the first RDA axis (*Operculodinium centrocarpum* and *Quinquecuspis concreta*) and the second RDA axis (*Pentapharsodinium dalei* and *Spiniferites ramosus*).....106
- Figure 10. RDA results of EFF, SB and GS data (i.e. DS1) showing ordination of species and environmental variables on axes 1 and 2 (respectively 31.2 % and 6.4 % of species data variance).....107
- Figure 11. RDA results of GS data (i.e. DS2) showing ordination of species and environmental variables on axes 1 and 2 (respectively 23.8 % and 15.4 % of species data variance).....108
- Figure 12. Map of the distribution of assemblage zones 1, 2 and 3 within the GS...109
- Figure 13. Results of the validation exercise for the reconstruction of temperature, salinity and productivity using the modern analogue technique.....110
- Figure 14. Map of site locations of the large data set (n = 123) used for the validation exercise.....111

Figure 15. Results of Principal Components Analysis (PCA) carried out on the environmental variables in the $n = 123$ data set.....112

Figure 16. Results of the validation exercise for the reconstruction of temperature, salinity and productivity for the data set $n=123$, using the modern analogue technique.....113

CHAPITRE 3

Figure 1: Location of surface sediment (core-top) samples in the “ $n=1171$ ” reference dinocyst database.....167

Figure 2: Seasonal and annual distribution maps of primary productivity based on satellite observations of chlorophyll.....168

Figure 3: Maps showing the difference between MODIS and CZCS data (cf. figure 2).....169

Figure 4: Results of CCA analysis applied to the Arctic dataset.....170

Figure 5: Results of CCA analysis applied to the North Atlantic dataset.....171

Figure 6: Results of CCA analysis applied to the North Pacific dataset.....172

Figure 7: Results of CCA analysis applied to the Northern Hemisphere dataset.....173

Figure 8: Map showing the distribution of the minimum distance of the closest analogue in the case of the “ $n=1171$ ” database.....174

Figure 9: Results of cross-validation tests using the leave-one-out technique for the North Atlantic dataset.....175

Figure 10: Results of cross-validation tests using the leave-one-out technique for the North Pacific dataset.....176

Figure 11: Results of cross-validation tests using the leave-one-out technique for the Northern Hemisphere “ $n=1171$ ” dataset.....177

Figure 12: Maps showing anomalies from dinocyst-based reconstruction (difference between observed and estimated) using annual and seasonal MODIS data (left panel) and the annual and seasonal differences between CZCS and MODIS modern data (right panel).....178

Figure 13: Northern Hemisphere and Core HU 91-045-094 samples scores of the two first ordination axes as generated by correspondence analysis.....	179
Figure 14: Percentages of main dinocyst taxa and sample scores of CA axes 1, 2 and 3 in core HU91-045-094.....	180
Figure 15: Geochemical and micropaleontological data of core HU 91-045-094....	181
Figure 16: Reconstruction of paleoproductivity for the last 25 000 years from dinocyst data in core HU 91-045-094 based on MAT and using the “n = 1171” dinocyst database.....	182

LISTE DES TABLEAUX

CHAPITRE 1

Table 1. Sampling site location, sea surface temperature and salinity (NODC, 1994), annual productivity (Antoine et al, 1996), dinocyst concentrations and values for the two first principal components PC1 and PC2.....54

Table 2. Matrix of correlation between dinocyst assemblages and taxa and selected oceanographic parameters. The correlations are based on linear or logarithmic (Asterisks) relationship.....56

CHAPITRE 2

Table 1. List of sample sites with location, water depth, total cysts counted and cyst concentration.....114

Table 2. Results of ordination by Detrended Correspondence Analysis (DCA) and Redundancy Analysis (RDA) of DS1 and DS2 data sets, showing eigenvalues, variance of species data and species-environment relationships.....115

Table 3. Importance ranking of environmental variables by their marginal and conditional effects on dinocysts distribution in the GS, EFF and SB Inlets (DS1), as obtained by forward selection.....116

Table 4. Importance ranking of environmental variables by their marginal and conditional effects on dinocysts distribution in the GS (DS2), as obtained by forward selection.....117

Table 5. Root Mean Square Error (RMSE) and the coefficient of correlation between observed and estimated values (r^2) of the environmental variables tested by the cross-validation exercises using modern analogue technique (MAT) and multiple regression technique (MRT).....118

Table 6. Mean seasonal SST, SSS (NODC, 2001), chlorophyll and nutrient concentrations (NODC, 2001; STRATOGEM, 2005) and annual primary productivity (Antoine et al, 1996) of surface water of estuarine sites (Seymour-Belize Inlets, Georgia Strait and Effingham Inlet) and oceanic sites (OSU 1 to 75).....119

CHAPITRE 3

Table 1: List of dinocyst taxa used in this study with abbreviations, occurrences and percentage ranges. The heterotrophic taxa are marked by asterisks (*). 183

Table 2: Table summarizing the ranges of SST, SSS and sea-ice cover for the North Atlantic, North Pacific and Arctic databases 184

Table 3: Results of forward selection and Monte Carlo permutation test for the Arctic, North Atlantic, North Pacific and the Northern Hemisphere datasets. Asterisks indicate parameters having VIF value >10 185

Table 4: Table summarizing the coefficient of correlations between observed and estimated values and the RMSE (accuracy of reconstruction), as obtained from the cross-validation test with the Northern Hemispheric dataset using both CZCS and MODIS data. The standard deviation of the residual between MODIS and CZCS data is shown for comparison with RMSE yielded by cross-validation tests. 186

LISTE DES PLANCHES PHOTOGRAPHIQUES

Plate 1. 1-3, cf. *Echinidinium granulatum*; 4-6, *Echinidinium* spp.; 7-9, Cysts of *Protoperidinium americanum*; 10, *Votadinium calvum*; 11, *Votadinium spinosum*; 12, *Quinquecuspis concreta*; 13, *Selenopemphis quanta*; 14-15, Cyst of *Polykrikos kofoidii*.....57

Plate 2. 1-3, *Impagidinium strialatum*; 4, *Impagidinium aculeatum*; 5, *Spiniferites mirabilis*; 6, *Nematosphaeropsis labyrinthus*; 7-9, Cyst of *Pentapharsodinium dalei*; 10-11, *Operculodinium centrocarpum*; 12, *Pyxidinoopsis reticulata*.....58

RÉSUMÉ GÉNÉRAL

La productivité primaire océanique joue un rôle important dans les processus d'échange du carbone entre l'océan et l'atmosphère. Elle constitue une contribution majeure à la séquestration du CO₂ atmosphérique, l'un des principaux gaz à effet de serre. La reconstitution de la paléoprodutivité à partir de séquences sédimentaires marines peut donc fournir des réponses à de nombreuses questions concernant les mécanismes impliqués dans les changements climatiques. Elle peut être extrêmement utile dans le domaine de la modélisation biogéochimique puisqu'elle permet de comprendre les mécanismes contrôlant la production, l'exportation et l'enfouissement du carbone à long terme. Cependant, l'estimation quantitative de la paléoprodutivité à partir de séquences sédimentaires marines constitue un défi qui ne pourra être relevé que par le développement de traceurs qui ne sont pas affectés par les différents processus de dégradation et de dissolution dans la colonne d'eau et dans le sédiment.

L'objectif principal de cette thèse est de développer un traceur micropaléontologique pour des reconstitutions quantitatives de la paléoprodutivité. Il s'agit des kystes de dinoflagellés (ou dinokystes) qui, grâce à leur extrême résistance à la dissolution et leur abondance dans le sédiment, constituent un outil extrêmement important dans le domaine de la paléocéanographie à l'échelle du quaternaire. Nous avons exploré, dans le cadre de ce travail, le potentiel des kystes de dinoflagellés préservés dans les sédiments comme traceurs quantitatifs des paramètres hydrographiques et de la paléoprodutivité marine. Nous avons choisi d'étudier leur distribution dans les sédiments de surface de l'hémisphère nord en relation avec les conditions hydrographiques et trophiques du milieu. Le but est d'évaluer la contribution des conditions trophiques au contrôle de la distribution des assemblages des dinokystes dans le sédiment. Notre étude a été réalisée selon trois volets.

Le premier volet a consisté en l'analyse d'échantillons de sédiments de surface prélevés dans le Golfe d'Alaska et le long des marges nord-est américaines, qui se caractérisent par un gradient de productivité associé aux upwellings. Ce volet visait à comprendre la distribution des dinokystes le long d'un gradient de productivité et d'upwelling dans un contexte océanique et néritique. Le deuxième volet consistait en l'analyse d'échantillons de sédiments de surface répartis dans les milieux estuariens et côtiers de la Colombie Britannique. Il visait à illustrer la distribution des assemblages dans un milieu très productif, influencés à la fois par des apports en éléments nutritifs d'origine naturelles (upwelling) et anthropique. Enfin, le troisième volet est une compilation de données palynologique, hydrographiques et de productivité primaire de 1171 sites dans l'hémisphère nord pour développer une base de données de référence hémisphérique à des fins de reconstitutions de la productivité par la méthode des meilleurs analogues modernes.

Dans le Pacifique du Nord-est, l'étude palynologique de 76 échantillons de sédiments de surface provenant des milieux néritiques et océanique a permis de montrer que les taxons liés à une productivité hétérotrophe dominent les assemblages des zones côtières influencées par l'upwelling alors que les sites associés aux zones oligotrophes océaniques sont dominés par les taxons autotrophes. Les analyses multivariées démontrent que, dans ce secteur, la distribution des assemblages de dinokystes est liée essentiellement à la productivité primaire et à l'intensité de l'upwelling. Elles démontrent également l'existence de liens avec la température hivernale qui, à une échelle régionale n'est pas affectée par l'upwelling contrairement à la température estivale qui est uniformisée sous l'effet de l'upwelling saisonnier.

Dans les milieux estuariens de la Colombie Britannique, incluant le détroit de Géorgie (GS) et les inlets d'Effingham (EFF), de Seymour et de Belize (SB), l'analyse de 60 échantillons de sédiment de surface montre que les taxons autotrophes dominent les assemblages dans les zones de productivité primaire relativement élevée (EFF et SB) alors que les protopéridinales et les gymnodinales, associés à une productivité hétérotrophe dominent les assemblages du détroit de Géorgie où la productivité est moindre. Les analyses multivariées montrent que la distribution des assemblages est significativement liée à la productivité primaire, la température de l'eau de surface et la concentration de silice pendant le printemps. Dans le détroit de Géorgie, les analyses de redondance montrent que la distance par rapport à la côte, la distance par rapport au port de Vancouver, la salinité de l'eau de surface, la concentration en phosphate et la productivité durant le printemps constituent les paramètres les plus déterminants. Par ailleurs, dans le panache du fleuve Fraser, les zones près du port de Vancouver, caractérisées par des apports continentaux élevés, une productivité printanière élevée et une stratification accrue sont marquées par l'abondance de *Pentapharsodinium dalei* alors que tous les protopéridinales et les gymnodinales dominent les assemblages des zones distales associées à une masse d'eau constituée par un mélange des eaux douces provenant du fleuve Fraser et des eaux salées issues de l'upwelling. Dans ce contexte, il est probable que la stratification des masses d'eau joue un rôle important, qu'il est toutefois difficile de quantifier. Des tests de validation utilisant la méthode des analogues modernes démontrent que les assemblages de dinokystes peuvent être utilisés pour reconstituer d'une manière quantitative la productivité primaire, la température et la salinité de surface à une échelle régionale.

À l'échelle de l'hémisphère nord, une base de données de référence de sédiments modernes a été utilisée pour explorer le potentiel des assemblages de dinokystes comme traceurs de productivité primaire. La base de données inclut 1171 sites provenant de l'Atlantique Nord (n = 483), de l'Océan Arctique (n = 401) et du Pacifique Nord (n = 287). Pour établir des liens entre les assemblages de dinokystes et la productivité, nous avons utilisé deux jeux de données de productivité moderne issues de deux programmes d'observation de la couleur de la chlorophylle par

satellite. L'une représentant une moyenne des mesures effectuées entre 1978 et 1989 (CZCS) et l'autre, une moyenne de données correspondant à la période de 2002 à 2005 (MODIS). Des analyses canoniques de correspondance ont été effectuées avec 62 taxons et huit paramètres environnementaux (température saisonnière et salinité saisonnière de l'eau de surface, couvert de glace de mer et productivité primaire saisonnière et annuelle). Les résultats montrent une relation étroite entre les assemblages et la productivité primaire notamment dans l'Atlantique Nord, dans le Pacifique Nord et à l'échelle hémisphérique. Toutefois, cette relation n'est pas la même dans tous les bassins de l'hémisphère nord. Des tests de validation (régressions linéaires entre les valeurs observées et estimées), en utilisant la méthode des meilleurs analogues, montrent des coefficients de corrélation généralement $> 0,9$ et des précisions de reconstitution de $\pm 11-25\%$, selon la base de données de productivité utilisée. De telles précisions montrent que la productivité peut être reconstituée avec une erreur inférieure à la différence entre les données de productivité instrumentales de MODIS et de CZCS.

L'ensemble des résultats de notre étude met en évidence l'intérêt des kystes de dinoflagellés pour reconstituer quantitativement la productivité primaire à l'échelle du quaternaire.

Mots clés : kystes de dinoflagellés, paléoprodutivité, reconstitution quantitative, Pacifique du Nord-est, Hémisphère Nord.

INTRODUCTION GÉNÉRALE

La productivité primaire océanique compte pour à peu près 50% de la productivité totale de la biosphère (e.g., Field et al., 1998). Les plus récentes estimations de la productivité primaire océanique sont de l'ordre de 45-60 Gt C an⁻¹ (Longhurst et al., 1995; Antoine et al., 1996; Field et al., 1998; Gregg et al., 2003). Généralement 80 à 90% de cette production est recyclée dans la couche euphotique, notamment par la respiration bactérienne. Le reste est exporté (~6-16 Gt C an⁻¹) vers l'océan profond sous forme de carbone organique particulaire, de carbone organique dissous et de carbonate de calcium. Finalement, une petite fraction de la production primaire (~0,2 Gt C an⁻¹) s'enfouit dans le sédiment et représente un puits de carbone. La séquestration du carbone dans l'océan, associée à l'activité biologique marine, a été souvent considérée comme un paramètre ayant joué un rôle significatif sur les fluctuations du CO₂ atmosphérique pendant les périodes glaciaires-interglaciaires du Quaternaire (e.g., Sarnthein et al., 1988; Berger et al., 1989; Thunell et Sauter, 1992; Brink et al., 1995; Schneider et Muller, 1995; Sigman et Boyle, 2000).

Depuis le développement de la méthode de ¹⁴C pour évaluer la production primaire océanique par Steemann Nielsen (1952), plusieurs milliers de mesures de productivité ont été effectuées dans les océans aux fins d'estimation de la productivité océanique globale. Les compilations de ces mesures ont permis la publication d'un certain nombre de travaux qui ont fournis des estimations très différentes les unes des autres, allant de 20 à 45 GT C an⁻¹ (cf. Sundquist, 1985). Citons par exemple les estimations de 23 Gt C an⁻¹ par Koblentz-Mishke et al. (1970), de 27 Gt C an⁻¹ par Walsh et al. (1988) et de 29,6 GT C an⁻¹ par Berger (1989). Tous ces travaux se sont basé sur un grand nombre d'extrapolations et sont limités par une couverture spatiale et temporelle incomplète. Les premières estimations de la chlorophylle océanique par satellite ont été réalisées par le programme Coastal Zone Color Scanner (CZCS) de la

NASA entre 1978 et 1989. L'utilisation des données de chlorophylle issues de ce programme au début des années 1990s a rendu possible des estimations de la productivité océanique basées sur de meilleures couvertures spatiales. Ainsi, Antoine et al. (1996) et Behrenfeld et Falkowski (1997) ont développé des méthodes d'intégrations pour la quantification de la productivité primaire à partir de données satellitaires. Ces nouvelles données ont permis des estimations de la productivité marine comprises entre 45 et 53 Gt C an⁻¹ (Longhurst et al., 1995; Antoine et al., 1996; Field et al., 1998). Le programme CZCS permet de prendre en considération la quasi-totalité des régions océaniques et fournit des mesures pour toutes les saisons. Cependant des faiblesses demeurent en ce qui concerne les hautes latitudes, les régions côtières et les régions caractérisées par un couvert nuageux persistant. En effet, plusieurs études ont montré que CZCS sous-estime les concentrations de chlorophylle océanique (e.g., Thomas et al., 2001; Gregg et Conkright, 2002; Davenport et al., 2002 ; Gregg et al., 2003). En revanche, le programme "Sea-viewing Wide Field-of-view Sensor" (SeaWiFS), lancé en 1997 et le programme MODerate resolution Imaging Spectroradiometer (MODIS), lancé en 2000 permettent une couverture de l'océan global presque complète et des estimations plus détaillées et plus fiables de la chlorophylle (cf. Werdeli et al., 2003).

L'estimation de la productivité primaire océanique a permis aux modélisateurs de quantifier les processus de transport du carbone dans la colonne d'eau (Najjar et al., 1992; Six et Maier-Reimer, 1996; Lampitt et Antia, 1997; Palmer et Totterdell, 2001; Ito et al., 2005) et de son transfert entre l'océan et l'atmosphère (e.g., Schimel et al., 1995; Sarmiento et Le Quéré, 1996; Six et Maier-Reimer, 1996). La reconstitution de la productivité passée peut donc contribuer à retracer l'histoire des échanges de CO₂ entre l'océan et l'atmosphère et offre l'opportunité d'évaluer la contribution de la pompe biologique aux changements climatiques et océanographiques. La paléoprodutivité est, en effet, un paramètre nécessaire pour les modèles physiques

et biogéochimiques qui visent à évaluer la variabilité passée du cycle de carbone en relation avec les changements climatiques.

Parmi les traceurs de la paléoproduktivité, les microfossiles préservés dans les sédiments ont été largement utilisés par les paléocéanographes, notamment avec les développements méthodologiques impliquant les fonctions de transfert (e.g. Imbrie et Kipp, 1971) qui ont transformé la paléocéanographie d'une science qualitative, ou semi-quantitative, à une science quantitative. Les données de productivité primaire issues du programme CZCS ont été souvent utilisées pour développer des fonctions de transfert utilisant les assemblages de foraminifères ou de coccolites pour des fins de reconstitutions quantitatives de la paléoproduktivité à partir de carottes sédimentaires dans l'océan Indien (Beaufort et al., 1997, 1999, 2001; Cayre et al., 1999; Schulte et Bard, 2003; Ivanova et al., 2003), l'Océan Atlantique (Henriksson, 2000; Davenport et al., 2002) et l'Océan Pacifique (Loubere, 1999, 2002; Beaufort et al., 2001). D'autres traceurs géochimiques de la paléoproduktivité ont été développés ces dernières décennies (cf. Sarnthein et al., 1988; Dymond et al., 1992; Francois et al., 1995; Fischer et Wefer, 1999; Mackensen et al., 2000; Eagle et al., 2003 ; Lazarus et al., 2006; Bradtmiller et al., 2006). Cependant, plusieurs de ces traceurs géochimiques (e.g., carbone organique, CaCO_3 , baryum, rapport Th/Pa, composition isotopique de carbone) et biologiques (e.g., microfossiles de nature minérale, biomarqueurs) sont difficilement utilisables à cause des processus de transport, de sédimentation et de dégradations biogéochimiques dans la colonne d'eau et dans le sédiment (Dymond et al., 1992; Nelson et al., 1995; McCorkle et al., 1995; Francois et al., 1995; 2004 ; Paytan et al, 1996; Meyers, 1997; Rühlemann, 1999; Klump et al., 2000 ; Gallinari et al., 2002; Eagle et Paytan, 2006).

Le travail de cette thèse présente le potentiel et les avantages des kystes organiques de dinoflagellés (ou dinokystes), préservés dans le sédiment, comme outil micropaléontologique de reconstitution de la productivité primaire, aussi bien dans

les milieux océaniques et néritiques que dans les systèmes côtiers et estuariens. C'est donc, dans l'optique d'une meilleure connaissance des paramètres régissant la distribution des dinokystes dans les sédiments de surface dans l'hémisphère nord en générale et dans le Pacifique du Nord-est en particulier que se place mon travail de thèse. Mon objectif principal est de développer une base de données de référence des dinokystes et de vérifier que ces traceurs, composés de matière organique réfractaire, peuvent servir comme outil de reconstitution quantitative de la productivité primaire.

Les kystes de dinoflagellés

Les dinoflagellés sont des protistes algaires appartenant à la division des Dinoflagellata (ou Pyrrophyta) et à la classe des Dinophyceae. Ils constituent des microorganismes à mode de nutrition le plus souvent autotrophe mais un grand nombre d'entre eux peuvent être hétérotrophes et certains mixotrophes. Les dinoflagellés constituent également l'un des trois groupes majeurs du phytoplancton marin (avec les coccolithophores et les diatomées), responsable de la production primaire océanique.

Les dinoflagellés ont la particularité de produire, durant leur cycle biologique, des kystes qui constituent un stade de dormance suite à la reproduction sexuée (e.g., Wall et Dale, 1968; Taylor, 1987). Les kystes d'environ 15 à 20% des dinoflagellés sont constitués d'une membrane organique (sporo-pollénine) extrêmement résistante et fossilisable et présentent un intérêt particulier en micropaléontologie puisqu'ils ne sont pas affectés par la dissolution comme les microfossiles à test minéral. Depuis l'essor de la paléocéanographie moderne, une attention particulière a été accordée aux kystes de dinoflagellés comme traceur paléocéanographique dans tous les domaines océaniques, depuis les zones tropicales jusqu'aux zones polaires. Leur utilisation en paléocéanographie permet de s'affranchir des problèmes de dégradation de la matière

organique durant les processus de sédimentation (e.g., Meyers, 1997) et de la dissolution du CaCO_3 et de la silice biogénique dans la colonne d'eau (e.g., Archer et al., 1989; Nelson et al., 1995; Gehlen et al., 2005). De nombreux travaux traitant de la distribution des dinokystes dans les sédiments de surface ont permis de démontrer que les dinokystes constituent d'excellents traceurs des paramètres hydrographiques de surface, en particulier de la température, la salinité et la durée saisonnière du couvert de glace de mer, et ce dans les moyennes et hautes latitudes de l'océan Atlantique (e.g., Marret, 1994; de Vernal et al., 1997, 2001, 2005; Rochon et al., 1999; Marret et al., 2004), dans les moyennes et hautes latitudes des l'océan Indien (Marret et de Vernal, 1997; Zonneveld, 1997), ainsi que dans les milieux arctiques et subarctique (Matthiessen, 1995; de Vernal et al., 2001, 2005; Radi et al., 2001). Par ailleurs, certaines études ont montré que les dinokystes peuvent également donner une estimation de l'intensité des upwellings côtiers (Powell et al., 1990, Lewis et al., 1990; Dale, 1996; Zonneveld, 1997; Zonneveld et al., 2001) et être de bons traceurs de productivité primaire tel que démontré dans les zones côtières des marges scandinaves (Dale et Fjellså, 1994; Thorsen et Dale, 1997; Dale, 2001) et à l'échelle de l'Atlantique Nord (Devillers et de Vernal, 2000). En général, les kystes de dinoflagellés hétérotrophes sont de plus en plus considérés comme traceurs indirects de la productivité primaires (e.g., Zonneveld et al., 2001; Sangiorgi et al., 2002). Cependant la réponse des différents taxons de dinokystes aux conditions environnementales particulières ainsi que la façon dont ils témoignent des conditions du milieu peuvent différer d'une région à une autre (Matsuoka, 1999; Pospelova et al., 2002). Dans les domaines estuariens et côtiers, les assemblages de dinokystes peuvent refléter l'état d'eutrophisation du milieu (Dale, 1996, 2001; Thorsen et Dale, 1997; Dale et al., 1999; Matsuoka, 1999; Pospelova et al., 2002, 2004, 2005).

Dans le Pacifique, toutefois, hormis quelques rare travaux réalisés dans les marges japonaises par Matsuoka (1985, 1987, 1992, 1999) dans la mer Jaune et la mer de Chine (Cho et Matsuoka, 2001), dans la mer de Béring (Radi et al., 2001) et dans le

fjord d'Effingham, sur la marge ouest de l'île de Vancouver (Kumar et Patterson, 2002), nos connaissances sur la distribution et la taxinomie des dinokystes restent très limitées.

Le Pacifique du Nord-est – Contexte régional

Les grandes fluctuations des conditions hydrographiques dans le Pacifique Nord sont liées à la position et à l'intensité de l'anticyclone du Pacifique Nord et de la dépression des Aléoutiennes qui contrôlent la circulation océanique locale (Huyer, 1983; Trenberth et Hurrell, 1994; Mock et al., 1998; Miller et Schneider, 2000). Une forte intensité du cyclone des Aléoutiennes combinée au ralentissement de l'anticyclone du Pacifique Nord sont responsables de l'affaiblissement du courant de Californie induisant des eaux superficielles plus chaudes et pauvres en éléments nutritifs (Mantua et al., 1997). Il en résulte une réduction importante de la production primaire et secondaire (e.g., Roemmich et McGowan, 1995; Tanasichuk, 1998). Par contre, l'affaiblissement de la dépression des Aléoutiennes, son déplacement vers le Nord-ouest et l'intensification de l'anticyclone du Pacifique Nord induisent un courant de Californie plus vigoureux, favorisant ainsi l'upwelling côtier qui se traduit par une production marine plus importante (Mantua et al., 1997; Mackas et al., 2001; Peterson et Schwing, 2003). Ces variations dans l'intensité de l'upwelling semblent contrôler les stocks de poissons à intérêt commercial dans les eaux côtières du Pacifique Nord-oriental (Baumgartner et al., 1992; Beamish et Bouillon, 1993; Glavin, 1996; O'Connell et Tunnicliffe, 2001; Dallimore, 2001) et seraient marquées par des oscillations décennales appelées PDO (Pacific Decadal Oscillations; War et Thomson, 1991; Polovina et al., 1995; Mantua et al., 1997; Hare et Mantua, 2000; Pierce et al., 2001). Toutefois, l'évolution à moyen ou à long terme (de 10^1 à 10^4 ans) de ces variations est encore mal connue. Finney et al. (2002) et Tunnicliffe et al.

(2001) ont montré que les variations dans le stock de poissons sur les 2000 dernières années dans le Pacifique du Nord-Est seraient liées aux changements dans le système atmosphère-océan associé à la migration des deux cellules atmosphériques. En plus des variations naturelles, l'environnement côtier et estuarien de la Colombie Britannique a été largement perturbé par le développement industriel et l'augmentation des populations humaines (e.g., Key, 1989; Mackas et Harrison, 1997), ce qui a eu une incidence directe sur la productivité marine incluant le phytoplancton, les mollusques et le stock de poissons à intérêt commercial. Les eaux usées provenant des égouts municipaux, des industries papetières et minières, du lessivage des terres agricoles et des stations d'épuration constituent la principale source de pollution marine en Colombie britannique (Lorimer, 1984; Key, 1989; Mackas et Harrison, 1997; Rideout et al., 2000). Les milieux estuariens de l'île de Vancouver se caractérisent, par une large gamme de concentration en chlorophylle durant la période estivale avec des valeurs de 1-3 $\mu\text{g l}^{-1}$ au sud du détroit de Géorgie et de 10-20 $\mu\text{g l}^{-1}$ dans l'estuaire du Fraser. Les concentrations en nitrates+nitrites y varient entre 18 et 27 μM et la concentration en oxygène dissous dans l'eau profonde peut atteindre 1,5 ml l^{-1} . De telles valeurs sont proches des valeurs seuils d'une eutrophisation élevée selon le "NOAA's Estuarine Eutrophication Survey" (Bricker et al., 1999).

Les enrichissements en substances nutritives azotées et phosphorées induisent, en général, une modification de la composition du phytoplancton, qui se caractérise alors par la dominance des dinoflagellés par rapport aux diatomées. En plus, les milieux marins côtiers se caractérisent par des conditions hydrodynamiques particulières telles que la proximité des panaches fluviaux, la stratification thermique ou haline des eaux et l'absence de turbulence qui confère au milieu une stabilité verticale favorable au développement des blooms de dinoflagellés. Ces conditions contribuent souvent à la prolifération de taxons opportunistes toxiques responsables des marées rouges

(Paerl, 1988; Livingston, 2001; ICES, 2002; Varekamp et al., 2003). Le long des marges orientales des océans Atlantique et Pacifique, ces blooms coïncident en général avec une baisse de l'intensité de l'upwelling et une augmentation de la température de l'eau. Le réchauffement global qui agit sur la circulation atmosphérique et océanique contribue à l'amplification de tels phénomènes (Cloern et al., 2005).

Le Pacifique du Nord-Est représente donc un domaine océanographique unique, avec des zones de haute productivité le long de la côte ouest américaine influencée par des upwellings saisonniers. Cette situation exceptionnelle permet de mieux appréhender les variations spatiales de la composition des assemblages de dinokystes en relation avec la productivité primaire. L'étude de la distribution des kystes de dinoflagellés dans les milieux estuariens de la Colombie Britannique qui se caractérisent par des apports considérables en éléments nutritifs à la fois d'origine naturelle (upwelling) et anthropiques (rejets urbain et industriels) permet de voir si les assemblages de dinokystes préservés dans le sédiment peuvent aider à distinguer l'influence naturelle et anthropique sur l'écosystème marin côtier de cette région.

Objectifs

Dans ce contexte, soit celui des marges orientales du Pacifique, les objectifs principaux de cette thèse sont:

(1) faire l'inventaire de la distribution des kystes de dinoflagellés dans les sédiments de surface du Pacifique du Nord-Est incluant les milieux océaniques, néritiques et estuariens,

(2) décrire la variabilité spatiale des assemblages le long de gradients de paramètres physico-chimiques et trophiques des eaux de surface. L'étude des sédiments estuariens de la Colombie Britannique permettrait d'évaluer les effets de la pollution anthropogénique sur les populations de dinokystes. Cette étude nous offre également l'opportunité d'aborder quelques questions sur la taxinomie et les affinités écologiques de certains taxa de dinokystes et de les comparer avec d'autres régions polluées comme les fjords norvégiens, le milieu côtier de Massachusetts et le port de Tokyo (Dale et al., 1999; Matsuoka, 1999; Pospelova et al., 2002),

(3) définir, à l'aide de traitements statistiques (différentes analyses multivariées), des liens entre les assemblages de dinokystes et les conditions du milieu, soit les conditions hydrographiques, la concentration en éléments nutritifs, la concentration en chlorophylle, la productivité primaire et l'intensité des upwellings. Le but est de voir si les assemblages de dinokystes dans le sédiment peuvent enregistrer la productivité primaire et l'intensité de l'upwelling indépendamment des paramètres hydrographiques,

(4) évaluer la validité et la robustesse de fonctions de transfert se basant sur les assemblages de dinokystes pour reconstituer la paléoprodutivité.

Pour répondre à ces objectifs, un total de 165 échantillons de sédiments de surface du Pacifique du Nord-est a fait l'objet de traitements et d'analyses palynologiques dans le cadre de ce travail. 76 de ces échantillons proviennent des milieux océaniques et néritiques incluant le golfe d'Alaska et les marges ouest américaines, 60 échantillons proviennent des milieux estuariens de la Colombie Britannique incluant le détroit de Géorgie et les fjords d'Effingham et de Seyour-Belize et 30 échantillons proviennent des milieux côtiers du golfe de Tehuantepec au large du Mexique et du golfe de Californie (Baie de la Paz). Les résultats sont reportés dans les deux premiers

chapitres de cette thèse. Des résultats additionnel d'ordre taxinomiques concernant la particularité de certains taxons, ainsi que la description d'une nouvelles espèce, observée notamment dans le golfe de Californie et le golfe de Tehuantepec, seront soumis sous peu pour publication dans la revue "Palynology". Enfin, des compilations de données modernes de productivité et de de données palynologiques de 1171 échantillons de sédiments de surface ont été réalisées pour définir des liens entres les assemblages de dinokystes et la productivité primaire à l'échelle de l'hémisphère nord et tester les fonctions de transfert basées sur la méthode des meilleurs analogues (Overpeck et al., 1985; Guiot, 1990).

CHAPITRE I

DINOCYST DISTRIBUTION IN SURFACE SEDIMENTS FROM THE NORTHEASTERN PACIFIC MARGIN (40-60 °N) IN RELATION TO HYDROGRAPHIC CONDITIONS, PRODUCTIVITY AND UPWELLING

Taoufik Radi¹ and Anne de Vernal¹

¹GEOTOP, Uqam, C. P. 8888, succ. Centre ville, Montréal (Qc). H3C 3P8 Canada
Fax : 514 987 3635

Article publié en 2004 dans la revue *Review of Palaeobotany and Palynology*,
volume 128, 169-193.

Résumé

Soixante seize échantillons de sédiments de surface provenant des marges nord-occidentales américaines, entre 40°N et 60°N, ont fait l'objet d'analyses pour leur contenu palynologique. Le but est d'établir des liens entre la distribution régionale des assemblages de dinokystes et les conditions environnementales (température et salinité des eaux de surface, productivité primaire et upwelling). Les résultats illustrent des concentrations de dinokystes pouvant atteindre 34 000 kystes cm⁻³, notamment dans les zones néritiques et une diversité taxinomique relativement élevée, avec trente deux taxons identifiés. Les assemblages incluent des kystes des dinoflagellés autotrophes et hétérotrophes. *Brigantedinium* spp. accompagné par d'autres taxons hétérotrophes comme *Votadinium* spp., *Quinquecuspis concreta*, *Trinovantedinium variable* et *Lejeunecysta* spp. domine les assemblages des zones côtières influencées par l'upwelling saisonnier. Les sites océaniques sont dominés par les taxons autotrophes, représentés principalement par *Operculodinium centrocarpum*, *Pyxidinoopsis reticulata*, *Nematosphaeropsis labyrinthus* et *Impagidinium aculeatum* vers le Sud, et par *O. centrocarpum*, *Pentapharsodinium dalei*, *Spiniferites ramosus* et *Spiniferites elongatus* dans le Golfe d'Alaska. L'analyse en composantes principales montre que la distribution régionale des assemblages de dinokystes est liée essentiellement à la productivité primaire, à l'intensité de l'upwelling et à la température de surface en hiver.

Mots clés : Pacifique du Nord-Est, productivité, upwelling, dinokystes.

Abstract

Seventy-six surface marine sediment samples from the northwest margin of North America, between 40°N and 60°N, were analysed for their palynological content in order to document the regional distribution of dinocyst assemblages and their relationships with environmental conditions (sea-surface temperature and salinity, productivity and upwelling). The results illustrate a high concentration of dinocysts, notably in the neritic area (up to 34 000 cysts cm⁻³) and a relatively high species diversity with thirty-two taxa identified. The assemblages include cysts of both autotrophic and heterotrophic species. *Brigantedinium* spp. accompanied by other heterotrophic taxa such as *Votadinium* spp., *Quinquecuspis concreta*, *Trinovantedinium variabile* and *Lejeunecysta* spp. dominate in the nearshore areas influenced by seasonal upwelling. The offshore sites are dominated by autotrophic taxa represented mainly by *Operculodinium centrocarpum*, *Pyxidinopsis reticulata*, *Nematosphaeropsis labyrinthus* and *Impagidinium aculeatum* in the south, and by *O. centrocarpum*, *Pentapharsodinium dalei*, *Spiniferites ramosus* and *Spiniferites elongatus* in the Gulf of Alaska. Principal component analysis demonstrates that the regional distribution of dinocyst assemblages is controlled by the primary productivity and upwelling, and by the winter temperature gradient.

Keywords: northeastern Pacific, productivity, upwelling, dinocyst assemblages.

1.1 Introduction

During the last decades, the growing interest in climate and environmental changes has motivated many studies aiming at documenting short- to long-term oceanic variations. The organic-walled dinoflagellate cysts (or dinocysts), which are generally well preserved in marine sediments, have been revealed to be a good proxy for the reconstruction of hydrographical changes at a millennial scale. In the northern North Atlantic and adjacent seas, it has been shown that close relationships link the dinocyst assemblages and sea-surface temperature (SST), salinity, and seasonal duration of sea-ice cover (*e.g.*, Turon, 1984; Matthiessen, 1995; Rochon et al., 1999; de Vernal et al., 1994, 1997, 2001). Some relationships with primary productivity and nutrients have also been reported to exist in the northern North Atlantic (Devillers and de Vernal, 2000) and in coastal areas of the Scandinavian margins (Dale and Fjellsa, 1994; Thorsen and Dale, 1997; Dale, 2001). In contrast to the North Atlantic (which has been intensively studied with regard to modern and Quaternary dinocyst assemblages), the modern distribution of dinocysts in the northern North Pacific is still poorly documented. The few studies of modern dinocyst assemblages that are available concern the coastal zones of Japan (Matsuoka, 1985, 1987, 1992, 1999), the Yellow Sea and East China Sea (Cho and Matsuoka, 2001), the coastal zones of British Columbia (Kumar and Patterson, 2001; Mudie et al., 2002) and the Bering Sea (Radi et al., 2001).

Here, we report on the dinocyst content of seventy-six surface sediment samples, collected from 40°N to 60°N and from 124°W to 150°W (Fig.1 and Table 1). The results permit further documentation of the recent distribution of dinocysts in the northeastern Pacific. One of the aims of this study is to determine whether the regional environmental conditions, *i.e.* temperature, salinity, seasonality, productivity and upwelling, govern the distribution of dinoflagellate cysts. Given the context of

seasonal upwelling along the west coast of North America, special attention has been given to the relationship between the distribution of dinocysts, productivity and upwelling. Dinocysts have been shown to be good tracers of upwelling (Powell et al., 1990; Lewis et al., 1990; Dale, 1996; Zonneveld, 1997a, 1997b, Zonneveld et al., 1997, 2001). The ultimate goal of this study is to contribute to the establishment of a modern data set for the North Pacific suitable for quantitative reconstructions of past sea-surface conditions, which could include upwelling and productivity, in addition to hydrographical parameters.

1.2 Method

1.2.1 Sampling and laboratory procedure

The seventy-six surface sediment samples were collected either by gravity coring or box coring (cf. Table 1). Sediments were sub-sampled from the Oregon State University (OSU) archives, between 0 and 3 cm down in the core and prepared for palynological analysis following the standard procedure of the micropaleontological laboratory at GEOTOP (cf. de Vernal et al., 1999) as summarised below.

Two to five cm³ of wet sediment were sieved at 10 and 106 µm in order to remove coarse sand, fine silt and clay particles. The 10-106 µm fraction was treated with HCl (10%) and HF (49%) to dissolve carbonate and silica particles. The residue was ultimately sieved at 10 µm and mounted between a slide and cover slide in glycerine gel. Dinocysts were identified and systematically counted using a transmitted light microscope at 250x to 1000x magnification. The concentration of dinocysts was evaluated using the marker-grain method (Matthews, 1969), which yields results accurate to about 90% for a 0.95 confidence interval (de Vernal et al., 1987). In most samples, more than 300 cysts were identified, with the exception of offshore samples

BB311-36, BB311-29, BB311-50, Y70-4-60 and W9009A-30, in which less than 100 specimens were counted (Table 1).

1.2.2 Nomenclature of dinoflagellate cysts

The taxonomical nomenclature of dinocyst used here conforms to that presented in Radi et al. (2001) after Rochon et al. (1999). The assemblages also include cysts we attribute to *Echinidinium granulatum* (Plate 1), which was described by Zonneveld (1997a). The specimens we observed in our samples are similar to those from the Arabian Sea as illustrated in Zonneveld (1997a) with clear granulate cell wall, acuminate and hollow processes. However, in our material, the archeopyle was very difficult to observe because of badly oriented specimens. Thus, we refer these specimens to “cf. *E. granulatum*”. Three specimens probably belonging to *Echinidinium*, but not to *E. granulatum*, were also encountered in sample TT68-18. These specimens are small and spherical with non-tabular and acuminate processes (25-30 μm of central body diameter, 5 μm of processes length; Plate 1). They were excluded from statistical analysis due to their rare occurrence. Brownish specimens surrounded by apical and antapical horns belonging to protoperidinales, for which determination at the genus level was difficult due to poor preservation and/or orientation are grouped under the label “undifferentiated Protoperidinioids”. Some taxa were grouped because of morphological convergence and/or difficulties in seeing the archeopyle, e.g. *Brigantedinium* spp. which include *Brigantedinium simplex* and *Brigantedinium cariacense*. *Spiniferites elongatus*, *Spiniferites frigidus* and *Rottnestia amphicavata* are grouped under *Spiniferites elongatus* s.l. (cf. Rochon et al., 1999). *Operculodinium centrocarpum* s.l. includes all the morphotypes described in de Vernal et al. (2001) and Radi et al. (2001).

1.2.3 Statistical methods

Multivariate analyses were performed using the principal components analysis (PCA) software of Guiot and Goeury (1996). The PCA is a commonly used technique for studies dealing with variations of environmental parameters and their influence upon animal or vegetal populations. We chose PCA because it is a method of ordination, which yields projections according to a limited number of orthogonal axes (principal components) and therefore permits us to distinguish grouping of samples that may be related to particular environmental conditions. For data treatment, the percentages of dinocysts were ln-transformed in order to increase the weight of the taxa with low percentages, which generally have narrow ecological preferences, and to diminish the importance of ubiquitous taxa, which often dominate the assemblages.

1.2.4 Hydrographical data

The temperature and salinity data of surface water (water depth = 0 m) were compiled from the data set of the National Oceanographic Data Center (NODC, 1994), which includes data collected between 1930 and 1994. Compilation was made to calculate mean values for all measurements available within one degree square. Productivity data are from Antoine et al. (1996) and were estimated from satellite observations of the chlorophyll distribution. The upwelling index (UI) used here is from the Pacific Fisheries Environmental Laboratory (PFEL) of the National Oceanographic and Atmospheric administration (NOAA). The calculation of UI is based upon the offshore Ekman transport due to geostrophic wind stress, which is derived from surface atmospheric pressure fields. The mass transport of the surface water is 90° to the right of the wind direction in the Northern Hemisphere. Ekman transports are resolved into components parallel and normal to the local coastline orientation. The

magnitude of the offshore component is considered to be an index of the amount of upwelled water. UI in PFEL's data set is represented in term of $\text{m}^3 \text{s}^{-1}$ per 100 m of coastline and includes six-hourly and monthly data from 1967 to 2001. More information is available from the PFEL web site (<http://www.pfeg.noaa.gov/index.html>).

1.3 Oceanographic settings

1.3.1 Atmospheric circulation

Atmospheric circulation in the northeastern Pacific is characterized by the anticyclonic North Pacific high and the cyclonic Gulf of Alaska-Aleutian low-pressure cells (Thomson, 1981; Rienecker and Ehret, 1988; Trenberth and Hurrell, 1994; Mock et al., 1998). In winter, the strong intensity of the Aleutian low generates cyclonic winds, which dominate from autumn to early spring. The anticyclonic North Pacific high occurs all the year, but its intensity is highest in summer, thus generating anticyclonic wind. As a consequence, the dominant winds originate from the west in winter and from the northwest in summer.

1.3.2 Surface water circulation

The configuration of wind contributes to the formation of the Alaska and California currents, which are derived respectively from the Subarctic and North Pacific currents (Huyer, 1983; Mock et al., 1998; Fig. 1). Along the California and Oregon coasts, strong summer wind from the northwest results in offshore Ekman transport. As a consequence, upwelling of cold nutrient-rich water occurs along the eastern margin of

the North Pacific as far north as Vancouver Island (Thomson, 1981; Huyer, 1983). Upwelling shows a pronounced seasonal cycle and occurs from April to September. It is stronger in the northern part of the Californian current and decreases towards the north. No upwelling occurs along the coast of the Gulf of Alaska (Fig. 2).

1.3.3 Productivity

A wide range of biological production rates characterize the study area. The open ocean sites are characterized by low productivity ($<100 \text{ gC m}^{-2} \text{ yr}^{-1}$), whereas the coastal areas record primary productivity up to $500 \text{ gC m}^{-2} \text{ yr}^{-1}$ (Antoine et al., 1996), the highest values being recorded in seasonal upwelling areas along the British Columbia and California coasts (Figs. 2 and 3). In these regions there are two major blooms of phytoplankton during the year: the spring bloom, which is principally associated with diatoms, and the summer to late summer bloom resulting from mixed phytoplankton growth including dinoflagellates (Thomson, 1981). These two blooms typically occur from April to June and from June to September, respectively (Fig. 4).

1.3.4 Temperature and salinity

Except in the Gulf of Alaska, which is characterized by relatively cold water, the eastern margin of the North Pacific is occupied by temperate waters. In the study area, sea-surface temperature (SST) ranges between 4 and 11.4°C in winter, with a decreasing gradient from the south to the north. In summer, SST ranges from 12 to 19°C (Fig. 5) with an east to west gradient, i.e. with colder water along the coastal areas (Thomson 1981) as a result of seasonal upwelling (Fig. 3).

Mean annual salinity is relatively low in the northeastern Pacific since precipitation exceeds evaporation. As a result, the water column is characterized by a strong stratification with a sharp halocline (Warren, 1983). In the study area, salinity ranges from 31 to 33 in August, with the exception of three sites (SUSP5-02, SUSP5-05, Y7409-02) close to Kenai Peninsula and the Columbia River end member, which are marked by a very low salinity (Fig. 5).

1.4 Dinoflagellate cyst distribution

The dinocyst concentration in surface sediment samples ranges from 200 to 34 000 cysts cm^{-3} (Fig. 6 and Table 1) with the highest values observed in the neritic areas. Offshore areas show relatively low concentrations and low species richness. In general, heterotrophic-related taxa are dominant in the coastal zone. They include protopteridinales (*Brigantedinium* spp., *Quinquecuspis concreta*, *Votadinium* spp., *Lejeunecysta* spp., *Selenopemphix* spp.) as well as gymnodiniales (cysts of *Polykrikos kofoidii*). Autotrophic-related taxa such as *Operculodinium centrocarpum*, *Nematosphaeropsis labyrinthus*, *Pyxidinopsis reticulata* and *Impagidinium aculeatum* mainly occur in the offshore area (Fig. 7; Plates 1 and 2).

Results of the PCA show that the two first principal components represent respectively 80.4 and 7.1% of the variance (Fig. 8). Each of the other components explains less than 3% of the variance and they are therefore considered to represent a non-significant part of variation in the assemblages.

All the heterotrophic-related taxa, including protopteridinales and gymnodinales taxa, are ordinated on the negative side of the first principal component axis (PC1), whereas most gonyaulacales taxa (*O. centrocarpum*, *Nematosphaeropsis labyrinthus*, *Impagidinium aculeatum* and *I. pallidum*) are ordinated on the positive side (Fig. 8). The PC1 values show a distal-proximal gradient with very high values at nearshore sites along the west coast of America (Fig. 9a). The second principal component (PC2) illustrates an opposition between temperate taxa (*Impagidinium strialatum*, *I. sphaericum*, *I. paradoxum*, *I. patulum*, *I. aculeatum* and *Spiniferites mirabilis*) and cold-water or ubiquitous taxa (*Spiniferites elongatus*, *S. ramosus*, *Spiniferites* spp. and cysts of *Pentapharsodinium dalei*; Fig. 8). PC2 illustrates a latitudinal gradient showing the highest values in the Gulf of Alaska (Fig. 9b).

Based on the relative abundance of taxa and the results of the PCA, five assemblage zones are defined (Figs. 6-10):

Assemblage zone I occurs in the Gulf of Alaska where the surface water is marked by a low temperature of about 4°C in February and 10°C in August. Dinocyst concentrations are variable from 145 to 13 500 cysts cm⁻³. The assemblage composition in this zone is dominated by *Brigantedinium* spp., *Spiniferites ramosus*, *S. elongatus*, *Spiniferites* spp., cysts of *Pentapharsodinium dalei* and *Operculodinium centrocarpum*. It is also characterized by high PC2 values (Fig. 10). This assemblage is similar to the modern one in the southern Bering Sea (Radi et al., 2001) with respect to species composition and relative abundance of taxa, except for the lack of *Nematosphaeropsis labyrinthus*, which occurs only in the Gulf of Alaska.

Assemblage zone II occurs in the coastal zones of Vancouver Island, where primary productivity is high because of coastal upwelling. Dinocyst concentration (up to

34000 cysts cm^{-3}) and species richness are high. The assemblage shows some similarities to lower-latitude assemblages from the Atlantic Ocean, such as the coastal zones of the Gulf of Guinea (Marret, 1994). This assemblage is characterized by the dominance of *Brigantedinium* spp. and other protoperidinian heterotrophic taxa. It is marked by negative scores of PC1. This assemblage is comparable to the one described from surface sediment samples collected in Effingham Inlet, along the Vancouver Island coast (Kumar and Patterson, 2001) and in the Strait of Georgia (Guilbault et al., 2003).

Assemblage zone III corresponds to the open ocean domain at middle latitudes where primary productivity is low ($<180 \text{ gC m}^{-2} \text{ yr}^{-1}$). Dinocyst concentration in this zone is relatively low (300-9000 cysts cm^{-3}). The assemblage includes most species found in the Atlantic Ocean at the same latitude (cf. Rochon et al., 1999). It is characterized by the dominance of the autotrophic taxa *Operculodinium centrocarpum*, *Nematosphaeropsis labyrinthus* and *Pyxidinosia reticulata*. This assemblage is distinguished on the basis of positive PC1 values.

Assemblage zone IV is associated with the coastal zone off North California and Oregon, where there is a high productivity related to upwelling. The assemblage is largely dominated by *Brigantedinium* spp. and other heterotrophic taxa. PC1 shows negative scores and the overall assemblage is comparable to that of assemblage zone II. However, assemblage IV is distinguished by PC1 values that are slightly less negative than for assemblage zone II, and by the occurrence of warm taxa such as *Impagidinium paradoxum* and *I. aculeatum*, which relate to relatively warm sea-surface conditions.

Finally, assemblage zone V corresponds to the open ocean domain in the southern part of the study area. Dinocyst concentrations are low ($<1300 \text{ cysts cm}^{-3}$) and the

assemblage is dominated by *Operculodinium centrocarpum* (reaching up to 80% of the sum) and *Impagidinium aculeatum* (up to 30%), which are accompanied by *I. patulum* and *I. paradoxum* also showing relatively high percentages. This assemblage zone is distinguished by positive PC1 scores and negative PC2 scores.

1.5 Discussion

1.5.1 Relationships between dinocyst assemblages and environmental conditions

In order to explore the relationships between the distribution of dinocysts and the selected oceanographic parameters, a matrix of correlation was developed (see Table 2). On the whole, there is no strong correlation between individual taxa percentages and the selected hydrographic parameters. Nevertheless, *Spiniferites elongatus* shows a negative relationship with the February SST, whereas *Impagidinium aculeatum* seems to be positively related to August SST. A stronger relationship apparently exists between some of the taxa and the productivity: *Brigantedinium* spp., *Quinquecuspis concreta*, *Islandinium minutum*, *Votadinium* spp., *Selenopemphix* spp. and cysts of *Polykrikos kofoidii* are positively linked with productivity, and there is a significant correlation between the total percentage of heterotrophic taxa and the primary productivity ($R = 0.76$) or the upwelling intensity ($R = 0.80$; cf. Fig. 11). Moreover the assemblages, as quantified through principal component analysis, show a very strong relationship between PC1 and productivity ($R = -0.88$) and the total percentages of heterotrophic taxa ($R = 0.91$; Fig. 12). Although more equivocal, there seems to be a link between the mean UI in summer (June to September) and PC1 (Fig. 13).

The PC2 distribution shows a latitudinal pattern in dinocyst assemblages (Fig. 9b). It seems to be explained by sea-surface conditions in winter as illustrated by the significant correlation between the PC2 and the February SST ($R = -0.79$; Fig. 14). In contrast, no clear relationship can be shown between August SST and the dinocyst assemblages or PC2, likely because the upwelling during summer, which is stronger in the south, results in limited gradient of temperature over the study area (see Fig. 6). The small range of sea-surface salinity in the study area does not permit us to illustrate accurately the relationship between the salinity and the dinocyst assemblages.

1.5.2 Dinocyst taxa and assemblages versus upwelling

Dinocyst assemblages dominated by cysts of heterotrophic taxa, notably cysts of *Protoperidinium* species, have been reported in various low-latitude upwelling zones characterized by high productivity and nutrient availability. They include the Gulf of Guinea (Marret, 1994), the Benguela upwelling region (Zonneveld et al., 2001), the Arabian Sea (Zonneveld, 1997a, 1997b; Zonneveld et al., 1997), the Peruvian coast (Lewis et al., 1990, Powell et al., 1990), and the Iberian west coast (Sprangers et al., 2004). The dominance of heterotrophic taxa was also reported from high-latitude environments such as the eastern margin of Greenland (Rochon et al., 1999) and the high-productivity area of the north water polynya that is related to upwelling (Hamel et al., 2002). In all cases, the abundance of heterotrophic-related taxa is most likely the result of food availability, notably diatoms (Jacobson and Anderson, 1986) whereas the low production of autotrophic dinoflagellates could be related to competition with the blooming diatom populations. In the North Pacific Ocean, the spring bloom of diatoms likely constitutes the major source of food for heterotrophic dinoflagellates.

Although the heterotrophic taxa dominance seems to be a common characteristic of upwelling regions, the assemblages of the northeastern Pacific upwelling zone (assemblage zones II and IV) show some particularities:

The northeastern Pacific assemblages differ from those of other high-latitude upwelling and polynyas (Rochon et al., 1999; Hamel et al., 2002) by their high species richness amongst protoperidinales, with significant occurrences of *Votadinium* spp., *Lejeunecysta* spp., *Quinquecuspis concreta* and *Echinidinium granulatum* (Fig. 7; Plate 1).

Lingulodinium machaerophorum is totally absent from the northeastern Pacific, although it is a common to dominant taxon in most if not all upwelling areas of low to middle latitudes such as the African west coast (Marret, 1994; Zonneveld et al., 2001), the northwest Iberian coast (Sprangers et al., 2004), the Arabian Sea (Zonneveld, 1997a, 1997b; Zonneveld et al., 1997) and the Peruvian coast (Lewis et al., 1990).

The cyst of *Polykrikos kofoidii*, which characterizes upwelling zones of the northeastern Pacific (up to 8%), records high percentages in other upwelling zones from the Atlantic Ocean (Marret, 1994; Zonneveld et al., 2001) and occurs in other areas of the North Pacific, such as the southeastern Bering Sea (Radi et al., 2001) and the coastal zones of Japan (Matsuoka, 1985, 1987; Matsuoka and Cho, 2000). However, in the Pacific, it was not observed in the Peruvian upwelling zone (Lewis et al., 1990).

1.6 Conclusion

The results of this study provide new information on the regional distribution of dinocyst assemblages and their relationships with environmental conditions in the northeastern Pacific. Productivity largely linked to seasonal upwelling constitutes the major parameter controlling the distribution pattern of dinocyst assemblages on a regional scale. In particular, the increase in relative abundance of heterotrophic taxa in the coastal zones appears closely related to prey availability (diatoms), which is the result of high primary productivity. In addition, the distribution pattern of dinocyst assemblages follows a latitudinal gradient that illustrates the importance of winter sea-surface temperature.

On this basis, the results of this study can be used together with results of previous work reporting on the dinocyst assemblages in Bering Sea (Radi et al., 2001) and the coastal areas of British Columbia (Kumar and Patterson, 2002) in order to establish a reference dinocyst database for the northern North Pacific Ocean. Such a database could eventually be used to reconstruct quantitatively sea-surface conditions including productivity in the northern Pacific, thus contributing to extend the potential of dinocysts assemblages as environmental tracers.

1.7 Acknowledgements

We are grateful to the Oregon State University for access to samples (NSF grant OCE97-12024) and to B. Conard for the subsampling of core tops. We are also grateful to J. McKay and F. Marret for the critical reading of the earlier manuscript.

We thank J. Powell and D. Hernández-Becerril for the review of the manuscript. The Natural Science and Engineering Council (NSERC) of Canada have supported this research, notably through the Climate System History and Dynamics (CSHD) project.

1.8 References

Antoine, D., André, J.M., Morel, A., 1996. Oceanic primary production. 2. Estimation at global scale from satellite (costal zone colour scanner) chlorophyll. *Global Biogeochemical Cycles* 10, 57-69.

Cho, H.-J., Matsuoka, K., 2001. Distribution of dinoflagellate cysts in surface sediments from the Yellow Sea and East China Sea. *Marine Micropaleontology* 42, 103-123.

Dale, B., Fjellsa, A., 1994. Dinoflagellate cysts as paleoproductivity indicators: state of the art, potential and limits. In: Zahn, R., Pedersen, T., Kaminski, M., Labeyrie, L. (Eds.), *Carbon cycling in the glacial Ocean: constrains on the ocean's role in global change*. Berlin, Springer-Verlag, 521-537.

Dale, B., 1996. Dinoflagellate cysts ecology: modelling and geological applications. In: Jansonius, J., McGregor, D. (Eds.), *Palynology: principles and applications*. The American Association of Stratigraphic Palynologists Foundation. Salt Lake City, 1249-1276.

Dale, B., 2001. Marine dinoflagellate cysts as indicators of eutrophication and industrial pollution: a discussion. *The Science of the Total Environment* 264, 235-240.

de Vernal, A., Larouche, A., Richard, P.J.H., 1987. Evaluation of palynomorph concentrations: do the aliquot and the marker-grain methods yield comparable results? *Pollen et Spores* 29, 291-304.

de Vernal, A., Turon, J.-L., Guiot, J., 1994. Dinoflagellate cyst distribution in high-latitude marine environments and quantitative reconstruction of sea-surface salinity, temperature, and seasonality. *Canadian Journal of Earth Sciences* 31, 48-62.

de Vernal, A., Rochon, A., Turon, J.-L., Matthiessen, J., 1997. Organic-walled dinoflagellate cysts: palynological tracers of sea-surface conditions in middle to high latitude marine environments. *Geobios* 30, 905-920.

de Vernal, A., Henry, M., Bilodeau, G., 1999. *Technique de préparation et d'analyse en micropaléontologie*. Unpublished report, Les Cahiers du GEOTOP, Université du Québec à Montréal 3, 41 pp.

de Vernal, A., Henry, M., Matthiessen, J., Mudie, P.J., Rochon, A., Boessenkool, K., Eynaud, F., Grøsfjeld, K., Guiot, J., Hamel, D., Harland, R., Head, M.J., Kunz-

Pirrung, M., Levac, E., Loucheur, V., Peyron, O., Pospelova, V., Radi, T., Turon, J.-L., Voronina E., 2001. Dinocyst assemblages as tracer of sea-surface conditions in the northern North Atlantic, Arctic and sub-Arctic seas: the "n = 677" database and derived transfer functions. *Journal of Quaternary Science* 16, 681-698.

Devillers, R., de Vernal, A., 2000. Distribution of dinocysts in surface sediments of the northern North Atlantic in relation with nutrients and productivity in surface waters. *Marine Geology* 166, 103-124.

Guilbault, J.P., Barrie, J.V., Conway, K., Lapointe, M., Radi, T., 2003. Paleoenvironments associated with the deglaciation process in the Strait of Georgia, off British Columbia: microfaunal and microfloral evidence. *Quaternary Science Reviews* 22, 839-857.

Guiot, J., Goeury, C., 1996. PPPbase, a software for statistical analysis of paleoecological data. *Dendrochronologia* 14, 295-300.

Hamel D., de Vernal, A., Hillaire-Marcel, C., Gosselin, M., 2002. Organic-walled microfossils and geochemical tracers: sedimentary indicators of productivity change in the North Water and northern Baffin Bay (high Arctic) during the last centuries. *Deep Sea Research II* 49, 5277-5295.

Huyer, A., 1983. Coastal upwelling in the California current system. *Progress in Oceanography* 12, 259-284.

Jacobson, D., Anderson, D., 1986. Thecate heterotrophic dinoflagellates: Feeding behaviour and mechanics. *Journal of Phycology* 22, 249-258.

Kumar, A., Patterson, T., 2002. Dinoflagellate cyst assemblages from Effingham Inlet, Vancouver Island, British Columbia, Canada. *Palaeogeography, Palaeoclimatology, Palaeoecology* 180, 187-206.

Lewis, J., Dodge, J.D., Powell, A.J., 1990. Quaternary dinoflagellate cysts from the upwelling system offshore Peru, Hole 686B, ODP Leg 112. In Suess, E., von Huene, R., et al. (eds.), *Proceeding of the Ocean Drilling Program. Scientific Results* 112, 323-327.

Marret, F., 1994. Distribution of dinoflagellate cysts in recent marine sediments from the east Equatorial Atlantic (Gulf of Guinea). *Review of Palaeobotany and Palynology* 84, 1-22.

Matsuoka, K., 1985. Organic-walled dinoflagellate cysts from surface sediments of Nagasaki Bay and Senzaki Bay, West Japan. *Bulletin of the Faculty of Liberal Arts, Nagasaki University* 25, (2), 21-115.

Matsuoka, K., 1987. Organic-walled dinoflagellate cysts from surface sediments of Akkeshi Bay and Lake Saroma, North Japan. *Bulletin of the Faculty of Liberal Arts, Nagasaki University* 28, (1), 35-123.

Matsuoka, K., 1992. Species diversity of modern dinoflagellate cysts in surface sediments around the Japanese islands. In: Head, M.J.; Wrenn, J.H. (eds.), *Neogene and Quaternary dinoflagellate cysts and acritarchs*. American Association of Stratigraphic Palynologists Foundation, Dallas, TX, pp. 33-53.

Matsuoka, K., 1999. Eutrophication process recorded in dinoflagellate cyst assemblages - a case of Yokohama Port, Tokyo Bay, Japan. *The Science of the Total Environment* 231, 17-35.

Matsuoka, K., Cho, H.J., 2000. Morphological variation in cyst of gymnodinialean dinoflagellate *Polykrikos*. *Micropaleontology* 46, 360-364.

Matthews, J., 1969. The assessment of a method for the determination of absolute pollen frequencies. *New Phytologist* 68, 161-166.

Matthiessen, J., 1995. Distribution patterns of dinoflagellate cysts and other organic-walled microfossils in recent Norwegian-Greenland Sea sediments. *Marine Micropaleontology* 24, 307-334.

Mock, C.J., Bartlein, P.J., Anderson, P.M., 1998. Atmospheric circulation patterns and spatial climatic variations in Beringia. *International Journal of Climatology* 10, 1085-1104.

Mudie, P.J., Rochon, A., Levac, E., 2002. Palynological records of red tide-producing species in Canada: past trends and implications for the future. *Palaeogeography, Palaeoclimatology, Palaeoecology* 180, 159-186.

NODC, 1994. *World Ocean Atlas*. National Oceanic and Atmospheric Administration, Boulder, Colorado, CD-ROM data set.

Powell, A.J., Dodge, J.D., Lewis, J., 1990. Late Neogene to Pleistocene palynological facies of the Peruvian continental margin upwelling, Leg 112. In Suess, E., von Huene, R., et al. (eds.), *Proceeding of the Ocean Drilling Program. Scientific Results* 112, 297-321.

- Radi, T., de Vernal, A., Peyron, O., 2001. Relationships between dinocyst assemblages in surface sediments and hydrographic conditions in the Bering and Chukchi seas. *Journal of Quaternary Science* 16, 667-680.
- Rienecker, M., Ehret, L., 1988. Wind stress curl variability over the North Pacific from the comprehensive Ocean-Atmosphere data set. *Journal of Geophysical Research* 96, 5069-5077.
- Rochon, A., de Vernal, A., Turon, J.-L., Matthiessen, J., Head, M.J., 1999. Distribution of dinoflagellate cysts in surface sediments from the North Atlantic Ocean and adjacent seas in relation to sea-surface parameters. *American Association of Stratigraphic Palynologists, Contribution Series* 35, 152 pp.
- Sprangers, M., Dammers, N., Brinkhuis, H., van Weering, T.C.E., Lotter, A.F., 2004. Modern organic walled dinoflagellate cyst distribution offshore NW Iberia; tracing the upwelling system. *Review of Palaeobotany and Palynology* 128, 97-106.
- Thomson, R.E., 1981. Oceanography of the British Columbia coast. *Canadian Special Publication of Fisheries and Aquatic Sciences*, Ottawa, ON, 56, 291 pp.
- Thorsen, T.A., Dale, B., 1997. Dinoflagellate cysts as indicators of pollution and past climate in a Norwegian fjord. *The Holocene* 7, 433-446.
- Trenberth, K.E., Hurrell, J.W., 1994. Decadal atmosphere-ocean variations in the Pacific. *Climate Dynamics* 9, 303-319.
- Turon, J.-L. 1984. Le palynoplancton dans l'environnement actuel de l'Atlantique nord-oriental. Évolution climatique et hydrologique depuis le dernier maximum glaciaire. *Mémoire de l'Institut de Géologie du bassin d'Aquitaine*, Bordeaux, 17, 313 pp.
- Warren, B.A., 1983. Why is no deep water formed in the North Pacific? *Journal of Marine Research* 41, 327-347.
- Zonneveld, K., 1997a. New species of organic walled dinoflagellate cysts from modern sediments of the Arabian Sea (Indian Ocean). *Review of Paleobotany and palynology* 97, 319-337.
- Zonneveld, K., 1997b. Dinoflagellate cyst distribution in surface sediments from the Arabian Sea (northwestern Indian Ocean) in relation to temperature and salinity gradients in the upper water column. *Deep-Sea Research II* 6-7, 1411-1443.

Zonneveld, K., Ganssen G., Troelstra, S., Versteegh, G.J.M., Visscher, H., 1997. Mechanisms forcing abrupt fluctuations of the Indian Ocean summer monsoon during the last deglaciation. *Quaternary Science Reviews* 16, 187-201.

Zonneveld, K., Hoek, R.P, Brinkhuis, H., Willems, H., 2001. Geographical distribution of organic-walled dinoflagellate cysts in surficial sediments of the Benguela upwelling region and their relationship to upper ocean conditions. *Progress in Oceanography* 48, 25-75.

1.9 Figure captions

Figure 1. Location map of study sites (dots). The arrows indicate the mean pathway of the surface currents. Isobaths indicate water depth at 200 and 1000 meters.

Figure 2. Seasonal change in productivity and upwelling index (UI) at selected coastal sites. Productivity data are from Antoine et al. (1996). The UI data are from the PFEL data set of NOAA (<http://www.pfeg.noaa.gov/index.html>). UI data represent mean values calculated from 1967 to 2001. UI is expressed in term of $\text{m}^3 \text{s}^{-1}$ per 100 m of coastline.

Figure 3. Sea-surface temperature in August plotted against annual primary productivity. Black dots indicate sites with low temperature and high productivity, which corresponds to upwelling situation.

Figure 4. Seasonal variation in primary productivity (Antoine et al., 1996) and temperature (NODC, 1994) at selected sites. Black arrows indicate the spring bloom and white arrows indicate the summer to late summer bloom. AP = Annual primary productivity in term of $\text{gC m}^{-2} \text{yr}^{-1}$.

Figure 5. Relationship between sea-surface temperature in August, sea-surface temperature in February and sea-surface salinity in August. Black dots indicate sites characterized by fresh water input and thus by particularly low salinity.

Figure 6. Diagram illustrating the percentages of all dinocyst taxa except *Bitectatodinium tepikiense* and *Echinidinium* spp., which occur only occasionally. On the right of the diagram are indicated the total cyst concentration, the two first

principal components (PC1 and PC2) which respectively represent 80.4% and 7.1% of the variance, the sea-surface temperature and the primary productivity.

Figure 7. Maps showing the percentages of dinocyst taxa in the northeastern Pacific.

Figure 8. Ordination of each taxon based on the two first principal component axes. The white diamonds represent cysts of autotrophic taxa and the black diamonds, cysts of heterotrophic taxa.

Figure 9. Maps showing the geographical distribution of PC1 and PC2 values.

Figure 10. Definition of dinocyst assemblages according to PC1 and PC2. PC1 permits the separation of neritic and oceanic areas, whereas PC2 exhibits a latitudinal gradient.

Figure 11. Relationship between the percentages of heterotrophic taxa and productivity and mean UI in summer (average over June, July, August and September). Only coastal sites, where a UI can be generated, are represented. The coefficients of correlations were calculated based on a logarithmic relationship.

Figure 12. Relationship between PC1 and the annual primary productivity and the percentages of heterotrophic taxa. The coefficient of correlation was calculated based on a logarithmic curve (PC1 versus Productivity) and a linear relationship (PC1 versus heterotrophic taxa percentages).

Figure 13. Relationship between the summer UI and PC1. Only coastal sites, where a UI can be generated, are represented. The coefficient of correlation was calculated based on a linear relationship.

Figure 14. Relationship between PC2 and productivity. The coefficient of correlation is calculated after a linear regression.

1.10 Table captions

Table 1. Sampling site location, sea surface temperature and salinity (NODC, 1994), annual productivity (Antoine et al, 1996), dinocyst concentrations and values for the two first principal components PC1 and PC2.

Table 2. Matrix of correlation between dinocyst assemblages and taxa and selected oceanographic parameters. The correlations are based on linear or logarithmic (Asterisks) relationship.

1.11 Plate captions

Plate 1. Scale bar is 10 μm . Sample number is followed by the England Finder coordinates.

1-3, cf. *Echinidinium granulatum*. 1-2, W8809A-3, L43/2-4. 3, W8809A-53, F52/2

4-6, *Echinidinium* spp. 4, W8809A-53, B50/3. 5-6, TT68-18, H19/2.

7-9, Cysts of *Protoperidinium americanum*. TT68-18, B55. 7, apical view showing apical surface and archeopyle. 8, antapical surface. 9, optical section showing outer wall.

10, *Votadinium calvum*. TT68-18, E25/1.

11, *Votadinium spinosum*. Y7409-2, T50/1-3.

12, *Quinquecuspis concreta*. TT68-18, D18/3. Dorsal view showing striations on the wall surface.

13, *Selenopemphis quanta*. Y74-1-8, J39/1.

14-15, Cyst of *Polykrikos kofoidii*. TT68-18. 14, E55/3. 15, C39/4.

Plate 2. Scale bar is 10 μm . Sample number is followed by the England Finder coordinates.

1-3, *Impagidinium striatum*. Y74-1-8, F47/3. 1, Ventral view. 2, dorsal view. 3, mid focus.

4, *Impagidinium aculeatum*. 7407-4, S39.

5, *Spiniferites mirabilis*. TT49-22, L16/2.

6, *Nematosphaeropsis labyrinthus*. TT53-005, Q17.

7-9, Cyst of *Pentapharsodinium dalei*. W8808A-3, B12/4. 7, Ventral view. 8, dorsal view. 9, mid focus.

10-11, *Operculodinium centrocarpum*. W8809A-3, F12/4. 10, Dorsal surface showing archeopyle. 11, mid focus.

12, *Pyxidinoopsis reticulata*. TT39-17, E30.

Figure 1

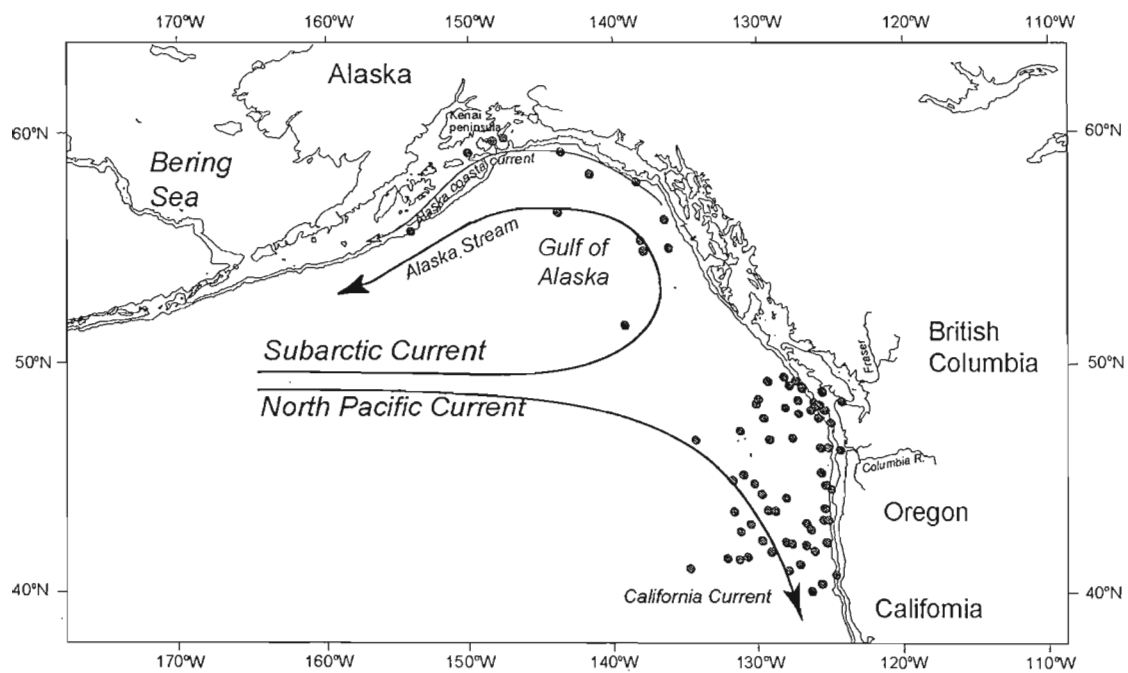


Figure 2

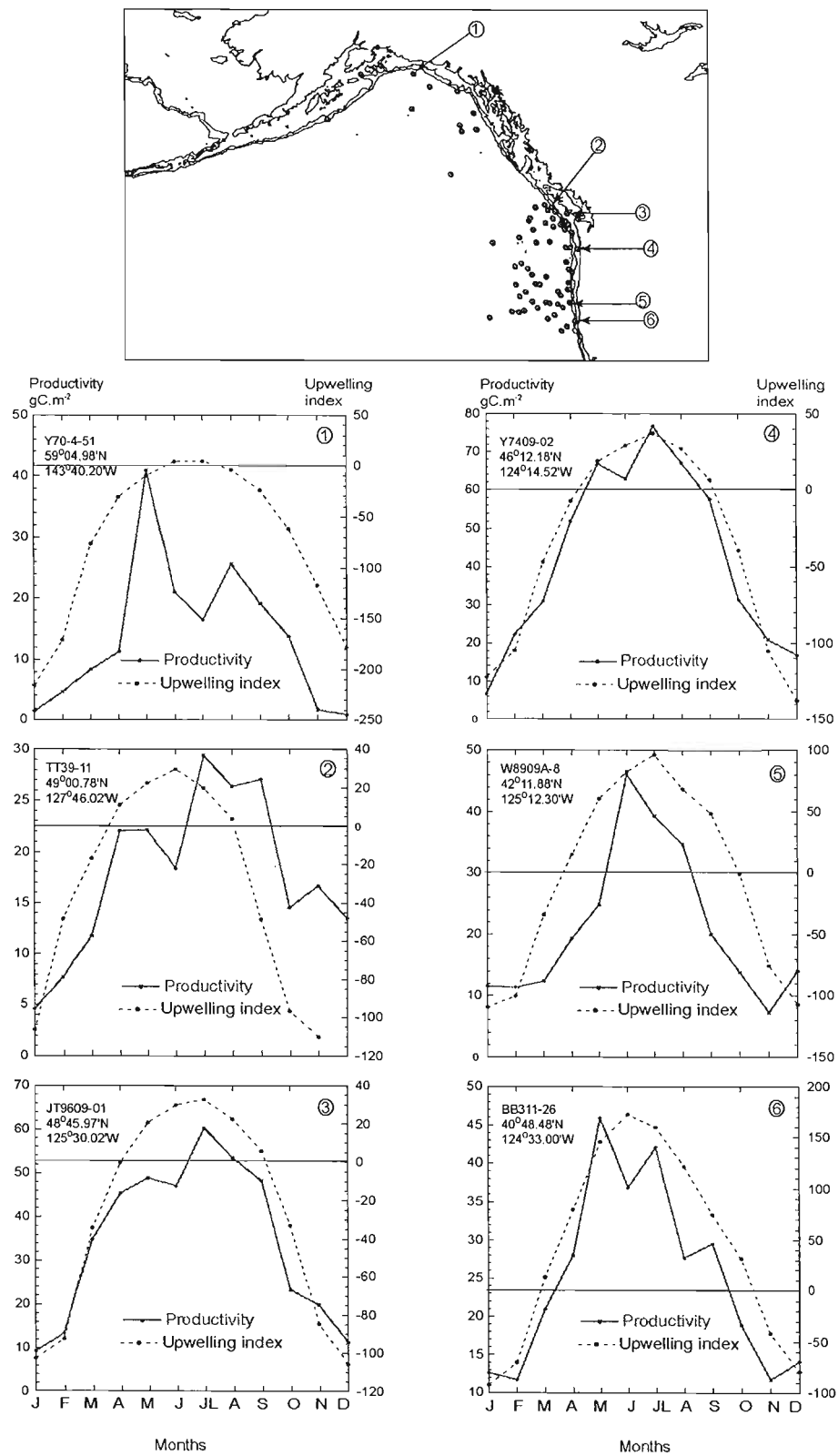


Figure 3

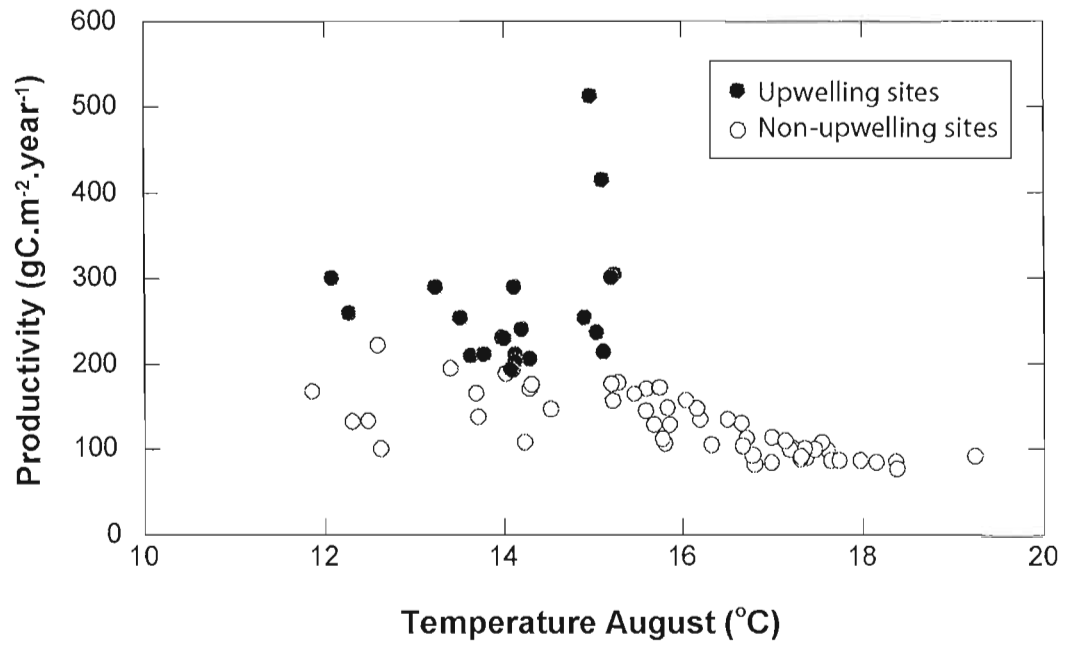


Figure 4

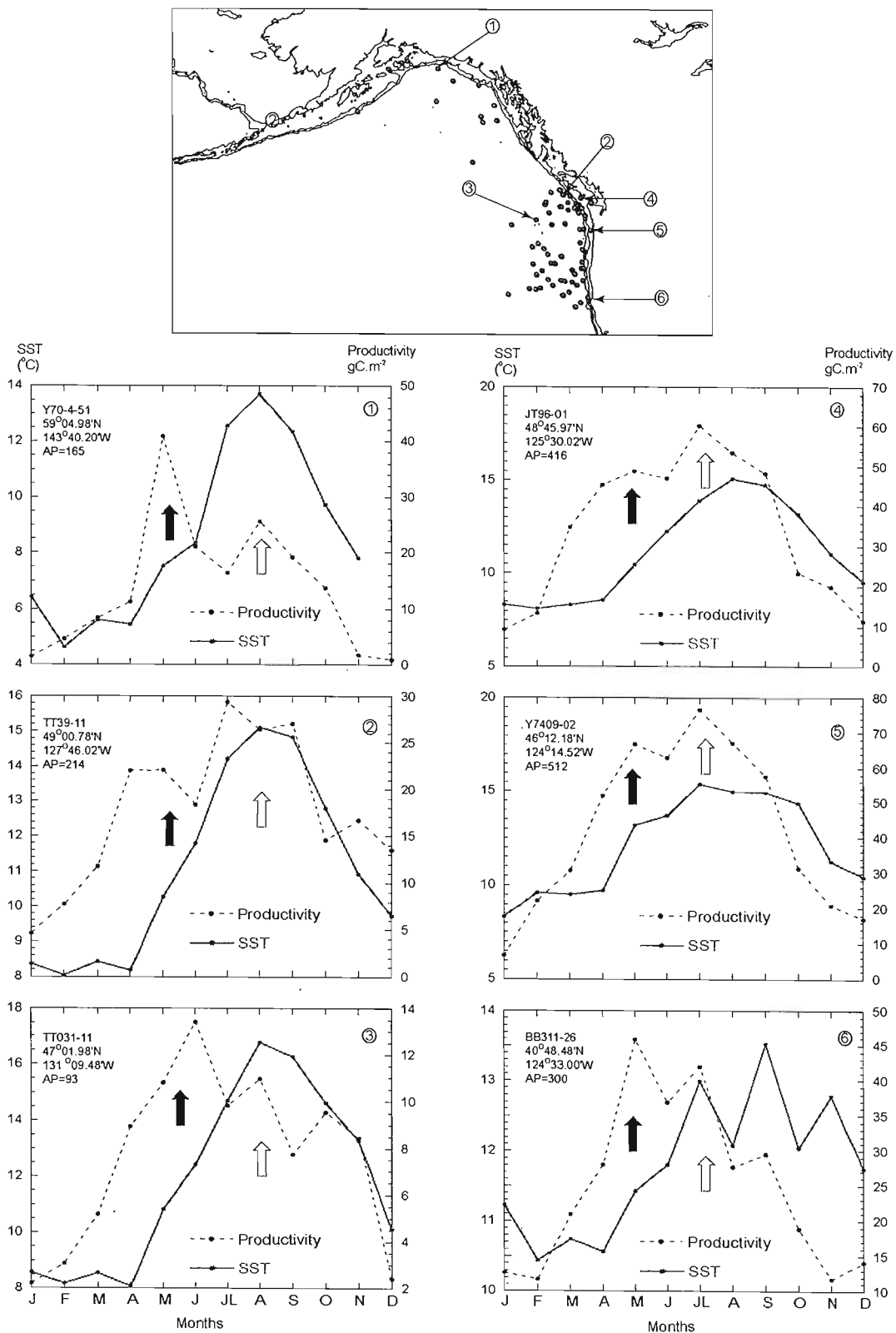


Figure 5

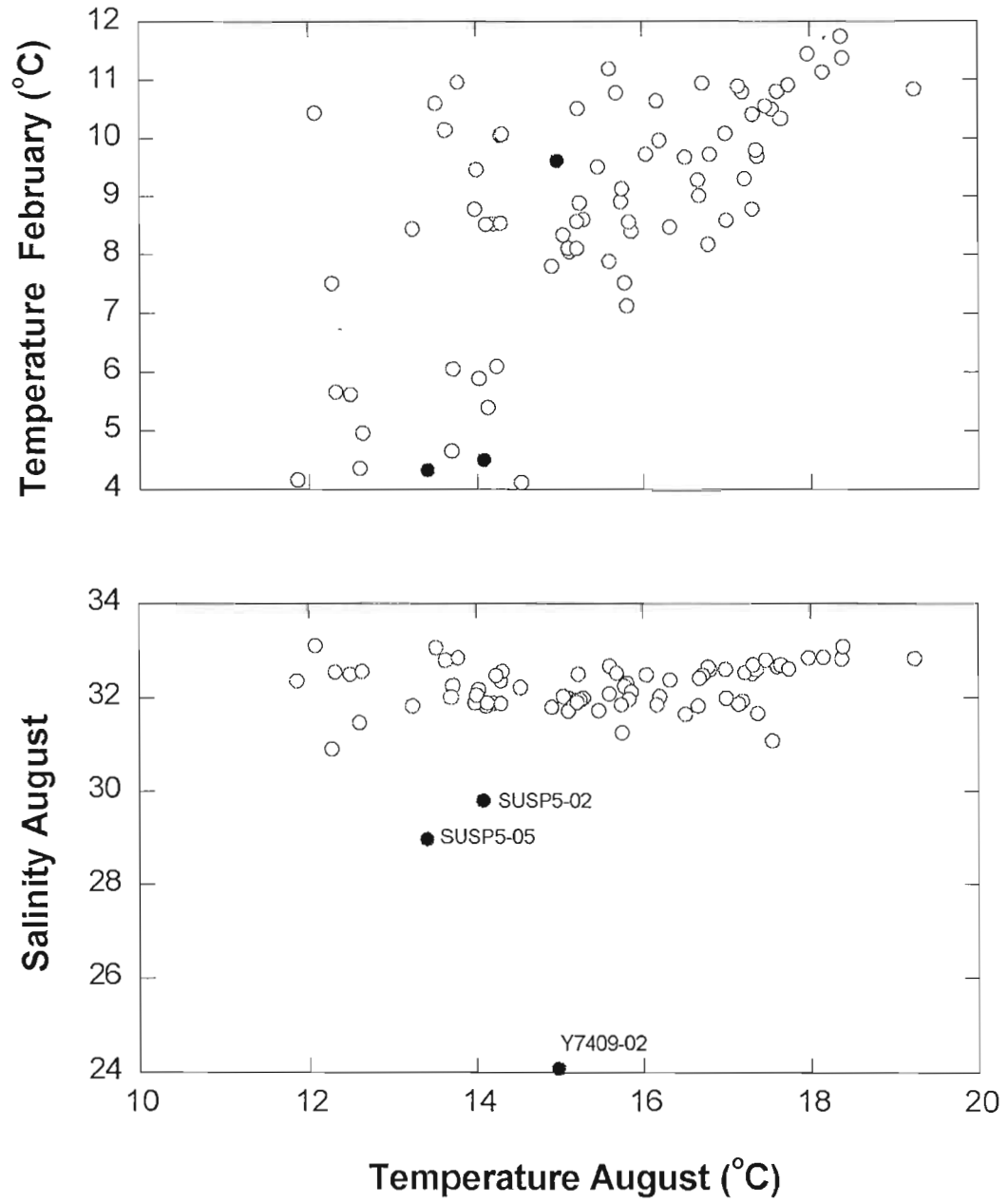


Figure 6

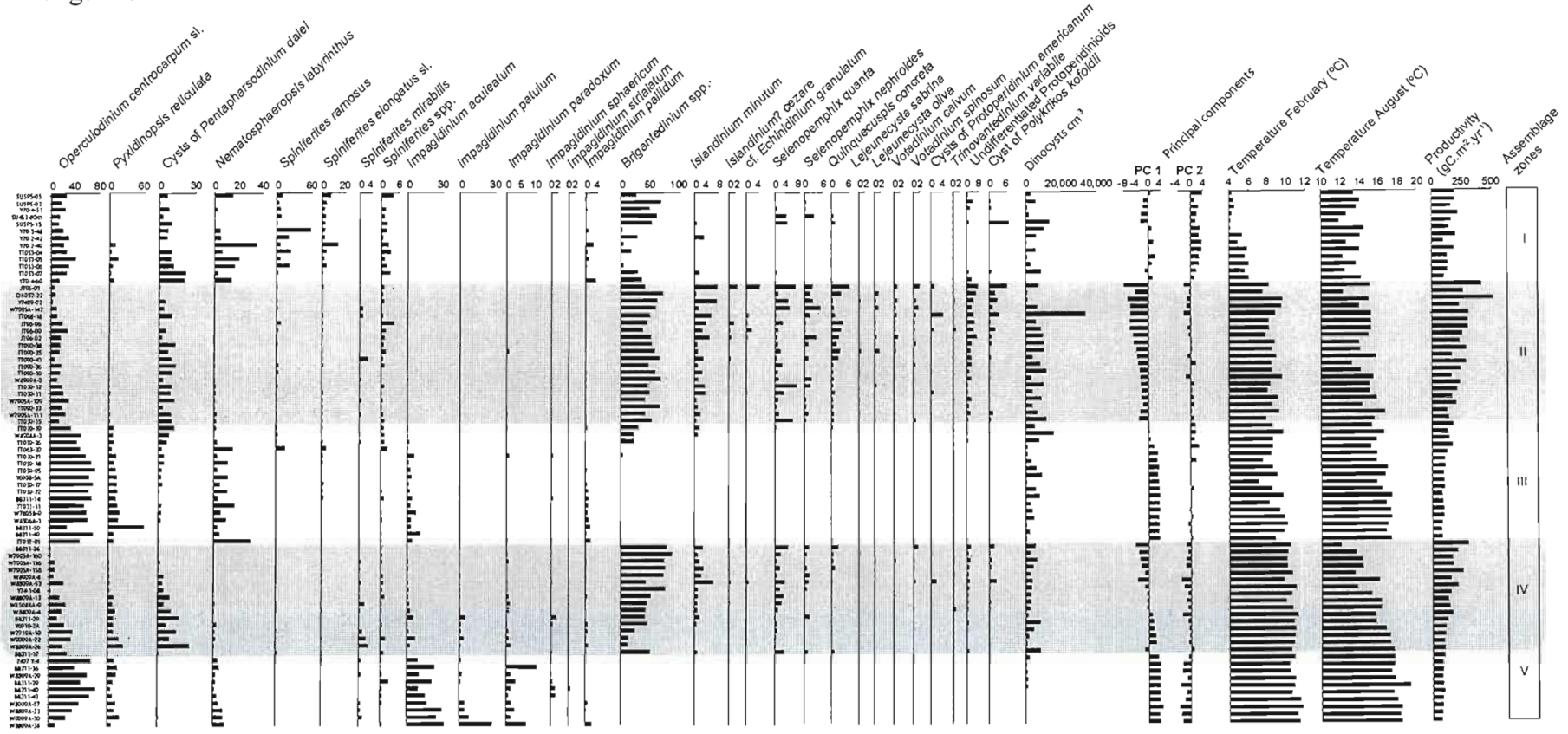


Figure 7

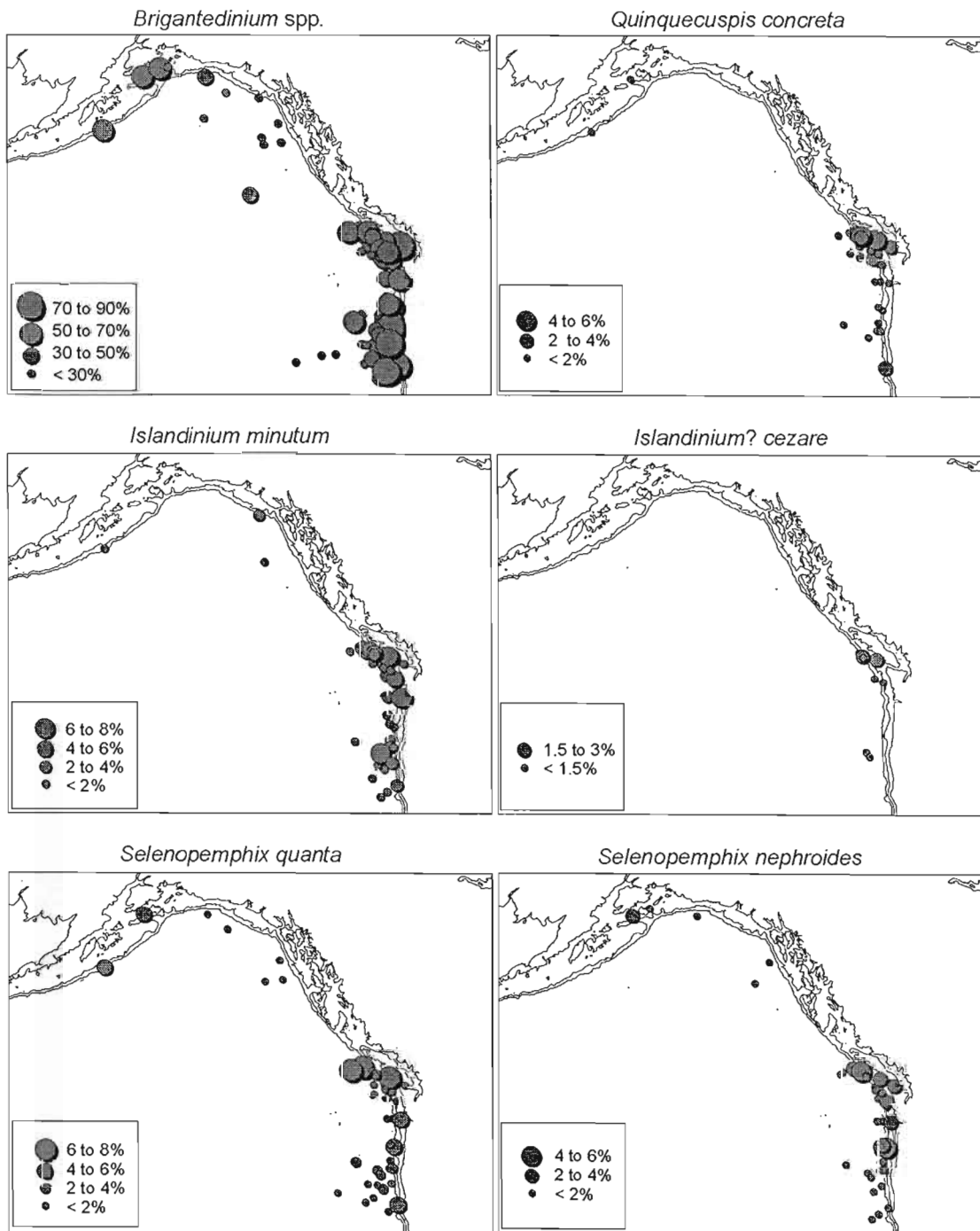


Figure 7 - continued

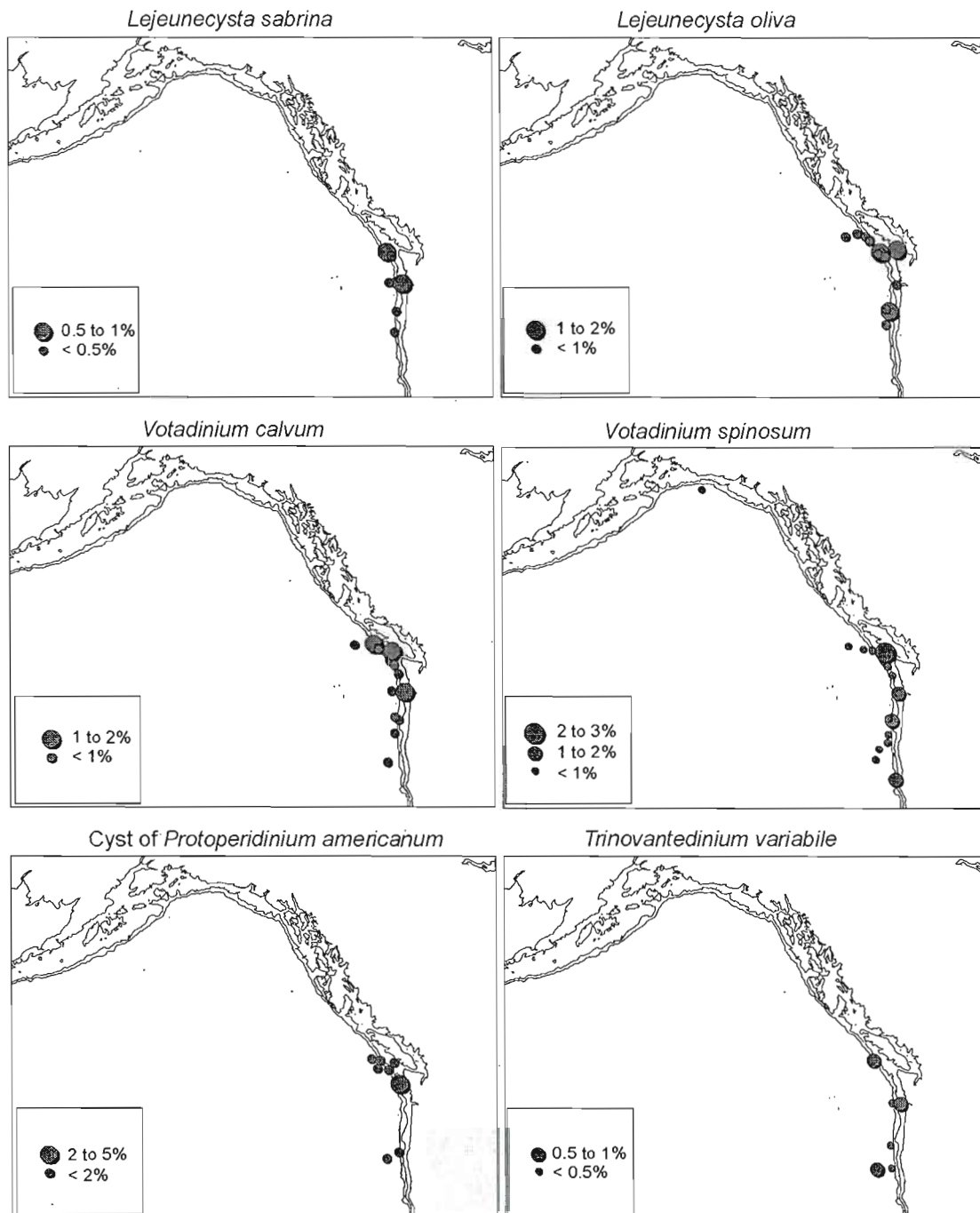


Figure 7 - continued

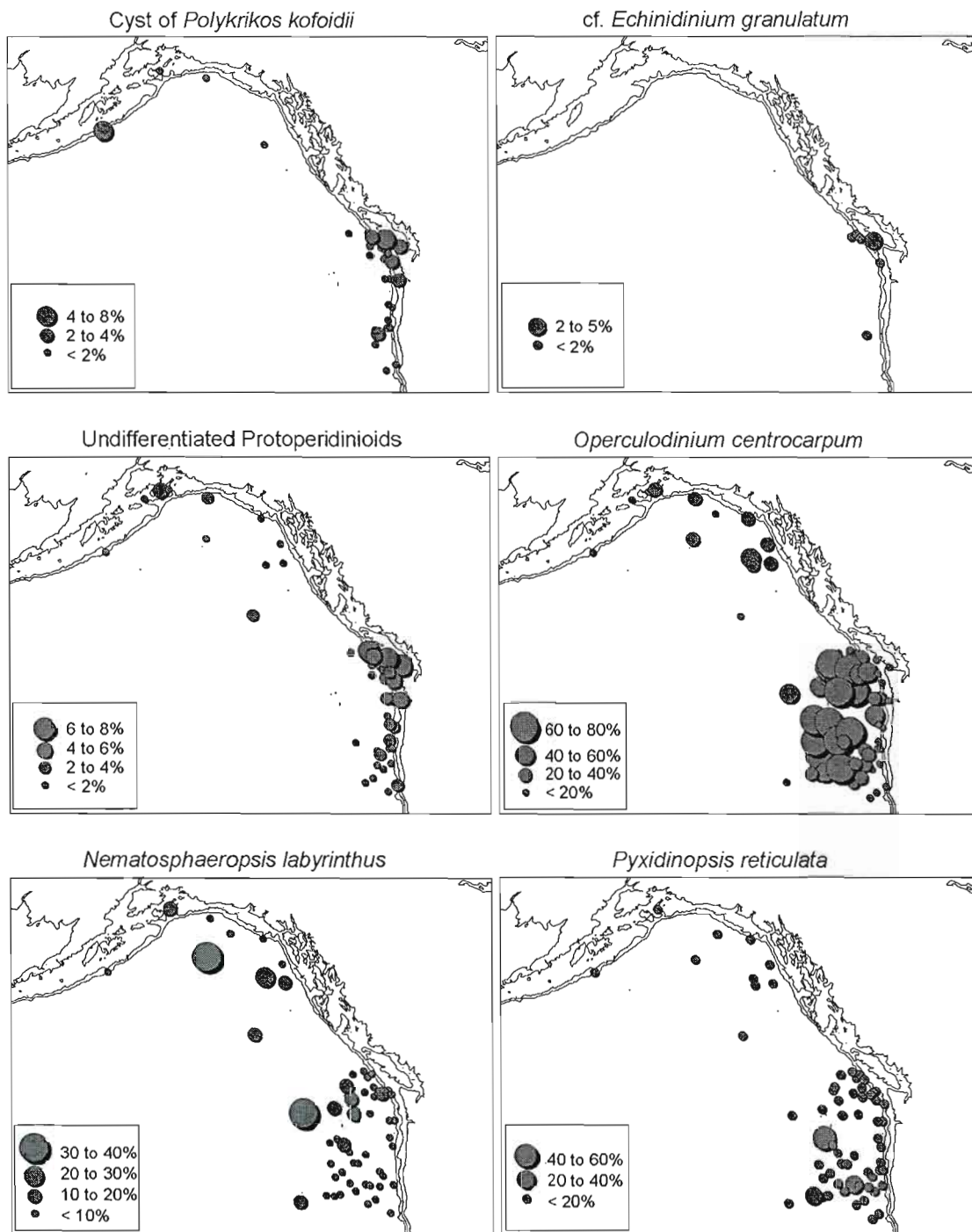


Figure 7 - continued

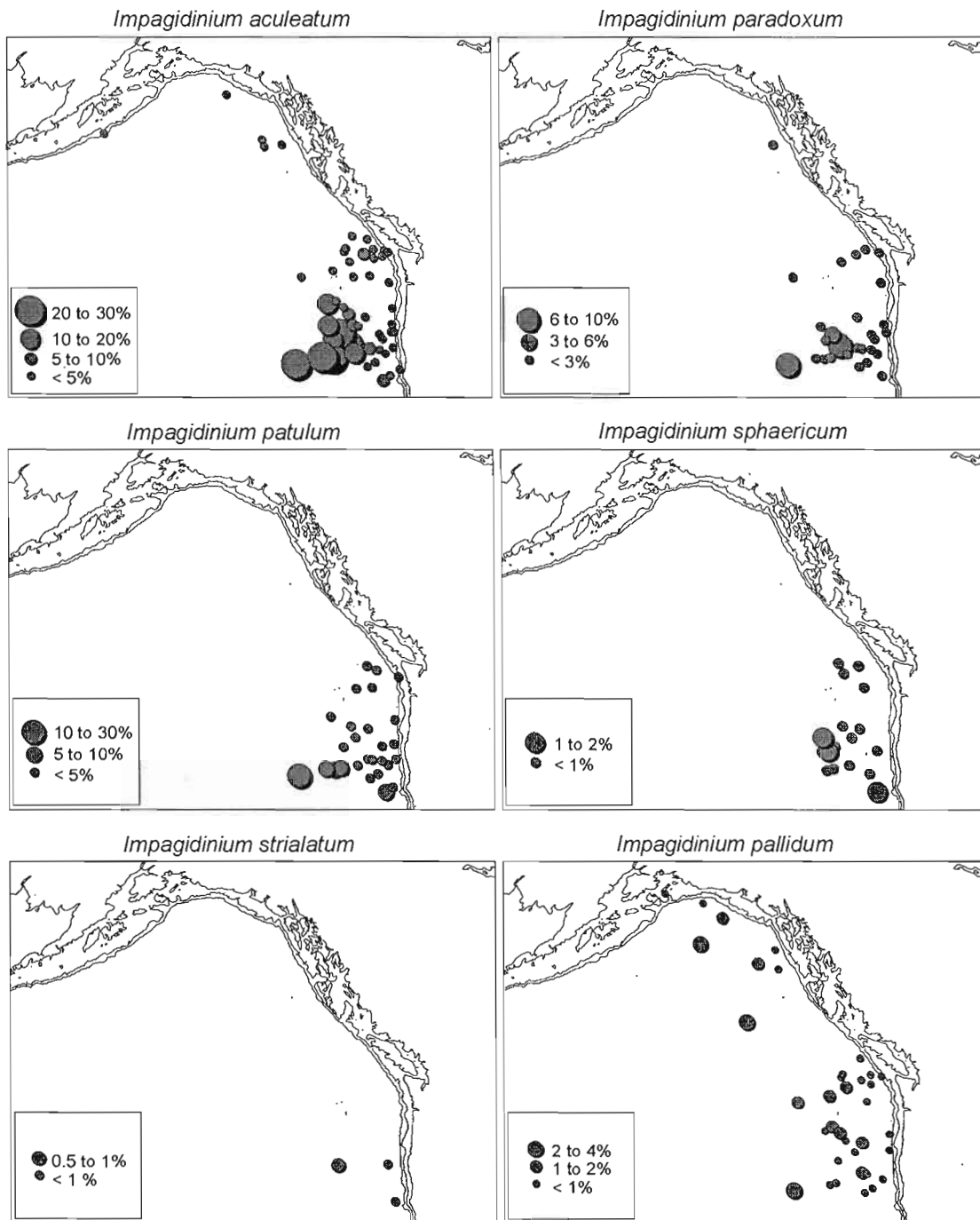


Figure 7 - continued

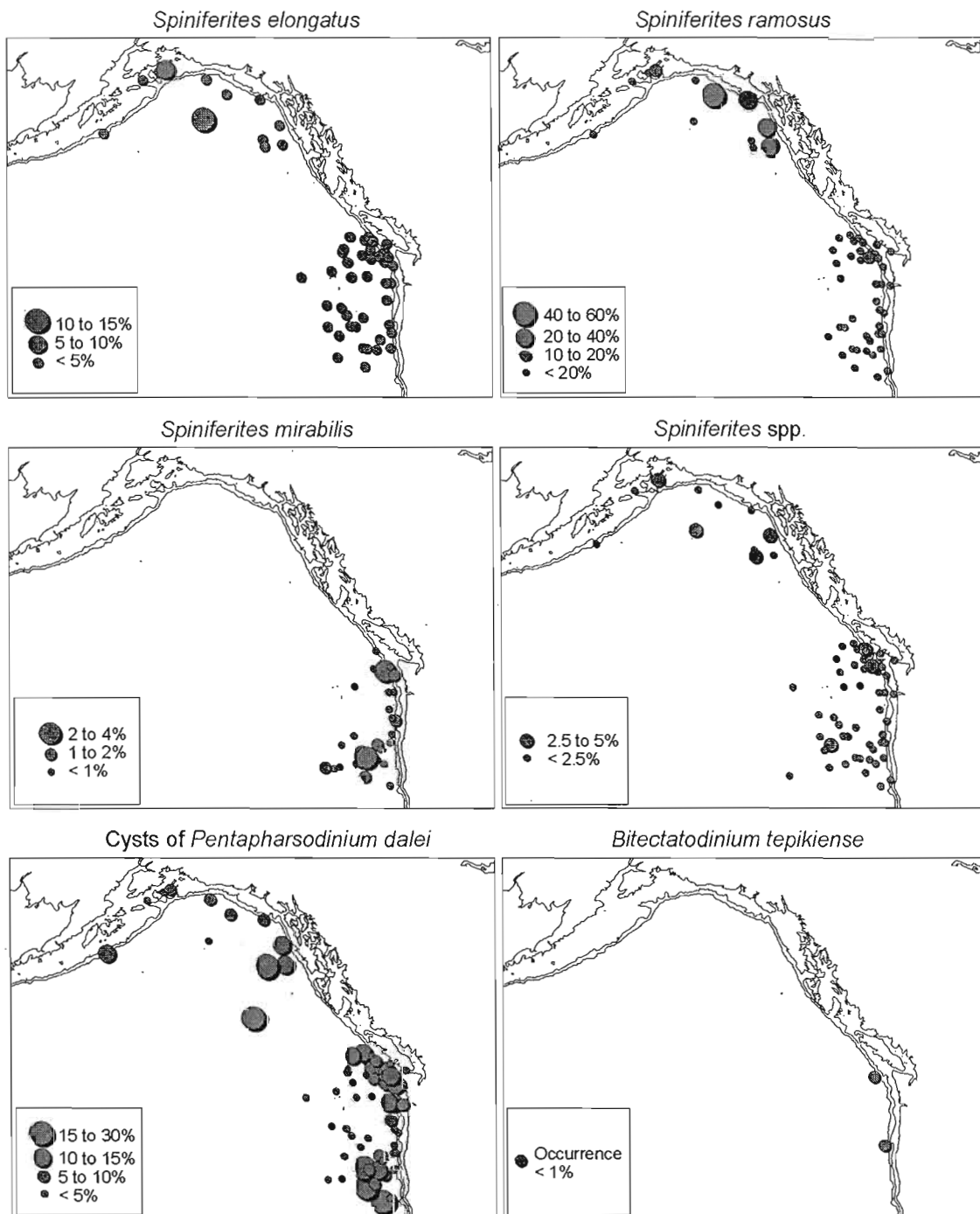


Figure 8

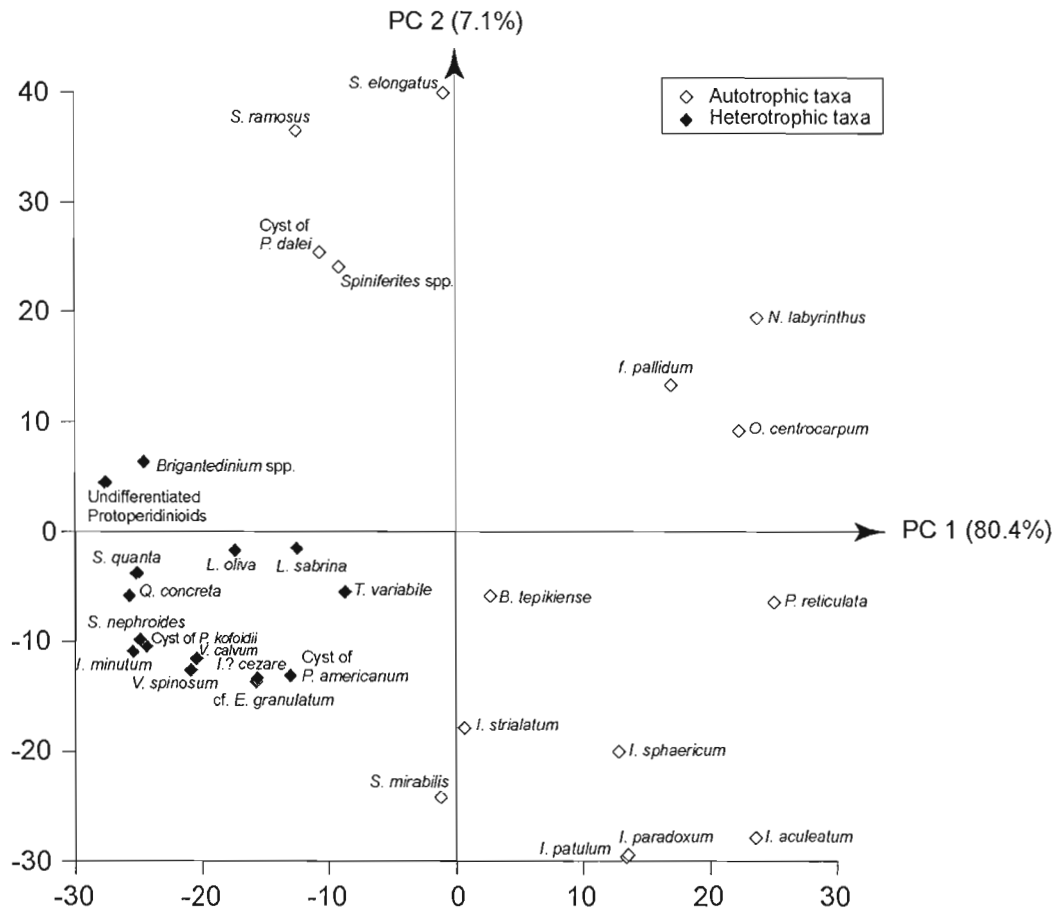


Figure 9

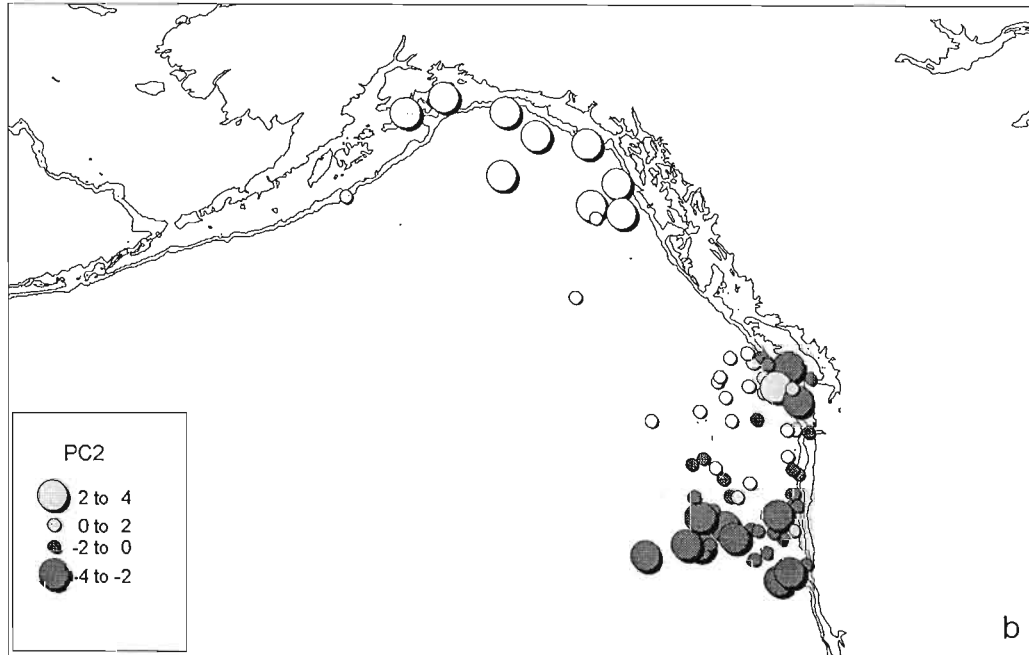
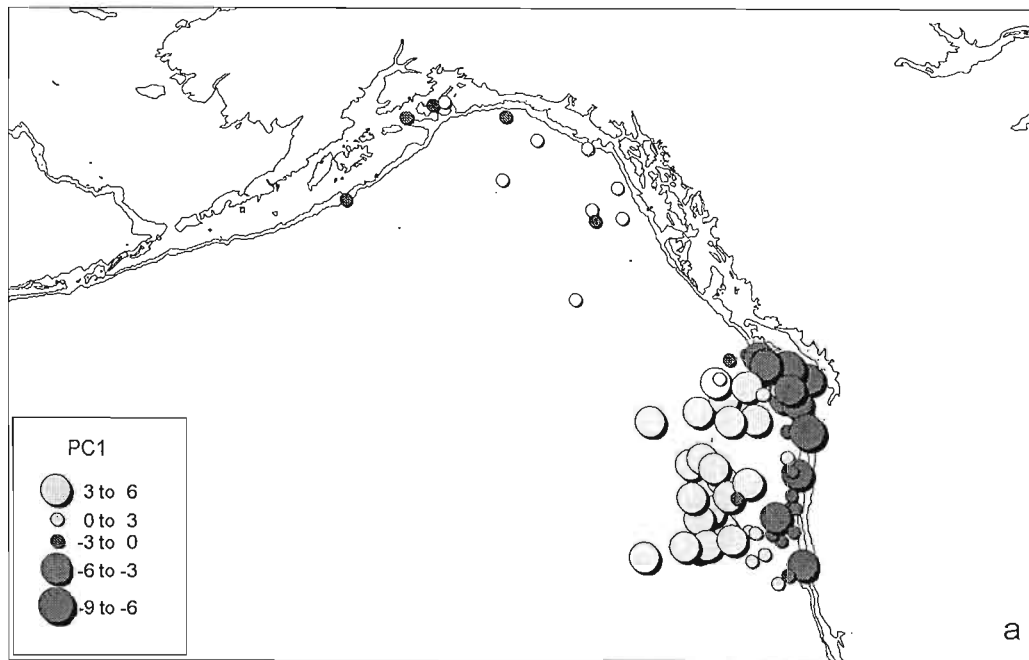


Figure 10

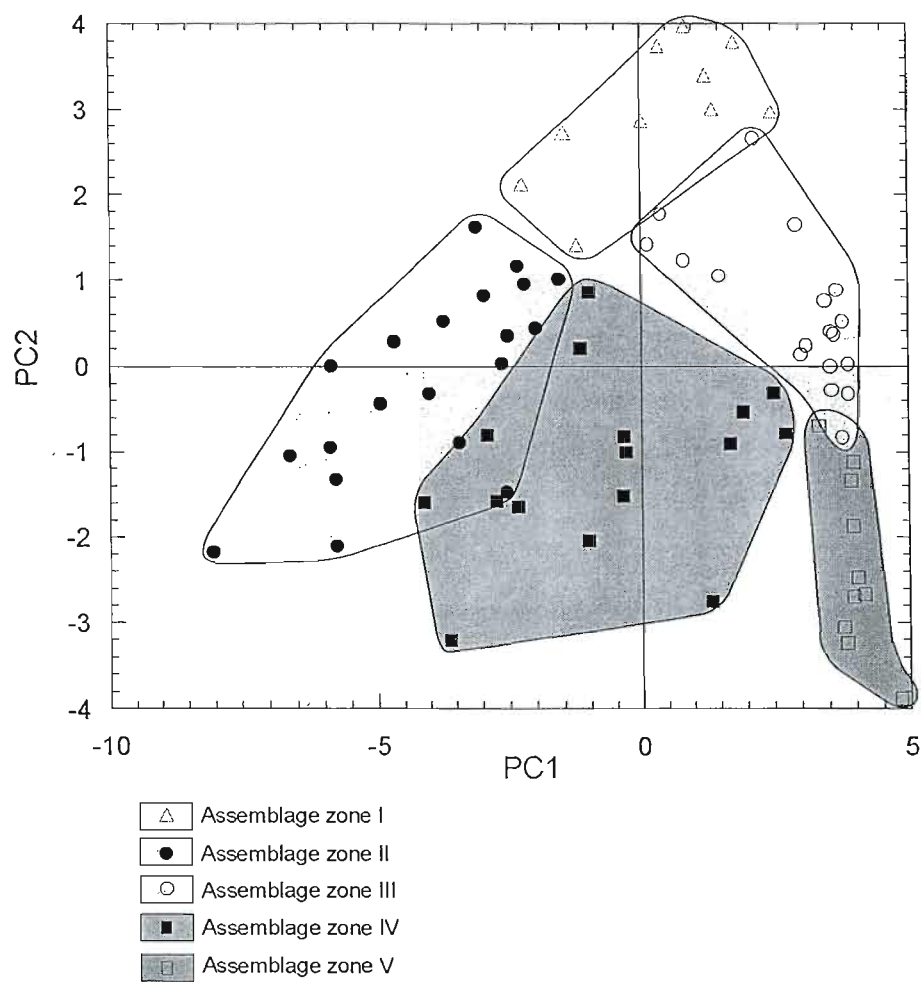


Figure 11

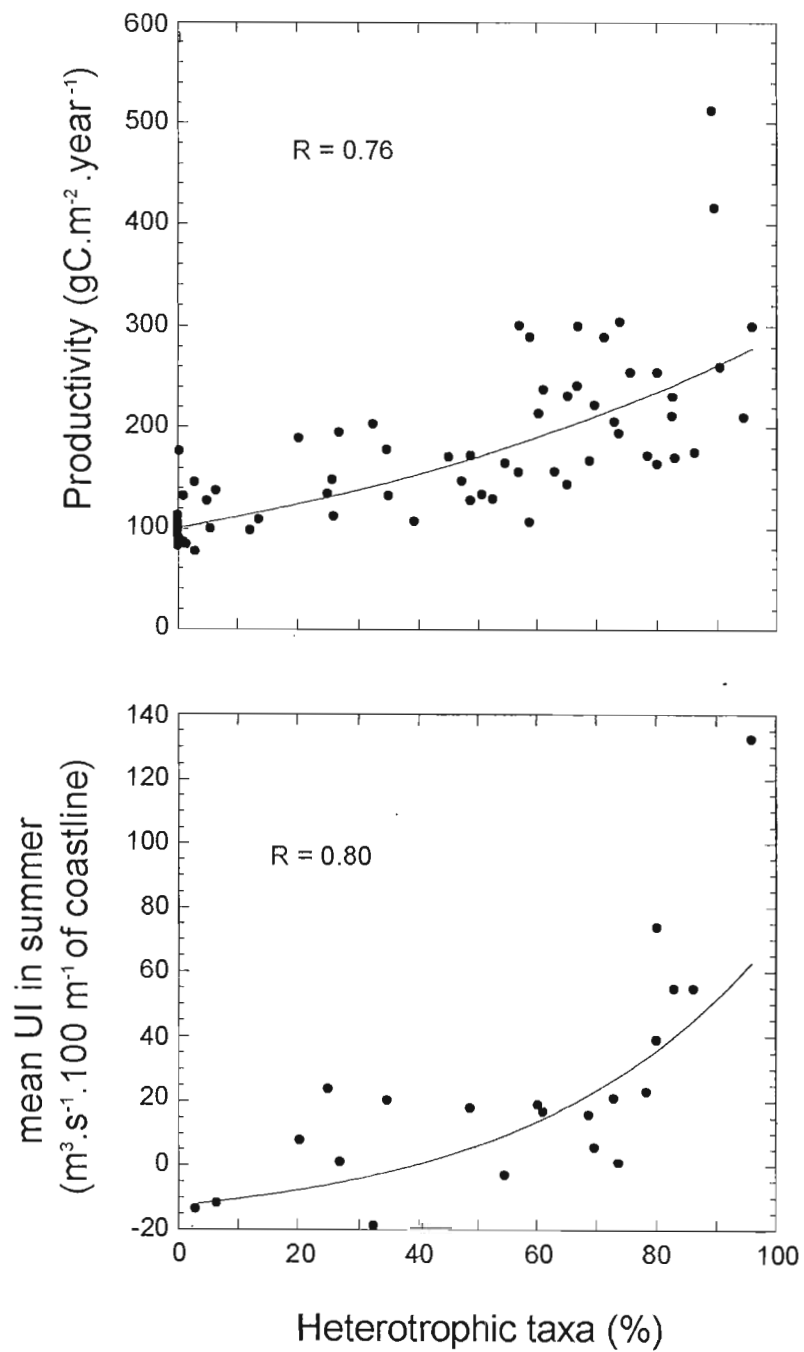


Figure 12

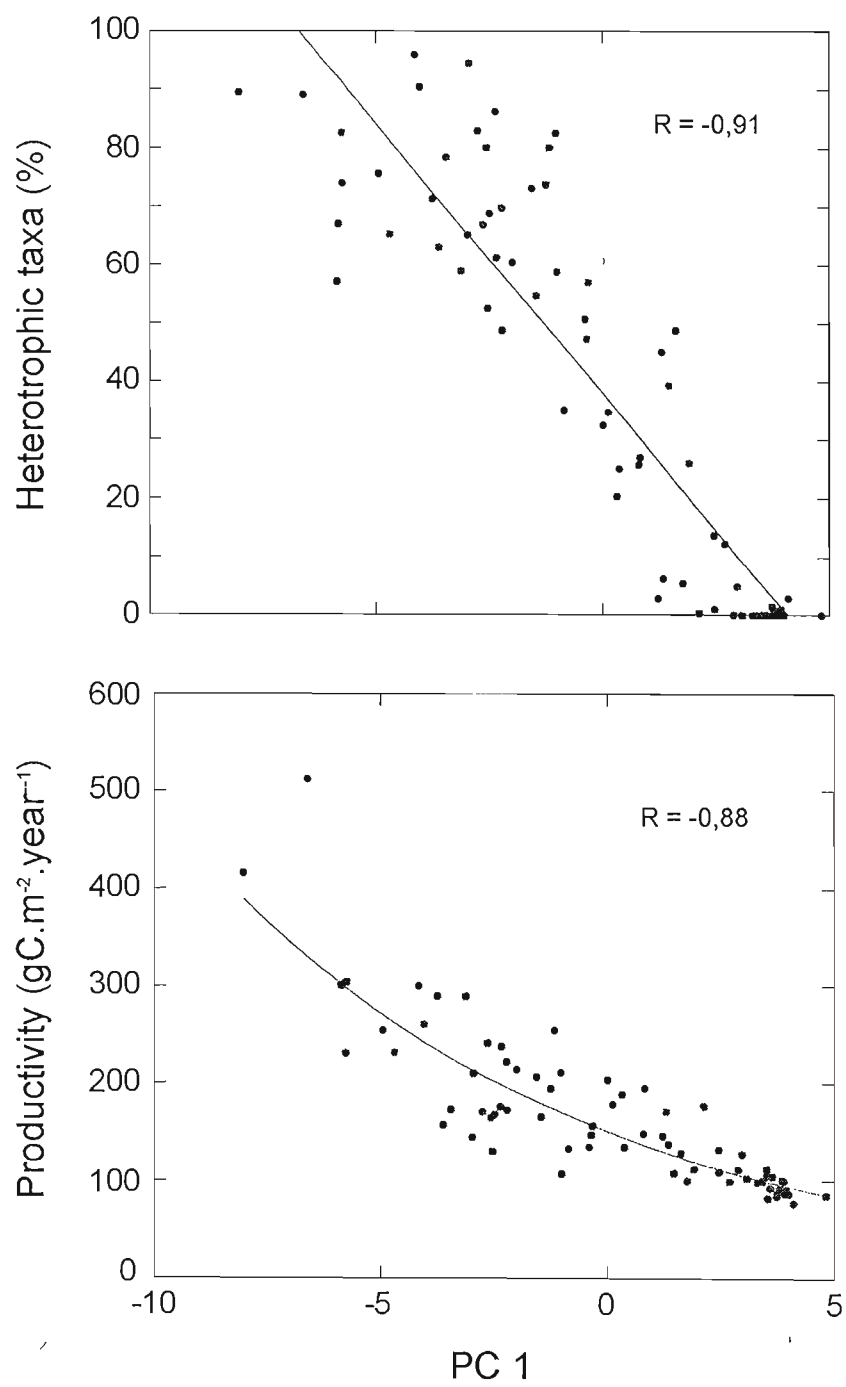


Figure 13

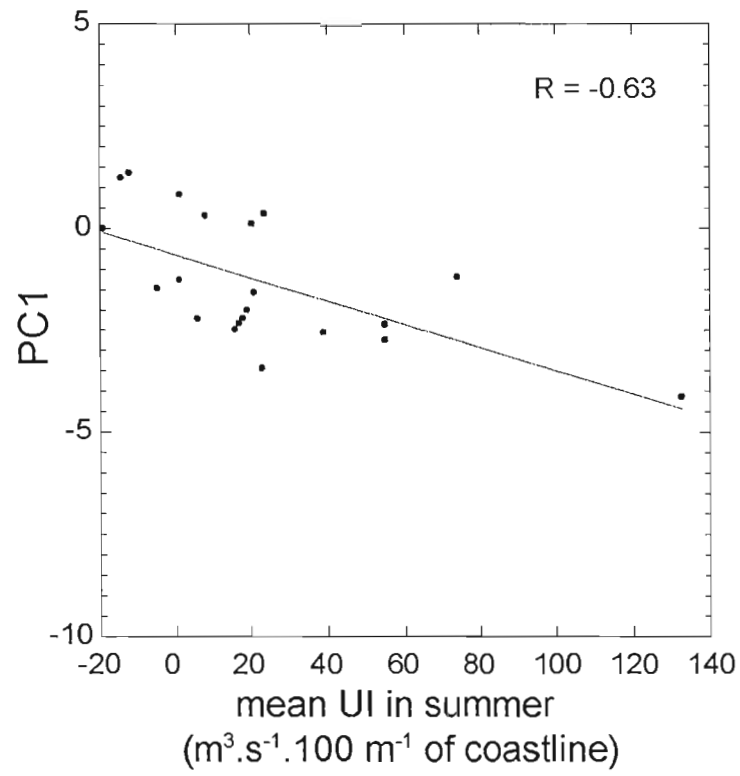


Figure 14

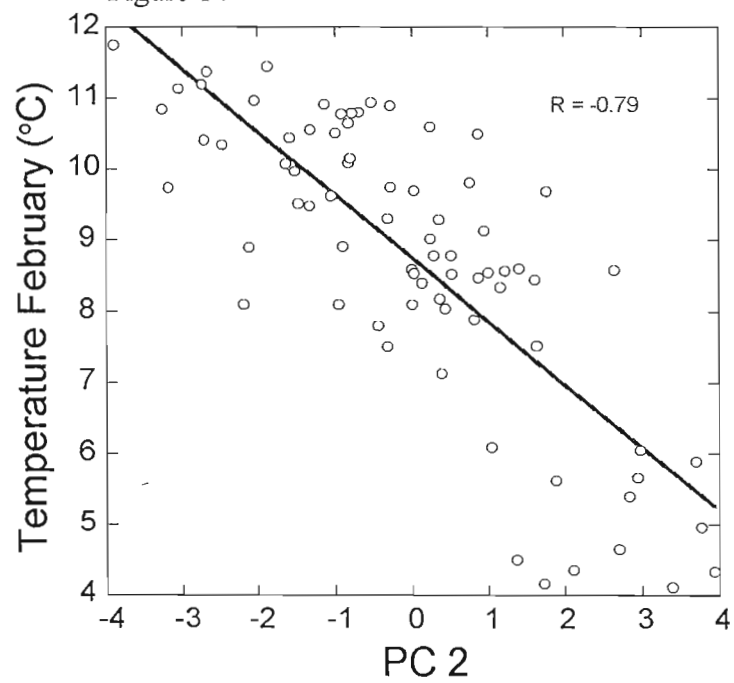


Table 1

Site	Laboratory number	Coring device	Latitude	Longitude	Water depth (m)	Temperature February (°C)	Temperature August (°C)	Salinity August	Dinocysts count	Dinocyst concentration (cysts cm ⁻³)	Annual productivity (gC m ⁻³ yr ⁻¹)	PC1 80.4 % of the variance	PC2 7.1 % of the variance
SUSP5-05	1592-4	Gravity	59°40.98'N	148°34.98'W	110	4.3	13.4	29.0	246	2821	195.0	0.84	3.93
SUSP5-02	1592-3	Gravity	59°33.30'N	147°18.48'W	190	4.5	14.1	29.8	322	5704	194.1	-1.25	1.38
Y70-4-51	1594-4	Gravity	59°04.98'N	143°40.20'W	3650	4.6	13.7	32.0	301	1053	165.3	-1.46	2.71
SU453-8Oct	1592-1	Gravity	59°02.40'N	150°00.00'W	198	4.3	12.6	31.5	174	1810	222.1	-2.21	2.11
SUSP5-15	1592-5	Gravity	55°41.22'N	153°57.00'W	1590	4.2	11.9	32.3	51	13510	167.4	-2.46	1.73
Y70-3-48	1594-3	Gravity	58°07.80'N	141°40.92'W	3636	4.1	14.5	32.2	39	10460	146.2	1.25	3.39
Y70-2-42	15942+1737-6	Gravity	57°48.12'N	138°23.40'W	2912	5.4	14.1	31.9	277	5810	203.5	0.01	2.84
Y70-2-40	1494-1	Gravity	56°30.18'N	143°52.62'W	3827	5.0	12.6	32.5	137	415	100.1	1.81	3.77
TT053-04	1531-1	Gravity	56°11.52'N	136°26.40'W	2575	5.9	14.0	32.2	134	5716	188.7	0.32	3.70
TT053-05	1531-2	Gravity	55°18.00'N	138°06.18'W	2997	5.7	12.3	32.5	322	975	132.2	2.50	2.94
TT053-06	1531-3	Gravity	54°58.98'N	136°07.50'W	2760	6.1	13.7	32.2	51	2696	137.6	1.37	2.98
TT053-07	1531-4	Gravity	54°51.18'N	137°53.58'W	3139	5.6	12.5	32.5	148	9179	133.0	-0.86	1.90
Y70-4-60	1588-4	Gravity	51°37.98'N	139°12.18'W	3707	6.1	14.2	32.5	149	145	107.7	1.50	1.05
JT96-01mc2	1183-1	Multicore	48°45.97'N	125°30.02'W	115	8.1	15.1	31.7	141	7142	415.6	-8.03	-2.17
OA057-22	1591-6	Gravity	48°21.30'N	124°08.40'W	311	7.5	12.3	30.9	238	1126	260.2	-4.01	-0.32
Y7409-02	1639-6+1588-5	Gravity	46°12.18'N	124°14.52'W	79	9.6	15.0	24.1	315	1057	512.2	-6.62	-1.05
W7905A-142	1533-5	Gravity	44°30.00'N	124°54.00'W	456	9.5	14.0	32.0	302	6717	230.8	-5.78	-1.33
TT068-18	1740-5	Gravity	47°22.98'N	124°54.78'W	1240	8.9	15.2	31.9	353	33563	304.1	-5.76	-2.11
JT96-06mc2	1183-4	Multicore	48°58.73'N	126°52.68'W	721	8.1	15.2	31.9	412	5472	300.6	-5.86	0.00
JT96-09mc3	1177-5	Multicore	48°54.72'N	126°53.40'W	920	8.1	15.2	31.9	303	8732	300.6	-5.89	-0.95
JT96-02bc	1183-6	Box	49°13.07'N	127°18.61'W	1340	7.8	14.9	31.8	302	10149	254.4	-4.94	-0.44
TT090-38	1532-5	Gravity	47°56.10'N	125°21.30'W	752	8.8	14.0	31.9	333	10477	231.1	-4.67	0.28
TT090-35	1532-3	Gravity	48°10.98'N	125°46.20'W	963	8.5	14.1	31.8	228	10540	289.3	-3.72	0.52
TT090-41	1532-6	Gravity	47°36.12'N	125°45.48'W	1444	8.9	15.7	31.8	344	3835	172.4	-3.42	-0.90
TT090-36	1532-4	Gravity	48°12.60'N	125°41.10'W	569	8.4	13.2	31.8	651	8595	289.3	-3.09	1.62
TT090-10	1532-1	Gravity	48°18.12'N	126°03.30'W	1013	8.5	14.2	31.9	323	11795	241.2	-2.61	0.03
W8909A-2	1539-2	Box	44°40.32'N	125°16.80'W	2050	9.5	15.5	31.7	368	3299	164.5	-2.54	-1.47
TT039-12	1592-6	Gravity	49°23.82'N	128°08.40'W	2341	8.3	15.0	32.0	327	10206	237.5	-2.32	1.16
TT039-11	1586-3	Gravity	49°00.78'N	127°46.02'W	2480	8.0	15.1	32.0	319	3995	214.2	-1.98	0.44
W7905A-109	1533-3	Gravity	46°18.00'N	125°06.90'W	1670	9.1	15.8	31.3	306	8899	172.2	-2.20	0.95
TT090-33	1532-2	Gravity	48°05.88'N	126°01.02'W	1474	8.5	14.3	31.9	314	3873	206.0	-1.56	1.01
W7905A-111	1533-4	Gravity	46°17.70'N	125°36.78'W	2286	9.3	16.7	31.8	312	6510	129.8	-2.51	0.35
TT039-15	1587-2	Gravity	49°12.60'N	129°14.58'W	2396	7.9	15.6	32.1	320	11736	144.2	-2.95	0.82
TT039-19	1587-4	Gravity	48°23.40'N	127°09.18'W	2555	8.6	15.3	32.0	319	5038	178.0	0.13	1.42
W8908A-3	1659-3	Gravity	45°13.08'N	125°34.50'W	2649	9.7	16.5	31.6	296	15880	134.4	0.38	1.77
TT039-26	1588-1	Gravity	47°48.00'N	127°07.32'W	2520	8.6	15.8	32.0	301	7608	148.2	0.82	1.23
TT063-20	1531-5	Gravity	47°56.88'N	126°16.32'W	1838	8.6	15.2	31.9	304	1139	176.5	2.17	2.66
TT039-21	1740-4	Gravity	48°03.78'N	128°03.42'W	2575	8.4	15.9	32.1	297	998	128.1	3.01	0.13
TT039-18	1593-1	Gravity	48°26.22'N	129°52.20'W	2765	7.5	15.8	32.2	337	3001	111.7	2.93	1.65
TT039-05	1587-1	Gravity	46°43.20'N	127°32.52'W	2665	8.6	17.0	32.0	130	6136	112.8	3.54	-0.01
Y6908-5A	1659-1+1593-5	Gravity	46°39.12'N	129°07.98'W	2600	9.0	16.7	32.4	342	9281	103.1	3.11	0.24
TT039-17	1740-3	Gravity	48°13.80'N	130°01.80'W	2793	7.1	15.8	32.3	309	346	105.9	3.55	0.39
TT039-22	1587-6	Gravity	47°35.22'N	129°30.42'W	2566	8.5	16.3	32.4	330	5630	104.8	3.65	0.88
BB311-14	1659-4+1589-2	Gravity	44°07.02'N	127°58.98'W	2835	9.7	17.4	31.7	335	7797	89.4	3.88	0.02
TT031-11	1586-6	Gravity	47°01.98'N	131°09.48'W	3056	8.2	16.8	32.6	317	2742	92.6	3.62	0.37
W7605B-9	1533-1	Gravity	44°16.80'N	129°39.30'W	3208	9.3	17.2	32.5	317	3734	101.1	3.87	-0.32

Table 1 - continued

Site	Laboratory number	Coring device	Latitude	Longitude	Water depth (m)	Temperature February (°C)	Temperature August (°C)	Salinity August	Dinocysts count	Dinocyst concentration (cysts cm ⁻³)	Annual productivity (gC m ⁻² yr ⁻¹)	PC1 80.4 % of the variance	PC2 7.1 % of the variance
W8506A-1	1538-1	Gravity	44°43.80'N	130°09.42'W	2623	9.8	17.4	32.6	313	4662	100.1	3.45	0.76
BB311-50	1736-6	Gravity	45°07.20'N	130°55.50'W	2853	10.1	17.0	32.6	311	315	84.3	3.76	-0.83
BB311-49	1591-4	Gravity	44°52.98'N	131°40.02'W	3603	9.7	16.8	32.6	382	2378	82.0	3.57	-0.29
TT017-01	1586-4	Gravity	46°39.78'N	134°16.02'W	3909	8.8	17.3	32.5	365	496	87.8	3.77	0.51
BB311-26	1589-4	Gravity	40°48.48'N	124°33.00'W	530	10.4	12.1	33.1	323	5363	300.1	-4.12	-1.58
W7905A-160	1540-5	Gravity	43°09.90'N	125°05.22'W	1476	10.1	13.6	32.8	269	2449	210.1	-2.93	-0.81
W7905A-156	1533-6	Gravity	43°40.08'N	125°19.20'W	1987	10.0	14.3	32.3	316	6304	170.6	-2.73	-1.57
W7905A-158	1540-6	Gravity	43°10.08'N	125°24.18'W	3174	10.1	14.3	32.6	321	4047	175.5	-2.34	-1.63
W8909A-8	1539-4	Gravity	42°11.88'N	125°12.30'W	2440	10.6	13.5	33.1	136	2483	254.6	-1.17	0.23
W8809A-53	1539-1+1740-6	Gravity	42°44.70'N	126°15.48'W	2408	9.7	16.0	32.5	353	3420	156.9	-3.58	-3.19
Y74-1-08	1659-4+1594-5	Gravity	40°25.32'N	125°31.02'W	2943	11.0	13.8	32.8	336	3048	211.3	-1.03	-2.04
W8809A-13	1536-5	Gravity	41°49.98'N	126°00.00'W	3079	10.5	15.2	32.5	329	2686	156.0	-0.32	-0.99
W8508AA-9	1538-2	Gravity	43°01.80'N	126°34.68'W	3092	10.0	16.2	32.0	316	2633	134.2	-0.40	-1.52
W8809A-4	1538-6	Gravity	42°05.22'N	126°36.00'W	3389	10.6	16.2	31.8	303	2375	147.0	-0.36	-0.83
BB311-29	1589-5+1639-4	Gravity	40°06.00'N	126°10.50'W	3840	11.2	15.6	32.7	302	1283	170.8	1.34	-2.74
Y6910-2A	1660-3+1593-6	Gravity	41°16.02'N	127°01.02'W	2615	10.8	15.7	32.5	322	8428	128.4	1.66	-0.92
W7710A-10	1533-2	Gravity	40°59.52'N	127°48.30'W	2707	10.9	16.7	32.5	67	4220	112.2	1.95	-0.53
W9009A-22	1539-5	Box	42°09.12'N	127°34.38'W	2848	10.9	17.1	31.9	415	1557	109.3	2.50	-0.29
W8809A-26	1536-6	Gravity	42°12.78'N	128°00.42'W	3034	10.8	17.2	31.9	322	669	99.1	2.74	-0.78
BB311-17	1589-3	Gravity	43°33.00'N	128°45.00'W	3347	10.5	17.5	31.1	218	8459	106.7	-1.01	0.87
7407 Y-4	1589-1+1660-1	Gravity	43°34.98'N	129°13.68'W	3271	10.8	17.6	32.7	148	1932	98.5	3.35	-0.69
BB311-36	1737-1	Gravity	42°17.22'N	129°37.02'W	3155	10.3	17.6	32.7	382	306	86.8	4.01	-2.47
W8809A-29	1538-3	Gravity	41°48.18'N	129°00.30'W	3288	10.4	17.3	32.7	247	1007	91.2	3.96	-2.71
BB311-39	1591-1	Gravity	42°58.98'N	130°24.48'W	3475	10.9	17.7	32.6	56	1271	86.8	3.95	-1.14
BB311-40	1737-5	Gravity	42°39.48'N	131°07.02'W	3530	10.8	19.3	32.8	304	906	91.9	3.82	-3.27
BB311-43	1737-4	Gravity	43°31.50'N	131°34.02'W	3475	10.5	17.5	32.8	174	567	99.7	3.90	-1.32
W8909A-57	1539-3	Gravity	41°34.98'N	130°37.02'W	3330	11.4	18.0	32.8	182	534	86.5	3.95	-1.87
W8809A-33	1538-4	Gravity	41°28.62'N	131°13.20'W	3589	11.7	18.4	32.8	239	481	84.8	4.83	-3.90
W9009A-30	1539-6	Box	41°31.32'N	132°02.52'W	3715	11.1	18.2	32.9	173	327	83.9	3.77	-3.05
W8809A-38	1538-5	Gravity	41°04.68'N	134°39.30'W	3928	11.4	18.4	33.1	369	233	76.6	4.12	-2.67

Table 2

	Temperature February	Temperature August	Salinity August	Productivity	Upwelling index	PC1	PC2
PC1	0.20	0.59	0.38	-0.88*	-0.63	1	10 ⁻⁵
PC2	-0.79	0.52	0.19	0.02	-0.76	10 ⁻⁵	1
Heterotrophic taxa percentages	-0.07	-0.60	-0.30	0.76*	0.80*	-0.91	-0.05
<i>Operculodinium centrocarpum</i> sl.	0.14	0.61	0.22	-0.61	-0.54	0.75	0.03
<i>Pyxidinosia reticulata</i>	0.3	0.49	0.25	-0.55	-0.11	0.65	-0.17
Cyst of <i>Pentaparsodinium dalei</i>	-0.21	-0.29	-0.06	0.08	-0.5	-0.18	0.29
<i>Nematosphaeropsis labyrinthus</i>	-0.29	0.03	0.13	-0.39	-0.45	0.5	0.4
<i>Spiniferites ramosus</i>	-0.52	-0.27	-0.06	0.06	-0.49	-0.01	0.55
<i>Spiniferites elongatus</i> sl.	-0.62	-0.38	-0.14	-0.02	-0.57	0.05	0.64
<i>Spiniferites mirabilis</i>	0.34	0.27	0.04	-0.15	0.08	-0.01	-0.32
<i>Spiniferites</i> spp.	-0.43	-0.34	-0.18	0.21	-0.36	-0.2	0.5
<i>Impagidinium aculeatum</i>	0.49	0.65	0.3	-0.47	0.46	0.59	-0.53
<i>Impagidinium patulum</i>	0.34	0.36	0.18	-0.24	0.42	0.29	-0.36
<i>Impagidinium paradoxum</i>	0.34	0.42	0.19	-0.3	0.07	0.35	-0.4
<i>Impagidinium sphaericum</i>	0.3	0.36	0.16	-0.24	0	0.33	-0.34
<i>Impagidinium pallidum</i>	-0.12	0.12	0.17	-0.41	-0.33	0.45	0.2
<i>Brigantedinium</i> spp.	-0.06	-0.61	-0.26	0.65	0.66	-0.83	-0.07
<i>Islandinium minutum</i>	0.04	-0.24	-0.37	0.76	0.45	-0.76	-0.25
<i>Selenopemphix nephroides</i>	-0.01	-0.32	-0.29	0.59	0.38	-0.68	-0.19
<i>Selenopemphix quanta</i>	-0.06	-0.33	-0.23	0.58	0.31	-0.68	-0.09
<i>Quinquecuspsis concreta</i>	-0.09	-0.29	-0.13	0.67	0.59	-0.73	-0.15
<i>Lejeunecysta sabrina</i>	0.06	-0.15	-0.45	0.45	-0.03	-0.4	-0.03
<i>Lejeunecysta oliva</i>	-0.04	-0.27	-0.25	0.47	0.05	-0.49	-0.02
<i>Votadinium calvum</i>	0.01	0.14	-0.41	0.67	0.24	-0.66	-0.21
<i>Votadinium spinosum</i>	0.38	0.24	-0.22	0.63	0.76	-0.64	0.23
Cyst of <i>Protoperidinium americanum</i>	0.01	-0.03	0	0.31	-0.02	-0.35	-0.23
Undifferentiated Protoperidinioids	-0.18	-0.43	-0.38	0.75	0.34	-0.85	-0.09
Cyst of <i>Polykrikos kofoidii</i>	-0.19	-0.32	-0.24	0.53	0.15	-0.59	-0.15

Plate 1

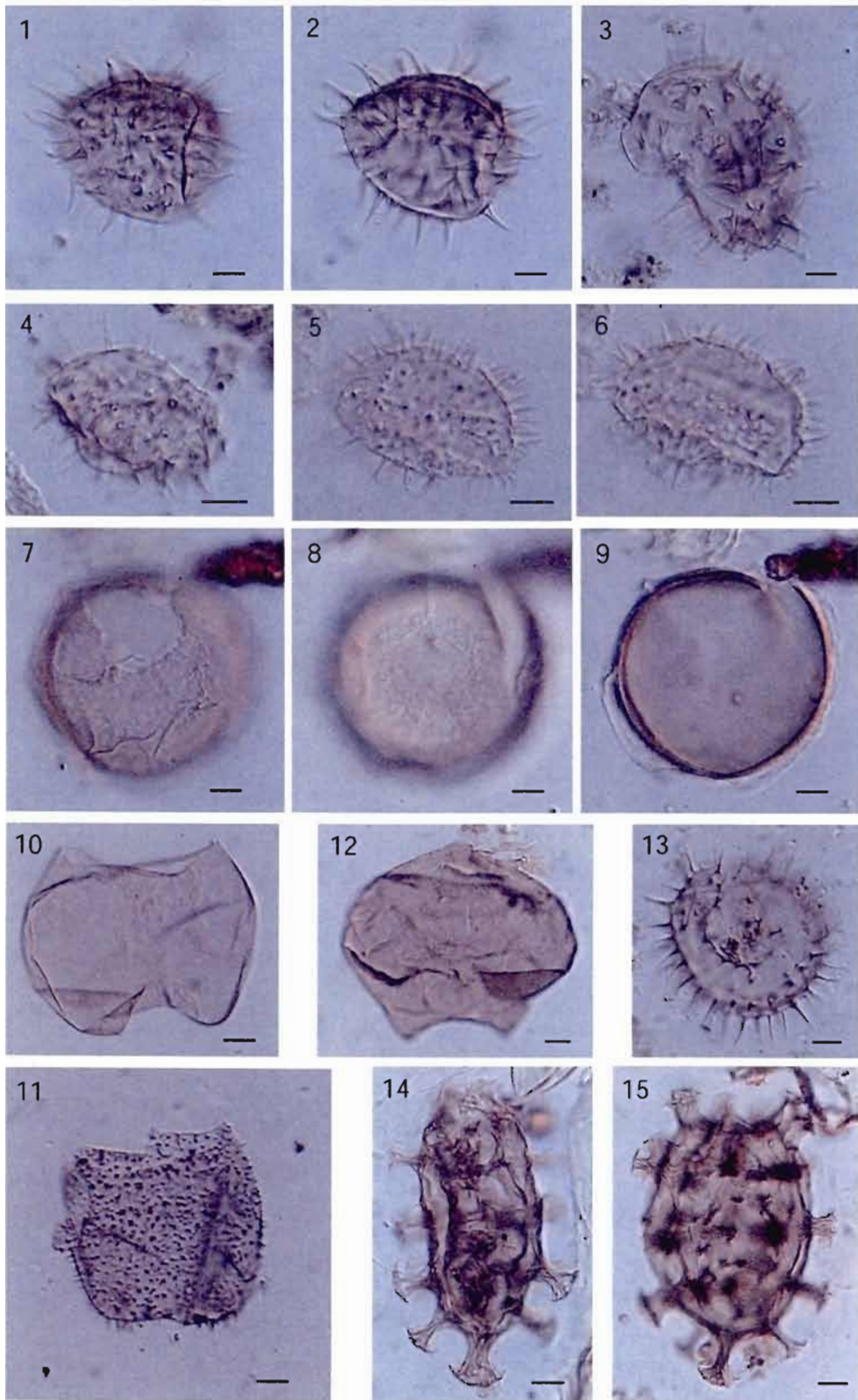
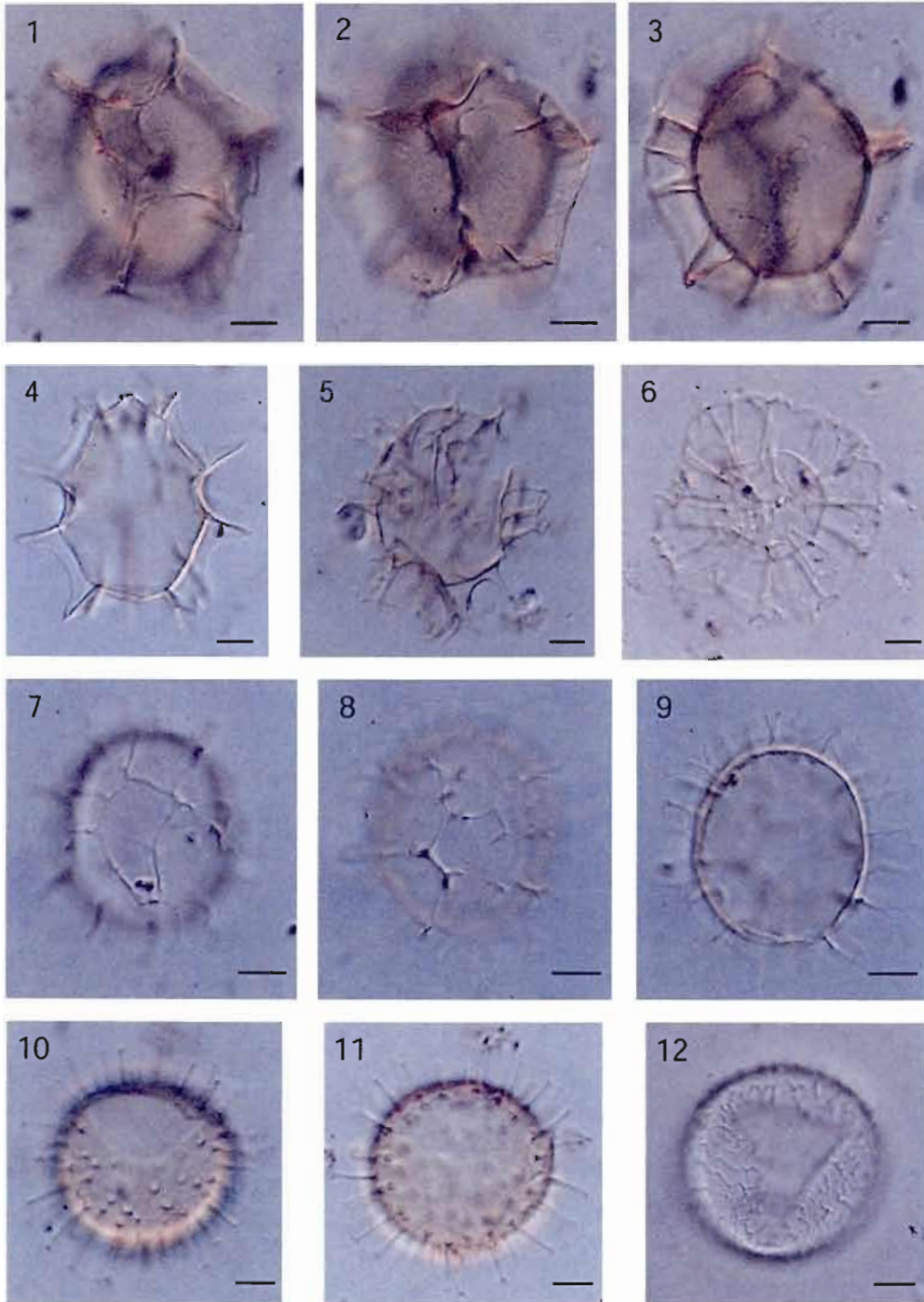


Plate 2



CHAPITRE II

DINOFLAGELLATE CYSTS AS INDICATORS OF WATER QUALITY AND PRODUCTIVITY IN BRITISH COLUMBIA ESTUARINE ENVIRONMENTS

Taoufik Radi¹, Vera Pospelova², Anne de Vernal¹, J. Vaughn Barrie³

¹ Centre de recherche en géochimie et géodynamique (GEOTOP-UQAM & McGill)
Université du Québec à Montréal, Case postale 8888, Succursale Centre-ville
Montréal, Qc, Canada, H3C 3P8

² School of Earth and Ocean Sciences, University of Victoria, Petch 168, P.O. Box 3055 STN CSC,
Victoria, BC, Canada, V8W 3P6

³ Geological Survey of Canada - Pacific, Institute of Ocean Sciences, P.O. Box 6000, Sidney, BC,
Canada, V8L 4B2

Article publié en 2007 dans la revue *Marine Micropaleontology*, volume 62, 269-297.

Résumé

Des analyses palynologiques de 60 échantillons de sédiments de surface des milieux estuariens de la Colombie Britannique, incluant le détroit de Géorgie (GS) et les inlets d'Effingham (EFF), de Seymour et de Belize (SB), ont été effectuées pour illustrer la distribution des kystes de dinoflagellés et leur relation avec les conditions hydrographiques, la productivité primaire et la concentration en éléments nutritifs dans les eaux de surface. EFF et SB sont caractérisés par la dominance des taxons autotrophes, notamment *Operculodinium centrocarpum* alors que les protopéridinales et les gymnodinales, associés à une productivité hétérotrophe, dominent les assemblages du GS. Les analyses multivariées montrent que cette distribution est liée à la productivité primaire, la température et la concentration en silice pendant le printemps. L'abondance des taxons hétérotrophes dans les inlets d'EFF et de SB est associée à une productivité primaire élevée et à de faibles températures estivales, illustrant l'upwelling côtier. Les taxons hétérotrophes qui caractérisent le GS semblent liés à une productivité moindre, une température estivale élevée et des concentrations élevées en silice durant le printemps. Les analyses multivariées, effectuées uniquement sur les échantillons du GS, montrent que la distance par rapport à la côte, la distance par rapport au port de Vancouver, la température, la concentration en phosphate et la productivité primaire durant le printemps, constituent les paramètres les plus déterminants. Les taxons autotrophes sont plus abondants dans les sites côtiers peu profonds. Toutefois, le long d'un gradient de productivité et de salinité, *Spiniferites ramosus* et *Pentapharsodinium dalei* semblent inversement corrélés. En effet, *P. dalei* est particulièrement abondant dans le panache du fleuve Fraser, aux alentours du port de Vancouver, près des côtes densément peuplées de la Colombie Britannique où l'apport continental et la productivité printanière sont élevées alors que la salinité y est très faible. *S. ramosus* montre son abondance maximale dans les marges ouest du GS. Les protopéridinales et les gymnodinales dominent les assemblages des zones distales dans le centre et le sud du GS. Ces zones sont associées à une masse d'eau constituée par un mélange des eaux douces provenant du fleuve Fraser et des eaux salées issues de l'upwelling. La relation entre les assemblages de dinokystes et la productivité primaire dans ces zones estuariennes diffère des zones néritiques et océaniques où l'abondance des taxons hétérotrophes est souvent associée à des upwellings intenses et à une productivité élevée. Les résultats des tests de validation basés sur la méthode des analogues modernes suggèrent que les assemblages de dinokystes peuvent être utilisés pour reconstituer la productivité primaire, à l'instar de la température et de la salinité de surface.

Mots clés : dinokystes, estuaires, Colombie Britannique, productivité, température de surface, salinité de surface, nutriments.

Abstract

Palynological analyses of 60 surface sediment samples from estuarine environments near Vancouver Island, including the Georgia Strait (GS) and the Effingham (EFF) and the Seymour-Belize (SB) Inlets were performed in order to document the distribution of dinoflagellate cyst assemblages and their relationship to hydrographic conditions, productivity and nutrient concentrations. We tested transfer functions using the analogue method, and suggest that dinocyst assemblages can be used to reconstruct productivity, temperature and salinity. The EFF and SB Inlets are characterized by a dominance of autotrophic taxa, particularly *Operculodinium centrocarpum*, whereas the Protoperidinioid and gymnodinial heterotrophic taxa such as *Quinquecuspis concreta* and *Brigantedinium* spp. dominate the assemblages of the GS. Multivariate analysis shows that this distribution is closely linked to primary productivity, sea surface temperature (SST) and spring silica concentration. The abundance of autotrophic taxa in the EFF and SB Inlets is associated with high primary productivity and low summer SST, indicating summer upwelling of coastal British Columbia, whereas the heterotrophic taxa that characterize the GS assemblages are related to low productivity, high summer SST and high silica concentration during spring. Multivariate analysis shows that the most important environmental parameters related to dinocyst distribution in the restricted embayment of the GS, are distance to shore, distance to Vancouver Harbor, spring sea surface salinity (SSS), spring phosphate concentration and spring productivity. The autotrophic taxa are generally more common in coastal and shallow waters, but *Spiniferites ramosus* and *Pentapharsodinium dalei* show an opposite correlation to spring productivity and salinity. *P. dalei* is particularly abundant around Vancouver Harbor, near highly urbanized shores and within the Fraser River plume, where salinity is low and spring productivity and continental runoff are high. *S. ramosus* show its highest abundance on the western coast of GS. Protoperidinioid and gymnodinial cysts characterize distal zones within the central and southern GS that are associated with a mixture of brackish waters coming from the Fraser River and deep upwelling waters entering the GS via Juan de Fuca Strait. The relationship between dinoflagellate cyst assemblages and primary productivity in these estuarine systems differs from that in oceanic and outer neritic zones, where the abundance of heterotrophic taxa is commonly associated with upwelling and high productivity.

Keywords: dinoflagellate cysts, estuaries, British Columbia, productivity, sea-surface temperature, sea-surface salinity, nutrients.

2.1 Introduction

Estuaries act as nutrient traps, receiving high organic and inorganic inputs from rivers, resulting in high primary productivity. Globally, estuarine systems have been the focus of research programs aimed at understanding the relationships between their physical environments and their biota, as well as anthropogenic influences on both (e.g., Bricker et al., 1999).

Several papers on the relationships between dinoflagellate cysts (dinocysts) and environmental conditions published in the last decade highlight the potential for dinocyst assemblages in surface sediment to serve as proxies of anthropogenic eutrophication (e.g., Thorsen and Dale, 1997; Dale, 1996, 2001; Dale et al., 1999; Matsuoka, 1999; Pospelova et al., 2002, 2004, 2005). A high relative abundance of *Lingulodinium machaerophorum* and *Selenopemphix quanta* has been associated with eutrophication in estuarine and coastal ecosystems (e.g., Saetre et al., 1997; Dale et al., 1999, 2002; Sangiorgi and Donders, 2004), but these species respond inversely to anthropogenic eutrophication in some particular estuaries. For instance, their relative abundances increase with eutrophication in the shallow estuaries of Massachusetts (Pospelova et al., 2002) but decrease with eutrophication in Tokyo Bay (Matsuoka, 1999). Thus, the interpretation of specific ecological requirements is not indisputable. In coastal upwelling zones, an increase in relative abundance of Protoperidinioid heterotrophic cysts is often interpreted as the result of an increase in primary productivity and upwelling intensity (Lewis, 1990; Marret, 1994; Zonneveld, 1997a; Zonneveld et al., 1997; 2001; Dale et al., 2002; Radi and de Vernal, 2004; Pospelova et al., 2006), however this interpretation cannot be extrapolated to estuarine systems (Pospelova et al., 2002).

In this study we documented the relationships between modern sediment dinocyst assemblages and parameters such as sea surface temperature (SST), sea surface

salinity (SSS), primary productivity and nutrient concentrations in the Georgia Strait (GS) and the Seymour-Belize (SB) and Effingham (EFF) Inlets (Fig. 1, Table 1), British Columbia (Canada). These estuaries are characterized by high primary productivity ($>260 \text{ gC m}^{-2} \text{ yr}^{-1}$) that sustains commercial fisheries (Ware and Thomson, 1991; Beamish and Bouillon, 1993; Robinson and Ware, 1999; Beamish et al., 1999; Mackas et al., 2001). The three studied areas have different oceanographic settings and are characterized by different mechanisms of nutrient enrichment. The nitrogen budget for GS is influenced by mixing due to estuarine and tidal currents. The natural nitrogen input from upwelling is about ten times higher than the anthropogenic input via the Fraser River (Harrison et al., 1994; Mackas and Harrison., 1997). However, inlets and fjords that have low flushing rates and/or are adjacent to urban centers, such as Burrard Inlet, are sensitive to anthropogenic nutrient input (Kay, 1989; West et al., 1994; Schmitt et al., 1994; Harrison et al., 1994; Mackas and Harrison, 1997). SB and EFF Inlets are not subjected to any significant anthropogenic nutrient input (Thomson, 1981).

Documenting the distribution of dinocysts in these estuaries provides an opportunity to discriminate between oceanic and terrestrial influences, and between natural and anthropogenic nutrient enrichment on dinocyst production, which can eventually provide a basis for paleoceanographic reconstructions in near-shore Quaternary sediments. The ultimate goal of this work is to establish a modern data set of dinocyst assemblages to reconstruct quantitatively environmental parameters in estuarine systems by using the modern analogue method (e.g. Guiot, 1990; de Vernal et al., 2001).

2.2 Regional setting

2.2.1 Seymour-Belize and Effingham Inlets

The SB and EFF Inlets are wide fjords located on the southwestern coast of Vancouver Island and the mainland of British Columbia, respectively, and directly connected to the Pacific Ocean (Fig. 1). Both inlets are similar in their oceanographic characteristics and fairly typical examples of most BC fjords, which are directly influenced by ocean waters. The maximum water depth recorded in the SB and EFF Inlets is about 350 and 210 m respectively. The inlets are partially mixed estuaries, due to active tidal action and relatively low continental runoff. The oceanographic regime of the northeastern Pacific, linked to the atmospheric circulation pattern of the North Pacific, constitutes the main control on their oceanographic setting. The North Pacific summer high-pressure atmospheric cell results in strong northerly winds, which in combination with the strong, southerly flowing California current enhances Ekman transport of surface waters, producing strong upwelling. The upwelling intensity can reach 20 to 40 m³ s⁻¹ per km of coastline from July through September (NOAA; <http://www.pfeg.noaa.gov/index.html>), and its influence can be seen in the distribution of temperature, salinity and productivity (Fig. 2). This seasonal upwelling is the principal mechanism providing nutrients to the inlets and coastal zones of BC (Thomson, 1981; Thomson et al., 1989; Mantua et al. 1997; Thomson and Gower, 1998). Inlets have high primary productivity, low surface water temperatures and high salinity during summer (Fig. 3).

The low population density and low levels of agricultural activity, in addition to limited runoff (<14 m³ s⁻¹) in the EFF and SB Inlets (Pickard, 1963) probably result in a minimal impact of human activity on nutrient inputs (Thomson, 1981).

Bottom waters in both inlets are subject to anoxic to hypoxic conditions, with oxygen concentration below 1.8 ml l^{-1} , thus limiting benthic fauna and resulting in the preservation of laminated sediments (Patterson et al., 2000).

2.2.2 Georgia Strait

Georgia Strait represents a semi-enclosed, broad, shallow basin (222 km long; 28 km wide, 6900 km² approx. area), which separates Vancouver Island from the mainland of BC (Fig. 1). Average and maximum water depths are 155 m and 420 m respectively (Thomson, 1981). Its shores are the most densely populated region of BC (75% of total), with three million inhabitants (Statistics Canada; <http://www.statcan.ca>). The GS has intensive shipping traffic as the most used marine channel in BC. Urban development, with its associated industrial and commercial activities, contributes significantly to marine environmental degradation (Key, 1989; Mackas and Harrison, 1997). For instance, inputs from rivers, sewage, groundwater discharges and atmospheric deposition amount to $\sim 285 \text{ t N day}^{-1}$ (Yin et al., 1995; Mackas and Harrison, 1997) and nutrient concentrations are high (Fig. 4). Enhanced productivity results in chlorophyll concentrations reaching as high as $20 \mu\text{g l}^{-1}$ in the Fraser plume. Primary productivity in GS ranges from 260 to 290 $\text{gC m}^{-2} \text{ yr}^{-1}$ on average, as derived from satellite observations (Antoine et al., 1996). The GS has noticeable gradients of nutrient concentrations, due to the Fraser River input and exchanges with the open ocean, mainly through the southern passage. The Southern GS is characterized by higher nutrient concentrations during the winter (Fig. 4), lower ones in the summer, probably because of nutrient uptake by phytoplankton. Dissolved oxygen concentration in the bottom waters ranges between 1.5 and 3 ml l^{-1} (Fig 5).

The Fraser River drains approximately 25% of BC and contributes 75% of the freshwater flowing into the GS. Its annual flow is about 140 km^3 , i.e. $\sim 11,000 \text{ m}^3 \text{ s}^{-1}$

during summer (June-July) and $\sim 1000 \text{ m}^3 \text{ s}^{-1}$ during winter (February-March), averaging $4400 \text{ m}^3 \text{ s}^{-1}$ (Mosher and Thomson, 2002). The Fraser River also delivers about 10 to $30 \times 10^9 \text{ kg yr}^{-1}$ of particulate matter (Johannessen et al., 2003).

Dissolved and particulate organic carbon are mainly derived from *in situ* primary production ($855 \times 10^6 \text{ kg yr}^{-1}$) and the Fraser River discharge ($550 \times 10^6 \text{ kg yr}^{-1}$), while other rivers ($200 \times 10^6 \text{ kg yr}^{-1}$), and anthropogenic sources ($120 \times 10^6 \text{ kg yr}^{-1}$) account for less (Johannessen et al., 2003).

The water column is highly stratified, especially within the brackish plume of the Fraser River (Figs. 5 and 6). The freshwater influx in the central and southern parts of the GS is characterized by a classical two layers estuarine exchange with the open ocean. The upper layer is less than about 50 m thick and is characterized by strong seasonal and latitudinal variation in SST (13 to 16°C in August, 6 to 7°C in February; Fig. 2). In the lower layer, temperatures are about 8 to 9.5°C over the entire basin (Fig. 5), and are nearly uniform throughout the year (Thomson, 1981; Masson, 2006). Brackish-low salinity upper waters circulate toward the Strait of Juan de Fuca, whereas deep ocean water circulates northwards (Thomson, 1981; LeBlond, 1983; Pawlowicz and Farmer, 1998; Fig. 7). This pattern is enhanced during the summer by the Fraser River freshet and intensive upwelling, but can be modified by tidal mixing and tidal streams (Thomson, 1981; LeBlond et al., 1991; Marinone and Pond, 1996). In spring and summer, the Fraser River freshet forms a strong brackish layer over a large area of the GS (Fig. 6), creating a stable stratification in combination with increased air temperature. Summer upwelling occurs along the Northeastern Pacific margin and Juan de Fuca Strait, and cold upwelled waters reach the southern part of the GS where they mix with brackish Fraser River water (Fig. 7). Currents, hydrographic conditions, and nutrient concentrations show considerable seasonal and inter-annual fluctuations (Masson and Cummins, 2000; Masson, 2002), but the inter-

annual or inter-decadal variability has only a small effect on phytoplankton communities and productivity in the study area (Li et al., 2000).

2.3 Materials and Methods

2.3.1 Sampling and laboratory treatments

All samples (Fig. 1; Table 1) were taken from the upper few centimetres of gravity or box cores, which were collected during various cruises onboard the Canadian Coast Guard Ships (CCGS) Victor or John P. Tully (see Table 1). Sedimentation rates generally range from 0.5 to 2 cm yr⁻¹, but can reach as much as 10 cm yr⁻¹ in the Fraser delta (Evoy et al., 1993; Hart et al., 1998; Patterson et al., 2000). We therefore assumed that the surface sediment samples represented about five years of deposition or less, and thus “modern” conditions.

Samples for palynological treatments were processed at the Centre de recherche en géochimie et en géodynamique (GEOTOP) of the Université du Québec à Montréal (UQAM) using standard procedures (de Vernal et al., 1999). Five cm³ of wet sediment was sieved to remove coarse silt, sand (106 µm sieve) and clay particles (10 µm sieve). To dissolve carbonate and silica particles, the 10-106 µm fraction was treated with warm (~40°C) HCl (10%) and HF (49%). HCl digestion lasted no longer than 20 min to avoid degradation of sensitive taxa. The residue was sieved at 10 µm and mounted between a slide and cover slide in glycerin gel. Dinocysts were identified and counted using light microscopy at 250x to 1000x. More than 200 cysts were identified and counted in most samples (Table 1). Cyst concentrations, per gram of dry weight sediment (cysts g⁻¹), were assessed using the marker grain method (Mathews, 1969).

2.3.2 Dinoflagellate cysts nomenclature

The taxonomical nomenclature follows Rochon et al. (1999), Head et al. (2001), and Pospelova and Head (2002). The assemblages include cysts of *Polykrikos kofoidii*, described by Morey-Gains and Ruse (1980), Matsuoka (1987) and Matsuoka and Cho (2000). Additional remarks upon northern and northeastern Pacific specimens are given in Radi et al. (2001) and Radi and de Vernal (2004), with illustrations. The original descriptions from Zonneveld (1997b), Zonneveld and Jurkschat (1999) and Head (2002) were used to identify *Echinidinium* species and *Bitectatodinium spongium*. Many specimens belonging to the Protoperidinales were grouped into 'Protoperidinioid' due to the difficulty in identifying at species or genus level. *Brigantedinium simplex* and *Brigantedinium cariacoenae* are grouped into *Brigantedinium* spp. because archeopyles were often not observed due to orientation. Rare specimens of the *O. centrocarpum*-morphotype short processes (de Vernal et al., 2001) were observed and were grouped with *O. centrocarpum*. Only rare specimens of *Impagidinium paradoxum*, *Nematosphaeropsis labyrinthus*, *Spiniferites mirabilis*, *Operculidium janduchenei*, *Echinidinium zonneveldiae* and *Islandinium brevispinosum* were observed, and excluded from the statistical analysis.

2.3.3 Sources of environmental data

Sea surface temperature, sea surface salinity, nutrient concentrations and chlorophyll data (0 m) were obtained from the World Ocean Atlas 2001 CD-ROM (WOA01) of the National Oceanographic Data Center (NODC, 2001; http://www.nodc.noaa.gov/O_C5/WOA01/pr_woa01.html). CD-ROM documentation, as well as data statistics, analyses and compilation of the *in situ* measurements made until 2001 are documented in Conkright et al. (2002a, 2002b), Stephens et al. (2002) and Boyer et al. (2002). Productivity levels were estimated using the algorithms developed by

Antoine et al. (1996) and Antoine and Morel (1996) based on chlorophyll concentration provided by satellite observations (Coastal Zone Color Scanner, CZCS). The relationship between radiance and marine photosynthesis is given in Morel (1978, 1991). Primary productivity in the productive layer was computed from the integrated chlorophyll content of the water column and the photosynthetically active radiation (cf. Antoine et al., 1996; Antoine and Morel, 1996). In the GS, additional nutrient data were compiled from measurements made between 2002 and 2005 through the Strait of Georgia Ecosystem Modeling (STRATOGEM) project (<http://www.stratogem.ubc.ca/data.html>). Monthly and seasonal averages were calculated for all parameters cited above. However, in some cases, the measurement locations are not the same as our sites, so we interpolated that data using the MapInfo program and the “Inverse Distance Weighting” (IDW) technique (<http://extranet.mapinfo.com>).

2.3.4 Multivariate analyses

Statistical analyses were done using CANOCO for Windows 4.0. (ter Braak and Smilauer, 1998). Because of heterogeneity in the distribution of our sampling sites, two data sets were defined for multivariate analysis: data set DS1 includes all samples of GS, and the EFF and SB Inlets (60 samples and 25 taxa), while data set DS2 includes only GS samples (40 samples and 25 taxa). In order to test the nature of variability of dinocyst assemblages, Detrended Correspondence Analyses (DCA) were done on both data sets. The length of the first gradient, which is given in standard deviation (S.D.) units, is 1.99 and 1.43 for DS1 and DS2 respectively (Table 2), indicates that dinocyst percentages show linear variation within the study area, conditions that are suitable for indirect analyses (Principal Component Analysis, PCA) or direct analyses (Redundancy Analysis, RDA), which is the linear equivalent of Canonical Correspondence Analysis (Jongman et al., 1995; ter Braak and

Smilauer, 1998). RDA allows us to extract the most significant synthetic gradient from field data on dinocyst communities and environmental variables.

RDA was performed on the DS1 and DS2 data sets with all environmental parameters available. For DS1, 21 environmental variables were used, including seasonal sea surface temperature (SST) and salinity (SSS), seasonality of temperature and salinity (difference between winter and summer), seasonal and annual primary productivity, phosphate and nitrate concentrations during spring, silica concentration during spring and summer, chlorophyll concentration during summer and water depth. For DS2, phosphate, nitrate and silica data were available for all seasons. Distance from the shore and distance from Vancouver Harbor were also added to the RDA analyses. All dinocyst and environmental data used in these analyses are included in Appendice A, which can be found, in the online version, at doi:10.1016/j.marmicro.2006.002.

Forward selection was used to reduce the set of variables to a smaller set sufficient to explain variation in species composition. The environmental variables were ranked by importance on the basis of the fit for each separate variable as the only environmental variable (marginal effect), and on the basis of the fit that each separate variable gave in conjunction with the variables already selected (conditional effect). The statistical significance of each variable was tested using a Monte Carlo permutation test under the null model with 199 random permutations. Environmental variables were deemed significantly related to the species data when P -value was less than 0.05.

2.3.5 Transfer functions and validation exercises

In order to evaluate the potential to reconstruct SST, SSS and productivity, from data on the dinocyst assemblage, transfer functions were tested using the multiple regression technique (MRT) and the modern analogue technique (MAT).

The MRT-based transfer function was made using JMP 5.1 software (<http://www.jmpin.com>). For the MAT, fossil assemblages were compared with a database of modern assemblages in order to find the best analogues according to the coefficient of similarity. The environmental values corresponding to the best analogues were then weighted by this coefficient to reconstruct paleoenvironments (see Overpeck et al., 1985; Guiot 1990). Validation tests were made using the 3PBase software (Guiot and Goeury, 1996; <http://www.imep-cnrs.com/pages/3pbase.htm>). Evaluation of the adequacy of each approach was made by comparing reconstructed and observed values using the Jackknife (or leave-one-out) method, where estimates are obtained by removing one site from the calibration data set. Each estimate was thus based on $n-1$ observations (cf. Efron and Gong, 1983). Accuracy of the approach was assessed by the coefficient of correlation between estimated and observed values, and the standard deviation of the difference between reconstructed and observed values, which is the equivalent of the Root Mean Square Error (RMSE).

2.4 Results

2.4.1 Dinocyst concentration and assemblages

Palynomorphs in general and dinocysts in particular, were abundant and well preserved. In the GS, dinocyst concentrations varied between 400 and 13,000 cysts g^{-1} , with an average of 3154 cysts g^{-1} . Such concentrations are comparable to values

observed in some European (e.g., Dale et al., 1999; Harland et al., 2004a, 2004b) and North American (Pospelova et al., 2004, 2005) estuaries, but are low in comparison to values for the EFF and SB Inlets which were commonly higher than 25,000 cysts g^{-1} , and up to as much as 137,000 cysts g^{-1} in the EFF Inlet (Table 1).

Dinocyst assemblages in all samples were characterized by relatively high species diversity, with a total of 35 taxa identified and systematically counted (Fig. 8). The EFF and SB Inlets were characterized by similar associations, with dominance of *O. centrocarpum*, whereas the GS was characterized by the dominance of heterotrophic Protoperidinioid taxa such as *Q. concreta* and *Brigantedinium* spp. In the GS some taxa, e.g. *P. dalei* and *Spiniferites ramosus* showed positive or negative gradients in relative abundance from Vancouver Harbor to offshore (Figs. 8 and 9).

2.4.2 Multivariate analyses

The results of forward selection (Tables 3 and 4) showed environmental variables ranked by their importance when analyzed separately (marginal effect) or in conjunction with other variables (conditional effect). The importance of variables according to their eigenvalues was not the same for the marginal and conditional effects due to co-variability. For example, in the DS1 (Table 3), summer chlorophyll had a higher eigenvalue when analyzed singly ($\lambda=0.28$) than when analyzed with other parameters ($\lambda=0.02$) because a large part of the chlorophyll effect can be explained by summer productivity. The conditional effect of chlorophyll was thus ordered tenth with $\lambda=0.02$ and P -value = 0.18 (Table 3). Only variables with statistically significant P -values (<0.05) were selected. The RDA ordination diagrams for DS1 and DS2 are shown in figures 10 and 11.

The results of the RDA (DS1; Fig. 10; Tables 2 and 3) show that the first ordination axis, explaining 31.2 % of the variance, is significantly and positively correlated with

annual and summer primary productivity, winter temperature and autumn salinity, and negatively correlated with water depth, summer temperature and dissolved silica concentration in spring and summer. The distribution of species along the first axis shows that autotrophic taxa, particularly *O. centrocarpum*, are ordinated on the positive side, whereas *Q. concreta*, *Brigantedinium* spp. and other heterotrophic Protoperidinioid cysts are ordinated on the negative side. The second axis explaining 6.4 % of the variance, shows opposite ordinations of *P. dalei* and *S. ramosus*, and is not clearly correlated with any environmental variable (Fig. 10).

For the DS2 data set (only GS samples), results of the RDA show that only seven of the 34 environmental variables tested are statistically significant ($P < 0.05$; Fig. 11, Table 4). The first ordination axis (23.8% of the species data variance), which mainly separates autotrophic from heterotrophic Protoperidinioid taxa, is negatively correlated with the distance from the shore. Silica concentration during summer and water depth show a significant relationship with the first ordination axis but the coefficient of correlation is relatively low (Table 4, Fig. 11). All autotrophic taxa, including *O. centrocarpum*, *P. dalei* and *S. ramosus*, are ordinated positively along axis 1 (Fig. 11), with highest abundances in shallow, coastal stations. Heterotrophic Protoperidinioid taxa, such as *Q. concreta*, *Selenopemphix nephroides*, *Selenopemphix quanta* and *Polykrikos kofoidii* are ordinated negatively along axis 1, with their highest abundances in areas of southern and central GS far from shore. The second ordination axis (15.4% of the variance), which separates *P. dalei* and *S. ramosus*, is positively correlated with spring productivity (Fig. 11) and negatively correlated with distance to Vancouver Harbor, SSS and phosphate concentration during spring. The relative abundance of different taxa, along with the RDA axes scores, allow us to distinguish three assemblages in the GS (Figs. 8, 11 and 12):

Assemblage zone 1 is characterized by relatively low cyst concentrations, ranging from 240 to 1700 cysts g^{-1} (average = 974 cysts g^{-1}). These assemblages are

characterized by high percentages of *P. dalei* (up to 30 %). RDA axes 1 and 2 show positive values. This assemblage zone seems to be related to urbanization, and is associated with the Fraser River Plume.

Assemblage zone 2 is characterized by a slightly higher cyst concentration, with an average of ~ 1800 cysts g^{-1} . *Q. concreta*, *Brigantedinium* spp. and other protoperidinal cysts dominate the assemblages. The first ordination axis shows negative scores. This zone is associated with the central and southern GS, and thus perhaps influenced by upwelled oceanic water during summer.

Assemblage zone 3 is characterized by high dinocyst concentrations (up to 13,000 cysts g^{-1}), high percentages of *S. ramosus* (40% at station V53), *O. centrocarpum*, *S. elongatus* and *Spiniferites* spp. Percentages of *Q. concreta* and *Brigantedinium* spp. are relatively low. The second ordination axis shows negative scores. Assemblage zone 3 is associated with the western side of the GS, i.e., not affected by the direct influence of Fraser River.

2.4.3 Evaluation of transfer function for estimating SST, SSS and productivity

Results of cross-validation exercises done with DS1 by the modern analogue technique (Fig. 13) represent reconstructions versus observations for SST, SSS and productivity, the most important parameters associated with dinocyst distribution in GS, EFF and SB Inlets (see Figs. 10 and 11). Although the number of modern samples used is limited (60 samples), this exercise yields a relatively good correlation ($r^2 > 0.86$) and low RMSE (Table 5). In order to test the reliability of the approaches further, we cross-validated using a larger data set by adding sites representative of neritic and oceanic domains of the northeastern Pacific, between 40 to 50°N (data from Radi and de Vernal, 2004) for a total of 123 sites (Fig. 14). This data set is

therefore representative of a domain with wider ranges of environmental variables (Table 6).

In order to verify co-variation between all parameters, we did a PCA upon all environmental variables listed in table 6. Nutrient and chlorophyll concentrations were significantly correlated with SST or SSS (Fig. 15). Seasonal SSS and winter SST also showed co-variation, mostly due to the relative influence of upwelling that determines the stratification of upper waters, and thus the salinity and thermal inertia at the surface. Nevertheless, both the winter SST and SSS were reconstructed. We considered only primary productivity, SST and SSS parameters for further reconstructions (Fig. 16).

Overall, the modern analogue technique (MAT) and the multiple regression technique (MRT) yielded comparable reconstructions with both DS1 (n=60) and the large data set (n=123), but the coefficient of correlation between reconstructed and observed values was higher, and the RMSE was lower, when using the MAT for SST and SSS (Table 5). Also, reconstruction of the primary productivity with MAT was more accurate than that made with MRT, especially when using the larger data set (n=123) as shown by the RMSE values (Table 5).

2.5 Discussion

2.5.1 Composition of assemblages

Dinocyst assemblages of estuarine environments of BC are characterized by the absence of open ocean taxa such as *Pyxidinosia reticulata* and *Impagidinium* species, which are common in the northeastern Pacific margins (Radi and de Vernal, 2004). In general, our assemblages resemble those from coastal zones of eastern and

western North Atlantic (e.g., Harland et al., 2004a, 2004b; Pospelova et al., 2005), but the GS and the EFF-SB Inlets are differentiated by the occurrence of *Echinidinium* species and the absence of *L. machaerophorum*.

Echinidinium spp. are rarely reported at middle to high latitudes in the North Atlantic, but are frequent in warm environments such as the northern Arabian Sea and along West African margins, where they are associated with high nutrient input (Zonneveld, 1997b; Zonneveld and Brummer, 2000; Susek et al., 2005). *Echinidinium* spp. are found (up to 5%) in most of the samples (see Fig. 8) from EFF, SB and GS, which indicates that these species are not restricted to warm environments, but are related to high productivity in areas with or without upwelling (see also Targarona et al., 1999; Vink et al., 2000; Zonneveld et al., 2001).

2.5.2 Dinocyst concentrations and distribution versus environmental parameters

In some estuarine systems, such as the Oslo Fjord (Norway), an increase in dinocyst concentration, along with an increase in relative abundance of the autotrophic taxon *L. machaerophorum* have been interpreted as indicating high anthropogenic nutrient input, or eutrophication (Dale and Fjelså, 1994; Dale et al., 1999). In Yokohama Port, an increase of dinocyst concentration combined with an increase of heterotrophic taxa is also interpreted as indicating eutrophication (Matsuoka, 1999). Low concentrations of dinocysts, combined with dominant heterotrophic taxa indicate industrial pollution within Frier Fjord in south-western Norway (Sætre et al., 1997). Sætre et al. (1997) argued that the increase in heterotrophic taxa reflected food availability (e.g. diatoms), which fosters heterotrophic dinoflagellates, or reduced light penetration in the water column that discriminates against autotrophic taxa. The response of assemblages may therefore differ from one region to another, depending upon the exact form of eutrophication (see Dale, 1999 and Matsuoka, 2001 for a discussion).

The GS, which is more strongly affected by human activities than the EFF and SB Inlets, has lower concentrations and higher percentages of heterotrophic dinocysts, quite similar to the Frier Fjord (Sætre et al., 1997).

Overall, the relationship between primary productivity or nutrient concentration and dinocyst concentration has not yet been clearly established quantitatively in oceanic or estuarine domains. Nevertheless, in many upwelling zones, cysts of heterotrophic species dominate the assemblages (e.g. Lewis et al., 1992; Dale et al., 2002; Radi and de Vernal, 2004). On this basis, Kumar and Patterson (2002) linked the increase in relative abundance of heterotrophic taxa in the outer basin of the EFF Inlet to high nutrient input due to upwelling. Our results show that the high productivity area of the EFF and SB Inlets is characterized by high dinocyst concentrations (Table 1), but not necessarily by high percentages of heterotrophic *Protoperidinioid* taxa (Fig. 8). This observation is important, because it illustrates the existence of relationships between dinocyst distribution and productivity in estuarine systems, which differs from that of marginal oceanic upwelling areas as documented previously (Marret, 1994; Zonneveld, 1997a; Zonneveld et al., 1997; 2001; Dale et al., 2002; Radi and de Vernal, 2004).

Axis 1 of the RDA carried out on DS1, which separates GS (low scores) from EFF-SB (high scores; Fig. 10), corresponds to two distinct regimes of nutrient enrichment and productivity. The EFF and SB Inlets face the open ocean and may thus be more influenced by regional coastal processes, including the intense summer upwelling. This configuration, together with low continental runoff, results in relatively high SSS and low summer SST, in addition to high productivity. The opposite ordination of autotrophic and heterotrophic taxa along axis 1 illustrates that there is a high relative abundance of heterotrophic *Protoperidinioid* taxa at the lower productivity sites. Both silica concentration (during spring and summer) and heterotrophic taxa are ordinated along the negative side of this axis, corresponding to the GS domain. This

suggests that heterotrophic dinoflagellates in GS produce more cysts during spring and summer, when brackish water from the Fraser River and upwelled water from the open ocean are strongly mixed in the upper layers, resulting in relatively high SST and high silica concentration. This interpretation assumes that the increase in heterotrophic Protopridinioid cysts could be supported by the spring bloom of diatoms, which are prey for heterotrophic dinoflagellates (Jacobson and Anderson, 1986; Gaines and Elbrachter, 1986) and usually bloom earlier than other phytoplankton groups (Harrison et al., 1983; Li et al., 2000). This shows that the Autotrophic/Heterotrophic ratio cannot be used without qualification as productivity or upwelling signal.

In coastal waters, upwelling and productivity often represent two covariant parameters that cannot be dissociated, but estuarine systems adjacent to upwelling cells, such as the GS, are characterized by two sources of nutrients (upwelling and continental runoff) and a large gradient in salinity (17 to 27). This gradient makes it possible to separate the influence of nutrients brought in by upwelling from that of nutrients brought in by continental runoff over a region characterized by a nearly uniform primary productivity. The abundance of autotrophic taxa in assemblages zones 1 and 3 within the GS is more likely related to coastal and shallow environments, where continental runoff and water column stratification are strong, especially within the area of the Fraser River plume (see Figs. 5, 6 and 7), as supported by the RDA showing a negative correlation between axis 1 and the distance to the shore and water depth (Fig. 11). The increase in percentage of heterotrophic taxa (assemblage zone 2; Figs. 11 and 12) in the central and southern part of GS is more likely associated with deeper and less stratified waters, as illustrated by the ordination of both distance to the shore and water depth on the negative side of the axis 1. Both axes 1 and 2 are negatively correlated with SSS and phosphate concentrations during spring, indicating that assemblage zone 2 may be associated with relatively high SSS and phosphate concentration during spring, and high silicate

concentration during summer (Fig. 11), from surface waters consisting of brackish water mixed with saline upwelled water.

High percentages (up to 30%) of *P. dalei* in the Fraser River plume and close to Vancouver Harbor characterize assemblage zone 1 (Figs. 11 and 12). This species has been recorded to be abundant in fjords and estuarine environments adjacent to the North Atlantic (Dale, 1976, 1977; Nehring, 1997; Persson et al., 2000), and is a common component of the spring phytoplankton bloom in Norwegian and Swedish fjords (Dale, 1977; Harland et al., 2004a). Little is known about the ecological affinities of this taxon in estuarine systems, but Harland et al. (2004b) suggested that it is opportunistic in zones of high anthropogenic nutrient inputs. Our results show that low salinity and high spring productivity, corresponding to the beginning of fresh water input in the Burrard Inlet (Vancouver Harbor), seem to be the most favorable for this taxon. The highly significant correlation between axis 2 and distance to Vancouver Harbor (Fig. 11), which represents the most densely populated region, suggests that human activity may strongly influence dinocyst distribution, but we do not find a positive correlation between nutrient concentrations and axis 2. This is probably because the largest source of nutrients in GS comes from the Pacific Ocean through Juan de Fuca Strait during upwelling season (Mackas and Harrison, 1997). Phosphate concentration during spring, silica concentration during summer and heterotrophic taxa show the same negative ordination along axes 1 and 2 (Fig. 11), illustrating the high phosphate and silica concentrations and high percentages of heterotrophic taxa far from Vancouver Harbor (Fig. 11). The negative correlation between silica concentration and axes 1 and 2 probably illustrates the influence of upwelling upon dinocyst assemblages, as silica is not abundant in anthropogenic effluents (sewage or agricultural runoff) as are nitrate and phosphate (cf. Anderson et al., 2002). Nitrate loading by human activity does certainly influence dinocyst distribution by favoring autotrophic taxa near Vancouver Harbor, but this signal is not easy to detect because of the high nutrient inputs from upwelling. Thus, we

assume that this signal is encoded in salinity. Finally, the dominance of gonyaulacales at the mouth of the Fraser River and the higher abundance of protoperidiniids at sites distal from the river seems to be typical of environments influenced by both upwelling and high river discharge, as documented for assemblages of the Congo River plume and the upwelling region of East Africa (Dale et al. , 2002).

2.5.3 Quantitative approaches for the reconstruction of sea-surface parameters

The composition of dinocyst assemblages along the coast of BC is closely associated with environmental parameters, especially SST, SSS and productivity. Therefore, it should be possible to use assemblage information in paleoceanographical reconstruction. Validation exercises done on the DS1 data set illustrate the identity of assemblages and their significance in terms of environmental conditions (Figure 13), and demonstrate the accuracy of the approaches on a regional scale, especially when using the modern analogue technique (Table 5). Modern analogue technique is also reliable for reconstructions of sea surface conditions when using a larger data set (i.e. the n=123 data set). A less accurate reconstruction with multiple regressions technique is probably due to the fact that this approach is based on the assumption of a linear species-environment response, which does not apply here. Annual primary productivity is reconstructed with a coefficient of correlation (r^2) of 0.90 and a root mean square error (RMSE) of $\pm 28 \text{ gC m}^{-2} \text{ yr}^{-1}$ (Fig. 16), close to the standard deviation of values estimated using chlorophyll data, i.e. $\pm 17\%$ (Antoine and Morel, 1996). SST could be reconstructed with a reasonable degree of accuracy within the range of inter-annual variability ($r^2 = 0.85$, RMSE = $\pm 0.60 \text{ }^\circ\text{C}$ for winter SST; $r^2 = 0.72$, RMSE = $\pm 0.72 \text{ }^\circ\text{C}$ for summer SST; Fig. 16). The standard deviation of measured SST for each month varies between ± 0.7 and $\pm 1.2^\circ\text{C}$ in winter and between ± 1.5 and $\pm 2.8^\circ\text{C}$ in summer, depending upon site location (NOEC, 2001), indicating that variability of SST is close to the RMSE of our validation tests. The

reconstruction of salinity shows a larger scatter, with RMSEs of about ± 0.87 and ± 1.98 for winter and summer respectively (Fig. 16). The scatter is larger in the low salinity range influenced by continental runoff. Nevertheless, the RMSEs are lower than the standard deviations of measured salinity, which vary between ± 3.31 and ± 5.7 in winter and between ± 4.62 and ± 9.90 in summer (NODC, 2001). This extremely high variability in SSS is probably related to the variable influence of upwelling intensity and freshwater input from the Fraser River.

2.6 Conclusion

Dinocyst distribution in the estuarine systems of BC shows diversified assemblages with distinct associations. The highly productive EFF and SB Inlets are characterized by dominant autotrophic taxa, whereas GS assemblages are dominated by heterotrophic taxa. GS assemblages also show variation corresponding to spring productivity and the salinity gradient. In the GS, the autotrophic taxa, including *P. dalei*, *S. ramosus* and *O. centrocarpum*, apparently characterize coastal stratified water under the influence of continental runoff, whereas the heterotrophic Protoperidinioid taxa are common in areas influenced by upwelled marine waters. In addition, high percentages of *P. dalei* close to Vancouver Harbor in the GS could be associated with the proximity to the highly urbanized shore, but also to freshwater input via the Fraser River during spring, which causes an increase in productivity. Our results provide evidence that there is a strong relationship between productivity, SST and SSS, and dinocyst distribution in surface sediments of estuarine systems of the northeastern Pacific.

2.7 Acknowledgments

We thank the Geological Survey of Canada, Sidney BC, and particularly Audrey Dallimore and Kim Conway for providing us with sedimentary samples. We gratefully acknowledge John Dower, Debby Ianson, Joe Linguanty for helping us to obtain water quality data. VP is most grateful to L. Page (University of Victoria) for providing her with a microscope facility. We are grateful to the Coastal Color Zone Project and the Distributed Active Archive Center at the Goddard Space Flight Center, Greenbelt, MD 20771 sponsored by NASA's Mission to Planet Earth Program. The Natural Sciences and Engineering Research Council of Canada (NSERC) and the Fonds pour la Formation de Chercheurs et d'aide à la Recherche du Québec (FCAR) funded this study. The critical and constructive comments of reviewers Dr. K.A.F. Zonneveld and Dr. F. Marret were very helpful in improving this paper.

2.8 References

- Anderson, D.M., Gilbert, P.M., Burkholder, J.M., 2002. Harmful algal blooms and eutrophication: nutrient sources, composition, and consequences. *Estuaries* 25, 704-726.
- Antoine, D., Morel, A., 1996. Oceanic primary production. 1. Adaptation of a spectral light photosynthesis model in view of application to satellite chlorophyll observations. *Global Biogeochemical Cycles* 10, 43-55.
- Antoine, D., André, J.M., Morel, A., 1996. Oceanic primary production. 2. Estimation at global scale from satellite (costal zone colour scanner) chlorophyll. *Global Biogeochemical Cycles* 10, 57-69.
- Barker, M.L., 1974. Water resources and related land uses: Strait of Georgia-Puget Sound basin. Lands Directorate, Department of Environment, Geographical paper, vol. 56. Ottawa, 55 pp.
- Beamish, R.J., Bouillon, D.R., 1993. Pacific salmon production trends in relation to climate. *Canadian Journal of Fisheries and Aquatic Sciences* 50, 1002-1016.
- Beamish, R.J., McFarlane, G.A., Thomson, R.E., 1999. Recent declines in the recreational catch of coho salmon (*Oncorhynchus kisutch*) in the Strait of Georgia are related to climate. *Canadian journal of Fisheries and Aquatic Science* 56, 506-515.
- Boyer, T.P., Stephens, C., Antonov, J.I., Conkright, M.E., Locarnini, R.A., O'Brien, T.D., Garcia, H.E., 2002. World Ocean Atlas 2001, Volume 2: Salinity. In: Levitus, S. (Ed.), NOAA Atlas NESDIS 50, U.S. Government Printing Office, Washington.
- Bricker, S.B., Clement, C.G., Pirhalla, D.E., Orlando, S.P., Farrow, D.R.G., 1999. National Estuarine Eutrophication Assessment: Effects of Nutrient Enrichment in the Nation's Estuaries. NOAA National Ocean Service, Silver Spring, MD.
- Conkright, M.E., Antonov, J.I., Baranova, O., Boyer, T.P., Garcia, H.E., Gelfeld, R., Johnson, D., Locarnini, R.A., Murphy, P.P., O'Brien, T.D., Smolyar, I., Stephens, C., 2002a. World Ocean Database 2001, Vol. 1: Introduction. Levitus, S., (Ed), NOAA Atlas NESDIS 42, U.S. Government Printing Office, Washington, D.C., 167 pp.
- Conkright, M.E., Locarnini, R.A., Garcia, H.E., O'Brien, T.D., Boyer, T.P., Stephens, C., Antonov, J.I., 2002b. World Ocean Atlas 2001: Objective Analyses, Data Statistics, and Figures, CD-ROM documentation. National Oceanographic Data Center, Silver Spring, MD.

Dale, B., 1976. Cyst formation, sedimentation and preservation: factors affecting dinoflagellate assemblages in recent sediments from Trondheimsfjord, Norway. *Review of Palaeobotany and Palynology* 22, 39-60.

Dale, B., 1977. New observation of *Peridinium faroense* Paulsen (1905) and classification of small orthoperidinoid dinoflagellates. *British Phycological Journal* 12, 241-253.

Dale, B., 1996. Dinoflagellate cysts ecology: modelling and geological applications. In: Jansonius, J., McGregor, D. (Eds.), *Palynology: principles and applications*. The American Association of Stratigraphic Palynologists Foundation, Salt Lake City, pp. 1249-1276.

Dale, B., 2001. Marine dinoflagellate cysts as indicators of eutrophication and industrial pollution: a discussion. *The Science of the Total Environment* 264, 235-240.

Dale, B., Fjellså, A., 1994. Dinoflagellate cysts as paleoproductivity indicators: state of the art, potential and limits. In: Zahn, R., Pedersen, T., Kaminski, M., Labeyrie, L. (Eds.), *Carbon cycling in the glacial Ocean: constraints on the ocean's role in global change*. Springer-Verlag, Berlin, pp. 521-537.

Dale B., Thorsen T.A., Fjellså, A., 1999. Dinoflagellate cysts as indicators of cultural eutrophication in the Oslofjord, Norway. *Estuarine Coastal and Shelf Sciences* 48, 371-382.

Dale, B., Dale, A.L., Jansen, F.J. H., 2002. Dinoflagellate cysts as environmental indicators in surface sediments from the Congo deep-sea fan and adjacent regions. *Palaeogeography Palaeoclimatology Palaeoecology* 185, 309-338.

de Vernal, A., M. Henry, Bilodeau, G., 1999. Techniques de préparation et d'analyse en micropaléontologie. *Les Cahiers du GEOTOP*, n° 3. Université du Québec à Montréal, Montréal, 41 pp.

de Vernal, A., Henry, M., Matthiessen, J., Mudie, P.J., Rochon, A., Boessenkool, K., Eynaud, F., Grøsfjeld, K., Guiot, J., Hamel, D., Harland, R., Head, M.J., Kunz-Pirrung, M., Levac, E., Loucheur, V., Peyron, O., Pospelova, V., Radi, T., Turon, J.-L., Voronina E., 2001. Dinocyst assemblages as tracer of sea-surface conditions in the northern North Atlantic, Arctic and sub-Arctic seas: the "n = 677" database and derived transfer functions. *Journal of Quaternary Science* 16, 681-698.

- Efron, B., Gong, C., 1983. A Leisurely Look at the Bootstrap, the Jackknife, and Cross validation. *The American Statistician* 37, 36-48.
- Evoy, R.W., Moslow, T.F., Patterson, R.T., Luternauer, J.L., 1993. Patterns and variability in sediment accumulation rates, Fraser River delta foreslope, British Columbia, Canada. *Geo-Marine Letters* 13, 212-218.
- Gaines, G., Elbrachter, M., 1986. Heterotrophic nutrition. In: Taylor, F.J.R., (Ed.), *The Biology of Dinoflagellates*, pp. 224-268. Blackwell Scientific Publications, Oxford.
- Guiot, J., 1990. Methodology of the last climatic cycle reconstruction in France from pollen data. *Palaeogeography Palaeoclimatology Palaeoecology* 80, 49-69.
- Guiot, J., Goeury, C., 1996. PPPbase, a software for statistical analysis of paleoecological data. *Dendrochronologia* 14, 295-300.
- Harland, R., Nordberg, K., Filipsson, H.L., 2004a. The seasonal occurrence of dinoflagellate cysts in surface sediments from Koljö Fjord, west coast of Sweden - a note. *Review of Palaeobotany and Palynology* 128, 107-117.
- Harland, R., Nordberg, K., Filipsson, H.L., 2004b. A high-resolution dinoflagellate cyst record from latest Holocene sediment in Koljö Fjord, Sweden. *Review of Palaeobotany and Palynology* 128, 119-141.
- Harrison, P.J., Fulton, J.D., Taylor, F.J.R., Persons, T.R., 1983. Review of the biological oceanography of the Strait of Georgia: pelagic environment. *Canadian Journal of Fisheries and Aquatic Sciences* 40, 1064-1094.
- Harrison, P.J., Mackas, D.L., Frst, B.W., Macdonald, R.W., Crecelius, E.A., 1994. An assessment of nutrients, plankton and some pollutants in the water column of Juan de Fuca Strait, Strait of Georgia and Puget Sound and their transboundary transport. In: Wilson, R.C.H., Beamish, R.J., Aitkens, F., Bell, J. (Eds.), *Review of the marine environment and biota of Strait of Georgia, Puget Sound and Juan de Fuca Strait. Proceeding of the BC/Washington Symposium on the Marine Environment*, Canadian technical report of Fisheries and Aquatic Science 1948, pp. 138-172.
- Hart, B.S., Hamilton, T.S., Barrie, J.V., 1998. Sedimentation rates and patterns on deep water delta (Fraser Delta, Canada); integration of high-resolution seismic stratigraphy, core lithofacies, and ¹³⁷Cs fallout stratigraphy. *Journal of Sedimentary Research* 68, 556-568.

- Head, M.J., 2002. *Echinidinium zonneveldiae* sp. nov., a dinoflagellate cyst from the Late Pleistocene of the Baltic Sea, northern Europe. *Journal of Micropalaeontology* 21, 169-173.
- Head, M.J., Harland, R., Matthiessen, J., 2001. Cold marine indicators of the late quaternary: the new dinoflagellate cyst genus *Islandinium* and related morphotypes. *Journal of Quaternary Science* 16, 621-636.
- Jacobson, D., Anderson, D., 1986. Thecate heterotrophic dinoflagellates: Feeding behaviour and mechanics. *Journal of Phycology* 22, 249-258.
- Johannesen, S.C., Macdonald, R.W., Paton, D.W. 2003. A sediment and organic carbon budget for the greater Strait of Georgia. *Estuarine Coastal and Shelf Science* 56, 845-860.
- Jongman, R.H.G., Ter Braak, C.J.F., Van Tongeren, O.F.R., 1995. *Data analysis in community and landscape ecology*. Cambridge University Press, Cambridge.
- Key, B.H., 1989. *Pollutants in British Columbia's Marine Environment*. Environment Canada. Report no. 89-1, Ottawa, 61 pp.
- Kumar, A., Patterson, T., 2002. Dinoflagellate cyst assemblages from Effingham Inlet, Vancouver Island, British Columbia, Canada. *Palaeogeography Palaeoclimatology Palaeoecology* 180, 187-206.
- LeBlond, P.H., 1983. The Strait of Georgia: functional anatomy of a coastal sea. *Canadian Journal of Fisheries and Aquatic Sciences* 40, 1033-1063.
- LeBlond, P.H., Ma, H., Doherty, F., Pond, S., 1991. Deep and intermediate water replacement in the Strait of Georgia. *Atmosphere-Ocean* 29, 288-312.
- Lewis, J., Dodge, J.D., Powell, A.J., 1990. Quaternary dinoflagellate cysts from the upwelling system offshore Peru, Hole 686B, ODP Leg 112. In Suess, E., von Huene, R., et al. (eds.), *Proceeding of the Ocean Drilling Program. Scientific Results* 112, pp. 323-327.
- Li, M., Gargett, A., Denman, K., 2000. What determines seasonal and interannual variability of phytoplankton and zooplankton in strongly estuarine systems? Application to the semi-enclosed estuary of Strait of Georgia and Juan de Fuca Strait. *Estuarine, Coastal and Shelf Science* 50, 467-488.

- Mackas, D.L., Harrison, P.J., 1997. Nitrogenous nutrient sources and sinks in the Juan de Fuca Strait/Strait of Georgia/Puget sound estuarine system: Assessing the potential eutrophication. *Estuarine, Coastal and Shelf Science* 44, 1-21.
- Mackas, D.L., Thomson, R.E., Galbraith, R.E., 2001. Changes in the zooplankton community of the British Columbia continental margin, 1985-1999, and their covariation with oceanographic conditions. *Canadian Journal of Fisheries and Aquatic Sciences* 58, 685-702.
- Mantua, N.J., Hare, S.R., Zhang, Y., Wallace, J.M., Francis, R.C., 1997. A Pacific Interdecadal Climate Oscillation with Impacts on Salmon Production. *Bulletin of the American Meteorological Society* 78, 1069-1079.
- Marinone, S.G., Pond, S., 1996. A three-dimensional model of deep water renewal and its influence on residual currents in the central Strait of Georgia, Canada. *Estuarine, Coastal and Shelf Science* 43, 183-204.
- Marret, F., 1994. Distribution of dinoflagellate cysts in recent marine sediments from the east Equatorial Atlantic (Gulf of Guinea). *Review of Palaeobotany and Palynology* 84, 1-22.
- Masson, D., 2002. Deep Water Renewal in the Strait of Georgia. *Estuarine, Coastal and Shelf Science* 54, 115-126.
- Masson, D., 2006. Seasonal water mass analysis for the Strait of Juan de Fuca and Georgia. *Atmosphere-Ocean* 44, 1-15.
- Masson, D., Cummins, P.F., 2000. Fortnightly modulation of the estuarine circulation in Juan de Fuca Strait. *Journal of Marine Research* 58, 439-463.
- Mathews, J., 1969. The assessment of a method for the determination of absolute pollen frequencies. *New Phytologist* 68, 161-166.
- Matsuoka, K., 1987. Organic-walled dinoflagellate cysts from surface sediments of Akkeshi Bay and Lake Saroma, North Japan. *Bulletin of the Faculty of Liberal Arts, Nagasaki University*, 28, 1, 35-123.
- Matsuoka, K., 1999. Eutrophication process recorded in dinoflagellate cyst assemblages - a case of Yokohama Port, Tokyo Bay, Japan. *The Science of the Total Environment* 231, 17-35.

- Matsuoka, K. 2001. Further evidence for a marine dinoflagellate cyst as an indicator of eutrophication in Yokohama Port, Tokyo Bay, Japan. Comments on a discussion by B. Dale. *The Science of the Total Environment* 264, 221-233.
- Matsuoka, K., Cho, H.J., 2000. Morphological variation in cyst of gymnodinialean dinoflagellate *Polykrikos*. *Micropaleontology* 46, 360-364.
- Morel, A. 1978. Available, usable and stored radiant energy in relation to marine photosynthesis. *Deep Sea Research* 25, 673-688.
- Morel, A. 1991. Light and marine photosynthesis: a spectral model with geochemical implications. *Progress in Oceanography* 26, 263-306.
- Morey-Grains, G., Ruse, R.H., 1980. Encystment and reproduction of the predatory dinoflagellate, *Polykrikos kofoidii* Chatton (Gymnodiniales). *Phycologia* 19, 230-236.
- Mosher, D.C., Thomson, R.E., 2002. The Foreslope Hills: large-scale, fine-grained sediment waves in the Strait of Georgia, British Columbia. *Marine Geology* 192, 275-295.
- Nehring, S., 1997. Dinoflagellate resting cysts from recent German coastal sediments. *Botanica Marina* 40, 307-324.
- NODC, 2001. World Ocean Atlas 2001, CD-ROMs data set, National Oceanographic Data Center, Silver Spring, MD.
- Overpeck, J., Webb, T., Prentice, I.C., 1985. Quantitative interpretation of fossil pollen spectra: dissimilarity coefficients and the method of modern analogs. *Quaternary Research* 23, 87-108.
- Patterson, R.T., Guilbault, J.-P., Thomson, R.E., 2000. Oxygen level control on foraminiferal assemblage distribution in Effingham Inlet, Vancouver Island, British Columbia. *Journal of Foraminiferal Research* 30, 321-335.
- Pawlowicz, R., Farmer, D.M., 1998. Diagnosing vertical mixing in a two-layer exchange flow. *Journal of Geophysical Research* 103, 30695-30712.
- Persson, A., Godhe, A., Karlson, B., 2000. Dinoflagellate cysts in recent sediments from the West coast of Sweden. *Botanica Marina* 43, 69-79
- Pickard, G.L., 1963. Oceanographic characteristics of inlets of Vancouver Island, British Columbia. *Journal of the Fisheries Research Board of Canada* 20, 1109-1144.

- Pospelova, V., Head, M.J., 2002. *Islandinium brevispinosum* sp. nov. (Dinoflagellata), a new organic-walled dinoflagellate cyst from modern estuarine sediments of New England (USA). *Journal of Phycology* 38, 593-601.
- Pospelova, V., Chmura, G.L., Boothman, W.S., Latimer, J.S., 2002. Dinoflagellate cyst records and human disturbance in two neighboring estuaries, New Bedford Harbor and Apponagansett Bay, Massachusetts (USA). *The Science of the Total Environment* 298, 81-102.
- Pospelova, V., Chmura, G.L., Walker, H.A., 2004. Environmental factors influencing spatial distribution of dinoflagellate cyst assemblages in shallow lagoons of southern New England (USA). *Review of Palaeobotany and Palynology* 128, 7-34.
- Pospelova, V., Chmura, G.L., Boothman, W., Latimer, J.S., 2005. Spatial distribution of modern dinoflagellate cysts in polluted estuarine sediments from Buzzards Bay (Massachusetts, USA) embayments. *Marine Ecology Progress Series* 292, 23-40.
- Pospelova, V., Pedersen, T.F., de Vernal, A., 2006. Dinoflagellate cysts as indicators of climatic and oceanographic changes during the past 40 kyr in the Santa Barbara Basin, southern California. *Paleoceanography* 21, 1-16.
- Radi, T., de Vernal, A., 2004. Dinocyst distribution in surface sediments from the northeastern Pacific margin (40-60 °N) in relation to hydrographic conditions, productivity and upwelling. *Review of Palaeobotany and Palynology* 128, 169-193.
- Radi, T., de Vernal, A., Peyron, O., 2001. Relationships between dinocyst assemblages in surface sediments and hydrographic conditions in the Bering and Chukchi seas. *Journal of Quaternary Science* 16, 667-680.
- Robinson, C.L.K., Ware, D.M., 1999. Simulated and observed response of the southwest Vancouver Island pelagic ecosystem to oceanic conditions in the 1990s. *Canadian Journal of Fisheries and Aquatic Sciences* 56, 2433-2443.
- Rochon, A., de Vernal, A., Turon, J.-L., Matthiessen, J., Head, M.J., 1999. Distribution of dinoflagellate cysts in surface sediments from the North Atlantic Ocean and adjacent seas in relation to sea-surface parameters. *American Association of Stratigraphic Palynologists, Contribution Series* 35, 152 pp.
- Sætre, M.L.L., Dale, B., Abdullah, M.I., Sætre, G.-P., 1997. Dinoflagellate cysts as possible indicators of industrial pollution in a Norwegian fjord. *Marine Environmental Research* 44, 167-189.

- Sangiorgie, F., Donders, T.H., 2004. Reconstructing 150 years of eutrophication in the north western Adriatic Sea (Italy) using dinoflagellate cysts, pollen and spores. *Estuarine, Coastal and Shelf Science* 60, 69-79.
- Schmitt, C., Schweigert, J., Quinn, T.P., 1994. Anthropogenic influence on fish populations of the Georgia Basin. In: Wilson, R.C.H., Beamish, R.J., Aitkens, F., Bell, J. (Eds.) *Review of the marine environment and biota of Strait of Georgia, Puget Sound and Juan de Fuca Strait. Proceeding of the BC/Washington Symposium on the Marine Environment, Canadian technical report of Fisheries and Aquatic Science* 1948, pp. 218-255.
- Stephens, C., Antonov, J.I., Boyer, T.P., Conkright, M.E., Locarnini, R.A., O'Brien, T.D., Garcia, H.E., 2002. *World Ocean Atlas 2001, Volume 1: Temperature*. In: Levitus, S. (Ed.), *NOAA Atlas NESDIS 49*. U.S. Government Printing Office, Wash., D.C., 167 pp., CD-ROMs.
- Susek, E., Zonneveld, K.A.F., Fischer, G., Versteegh, G.J.M., Willems, H., 2005. Organic-walled dinoflagellate cyst production in relation to upwelling intensity and lithogenic influx in the Cape Blanc region (off north-west Africa). *Phycological Research* 53, 97-112.
- Targarona, J., Warnaar, J., Boessenkool, K.P., Brinkhuis, H., Canals, M., 1999. Recent dinoflagellate cyst distribution in the North Canary Basin, NW Africa. *Grana* 38, 170-178.
- ter Braak, C.J.F., Smilauer, P., 1998. *Canoco reference manual and user's guide to Canoco for Windows, software for canonical community ordination (version 4)*. Centre for Biometry, Wageningen, 351 pp.
- Thomson, R.E., 1981. *Oceanography of the British Columbia coast*. Canadian Special Publication of Fisheries and Aquatic Sciences 56, Sidney, 291 pp.
- Thomson, R.E., Gower, J.F.R., 1998. A basin-scale oceanic instability event in the Gulf of Alaska. *Journal of Geophysical Research-Oceans* 103, 3033-3040.
- Thomson, R.E., Hickey, B.M., LeBlond, P.H. 1989. The Vancouver Island coastal current: fisheries barrier and conduit. In: Beamish, R.J., MacFarlane, G.D. (eds.), *Effect of Ocean variability on recruitment and an evaluation of parameters used in stock assessment models*. Canadian Special Publication of Fisheries and Aquatic Sciences 108, Ottawa, pp. 265-296.
- Thorsen, T.A., Dale, B., 1997. Dinoflagellate cysts as indicators of pollution and past climate in a Norwegian fjord. *The Holocene* 7, 433-446.

Vink, A., Zonneveld, K.A.F., Willems, H., 2000. Organic-walled dinoflagellate cysts in western equatorial Atlantic surface sediments: distribution and their relation to environment. *Review of Palaeobotany and Palynology* 112, 247-286.

Ware, D.M., Thomson, R.E., 1991. Link between long-term variability in upwelling and fish production in the northeast Pacific Ocean. *Canadian Journal of Fisheries and Aquatic Sciences* 48, 2296-2306.

West, P., Fyles, T.M., King, B., Peeler, D.C., 1994. The effects of human activity on the marine environment of the Georgia Basin: present waste loading and future trends. In: Wilson, R.C.H., Beamish, R.J., Aitkens, F., Bell, J. (Eds.), *Review of the marine environment and biota of Strait of Georgia, Puget Sound and Juan de Fuca Strait*. Proceeding of the BC/Washington Symposium on the Marine Environment, Canadian technical report of Fisheries and Aquatic Science 1948, pp. 9-35.

Yin, K., Harrison, P.J., Pond, S., Beamish, R.J., 1995. Entrainment of nitrate in the Fraser River estuary and its biological implications, II. Effects of spring vs. neap tides and river discharge. *Estuarine, Coastal and Shelf Science* 40, 529-544.

Zonneveld, K.A.F., 1997a. Dinoflagellate cyst distribution in surface sediments from the Arabian Sea (northwestern Indian Ocean) in relation to temperature and salinity gradients in the upper water column. *Deep-Sea Research II*, 6-7, 1411-1443.

Zonneveld, K.A.F., 1997b. New species of organic walled dinoflagellate cysts from modern sediments of the Arabian Sea (Indian Ocean). *Review of Palaeobotany and palynology* 97, 319-337.

Zonneveld, K.A.F., Brummer, G.J.A., 2000. Palaeoecological significance, transport and preservation of organic-walled dinoflagellate cysts in the Somali Basin, NW Arabian Sea. *Deep Sea Research II* 47, 2229-2256.

Zonneveld, K.A.F., Jurkschat, T., 1999. *Bitectatodinium spongium* (Zonneveld, 1997) Zonneveld et Jurkschat, comb. nov. from modern sediments and sediment trap samples of the Arabian Sea (northwestern Indian Ocean): taxonomy and ecological affinity. *Review of Palaeobotany and Palynology* 106, 153-169.

Zonneveld, K.A.F., Ganssen G., Troelstra, S., Versteegh, G.J.M., Visscher, H., 1997. Mechanisms forcing abrupt fluctuations of the Indian Ocean summer monsoon during the last deglaciation. *Quaternary Science Reviews* 16, 187-201.

Zonneveld, K.A.F., Hoek, R.P, Brinkhuis, H., Willems, H., 2001. Geographical distribution of organic-walled dinoflagellate cysts in surficial sediments of the Benguela upwelling region and their relationship to upper ocean conditions. *Progress in Oceanography* 48, 25-75.

2.9 Figure captions

Figure 1. Map of study area showing sampling site locations (dots) within EFF, SB and GS (A). Arrows indicate main summer surface circulation pattern. Regional surface circulation pattern for the GS is shown in (B) where grey arrows indicate circulation of brackish Fraser River water, mixing with saline oceanic water from Juan de Fuca Strait and discovery Pass. Isolines of equal mean tidal range are indicated in (C) (compiled from Barker, 1974; Thomson, 1981 and Thomson et al., 1989)

Figure 2. SST, SSS and productivity distributions in the coastal waters of BC. February and August SST and SSS data are from The World Ocean Atlas (2001). Productivity data are from Antoine et al. (1996) based on satellite observation of the chlorophyll yielded by the CZCS program.

Figure 3. Summer SSS plotted against summer SST, winter SST and summer productivity in the GS (diamonds), SB Inlets (squares) and EFF Inlet (circles).

Figure 4. Winter and summer distribution maps of nitrate, phosphate and silica concentrations in the surface water of the GS. Data are from STRATOGEM (Strait of Georgia Ecosystem Modeling project; <http://www.stratogem.ubc.ca/data.html>) and the World Ocean Atlas (2001).

Figure 5. Average distribution of temperature (a) and dissolved oxygen (b) in the water column along the Georgia Strait and Juan de Fuca Strait. Data are from Masson (2006) and represent average of measurements made between 1999 and 2003 at 20 stations.

Figure 6. Satellite images of suspended sediment in the Georgia Strait, from the AVHRR (Very High Resolution Radiometer) aboard a NOAA weather satellite, showing the extent of the Fraser River plume in February, May and August 2002. The images are from the Fisheries and Oceans Canada - Pacific Region web site (http://www-sci.pac.dfo-mpo.gc.ca/osap/data/default_e.htm).

Figure 7. Diagram showing the basic physical mechanisms of water circulation in the Georgia Strait and Juan de Fuca Strait. Grey arrows represent upwelled water coming from Juan de Fuca Strait and mixing with brackish Fraser River water in the central and southern parts of the Georgia Strait (adapted from Thomson, 1981)

Figure 8. Percentages diagram of dinocyst taxa (except *Operculodinium janduchenei*, *Impagidinium paradoxum* and *Islandinium brevispinosum*, which only occur in very low numbers).

Figure 9. Percentage distributions of the most important taxa in the GS, according to their ordination upon the first RDA axis (*Operculodinium centrocarpum* and *Quinquecuspis concreta*) and the second RDA axis (*Pentapharsodinium dalei* and *Spiniferites ramosus*)

Figure 10. RDA results of EFF, SB and GS data (i.e. DS1) showing ordination of species and environmental variables on axes 1 and 2 (respectively 31.2 % and 6.4 % of species data variance). Only statistically significant environmental variables ($P < 0.05$) are displayed. Bottom panel illustrates the sample scores of the two ordination axes.

Figure 11. RDA results of GS data (i.e. DS2) showing ordination of species and environmental variables on axes 1 and 2 (respectively 23.8 % and 15.4 % of species data variance). Only statistically significant environmental variables ($P < 0.05$) are

displayed. Dist. shore = distance from the shore, Dist. Van. Harbor = distance from Vancouver Harbor, Spring PO = phosphate concentration during spring. Bottom panel illustrates sample scores of the two ordination axes and the definition of assemblage zones 1, 2 and 3.

Figure 12. Map of the distribution of assemblage zones 1, 2 and 3 within the GS.

Figure 13. Results of the validation exercise for the reconstruction of temperature, salinity and productivity using the modern analogue technique. Data set DS1 ($n = 60$) includes EFF-SB Inlets and the GS. Because of the small size of the data set, only three analogues were retained for the reconstructions.

Figure 14. Map of site locations of the large data set ($n = 123$) used for the validation exercise. This data set includes, in addition to EFF-SB Inlets and GS, 63 sites offshore of BC spanning coastal and oceanic domains (data from Radi and de Vernal, 2004). Filled circles correspond to data from Radi and de Vernal (2004) and open circles indicate data from this study.

Figure 15. Results of Principal Components Analysis (PCA) carried out on the environmental variables in the $n = 123$ data set. The two axes represent respectively 61.8% and 23.4% of the total variance. Note that dinocyst data are excluded from this analysis, which allows us to identify the environmental variables that may co-vary and therefore allows us to select adequately the parameters that are to be used during reconstructions. The matrix of correlation coefficients (bottom) is based on linear relationships between the environmental parameters used in this PCA.

Figure 16. Results of the validation exercise for the reconstruction of temperature, salinity and productivity for the data set $n=123$, using the modern analogue technique.

Because of the small size of the data set, only 3 analogues were retained for the reconstructions.

2.10 Table captions

Table 1. List of sample sites with location, water depth, total cysts counted and cyst concentration. Samples of SB Inlets (SB1 to SB10) are from cores collected during summer 2003 onboard the CCGS Victor. Samples of the GS, labeled "T" and "V", were collected during the CCGS John P. Tully and CCGS Victor cruises in summers 1992 and 2002. Samples of EFF Inlet (EF8 to EF27) were collected during the CCGS John P. Tully cruise in summer 1997.

Table 2. Results of ordination by Detrended Correspondence Analysis (DCA) and Redundancy Analysis (RDA) of DS1 and DS2 data sets, showing eigenvalues, variance of species data and species-environment relationships for the first two axes.

Table 3. Importance ranking of environmental variables by their marginal and conditional effects on dinocysts distribution in the GS, EFF and SB Inlets (DS1), as obtained by forward selection. λ is the eigenvalue explained by environmental variable. *P*-value is the significance level of the conditional effect, as obtained by Monte Carlo permutation test under the null model with 199 random permutations.

Table 4. Importance ranking of environmental variables by their marginal and conditional effects on dinocysts distribution in the GS (DS2), as obtained by forward selection. λ is the eigenvalue explained by environmental variable, *P*-value is the significance level of the conditional effect, as obtained by Monte Carlo permutation test under the null model with 199 random permutations.

Table 5. Root Mean Square Error (RMSE) and the coefficient of correlation between observed and estimated values (r^2) of the environmental variables tested by the cross-validation exercises using modern analogue technique (MAT) and multiple regression technique (MRT). The small data set (DS1+DS2) includes EFF-SB Inlets and GS alone, whereas the large data set (n=123) includes, in addition to EFF-SB Inlets and GS, 63 sites offshore BC spanning coastal and oceanic domains (data from Radi and de Vernal, 2004).

Table 6. Mean seasonal SST, SSS (NODC, 2001), chlorophyll and nutrient concentrations (NODC, 2001; STRATOGEM, 2005) and annual primary productivity (Antoine et al., 1996) of surface water of estuarine sites (Seymour-Belize Inlets, Georgia Strait and Effingham Inlet) and oceanic sites (OSU 1 to 75)

Figure 1

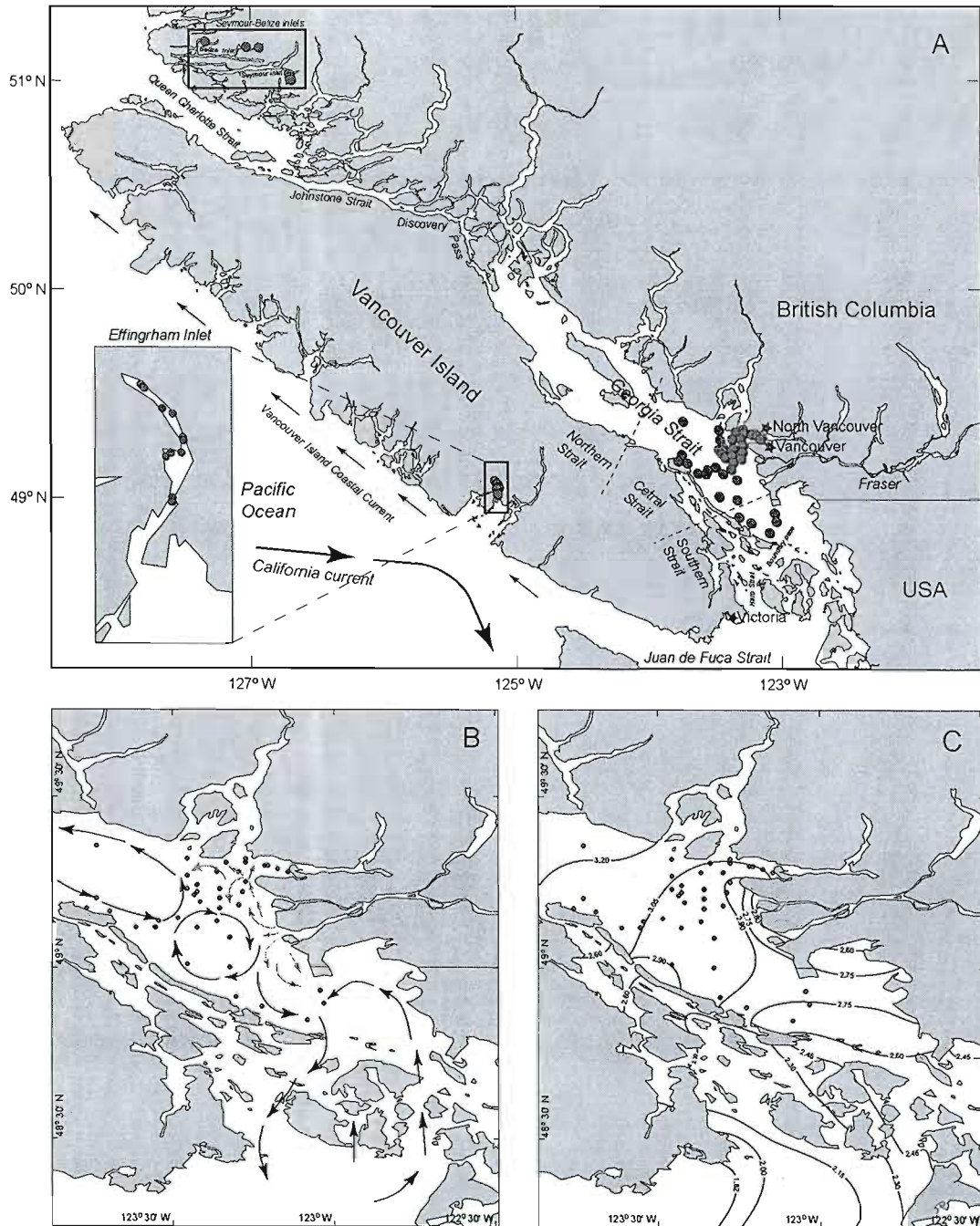


Figure 2

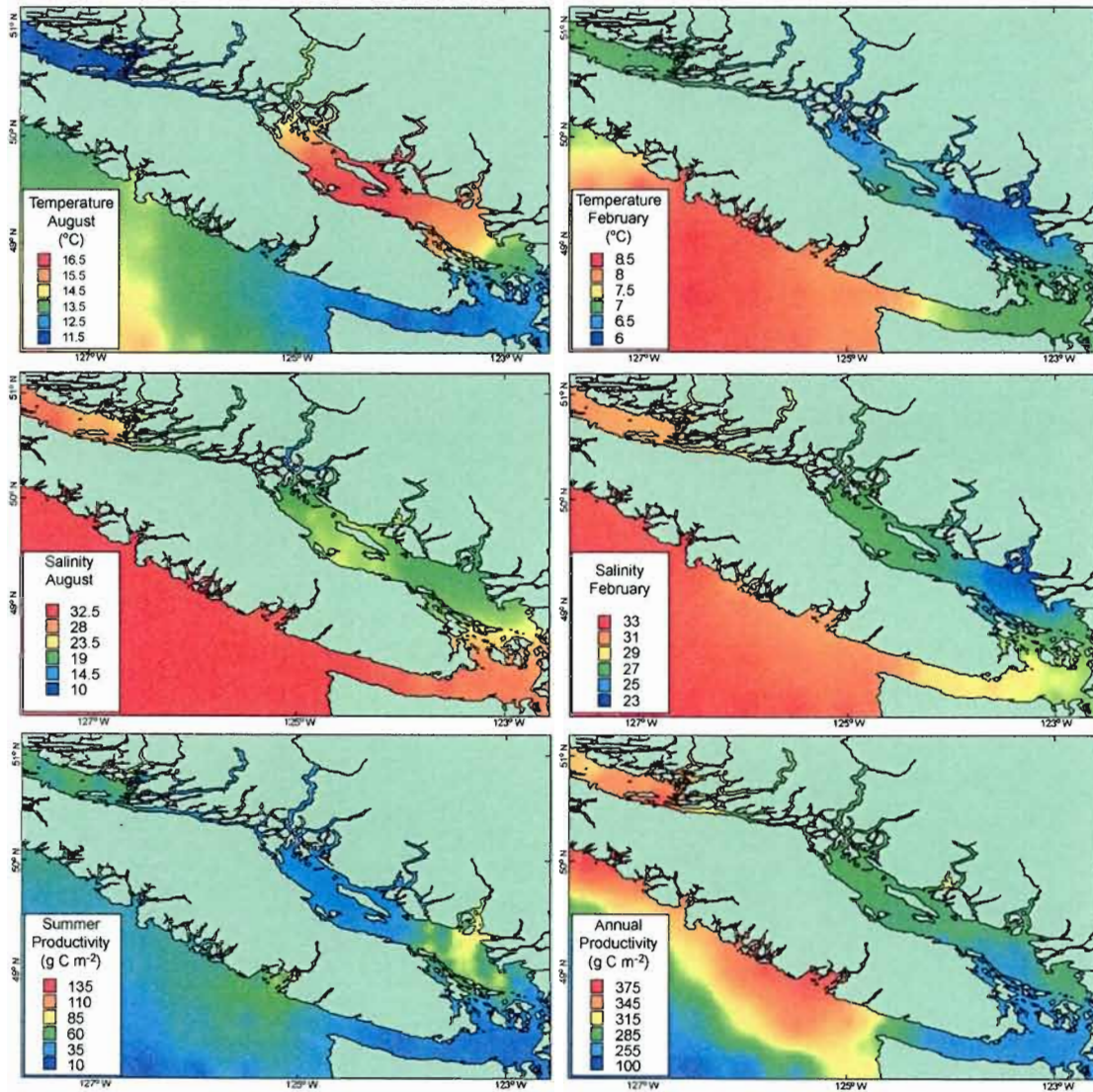


Figure 3

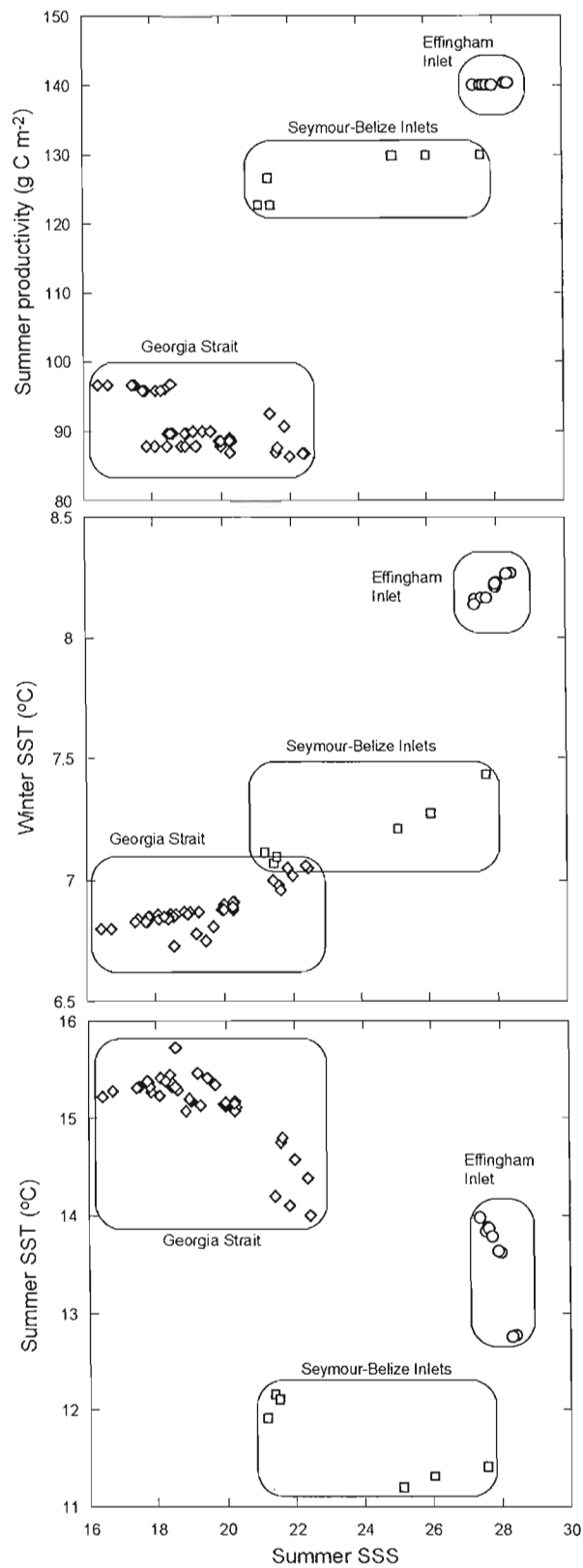


Figure 4

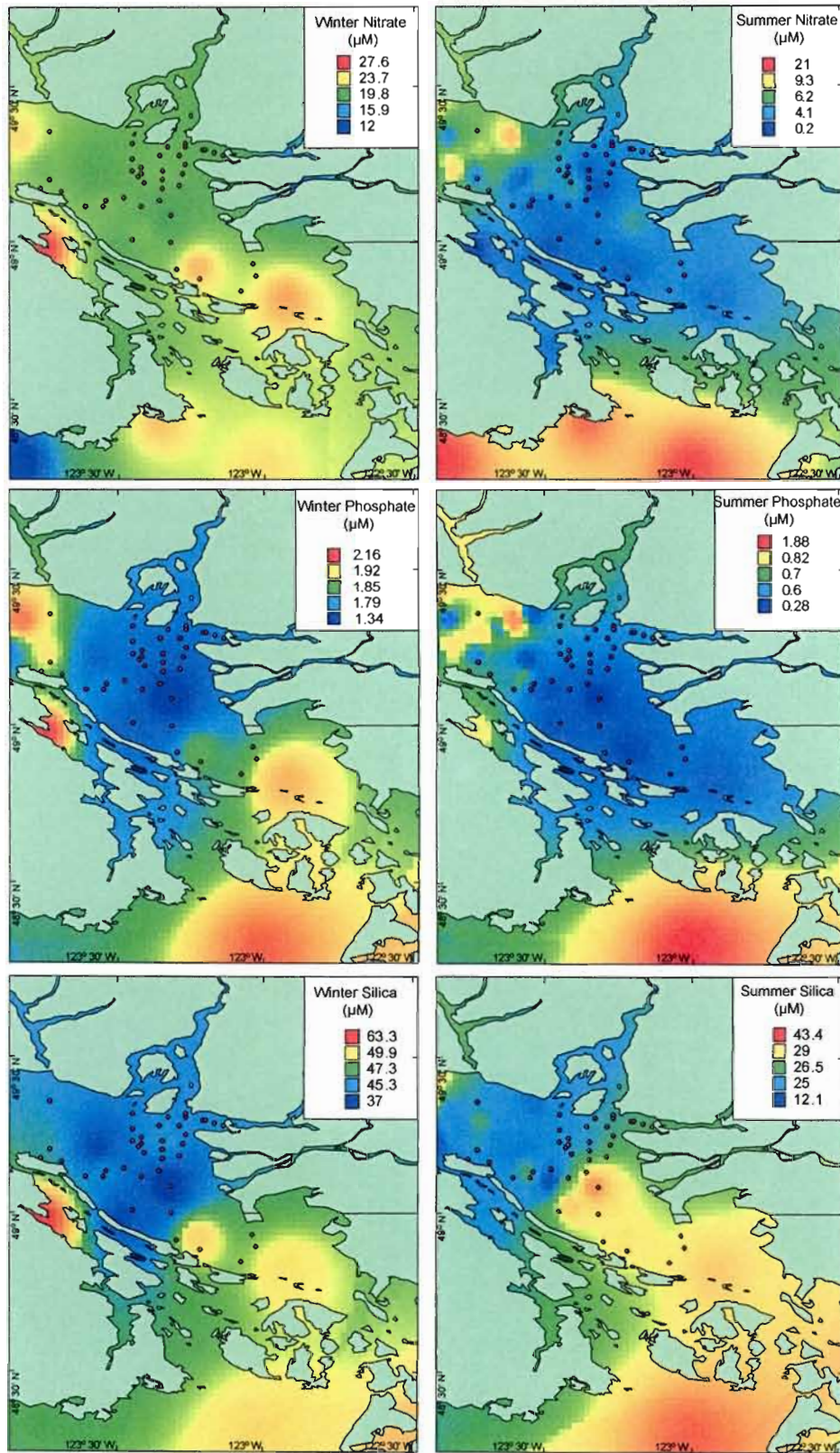


Figure 5

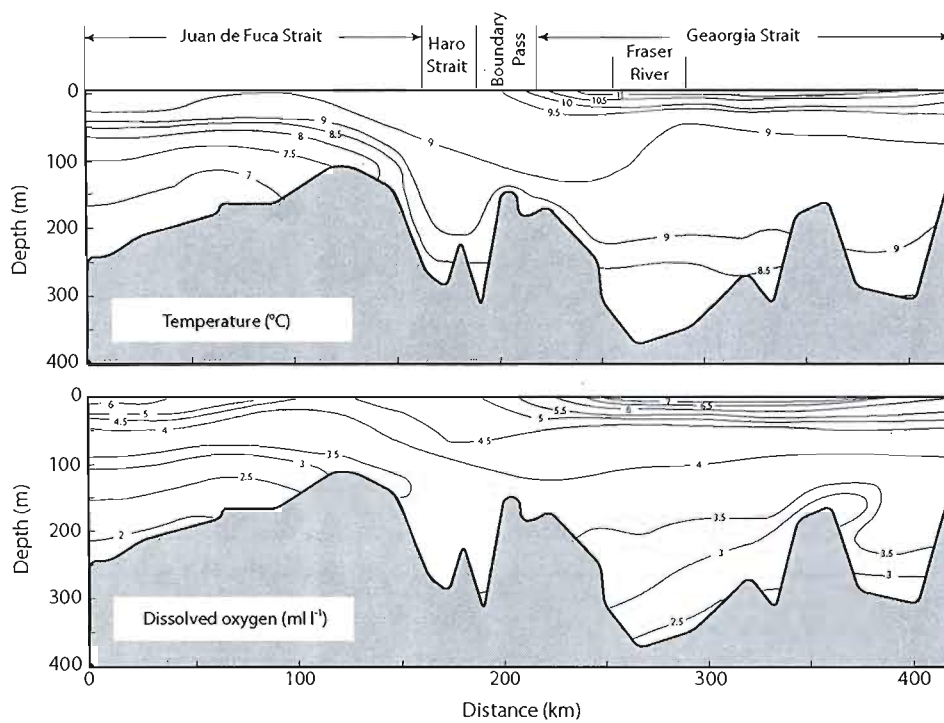


Figure 6

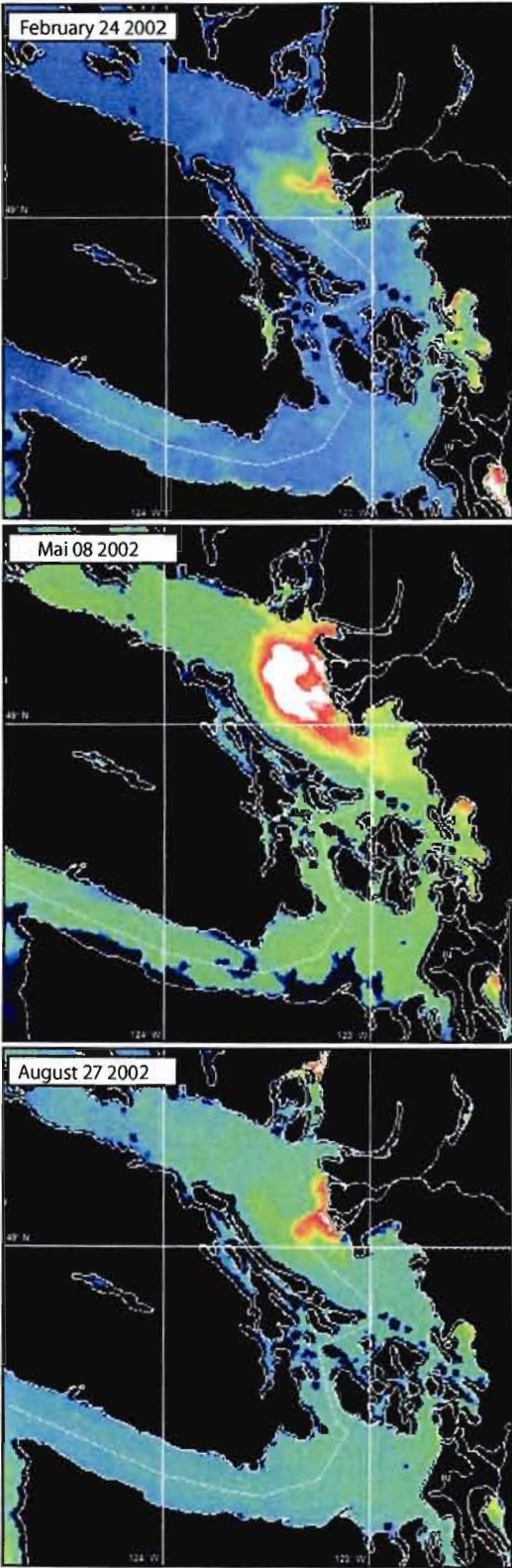
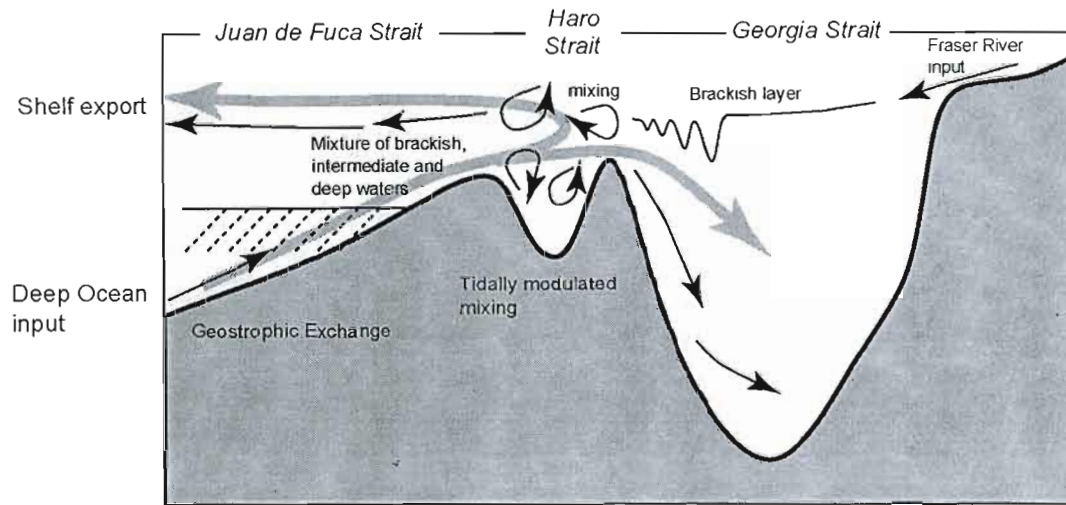


Figure 7



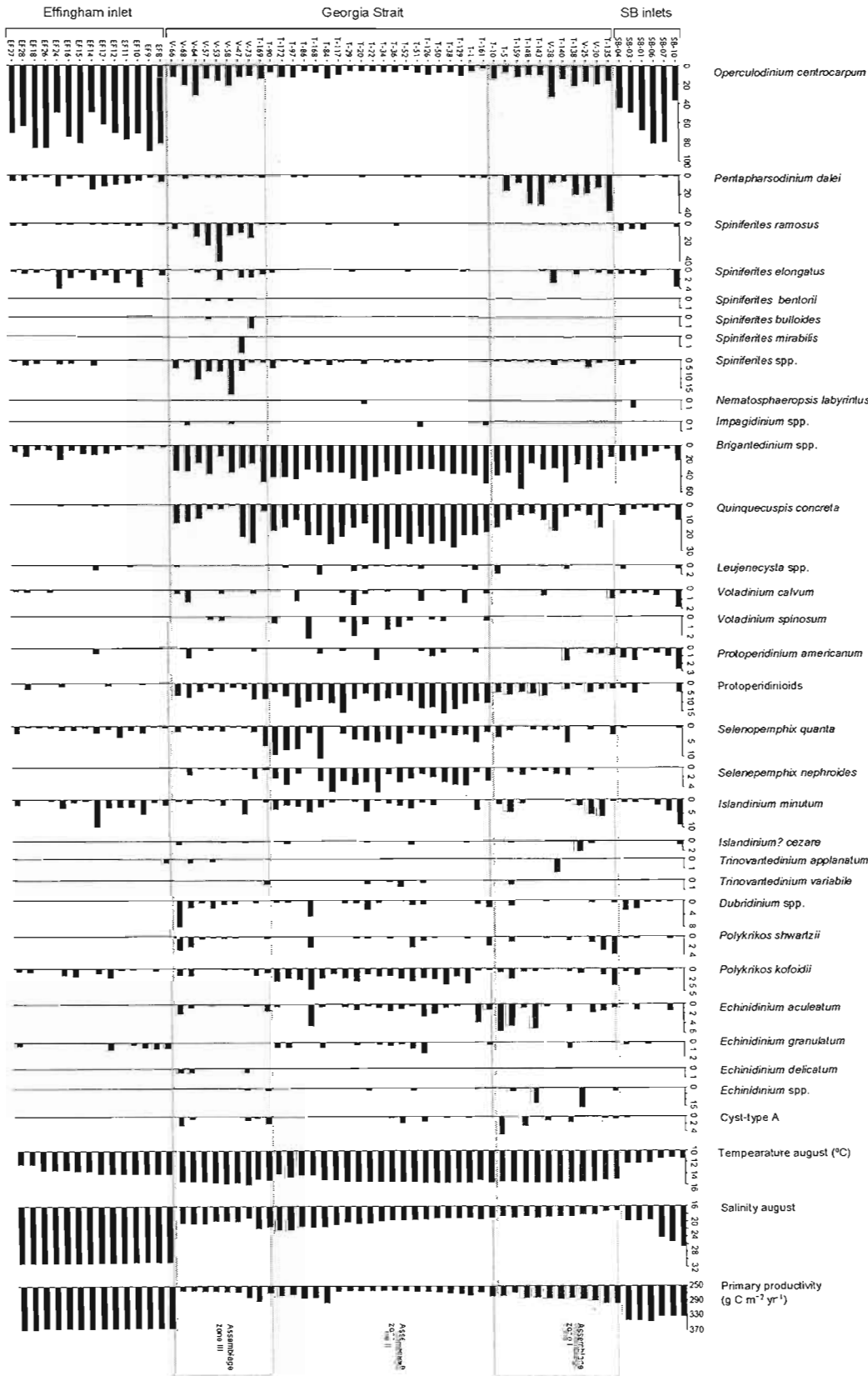


Figure 8

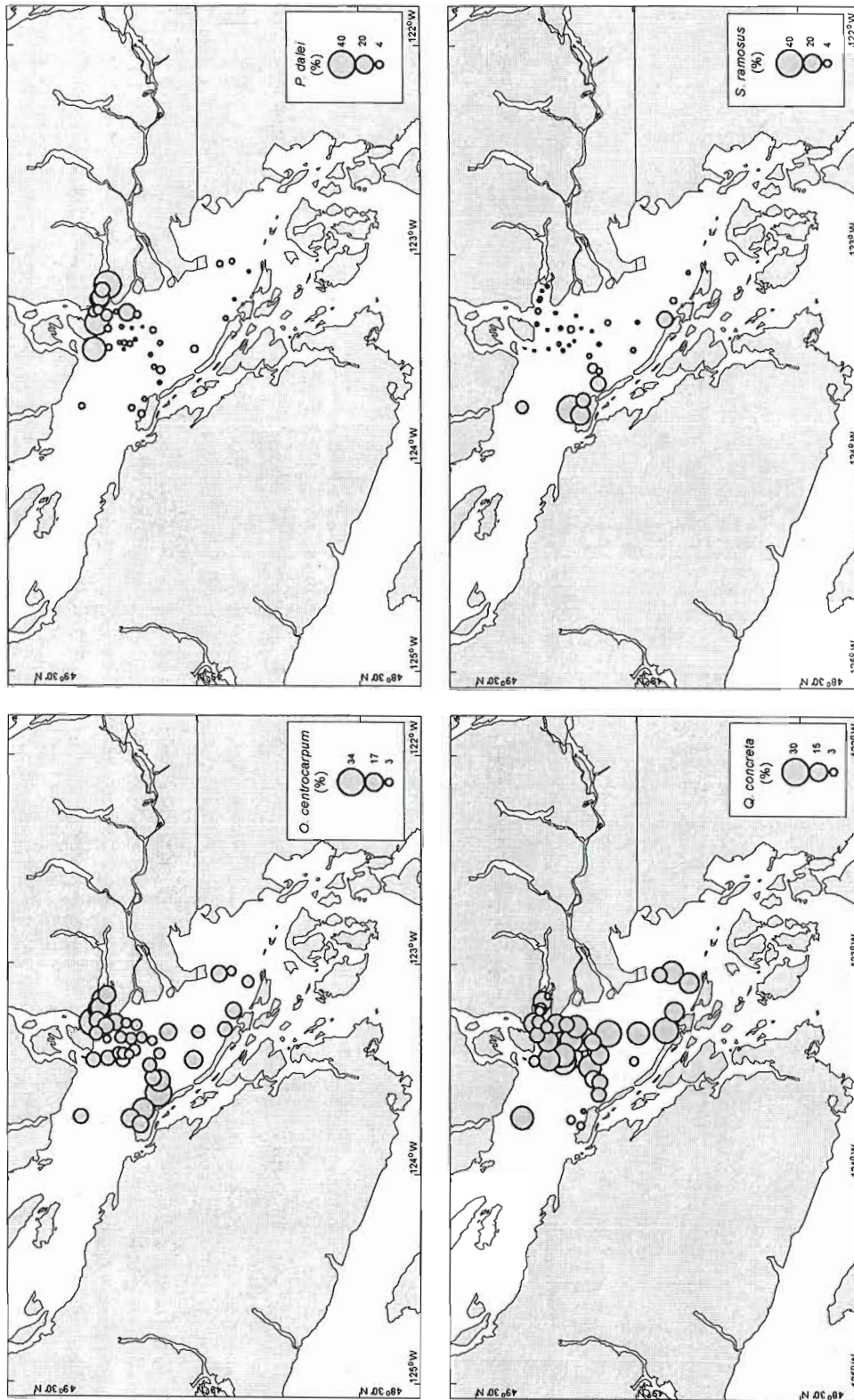


Figure 9

Figure 10

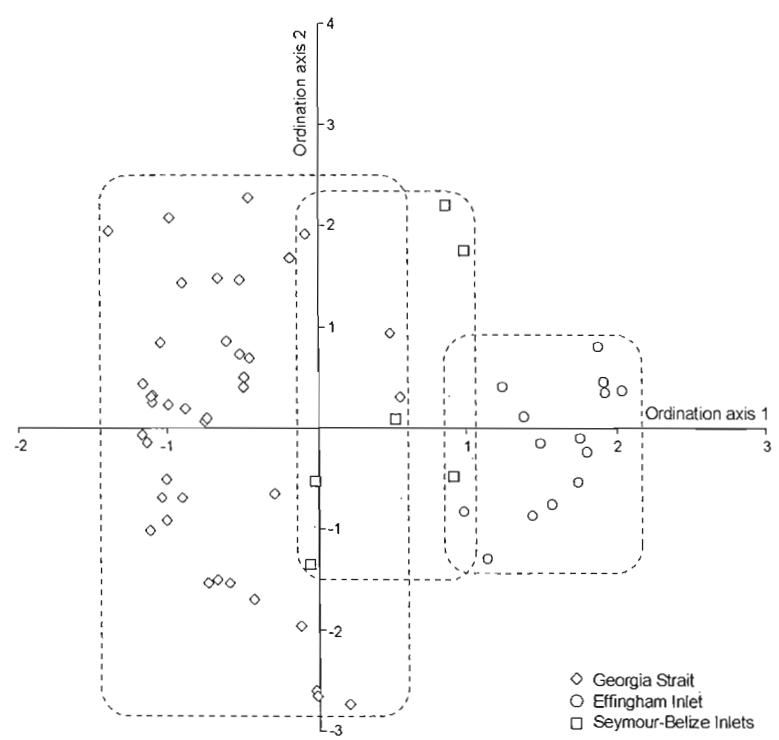
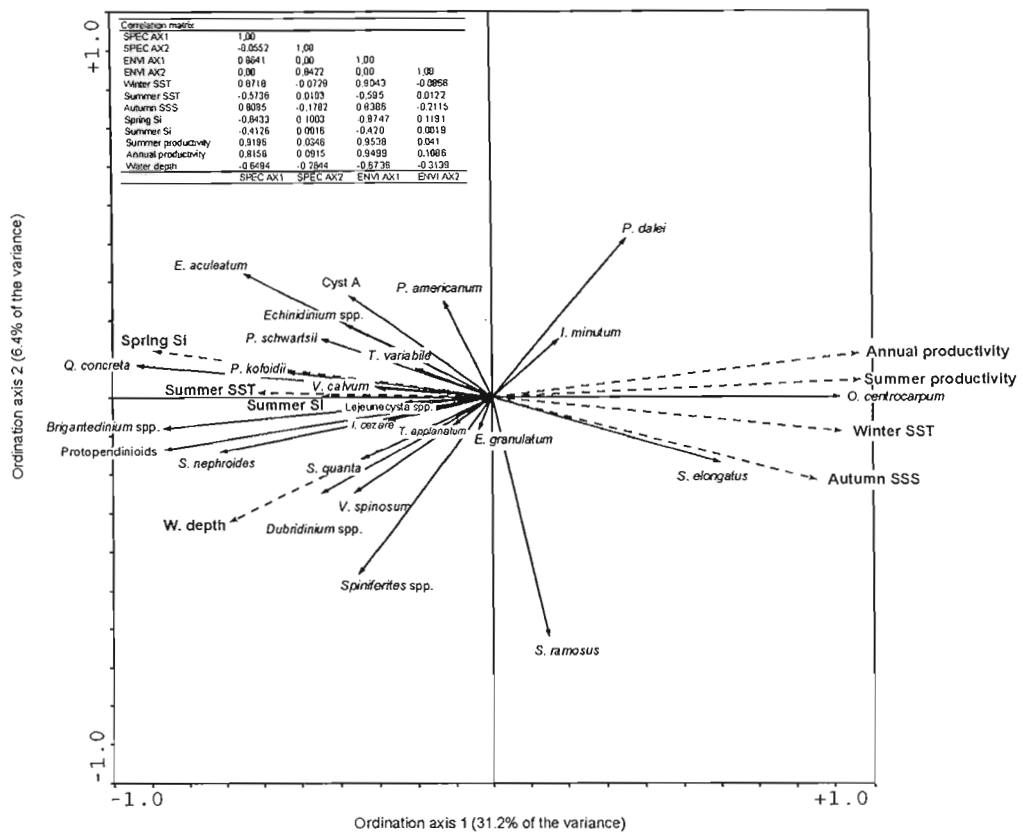


Figure 11

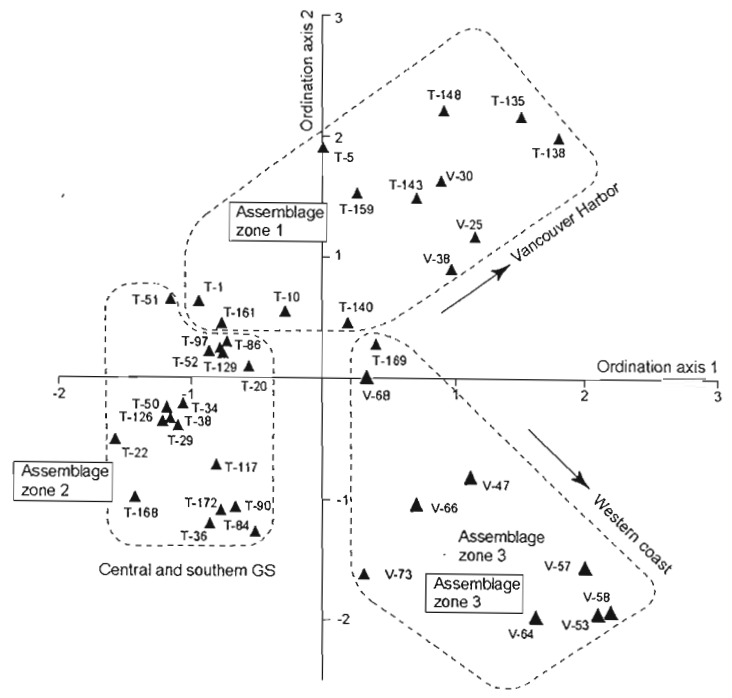
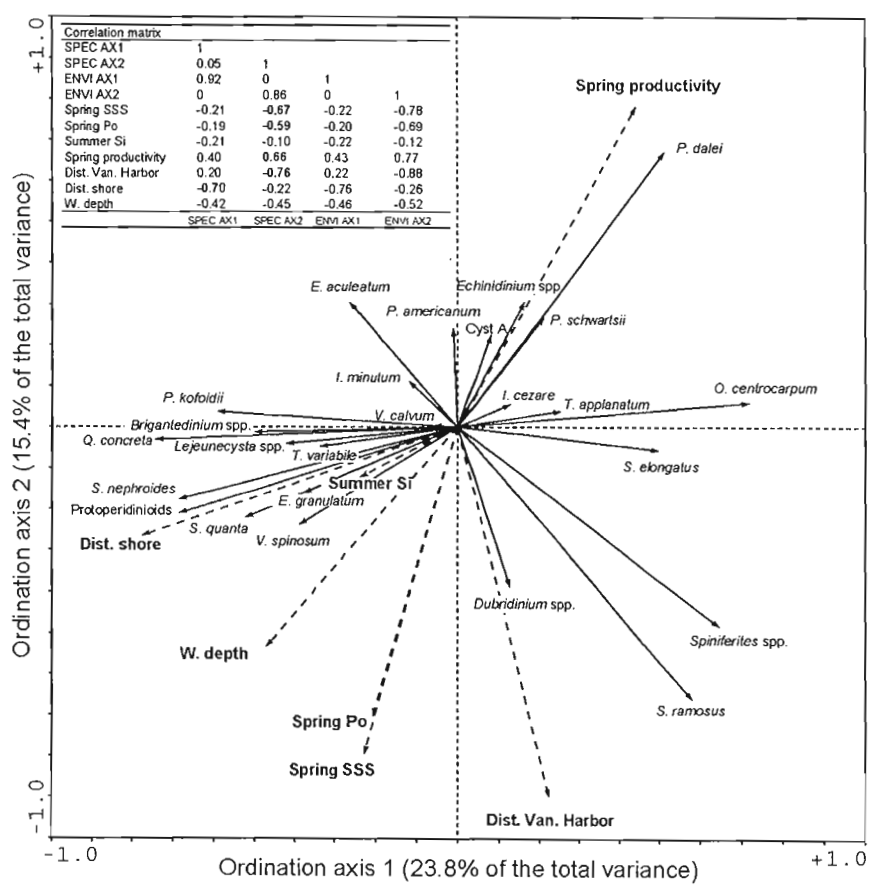


Figure 12

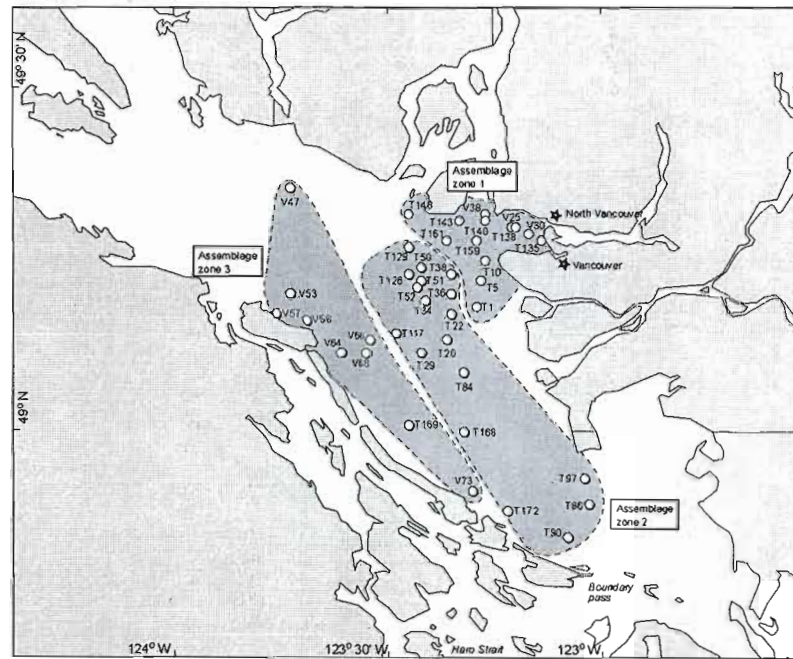
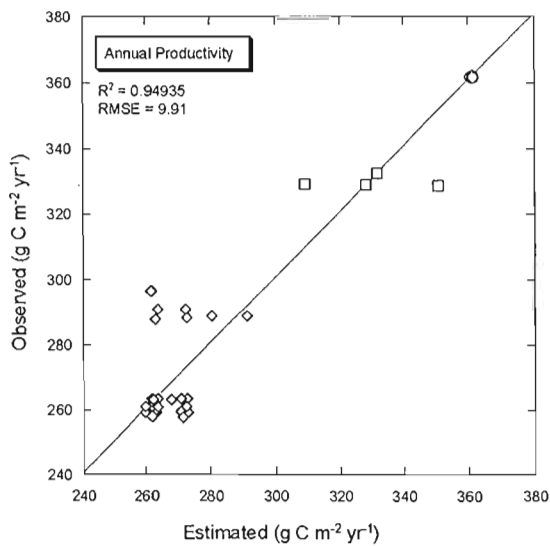
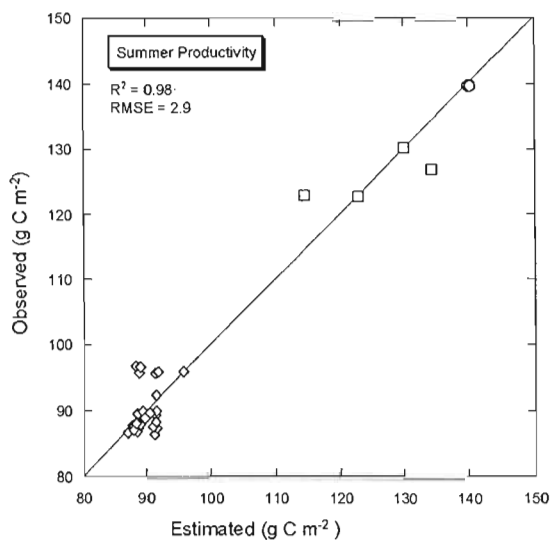
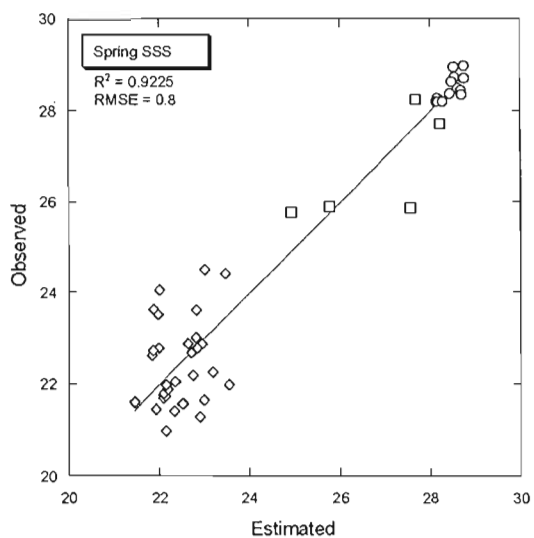
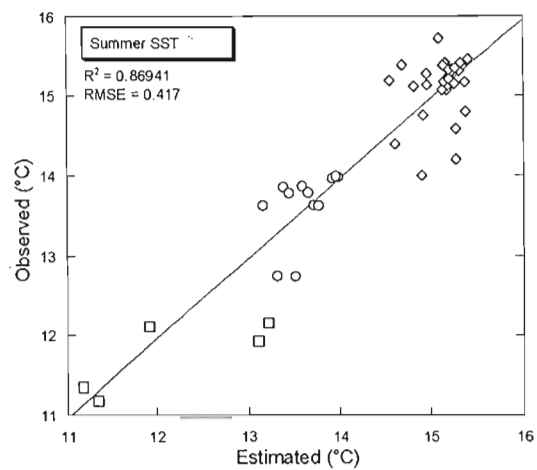
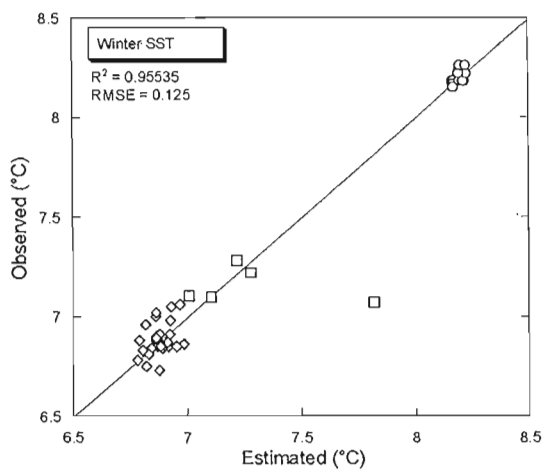


Figure 13



- Effingham Inlet
- Seymour-Belize inlets
- ◇ Georgia Strait

Figure 14

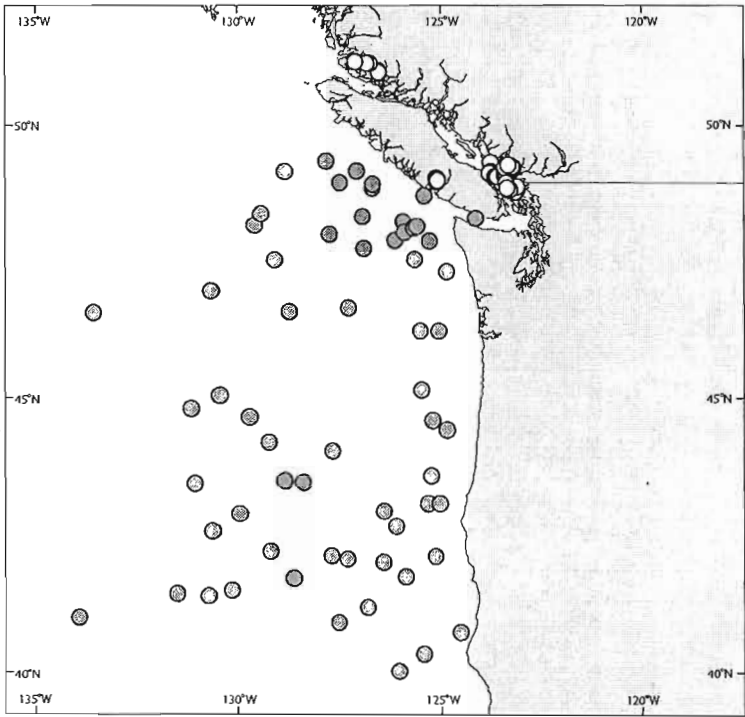
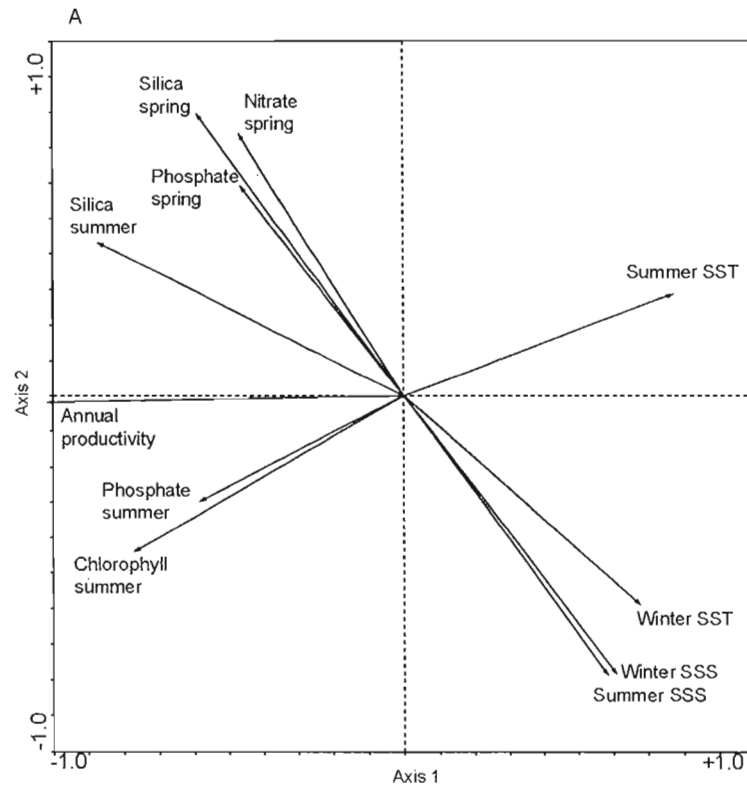


Figure 15



B

	winter SST	winter SSS	summer SST	summer SSS	Annual productivity	Nitrate spring	Phosphate spring	Phosphate summer	Silica spring	Silica summer
Winter SST	-									
Winter SSS	0.83	-								
Summer SST	0.45	0.14	-							
Summer SSS	0.84	0.97	0.16	-						
Annual productivity	-0.65	-0.59	-0.76	-0.56	-					
Nitrate spring	-0.65	-0.82	-0.17	-0.77	0.45	-				
Phosphate spring	-0.69	-0.63	-0.38	-0.67	0.44	0.72	-			
Po summer	-0.27	-0.05	-0.70	-0.08	0.57	0.03	0.28	-		
Silica spring	-0.81	-0.94	-0.22	-0.90	0.57	0.85	0.71	0.05	-	
Silica summer	-0.85	-0.81	-0.62	-0.80	0.85	0.65	0.65	0.50	0.79	-
Chlorophyll summer	-0.23	-0.13	-0.65	-0.11	0.77	0.04	0.07	0.69	0.08	0.53

Figure 16

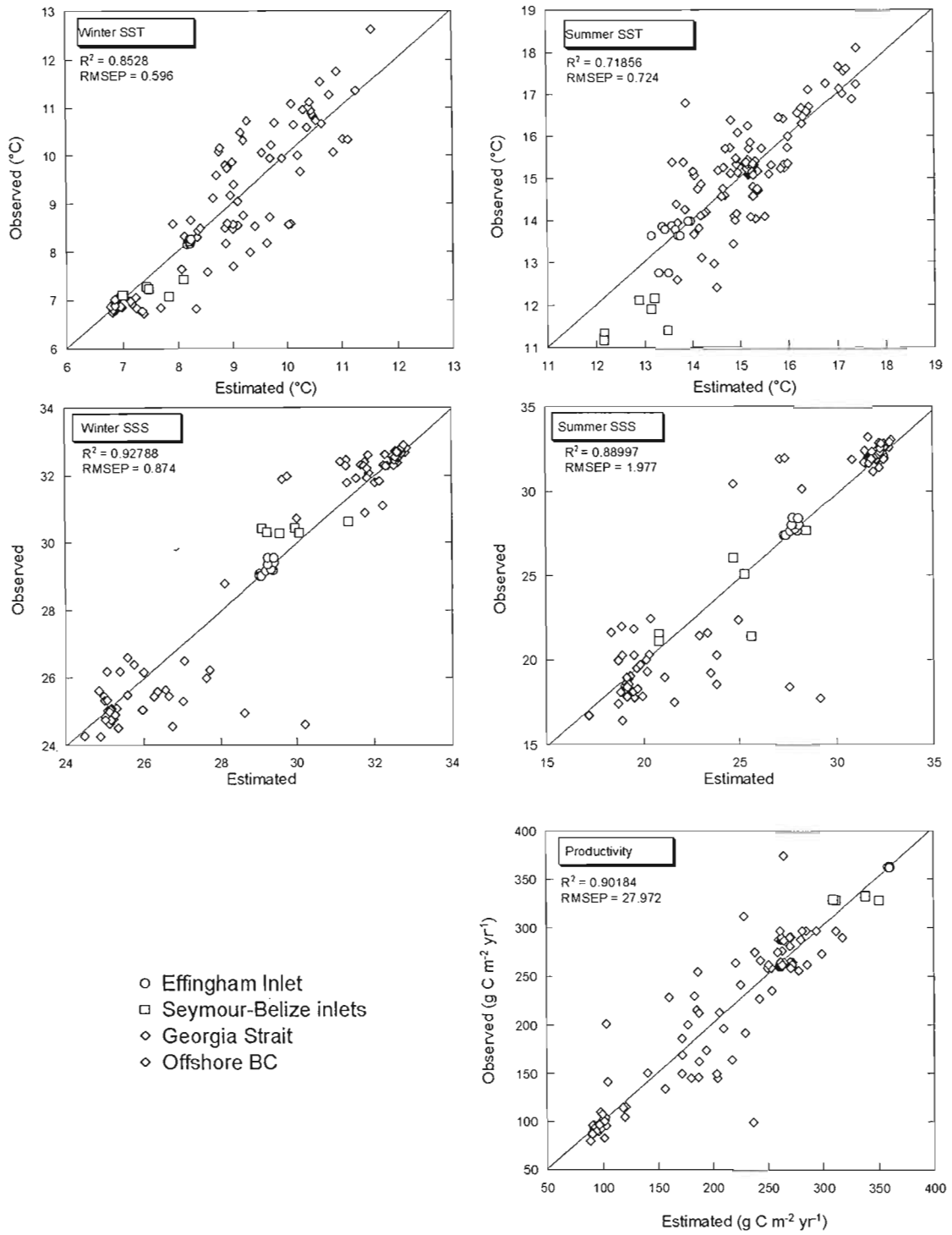


Table 1

Station number	Latitude	Longitude	Water depth (m)	Laboratory number	Count	cysts g ⁻¹
SB-10	51.20	-127.35	164	1908-4	109	34 955
SB-07	51.17	-127.04	151	1908-3	188	66 391
SB-06	51.17	-126.95	131	1908-2	147	25 037
SB-01	51.04	-126.72	241	1907-5	325	8617
SB-03	51.02	-126.71	241	1907-6	239	29 568
SB-04	51.01	-126.71	211	1908-1	246	51 918
T-135	49.29	-123.16	13	1873 -5	103	549
V-30	49.30	-123.19	25	1912 -6	130	1060
V-25	49.31	-123.22	54	1912 -5	152	1114
T-138	49.31	-123.23	54	1862 -3	88	922
T-140	49.32	-123.29	129	1873 -6	125	833
V-38	49.33	-123.29	125	1913 -2	68	677
T-143	49.32	-123.35	184	1874 -1	316	1693
T-148	49.33	-123.47	257	1862 -4	150	1680
T-159	49.29	-123.31	107	1874 -2	112	577
T-5	49.23	-123.30	96	1871 -2	172	1369
T-10	49.26	-123.29	66	1871 -3	104	243
T-129	49.28	-123.47	178	1873 -4	210	1172
T-161	49.29	-123.38	251	1874 -3	240	1421
T-1	49.19	-123.31	100	1871 -1	183	1377
T-38	49.24	-123.37	241	1872 -1	216	1429
T-50	49.25	-123.44	256	1872 -2	354	1355
T-126	49.24	-123.47	310	1873 -3	287	2781
T-51	49.23	-123.44	302	1872 -3	323	3014
T-52	49.22	-123.45	302	1872 -4	210	1342
T-36	49.21	-123.37	243	1861 -4	259	2719
T-34	49.20	-123.43	289	1871 -6	346	2870
T-22	49.18	-123.37	217	1871 -5	322	2226
T-20	49.14	-123.38	167	1871 -4	225	2031
T-29	49.12	-123.44	288	1861 -3	244	1937
T-117	49.15	-123.50	335	1873 -2	315	2030
T-84	49.09	-123.34	136	1873 -1	78	423
T-168	49.00	-123.34	211	1862 -5	139	1910
T-86	48.89	-123.05	155	1861 -6	43	512
T-97	48.93	-123.06	128	1862 -2	79	483
T-172	48.88	-123.24	198	1862 -6	137	2013
T-90	48.84	-123.10	200	1862 -1	134	2977
V-47	49.37	-123.75	192	1913 -4	225	1947
V-58	49.17	-123.71	210	1915 -3	270	3894
V-53	49.21	-123.75	164	1915 -1	225	13 156
V-57	49.18	-123.78	200	1915 -2	291	6099
V-64	49.12	-123.63	210	1915 -6	318	1719
V-68	49.12	-123.57	265	1916 -2	225	1663
V-66	49.14	-123.56	265	1916 -1	240	2073
T-169	49.01	-123.47	228	1874 -5	197	1024
V-73	48.91	-123.32	150	1916 -4	240	1303
EF8	49.09	-125.18	58	1563 -5	228	49 710
EF9	49.09	-125.18	59	1563 -6	305	91 837
EF10	49.09	-125.18	62	1564 -1	133	42 347
EF11	49.09	-125.18	64	1564 -2	250	64 208
EF12	49.08	-125.17	66	1564 -3	176	44 943
EF13	49.07	-125.16	105	1564 -4	293	73 536
EF14	49.07	-125.15	121	1564 -5	233	58 409
EF15	49.06	-125.15	51	1564 -6	308	105 151
EF16	49.06	-125.15	55	1567 -1	328	17 277
EF24	49.05	-125.16	123	1567 -3	305	37 301
EF26	49.05	-125.15	108	1567 -4	317	137 054
EF18	49.05	-125.16	22	1567 -2	144	10 679
EF28	49.02	-125.16	135	1567 -6	325	84 878
EF27	49.02	-125.16	115	1567 -5	337	125 351

Table 2

Analysis	DS1 (60 samples, 25 taxa)			DS2 (40 samples, 25 taxa)			
	Axis 1	Axis 2	Total inertia	Axis 1	Axis 2	Total inertia	
DCA	Eigenvalues	0.42	0.50	1.031	0.21	0.14	0.736
	Lengths of gradient	1.99	1.83		1.43	1.70	
	Cum. percentage variance of species data	41.4	55.8		28.6	48.1	
Multivariate analysis adopted		RDA with 21 environmental variables			RDA with 34 environmental variables		
RDA	Eigenvalues	0.31	0.065	1.000	0.24	0.15	1.000
	Species-environment correlations	0.97	0.875		0.92	0.86	
	Cumulative percentage variance of species data	31.2	37.6		23.8	39.2	
	of species-environment relation	51.1	61.6		47.8	78.7	

Table 3

Marginal Effects		Conditional Effects		
Variable	λ	Variable	λ	<i>P</i> -value
Summer productivity	0.28	Summer productivity	0.28	0.005
Annual productivity	0.28	Winter SST	0.05	0.005
Summer chlorophyll-a	0.27	Autumn SSS	0.05	0.005
Winter SST	0.26	Summer SST	0.03	0.005
Spring silica	0.25	Water depth	0.03	0.005
Spring SSS	0.24	Annual productivity	0.02	0.005
Summer SSS	0.24	Summer Silica	0.02	0.025
Autumn SSS	0.23	Spring Silica	0.02	0.040
Winter SSS	0.22	Autumn productivity	0.01	0.050
Spring productivity	0.22	Summer chlorophyll-a	0.02	0.180
SST seasonality	0.20	Winter productivity	0.01	0.110
Winter productivity	0.19	Autumn SST	0.01	0.410
Autumn SST	0.19	Spring SSS	0.01	0.275
SSS seasonality	0.17	Spring SST	0.01	0.555
Autumn productivity	0.16	Spring phosphate	0.01	0.185
Water depth	0.15	Spring productivity	0.01	0.560
Summer SST	0.13	Summer SSS	0.01	0.780
Spring SST	0.08	Spring nitrate	0.01	0.835
Summer silica	0.07	Winter SSS	0.00	0.950
Spring phosphate	0.06			
Spring nitrate	0.02			

Table 4

Marginal Effects		Conditional Effects (GS, n=40)		
Variable	λ	Variable	λ	P- value
Distance to the shore	0.15	Distance to the shore	0.15	0.005
Spring productivity	0.14	Dist. Van. Harbor	0.14	0.005
Summer productivity	0.14	Summer silica	0.06	0.005
Annual productivity	0.13	Water depth	0.04	0.005
Winter productivity	0.13	Spring productivity	0.04	0.025
Dist. Van. Harbor	0.13	Spring SSS	0.04	0.005
Autumn SSS	0.13	Spring phosphate	0.03	0.045
Winter SSS	0.12	Spring SST	0.02	0.165
Spring SSS	0.11	Spring nitrate	0.02	0.28
Summer SSS	0.11	Summer nitrate	0.01	0.445
Water depth	0.10	Autumn SST	0.02	0.125
Autumn productivity	0.10	Spring silica	0.02	0.35
SSS seasonality	0.10	Winter phosphate	0.02	0.35
Spring phosphate	0.09	SST seasonality	0.01	0.455
Winter chlorophyll-a	0.09	Autumn SSS	0.02	0.335
Winter SST	0.08	Winter SST	0.02	0.205
Autumn silica	0.07	Spring chlorophyll-a	0.02	0.215
Spring silica	0.07	Summer SSS	0.01	0.325
SST seasonality	0.07	Summer productivity	0.02	0.275
Summer phosphate	0.07	Summer phosphate	0.02	0.16
Summer SST	0.06	Winter chlorophyll-a	0.02	0.365
autumn phosphate	0.06	Annual productivity	0.01	0.39
Spring SST	0.06	Winte productivity	0.02	0.27
Winter silica	0.05	Autumn silica	0.02	0.275
Autumn nitrate	0.05	Winter SSS	0.01	0.795
Winter nitrate	0.05	Winter silica	0.02	0.23
Spring nitrate	0.05	Winter nitrate	0.01	0.68
Spring chlorophyll-a	0.05	Autumn chlorophyll-a	0.01	0.615
Winter phosphate	0.05	Autumn phosphate	0.01	0.605
Summer chlorophyll-a	0.04	Autumn productivity	0.01	0.62
Automn SST	0.04	Summer chlorophyll-a	0.01	0.84
Summer nitrate	0.03			
Summer silica	0.03			
Autumn chlorophyll-a	0.02			

Table 5

	DS1 (n = 60)				Large data set (n = 123)			
	MAT		MRT		MAT		MRT	
	r^2	RMSEP	r^2	RMSEP	r^2	RMSEP	r^2	RMSEP
Winter SST	0.96	0.12°C	0.91	0.22°C	0.85	0.60 °C	0.88	0.65°C
Summer SST	0.87	0.42°C	0.81	0.67°C	0.72	0.72°C	0.73	0.85°C
Winter SSS	0.95	0.45	0.93	0.75	0.93	0.874	0.92	1.09
Summer SSS	0.88	1.33	0.91	1.52	0.89	1.977	0.94	1.80
Annual primary productivity	0.95	9.91 gC m ⁻²	0.95	12.36 gC m ⁻²	0.90	27.97 gC m ⁻²	0.83	44.47 gC m ⁻²

Table 6

Station number	Longitude	Latitude	Winter SST (°C)	Winter SSS	Summer SST (°C)	Summer SSS	Annual productivity (gC m ⁻² yr ⁻¹)	Spring nitrate (μM)	Spring phosphate (μM)	Summer phosphate (μM)	Spring silica (μM)	Summer silica (μM)	Summer chlorophyll (μg l ⁻¹)
SB-10	-127.35	51.20	7.43	30.63	11.40	27.66	296.86	1.00	1.00	1.00	12.00	33.00	3.98
SB-07	-127.04	51.17	7.28	30.42	11.34	26.06	331.94	4.00	1.00	1.00	12.00	33.00	4.47
SB-06	-126.95	51.17	7.22	30.28	11.17	25.10	331.94	3.00	1.02	1.02	12.10	33.00	4.47
SB-01	-126.72	51.04	7.07	30.28	12.16	21.40	328.12	3.00	1.27	1.27	12.10	33.00	6.87
SB-03	-126.71	51.02	7.10	30.30	12.12	21.48	328.12	3.00	1.27	1.27	12.10	33.00	6.87
SB-04	-126.71	51.01	7.11	30.39	11.92	21.16	328.12	3.00	1.28	1.28	12.10	33.00	6.08
T-135	-123.16	49.29	6.80	24.25	15.22	16.41	296.73	10.76	1.03	0.58	28.61	26.28	2.50
V-30	-123.19	49.30	6.80	24.27	15.28	16.71	296.73	10.81	1.02	0.58	28.40	26.08	2.50
V-25	-123.22	49.31	6.83	24.50	15.31	17.42	296.73	10.89	1.03	0.58	28.86	25.94	2.50
T-138	-123.23	49.31	6.84	24.55	15.32	17.50	296.73	10.89	1.03	0.58	28.86	25.94	2.50
T-140	-123.29	49.32	6.83	24.62	15.37	17.77	290.34	11.15	1.10	0.59	29.08	25.47	2.50
V-38	-123.29	49.33	6.83	24.61	15.38	17.73	290.34	11.15	1.10	0.59	29.08	25.47	2.52
T-143	-123.35	49.32	6.84	24.74	15.41	18.12	290.34	11.75	1.19	0.60	29.29	25.14	2.53
T-148	-123.47	49.33	6.84	24.84	15.44	18.40	287.89	10.69	1.02	0.62	23.03	24.12	2.83
T-159	-123.31	49.29	6.85	24.74	15.32	17.81	290.34	11.44	1.18	0.57	30.48	25.56	2.50
T-5	-123.30	49.23	6.86	24.84	15.23	18.09	259.84	10.93	1.13	0.54	30.95	26.31	2.43
T-10	-123.29	49.26	6.85	24.76	15.27	17.85	259.84	11.10	1.12	0.56	30.22	25.93	2.45
T-129	-123.47	49.28	6.85	24.94	15.38	18.40	287.89	12.31	1.22	0.60	26.24	24.39	2.82
T-161	-123.38	49.29	6.85	24.89	15.38	18.28	290.34	14.09	1.49	0.58	33.21	25.12	2.53
T-1	-123.31	49.19	6.87	24.93	15.07	18.85	259.84	10.43	0.89	0.51	30.52	27.01	2.41
T-38	-123.37	49.24	6.86	24.96	15.32	18.45	259.84	11.50	1.47	0.55	33.84	25.10	2.48
T-50	-123.44	49.25	6.86	24.98	15.33	18.47	264.80	12.13	1.21	0.58	27.64	24.85	2.46
T-126	-123.47	49.24	6.85	24.98	15.32	18.55	264.80	12.06	1.16	0.56	24.54	24.53	2.78
T-51	-123.44	49.23	6.86	25.03	15.29	18.61	264.80	12.13	1.12	0.56	26.26	24.85	2.44
T-52	-123.45	49.22	6.86	25.05	15.20	18.96	264.80	10.61	0.88	0.55	18.31	24.52	2.44
T-36	-123.37	49.21	6.86	25.04	15.18	18.98	259.84	8.74	1.29	0.53	32.77	25.18	2.45
T-34	-123.43	49.20	6.87	25.08	15.17	19.04	264.80	9.33	0.84	0.52	24.27	24.98	2.40
T-22	-123.37	49.18	6.87	25.09	15.13	19.29	259.84	9.65	0.66	0.49	30.38	27.06	2.45
T-20	-123.38	49.14	6.90	25.44	15.12	19.99	259.84	9.20	0.74	0.43	30.48	30.94	2.45
T-29	-123.44	49.12	6.91	25.48	15.11	20.29	261.96	5.60	0.60	0.46	27.98	26.77	2.40
T-117	-123.50	49.15	6.88	25.32	15.14	19.94	261.96	4.91	0.60	0.48	17.11	21.46	2.74
T-84	-123.34	49.09	6.91	25.45	15.07	20.26	258.42	10.09	0.79	0.36	36.85	36.00	2.47
T-168	-123.34	49.00	6.98	25.63	14.75	21.58	258.42	14.32	1.89	0.45	31.34	30.15	1.91
T-86	-123.05	48.89	7.05	26.17	14.10	21.84	281.18	13.08	1.20	0.52	28.50	29.44	2.82
T-97	-123.06	48.93	7.00	25.58	14.20	21.41	287.33	13.04	1.23	0.52	28.17	29.20	2.54
T-172	-123.24	48.88	7.06	26.48	14.39	22.37	262.00	14.62	0.96	0.41	23.76	29.63	2.35
T-90	-123.10	48.84	7.05	26.58	14.00	22.44	262.00	13.04	1.11	0.52	27.97	29.29	2.35

Table 6 - continued

Station number	Longitude	Latitude	Winter SST (°C)	Winter SSS	Summer SST (°C)	Summer SSS	Annual Productivity (gC m ⁻² yr ⁻¹)	Spring nitrate (μM)	Spring phosphate (μM)	Summer phosphate (μM)	Spring silica (μM)	Summer silica (μM)	Summer chlorophyll (μg l ⁻¹)
V-47	-123.75	49.37	6.73	25.98	15.72	18.56	286.68	8.10	0.83	0.81	19.61	25.06	2.63
V-58	-123.71	49.17	6.81	26.37	15.34	19.70	264.41	8.41	1.01	0.65	20.33	23.94	2.58
V-53	-123.75	49.21	6.78	26.21	15.46	19.21	264.41	9.32	0.93	0.54	20.55	25.19	2.66
V-57	-123.78	49.18	6.75	26.15	15.41	19.48	262.00	8.90	0.94	0.69	20.70	24.01	2.64
V-64	-123.63	49.12	6.88	25.43	15.17	20.26	261.74	6.91	0.59	0.61	22.05	24.63	2.69
V-68	-123.57	49.12	6.89	25.33	15.15	20.25	261.96	5.57	0.47	0.46	23.81	25.53	2.72
V-66	-123.56	49.14	6.88	25.30	15.16	19.99	261.96	5.57	0.41	0.53	25.14	25.69	2.74
T-169	-123.47	49.01	6.96	25.61	14.80	21.63	260.21	11.47	1.14	0.42	30.42	30.34	2.08
V-73	-123.32	48.91	7.02	26.17	14.58	21.99	258.11	13.60	0.89	0.46	22.85	29.20	2.37
EF8	-125.18	49.09	8.17	29.04	13.98	27.36	361.46	1.10	0.58	1.07	12.47	25.92	8.28
EF9	-125.18	49.09	8.17	29.04	13.98	27.36	361.46	1.10	0.58	1.07	12.47	25.92	8.28
EF10	-125.18	49.09	8.17	29.07	13.98	27.36	361.46	1.10	0.58	1.07	12.47	25.92	8.28
EF11	-125.18	49.09	8.15	29.01	13.98	27.36	361.46	1.10	0.58	1.07	12.47	25.92	8.28
EF12	-125.18	49.09	8.15	29.01	13.98	27.36	361.46	1.10	0.58	1.07	12.47	25.92	8.28
EF13	-125.16	49.07	8.17	29.16	13.87	27.60	361.46	1.10	0.63	0.89	12.49	25.92	8.68
EF14	-125.16	49.07	8.17	29.18	13.85	27.63	361.46	1.10	0.64	0.92	12.49	26.22	8.68
EF15	-125.15	49.06	8.17	29.21	13.78	27.76	361.46	1.10	0.67	0.92	13.42	26.22	8.69
EF16	-125.15	49.06	8.17	29.21	13.78	27.76	361.46	1.10	0.67	0.92	13.42	26.22	8.70
EF24	-125.16	49.05	8.23	29.42	13.63	27.99	361.46	11.45	0.73	0.89	14.14	25.92	8.52
EF26	-125.15	49.05	8.22	29.35	13.63	27.96	361.46	11.45	0.73	0.92	14.14	26.22	8.52
EF18	-125.16	49.05	8.22	29.41	13.63	27.98	361.46	11.45	0.73	0.92	14.14	26.22	8.52
EF28	-125.16	49.02	8.27	29.55	12.75	28.40	361.46	11.45	0.77	0.93	14.91	24.77	8.24
EF27	-125.16	49.02	8.27	29.55	12.75	28.37	361.46	11.45	0.77	0.94	14.91	25.00	8.45
OSU1	-129.23	43.58	10.68	32.61	17.11	32.00	96.04	1.01	0.54	0.52	3.43	2.17	1.01
OSU2	-127.98	44.12	9.86	32.59	16.41	32.06	101.17	0.85	0.78	0.40	1.50	2.20	1.92
OSU3	-128.75	43.55	10.48	32.62	16.79	31.75	99.32	1.07	0.54	0.41	3.49	3.33	1.32
OSU4	-124.55	40.81	10.72	32.46	12.59	33.21	311.63	8.86	1.20	0.72	13.87	11.80	5.86
OSU5	-126.18	40.10	11.26	32.65	15.70	32.64	162.57	3.36	0.56	0.51	6.79	2.00	3.21
OSU6	-129.62	42.29	10.34	32.67	17.23	32.61	93.29	0.05	0.45	0.50	2.00	2.32	1.46
OSU7	-130.41	42.98	10.81	32.66	17.25	32.58	91.81	0.02	0.50	0.49	2.00	1.94	1.17
OSU8	-131.12	42.66	10.86	32.80	17.66	32.74	90.92	0.95	0.49	0.54	2.96	1.50	1.26
OSU9	-131.57	43.53	10.58	32.78	17.01	32.71	96.31	1.20	0.52	0.46	3.47	1.00	1.15
OSU10	-131.67	44.88	9.94	32.73	16.70	32.59	82.74	0.00	0.42	0.47	1.50	4.00	1.05
OSU11	-130.93	45.12	10.06	32.62	16.55	32.59	86.47	1.53	0.67	0.47	6.50	4.00	1.02
OSU12	-124.14	48.36	7.64	28.79	12.41	30.43	235.58	10.61	1.39	1.91	25.64	34.19	3.39
OSU17	-134.27	46.63	9.05	32.52	15.24	32.57	89.77	7.00	0.63	0.66	11.00	7.05	0.02
OSU18	-131.16	47.03	8.53	32.63	15.99	32.47	92.36	0.20	0.92	0.74	10.88	4.67	0.26
OSU19	-127.54	46.72	8.72	32.50	16.29	32.14	110.18	1.13	0.66	0.40	4.89	4.46	0.13
OSU20	-127.77	49.01	8.30	32.30	14.59	32.06	215.66	0.55	0.66	0.45	11.19	10.55	2.07
OSU21	-128.14	49.40	8.47	32.29	14.04	32.08	228.88	0.35	0.47	0.43	14.38	12.11	2.83

Table 6 - continued

Station number	Longitude	Latitude	Winter SST (°C)	Winter SSS	Summer SST (°C)	Summer SSS	Annual Productivity (gC m ⁻² yr ⁻¹)	Spring nitrate (μM)	Spring phosphate (μM)	Summer phosphate (μM)	Spring silica (μM)	Summer silica (μM)	Summer chlorophyll (μg l ⁻¹)
OSU22	-129.24	49.21	7.99	32.39	15.21	32.10	144.82	2.47	0.71	0.41	5.96	2.50	0.27
OSU23	-130.03	48.23	7.58	32.51	15.33	32.18	104.52	2.96	0.80	0.67	7.74	5.00	1.51
OSU24	-129.87	48.44	7.70	32.45	15.31	32.20	107.61	3.12	0.81	0.63	7.83	5.82	1.48
OSU25	-127.15	48.39	8.49	32.27	14.71	32.01	185.79	0.55	0.59	0.44	6.59	3.86	1.73
OSU26	-128.06	48.06	8.18	32.38	15.35	32.05	141.26	1.60	0.70	0.52	5.00	5.33	2.16
OSU27	-129.51	47.59	8.17	32.55	15.10	32.31	100.10	4.38	0.89	0.66	6.50	3.50	1.30
OSU28	-127.12	47.80	8.58	32.39	15.23	32.02	150.48	1.53	0.63	0.41	7.00	5.50	1.67
OSU33	-126.27	47.95	8.65	32.29	14.76	31.95	201.22	0.77	0.67	0.50	9.41	10.90	3.00
OSU34	-124.91	47.38	9.40	30.87	14.87	31.66	287.81	0.81	0.55	0.55	13.67	7.77	1.58
OSU35	-126.06	48.30	8.55	31.78	13.84	31.86	276.37	0.75	0.62	0.61	8.73	13.60	3.78
OSU36	-126.02	48.10	8.56	32.06	14.09	31.92	230.17	0.57	0.67	0.57	9.95	13.47	3.88
OSU37	-125.77	48.18	8.57	31.82	13.67	31.89	266.57	0.50	0.69	0.79	9.84	16.21	4.26
OSU38	-125.69	48.21	8.43	31.77	13.11	31.88	274.87	2.80	0.73	0.87	11.07	17.93	4.10
OSU39	-125.36	47.94	8.76	31.92	13.81	31.96	274.87	1.73	0.66	0.89	10.07	18.29	3.79
OSU40	-125.76	47.60	9.18	32.31	15.25	31.93	191.69	0.62	0.69	0.55	8.64	8.11	1.56
OSU41	-129.66	44.28	10.31	32.55	16.59	32.58	95.64	1.18	0.52	0.47	3.55	1.79	0.08
OSU42	-127.81	40.99	10.95	32.72	16.55	32.48	115.26	3.50	0.45	0.44	6.00	2.00	2.38
OSU43	-125.12	46.30	9.74	31.09	15.70	31.17	200.33	0.63	0.48	0.42	14.20	11.53	3.04
OSU44	-125.61	46.30	9.80	32.28	16.25	31.84	145.96	0.51	0.53	0.40	7.27	3.96	2.79
OSU45	-124.90	44.50	9.59	32.28	14.26	31.71	226.96	1.43	0.50	0.44	8.45	8.58	3.95
OSU46	-125.32	43.67	9.94	32.55	14.76	31.98	196.48	0.18	0.48	0.57	5.00	6.00	2.95
OSU47	-125.40	43.17	10.00	32.56	14.57	32.15	212.96	0.24	0.56	0.53	4.10	6.20	2.07
OSU48	-125.09	43.17	10.08	32.41	13.94	32.42	241.66	0.26	0.56	0.62	3.75	10.29	2.11
OSU49	-130.16	44.73	10.16	32.58	16.44	32.57	96.75	1.33	0.43	0.49	3.00	1.00	0.50
OSU50	-126.58	43.03	10.07	32.58	16.08	31.89	145.14	0.75	0.47	0.45	2.00	3.50	2.36
OSU51	-126.00	41.83	10.66	32.64	15.07	32.38	169.27	3.18	0.59	0.40	5.98	4.50	1.95
OSU52	-128.01	42.21	10.93	32.71	16.67	32.18	104.57	1.75	0.46	0.43	4.49	3.00	2.05
OSU53	-129.01	41.80	10.33	32.65	16.88	32.62	93.09	0.05	0.51	0.46	2.50	2.00	1.80
OSU54	-131.22	41.48	11.75	32.82	17.55	32.86	88.84	1.69	0.39	0.40	3.41	1.57	1.42
OSU55	-134.66	41.08	12.62	32.81	18.10	33.06	79.28	0.13	0.37	0.48	4.63	2.61	0.06
OSU56	-126.60	42.09	10.72	32.66	15.85	32.18	149.89	2.33	0.56	0.37	4.58	4.00	2.26
OSU57	-126.26	42.75	10.22	32.60	15.35	32.35	163.94	1.00	0.48	0.58	1.00	2.50	2.20
OSU58	-125.58	45.22	9.73	32.20	16.38	31.66	149.55	0.23	0.52	0.33	7.88	5.41	0.32
OSU59	-125.28	44.67	9.66	32.45	15.48	31.40	174.18	0.64	0.44	0.37	7.38	6.69	3.92
OSU60	-130.62	41.58	11.53	32.80	17.13	32.85	89.69	2.00	0.46	0.44	3.36	1.00	1.51
OSU61	-125.21	42.20	10.64	32.57	13.44	32.88	254.88	8.00	0.64	0.64	12.00	5.45	0.40
OSU62	-127.57	42.15	11.01	32.68	16.46	32.21	114.51	1.47	0.55	0.37	4.83	3.00	2.23
OSU63	-132.04	41.52	11.35	32.90	17.61	32.92	87.27	1.51	0.26	0.45	3.00	2.01	1.25
OSU64	-129.13	46.65	9.12	32.55	15.72	32.32	100.32	2.55	0.72	0.63	6.00	4.27	0.18
OSU65	-127.02	41.27	11.07	32.70	15.70	32.55	134.16	3.50	0.45	0.39	6.00	2.50	2.50
OSU70	-125.52	40.42	11.11	32.69	14.16	32.83	212.39	4.49	0.50	0.82	8.25	2.00	3.87
OSU72	-125.50	48.77	8.32	30.71	12.97	30.14	373.63	4.27	0.70	0.81	14.67	22.49	5.91
OSU73	-126.89	48.91	8.59	31.91	14.16	31.92	255.83	1.52	0.68	0.57	9.73	12.74	2.73
OSU74	-126.88	48.98	8.58	31.88	14.11	31.91	273.06	1.52	0.68	0.57	9.73	12.74	2.73
OSU75	-127.31	49.22	8.49	31.97	14.08	31.96	263.85	1.22	0.67	0.54	10.56	12.11	2.54

CHAPITRE III

DINOCYSTS AS A PROXY OF PRIMARY PRODUCTIVITY IN MID-HIGH LATITUDES OF THE NORTHERN HEMISPHERE

Taoufik Radi¹, Anne de Vernal¹

¹Centre de recherche en géochimie et géodynamique (GEOTOP-UQAM & McGill)
Université du Québec à Montréal, Case postale 8888, Succursale Centre Ville
Montréal, Qc, Canada, H3C 3P8

Manuscrit accepté pour publication dans la revue *Marine Micropaleontology*

Résumé

Une base de données de référence de sédiments modernes a été utilisée pour explorer l'utilisation potentielle des assemblages de dinokystes préservés dans les sédiments comme traceurs de productivité primaire. La base de données inclut 1171 sites provenant de l'Atlantique Nord (n = 483), de l'océan Arctique (n = 401) et du Pacifique Nord (n = 287). Nous avons compilé deux jeux de données de productivité primaire moderne, issues d'observations satellitaires de la chlorophylle: (1) les données du programme Coastal Zone Color Scanner (CZCS) qui représentent une moyenne des mesures effectuées entre 1978 et 1989 et (2) les données du programme MODerate resolution Imaging Spectroradiometer (MODIS) qui représentent des données correspondant à la période entre 2002 et 2005. Nous avons utilisé des Analyses Canoniques de Correspondances (ACC) avec 62 taxons de dinokystes et huit paramètres environnementaux (la salinité d'hiver et d'été, la température d'hiver et d'été, le couvert de glace de mer, la productivité primaire estivale, hivernale et annuelle). Les résultats de l'ACC montrent que la productivité primaire est un paramètre déterminant des assemblages de dinokystes à l'échelle de l'Atlantique Nord, du Pacifique Nord et à l'échelle hémisphérique. Dans le Pacifique, la relation entre la productivité et la distribution des dinokystes est particulièrement élevée. Des tests de validation, basés sur la méthode des analogues modernes, ont été effectués afin d'évaluer le potentiel des dinokystes comme traceurs quantitatifs de paléoprodutivité. Les résultats montrent qu'à l'exception de l'océan Arctique, qui est caractérisé généralement par de faibles productivités, la productivité peut être reconstituée avec une erreur de $\pm 11-25\%$, selon la base de données de productivité utilisée. La meilleure performance est obtenue pour la reconstitution de la productivité hivernale en utilisant les données de MODIS. Dans tous les cas, les erreurs de prédiction issues des tests de validation sont inférieures à la différence entre les données de productivité de MODIS et de CZCS. La reconstitution à partir d'une carotte sédimentaire prélevée dans le Nord-Ouest de l'Atlantique Nord (HU 91-045-094) montre une grande variabilité de la productivité durant les derniers 25 000 ans. Les reconstitutions suggèrent de faibles productivités durant l'intervalle glaciaire, notamment durant les événements d'Heinrich et le Dryas Récent ($100 \text{ gC m}^{-2} \text{ an}^{-1}$) et une productivité élevée au début de l'Holocène ($350 \text{ gC m}^{-2} \text{ an}^{-1}$).

Mots clés : kystes de dinoflagellés, paléoprodutivité, reconstitution quantitative, hémisphère nord.

Abstract

In order to explore the potential of dinocyst assemblages in marine sediment as a proxy for primary productivity, we analyzed a reference “modern” database including 1171 sites from the North Atlantic Ocean ($n = 483$), the Arctic Ocean ($n = 401$) and the North Pacific Ocean ($n = 287$). We compiled two sets of primary productivity data derived from satellite observations: (1) The dataset from the Coastal Zone Color Scanner (CZCS) program applied to observations from 1978 to 1989 and (2) the data set from the MODerate resolution Imaging Spectroradiometer (MODIS) program using observations from 2002 to 2005. We performed canonical correspondence analysis (CCA) on a data matrix that included 62 dinocyst taxa and eight sea-surface parameters (winter and summer salinity, winter and summer temperature, sea-ice cover, summer, winter and annual primary productivity). CCA results show that primary productivity is a determinant parameter of dinocyst assemblages (including both phototrophic and heterotrophic taxa) in the North Atlantic, North Pacific, and at hemispheric scale. In the North Pacific, the relationship between productivity and dinocyst assemblages is particularly strong. We tested the modern analogue technique to reconstruct productivity using the North Atlantic, North Pacific, Arctic and hemispheric dinocyst datasets. With the exception of the Arctic Ocean alone, which is characterized by overall low productivity, productivity can be estimated with an accuracy (Root Mean Square Error = RMSE) of ± 11 -25%. The best performance is obtained for reconstruction of winter productivity from the MODIS data. It is noteworthy that the RMSE for all estimated productivity parameters is narrower than the mean differences between productivity data derived from the MODIS and CZCS datasets. Therefore, we conclude that dinocysts can be used to reconstruct productivity with an accuracy equivalent to that of primary productivity estimated from satellite observations. Application of the approach in a sedimentary core from the northwest North Atlantic (core HU 91-045-094) revealed large amplitude variations of productivity over the last 25 000 years. The use of both MODIS and CZCS datasets indicate generally low productivity during the glacial stage, especially during the Younger Dryas and Heinrich events, with annual productivity of less than 100 gC m^{-2} . The reconstructions also suggest higher productivity during the early Holocene, especially based on the MODIS data that suggest annual values of up to 350 gC m^{-2} .

Keywords: dinoflagellate cysts, paleoproductivity, quantitative reconstruction, Northern Hemisphere.

3.1 Introduction

The rising atmospheric concentration of the greenhouse gas CO₂ is a source of concern, and exchange of the gas between ocean and atmosphere remains poorly quantified. It is generally thought that the biological pump and oceanic primary productivity play a determinant role on global carbon budget, at time scales ranging from millennia to millions of years (e.g., Knox and McElroy, 1984; Sarmiento and Toggweiler, 1984; Barnola et al., 1987; Sarnthein et al., 1988; Berger et al., 1989; Ikeda and Takija, 2002). In the modern ocean, photosynthetic carbon fixation by marine phytoplankton is about 45-63 Gt C yr⁻¹, and accounts for roughly half the global biospheric productivity (Field et al., 1998; Behrenfeld et al., 2001). About 30% of this carbon is exported below the euphotic zone and ~0.4% is buried in sediment. At the scales of the last millennia to the last several millions of years, organic carbon accumulation rates and tracers of production such as barium suggest large variation in the amplitude of biological productivity (e.g., Lyle et al., 1988; Pedersen et al., 1988, 1991; Mix, 1989; Sarnthein et al., 1992; Paytan and Kastner, 1996). However, whereas the measurement of buried carbon is relatively easy, the evaluation of past productivity is still a challenge.

In order to evaluate past productivity quantitatively, several approaches have been used (Muller et al., 1983; Sarnthein, 1988, Berger et al., 1989; Meyers, 1997; Wefer et al., 1999; Fischer et al., 2000). Organic carbon content in sediment has commonly been used as index of paleoproductivity, based on empirical relationships between fluxes or percentages of total organic carbon in sediment and net primary productivity (Muller and Suess, 1979; Muller et al., 1983; Sarnthein et al., 1988; Berger et al., 1989), leading to regional transfer functions (Muller et al., 1983; Sarnthein et al., 1988, 1992; Fischer et al., 2000). However, the use of organic carbon for estimating paleoproductivity is limited both by oxidation through the water column, and degradation in the sediment (Meyers, 1997; Rühlemann, 1999). Even in anoxic

sediment, the concentration of organic carbon declines exponentially with depth in the sediment suggesting that degradation can occur despite favourable conditions of preservation (e.g., Emerson and Hedges, 1988, 2003).

Other proxies of paleoproductivity are based on remains of planktic or benthic organisms such as foraminiferal tests, diatom frustules or coccoliths (see Berger et al., 1989; Wefer et al., 1999 and Fischer and Wefer, 1999 for an overview). The use of microfossils as paleoproductivity proxies is based on the isotopic or chemical composition of their calcareous tests ($\delta^{13}\text{C}$, Cd/Ca), opal abundance (e.g., Mackensen et al., 2000; Lazarus et al., 2006), or on the relative abundances of species (e.g., Loubere, 1991, 1994, 1999, 2002; Abrantes et al., 1994; Naidu and Malmgren, 1996; Beaufort et al., 1997, 1999, 2001; Loubere and Fariduddin, 1999; Almogi-Labin et al., 2000; Vénec-Peyré and Caulet, 2000). However, microfossil remains composed of CaCO_3 are subjected to dissolution in deep water under high pCO_2 conditions due to poor ventilation. Biogenic remains composed of opal are also subject to dissolution because of undersaturation of marine water with respect to dissolved silicon (Nelson et al., 1995; Gallinari et al., 2002). Accumulation rates of opal have been used to infer productivity but biases due to abiotic sources of silica (terrigenous, volcanic) and dissolution often result in equivocal data (e.g., Ragueneau et al., 2000). The $\Delta\delta^{13}\text{C}$ (deep versus surface water) as inferred from planktonic and benthic foraminifera that has been used as a productivity index (Shackleton et al., 1983) is also equivocal because it may respond to vertical mixing of water masses in addition to productivity and because dissolution seems to remove ^{13}C preferentially from benthic foraminifer tests (McCorkle et al., 1995). Moreover, benthic foraminifera show marked interspecific differences and vital effects. To overcome the problem linked to dissolution, some abiotic proxies were used, including the total sedimentary barium (Dymond et al., 1992; François et al., 1995; Dymond and Collier, 1996; Jeandel et al., 2000; Eagle et al., 2003) or the isotopic composition of thorium and protactinium (e.g., Bradtmiller et al., 2006), but these geochemical proxies have other limitations

dues to their physical and chemical behaviours, notably in upwelling areas or near hydrothermal vents (Von Breymann et al., 1992; Dymond et al., 1992; François et al., 1995, 2004; Paytan et al., 1996; Klump et al., 2000). Finally, on the basis of ocean productivity estimates from space (Antoine et al., 1996; Behrenfeld and Falkowski, 1997), it has been possible to calibrate a few regional datasets to develop transfer functions for reconstructing paleoproductivity using assemblages of foraminifera (Loubere, 1996, 1999, 2002; Loubere and Fariduddin, 1999; Cayre et al., 1999; Ivanova et al., 2003) or coccoliths (Beaufort et al., 1997, 1999, 2001).

Here, we are exploring a micropaleontological approach for quantifying past productivity on the basis of dinoflagellate cyst assemblages. Many dinoflagellate species (about 20%) produce fossilisable organic-walled cysts (=dinocysts) during their biological cycle in relation with sexual reproduction (e.g., Wall and Dale, 1968; Dale, 1983; Taylor, 1987). The wall cysts are mostly composed of a condensed macromolecular structure that is predominantly aromatic and aliphatic in composition (e.g., Kokinos et al., 1998). Due to this chemical composition, the cysts are extremely resistant to dissolution in the sediment unlike siliceous or carbonate remains. The development of the modern dinocyst database has permitted illustration of close relationships between dinocyst distribution and sea-surface parameters such as temperature, salinity or sea-ice cover (e.g., de Vernal et al., 1997, 2001, 2005; Rochon et al., 1999). Relationships between cyst fluxes or assemblages and primary productivity or upwelling intensity have been also documented from North Atlantic data sets (Dale and Fjelsä, 1994; Marret, 1994; Devillers and de Vernal, 2000), North Pacific (Radi and de Vernal, 2004; Radi et al., 2007; Pospelova et al., in press) and the northern Indian Ocean (Zonneveld, 1997a).

In this paper we use an updated hemispheric data set “n = 1171” of modern samples from the North Atlantic, Arctic and North Pacific oceans (Fig. 1; de Vernal et al.,

1997, 2001, 2005), in order to explore empirically the relationship of dinocyst assemblages and primary productivity.

3.2 Methodology

3.2.1 Dinocyst data bases

The dinocyst data used in this work result from palynological analysis performed in 1171 surface sediment samples after standardization of procedures for palynological preparations (de Vernal et al., 2005), which exclude the use of oxidation techniques to avoid selective degradation of more sensitive cyst taxa such as those produced by protoperidinales (cf. Marret, 1993). Samples are from the North Atlantic Ocean and adjacent seas ($n = 483$), the Arctic Ocean and sub-arctic seas ($n = 401$) and the North Pacific Ocean including estuarine environments of British Columbia and California ($n = 287$), as illustrated in figure 1. This dataset constitutes an update of the “ $n = 940$ ” dataset (cf. de Vernal et al., 2005). It includes additional samples from the North Atlantic, the St. Lawrence Estuary, Hudson Bay (Ladouceur, 2007), Beaufort Sea (Richerol and Rochon, submitted) and the northeastern Pacific Ocean (Kielt, 2007; Radi et al., 2007; Pospelova et al., in press). Surface samples were collected in the uppermost 1 or 2 cm of box or gravity cores. They represent a few tens to thousand of years depending upon sedimentation rates and mixing due to bioturbation. Dinocyst data are archived at GEOTOP (<http://www.geotop.uqam.ca>).

The taxonomy of dinocysts used here conforms to that presented in Zonneveld (1997b), Zonneveld and Jurkschat (1999), Rochon et al. (1999), de Vernal et al. (2001), Head et al., (2001, 2006), Radi et al., (2001, 2007), Head (2002) Pospelova and Head (2002) and Radi and de Vernal (2004). A total of 74 dinocyst taxa were identified, of which 38 are related to a phototrophic productivity and 36 to an

heterotrophic productivity (cf. Table 1). The phototrophic dinoflagellates contribute with other primary producers (mostly diatoms and coccolithophorids) to the marine primary productivity (e.g., Parsons et al., 1984) whereas heterotrophic ones are reported to be dependant of diatoms by feeding on them (Jacobson and Anderson, 1986; Gaines and Elbrächter, 1986). The list of all taxa and corresponding abbreviations is presented in table 1. After grouping, 62 taxa were used for statistical analysis and cross-validations tests. Among the taxa, 41 occur in both North Atlantic Ocean and North Pacific Ocean (see Table 1). A few appear exclusive of the North Pacific (cf. *Echinidinium delicatum*, *Echinidinium aculeatum* and *Bitectatodinium spongium*) in the “n=1171” database. However, they are reported to occur in some upwelling zones such as the Arabian Sea and southwestern African margin (Zonneveld, 1997a, 1997b; Zonneveld and Jurkschat, 1999; Zonneveld and Brummer, 2000; Marret and Zonneveld, 2003). *Polykrikos* cf. *kofoidii* seems to be endemic in the North Pacific Ocean since no occurrences are known elsewhere. *Trinovantedinium variabile* characterizes northeastern Pacific margins and is not recorded in the modern North Atlantic and Arctic Oceans, but it was reported to occur in the Miocene and Pliocene sediments of southern North Sea (e.g., Louwye et al., 2004, 2007). In our database, *Xandarodinium xanthum*, cysts of *Gymnodinium catenatum* and *Gymnodinium nolleri* are present only in the Northern Atlantic but they are reported also in the China Sea and coastal environments of Japan (Matsuoka, 1987; Cho and Matsuoka, 2001; Marret and Zonneveld, 2003; Wang et al., 2004). *Spiniferites ramosus* type *granosus* is exclusively recorded in the Mediterranean Sea. In modern sediments, *Achomosphaera* spp. is only recorded from the North Atlantic Ocean. Finally the Arctic and quadrangular morphotypes of *Polykrikos* sp. and *Echinidinium karaense* seem to be characteristic of the Arctic and subarctic zones.

3.2.2 Hydrographic and productivity data

3.2.2.1 Hydrographic data

Sea-surface temperature (SST) and salinity (SSS) data were compiled from the World Ocean Atlas (WOA, 2001). Mean summer and winter SST and SSS were defined with a radius of 30 nautical miles around each station. Sea-ice cover data are compiled after data spanning 1954-2000 as provided by the National Snow and Ice Data Center (NSIDC) in Boulder. We used the number of months per year with more than 50% sea-ice concentration that correlates with the annual concentration (cf. de Vernal et al., 2001). The ranges of SST, SSS and sea-ice cover for the North Atlantic, North Pacific and Arctic databases are presented in Table 2.

3.2.2.2 Productivity data

In this paper, we used two productivity datasets resulting from satellite observation of water properties of the oceans. The first one is from estimates using the Laboratoire de Physique et Chimie Marine (LPCM) model, based on chlorophyll concentration as well as physical properties of the water column provided by satellite observations of the Coastal Zone Color Scanner (CZCS) program (Antoine et al., 1996; Antoine and Morel, 1996). The CZCS program was developed by NASA and launched on the Nimbus 7 satellite in October 1978. During its 8 years lifetime (i.e. from October 1978 to June 1986), CZCS acquired several tens of thousands of images of the ocean surface. Primary productivity was estimated with a spatial resolution of $1/6^\circ$ of latitude by $1/6^\circ$ of longitude. Original Productivity data in Hierarchical Data Format (HDF) are available at: <http://marine.rutgers.edu/opp/Database/Database2.html>. The second dataset comprises productivity data calculated with the Vertical Generalized Production Model (VGPM) described by Behrenfeld and Falkowski (1997) using the

2002-2005 chlorophyll data provided by the MODerate resolution Imaging Spectroradiometer (MODIS) program. MODIS was launched by NASA in June 2000 and was designed for a 6 year life time. Computed productivity data are archived as MODIS Ocean level 4 primary productivity binned products (Level 4 data collection) with 4.63 km spatial resolution. The files in this data collection are stored in HDF in the MODIS web site (<http://daac.gsfc.nasa.gov>).

The LPCM and VGPM are both using bio-optical properties to estimate the carbon uptake by photosynthesis in relation to solar radiance, day length in addition to physical properties of water column including temperature, turbulence and euphotic depth. However, productivity in some coastal areas may be overestimated by both sensors due the effect of colored dissolved organic matter (Morel, 1978, 1991). The effect of water temperature and photosynthesis is computed differently with each model, as described by Antoine and Morel (1996) and Behrenfeld and Falkowski (1997), respectively.

At sites with no available productivity data, simple interpolation techniques were used. Most of the interpolated data are located in the Arctic Ocean where productivity is very low, sometimes below detection levels. Monthly productivity data derived from both CZCS and MODIS sensors were compiled from original databases and the seasonal and annual distribution of productivity over the Northern Hemisphere is presented in Figure 2. The data used in this study are archived at UQAM using a relational database management system, built using an SQL Server.

Comparison between CZCS-derived and MODIS-derived productivity data show considerable discrepancies, with generally higher productivity values yielded by MODIS (Fig. 3). The difference of productivity values between the two sensors can reach as much as 200 g C m^{-2} seasonally and 600 g C m^{-2} annually in some regions (Fig. 3). The largest difference occurs in areas of mid- and high-latitudes, such as the

Baltic Sea and around Iceland. Nevertheless, the spatial heterogeneity in primary productivity is comparable with both sensors, which show high productivity in coastal and upwelling regions and generally low productivities in the Arctic region (Figs. 2-3).

The LPCM and VGPM algorithms used to generate productivity values can explain the discrepancies between the CZCS and MODIS data, but only to some extent. The global estimates of productivity using the same chlorophyll data yield very close values, with slightly lower estimates with VGPM ($43.5 \text{ Gt C yr}^{-1}$) than LPCM ($46.9 \text{ Gt C yr}^{-1}$; Antoine et al., 1996; Behrenfeld and Falkowski, 1997). These values are close to those from other models using the same chlorophyll data (i.e. $50.2 \text{ Gt C yr}^{-1}$; cf. Longhurst et al., 1995). Although the different methods yield consistent global annual productivity estimates ranging between 43.5 and 50.2 Gt C , they result in important regional differences. In particular, with respect to the global productivity, the LPCM data show a larger contribution of the Pacific Ocean than the North Atlantic and Arctic oceans.

This discrepancy is possibly also related to the difference in the CZCS and MODIS data acquisition processes. It has been demonstrated that CZCS underestimated chlorophyll concentrations due to the data sparseness and to the poor data quality of Polar Regions and coastal zones (e.g., Gregg and Conkright, 2001; Thomas, 2001; Conkright and Gregg, 2003; Werdeli et al., 2003). Difference in productivity between the 1980s and the 2000s could also explain the difference in the CZCS and MODIS datasets although there is debate about this. Based on satellite and in situ measurements, Gregg and Conkright (2002) showed that spatial distributions and seasonal variabilities in ocean chlorophyll were roughly similar from 1979 to 2000, and Gregg et al. (2003) suggested that annual primary productivity in the ocean has even declined (more than 6%) since the early 1980's, notably in the northern high latitudes due to higher SST and lower atmospheric iron deposition. However, a more

recent study by Antoine et al. (2005) suggests in contrast that global productivity between the 1980s and the 2000s increased by about 20%.

3.2.3 Statistical treatment and transfer function

In order to explore the relationship between dinocyst assemblages and productivity at different basin scales, the “n = 1171” data set was split into three sub-datasets defined as follows (Fig. 1):

- (1) The Arctic data set includes 401 sites and 37 taxa. It represents the domain located north of the Arctic Polar Circle (i.e. between 66 and 82°N).
- (2) The North Atlantic data set includes 483 sites and 53 taxa. It represents the North Atlantic Ocean (between 28 and 66°N) including the Mediterranean Sea, Hudson Bay, Gulf and Estuary of St. Lawrence and Norwegian Fjords.
- (3) The North Pacific dataset includes 287 sites and 55 taxa. This dataset represents the domain located between 14 and 66 °N in the northeastern Pacific. It includes also the Bering Sea and estuarine regions of British Columbia and California.

For each data set, detrended correspondence analyses (DCA) were used to identify the type of function between assemblages and environmental variables (ter Braak and Smilauer, 1998). Here, the results show unimodal type function, which makes traditional linear-based multivariate methods, such as Partial Least Squares (PLS) or Principal Component Analyses (PCA) unsuitable (Jongman et al., 1995; ter Braak and Smilauer, 1998). Therefore, we have used Canonical Correspondence Analysis (CCA) which is the most suitable multivariate analysis since it implies unimodal responses of taxa to environmental influences (Jongman et al., 1995). CCA is a

constrained ordination method build on the method of weighted averaging of indicator species and on the ordination method of correspondence analysis (CA; Hill, 1974, ter Braak and Verdonschot, 1995). It provides a general framework for estimation and statistical testing of the effects of environmental variables (Gauch, 1982; Jongman et al., 1995). In contrast to CA, CCA allows environmental data to be incorporated into the analysis. By coupling the two datasets (species and environment) CCA extracts from the environmental variables synthetic gradients (ordination axes) that maximize the separation among species. Thus, the axes of the final ordination are restricted to the linear combinations of environmental variables, rather than simply reflecting dimensions of the greatest variability in the species data as is the case for the CA. In this way these two data sets (species and environment) are directly related (ter Braak, 1986). The canonical coefficients, from which the canonical scores of each variable are calculated, constitute standardized canonical weights of species and environmental variables and illustrate the contribution of each variable to the canonical axes. The species, represented by their statistical weight along each axis, as well as the signs and relative magnitude of intra-set correlations (correlation coefficients between the environmental variables and the ordination axes) allow inferring the relative importance of each environmental variable for the prediction of taxa composition.

Eleven environmental variables (winter and summer SST and SSS, sea-ice cover, winter, summer and annual MODIS and CZCS productivity) were used in these analyses. In order to test the significance of each variable and to avoid variables that are highly inter-correlated, the CCA analysis for all data sets was performed using manual forward selection option by applying 199 Monte Carlo randomizations. The importance of environmental variables is given by the amount of variance they explain. Their significances are determined by the P-value generated from Monte Carlo tests. Forward selection option allows ranking environmental variables in their importance for determining the taxa composition (ter Braak and Verdonschot, 1995).

In a first step, CCA was applied with each variable as the only variable and eigenvalue and p-value for this variable are obtained. Each environmental variable is thus ranked by its marginal effect, which is defined on the basis of the fit of each variable taken individually. In a second step, the best variable is selected and all other variables are ranked according to their conditional effect, which is defined on the basis of the fit of each individual variable in conjunction with the variable already selected. During the forward selection, environmental variables resulting in variance inflation factor (VIF) higher than 10 are assumed to be significantly correlated to other variables already selected (Montgomery and Peck, 1982; ter Braak and Smilauer, 1998). In general, high VIFs indicate multicollinearity among the environmental variables. If the VIF of a variable is higher than 20, the variable is almost perfectly correlated with the other variables and therefore its interpretation is not relevant (ter Braak, 1986).

The dinocyst data are ln-transformed in order to increase the weight of accompanying taxa that usually have narrower tolerance to environmental variables than ubiquitous taxa that often dominate the assemblages. Because of their different units, environmental variables are transformed within the CCA analyses such that each variable has a mean of zero and standard deviation of one.

For reconstruction purposes, we used the modern analogue technique (MAT). The method is based on calculation of an algebraic distance (coefficient of dissimilarity or squared chord distance) between fossil and modern assemblages. Every fossil assemblage is compared with modern ones in the reference database in order to find the best possible analogues. The productivity values of the best analogues according to the coefficient of dissimilarity are then weighted by this coefficient to reconstruct paleoproductivity. The background of the technique is reported in Overpeck et al. (1985) and Guiot (1990). Additional remarks concerning the approach are given in de Vernal et al. (2001, 2005). The advantage of the MAT is that there is no assumption

of quantitative relationships between assemblages and reconstructed parameters as is the case with calibration techniques (e.g., Guiot and de Vernal, 2007). In order to assess the accuracy of MAT for reconstructing productivity, cross-validation tests were performed using the leave-one-out or Jackknife method (cf. Efron and Gong, 1986). Estimated values were then compared to instrumental ones. The accuracy of the approach is assessed by the coefficient of correlation between estimated and observed values, and the root mean square error (RMSE) which is the standard deviation of the residuals between reconstructed and observed values.

Finally, reconstruction of past productivity is made using the Pleistocene-Holocene record of core HU 91-045-94 from the Northwest North Atlantic (50°12'N - 45°41'W; 3448 m water depth). This core is well dated and has been intensively studied for paleoceanographic purposes (e.g., Hillaire-Marcel et al., 1994; Stoner et al., 1998; de Vernal et al., 2000; Hillaire-Marcel and Bilodeau, 2000; Solignac et al., 2004; de Vernal and Hillaire-Marcel, 2006).

3.3 Results of CCA analyses - relationship between assemblages and productivity

3.3.1 Arctic Ocean

Figure 4 shows the CCA results when considering the Arctic Ocean alone (n = 401). The first two axes explain 29.5 % of the taxa variance, and 78.8 % of the canonical variance. The positioning of the environmental parameters in figure 4 show that the first CCA axis, which explains 22.7 % of the taxa variance, is positively correlated with sea-ice cover (R = 0.68; Fig. 4). Summer SST, winter SST and annual productivity seem to play a role as illustrated by their negative correlation with CCA axis 1 (R = -0.68, R = -0.56, R = -0.54 respectively). Some heterotrophic taxa such as *Brigantedinium* spp., *Islandinium minutum*, *Islandinium? cezare*, *Polykrikos kofoidii*

and the Arctic morphotype of *Polykrikos* sp. are ordinated on the positive side of axis 1, whereas all other taxa are ordinated in the negative side. Summer SSS and winter productivity show opposite correlation with CCA axis 2, which explains 6.8 % of the taxa variance (Fig. 4). This axis is characterized by the strong ordination of *Impagidinium pallidum* and *Nematosphaeropsis labyrinthus* in the positive side and *Impagidinium paradoxum*, *Votadinium calvum* and *Pyxidinoopsis reticulata* in the negative side.

3.3.2 North Atlantic Ocean

The CCA of the North Atlantic data set ($n = 483$) shows that the two CCA axes explain 23.1 % of the dinocyst dataset variance and 64 % of the canonical variance. The best linear combination of environmental variables that describes the sample position along each axis is defined by the canonical coefficient (Fig. 5, Table 3). CCA axis 1 is strongly correlated with winter SST ($R = 0.92$), summer SST ($R = 0.80$), winter SSS ($R = 0.77$) and summer SSS ($R = 0.78$). The CCA axis 1 represents a gradient of SST with cold taxa such as *Echinidinium karaense* and *Islandinium minutum* ordinated negatively whereas warm taxa such as *Polysphaeridium zoharyi* are ordinated positively. This illustrates that hydrographical parameters constitute the most determinant parameters of the dinocyst distribution as proposed in a number of publications (for example, see de Vernal et al., 1994, 1997, 2001; Rochon et al., 1999). Nevertheless, the CCA axis 1 is also significantly correlated with summer productivity ($R = -0.66$). Annual productivity is the variable with highest correlation with CCA axis 2 ($R = 0.29$). That axis explains 5.3% of the dinocyst variance and 14.7 % of the canonical variance (Fig. 5). It is of note that Axis 2 represents a gradient that separates heterotrophic taxa (positive scores) from phototrophic ones (negative scores), thus illustrating a positive correlation between heterotrophic taxa such as *Selenopemphix quanta* or *Protopteridinium americanum* and productivity

(Fig. 5). The positive relationship between *S. quanta* and productivity in the North Atlantic Ocean was previously reported by Dale and Fjelsä (1994) and Devillers and de Vernal (2000).

3.3.3 North Pacific Ocean

In the North Pacific Ocean ($n = 287$), the two first CCA axes explain 29.7 % of the variance in the dinocyst data set and 66.5 % of the canonical variance. The CCA axis 1 (17.8 % of the taxa variance and 39.8 % of the canonical variance) is strongly correlated with winter and summer SST ($R = 0.83$ and 0.80 respectively) and winter productivity ($R = 0.68$). These three parameters best describe the score of spectra along this axis (Fig. 6 and Table 3). The second CCA axis explains 11.9 % of the total variance in the dinocyst dataset and 26.7 % of the canonical variance. As indicated by their canonical coefficients, summer and annual productivity ($R = 0.67$ and $R = 0.60$) constitute the greatest contribution to the score of spectra along this axis (Fig. 6, Table 3), although winter and summer SSS ($R = -0.49$ and $R = -0.48$) also contribute to the canonical variance. Several heterotrophic and phototrophic taxa have significant relationships with CCA axis 2 (Fig. 6). The highest CCA axis 1 scores characterize heterotrophic taxa such as *Polykrikos schwartzii*, *Islandinium minutum*, *Lejeunecyta* spp., *Votadinium calvum*, *V. spinosum*, *Quinquecuspis concreta* and *Trinovantedinium variabile*, whereas the negative scores along the CCA axis 2 correspond to phototrophic taxa exclusively. *Impagidinium* species together with *Pyxidinosia reticulata* and *Nematosphaeropsis labyrinthus* have the lowest weight (Fig. 6). The results illustrate that productivity is playing a major role in the dinocyst distribution in the North Pacific Ocean as documented previously from regional data sets (Radi and de Vernal 2004; Radi et al., 2007; Pospelova et al., in press).

3.3.4 Northern Hemisphere

When the entire Northern Hemisphere is analyzed as a whole ($n = 1171$), SST seems to be the most determinant parameter since it is strongly correlated with the first ordination axis that explains 12.6 % of the variance ($R = 0.92$ for winter SST and $R = 0.89$ for summer SST; Fig. 7). Cold taxa such as *Polykrikos* sp.-Arctic morphotype, *I. minutum* and *E. karaense* are strongly ordinated together with sea-ice cover in the negative side of axis 1 whereas the warm taxa such as *Lingulodinium machaerophorum*, *Impagidinium striatum*, *Spiniferites ramosus* cf. *granosus*, *Polysphaeridium zoharyi* and *Bitectatodinium spongium* have the highest score along the CCA axis 1. Results show also that the two first ordination axes separate taxa in distinct groups with most of the heterotrophic taxa being positively correlated with both axes (Fig. 7A). This is the case of *Echinidinium aculeatum*, *E. granulatum*, *E. delicatum*, *Islandinium brevispinosum*, *T. variabile*, *Q. concreta* and *Votadinium spinosum* (shaded zone of Fig. 7A). Winter and annual productivity are also positively correlated with CCA axes 1 and 2. Figure 7B also illustrates that the three oceans constitute three different domains with respect to assemblages in relation to hydrographic and productivity conditions. These domains, however, form continuums and share overlapped areas.

3.4 Discussion

3.4.1 Significance and co-variability of hydrographic parameters and productivity

In order to explore the statistical significance of each parameter (SST, SSS, sea-ice and productivity) and its relative importance with respect to the dinocyst assemblage

distribution, forward selection and Monte Carlo permutation test were applied to all data sets (Table 3). The results show that the most determinant parameters are not the same from one ocean to another, but that productivity plays an important role. In the North Atlantic Ocean, seasonal and annual productivities weight roughly the same ($\lambda = 0.06$ to 0.08), but less than SST and sea-ice cover. In the North Pacific Ocean, winter SST and annual productivity represent the two most important parameters with the highest eigenvalues according to the conditional effect ($\lambda = 0.35$ and 0.20 respectively). Finally, at the scale of the Northern Hemisphere, winter productivity is ranked 3rd ($\lambda = 0.31$) after winter and summer SSTs (Table 3).

On the whole, productivity does not co-vary with SST, SSS or sea-ice cover (see figures 4 to 7). However, the variance inflation factor (VIF) suggests that summer productivity may co-vary with summer SST at the scale of the Arctic Ocean (Table 3). In the North Atlantic dataset, winter, summer and annual productivities do not show any significant co-variation ($VIF < 10$), but winter SSS may co-vary with summer SST. In the North Pacific dataset, winter productivity, summer SST and SSS may be considered as co-variants according to their VIF although they show P-values < 0.05 . The North Pacific sites analyzed correspond to a strong gradient of summer and annual productivity due to seasonal upwelling along the coasts. Here, VIF shows that winter productivity co-varies with winter SST (see also Fig. 6). In the Northern Hemisphere dataset, only summer productivity generates a $VIF > 10$. This is due to the fact that summer productivity is inversely correlated with summer SSS (Fig. 7), which is probably due to the weight of coastal and estuarine sites characterized by extremely high productivity and low salinity related to riverine nutrient and fresh water inputs.

3.4.2 The use of dinocysts for quantitative reconstructions of paleoproductivity

The hemispheric dinocyst database analyzed here encompasses a wide range of primary productivity conditions from regions with extremely low productivity in Arctic areas with nearly permanent ice cover, to very high productivity upwelling zones and estuaries.

CCA results demonstrate close relationships between productivity and dinocyst assemblages at basin or hemispheric scales. On these grounds, dinocysts can be used as paleoproductivity tracers. However, the relationship between productivity and a given taxon may differ from one ocean to another. For example, *S. quanta* and *P. americanum* correlate with annual productivity in the North Atlantic Ocean, whereas *Q. concreta*, *V. calvum* and *V. spinosum* show strong relation with annual productivity in the North Pacific Ocean and *I. minutum* appears more characteristic of high productivity in the Arctic Ocean (Figs. 4-6). The results show that a taxon may show specific response to productivity depending upon areas of the world considered, as previously illustrated by Zonneveld (1997b) in the Indian Ocean, Zonneveld et al. (2001b) for the southwestern African margins, Pospelova et al. (2002, 2005) along the eastern American margins and Radi et al. (2007) for the British Columbia margins. The difference in assemblages from one ocean to another and the non uniform relationship between relative abundances of a given taxon and productivity can be related to several factors. They include a response different depending upon the combination of the various hydrographic parameters (sea-ice, salinity, temperature, seasonality, notably) as suggested by the regionalism of CCA results, in addition to possible endemism of some taxa and possible existence of cryptic species having similar morphology but dissimilar genetic and ecologic affinities. Given the generally higher dissolved oxygen concentration in bottom waters of North Atlantic than Pacific Ocean due to better ventilation, one may question the potential effect of selective degradation (cf. Zonneveld et al., 2001a) in the North Atlantic. However,

the taxa showing the strongest relationships with productivity in the North Pacific, North Atlantic or the Arctic Ocean are all belonging to the order of protoperidinales and are among the most sensitive taxa with respect to oxidation. Therefore, although some selective degradation cannot be totally ruled out, there is no evidence from the data set presented here that it is a parameter invalidating the relationship between productivity and dinocyst assemblages.

The regionalism in the distribution of taxa suggests we should be cautious with interpretation based on the presence-absence, or on the relative abundance of marker species. Transfer functions based on linear or modal relationships between a single species or a combination of species using calibration techniques can be misleading since such relationships vary depending upon the spatial domain considered. Therefore, the use of modern analogue technique (MAT) is probably the most adequate since it provides a reconstruction based on the degree of similarity between modern and fossil spectra and simply assumes that identical assemblages are likely to occur under identical conditions. Another advantage of MAT is the possibility to reconstruct a combination of parameters simultaneously. MAT and the leave-one-out technique were thus performed with both MODIS and CZCS datasets.

3.4.3 Accuracy of reconstructions based on MAT

The reconstruction is based on the selection of the five analogues having the lowest distances with the analyzed spectra of the database. In order to avoid no analogue situations, analogues are selected only if their distance is lower than a threshold value above which the analogy between spectra is considered insignificant (see de Vernal et al., 2001, 2005; Guiot and de Vernal, 2007). The reconstruction is based on the number of analogues being ≤ 5 . Here, for the “n = 1171” database, the mean distance between randomly taken pairs of spectra is 148.11 ± 70.89 and the threshold adopted

is thus 77.22. The assessment of the quality of analogues by their distance (Fig. 8) illustrates that 1.8 % of sites have poor modern analogues (distance > 50), and that 88.3 % of sites have analogues with distance < 30. This exercise points to some weaknesses of the modern database, in particular for areas of sparse coverage and regions characterized by high species diversity and heterogeneity in assemblages, such as along the margins of western America, Mexico, and the Iberic peninsula. Results of cross-validation tests using the leaving-one-out technique indicate reasonably good estimates of productivity especially for North Atlantic and North Pacific Oceans with coefficients of correlation between observed and estimated values greater than 0.90 for most parameters (Figs. 9-11). The accuracy of estimates seems lower in the Arctic Ocean, which is characterized by low productivity. The coefficient of correlation between estimated and observed values is higher when using MODIS data than the CZCS dataset, which could be due to a wider range of productivity values. Similarly, the absolute values of the RMSE of CZCS data are lower due to lower values of productivity.

The validation test with the Northern Hemisphere database shows that annual and seasonal productivity can be reconstructed, using MODIS data, with an accuracy of $\pm 11.5 \text{ gC m}^{-2}$ or 20.4 % for winter, $\pm 23.1 \text{ gC m}^{-2}$ or 25.5 % for summer and $\pm 54.9 \text{ gC m}^{-2}$ or 17.8 % for annual productivity (Table 4; Fig. 11). It is noteworthy that the RMSEs for all estimated productivity parameters (winter, summer and annual productivity) are lower than the difference between MODIS and CZCS data. The standard deviation of this difference is used here as an index of the accuracy of instrumentally derived values of modern productivity (Table 4). Comparison between anomalies from dinocyst-based reconstruction (observed minus reconstructed values using MODIS data) and the difference between CZCS and MODIS modern data (Fig. 12) shows that regions with low accuracy of reconstructions correspond also to large discrepancies between CZCS and MODIS data. In some cases, these regions are also characterized by poor analogue situations for a few spectra (cf. Fig. 8). Therefore, a

large part of the error in estimates is probably due to uncertainty in the actual modern productivity data, and could also be due, for some regions, to poorly documented dinocyst assemblages.

3.5 Example of application: core HU 91-045-094

An example of paleoproductivity reconstruction is shown here for the last 25 000 years in the northwestern North Atlantic (data from core HU 91-045-94; Fig. 1). This core has been studied with detail and stratigraphical data could be found notably in Hillaire-Marcel et al. (1994, 2001) and Hillaire-Marcel and Bilodeau (2000). Palynological data and dinocyst assemblages have been published by de Vernal et al. (2000).

In order to assess the affinity of down core assemblages with those of the Northern Hemispheric modern database ($n = 1171$), we performed correspondence analysis (CA) from a matrix including dinocyst data of both the “ $n = 1171$ ” and the core analyzed. The position of core assemblages in the overlapping zone between the North Atlantic, Arctic and North Pacific oceans (Fig. 13) indicates that the spectra of core HU 91-045-94 have affinities with the modern ones of the different oceans (Arctic, North Atlantic and North Pacific). The ordination of core samples along CA axes 1 and 2 suggests also that dinocyst variability during the last 25 ka in this area reflects an oscillation between Arctic-type conditions with high sea-ice cover and low productivity (low axis 1 scores and high axis 2 scores) and North Atlantic-type conditions with low sea-ice cover and high productivity (high axis 1 scores and low axis 2 scores). As discussed earlier in the text, CCA axis 1 (the canonical equivalent of CA axis 1) is positively correlated with winter productivity ($R = 0.72$), whereas CCA axis 2 illustrates salinity rather than productivity (see Fig. 7). CCA axis 3 explains only a small part of the variance of the dinocyst assemblages (5.3 % of the

taxa variance and 16.4 % of the canonical variance), but it also emphasize the importance of summer and annual productivity on the overall distribution (Fig. 7D).

The downcore variation in dinocyst taxa percentages together with the scores of the three first CA axes is shown in Figure 14. This variation expresses the dominance of *N. labyrinthus*, *Operculodinium centrocarpum*, *Brigantedinium* spp. and *I. minutum*. Although *Brigantedinium* spp. dominate the assemblages of some productive zones in middle to low latitudes of the Northern Hemisphere (Marret, 1994; Radi and de Vernal, 2004), its quasi-exclusive dominance in the high latitudes could result from harsh sea-surface conditions with an extensive sea-ice cover (Rochon et al., 1999; de Vernal et al., 2000). As inferred from CA scores (Fig. 14), the last glacial maximum (LGM), the Younger Dryas (YD) and the Heinrich events 1 and 2 (H1 and H2) are characterized by low CA axis 1 scores and high CA axis 3 scores suggesting low productivity. After the YD, low CA axis 3 and relatively higher CA axis 1 scores show a transition to more productive environmental conditions.

Core HU 91-045-094 is characterized by sedimentation rates of about $\sim 20 \text{ cm ka}^{-1}$ and relatively high organic carbon (C_{org}) contents (Fig. 15). However, C_{org} may represent terrigenous inputs in addition to marine productivity. High fluxes of reworked palynomorphs together with pollen and spores suggest that terrigenous inputs contribute significantly to the total C_{org} at that site during the glacial episode. C_{org} alone is therefore a poor tracer of past productivity in this context. CaCO_3 also derives from both detrital input originating from the Hudson Bay terrains, and biogenic materials (coccoliths, foraminiferal tests). The contribution of detrital CaCO_3 to the site is well illustrated in Heinrich layers (Fig. 15). The isotopic composition ($\delta^{13}\text{C}$) of the mesopelagic foraminifer (*Neogloboquadrina pachyderma*-left coiling) has been interpreted as a proxy for ventilation in the North Atlantic (e.g., Duplessy, 1978; Labeyrie and Duplessy, 1985) and it can not be used here as paleoproductivity tracer.

Hillaire-Marcel et al. (1994) showed that microfossil fluxes at this site are characterized by a high variability during the last 25 ka, illustrating low fluxes during the glacial periods and high productivity after 12 ka. This high productivity is illustrated by increase of about four orders of magnitude for diatoms, three orders of magnitudes for coccoliths and one order of magnitude for dinocysts. This extremely high variation in microfossil fluxes is due in part to dissolution and can not be transferred quantitatively in term of primary productivity.

Here, the modern analogue technique is applied to dinocyst data to permit reconstruction of important changes in productivity. It suggests generally high productivity during Holocene and lower productivity during the glacial episode, which is consistent with micropaleontological flux data (cf. Hillaire-Marcel et al., 1994). The transition from isotopic stage 2 to the Holocene, between 11.5 and 7 ka cal. BP is marked particularly by very high productivity (250 - 350 gC m⁻² year⁻¹). Low productivity (<100 g C m⁻² year⁻¹) is recorded during the LGM, the YD, H1 and H2 (Fig. 16). In general, our reconstructions for the glacial episode are consistent with micropaleontological data from core HU 91-045-94 as well as with qualitative estimates of past productivity in the North Atlantic using benthic and planktic foraminifera (Thomas et al., 1995; Rasmussen et al., 2002). The reconstructions we present, however, include a few peaks of high productivity during the glacial time. These peaks probably illustrate sea-ice edge conditions favourable for phytoplankton blooming as in modern polar and subpolar marine environments (Wilson et al., 1986; Niebauer et al., 1995; Stabino et al., 1998). The particularly high productivity reconstructed after 11.5 ka is a feature that is not depicted by all micropaleontological proxies but it seems consistent with the fluxes of dinocysts and organic linings of benthic foraminifers (Fig. 15). The amplitude of reconstructed changes differs significantly depending upon the reference productivity dataset. Our productivity reconstructions based on MODIS data for the LGM are consistent with North Atlantic

Ocean productivity simulated by a coupled climate-ecosystem model (Schmittner, 2005) under hypothesized conditions of reduced Atlantic Meridional Overturning (as during the LGM).

3.6 Conclusion

Primary productivity is a challenge to measure in the modern ocean and a fortiori to reconstruct in the past ocean. Here, we have shown that productivity is a determinant parameter on the distribution of dinocyst assemblages. The fact that different trophic levels are present within dinoflagellate populations seems to facilitate development of a better integrated picture of productivity. On these grounds, transfer functions can be used to infer past productivity from dinocyst assemblages. However, calibration techniques should be avoided because the relation between dinocyst assemblages and productivity is not the same from one basin to another and, therefore, can not be transferred into equations unequivocally. The modern analogue approach seems appropriate, especially since we may use a large reference modern database of dinocysts representative of a wide range of productivity conditions. Despite weaknesses for regions with low density of reference points, the “n=1171” dinocyst database can be used to reconstruct productivity with a reasonable accuracy of about $\pm 15\%$. Validation exercises using the modern analogue technique indicate that reconstructions of seasonal and annual productivity can be obtained from dinocysts, with an error of prediction lower than the difference between available modern productivity datasets (CZCS and MODIS). Both seasonal and annual productivity can be reconstructed in the North Atlantic dataset since these parameters appear independent of all others, which is not the case for the North Pacific, where winter productivity can not be interpreted independently from winter SST due to the co-variability of the two parameters.

Paleoproductivity reconstructed using a core from the Northwest North Atlantic illustrates low production during glacial time and higher productivity during the Holocene. This reconstruction is consistent with other available data. However, the range of variation differs significantly depending upon the modern productivity reference dataset used, likely because the difference in estimation of chlorophyll by CZCS and MODIS programs (Antoine et al., 2005). Cross-validation tests show that MODIS data are best reconstructed. Past productivity estimates using MODIS data are also more consistent with present and past productivity simulated using coupled models (Schmittner, 2005).

According to these results, we conclude that dinocyst assemblages can be used as quantitative paleoproductivity proxy using the modern analogue technique.

3.7 Acknowledgments

We thank L. Levesque for technical computer assistance in downloading and compiling the estimates of MODIS ocean productivity. We are grateful to the NASA Goddard Earth Sciences Distributed Active Archive Center (GES DAAC) for making CZCS and MODIS data available to the user community. This study is a contribution to the Polar Climate Stability Network supported by the Canadian Foundation for Climate and Atmospheric Sciences. Financial support from the Natural Sciences and Engineering Research Council (NSERC) of Canada and from the *Fonds de la Recherche sur la Nature et les Technologies* (FQRNT) of Québec is also acknowledged. We are grateful to the reviewers of the Journal and to Thomas Pedersen and Laurent Londeix for their constructive comments on the original manuscript.

3.8 References

- Abrantes, F., Winn, K., Sarnthein, M., 1994. Late Quaternary paleoproductivity variations in the NE and equatorial Atlantic: diatom and C_{org} evidence. In: Zahn, R., Pedersen, T.F., Kaminski, M.A., Labeyrie, L. (Eds.), *Carbon Cycling in the Glacial Ocean: Constraints on the Ocean's Role in Global Change*. Springer-Verlag, Berlin, 425-439.
- Almogi-Labin, A., Schmiedl, G., Hemleben, C., Siman-Tov, R., Segl, M., Meischner, D., 2000. The influence of the NE winter monsoon on productivity changes in the Gulf of Aden, NW Arabian Sea, during the last 530 ka as recorded by foraminifera. *Marine Micropaleontology* 40, 295-319.
- Antoine, D., Morel, A., 1996. Oceanic primary production. 1. Adaptation of a spectral light photosynthesis model in view of application to satellite chlorophyll observations. *Global Biogeochemical Cycles* 10, 43-55.
- Antoine, D., André, J.M., Morel, A., 1996. Oceanic primary production. 2. Estimation at global scale from satellite (costal zone colour scanner) chlorophyll. *Global Biogeochemical Cycles* 10, 57-69.
- Antoine, D., Morel, A., Howard, R.G., Banzon, V.F., Evans, R.H., 2005. Bridging ocean color observation of the 1980s and 2000s in search of long-term trends. *Journal of Geophysical Research* 110, C06009, doi: 10.1029/2004JC002620.
- Barnola, J.M., Raynaud, D., Korotkevich, Y.S., and Lorius, C., 1987. Vostok ice core provides 160,000-year record of atmospheric CO₂. *Nature* 329, 408-414.
- Beaufort, L., Lancelot, Y., Camberlin, P., Cayre, O., Bassinot, F., Labeyrie, L., 1997. Insolation cycles as a major control of equatorial Indian Ocean primary production. *Science* 278, 1451-1454.
- Beaufort, L., Bassinot, F., Vincent, E., 1999. Primary production response to orbitally induced variations of the southern oscillations in the Equatorial Indian Ocean. In Abrantes, F., Mix, A.C. (Eds.), *Reconstructing Ocean History: A Window into the Future*, Kluwer Academic/Plenum Publishers, New York, 245-272.
- Beaufort, L., de Gabriel-Thoron, T., Mix, A., Pisias, N., 2001. ENSO-like forcing on oceanic primary production during the late Pleistocene. *Science* 293, 2440-2444.
- Behrenfeld, M.J., Falkowski, P.G., 1997. Photosynthetic rates derived from satellite-based chlorophyll concentration. *Limnology and Oceanography* 42, 1-20.

- Behrenfeld, M.J., Randerson, J.T., McClain, C.R., Feldman, G.C., Los, S.O., Tucker, C.J., Falkowski, P.G., Field, C.B., Froin, R., Esuas, W.E., Kolber, D.D., Pollack, N.H., 2001. Biospheric primary production during an ENSO transition. *Science* 291, 2594-2597.
- Berger, W.H., Smetacek, V.S., Wefer, G., 1989. Ocean productivity and paleoproductivity - An overview. In: Berger, W.H., Smetacek, V.S., Wefer, G. (Eds.), *Productivity of the Ocean: Present and Past*. Life Sciences Research Report 14, Chichester, 1-34.
- Bradtmiller, L.I., Anderson, R.F., Fleisher, M.Q., Burckle, L.H., 2006. Diatom productivity in the equatorial Pacific Ocean from the last glacial period to the present: A test of the silicic acid leakage hypothesis. *Paleoceanography* 21, PA4201, doi:10.1029/2006 PA001282.
- Cayre, O., Beaufort, L., Vincent, E., 1999. Paleoproductivity in the equatorial Indian Ocean for the last 260,000 yrs: A transfert function based on planktonic foraminifera. *Quaternary Science Reviews* 18, 839-857.
- Cho, H.-J., Matsuoka, K., 2001. Distribution of dinoflagellate cysts in surface sediments from the Yellow Sea and East China Sea. *Marine Micropaleontology* 42, 103-123.
- Conkright, M.E., Gregg, W.W., 2003. Comparison of global chlorophyll climatologies: In situ, CZCS, Blended in situ-CZCS and SeaWiFS. *International Journal of Remote Sensing* 24, 969-991.
- Dale, B., 1983. Dinoflagellate resting cysts: 'Benthic planktona. In: Fryxell, G.A. (Ed.), *Survival strategy of the algae*, Cambridge University Press, Cambridge, 69-136.
- Dale, B., Fjellsä, A., 1994. Dinoflagellate cysts as paleoproductivity indicators: state of the art, potential and limits. In: Zahn, R., Pedersen, T., Kaminski, M., Labeyrie, L. (Eds.), *Carbon cycling in the glacial Ocean: constrains on the ocean's role in global change*. Berlin, Springer-Verlag, 521-537.
- de Vernal, A., Hillaire-Marcel, C., 2006. Provincialism in trends and high frequency changes in the northwest North Atlantic during the Holocene. *Global and Planetary Change* 54, 263-290.
- de Vernal, A., Turon, J.-L., Guiot, J., 1994. Dinoflagellate cyst distribution in high latitude marine environments and quantitative reconstruction of sea-surface salinity, temperature, and seasonality. *Canadian Journal of Earth Sciences* 31, 48-62.

de Vernal, A., Rochon, A., Turon, J.-L., Matthiessen, J., 1997. Organic-walled dinoflagellate cysts: palynological tracers of sea-surface conditions in middle to high latitude marine environments. *Geobios* 30, 905-920.

de Vernal, A., Hillaire-Marcel, C., Turon, J.-L., Matthiessen, J., 2000. Reconstruction of sea-surface conditions in the northern North Atlantic during the last glacial maximum based on dinocyst assemblages. *Canadian Journal of Earth Sciences* 37, 725-750.

de Vernal, A., Henry, M., Matthiessen, J., Mudie, P.J., Rochon, A., Boessenkool, K., Eynaud, F., Grøsfjeld, K., Guiot, J., Hamel, D., Harland, R., Head, M.J., Kunz-Pirring, M., Levac, E., Loucheur, V., Peyron, O., Pospelova, V., Radi, T., Turon, J.-L., Voronina E., 2001. Dinocyst assemblages as tracer of sea-surface conditions in the northern North Atlantic, Arctic and sub-Arctic seas: the "n = 677" database and derived transfer functions. *Journal of Quaternary Science* 16, 681-698.

de Vernal, A., Eynaud, F., Henry, M., Hillaire-Marcel, C., Londeix, L., Mangin, S., Matthiessen, J., Marret, F., Radi, T., Rochon, A., Solignac, S., Turon, J.-L., 2005. Reconstruction of sea-surface conditions at middle to high latitudes of the Northern Hemisphere during the Last Glacial Maximum (LGM) based on dinoflagellate cyst assemblages. *Quaternary Science Reviews* 24, 897-924.

Devillers, R., de Vernal, A., 2000. Distribution of dinocysts in surface sediments of the northern North Atlantic in relation with nutrients and productivity in surface waters. *Marine Geology* 166, 103-124.

Duplessy, J.C., 1978. Isotope studies. In: Gribbin, J. (Ed.), *Climate Change*. Cambridge University Press, 47-67.

Dymond, J., Collier, R., 1996. Particulate barium fluxes and their relationships to biological productivity. *Deep Sea Research Part II* 43, 1283-1308.

Dymond, J., Suess, E., Lyle, M., 1992. Barium in deep-sea sediment: a geochemical proxy for paleoproductivity. *Paleoceanography* 7, 163-181.

Eagle, M., Paytan, A., Arrigo, K.R., van Dijken, G., Murray, R.W., 2003. A comparison between excess barium and barite as indicators of carbon export. *Paleoceanography* 18, doi:10.1029/2002PA000793.

Efron, B., Gong, C., 1983. A Leisurely Look at the Bootstrap, the Jackknife, and Cross validation. *The American Statistician* 37, 36-48.

Emerson, S., Hedges, J., 1988. Processes controlling the organic carbon content of open ocean sediments. *Paleoceanography* 3, 621-634.

Emerson, S., Hedges, J., 2003. Sediment Diagenesis and Benthic Flux. In: Holland, H.D., Turekian, K.K. (Eds.), *Treatise on Geochemistry*, vol. 6. Elsevier-Pergamon, Oxford, 293-319.

Field, C.B., Behrenfeld, M.J., Randerson J.T., Falkowski, P., 1998. Primary Production of the biosphere: Integrating Terrestrial and Oceanic Components. *Science* 281, 237-240.

Fischer, G., Wefer, G. (Eds.), 1999. *Use of Proxies in Paleoceanography: Examples from the South Atlantic*. Springer-Verlag Berlin, 735 pp.

Fischer, V., Ratmeyer, V., Wefer, G., 2000. Organic carbon fluxes in the Atlantic and southern ocean: relationship to primary production compiled from satellite radiometer data. *Deep-Sea Research Part II* 47, 1961-1997.

François, R., Honjo, S., Manganini, S., Ravizza, G., 1995. Biogenic barium fluxes to the deep sea: implications for paleoproductivity reconstructions. *Global Biogeochemical Cycles* 9, 289-303.

François, R., Frank, Van der Loeff, M.M.R., Bacon, M.B., 2004. ^{230}Th normalization: An essential tool for interpreting sedimentary fluxes during the late Quaternary. *Paleoceanography* 19, PA1018, doi:10.1029/2003PA000939.

Gaines, G., Elbrächter, M., 1986. Heterotrophic nutrition. In: Taylor, F.J.R., (Ed.), *The Biology of Dinoflagellates*. Oxford: Blackwell Scientific Publications, 224-268.

Gallinari, M., Ragueneau, O., Corrin, L., DeMaster. D.J., Tréguer, P., 2002. The importance of water column processes on the dissolution properties of biogenic silica in deep-sea sediments. I. Solubility. *Geochimica et Cosmochimica Acta* 66, 2701-2717.

Gauch, H.G., 1982. *Multivariate analysis in community ecology*. Cambridge University Press, Cambridge. 298 pp.

Gregg, W.W., Conkright, M.E., 2001. Global seasonal climatologies of ocean chlorophyll: Blending in situ and satellite data for the Coastal Zone Color Scanner era. *Journal of Geophysical Research* 106, 2499-2515.

Gregg, W.W., Conkright, M.E., 2002. Decadal changes in global ocean chlorophyll. *Geophysical Research Letters* 29, doi:10.1029/2002GL014689.

- Gregg W.W., Conkright, M.E., Ginoux, P., O'Reilly, J.E., Casey, N.W., 2003. Ocean primary production and climate: Global decadal changes. *Geophysical Research Letters* 30, doi: 10.1029/2003GL016889.
- Guiot, J., 1990. Methods and programs of statistics for paleoclimatology and paleoecology. In: Guiot, J., Labeyrie, L. (Eds.), *Quantification des changements climatiques: méthode et programmes*. Institut National des Sciences de l'Univers (INSU-France), Monographie No 1, Paris.
- Guiot, J., de Vernal, A., 2007. Transfer functions - Methods for quantitative paleoceanography based on microfossils. In: Hillaire-Marcelle, C., de Vernal, A. (Eds.). *Late Cenozoic paleoceanography*, volume 1. Elsevier, 523-566.
- Head, M.J., 2002. *Echinidinium zonneveldiae* sp. nov., a dinoflagellate cyst from the Late Pleistocene of the Baltic Sea, northern Europe. *Journal of Micropalaeontology* 21, 169-173.
- Head, M.J., Harland, R., Matthiessen, J., 2001. Cold marine indicators of the late quaternary: the new dinoflagellate cyst genus *Islandinium* and related morphotypes. *Journal of Quaternary Science* 16, 621-636.
- Head, M.J., Lewis, J., de Vernal, A., 2006. The cyst of the calcareous Dinoflagellate *Scrippsiella trifida*: Resolving the fossil record of its organic wall with that of *Alexandrium tamarense*. *Journal of Paleontology* 80, 1-18.
- Hill, M.O., 1974. Correspondence analysis: a neglected multivariate method. *Applied Statistics* 23, 340-354.
- Hillaire-Marcel, C., Bilodeau, G., 2000. Instabilities in the Labrador Sea water mass structure during the last climatic cycle. *Canadian Journal of Earth Sciences* 37, 795-809.
- Hillaire-Marcel, C., de Vernal, A., Lucotte, M., Mucci, A., Bilodeau, G., Rochon, A., Vallières, S., Wu, G., 1994. Productivité et flux de carbone dans la mer du Labrador au cours des derniers 40 000 ans. *Canadian Journal of Earth Science* 31, 139-158.
- Hillaire-Marcel, C., de Vernal, A., Candon, L., Bilodeau, G., Stoner, J., 2001. Changes of potential density gradients in the Northwestern North Atlantic during the Last climatic cycle based on a multiproxy approach. In: Seidov, D. (Ed.), *The Oceans and Rapid Climate Changes: Past, Present and Future*. Geophysical Monograph Series 126, 83-100.

Ikeda, T., Tajika, E., 2002. Carbon cycling and climate change during the last glacial cycle inferred from the isotope records using an ocean biogeochemical carbon cycle model. *Global and Planetary Change* 35, 131-141.

Ivanova, E., Schiebel, R., Singh, A.D., Schmiedl, G., Niebler, H.-S., Hemleben, C., 2003. Primary production in the Arabian Sea during the last 135 000 years. *Palaeogeography, Palaeoclimatology, Palaeoecology* 197, 61-82.

Jacobson, D., Anderson, D., 1986. Thecate heterotrophic dinoflagellates: Feeding behaviour and mechanics. *Journal of Phycology* 22, 249-258.

Jeandel, C., Tachikawa, K., Bory, A., Dehairs, F., 2000. Biogenic barium in suspended and trapped material as a tracer of export production in the tropical NE Atlantic EUMELI sites. *Marine Chemistry* 71, 125-142.

Jongman, R.H.G., ter Braak, C.J.F., Van Tongeren, O.F.R. (Eds.), 1995. *Data analysis in community and landscape ecology*. Cambridge University Press, Cambridge, 299 pp.

Kielt, J.F., 2007. *Distribution des assemblages palynologiques et microfaunistiques le long des côtes ouest mexicaines*. Ms Thesis, Université du Québec à Montréal. Montreal.

Klump, J., Hebbeln, D., Wefer, G., 2000. The impact of sediment provenance on barium-based productivity estimates. *Marine Geology* 169, 259-271.

Kokinos, J.P., Eglinton, T.I., Goni, M.A., Boon, J.J., Martoglio, P.A., Anderson, D.M., 1998. Characterization of a highly resistant biomacromolecular material in the cell wall of a marine dinoflagellate resting cyst. *Organic Geochemistry* 28, 265-288.

Knox, F., McElroy, M.B., 1984. Changes in atmospheric carbon dioxide: influence of the marine biota at high latitude. *Journal of Geophysical Research* 89, 4629-4637

Labeyrie, L., Duplessy, J.C., 1985. Change in the oceanic $^{13}\text{C}/^{12}\text{C}$ ratio during the last 140,000 years: High latitude surface water records. *Palaeogeography, Palaeoclimatology, Palaeoecology* 50, 217-240.

Ladouceur, S., 2007. *Évaluation des changements hydrographiques de la Baie d'Hudson et du Bassin de Foxe au cours des derniers siècles à partir de traceurs palynologiques et micropaléontologiques*. Ms Thesis, Université du Québec à Montréal, Montreal.

- Lazarus, D., Bittniok, B., Diester-Haass, L., Meyers, P., Billups, K., 2006. Comparison of radiolarian and sedimentologic paleoproductivity proxies in the latest Miocene-Recent Benguela Upwelling System. *Marine Micropaleontology* 60, 269-294.
- Longhurst, A., Sathyendranath, S., Platt, T., Caverhill, C., 1995. An estimate of global primary production in the Ocean from satellite radiometer data. *Journal of Plankton Research* 17, 1245-1271.
- Loubere, P., 1991. Deep-sea benthic foraminiferal assemblage response to a surface ocean productivity gradient: A test. *Paleoceanography* 6, 193-204.
- Loubere, P., 1994. Quantitative estimation of surface ocean productivity and bottom water oxygen concentration using benthic foraminifera. *Paleoceanography* 9, 723-737.
- Loubere, P., 1996. The surface ocean productivity and bottom water oxygen signals in deep water benthic foraminiferal assemblages. *Marine Micropaleontology* 28, 247-261.
- Loubere, P., 1999. A multiproxy reconstruction of biological productivity and oceanography in the eastern equatorial Pacific for the past 30,000 years. *Marine micropaleontology* 37, 173-198.
- Loubere, P., 2002. Remote vs. local control of changes in eastern equatorial Pacific bioproductivity from the Last Glacial Maximum to Present. *Global and Planetary Changes* 35, 113-126.
- Loubere, P., Fariduddin, M., 1999. Quantitative estimation of global patterns of surface Ocean biological productivity and its seasonal variation timescales from centuries to millennia. *Global Biogeochemical Cycles* 13, 115-133.
- Louwey, S., Head, M.J., De Schepper, S., 2004. Dinoflagellate cyst stratigraphy and palaeoecology of the Pliocene in northern Belgium, southern North Sea Basin. *Geological Magazine* 141, 353-378.
- Louwey, S., De Schepper, S., Laga, P., Vandenberghe, N., 2007. Upper Miocene of the southern North Sea Basin (northern Belgium): a palaeoenvironmental and stratigraphical reconstruction using dinoflagellate cysts. *Geological Magazine* 144, 33-52.

Lyle, M., Murray, D.W., Finney, B.P., Dymond, J., Robbins, J.M., Brooksforce, K., 1988. The record of late Pleistocene biogenic sedimentation in the eastern tropical Pacific Ocean. *Paleoceanography* 3, 39-59.

Mackensen A., Schumacher S., Radke J, Schmidt, D.N., 2000. Microhabitat preferences and stable carbon isotopes of endobenthic foraminifera: clue to quantitative reconstruction of oceanic new production? *Marine Micropaleontology* 40, 233-258.

Marret, F., 1993. Les effets de l'acétolyse sur les assemblages de kystes de dinoflagellés, *Palynosciences* 2, 267-272.

Marret, F., 1994. Distribution of dinoflagellate cysts in recent marine sediments from the east Equatorial Atlantic (Gulf of Guinea). *Review of Palaeobotany and Palynology* 84, 1-22.

Marret, F., Zonneveld, K.A.F., 2003. Atlas of modern organic-walled dinoflagellate cyst distribution. *Review of Palaeobotany and Palynology* 125, 1-200.

Matsuoka, K., 1987. Organic-walled dinoflagellate cysts from surface sediments of Akkeshi Bay and Lake Saroma, North Japan. *Bulletin of the Faculty of Liberal Arts, Nagasaki University*, 28, 35-123.

McCorkle, D.C., Martin, P.A., Lea, D.W., Klinkhammer, G.P., 1995. Evidence of a dissolution effect on benthic foraminiferal shell chemistry: $\delta^{13}\text{C}$, Cd/Ca, Ba/Ca, and Sr/Ca results from the Ontong Java Plateau. *Paleoceanography* 10, 699-714.

Meyers, P.A., 1997. Organic geochemical proxies of paleoceanographic, paléolimnologic, and paleoclimatic processes. *Organic Geochemistry* 27, 213-250.

Mix, A.C., 1989. Influence of productivity variations on long-term atmospheric CO_2 . *Nature* 337, 541-544.

Montgomery, D.C., Peck, E.A., 1982. *Introduction to Linear Regression Analysis*. John Wiley and Sons, New York, 504 pp.

Morel, A., 1978. Available, usable and stored radiant energy in relation to marine photosynthesis. *Deep Sea Research* 25, 673-688.

Morel, A., 1991. Light and marine photosynthesis: a spectral model with geochemical implications. *Progress in Oceanography* 26, 263-306.

Muller, P.J., Suess, E., 1979. Productivity, sedimentation rate, and sedimentary organic matter. *Deep Sea Research* 26, 1347-1362.

Muller, P.J., Erlenkeuser, H., Von Grafenstein, R., 1983. Glacial-interglacial cycles in oceanic productivity inferred from organic carbon contents in eastern north Atlantic sediment cores. In: Thiede, J., Suess, E. (eds), *Coastal upwelling, its sediment record, Part B: Sedimentary records of ancient coastal upwelling*. Plenum press, New York, 65-398.

Naidu, P.D., Malmgren, B.A., 1996., A high-resolution record of late Quaternary upwelling along the Oman Margin, Arabian Sea based on planctonic foraminifera. *Paleoceanography* 11, 129-140.

Nelson, D.M., Tréguer, P., Brzezinski, M.A., Leynaert, A., Quéguiner, B., 1995. Production and dissolution of biogenic silica in the ocean: Revised global estimates, comparison with regional data and relationship with biogenic sedimentation. *Global Biogeochemical Cycles* 9, 359-372.

Niebauer, H.J., Alexander, V.A, Henrichs, S., 1995. Physical and biological oceanographic interaction in the Spring Bloom at the Bering Sea marginal ice edge zone. *Journal of Geophysical Research* 95, 22229-22242.

Overpeck, J., Webb, T., Prentice, I.C., 1985. Quantitative interpretation of fossil pollen spectra: dissimilarity coefficients and the method of modern analogs. *Quaternary Research* 23, 87-108.

Parsons, T.R., Takahashi, M., Hargrave, B., 1984. *Biological organic processes*. Pergamon Press, Oxford, UK, 330 pp.

Paytan, A., Kastner, M., 1996. Benthic Ba fluxes in the central equatorial Pacific, implications for the oceanic Ba cycle. *Earth and Planetary Science Letter* 142, 439-450.

Paytan, A., Kastner, M., Chavez, F.P., 1996. Glacial to interglacial fluctuation in productivity in the equatorial Pacific as indicated by marine Barite. *Science* 274, 1355-1357.

Pedersen, T.F., Pickering, M., Vogel, J.S., Southon, J.N., Nelson, D.E., 1988. The response of benthic foraminifera to productivity cycles in the eastern equatorial Pacific: Faunal and geochemical constraints on glacial bottom water oxygen levels. *Paleoceanography* 3, 157-168.

Pedersen, T.F., Nielsen, B., Pickering, M., 1991. The timing of Late Quaternary productivity pulses in the Panama Basin and implications for atmospheric CO₂. *Paleoceanography* 6, 657-677.

Pospelova, V., Head, M.J., 2002. *Islandinium brevispinosum* sp. nov. (Dinoflagellata), a new organic-walled dinoflagellate cyst from modern estuarine sediments of New England (USA). *Journal of Phycology* 38, 593-601.

Pospelova, V., Chmura, G.L., Boothman, W.S., Latimer, J.S., 2002. Dinoflagellate cyst records and human disturbance in two neighboring estuaries, New Bedford Harbor and Apponagansett Bay, Massachusetts (USA). *The Science of the Total Environment* 298, 81-102.

Pospelova, V., Chmura, G.L., Boothman, W., Latimer, J.S., 2005. Spatial distribution of modern dinoflagellate cysts in polluted estuarine sediments from Buzzards Bay (Massachusetts, USA) embayments. *Marine Ecology Progress Series* 292, 23-40.

Pospelova, V., de Vernal, A., Pedersen, T.F., 2008. Distribution of dinoflagellate cysts in surface sediments from the northeastern Pacific (43-25°N) in relation to sea-surface temperature, salinity, productivity and coastal upwelling. *Marine Micropaleontology*, in press.

Radi, T., de Vernal, A., 2004. Dinocyst distribution in surface sediments from the northeastern Pacific margin (40-60 °N) in relation to hydrographic conditions, productivity and upwelling. *Review of Palaeobotany and Palynology* 128, 169-193.

Radi, T., de Vernal, A., Peyron, O., 2001. Relationships between dinocyst assemblages in surface sediments and hydrographic conditions in the Bering and Chukchi seas. *Journal of Quaternary Science* 16, 667-680.

Radi, T., Pospelova, V., de Vernal, A., Barrie, J.V., 2007. Dinoflagellate cysts as indicators of water quality and productivity in British Columbia estuarine environments. *Marine Micropaleontology* 62, 269-297.

Ragueneau, O., Tréguer, P., Leynaert, A., Anderson, R.F., Brzezinski, M.A., DeMaster, D.J., Dugdale, R.C., Dymond, J., Fischer, G., François, R., Heinze, C., Maier-Reimer, E., Martin-Jézéquel, V., Nelson, D.M., Quéguiner, B., 2000. A review of the Si cycle in the modern ocean: Recent progress and missing gaps in the application of biogenic opal as a paleoproductivity proxy. *Global Planet Change* 26, 317-365.

Rasmussen, T.L., Thomson, E., Trolestra, S.R., Kuijpers, A., Prins, M.A., 2002. Millennial-scale glacial variability versus Holocene stability: changes in planktic and benthic foraminiferal faunas and ocean circulation in the North Atlantic during the last 60,000 years. *Marine Micropaleontology* 47, 143-176.

Richerol, T., Rochon, A. Decadal-scale sea ice history of the Mackenzie Trough (Beaufort Sea, Canada) over the last 300 years based on dinocyst data. *Marine Micropaleontology*, submitted.

Rochon, A., de Vernal, A., Turon, J.-L., Matthiessen, J., Head, M.J., 1999. Distribution of dinoflagellate cysts in surface sediments from the North Atlantic Ocean and adjacent seas in relation to sea-surface parameters. *American Association of Stratigraphic Palynologists, Contribution Series* 35, 152 pp.

Rühlemann, C., Müller, P.J., Schneider, R.R., 1999. Organic carbon and carbonate as paleoproductivity proxies: Examples from high and low productivity areas of the Tropical Atlantic. In: Fischer, G., Wefer, G., (Eds.), *Use of proxies in Paleoceanography: examples from the South Atlantic*. Springer-Verlag, Berlin, 315-344.

Sarmiento J.L., Toggweiler, J.R., 1984. A new model for the role of the oceans in determining atmospheric pCO₂. *Nature* 308, 621-624.

Sarnthein, M., Duplessy, J.-C., Fontugue, M.R., 1988. Global variations of surface ocean productivity in low and mid latitudes: influence on CO₂ reservoirs of the deep ocean and atmosphere during the last 21 000 years. *Paleoceanography* 3, 361-399.

Sarnthein, M., Pflaumann, U., Ross, R., Tiedemann, R., Winn, K., 1992. Transfer functions to reconstruct ocean palaeoproductivity: a comparison. In: Summerhayes, C.P., Prell, W.L., Emeis, K.C. (Eds.), *Upwelling Systems: Evolution since the early Miocene*. Geological Society Special Publication 64, London, 411-427.

Schmittner, A., 2005. Decline of the marine ecosystem caused by a reduction in the Atlantic overturning circulation. *Nature* 434, 628-633.

Shackleton, N.J., Hall, M.A., Line, J., Ceng, S., 1983. Carbon isotope data in core V19-30 (Carnegie Ridge, south of the Panama Basin) confirm reduced carbon dioxide concentration in the ice age atmosphere. *Nature* 306, 319-322.

Solignac, S., de Vernal, A., Hillaire-Marcel, C., 2004. Holocene sea surface conditions in the North Atlantic - contrasted trends and regimes between the eastern and western sectors (Labrador Sea vs. Iceland Basin). *Quaternary Science Reviews* 23, 319-334.

Stabino, P.J., Schumacher, R.F., Davis, R.F., Napp, J.M., 1998. Under-ice observations of water column temperature, salinity and spring phytoplankton dynamics: Eastern Bering Sea shelf. *Journal of Marine Research* 56, 239-255.

Stoner, J.S., Channell, J.E.T., Hillaire-Marcel, C., 1998. A 200 ka geomagnetic chronostratigraphy for the Labrador Sea: Indirect correlation of sediment record to SPECMAP. *Earth and Planetary Science letters* 159, 165-181.

Taylor, F.J.R., (Ed.), 1987. *The biology of dinoflagellates*. Botanical Monographs 21, Blackwell Scientific Publications, Oxford, 785 pp.

ter Braak, C.J.F., 1986. Canonical correspondence analysis: a new eigenvector technique for multivariate direct gradient analysis. *Ecology* 67, 1167-1179.

ter Braak, C.J.F., Smilauer, P., 1998. *Canoco reference manual and user's guide to Canoco for Windows, software for canonical community ordination (version 4)*. Centre for Biometry, Wageningen, 351 pp.

ter Braak, C.J.F., Verdonschot, P.F.M., 1995. Canonical correspondence analysis and related multivariate methods in aquatic ecology. *Aquatic Sciences* 57, 255-289.

Thomas, E., Booth, L., Maslin, M., Shackleton, N.J., 1995. Northeastern Atlantic benthic foraminifera during the last 45 000 years: Changes in productivity seen from the bottom up. *Paleoceanography* 10, 545-562.

Thomas, A.C., Carr, M.-E., Strub, P.T., 2001. Chlorophyll variability in Eastern Boundary Currents. *Geophysical Research Letters* 28, 3421-3424.

Véneç-Peyré, M.-T., Caulet, J.-P., 2000. Paleoproductivity changes in the upwelling system of Socotra (Somali Basin, NW Indian Ocean) during the last 72,000 years: evidence from biological signatures. *Marine Micropaleontology* 40, 321-344.

Von Breymann, M.T., Emeis, K.C., Suess, E., 1992. Water depth and diagenetic constraints on the use of barium as a paleoproductivity indicator. In: Summerhayes, C.P., Prell, W.L., Emeis, K.C. (Eds.), *Upwelling Systems: Evolution since the Early Miocene*. Geological Society of London, special publication 64, 273-284.

Wall, D., Dale, B., 1968. Modern dinoflagellate cysts and evolution of the Peridinales. *Micropaleontology* 14, 265-304.

Wang, Z., Matsuoka, M., Qi, Y., Chen, J., 2004. Dinoflagellate cysts in recent sediments from Chinese coastal waters. *Marine Ecology* 25, 4, 289-311.

Wefer, G., Berger, W.H., Bijma, J., Fischer, G., 1999. Clues to Ocean History: a brief overview of proxies. In: Fischer, G., Wefer, G. (Eds.), *Use of Proxies in Paleoceanography: Examples from the South Atlantic*. Springer-Verlag, Berlin, 1-68.

Werdeli, P.J., Bailey, S., Fargion, G., Pietras, C., Knobelspiesse, K., Feldman, G., McClain, C., 2003. Unique data repository facilitates ocean color satellite validation. *EOS Transactions* 84, 38, p. 377.

Wilson, D.L., Smith, W.O., Nelson, D.M., 1986. Phytoplankton bloom dynamics of the western Ross Sea ice edge. I. Primary productivity and specific production. *Deep Sea Research* 33, 1375-1387.

World Ocean Atlas, 2001. CD-ROMs data set, National Oceanographic Data Center, Silver Spring, MD.

Zonneveld, K.A.F., 1997a. Dinoflagellate cyst distribution in surface sediments from the Arabian Sea (northwestern Indian Ocean) in relation to temperature and salinity gradients in the upper water column. *Deep-Sea Research II* 6-7, 1411-1443.

Zonneveld, K.A.F., 1997b. New species of organic walled dinoflagellate cysts from modern sediments of the Arabian Sea (Indian Ocean). *Review of Palaeobotany and Palynology* 97, 319-337.

Zonneveld, K.A.F., Jurkschat, T., 1999. *Bitectatodinium spongium* (Zonneveld, 1997) Zonneveld and Jurkschat, comb. nov. from modern sediments and sediment trap samples of the Arabian Sea (northwestern Indian Ocean): taxonomy and ecological affinity. *Review of Palaeobotany and Palynology* 106, 153-169.

Zonneveld, K.A.F., Brummer, G.J.A., 2000. Palaeoecological significance, transport and preservation of organic-walled dinoflagellate cysts in the Somali Basin, NW Arabian Sea. *Deep Sea Research II*, 47, 2229-2256.

Zonneveld, K.A.F., Versteegh, G.J.M., de Lange, G.J., 2001a. Palaeoproductivity and post-depositional aerobic organic matter decay reflected by dinoflagellate cyst assemblages of the Eastern Mediterranean S1 sapropel. *Marine Geology* 172, 181-195.

Zonneveld, K.A.F., Hoek, R.P., Brinkhuis, H., Willems, H., 2001b. Geographical distribution of organic-walled dinoflagellate cysts in surficial sediments of the Benguela upwelling region and their relationship to upper ocean conditions. *Progress in Oceanography* 48, 25-75.

3.9 Figure captions

Figure 1: Location of surface sediment (core-top) samples in the “n=1171” reference dinocyst database. It constitutes an update of the “n=940” (de Vernal et al., 2005) and includes additional sites from St. Lawrence estuary, Hudson Bay (Ladouceur, 2007), Arctic Ocean (Richerol and Rochon, submitted), and Northeastern Pacific (Kieft, 2007; Radi et al., 2007; Pospelova et al., in press).

Figure 2: Seasonal and annual distribution maps of primary productivity based on satellite observations of chlorophyll. The CZCS productivity is from the LPCM model (Antoine et al., 1996) based on CZCS ocean color data averaging from 1979 to 1986. The MODIS productivity is from the VGPM model (Behrenfeld and Falkowseki, 1997) based on MODIS ocean color data averaging from 2002 to 20005.

Figure 3: Maps showing the difference between MODIS and CZCS data (cf. figure 2).

Figure 4: Results of CCA analysis applied to the Arctic dataset. A, ordination diagram of the dinocyst taxa (open dots, see Table 1 for abbreviations), represented by their niche center along axes 1 and 2. Environmental variables (arrows) are displayed by their correlation with the axes (direction of arrows) and by their importance in explaining the dinocyst distribution (length of arrows). They have been standardized to a mean of 0 and a standard deviation of 1 in order to remove arbitrariness in the units and make the canonical coefficients comparable among each other. W_SST, winter sea surface temperature; S_SST, summer sea surface temperature; W_SSS, winter sea surface salinity; S_SSS, summer sea surface salinity; ICE, duration of sea-ice cover; W_MODIS, winter productivity; S_MODIS, summer productivity; A_MODIS, annual productivity (according to MODIS data). Ordination of seasonal and annual productivity of CZCS data are not shown because they are

strongly correlated to MODIS ones. Dashed arrows represent the variable which may co-vary with other parameters as judged by the variance inflation factor (VIF, cf. CCA analysis). B, eigenvalues, species-environment correlation and variance of species data and species-environment relationship for the 4 first ordination axes. C, Correlation matrix between environmental parameters and the first 4 ordination axes.

Figure 5: Results of CCA analysis applied to the North Atlantic dataset; A, Diagram showing the ordination of the dinocyst taxa and environmental variables along the two first axes (see figure 4A for legend); B, eigenvalues, species-environment correlation and variance of species data and species-environment relationship for the four first ordination axes; C, Correlation matrix between environmental parameters and the first four ordination axes.

Figure 6: Results of CCA analysis applied to the North Pacific dataset. See legend of figure 5 for more explanation.

Figure 7: Results of CCA analysis applied to the Northern Hemisphere dataset; A, Diagram showing the ordination of the dinocyst taxa and environmental variables along the two first axes (see figure 4A for legend). The shaded zone point out a group of heterotrophic taxa that are positively correlated with CCA axes 1 and 2; B, Samples CCA axes 1 and 2 scores; C, eigenvalues, species-environment correlation and variance of species data and species-environment relationship for the four first ordination axes; D, Correlation matrix between environmental parameters and the first four ordination axes.

Figure 8: Map showing the distribution of the minimum distance of the closest analogue in the case of the “n=1171” database. This distance gives information about the quality of analogues and reconstructions. Note that the threshold for acceptable

analogue is 77.22. Numbers and percentages of sites corresponding to distance ranges are shown in parenthesis.

Figure 9: Results of cross-validation tests using the leave-one-out technique for the North Atlantic dataset. MAT was applied with both CZCS and MODIS data by a non-constrained selection of the best 5 analogues. The estimated versus observed values of seasonal and annual productivity and their respective coefficient of correlations and RMSEs are also shown. Note that scale differs according to the season and the modern productivity data set.

Figure 10: Results of cross-validation tests using the leave-one-out technique for the North Pacific dataset. See legend of figure 9 for more explanation.

Figure 11: Results of cross-validation tests using the leave-one-out technique for the Northern Hemisphere “n=1171” dataset. See legend of figure 9 for more explanation.

Figure 12: Maps showing anomalies from dinocyst-based reconstruction (difference between observed and estimated) using annual and seasonal MODIS data (left panel) and the annual and seasonal differences between CZCS and MODIS modern data (right panel).

Figure 13: Northern Hemisphere and Core HU 91-045-094 samples scores of the two first ordination axes as generated by correspondence analysis.

Figure 14: Percentages of main dinocyst taxa and sample scores of CA axes 1, 2 and 3 in core HU91-045-094.

Figure 15: Geochemical and micropaleontological data of core HU 91-045-094. Reworked palynomorphs, pollen and spores, dinocysts and organic linings of benthic

foraminifers are presented by their fluxes (number $\text{cm}^{-2} \text{ky}^{-1}$). Isotopic data and the chronology are from Hillaire-Marcel and Bilodeau (2000). Geochemical and micropaleontological data were reported by Hillaire-Marcel et al. (1994) and de Vernal et al. (2000). LGM, Last Glacial Maximum interval; YD, Younger Dryas; H1 and H2, Heinrich events 1 and 2.

Figure 16: Reconstruction of paleoproductivity for the last 25 000 years from dinocyst data in core HU 91-045-094 based on MAT and using the “n = 1171” dinocyst database. We used both MODIS productivity data (solid line) and CZCS data (dotted line). LGM, Last Glacial Maximum interval; YD, Younger Dryas; H1 and H2, Heinrich events 1 and 2.

3.10 Table captions

Table 1: List of dinocyst taxa used in this study with abbreviations, occurrences and percentage ranges. The heterotrophic taxa are marked by asterisks (*).

Table 2: Table summarizing the ranges of SST, SSS and sea-ice cover for the North Atlantic, North Pacific and Arctic databases.

Table 3: Results of forward selection and Monte Carlo permutation test for the Arctic, North Atlantic, North Pacific and the Northern Hemisphere datasets. λ is the eigenvalue explained by environmental variable. It represents the weighted contribution of each parameter. Note that P-value is lower than 0.05 for all parameters illustrating a significant relationships with dinocyst assemblages. Asterisks indicate parameters having VIF value >10 , and are thus considered to covary with other parameters.

Table 4: Table summarizing the coefficient of correlations between observed and estimated values and the RMSE (accuracy of reconstruction), as obtained from the cross-validation test with the Northern Hemispheric dataset using both CZCS and MODIS data. The standard deviation of the residual between MODIS and CZCS data is shown for comparison with RMSE yielded by cross-validation tests.

Figure 1

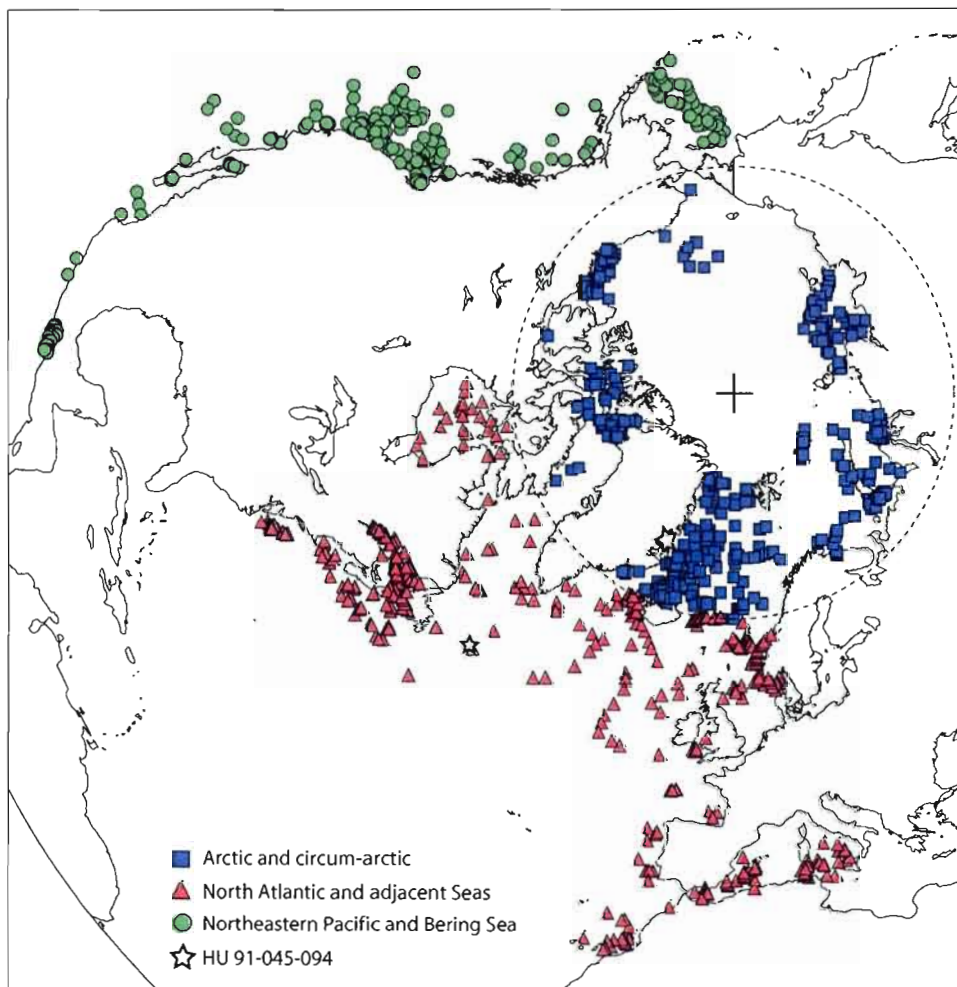


Figure 2

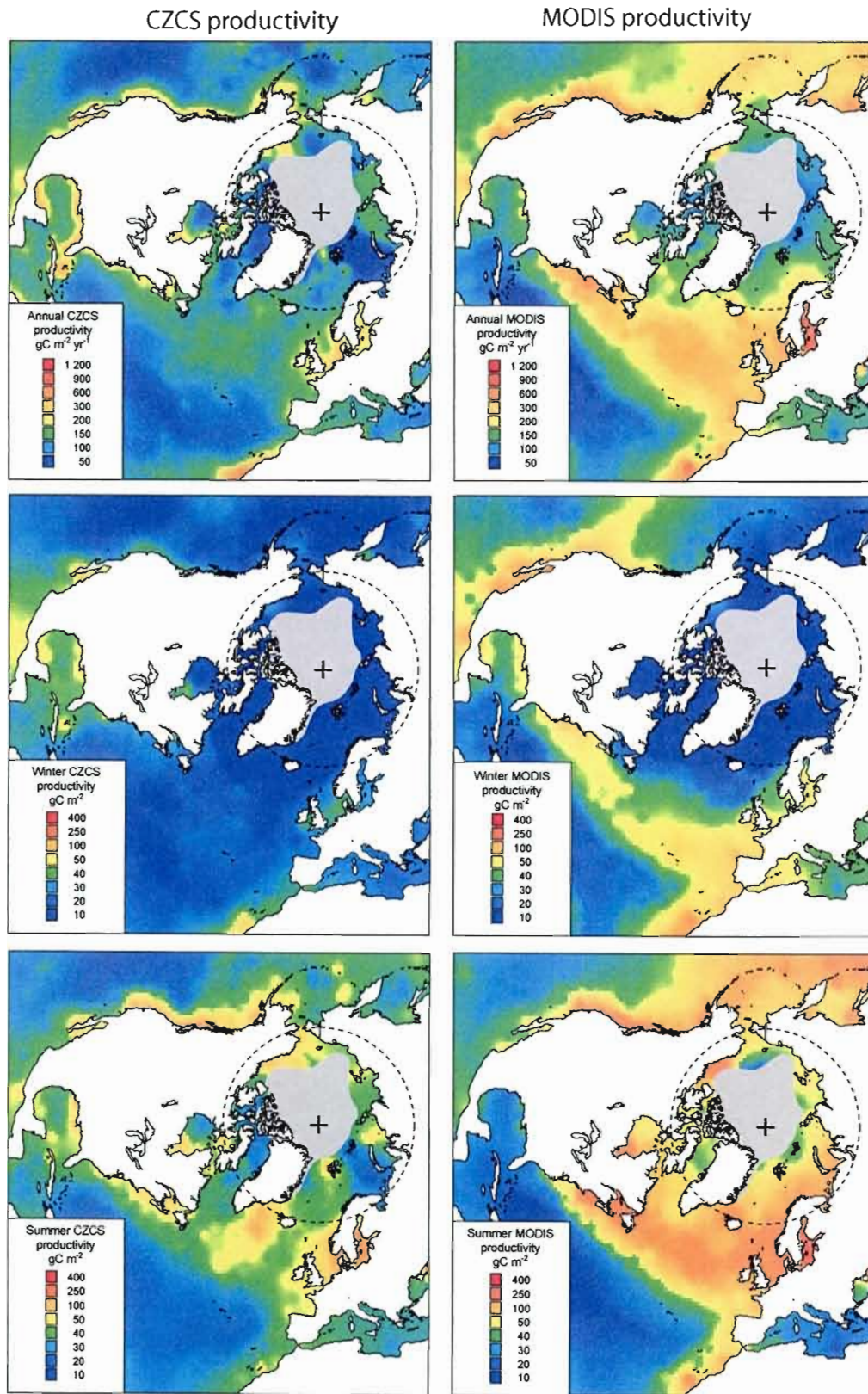


Figure 3

MODIS - CZCS

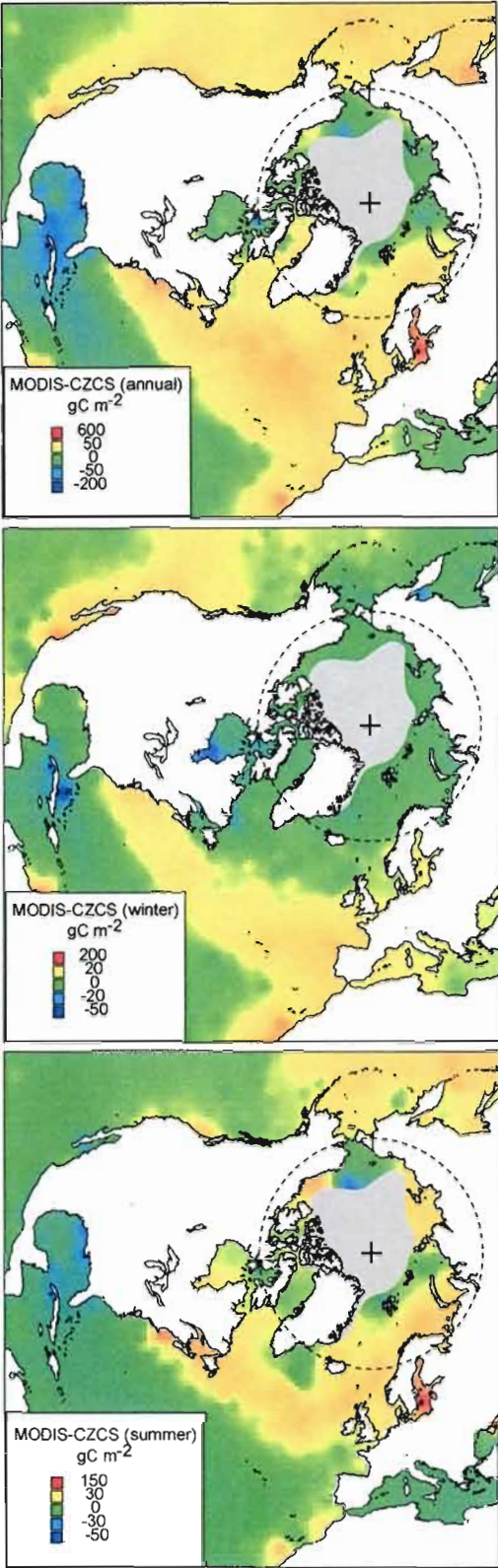
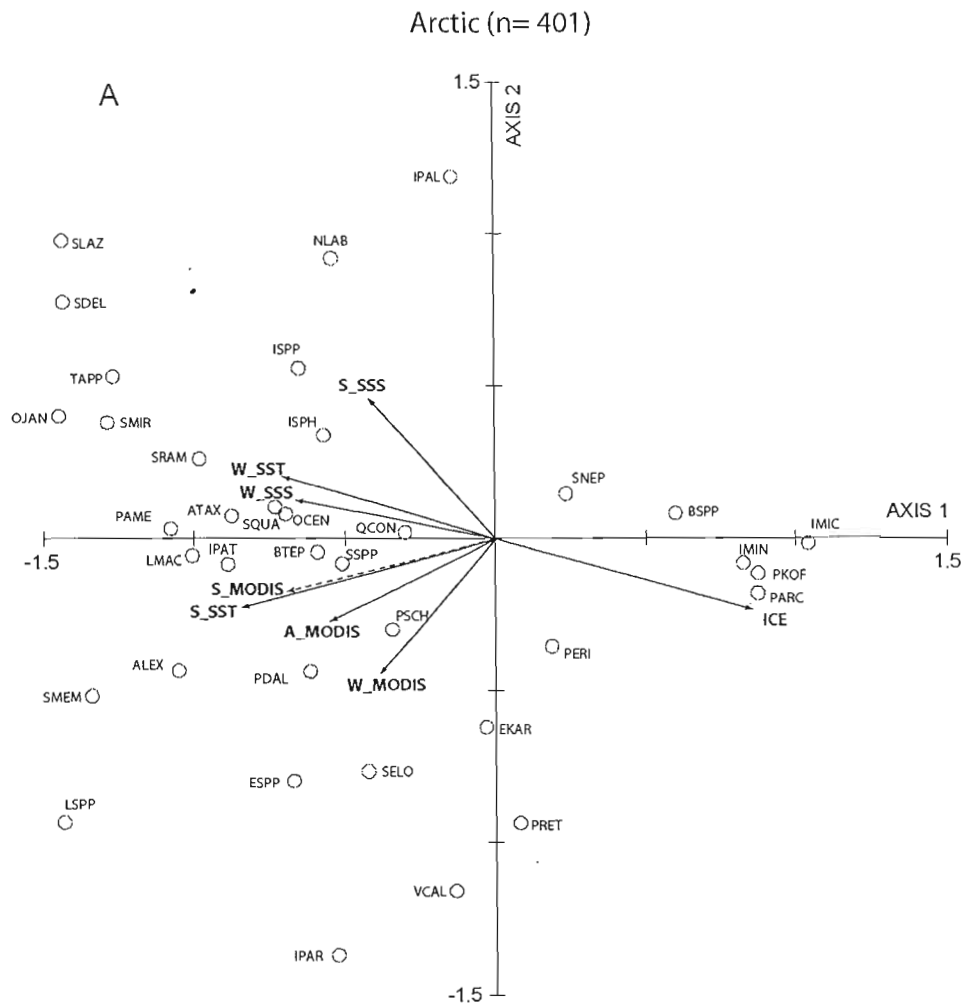


Figure 4



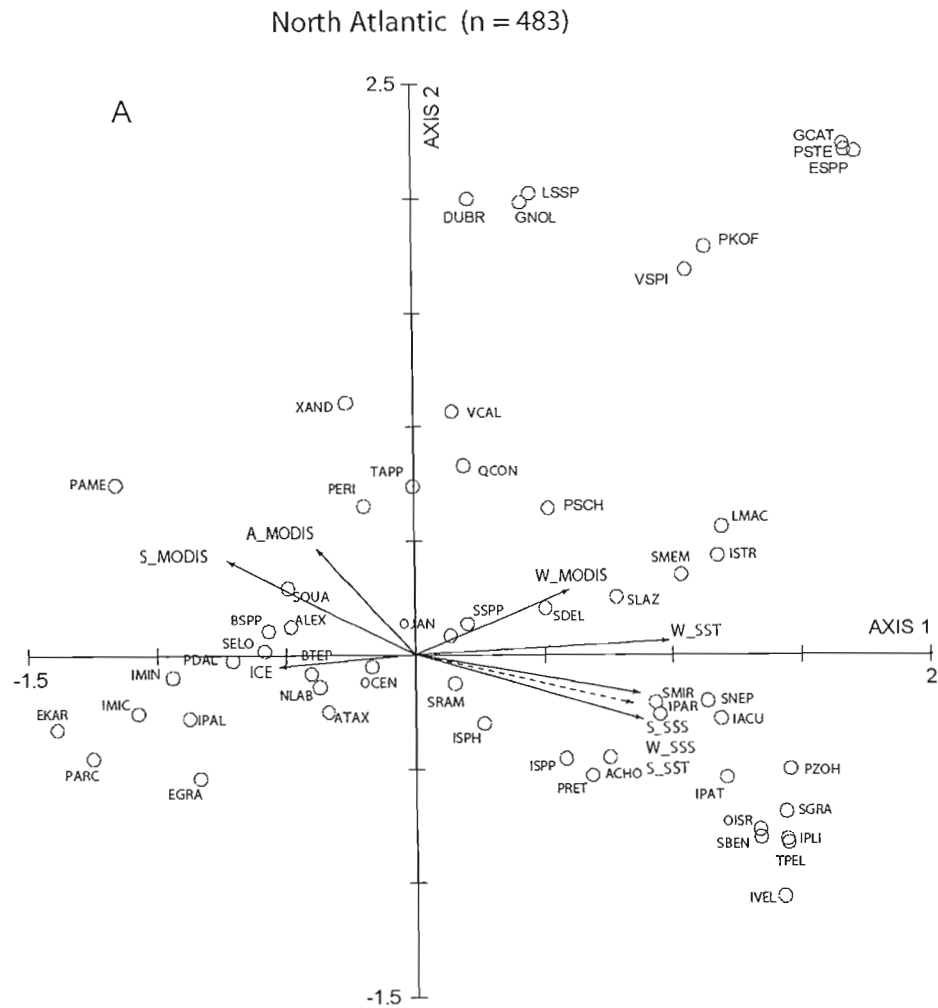
B

Axes	1	2	3	4	Total inertia
Eigenvalues:	0.478	0.143	0.062	0.054	2.102
Species-environment correlations:	0.835	0.645	0.626	0.525	
Cumulative percentage variance					
of species data:	22.7	29.5	32.5	35	
of species-environment relation:	60.7	78.8	86.7	93.6	

C

	SPEC AX1	SPEC AX2	SPEC AX3	SPEC AX4
W_MODIS	-0.2944	-0.2707	0.2147	-0.0758
S_MODIS	-0.4361	-0.17	0.0195	0.0853
A_MODIS	-0.537	-0.1102	0.0925	0.1275
W_SST	-0.5555	0.1207	0.2916	-0.017
W_SSS	-0.5174	0.0739	-0.268	-0.2488
S_SST	-0.6761	-0.1373	0.1626	0.1233
S_SSS	-0.3321	0.2741	-0.2492	-0.0975
ICE	0.679	-0.1423	0.0057	-0.1883

Figure 5



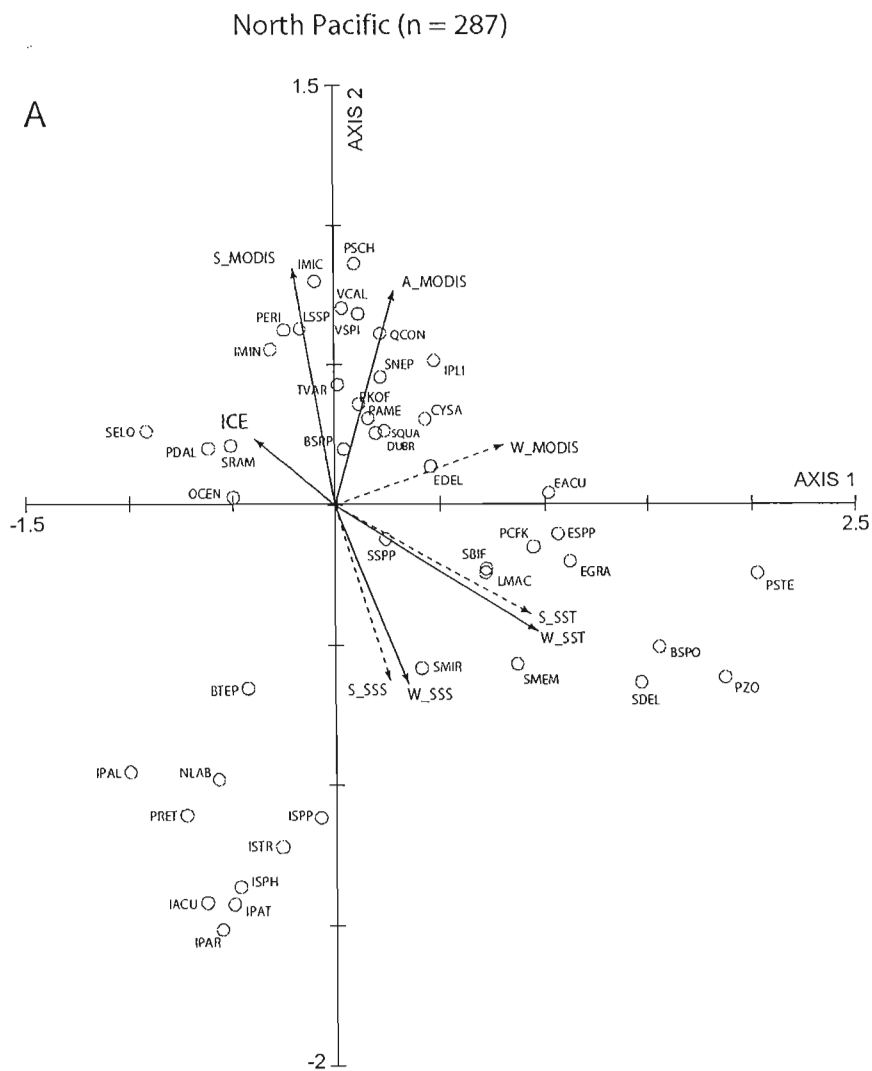
B

Axes	1	2	3	4	Total inertia
Eigenvalues:	0.477	0.142	0.112	0.081	2.676
Species-environment correlations:	0.961	0.683	0.786	0.718	
Cumulative percentage variance					
of species data:	17.8	23.1	27.3	30.3	
of species-environment relation:	49.3	64	75.5	83.9	

C

	SPEC AX1	SPEC AX2	SPEC AX3	SPEC AX4
W_MODIS	0.5336	0.1775	-0.1418	0.1955
S_MODIS	-0.6551	0.2607	-0.0284	0.1304
A_MODIS	-0.4101	0.2911	-0.1824	0.1202
W_SST	0.9171	0.0397	-0.1205	-0.0916
W_SSS	0.7743	-0.1268	-0.129	-0.1325
S_SST	0.8003	-0.1729	-0.1163	0.1231
S_SSS	0.7777	-0.1222	-0.2121	-0.1428
ICE	-0.4492	-0.0329	0.6644	0.0205

Figure 6



B

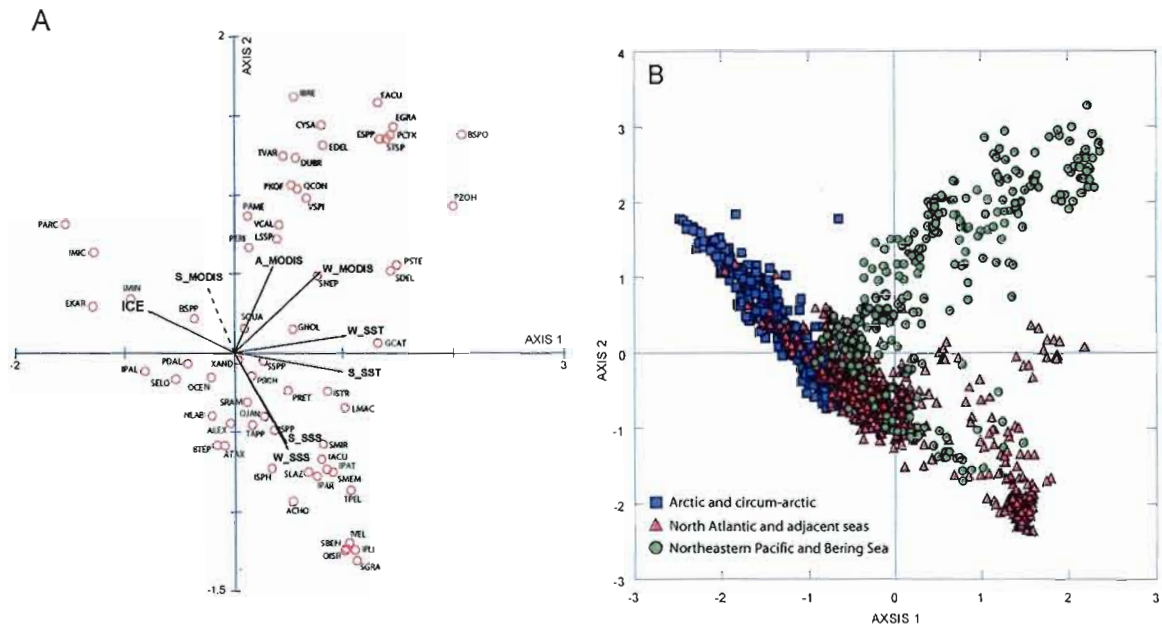
Axes	1	2	3	4	Total inertia
Eigenvalues:	0.388	0.26	0.125	0.08	2.183
Species-environment correlations:	0.93	0.845	0.753	0.771	
Cumulative percentage variance					
of species data:	17.8	29.7	35.4	39.1	
of species-environment relation:	39.8	66.5	79.3	87.5	

C

	SPEC AX1	SPEC AX2	SPEC AX3	SPEC AX4
W_MODIS	0.6843	0.1548	0.2386	-0.054
S_MODIS	-0.1796	0.6734	0.162	-0.3984
A_MODIS	0.237	0.5982	0.3544	-0.2588
W_SST	0.8301	-0.3444	-0.0167	-0.0727
W_SSS	0.2744	-0.493	0.0231	0.5069
S_SST	0.8044	-0.2955	-0.1074	-0.0628
S_SSS	0.1974	-0.4814	0.0375	0.511
ICE	-0.3016	0.1647	-0.3296	0.453

Figure 7

Northern Hemisphere (n = 1171)



C

Axes	1	2	3	4	Total inertia
Eigenvalues:	0.419	0.28	0.176	0.058	3.319
Species-environment correlations:	0.951	0.838	0.836	0.585	
Cumulative percentage variance					
of species data:	12.6	21.1	26.4	28.1	
of species-environment relation:	39	65.2	81.6	87.1	

D

	SPEC AX1	SPEC AX2	SPEC AX3	SPEC AX4
W_MODIS	0.7155	0.3999	-0.0931	-0.1089
S_MODIS	-0.1979	0.3026	-0.5526	-0.1727
A_MODIS	0.3228	0.422	-0.5242	-0.173
W_SST	0.9223	0.0827	0.133	0.0181
W_SSS	0.4527	-0.4758	-0.0774	0.23
S_SST	0.8932	-0.0932	0.0445	-0.0399
S_SSS	0.4321	-0.4498	0.0423	0.2418
ICE	-0.6881	0.2035	0.4959	0.0138

Figure 8

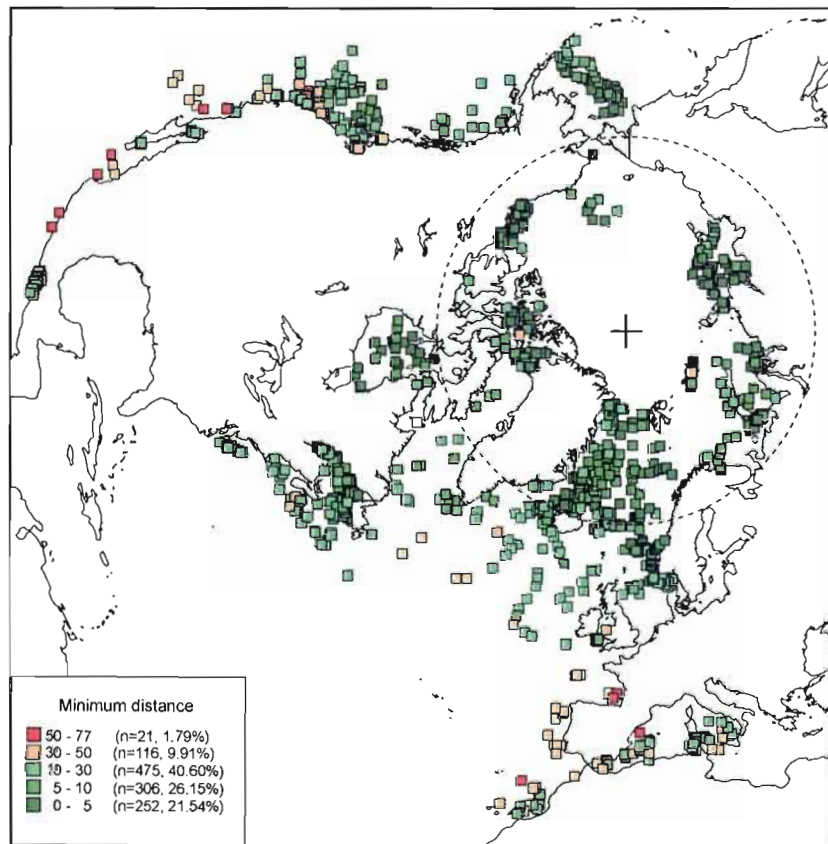


Figure 9

North Atlantic (n = 483)

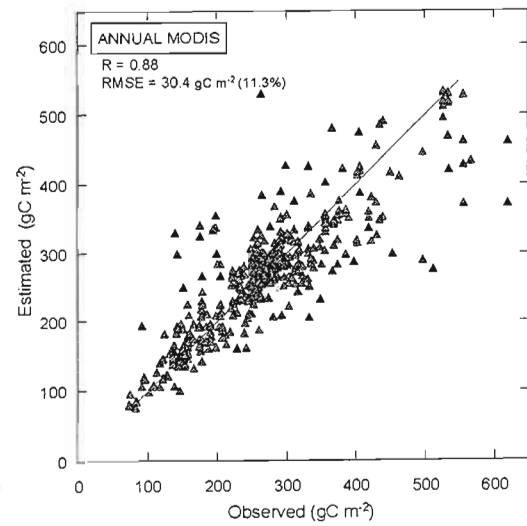
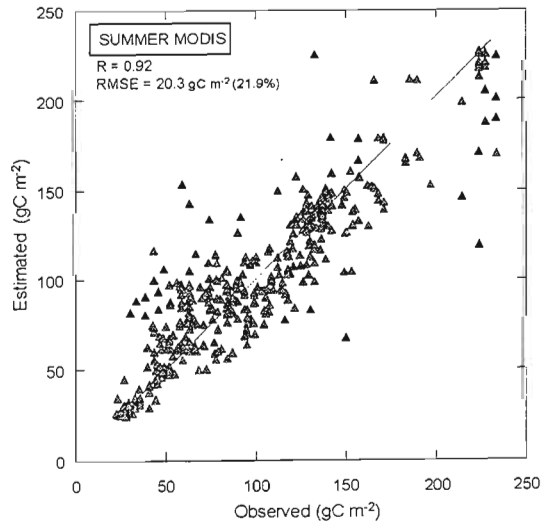
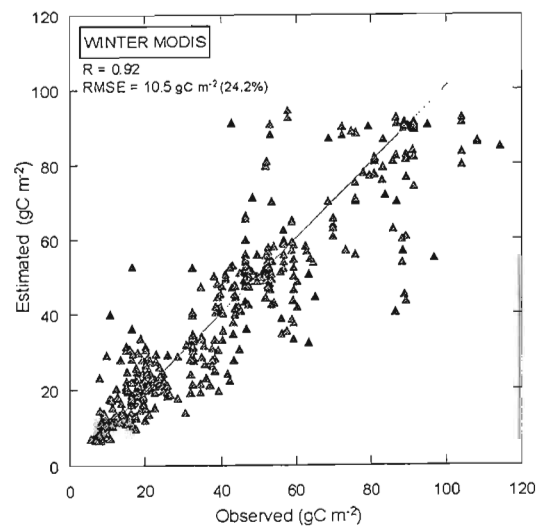
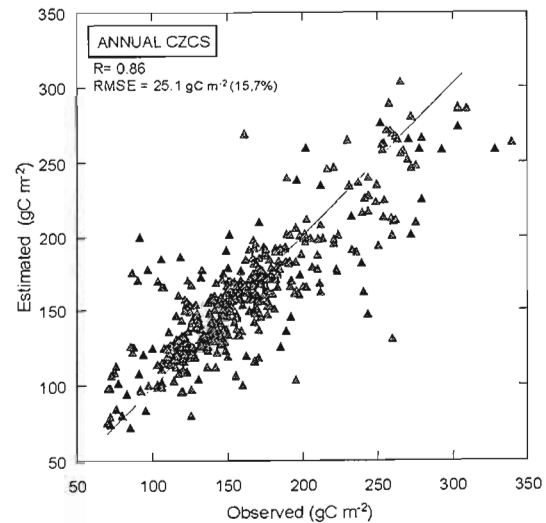
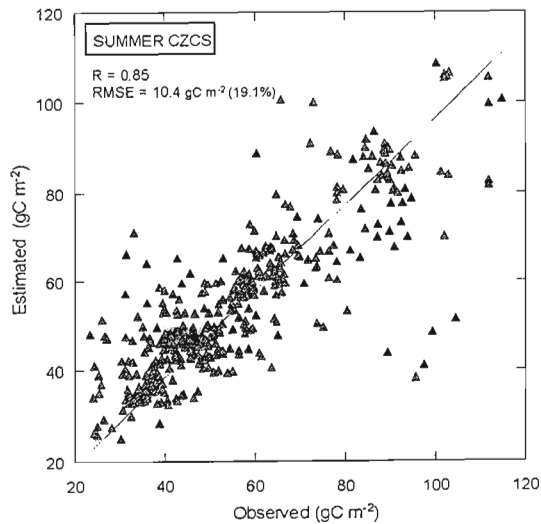
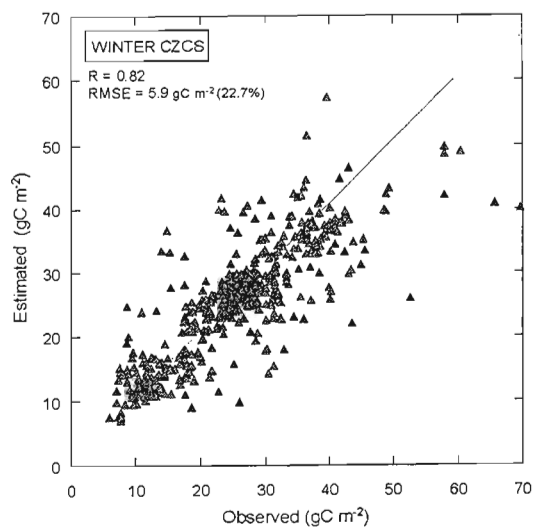


Figure 10

North Pacific (n = 287)

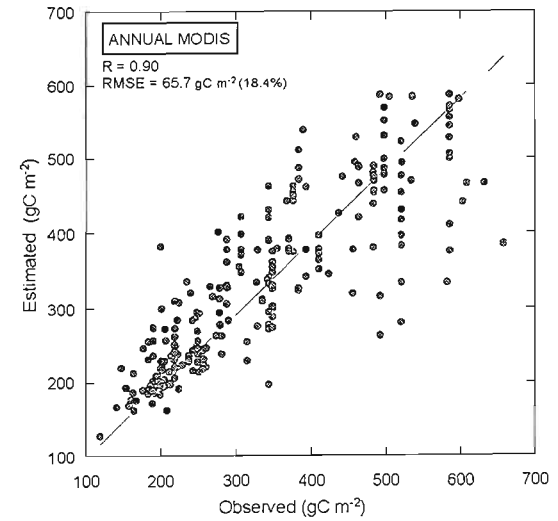
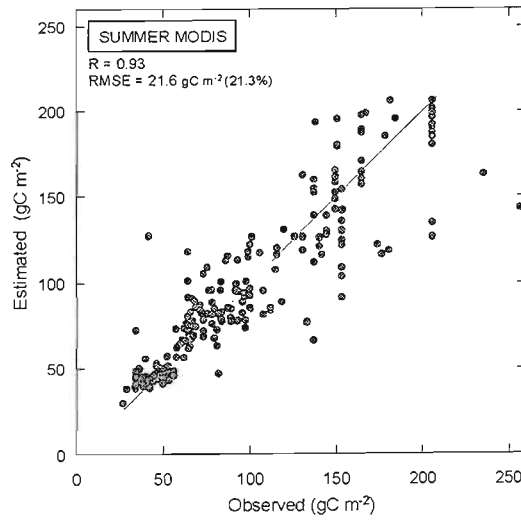
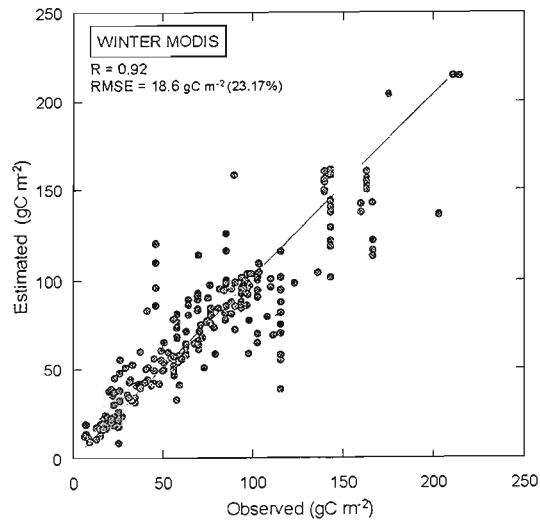
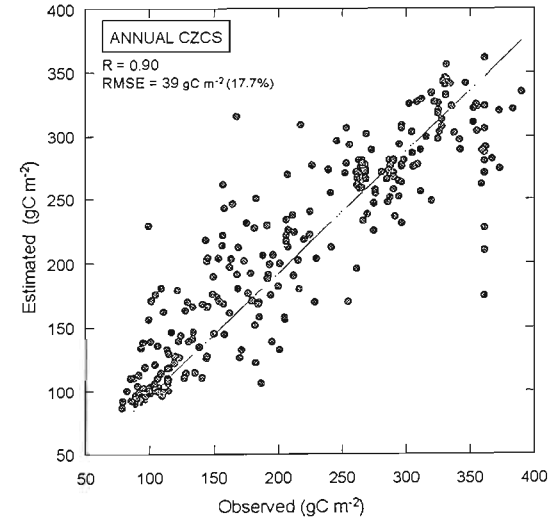
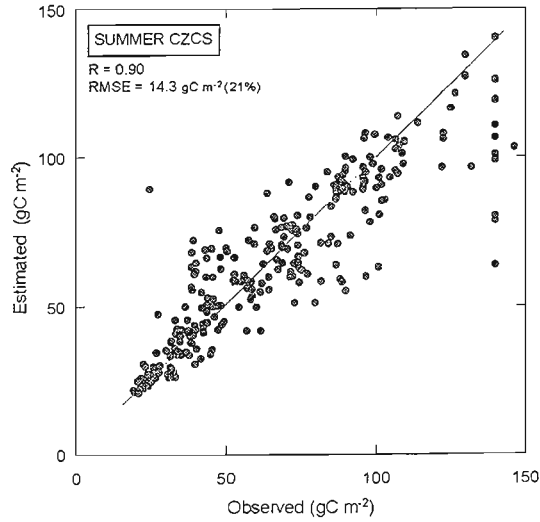
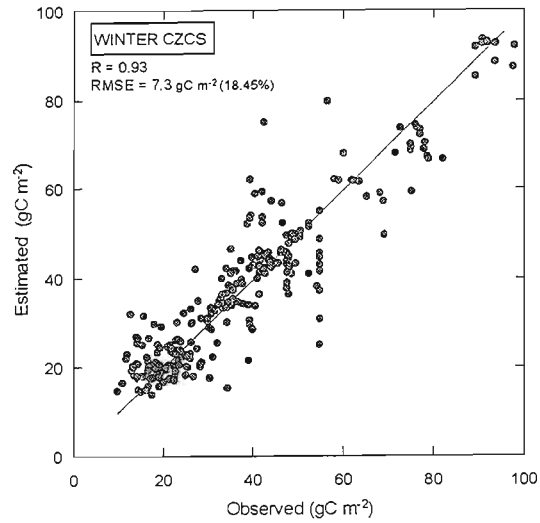


Figure 11

Northern Hemisphere (n = 1171)

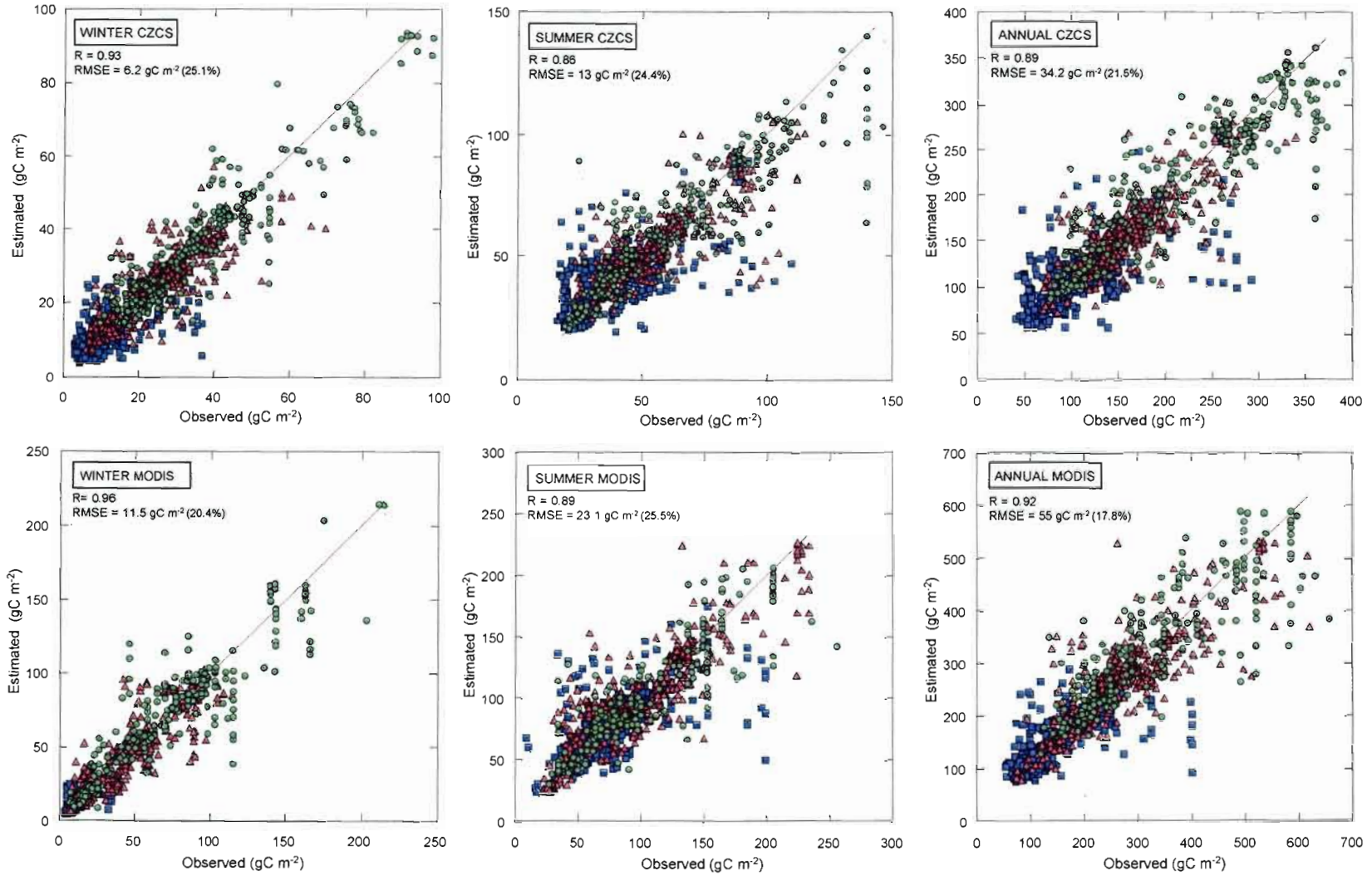


Figure 12

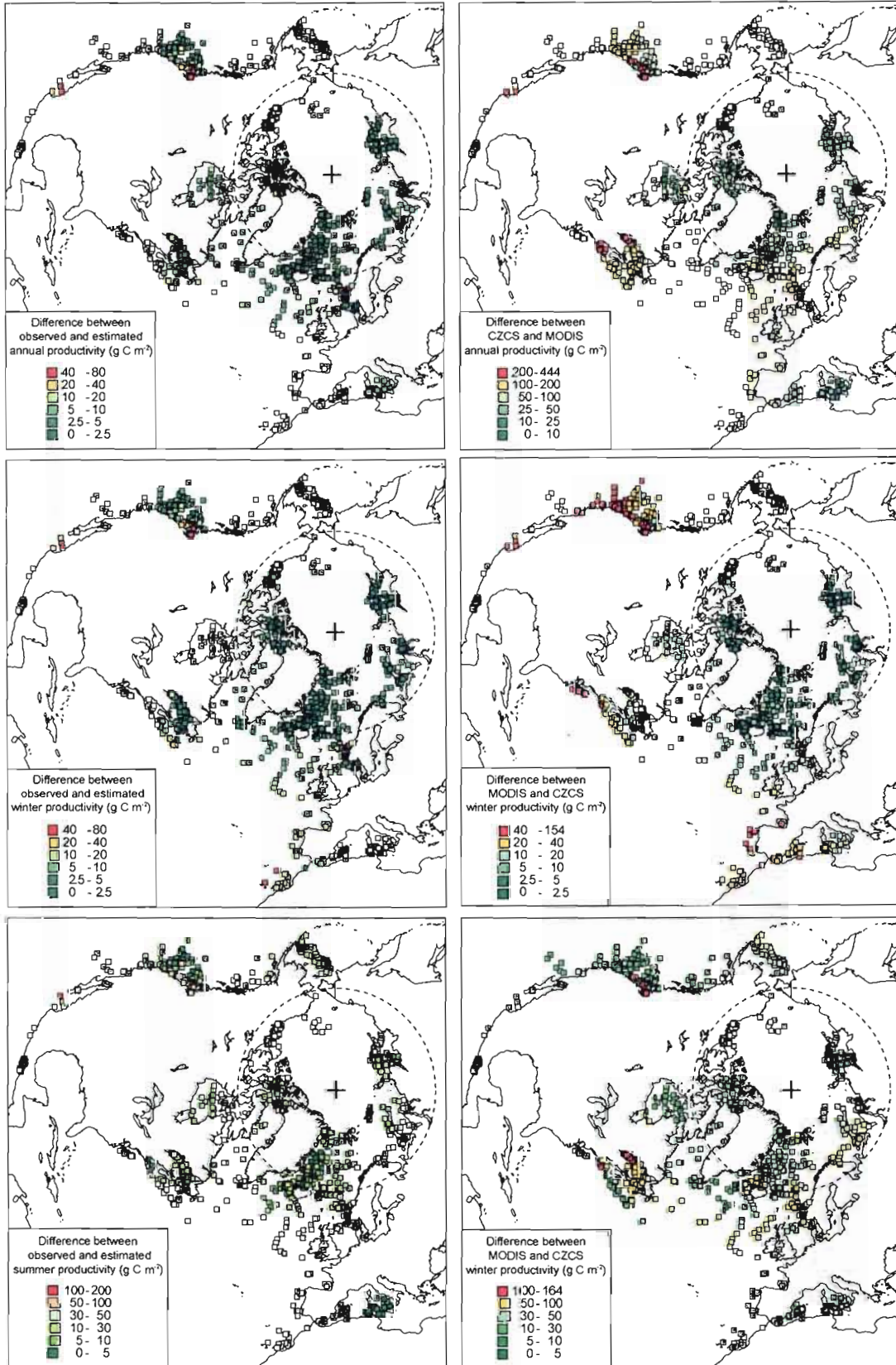


Figure 13

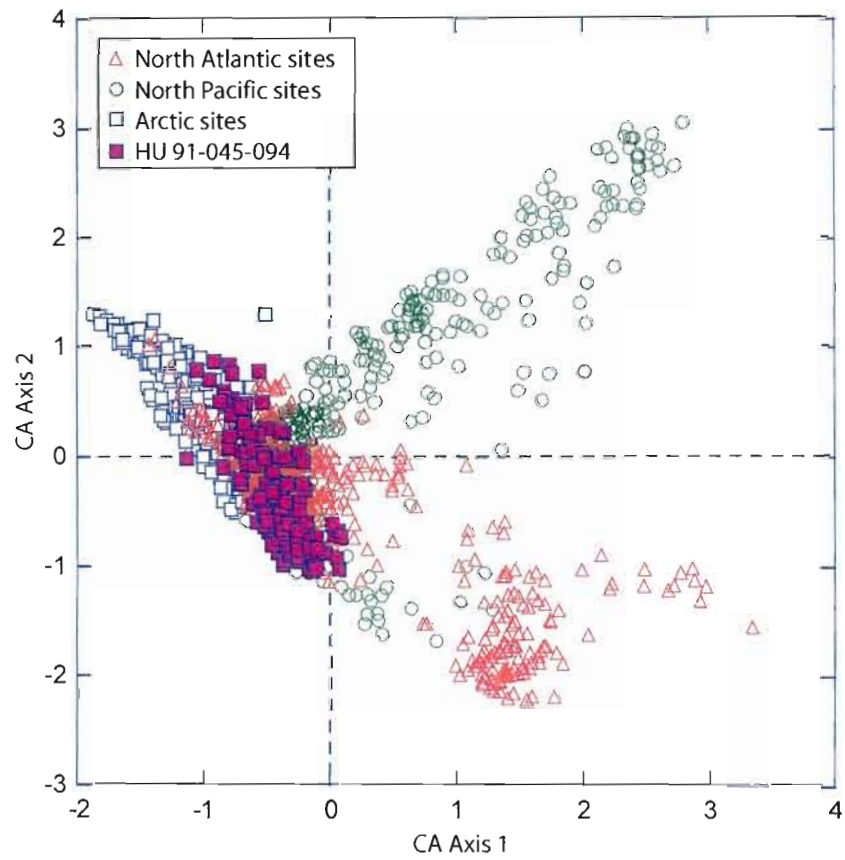


Figure 14

HU 91-045-094

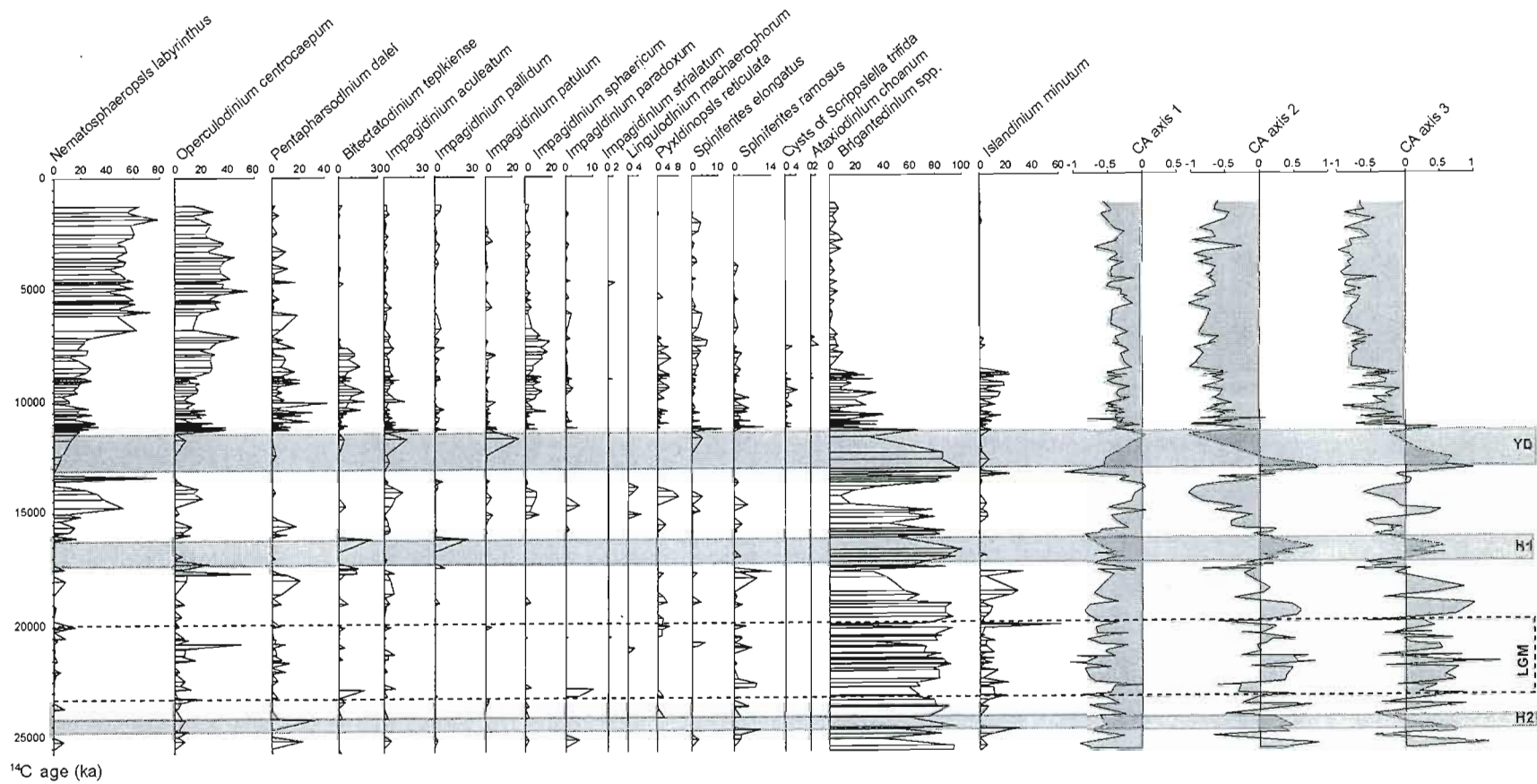


Figure 15

Core HU 91-045-094

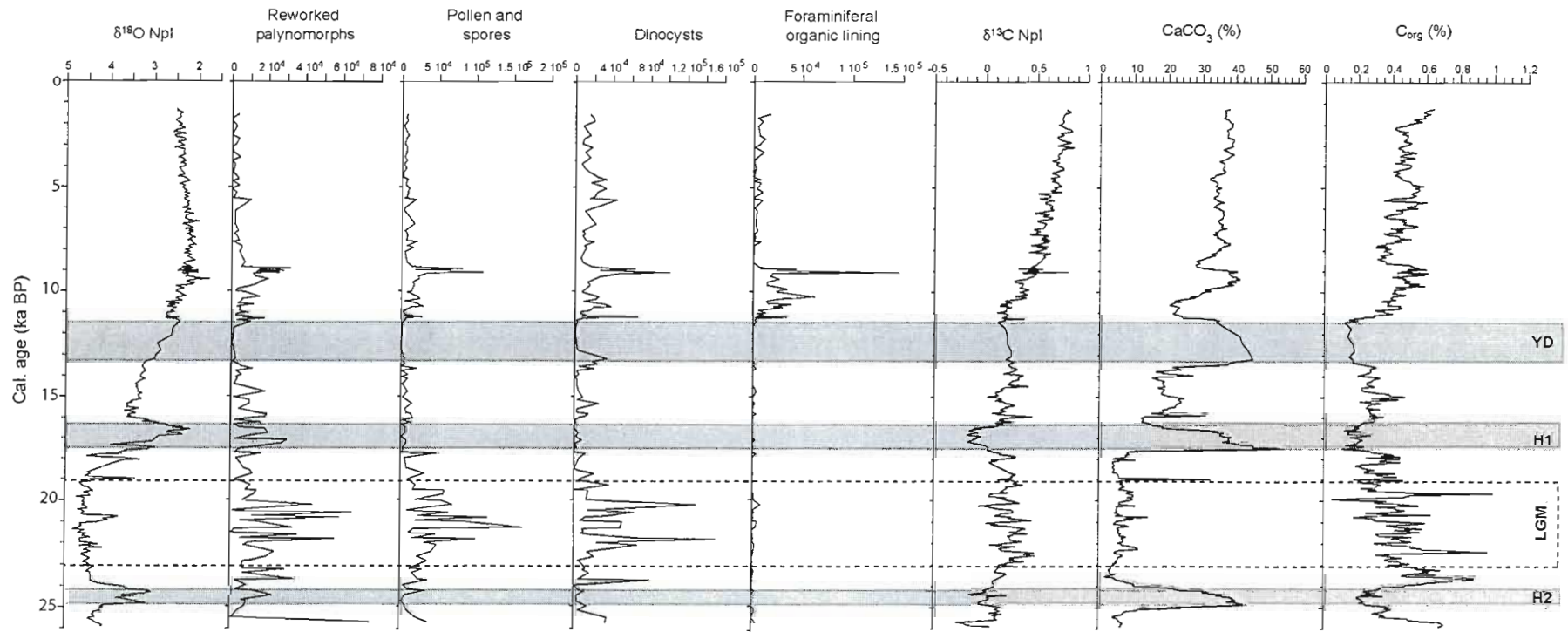


Figure 16

Core HU 91-045-094

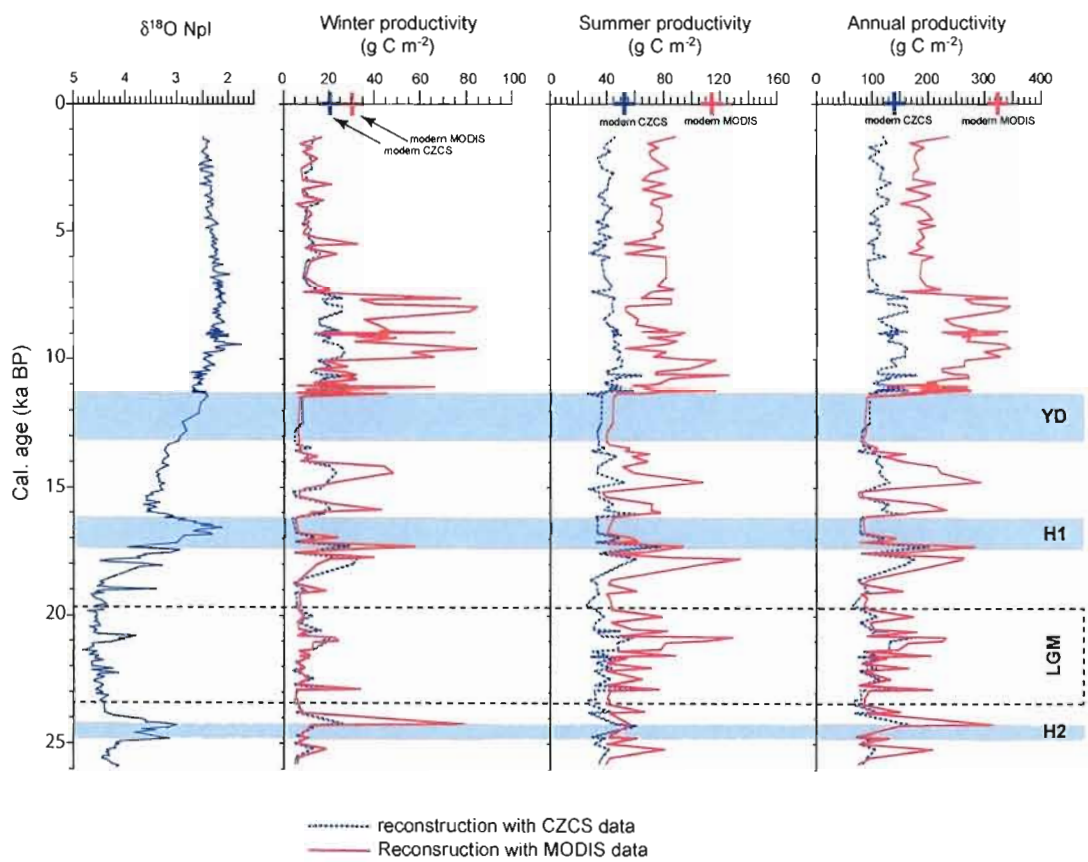


Table 1

Taxa name	Abbreviation	Notes	Occurrence	Percentage range
<i>Achomospaera</i> spp.	ACHO		Atlantic	0 - 5.26
<i>Ataxiodinium choane</i>	ATAX		Arctic, Atlantic, Pacific	0 - 3.38
<i>Bitectatodinium spongium</i>	BSPO		Pacific	0 - 62.5
<i>Bitectatodinium tepikiense</i>	BTEP		Arctic, Atlantic, Pacific	0 - 30
<i>Brigantedinium cariacense</i> *	BCAR	Grouped with <i>Brigantedinium</i> spp.	Arctic, Atlantic, Pacific	-
<i>Brigantedinium simplex</i> *	BSIM	Grouped with <i>Brigantedinium</i> spp.	Arctic, Atlantic, Pacific	-
<i>Brigantedinium</i> spp.*	BSPM		Arctic, Atlantic, Pacific	0 - 97.25
Cyst A*	CYSA		Pacific	0 - 4.9
Cyst of cf. <i>Scrippsiella trifida</i>	ALEX		Arctic, Atlantic, Pacific	0 - 17.15
Cyst of <i>Pentaparsodinium dalei</i>	PDAL		Arctic, Atlantic, Pacific	0 - 95.89
Cyst of <i>Polykrikos cf. kofoidii</i> *	PCFK		Pacific	0 - 13.19
Cyst of <i>Polykrikos kofoidii</i> *	PKOF		Arctic, Atlantic, Pacific	0 - 15.79
Cyst of <i>Polykrikos schwartzi</i> *	PSCH		Arctic, Atlantic, Pacific	0 - 77.19
Cyst of <i>Polykrikos</i> spp. - Arctic morphotype*	PARC		Arctic, Atlantic	0 - 14.82
Cyst of <i>Polykrikos</i> spp. - quadrangular morphotype*	PQUA	Grouped with cyst of <i>Polykrikos</i> spp. - Arctic morphotype	Arctic, Atlantic	-
Cyst of <i>Protooperidinium americanum</i> *	PAME		Arctic, Atlantic, Pacific	0 - 16.34
Cyst of <i>Protooperidinium nudum</i> *	PNUD	Grouped with <i>S. quanta</i>	Arctic, Atlantic, Pacific	-
<i>Dubridinium</i> spp.*	DUBR		Atlantic, Pacific	0 - 15.99
<i>Echinidinium aculeatum</i> *	EACU		Pacific	0 - 19.87
<i>Echinidinium karaense</i> *	EKAR		Arctic, Atlantic	0 - 8.33
<i>Echinidinium delicatum</i> *	EDEL		Pacific	0 - 11.52
<i>Echinidinium granulatum</i> *	EGRA		Atlantic, Pacific	0 - 21.72
<i>Echinidinium</i> spp.*	ESPP		Arctic, Atlantic, Pacific	0 - 31.19
<i>Gymnodinium catenatum</i> *	GCAT		Atlantic	0 - 48.98
<i>Gymnodinium nolleri</i> *	GNOL		Atlantic	0 - 0.74
<i>Impagidinium aculeatum</i>	IACU		Atlantic, Pacific	0 - 80
<i>Impagidinium pallidum</i>	IPAL		Arctic, Atlantic, Pacific	0 - 39.58
<i>Impagidinium paradoxum</i>	IPAR		Arctic, Atlantic, Pacific	0 - 13.65
<i>Impagidinium patulum</i>	IPAT		Arctic, Atlantic, Pacific	0 - 27.21
<i>Impagidinium pilicatum</i>	IPLI		Atlantic, Pacific	0 - 3.77
<i>Impagidinium sphaericum</i>	ISPH		Arctic, Atlantic, Pacific	0 - 8.77
<i>Impagidinium</i> spp.	ISPP		Arctic, Atlantic, Pacific	0 - 6.52
<i>Impagidinium striolatum</i>	ISTR		Atlantic, Pacific	0 - 24.83
<i>Impagidinium velorum</i>	IVEL		Atlantic, Pacific	0 - 2.38
<i>Islandinium brevispinosum</i> *	IBRE		Atlantic, Pacific	0 - 0.79
<i>Islandinium minutum</i> *	IMIN		Arctic, Atlantic, Pacific	0 - 96.83
<i>Islandinium? cesare</i> *	IMIC		Arctic, Atlantic, Pacific	0 - 32.26
<i>Lejeuncysta oliva</i> *	LOLI	Grouped with <i>Lejeuncysta</i> spp.	Arctic, Atlantic, Pacific	-
<i>Lejeuncysta sabrina</i> *	LSAB	Grouped with <i>Lejeuncysta</i> spp.	Atlantic, Pacific	-
<i>Lejeuncysta</i> spp.*	LSSP		Arctic, Atlantic, Pacific	0 - 2.36
<i>Lingulodinium machaerophorum</i>	LMAC		Arctic, Atlantic, Pacific	0 - 80.2
<i>Nematosphaeropsis labyrinthus</i>	NLAB		Arctic, Atlantic, Pacific	0 - 71.54
<i>O. centrocarpum</i> sensu Wall & Dale 1966 - short processes	OCSS	Grouped with <i>O. centrocarpum</i> sensu Wall & Dale 1966	Arctic, Atlantic, Pacific	-
<i>Operculodinium centrocarpum</i> sensu Wall & Dale 1966	OCEN		Arctic, Atlantic, Pacific	0 - 90.52
<i>Operculodinium centrocarpum</i> - Arctic morphotype	OARC	Grouped with <i>O. centrocarpum</i> sensu Wall & Dale 1966	Arctic, Atlantic, Pacific	-
<i>Operculodinium centrocarpum</i> - morphotype cesare	OCEZ	Grouped with <i>O. centrocarpum</i> sensu Wall & Dale 1966	Arctic, Atlantic, Pacific	-
<i>Operculodinium cf. janduchenei</i>	OJAN		Arctic, Atlantic, Pacific	0 - 3.45
<i>Operculodinium israelianum</i>	OISR		Atlantic, Pacific	0 - 12.81
<i>Polysphaeridium zoharyi</i>	PZOH		Atlantic, Pacific	0 - 40.48
<i>Protooperidinioids</i> *	PERI		Arctic, Atlantic, Pacific	0 - 16.62
<i>Protooperidinium stellatum</i> *	PSTE		Atlantic, Pacific	0 - 26.52
<i>Pyxidropsis reticulata</i>	PRET		Arctic, Atlantic, Pacific	0 - 60.78
<i>Quinquecuspis concreta</i> *	QCON		Arctic, Atlantic, Pacific	0 - 30.12
<i>Selenopemphix nephroides</i> *	SNEP		Arctic, Atlantic, Pacific	0 - 9.09
<i>Selenopemphix quanta</i> *	SQUA		Arctic, Atlantic, Pacific	0 - 21.52
<i>Spiniferites beherius</i>	SBEL	Grouped with <i>S. membranaceus</i>	Arctic, Atlantic, Pacific	-
<i>Spiniferites bentorii</i>	SBEN		Atlantic, Pacific	0 - 10.87
<i>Spiniferites bulloides</i>	SBUL	Grouped with <i>S. ramosus</i>	Arctic, Atlantic, Pacific	-
<i>Spiniferites delcatus</i>	SDEL		Arctic, Atlantic, Pacific	0 - 57.77
<i>Spiniferites elongatus</i>	SELO		Arctic, Atlantic, Pacific	0 - 47.99
<i>Spiniferites frigidus</i>	SFRI	Grouped with <i>S. elongatus</i>	Arctic, Atlantic, Pacific	-
<i>Spiniferites lazus</i>	SLAZ		Arctic, Atlantic	0 - 2.2
<i>Spiniferites membranaceus</i>	SMEM		Arctic, Atlantic, Pacific	0 - 23.38
<i>Spiniferites mirabilis-hyperacanthus</i>	SMIR		Arctic, Atlantic, Pacific	0 - 77
<i>Spiniferites ramosus</i>	SRAM		Arctic, Atlantic, Pacific	0 - 57.33
<i>Spiniferites ramosus</i> type granosus	SGRA		Atlantic	0 - 5.73
<i>Spiniferites</i> spp.	SSPP		Arctic, Atlantic, Pacific	0 - 23.97
<i>Steladanium</i> sp.*	STSP		Pacific	0 - 1.3
<i>Tectatodinium pellitum</i>	TPEL		Atlantic, Pacific	0 - 1.73
<i>Trinovantedinium applanatum</i> *	TAPP		Arctic, Atlantic, Pacific	0 - 20.24
<i>Trinovantedinium variabile</i> *	TVAR		Pacific	0 - 1.36
<i>Votadinium calvum</i> *	VCAL		Arctic, Atlantic, Pacific	0 - 2.8
<i>Votadinium spinosum</i> *	VSPI		Atlantic, Pacific	0 - 3.39
<i>Xandarodinium xanthum</i> *	XAND		Atlantic	0 - 0.88

Table 2

	Winter SST (°C)	Summer SST (°C)	Winter SSS	Summer SSS	Sea ice cover (months yr ⁻¹)
North Atlantic	-1.6 to 18.5	0.7 to 26	14.5 to 38	20.6 to 38.2	0 to 8.8
North Pacific	-1.7 to 27.8	6.7 to 30.5	23.11 to 35.4	16.4 to 35.9	0 to 4.7
Arctic	-2.1 to 6.7	-1.8 to 11.3	6.2 to 41.5	6.7 to 35.1	0 to 12

Table 3

Arctic				
Marginal Effects		Conditional Effects		
Variable	λ	Variable	λ	P-value
Sea ice	0.33	Sea ice	0.33	0.005
S_SST	0.33	W_MODID	0.13	0.005
W_SST	0.23	W_SSS	0.08	0.005
A_MODIS	0.21	S_SST	0.06	0.005
W_SSS	0.21	W_SST	0.05	0.005
S_MODIS*	0.15	A_MODIS	0.03	0.005
S_SSS	0.12	S_SSS	0.02	0.005
W_MODIS	0.10	S_MODIS*	0.02	0.005

North Atlantic				
Marginal Effects		Conditional Effects		
Variable	λ	Variable	λ	P-value
W_SST	0.44	W_SST	0.44	0.005
S_SST	0.35	Sea ice	0.10	0.005
S_SSS	0.34	S_SST	0.08	0.005
W_SSS*	0.33	W_MODIS	0.08	0.005
S_MODIS	0.26	S_MODIS	0.07	0.005
Sea ice	0.19	A_MODIS	0.06	0.005
W_MODIS	0.18	S_SSS	0.03	0.005
A_MODIS	0.14	W_SSS*	0.01	0.010

North Pacific				
Marginal Effects		Conditional Effects		
Variable	λ	Variable	λ	P-value
W_SST	0.35	W_SST	0.35	0.005
S_SST*	0.33	A_MODIS	0.20	0.005
W_MODIS*	0.24	Sea ice	0.10	0.005
S_MODIS	0.21	S_MODIS	0.07	0.005
A_MODIS	0.20	S_SST*	0.08	0.005
W_SSS	0.16	W_SSS	0.03	0.005
S_SSS*	0.14	W_MODIS*	0.02	0.005
Sea ice	0.11	S_SSS*	0.01	0.025

Northern Hemisphere				
Marginal Effects		Conditional Effects		
Variable	λ	Variable	λ	P-value
W_SST	0.40	W_SST	0.40	0.005
S_SST	0.38	Sea ice	0.19	0.005
W_MODIS	0.31	A_MODIS	0.17	0.005
Sea ice	0.30	S_SST	0.09	0.005
W_SSS	0.20	W_SSS	0.04	0.005
A_MODIS	0.20	W_MODIS	0.03	0.005
S_SSS	0.19	S_MODIS*	0.03	0.005
S_MODIS*	0.15	S_SSS	0.02	0.005

Table 4

	Coefficient of correlation between observed and estimated values		RMSE (accuracy of reconstruction)				Standard deviation (accuracy of intrumental measurements)	
	with CZCS data	with MODIS data	with CZCS data		with MODIS data		(residual, MODIS-CZCS)	
			value in gC m^{-2}	%	value in gC m^{-2}	%	value in gC m^{-2}	%
Winter productivity	0.93	0.96	6.22	25.11	11.52	20.4	26.77	47.4
Summer productivity	0.86	0.89	13.01	24.44	23.1	25.47	35.44	39.08
Annual productivity	0.89	0.92	34.16	21.51	54.97	17.85	87.5	28.4

CONCLUSION GÉNÉRALE

En jouant un rôle extrêmement important sur les échanges du CO₂ entre l'atmosphère et l'océan, la productivité primaire océanique constitue un paramètre clef dans les processus biogéochimique qui contrôlent le système climatique global (e.g. Boyd et Doney, 2002 ; Bopp et al., 2003; Ito et al., 2005). Elle est toutefois complexe, étant liée aux courants océaniques, à la turbulence, aux apports fluviaux et aux mélanges verticaux (upwelling) qui influencent les conditions hydrographiques et la distribution des éléments nutritifs.

Pendant les trois dernières décennies, les estimations de la productivité primaire par des observations satellitaires des océans ont permis d'étudier les variations de la productivité en relation avec les changements climatiques (cf. Gregg et Conkright, 2002 ; Gregg et al., 2003; Antoine et al., 2005). À la lumière de ces nouvelles données, issues notamment des programmes Sea-viewing Wide Field-of-view Sensor (SeaWiifs) et Moderate Resolution Imaging Spectroradiometer (MODIS) de la NASA, Behrenfeld et al. (2006) et Behrenfeld et Siegel (2007) ont démontré que la productivité primaire océanique globale est très bien corrélée avec les événements climatiques globaux comme par exemple les oscillations australes d'El Niño (ENSO). Ils ont montré également que la productivité globale de l'océan a diminué de 190 Tg C an⁻¹ entre 1999 et 2006. Cette variation a été associée à la variabilité climatique globale qui s'est caractérisée par une augmentation de la température et une diminution de l'intensité des upwellings accompagnée par une stratification accrue des masses d'eau dans les basses latitudes. Des simulations à partir des modèles couplés Océan-Atmosphère selon un scénario de doublement des concentrations de CO₂ atmosphérique suggèrent également un réchauffement global qui s'accompagnerait d'une diminution de productivité et de l'intensité des upwellings et une augmentation de la stratification (Bopp et al., 2001). À l'échelle du dernier cycle

climatique, des données géochimiques et de modélisation suggèrent une relation directe entre la productivité primaire et la ventilation de l'océan global (Toggweiler, 1999; Sigman et Boyle, 2000 ; Galbraith et al., 2007). Enfin, à l'échelle du dernier million d'années, des données de carbone organique dans le sédiment ainsi que d'autres traceurs comme le baryum suggèrent une grande variation dans l'amplitude de la productivité biologique (Lyle et al., 1988; Pedersen et al., 1988, 1991; Mix, 1989; Sarnthein et al., 1992; Paytan et Kastner, 1996). Toutefois, la reconstitution quantitative de la paléoprodutivité à partir de séquences sédimentaires demeure une tâche extrêmement difficile et délicate. En effet, l'utilisation du contenu en carbone organique dans le sédiment comme traceur de productivité (Muller et Suess, 1979; Muller et al., 1983; Sarnthein et al., 1988; Berger et al., 1989; Fischer et al., 2000) est limitée notamment par l'oxydation de la matière organique dans la colonne d'eau et dans le sédiment (Emerson et Hedges, 1988, 2003; Meyers, 1997; Rühlemann, 1999). Les microfossiles calcaires ou siliceux (e.g., tests de foraminifères et de diatomées) ont été largement utilisés comme traceurs qualitatifs ou quantitatifs de la paléoprodutivité, soit en utilisant les compositions chimiques ou isotopiques des tests (Mackensen et al., 2000; Lazarus et al., 2006) ou les proportions relatives des taxons dans les assemblages de foraminifères (Loubere, 1996, 1999, 2002; Loubere et Fariduddin, 1999; Cayre et al., 1999; Ivanova et al., 2003) ou de coccolithes (Beaufort et al., 1997, 1999, 2001). Cependant, les microfossiles composés de CaCO_3 peuvent être dissous sous des conditions de $p\text{CO}_2$ élevée en raison d'une ventilation limitée des masses d'eau. Les microfossiles siliceux sont également sensibles à la dissolution à cause de la sous-saturation de l'eau en silice (Nelson et al., 1995; Gallinari et al., 2002). Par ailleurs, la silice biogénique dans le sédiment est influencée, en plus de la dissolution, par des sources terrigènes et volcaniques (Ragueneau et al., 2000). D'autres traceurs géochimiques ont été développés tel le baryum biogénique (Dymond et al., 1992; François et al., 1995; Dymond et Collier, 1996; Jeandel et al., 2000; Eaigle et al., 2003) ou la composition isotopique du thorium et du protactinium (Bradtmiller et al., 2006), mais ces traceurs ont d'autres

limitations dues à notamment à leurs comportements physique et chimique dans les zones d'upwelling ou près des sources hydrothermales (Von Breymann et al., 1992; Dymond et al., 1992; François et al., 1995, 2004; Paytan et al., 1996; Klump et al., 2000). D'une façon générale, l'état de nos connaissances actuelles sur les différents traceurs de la productivité dans les archives sédimentaires marines laisse envisager qu'il est pertinent, sinon nécessaire de développer de nouvelles approches et de nouveaux traceurs si l'on veut aborder le sujet de la paléoprodutivité océanique comme paramètre clef dans les processus biogéochimique qui contrôlent système climatique global.

Dans le cadre de cette thèse, nous avons choisi d'explorer le potentiel des kystes de dinoflagellés comme traceurs quantitatifs de la productivité primaire. En effet, les dinoflagellés constituent, avec les diatomées et les coccolithophores, les principaux producteurs primaires des océans (Parsons et al., 1983) et ont la particularité d'inclure des espèces autotrophes et hétérotrophes. Ils représentent ainsi à la fois une image directe de la productivité via les espèces autotrophes et une image indirecte via les espèces hétérotrophes. En outre, les dinoflagellés occupent tous les milieux marins, allant des zones équatoriales aux zones polaires et des milieux estuariens aux milieux océaniques. Finalement, les composés aromatiques qui entrent dans la composition chimique des dinokystes permettent une meilleure préservation dans le sédiment contrairement aux microfossiles siliceux ou carbonatés.

Nous avons utilisé différentes approches et méthodes pour tester la validité et la robustesse des reconstitutions obtenues par les dinokystes. Les relations entre les assemblages et la productivité ont été évaluées par des analyses multivariées incluant les analyses en composantes principales (PCA), les analyses de redondance (RDA), les analyses de correspondance (CA) ou les analyses canoniques des correspondances (CCA). Des tests de permutations de Monte-Carlo ont été également effectuées pour évaluer le poids statistique de chaque relation et pour détecter d'éventuelles co-

variabilités entre les paramètres hydrographiques et la productivité (cf. Gauch, 1982; Jongman et al., 1995). Enfin, le degré de validité et l'erreur des reconstitutions par la méthode des meilleurs analogues modernes (MAT) ou par la méthode des régressions multiples (MRT) ont été obtenues en utilisant des validations selon la méthode de Jackknife (cf. Efron and Gong, 1983).

Grâce à ces traitements statistiques, nous avons exploré les relations entre la productivité et la distribution des assemblages de dinokystes dans les sédiments de surface à différentes échelles spatiales dans le Pacifique du Nord-est et dans l'hémisphère nord. À toutes ces échelles spatiales, nos résultats démontrent que la productivité primaire constitue un paramètre déterminant de la distribution des assemblages de dinokystes, que ce soit à une échelle régionale dans les milieux néritiques et océaniques le long des côtes ouest américaines (cf. Chapitre I), ou dans les milieux estuariens de la Colombie Britannique (cf. Chapitre II). Toutefois, la relation entre les assemblages et la productivité diffère de celle illustrée pour les zones néritiques et océaniques. Les résultats d'analyses de sédiments estuariens suggèrent que les assemblages de dinokystes peuvent également servir comme traceurs de l'enrichissement en éléments nutritifs d'origine naturelle (upwelling) ou anthropique (pollution marine).

À l'échelle des régions estuariennes, néritiques et océanique du Pacifique du Nord-est, notre étude a permis de dresser un patron détaillé de la distribution des dinokystes dans les sédiments de surface en contribuant à améliorer nos connaissances sur les particularités morphologiques et les affinités écologiques de certains taxons dans cette région jusqu' alors très peu étudiée de point de vue palynologique. Le Pacifique du nord-est se caractérise en effet par des assemblages très différents de ceux de l'Atlantique à des latitudes équivalentes. Certaines espèces semblent exclusives au Pacifique comme par exemple *Polykrikos* cf. *kofoidii* et *Stelladinium* sp. Le taxon *Polykrikos* cf. *kofoidi* se singularise par une petite taille et des processus plus

nombreux et relativement courts comparativement à *P. kofoidii*. Par ailleurs, *Stelladinium* sp. présente une morphologie proche de celle de *Stelladinium stellatum* mais diffère de celle-ci par la présence de bifurcations à la terminaison des processus le long du cingulum. Les sédiments du Pacifique du Nord-est se caractérisent également par la présence de plusieurs espèces connues uniquement dans la mer d'Arabie et dans l'océan austral mais qui n'ont jamais été observées dans les sédiments modernes de l'Atlantique Nord. Il s'agit de *Bitectatodinium spongium*, *Echinidinium aculeatum*, *Echinidinium granulatum*, *Echinidinium delicatum* et *Echinidinium zonneveldiae*. Nous avons démontré également un régionalisme dans les affinités écologiques des différents taxons. Par exemple *P. dalei* est lié à l'influence du fleuve Fraser dans l'environnement restreint du détroit de Géorgie (cf. Chapitre II) alors qu'il est considéré comme associé à la glace de mer dans la Mer de Béring (Radi et al., 2001). La relation entre un taxon particulier et la productivité peut varier également entre l'Atlantique et le Pacifique (cf. Chapitre III). Ces différences pourraient résulter des différences dans les propriétés physico-chimiques des masses d'eau des deux océans (conditions hydrographiques, stratification, courants). Elle pourrait résulter également des adaptations phénotypiques des différentes espèces aux océans Atlantique et Pacifique et/ou de l'existence des espèces cryptiques ayant un même phénotype mais des génotypes et des préférences écologiques différents. Dans cette optique, des analyses génétiques des spécimens du Pacifique appartenant à *Polykrikos*, *Echinidinium* et *Islandinium* seraient d'une grande utilité.

Depuis plus d'une décennie, le développement d'une base de données des assemblages de dinokystes dans l'hémisphère nord a rendu possible l'utilisation des dinokystes comme outil de reconstitutions quantitatives des conditions hydrographiques à l'échelle du quaternaire (cf. de Vernal et al., 2001, 2005). Nous avons amélioré la base de données par nos travaux sur l'Océan Pacifique (près de 165 sites représentatifs des milieux océaniques, néritiques et estuariens). La base de données compte actuellement 1171 sites répartis dans l'Atlantique Nord, l'Océan

Arctique et le Pacifique Nord. L'intégration des données du Pacifique Nord a permis d'élargir la gamme de conditions de productivité représentée dans la base de données, allant de valeurs extrêmement élevées dans les zones d'upwelling le long des marges ouest américaines à des valeurs extrêmement faibles dans les zones arctiques. Les analyses statistiques effectuées sur des régions et sur l'ensemble de cette nouvelle base de données démontrent que le signal de la productivité primaire est bien enregistré dans les assemblages de dinokystes, autorisant ainsi l'utilisation des fonctions de transfert. Toutefois, les méthodes basées sur des calibrations sont inadéquates puisque la relation entre les assemblages et la productivité n'est pas la même d'un bassin à un autre et d'un océan à un autre. Ici nous avons privilégié l'utilisation de la méthode des meilleurs analogues modernes (MAT; Overpeck et al., 1985; Guiot 1990). MAT permet d'éviter les problèmes liés aux régionalismes des assemblages puisque la reconstitution se base uniquement sur le degré de ressemblance entre les assemblages fossiles et les assemblages modernes plutôt que sur une équation liant les assemblages et la productivité comme c'est le cas pour les méthodes basées sur des bases de données de calibrations (e.g., MRT; PLS, WA-PLS). À l'échelle de l'Atlantique Nord, du Pacifique Nord et de l'ensemble de l'hémisphère nord, l'utilisation de la méthode des analogues modernes livre des résultats convaincants, avec des coefficients de corrélation (R) entre les valeurs estimées et mesurées supérieurs à 0,9. Cet exercice montre également que les reconstitutions de la productivité saisonnière et annuelle peuvent être obtenues avec une erreur de prédiction inférieure à la différence entre les données de productivités modernes issues des observations satellitaires de la chlorophylle. À l'échelle de l'hémisphère nord et de l'Atlantique Nord, les productivités saisonnière et annuelle semblent indépendantes des paramètres hydrographiques. Toutefois, en ce qui concerne le Pacifique Nord, la productivité hivernale ne peut être interprétée indépendamment de la température de l'eau de surface en raison de la co-variabilité de ces deux paramètres.

Sur ces bases, nous pouvons conclure que les assemblages de dinokystes dans les séries sédimentaires peuvent être utilisés comme traceurs quantitatifs de la paléoproduktivité en se basant sur la méthode des analogues modernes. Toutefois, l'exploration d'autres méthodes comme celle basée sur des surfaces de réponse (cf. Revised Analogue Methode, RAM) ou celle des réseaux neuronaux serait pertinente afin de vérifier la portée des reconstitutions effectuées par la méthode des analogues modernes. Une approche multi-proxy, intégrant par exemple des traceurs micropaléontologiques et géochimiques serait également très intéressante pour évaluer le potentiel des dinokystes comme traceur privilégié de la productivité.

L'analyse d'une carotte sédimentaire prélevée dans le Nord-ouest de l'Atlantique montre que les assemblages du dernier maximum glaciaire sont dominés par *Brigantedinium* spp. qui est associés aux zones de productivité élevée dans le Pacifique Nord. Toutefois, la reconstitution de la productivité illustre une faible productivité pendant l'épisode glaciaire et une productivité plus élevée pendant l'Holocène. En effet, les assemblages glaciaires ont plus d'analogues modernes dans l'océan Arctique que dans le Pacifique. De ce fait, ces résultats illustrent bien la robustesse de la méthode utilisée, notamment dans les hautes latitudes et met en évidence la nécessité de travailler avec une base de données de référence hémisphérique plutôt qu'avec une base de données régionale. La basse productivité pendant le dernier maximum glaciaire a été également signalée sur des bases qualitatives en utilisant des données micropaléontologiques (e.g., Thomas et al., 1995 ; Rasmussen et al., 2002 ; Nave et al., 2007) ou quantitatives en utilisant la modélisation biogéochimique (e.g., Schmittner, 2005).

Enfin, Bien que la base de données hémisphérique présentée ici soit représentative d'une large gamme de conditions de productivité dans les océans Atlantique, Pacifique et Arctique. Le régionalisme de la relation entre la distribution des dinokystes et la productivité souligne la pertinence de compléter cette base de

données notamment par des sites représentatifs du Pacifique du Nord-Ouest, du Golfe d'Alaska et des moyennes et basses latitudes des océans Atlantique et Pacifique.

BIBLIOGRAPHIE GÉNÉRALE

Antoine, D., André, J.-M., Morel, A., 1996. Oceanic primary production 2. Estimation at global scale from satellite (coastal zone color scanner) chlorophyll. *Global Biogeochemical Cycles* 10, 57-69.

Antoine, D., Morel, A., Howard, R.G., Banzon, V.F., Evans, R.H., 2005. Bridging ocean color observation of the 1980s and 2000s in search of long-term trends. *Journal of Geophysical Research* 110, C06009, doi: 10.1029/2004JC002620.

Archer, S.E., Reimers, C., 1989. Dissolution of calcite in deep-sea sediments-pH and O₂ microelectrode results, *Goechimica and Cosmochimica Acta* 53, 2831-2845.

Baumgartner, T.R., Soutar, A., Ferreira-Bartrina, V., 1992. Reconstruction of the history of Pacific sardine and northern anchovy populations over the past two millennia from sediments of the Santa Barbara Basin, California. *CalCOFI Reports* 33, 24-40.

Beamish, R.J., Bouillon, D.R., 1993. Pacific salmon production trends in relation to climate. *Canadian Journal of Fisheries and Aquatic Sciences* 50, 1002-1016.

Beaufort, L., Lancelot, Y., Camberlin, P., Cayre, O., Bassinot, F., Labeyrie, L., 1997. Insolation cycles as a major control of equatorial Indian Ocean primary production. *Science* 278, 1451-1454.

Beaufort, L., Bassinot, F., Vincent, E., 1999. Primary production response to orbitally induced variations of the southern oscillations in the Equatorial Indian ocean. In Abrantes, F., Mix, A.C. (Eds.) *Reconstructing Ocean History: A Window into the Future*, Kluwer Academic/Plenum Publishers, New York, 245-272.

Beaufort, L., de Gabriel-Thoron, T., Mix, A., Pisias, N., 2001. ENSO-like forcing on oceanic primary production during the late Pleistocene. *Science* 293, 2440-2444.

Behrenfeld, M.J., Falkowski, P.G., 1997. Photosynthetic rates derived from satellite-based chlorophyll concentration. *Limnology and Oceanography* 42, 1-20.

Behrenfeld, M.J., Siegel, D.A., 2007. Ocean Productivity – Climate Linkages imprinted in satellite observations. *Global Change NewsLetter* 68, 4-7.

- Behrenfeld, M.J., O'Malley, R.T., Siegel, D.A., McClain, C.R., Sarmiento, J.L., Feldman, G.C., Milligan, A.J., Falkowski, P.G., Letelier, R.M., Boss, E.S., 2006. Climate-driven trends in contemporary ocean productivity. *Nature* 444, 752-755.
- Berger, W.H., 1989. Global maps of ocean productivity. In Berger, W.H., Smetacek, V.S., Wefer, G. (Eds). *Productivity of the Ocean: Present and Past*. Life Sciences Research Report 14, Chichester, 429-455.
- Berger, W.H., Smetacek, V.S., Wefer, G., 1989. Ocean productivity and paleoproductivity - An overview. In Berger, W.H., Smetacek, V.S., Wefer, G. (Eds). *Productivity of the Ocean: Present and Past*. Life Sciences Research Report 14, Chichester: 1-34.
- Bopp, L., Monfray, P., Aumont, O., Dufresne, J.-L., Le Treut, H., Madec, G., Terray, L., Orr, J.C., 2001. Potential impact of climate change on marine export production. *Global Biogeochemical Cycles* 15, 81– 99.
- Bopp, L., Kohfeld, K.E., Le Quéré, C., Aumont, O., 2003. Dust impact on marine biota and atmospheric CO₂ during glacial periods, *Paleoceanography* 18, 1046, doi: 10.1029/2002PA000810.
- Boyd, P.W., Doney, S.C., 2002. Modelling regional responses by marine pelagic ecosystems to global climate change. *Geophysical Research Letters* 29, 16, 1806, doi:10.1029/2001GL014130.
- Bradt Miller, L.I., Anderson, R.F., Fleisher, M.Q., Burckle L.H., 2006. Diatom productivity in the equatorial Pacific Ocean from the last glacial period to the present: A test of the silicic acid leakage hypothesis. *Paleoceanography* 21, PA4201, doi:10.1029/2006 PA001282.
- Cayre, O., Beaufort, L., Vincent, E., 1999. Paleoproductivity in the equatorial Indian Ocean for the last 260,000 yrs: A transfer function based on planktonic foraminifera. *Quaternary Science Reviews* 18, 839-857.
- Bricker, S.B., Clement, C.G., Pirhalla, D.E, Orlando, S.P., Farrow, D.R.G., 1999. *National Estuarine Eutrophication Assessment: effects of nutrient enrichment in the nation's estuaries*. NOAA, National Ocean Service, Special Projects and the National Centers for Coastal Ocean Science. Silver Spring, MD, 71 pp.
- Brink, K.H., Abrantes, F.F.G., Bernal, P.A., Dugdale, R.C., Estrada, M., Hutchings, L., Jahnke, R.A., Muller, P.J., Smith, R.L., 1995. How do coastal upwelling systems operate as integrated physical, chemical, and biological systems and influence the geological records? The role of physical processes in defining the spatial structure of

biological and chemical variables. In Summerhayes, K.-C., Eims, M.V., Zeitzschel, B. (eds.). *Upwelling in the Ocean: modern processes and ancient records*. Environmental Sciences Research Report ES 18, Chichester, 103-124.

Cho, H.-J., Matsuoka, K., 2001. Distribution of dinoflagellate cysts in surface sediments from the Yellow Sea and East China Sea. *Marine Micropaleontology* 42, 103-123.

Cloern, J.E., Schraga, T.H., Lopez, C.B., Knowles, N., 2005. Climate anomalies generate an exceptional dinoflagellate bloom in San Francisco Bay. *Geophysical Research Letters* 32, doi: 10.1029/2005GL023321.

Dale, B., 1996. Dinoflagellate cysts ecology: modelling and geological applications. In: Jansonius, J., McGregor, D. (Eds.), *Palynology: principles and applications*. The American Association of Stratigraphic Palynologists Foundation, Salt Lake City, 1249-1276.

Dale, B., 2001. Marine dinoflagellate cysts as indicators of eutrophication and industrial pollution: a discussion. *The Science of the Total Environment* 264, 235-240.

Dale, B., Fjellså, A., 1994. Dinoflagellate cysts as paleoproductivity indicators: state of the art, potential and limits. In: Zahn, R., Pedersen, T., Kaminski, M., Labeyrie, L. (Eds.), *Carbon cycling in the glacial Ocean: constraints on the ocean's role in global change*. Springer-Verlag, Berlin, 521-537.

Dale, B., Thorsen, T.A., Fjellsa, A., 1999. Dinoflagellate cysts as indicators of cultural eutrophication in the Oslofjord, Norway. *Estuarine Coastal Shelf Science* 48, 371-382.

Dallimore, A., 2001. Late Holocene geologic, oceanographic, and climate history of an anoxic fjord: Effingham Inlet, west coast Vancouver Island. *Thèse de doctorat*, Carleton University, Ottawa, Ontario.

Davenport, R., Neuer, S., Helmke, P., Perez-Marrero, J., Llinas, O., 2002. Primary productivity in the northern Canary Islands region as inferred from SeaWiFS imagery. *Deep-Sea Research II* 49, 3481-3496.

de Vernal, A., Rochon, A., Turon, J.-L., Matthiessen, J., 1997. Organic-walled dinoflagellate cysts: palynological tracers of sea-surface conditions in middle to high latitude marine environments. *Geobios* 30, 905-920.

de Vernal, A., Henry, M., Matthiessen, J., Mudie, P. J., Rochon, A., Boessenkool, K., Eynaud, F., Grøsfjeld, K., Guiot, J., Hamel, D., Harland, R., Head, M. J., Kunz-Pirring, M., Levac, E., Loucheur, V., Peyron, O., Pospelova, V., Radi, T., Turon, J.-L., Voronina E., 2001. Dinocyst assemblages as tracer of sea-surface conditions in the northern North Atlantic, Arctic and sub-Arctic seas: the “n = 677” database and derived transfer functions. *Journal of Quaternary Science* 16, 681-698.

de Vernal, A., Eynaud, F., Henry, M., Hillaire-Marcel, C., Londeix, L., Mangin, S., Matthiessen, J., Marret, F., Radi, T., Rochon, A., Solignac, S., Turon, J.-L., 2005. Reconstruction of sea-surface conditions at middle to high latitudes of the Northern Hemisphere during the Last Glacial Maximum (LGM) based on dinoflagellate cyst assemblages. *Quaternary Science Reviews* 24, 897-924.

Devillers, R., de Vernal, A., 2000. Distribution of dinocysts in surface sediments of the northern North Atlantic in relation with nutrients and productivity in surface waters. *Marine Geology* 166, 103-124.

Dymond, J., Suess, E., Lyle, M., 1992. Barium in deep-sea sediment: a geochemical proxy for paleoproductivity. *Paleoceanography* 7, 163-181.

Dymond, J., Collier, R., 1996. Particulate barium fluxes and their relationships to biological productivity. *Deep Sea Research Part II* 43, 1283-1308.

Eagle, M., Paytan, A., 2006. Phase associations of barium in marine sediments. *Marine Chemistry* 100, 124-135.

Eagle, M., Paytan, A., Arrigo, K.R., van Dijken, G., Murray, R.W., 2003. A comparison between excess barium and barite as indicators of carbon export. *Paleoceanography* 18, 1021-1033.

Efron, B., Gong, C., 1983. A Leisurely Look at the Bootstrap, the Jackknife, and Cross validation. *The American Statistician* 37, 36-48.

Emerson, S., Hedges, J., 1988. Processes controlling the organic carbon content of open ocean sediments. *Paleoceanography* 3, 621-634.

Emerson, S., Hedges, J., 2003. Sediment Diagenesis and Benthic Flux. In: Holland, H.D., Turekian, K.K. (Eds.), *Treatise on Geochemistry*, vol. 6. Elsevier-Pergamon, Oxford, 293-319.

Field, C.B., Behrenfeld, M.J., Randerson, J.T., Falkowski, P.G., 1998. Primary Production of the biosphere: Integrating Terrestrial and Oceanic Components. *Science* 281, 237-240

- Finney, B.P., Gregory-Eaves, I., Douglas, M.S.V., Smol, J.P., 2002. Fisheries productivity in the northeastern Pacific Ocean over the past 2,200 years. *Nature* 416, 729-733.
- Fischer, G., Wefer, G. (Eds.), 1999. *Use of Proxies in Paleoceanography: Examples from the South Atlantic*. Springer-Verlag Berlin, 735 pp.
- Fischer, V., Ratmeyer, V., Wefer, G., 2000. Organic carbon fluxes in the Atlantic and southern ocean: relationship to primary production compiled from satellite radiometer data. *Deep-Sea Research Part II* 47, 1961-1997.
- François, R., Honjo, S., Manganini, S., Ravizza, G., 1995. Biogenic barium fluxes to the deep sea: implications for paleoproductivity reconstructions. *Global Biogeochemical Cycles* 9, 289-303.
- François, R., Frank, Van der Loeff, M.M.R., Bacon, M.B., 2004. ^{230}Th normalization: An essential tool for interpreting sedimentary fluxes during the late Quaternary. *Paleoceanography* 19, PA1018, doi:10.1029/2003PA000939.
- Galbraith, E.D., Jaccard, S.L., Pedersen, T.F., Sigman, D.M., Haug, G.H., Cook, M., Southon, J.R., François, R., 2007. Carbon dioxide release from the North Pacific abyss during the last deglaciation. *Nature* 449, 890 – 893.
- Gallinari, M., Ragueneau, O., Corrin, L., DeMaster, D.J., Tréguer, P., 2002. The importance of water column processes on the dissolution properties of biogenic silica in deep-sea sediments. I. Solubility. *Geochimica et Cosmochimica Acta* 66, 2701-2717. doi:10.1016/S0016-7037(02)00874-8.
- Gauch, H.G., 1982. *Multivariate analysis in community ecology*. Cambridge University Press, Cambridge, 298 pp.
- Gehlen, M., Bassinot, F.C., Chou, L., McCorkle, D., 2005. Reassessing the dissolution of marine carbonates: I. Solubility. *Deep Sea Research I* 52, 1445-1460.
- Glavin, T., 1996. *Dead Reckoning: confronting crisis in Pacific Fisheries*. Greystone Books, Vancouver.
- Gregg, W.W., Conkright, M.E., 2002. Decadal changes in global ocean chlorophyll. *Geophysical Research Letters* 29, doi:10.1029/2002GL014689.

Gregg W.W., Conkright, M.E., Ginoux, P., O'Reilly, J.E., Casey, N.W., 2003. Ocean primary production and climate: Global decadal changes. *Geophysical Research Letters* 30, doi: 10.1029/2003GL016889.

Guiot, J., 1990. Methods and programs of statistics for paleoclimatology and paleoecology. In: Guiot, J., Labeyrie, L., (eds.), *Quantification des changements climatiques: méthodes et programmes*. Institut National des Sciences de l'Univers (INSU-France), Paris, Monographie no 1, 253 pp.

Hare, S.R., Mantua, N.J., 2000. Empirical evidence for North Pacific regime shifts in 1977 and 1989. *Progress in Oceanography* 47, 103-145.

Henriksson, A.S., 2000. Coccolithophore response to oceanographic changes in the equatorial Atlantic during the last 200,000 year. *Palaeogeography, Palaeoclimatology, Palaeoecology* 156, 161-173.

Huyer, A., 1983. Coastal upwelling in the California current system. *Progress in Oceanography* 12, 259-284.

ICES (International Council for the Exploration of the Sea). 2002. Workshop on Contrasting Approaches to Understanding Eutrophication Effects on Phytoplankton, Rapport : ICES CM 2002/C:05, La Hague, Netherlands, 36 pp.

Imbrie, J., Kipp, N., 1971. A new micropaleontologic method for quantitative paleoclimatology. Application to a late Pleistocene Caribbean core. In: Turekian, K.K. (ed.), *The Late Cenozoic Glacial Ages*. Yale University, New Haven, 71-182.

Ito, T., Parekh, P., Dutkiewicz, S., Follows, N.J., 2005. The Antarctic Circumpolar Productivity Belt. *Geophysical Research Letters* 32, L13604, doi: 10.1029/2005GL023021

Ivanova, E., Schiebel, R., Singh, A.S., Gerhard, S., Niedler, H.S., Hemleben, C., 2003. Primary production in the Arabian Sea during the last 135 000 years. *Palaeogeography, Palaeoclimatology, Palaeoecology* 197, 61-82.

Jeandel, C., Tachikawa, K., Bory, A., Dehairs, F., 2000. Biogenic barium in suspended and trapped material as a tracer of export production in the tropical NE Atlantic EUMELI sites. *Marine Chemistry* 71, 125-142.

Jongman, R.H.G., ter Braak, C.J.F., Van Tongeren, O.F.R. (Eds.), 1995. *Data analysis in community and landscape ecology*. Cambridge University Press, Cambridge, 299 pp.

- Key, B.H., 1989. Les polluants dans le milieu marin de la Colombie Britannique. Rapport sur l'état des connaissances. Ottawa : Environnement Canada. Rapport sur l'état de l'environnement No. 89-1, 61 pp.
- Klump, J., Hebbeln, D., Wefer, G., 2000. The impact of sediment provenance on barium-based productivity estimates. *Marine Geology*, 169, 259-271.
- Koblentz-Mishke, O.J., Volkovinsky, V.V., Kabanova, J.G., 1970. Plankton primary production of the world ocean. In: Wooster, W.S., (Ed.), *Scientific Exploration of the South Pacific*, p. 183-193, National Academy of Sciences, Washington, D.C.
- Kumar, A., Patterson, T., 2002. Dinoflagellate cyst assemblages from Effingham Inlet, Vancouver Island, British Columbia, Canada. *Palaeogeography, Palaeoclimatology, Palaeoecology*, 180: 187-206.
- Lampitt, R.S., Antia, A.N., 1997. Particle flux in the deep seas: regional characteristics and temporal variability. *Deep Sea Research* 44, 1377-1403.
- Lazarus, D., Bittniok, B., Diester-Haass, L., Meyers, P., Billups, K., 2006. Comparison of radiolarian and sedimentologic paleoproductivity proxies in the latest Miocene–Recent Benguela Upwelling System. *Marine Micropaleontology* 60, 269-294.
- Lewis, J., Dodge, J.D., Powell, A.J., 1990. Quaternary dinoflagellate cysts from the upwelling system offshore Peru, Hole 686B, ODP Leg 112. In Suess, E., von Huene, R., et al. (eds.), *Proceeding of the Ocean Drilling Program. Scientific Results 112*, 323-327.
- Livingston, R.J., 2001. Eutrophication processes in coastal systems: origin and succession of plankton blooms and effects on secondary production in Gulf Coast estuaries. CRC Press, Washington, D.C., 327 pp.
- Longhurst, A., Sathyendranath, S., Platt, T., Caverhill, C., 1995. An estimate of global primary production in the ocean from satellite radiometer data. *Journal of Plankton Research* 17, 1245-1271.
- Lorimer, E.G., 1984. Review of selected marine municipal outfalls in British Columbia. Rapport régional de programme de Service de la protection de l'environnement, Environnement Canada, rapport no 84-4.
- Loubere, P., 1996. The surface ocean productivity and bottom water oxygen signals in deep water benthic foraminiferal assemblages. *Marine Micropaleontology* 28, 247-261.

Loubere, P., 1999. A multiproxy reconstruction of biological productivity and oceanography in the eastern equatorial Pacific for the past 30,000 years. *Marine micropaleontology* 37, 173-198.

Loubere, P., 2002. Remote vs. local control of changes in eastern equatorial Pacific bioproductivity from the Last Glacial Maximum to Present. *Global and Planetary Changes* 35, 113-126.

Loubere, P., Fariduddin, M., 1999. Quantitative estimation of global patterns of surface Ocean biological productivity and its seasonal variation timescales from centuries to millennia. *Global Biogeochemical Cycles* 13, 115-133.

Lyle, M., Murray, D.W., Finney, B.P., Dymond, J., Robbins, J.M., Brooksforce, K., 1988. The record of late Pleistocene biogenic sedimentation in the eastern tropical Pacific Ocean. *Paleoceanography* 3, 39-59.

Mackas, D.L., Harrison, P.J., 1997. Nitrogenous Nutrient sources and sinks in the Juan de Fuca Strait/ Strait of Georgia/Puget Sound Estuarine system : Assessing the potential for Eutrophication. *Estuarine, Coastal and Shelf Science*, 44, 1-21.

Mackas, D.L., Thomson, R.E., Galbraith, M. 2001. Changes in the zooplankton community of the British Columbia continental margin, 1985-1999, and their covariation with oceanographic conditions. *Canadian Journal of Fisheries and Aquatic Sciences*, 58, 685-702.

Mackensen A., Schumacher S., Radke J, Schmidt, D.N., 2000. Microhabitat preferences and stable carbon isotopes of endobenthic foraminifera: clue to quantitative reconstruction of oceanic new production? *Marine Micropaleontology* 40, 233-258.

Mantua, N.J., Hare, S.R., Zhang, Y., Wallace, J.M., Francis, R.C. (1997). A Pacific interdecadal climate oscillation with impacts on salmon production. *Bulletin of the Meteorological Society*, 78, 1069-1079.

Marret, F., 1994. Distribution of dinoflagellate cysts in recent marine sediments from the east Equatorial Atlantic (Gulf of Guinea). *Review of Paleobotany and Palynology* 84, 1-22.

Marret, F., de Vernal, A., 1997. Dinoflagellate cyst distribution in surface sediments of the southern Indian Ocean. *Marine Micropaleontology* 29, 367-392.

Marret, F., Eiriksson, J., Knudsen, K.L., Turon, J-L., Scourse, J.D., 2004. Distribution of dinoflagellate cyst assemblages in surface sediments from the

northern and western shelf of Iceland. *Review of Palaeobotany and Palynology*, 128, 35-53.

Matsuoka, K., 1985. Organic-walled dinoflagellate cysts from surface sediments of Nagasaki Bay and Senzaki Bay, West Japan. *Bulletin of the Faculty of Liberal Arts, Nagasaki University*, 25, 2, 21-115.

Matsuoka, K., 1987. Organic-walled dinoflagellate cysts from surface sediments of Akkeshi Bay and Lake Saroma, North Japan. *Bulletin of the Faculty of Liberal Arts, Nagasaki University*, 28, 1, 35-123.

Matsuoka, K., 1992. Species diversity of modern dinoflagellate cysts in surface sediments around the Japanese islands. In: Head, M. J., and Wrenn, J. H., (eds.), *Neogene and Quaternary Dinoflagellate Cysts and Acritarchs*. American Association of Stratigraphic Palynologists Foundation, Dallas, 33-53.

Matsuoka, K., 1999. Eutrophication process recorded in dinoflagellate cyst assemblages - a case of Yokohama Port, Tokyo Bay, Japan. *The Science of the Total Environment*, 231, 17-35.

Matthiessen, J., 1995. Distribution patterns of dinoflagellate cysts and other organic-walled microfossils in recent Norwegian-Greenland Sea sediments. *Marine Micropaleontology*, 24, 307-334.

McCorkle, D.C., Martin, P.A., Lea, D.W., Klinkhammer, G.P., 1995. Evidence of a dissolution effect on benthic foraminiferal shell chemistry: $\delta^{13}\text{C}$, Cd/Ca, Ba/Ca, and Sr/Ca results from the Ontong Java Plateau. *Paleoceanography*, 10, 699-714.

Meyers, P.A., 1997. Organic geochemical proxies of paleoceanographic, paleolimnologic, and paleoclimatic processes. *Organic Geochemistry*, 27, 213-250.

Miller, A.J., Schneider, N., 2000. Interdecadal climate regime dynamics in the North Pacific Ocean: theories, observations and ecosystem impacts. *Progress in Oceanography* 47, 355-379.

Mix, A.C., 1989. Influence of productivity variations on long-term atmospheric CO_2 . *Nature* 337, 541-544.

Mock, C.J., Bartlein, P.J., Anderson, P.M., 1998. Atmospheric circulation patterns and spatial climatic variations in Beringia. *International Journal of Climatology* 10, 1085-1104.

Muller, P.J., Erlenkeuser, H., Von Grafenstein, R., 1983. Glacial-interglacial cycles in oceanic productivity inferred from organic carbon contents in eastern north Atlantic sediment cores. In: Thiede, J., Suess, E. (eds), Coastal upwelling, its sediment record, Part B: Sedimentary records of ancient coastal upwelling. Plenum press, New York, 65-398.

Najjar, R.G., Sarmiento, J.L., Toggweiler, J.R., 1992. Downwards transport and fate of organic matter in the ocean: simulations with a general circulation model. *Global Biogeochemical Cycles* 6, 45-76.

Nave, S., Labeyrie, L., Gherardi, J., Caillon, N., Cortijo, E., Kissel, C., Abrantes, F., 2007. Primary productivity response to Heinrich events in the North Atlantic Ocean and Norwegian Sea. *Paleoceanography* 22, PA3216, doi:10.1029/2006PA001335.

Nelson, D.M., Tréguer, P., Brzezinski, M.A., Leynaert, A., Quéguiner, B., 1995. Production and dissolution of biogenic silica in the ocean: Revised global estimates, comparison with regional data and relationship with biogenic sedimentation. *Global Biogeochemical Cycles*, 9, 359-372.

O'Connell, J.M., Tunnicliffe, V., 2001. The use of sedimentary fish remains for interpretation of long-term population fluctuations. *Marine Geology*, 174, 177-195.

Overpeck, J., Webb, T., Prentice, I.C., 1985. Quantitative interpretation of fossil pollen spectra: dissimilarity coefficients and the method of modern analogs. *Quaternary Research* 23, 87-108.

Paerl, H.V., 1988. Nuisance phytoplankton blooms in coastal, estuarine, and inland waters. *Limnology and Oceanography*, 33, 823-847.

Palmer, J.R., Totterdell, I.J., 2001. Production and export in a global ocean ecosystem model. *Deep Sea Research* I48, 1169-1198

Parsons, T.R., Takahashi, M., Hargrave, B., 1984. Biological organic processes. Pergamon Press, Oxford, UK, 330 pp.

Paytan, A., Kastner, M., 1996. Benthic Ba fluxes in the central equatorial Pacific, implications for the oceanic Ba cycle. *Earth and Planetary Science Letter* 142, 439-450.

Paytan, A., Kastner, M., Chavez, F.P., 1996. Glacial to interglacial fluctuation in productivity in the equatorial Pacific as indicated by marine Barite. *Science* 274, 1355-1357.

- Pedersen, T.F., Pickering, M., Vogel, J.S., Southon, J.N., Nelson, D.E., 1988. The response of benthic foraminifera to productivity cycles in the eastern equatorial Pacific: Faunal and geochemical constraints on glacial bottom water oxygen levels. *Paleoceanography* 3, 157-168.
- Peterson, W.T., Schwing, F.B., 2003. A new climate regime in Northeast Pacific ecosystems. *Geophysical Research Letters* 30, 1896, doi:10.1029/2003GL017528.
- Pierce, D.W., Barnett, T. P., Schneider, N., Saravanan, R., Dommenget, D., Latif, M., 2001. The role of ocean dynamics in producing decadal climate variability in the North Pacific. *Climate Dynamics* 18, 51-70.
- Polovina, J.J., Mitchum, G.T., Evans, G.T., 1995. Decadal and basin-scale variation in mixed layer depth and the impact on biological production in the Central and North Pacific, 1960-1988. *Deep Sea Research I*, 42, 1701-1716.
- Pospelova, V., Chmura, G.L., Boothman, W.S., Latimer, J.S., 2002. Dinoflagellate cyst records and human disturbance in two neighbouring estuaries, New Bedford Harbor and Apponagansett Bay, Massachusetts (USA). *The Science of the Total Environment*, 298, 81-102.
- Pospelova, V., Chmura, G.L., Walker, H.A., 2004. Environmental factors influencing spatial distribution of dinoflagellate cyst assemblages in shallow lagoons of southern New England (USA). *Review of Palaeobotany and Palynology*, 128, 7-34.
- Pospelova, V., Chmura, G.L., Boothman, W., Latimer, J.S., 2005. Spatial distribution of modern dinoflagellate cysts in polluted estuarine sediments from Buzzards Bay (Massachusetts, USA) embayments. *Marine Ecology Progress Series*, 292, 23-40.
- Powell, A. J., Dodge, J. D., Lewis, J., 1990. Late Neogene to Pleistocene palynological facies of the Peruvian continental margin upwelling, Leg 112. In Suess, E., von Huene, R., et al. (eds.), *Proceeding of the Ocean Drilling Program. Scientific Results*, 112, 297-321.
- Radi, T., de Vernal, A., Peyron, O., 2001. Relationships between dinocyst assemblages in surface sediments and hydrographic conditions in the Bering and Chukchi seas. *Journal of Quaternary Science*, 16, 667-680.
- Ragueneau, O., Tréguer, P., Leynaert, A., Anderson, R.F., Brzezinski, M.A., DeMaster, D.J., Dugdale, R.C., Dymond, J., Fischer, G., François, R., Heinze, C., Maier-Reimer, E., Martin-Jézéquel, V., Nelson, D.M., Quéguiner, B., 2000. A review of the Si cycle in the modern ocean: Recent progress and missing gaps in the

application of biogenic opal as a paleoproductivity proxy. *Global Planet Change* 26, 317-365.

Rasmussen, T.L., Thomson, E., Trolestra, S.R., Kuijpers, A., Prins, M.A., 2002. Millennial-scale glacial variability versus Holocene stability: changes in planktic and benthic foraminiferal faunas and ocean circulation in the North Atlantic during the last 60,000 years. *Marine Micropaleontology* 47, 143-176.

Rideout, P., Taekema, B., Deniseger, J., Liboiron, R., McLaren, D., 2000. A water quality assessment of the Cowichan and Koksilah Rivers and Cowichan Bay. Rapport du Ministry of Environment, Lands and Parks Province of British Columbia, Pollution Prevention, Vancouver Island Region, 109 pp.

Rochon, A., de Vernal, A., Turon, J.-L., Matthiessen, J., Head, M.J., 1999. Distribution of dinoflagellate cysts in surface sediments from the North Atlantic Ocean and adjacent seas in relation to sea-surface parameters. *American Association of Stratigraphic Palynologists, Contribution Series* 35, 152 pp.

Roemmich, D., McGowan, J., 1995. Climatic warming and the decline of zooplankton in the California Current. *Science*, 267, 1324-1326.

Rühlemann, C., Müller, P.J., Schneider, R.R., 1999. Organic carbon and carbonate as paleoproductivity proxies: Examples from high and low productivity areas of the tropical Atlantic. In Fischer G., Wefer, G. (eds), *Use of Proxies in Paleoceanography: Examples from the South Atlantic*. Springer-Verlag, Berlin, 315-344.

Sangiorgi, F., Capotondi, L., Brinkhuis, H. 2002. A centennial scale organic-walled dinoflagellate cyst record of the last deglaciation in the South Adriatic Sea (Central Mediterranean). *Palaeogeography, Palaeoclimatology, Palaeoecology*, 186, 199-216.

Sarmiento, J.L., Le Quéré, C., 1996. Oceanic carbon dioxide uptake in a model of century-scale global warming. *Science* 274, 1346-1350.

Sarnthein, M., Duplessy, J.-C., Fontugue, M.R., 1988. Global variations of surface ocean productivity in low and mid latitudes: influence on CO₂ reservoirs of the deep ocean and atmosphere during the last 21 000 years. *Paleoceanography* 3, 361-399.

Sarnthein, M., Pflaumann, U., Ross, R., Tiedemann, R., Winn, K., 1992. Transfer functions to reconstruct ocean palaeoproductivity: a comparison. In: Summerhayes, C.P., Prell, W.L., Emeis, K.C. (Eds.), *Upwelling Systems: Evolution since the early Miocene*. Geological Society Special Publication 64, London, 411-427.

Schimel, D., Enting, I.G., Heimann, M., Wigley, T.M.L., Raynaud, D., Alves, D., Siegenthaler, U., 1995. CO₂ and the carbon cycle. In: Houghton, J.T., Meira Filho, L.G., Bruce, J., Lee, H., Callander, B.A., Haites, E., Harris, N., Maskell, K. (Eds.), *Climate Change 1994: Radiative Forcing of Climate Change and an Evaluation of the IPCC IS92 Emission Scenarios*. Cambridge University Press, Cambridge, pp. 35-71.

Schmittner, A., 2005. Decline of the marine ecosystem caused by a reduction in the Atlantic overturning circulation. *Nature* 434, 628-633.

Schneider, R.R., Muller, P.J., 1995. What role has upwelling played in the global carbon and climate cycles on a million-year time scale? In: Summerhayes, K.-C., Eims, M. V., Zeitzschel, B. (eds.), *Upwelling in the Ocean: modern processes and ancient records*. Environmental Sciences Research Report ES 18, Chichester, pp. 361-380.

Schulte, S., Bard, E. 2003. Past changes in biologically mediated dissolution of calcite above the chemical lysocline recorded in Indian Ocean sediments. *Quaternary Science Reviews* 22: 1757-1770.

Sigman, D. M., Boyle, E. A. 2000. Glacial/interglacial variations in atmospheric carbon dioxide. *Nature* 407, 859-869.

Six, K.D., Maier-Reimer, E., 1996. Effects of plankton dynamics on seasonal carbon fluxes in an ocean general circulation model. *Global Biogeochemical Cycles* 10, 559-583.

Stemann Nielsen, E., 1952. The use of radioactive carbon (¹⁴C) for measuring organic production in the Sea. *Journal du Conseil International pour l'Exploration de la Mer* 18, 117-140.

Sundquist, E.T., 1985. Geological perspectives on carbon dioxide and the carbon cycle. *Geophysical Monographs* 32, 5-59.

Tanasichuk, R.W., 1998. Interannual variations in the population biology and productivity of *Euphausia pacifica* in Barkley Sound, Canada with special reference to the 1992 and 1993 warm ocean years. *Marine Ecology Progress Series* 173, 181-195.

Taylor, F.J.R., (Ed.), 1987. *The biology of dinoflagellates*. Botanical Monographs, 21, Blackwell Scientific Publications, Oxford, 785 p.

- Thomas, E., Booth, L., Maslin, M., Shackleton, N.J., 1995. Northeastern Atlantic benthic foraminifera during the last 45 000 years: Changes in productivity seen from the bottom up. *Paleoceanography* 10, 545-562.
- Thomas, A.C., Carr, M.-E. Strub, P. T. 2001. Chlorophyll variability in Eastern Boundary Currents. *Geophysical Research Letters* 28, 18: 3421-3424.
- Thorsen, T.A., Dale, B., 1997. Dinoflagellate cysts as indicators of pollution and past climate in a Norwegian fjord. *The Holocene* 7, 433-446.
- Thunell, R., Sautter, L.R. 1992. Planktonic foraminiferal faunal and stable isotopic indices of upwelling. A sediment trap study in the San Pedro Basin, Southern California Bight. In: Summerhays, C.P., et al. (Ed.) *Upwelling Systems. Evolution since the Early Miocene*. Geological Society Special Publication 64, pp. 77-91.
- Toggweiler, J. R., 1999. Variation of atmospheric CO₂ by ventilation of the ocean's deepest water. *Paleoceanography* 14, 571-588.
- Trenberth, K.E., Hurrell, J.W., 1994. Decadal atmosphere-ocean variations in the Pacific. *Climate Dynamics* 9, 303-319.
- Tunnicliffe, V., O'Connell, J.M., McQuoid, M.R., 2001. A Holocene record of marine fish remains from the Northeastern Pacific. *Marine Geology* 174, 197-210.
- Varekamp, J.C., Thomas, E., Buchholtz-ten-Brink, M., Altabet, M.A., Cooper, C., 2003. Environmental change in Long Island Sound in the recent past: Eutrophication and climate change. International Working Meeting of the LIS Lobster Initiative, University of Connecticut. Storrs-Mansfield. Abstract.
- Wall, D., Dale, B., 1968. Modern dinoflagellate cysts and evolution of the Peridinales. *Micropaleontology* 14, 265-304.
- Walsh, I., Dymond, J., Collier, R., 1988. Rates of recycling of biogenic components of settling particles in the ocean derived from sediment trap experiments. *Deep Sea Research* 35, 43-58.
- Ware, D.M., Thomson, R.E., 1991. Link between long-term variability in upwelling and fish production in the northeast Pacific Ocean. *Canadian Journal of Fisheries and Aquatic Sciences*, 48, 2296-2306.
- Werdeli, P.J., Bailey, S., Fargion, G., Pietras, C., Knobelspiesse, K., Feldman, G., McClain, C., 2003. Unique data repository facilitates ocean color satellite validation. *EOS Transactions* 84, 38, p. 377.

Zonneveld, K.A.F., 1997. Dinoflagellate cyst distribution in surface sediments from the Arabian Sea (northwestern Indian Ocean) in relation to temperature and salinity gradients in the upper water column. *Deep-Sea Research II* 6-7, 1411-1443.

Zonneveld, K.A.F., Hoek, R. P, Brinkhuis, H., Willems, H., 2001. Geographical distribution of organic-walled dinoflagellate cysts in surficial sediments of the Benguela upwelling region and their relationship to upper ocean conditions. *Progress in Oceanography* 48, 25-75.

ANNEXE 1

Copie de l'article

PALEOENVIRONMENTS ASSOCIATED WITH THE DEGLACIATION
PROCESS IN THE STRAIT OF GEORGIA, OFF BRITISH COLUMBIA:
MICROFAUNAL AND MICROFLORAL EVIDENCE

Guilbault, J. P., Barrie, J. V., Conway, K, Lapointe, M., Radi, T.

Quaternary Science Reviews (2003), vol. 22, 839-857



PERGAMON

Quaternary Science Reviews 22 (2003) 839–857



QSR

Paleoenvironments of the Strait of Georgia, British Columbia during the last deglaciation: microfaunal and microfloral evidence

Jean-Pierre Guilbault^{a,*}, J. Vaughn Barrie^b, Kim Conway^b, Martine Lapointe^c,
Taoufik Radi^d

^aBRAQ-Stratigraphie, 10555 rue Meilleur, Montréal, QC, Canada H3L 3K4

^bGeological Survey of Canada, P.O. Box 6000, Sidney, BC, Canada, V8L 4B2

^c10220 Grande Allée, Appartement 1, Montréal, QC, Canada, H3L 2M1

^dGEOTOP, Université du Québec à Montréal, C.P. 8888, Montréal, QC, Canada, H3C 3P8

Received 21 May 2002; accepted 1 December 2002

Abstract

The Strait of Georgia is situated between Vancouver Island and the western Canadian mainland. It was deglaciated quickly, around 12,500 ¹⁴C yr BP, by in situ downwasting. The subsequent marine invasion has left glacial marine sediments with foraminifers, diatoms and dinocysts characterizing successive paleoenvironments recognizable basinwide. The first paleoenvironment represents near-ice conditions under the influence of the turbid meltwater plume marked by low algal productivity and few foraminifers, mostly *Elphidium excavatum*. Just off the plume, the second environment shows a peak of *Nonionellina labradorica* possibly resulting from an observed sudden increase in diatom numbers, mostly ice-dwelling forms implying a long annual sea-ice cover. Further away, *Cassidulina reniforme* increases, *N. labradorica* decreases while other calcareous foraminifer species colonize the area; there are fewer ice diatoms, more marine planktonic diatoms and dinocysts become more abundant. Finally, after 12,000 ¹⁴C yr BP, calcareous foraminifers are gradually replaced because of dissolution of calcium carbonate by a low-diversity arenaceous assemblage. At the same time, abundant planktonic diatoms and dinocysts indicate warmer surface temperature. The succession of fossils and environments compares well with modern, horizontal, off-glacier successions observed in fjords of the European Arctic.

Crown Copyright © 2003 Published by Elsevier Science Ltd. All rights reserved.

1. Introduction

Until recently, interpretation of deglacial foraminifer faunas was rather approximate due to a poor knowledge of modern equivalent environments which, unfortunately, are few (ex.: Elverhøi et al., 1980). Hald and Korsun (1997) and Korsun and Hald (1998, 2000) have made significant advances in that field thanks to careful study of near-ice foraminifer faunas in Novaya Zemlya and Svalbard, European Arctic. Their results have been very useful for the interpretation of our assemblages. By combining benthic foraminifer results with information supplied by planktonic organisms (diatoms and dinocysts) we have improved the reliability of paleoenvironmental interpretation.

Recently, the Geological Survey of Canada has undertaken the "Georgia Strait Geohazard Initiative" project, one of whose objectives is to map the distribution of different seafloor types in the Strait of Georgia, a sound situated between Vancouver Island and the west coast of Canada (Fig. 1). In addition to seismic lines, piston cores have been collected, of which 12 yielded biostratigraphic information about the deglaciation (Table 1). In this study, we report microfaunal and microfloral evidence that characterizes the paleoenvironments in the Strait of Georgia during the last deglaciation.

2. Physical setting and deglaciation of the Strait of Georgia

The Strait of Georgia stretches for approximately 220 km in a NW-SE direction between Vancouver Island and the mainland; the overall width varies from 25 to

*Corresponding author. Tel.: +1-514-331-9695.

E-mail address: jean-pierre.guilbault@sympatico.ca (J.-P. Guilbault).

URL: <http://www.elsevier.com/locate/quascirev>.

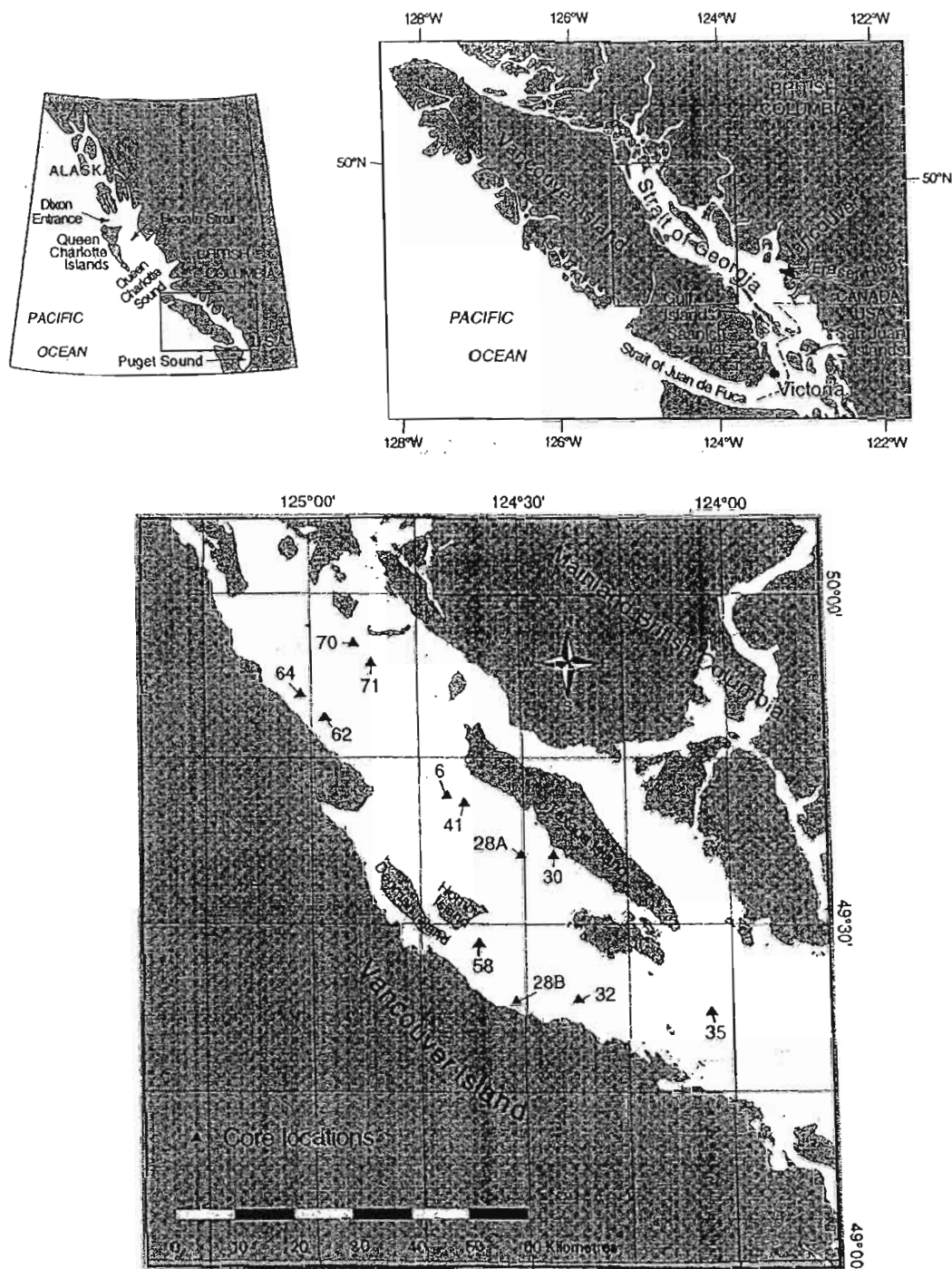


Fig. 1. Location of Strait of Georgia on the west coast of Canada and location of cores in Strait of Georgia.

55 km. The average depth of the Strait of Georgia is 155 m and the deepest point is 420 m (Thomson, 1981). Large areas of the strait lie at depths of 100–250 m,

which is where most of our cores come from. The strait connects with the open sea in the south first through the Gulf Islands and San Juan Islands and then through the

Table 1
Latitude, longitude and water depth of cores examined for this study

Core	Formal designation of core	Bathymetric depth of core (m)	Penetration (m)	Latitude (N)	Longitude (W)
6	TUL00A006	281	5.26	49° 41.76'	124° 40.91'
28A	TUL97B028	231	1.65	49° 36.41'	124° 30.46'
28B	TUL00A028	71	2.43	49° 23.201'	124° 31.609'
30	TUL97B030	170	0.36	49° 36.41'	124° 25.77'
32	TUL97B032	195	5.54	49° 23.40'	124° 22.45'
35	TUL97B035	244	3.24	49° 22.24'	124° 03.18'
41	TUL97B041	186	5.12	49° 40.96'	124° 38.50'
58	TUL92A058	178	6.75	49° 28.30'	124° 36.75'
62	TUL97B062	100	0.95	49° 49.09'	124° 58.43'
64	TUL97B064	102	2.37	49° 50.86'	125° 01.57'
70	TUL97B070	153	2.21	49° 55.53'	124° 54.00'
71	TUL97B071	179	5.65	49° 53.72'	124° 51.59'

Strait of Juan de Fuca (Fig. 1). Bottom topography in the Gulf/San Juan Islands area is complex but mostly shallower than 100 m, except for narrow, deep channels. The shallowest point along the main channel is at 140 m depth. This may be seen as a sill between the Strait of Juan de Fuca and the Strait of Georgia, but since it is about 3 km wide, it does not constitute a major conduit for ocean water. In the north, the Strait of Georgia connects with the open shelf of Queen Charlotte Sound through four narrow channels with sill depths of 40 m or less save for one at 90 m.

The strait is surrounded by mountains, those on the mainland being the highest. The mainland coast is dissected by deep silled fjords extending far inland. The Fraser River enters the southern end of the Strait, and drains a large part of southern and central British Columbia. The Fraser River delta is a thick pile of sediment which began accumulating about 8000–10,000 ¹⁴C yr BP (Clague, 1994). The delta's bottomset beds gradually covered an important area in the southern part of the strait, so that it is now impossible to core for sediments of the early deglacial period.

Modern circulation in the Strait of Georgia is characteristic of a partially mixed estuary with moderately strong tidal currents (2.6–3.4 m range), seasonally varying stratification and late summer deep-water density intrusions (LeBlond, 1983; Crean and Ages, 1971; Thomson, 1994). The oceanography of the Strait of Georgia can be broadly divided into two layers, above and below 50 m (Table 2). Temperatures are seasonally variable above 50 m but vary little underneath. In the northern strait (Texada Island and north), salinities vary little through the year, even in surface waters. In southern areas influenced by the Fraser River runoff, surface salinities vary considerably. This runoff reaches a maximum of 10,000 m³/s during the spring freshet and a minimum of around 1000 m³/s in late winter. The Fraser River accounts for about 80% of the mean annual freshwater discharge of 4400 m³/s into the Strait of Georgia (Mosher and Thomson, 2002). This

freshwater influx then develops the estuarine component of circulation in the southern strait that is characterized by a net outflow of low-salinity water toward Strait of Juan de Fuca in the upper layer (< 50 m depth) and a net northward inflow of high-salinity water in the underlying portion of the water column that reaches the Strait of Georgia in late summer (Mosher and Thomson, 2002). The influence of ocean water coming through the northern channels is limited to the northern strait, beyond our northernmost core.

During the last glacial maximum, the Cordilleran Ice Sheet extended over the Strait of Georgia and the whole of Vancouver Island. Ice flowing SE-ward along the axis of the Strait of Georgia was joined by ice coming out of the Fraser Valley and then divided into two tongues, one following Juan de Fuca Strait toward the ocean and the other going southward into the Puget Sound. The ice reached its southernmost extent around 16,900 calendric years BP (Porter and Swanson, 1998) or approximately 14,000 ¹⁴C yr BP. The earliest post-glacial dates from the Victoria and the Vancouver areas are not older than 12,700–12,800 ¹⁴C yr BP (James et al., 2002). Deglaciation of the Strait of Georgia seems to have taken place through in situ downwasting instead of northward retreat of a grounded ice front. The arguments in favor of downwasting are the limited amount of ice-rafted debris (IRD) and the absence of iceberg furrows and morainic ridges marking ice front positions on the floor of the strait (Barrie and Conway, 2002). In addition, multibeam swath bathymetry in the southern Strait of Georgia has recently shown possible eskers, kettles and kames (Geological Survey of Canada, unpublished results). Similar downwasting features have been reported on land around the edge of the basin by Fyles (1963).

The post-glacial marine limit around the Strait of Georgia (Dethier et al., 1995; Clague and James, 2002; James et al., 2002) indicates that the sites of our deep cores, now at 200 m, were at 350 m depth around 12,500 ¹⁴C yr BP.

Table 2
Seasonal variations of temperatures and salinities in the Strait of Georgia (data from Thomson, 1981)

Depth (m)	Temperature (°C)		Salinity (‰)	
	Max	Min	Max	Min
<i>Northern Strait (Texada Island and north)</i>				
0–50	15–20 (early Aug)	5–6 (Feb–Mar)	27–29	27–29
> 50	8–10	8–10	31.0 (winter)	30.5 (summer)
<i>Southern Strait</i>				
0–50	15–20 (early Aug)	5–6 (Feb–Mar)	29.5 (late winter)	< 15 (late May)
> 50	8–10	8–10	31.0 (winter)	30.5 (summer)

3. Lithostratigraphic setting

By comparing seismic and core data, Barrie and Conway (2000, 2002) developed a six-facies lithostratigraphic framework for the Quaternary sediments of the Strait of Georgia:

- (1) Thick, stratified pre-glacial sediments probably deposited in front of the advancing late Wisconsinan glacier.
- (2) Late Wisconsinan till.
- (3) Ice-proximal lithofacies composed of clay, sand laminae and occasional sand beds. The laminae have likely been deposited by turbidity currents. This lithofacies has probably accumulated close to the ice-water interface, within the reach of the turbid meltwater plume.
- (4) Ice-distal facies composed predominantly of massive gray silty clay, often bioturbated and containing some ice rafted debris (IRD). There is usually a non-bioturbated interval at the base of this unit whereas the IRD do not extend to the top. The lower part of this lithofacies contains many shells dated from 12,000 to 12,500 ¹⁴C yr BP. It is usually thinner than Lithofacies 3.
- (5) Post-glacimarine (“Holocene” in Barrie and Conway, 2000, 2002) olive to olive-gray marine muds, bioturbated, richer in organic matter than the underlying facies, but poorer in shells. The reduction in glacial rock flour (clay) marks the end of the glacimarine influence in the basin. Relationship with the Fraser flood clay (Conway et al., 2001) indicates that deposition of this facies probably began shortly before 10,000 ¹⁴C yr BP.
- (6) Post-glacimarine (“Holocene”) sands are gray to olive-gray sands present above the glacial clays in cores collected at depths less than 100 m.

4. Material and methods

Of the 12 piston cores considered here (Table 1), nine include the whole succession from the modern, through the Holocene and the ice-distal massive clays to

the ice-proximal laminated clays. One core (28A) lacks only the Holocene and two others (32 and 70) do not reach the contact between the massive clays and the laminated clays. Late Wisconsinan till has been identified in two cores (6 and 62). The 12 cores come from depths varying from 71 to 281 m; they vary in length from 40 to 670 cm. The sampling space is irregular but averages about 40 cm. A total of 74 foraminiferal samples, 24 diatom and 11 dinoflagellate cyst samples were collected and analyzed from the laminated facies up into the base of the post-glacimarine sediments.

Most foraminifer samples represented 2–3 cm of core length and 15–25 cm³. In sediments expected to yield few specimens (laminated clays), up to 45 cm³ were collected. Wet samples were sieved through a 63 µm sieve. Foraminifers were concentrated in a heavy liquid (density: 1.9). When necessary, the concentrated fossil residue was split into aliquots with a microsplitter until a fraction manageable for counting was obtained. The numbers of specimens per cm³ given in the distribution charts are thus extrapolations. For samples in which counts of ca. 500 or less were obtained, all specimens were counted.

Many samples yielded such large numbers of diatoms that foraminifers could not be seen. Excess diatoms were removed by first spreading the concentrated residue over a counting tray. The tray was then turned upside down and knocked upon so that heavier grains (including foraminifers) fell down, whereas diatoms remained stuck by static electricity. This procedure was repeated until most diatoms were removed and all foraminifers visible. We believe that negligible bias is introduced by this method.

For diatom analysis, 2 cm³ samples were collected, of which 1 g of dry sediment per sample was weighed and diluted in 50 ml of distilled water in a glass jar. An average of 0.2–0.5 ml was mounted for microscopic analysis on glass slides, using Norland Optical Adhesive as embedding medium. Apparently barren samples were further processed using gravity settling in order to further concentrate the diatoms. For each sample, a minimum of 300 valves was counted, where possible, along random transect lines.

Both the resting spores and the vegetative cells are included in the computation of diatom percentages and concentrations. Diatom concentrations are given in number of frustules per gram of dry sediment. They were calculated from sample density and number of counted valves per known subsample volume.

For palynological analysis, 5 cm³ of sediment were sieved at 10 and 120 µm to remove coarse sand and fine silt and clay particles. The 10–120 µm fraction was treated with HCl (10%) and HF (49%) to dissolve carbonate and silica particles. The residue was ultimately sieved at 10 µm and mounted between a slide and cover slide in glycerin gel. The concentration of palynomorphs was evaluated using the marker–grains method (Matthews, 1969). In most of the samples, more than 300 dinocysts were identified. The taxonomic nomenclature of dinocysts used here conforms to that presented in Radi et al. (2001). Specimens belonging to Protoperidinales, for which determination at the genus level was difficult due to the orientation and/or preservation, were grouped under the label “protoperidinioids”.

5. Results

5.1. Foraminifers

In all, 76 benthonic taxa were recorded from the glacial marine deposits (online appendix). Only six planktonic specimens were encountered; they were not identified.

A succession of five foraminiferal biofacies and two subfacies can be recognized in the Strait of Georgia cores; this succession is the same everywhere in the region of study. One late additional biofacies occurs in one core only. None of the cores show all the biofacies and subfacies; one biofacies or another may be missing mostly because of the wide sample spacing, but the biofacies always occur in the same order.

We will compare our microfossil zones to a succession of sedimentary events which tend to occur always in the same order, from bottom to top (Table 3): the end of the laminated clay facies, the first bioturbation, the last IRD, the change in sediment color from gray to olive-gray and the increase in grain size from silty clay to mud. The last two events may occur in any order.

From bottom to top, the biofacies are:

- (1) “scattered calcareous foraminifers”: This designates assemblages where only statistically insignificant numbers (< 50) of common calcareous glacial marine foraminifers can be found, only in the lower parts of cores. The numbers are too small to allow for defining a biofacies quantitatively, but it is convenient to group them for discussion purposes. These assemblages occur mostly in the laminated clay; only a few have been seen at the base of the non-laminated clay above, especially in core 35.
- (2) *Elphidium excavatum*-*Quinqueloculina stalkerii*: The major species are *E. excavatum* and *E. foraminosum*. *Q. stalkerii* is less numerous than the two elphidiids. A few specimens of other glacial marine species usually occur but species diversity and total population are always low. Biofacies 2 occurs in a patchy way, in-between samples yielding only scattered calcareous foraminifers. Only four samples with more than 50 specimens have been found, three in the laminated facies and one in the massive clay above, before the first bioturbation (Table 3). One sample at the base of core 58 (666 cm, Fig. 2) does not quite qualify for this biofacies, being composed of *E. foraminosum* and *Q. akneriana*. We will nevertheless consider that, being a miliolid, the last species is equivalent to *Q. stalkerii* and consider the sample as “? *E. excavatum*-*Q. stalkerii*”. Many of the *E. excavatum* specimens in Biofacies 2 have a characteristic morphology found nowhere else in our material, save occasionally at the very beginning of Biofacies 3; they are thus useful markers. Their umbilical area, instead of showing a

Table 3
Occurrence of biofacies in function of sedimentologic characteristics

Sedimentologic characteristics	The <i>E. excavatum</i> / <i>Q. stalkerii</i> ^a biofacies occurs		The <i>N. labradorica</i> biofacies occurs		The early <i>C. reniforme</i> biofacies occurs		The late <i>C. reniforme</i> biofacies occurs		The <i>E. advena</i> biofacies occurs		Assemblages with no calcareous foraminifera occur	
	Before ^b	After	Before	After	Before	After	Before	After	Before	After	Before	After
Increase in grain	in 5 cores		7	9			5		7	6	3	3
First olive sediment	5		7	9	1	4	2	5	5	4	3	
Last IRD	4		7	5	6	2	3		8		6	
First bioturbation	5		5	2	3	8	5		7		5	
Last laminac	3	2		7	1	9	5		9		6	

Occurrences: Number of cores where the biofacies occurs, regardless of the number of samples in each core.

Interval of maximum occurrence is highlighted.

^aIncludes the ?*E. excavatum*/*Q. stalkerii* sample at 666 cm in core 58.

^b“Before”: starting from the base of the core.

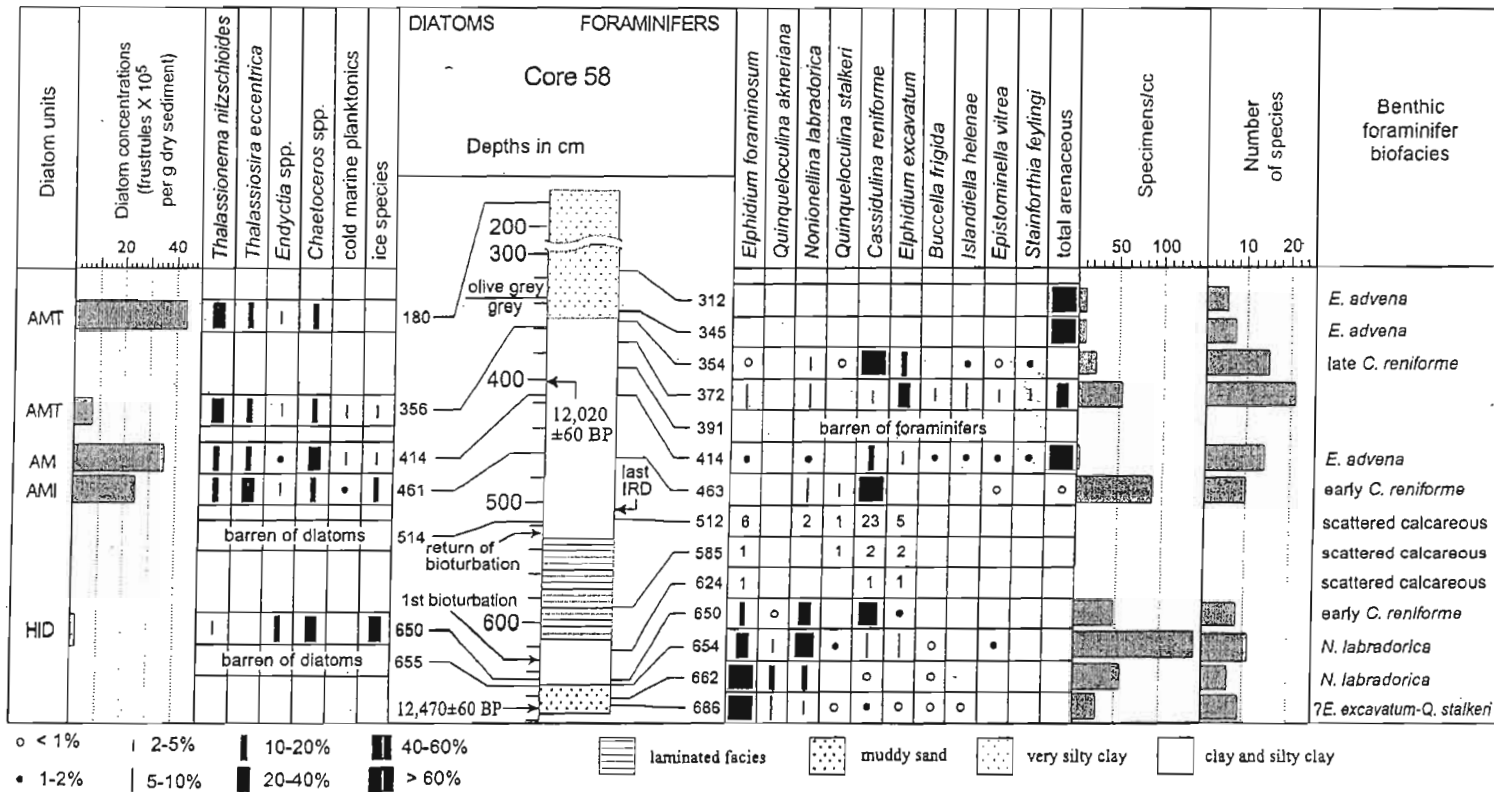


Fig. 2. Distribution of diatoms and foraminifers in core 58. When the specimens in a sample total less than 50, the number of specimens is shown instead of percentages. Acronyms for diatom units are: HID (high-ice-diatom species, not present in this core), AMI (abundant marine planktonics with few ice diatoms), AM (abundant marine planktonics), AMT (abundant marine planktonics with *T. nitzschioides*). Cold marine planktonics are *T. nordenskioldii* and *T. antarctica* resting spores.

Table 4

Radiocarbon dates on shells extracted from Strait of Georgia cores. Dates are corrected for an 800 years reservoir effect based on the corrections of Southon et al. (1990)

Laboratory number	Core	Depth in core (cm)	Lithologic unit	Corrected radiocarbon age (yr BP)	Dated material	Foraminifer biofacies
LLNL33802	58	402	ID	12,020 ± 60	<i>Rhabdus rectius</i>	Undiff. <i>C. reniforme</i>
LLNL33803	58	670	IP	12,470 ± 60	<i>Nuculana fossa</i>	? <i>E. excavatum</i> / <i>Q. stalkerii</i>
LLNL51003	28A	55	IP	12,380 ± 50	<i>Yoldia thraciaeformis</i>	Early <i>C. reniforme</i>
LLNL51004	30	19	IP	12,340 ± 50	<i>Yoldia martyria</i>	<i>N. labradorica</i>
LLNL52091	71	118	IP	12,310 ± 60	<i>Macoma lipara</i>	Early <i>C. reniforme</i>
TO-9315	6	104	ID	11,700 ± 80	Shell	Late <i>C. reniforme</i>
TO-9325	28B	97	ID	12,090 ± 100	Shell	Early <i>C. reniforme</i>
TO-9326	28B	151	IP	12,340 ± 90	<i>Nuculana minuta</i>	<i>N. labradorica</i>

Laboratories: LLNL = Lawrence Livermore National Laboratories; TO = University of Toronto; Lithologic units: IP = Ice proximal, ID = Ice distal.

prominent boss, is slightly depressed and partly or totally filled with papillae. The above-mentioned ?*E. excavatum*-*Q. stalkerii* sample is dated at 12,470 ± 60 ¹⁴C yr BP (Table 4).

- (3) *Nonionellina labradorica*: This biofacies is characterized by the highest percentage of *N. labradorica* in the succession and by the occasional abundance of *N. cf. turgida* and *N. digitata*. *E. foraminosum* and *E. excavatum* are highly variable. *Cassidulina reniforme* is a major species but it is less abundant than the sum of *Nonionella* and *Nonionellina*. *Q. stalkerii* is commonly present but never accounts for more than 10% of the assemblage. Diversities are low and assemblages are often limited to the species already mentioned. Biofacies 3 occurs at the base of the massive clay, mostly before the first bioturbation. There are two radiocarbon dates on this biofacies: 12,340 ± 50 and 12,340 ± 90 ¹⁴C yr BP (Table 4).
- (4) *Cassidulina reniforme*: *C. reniforme* is abundant and in most samples dominant, usually accounting for more than 50% of the fauna. The rest is composed of a larger number of species than Biofacies 3 and can be roughly subdivided into two successive subfacies: a *N. labradorica*-rich, early *C. reniforme* subfacies below and a *N. labradorica*-poor, late *C. reniforme* subfacies above. The abundant *N. labradorica* of the early part constitute the waning side of the *N. labradorica* peak of Biofacies 3. We set the limit between Biofacies 3 and 4 at the point where *C. reniforme* becomes more abundant than *N. labradorica*; this last species is never again more abundant than *C. reniforme* except in core 6. *Nonionella cf. turgida* and *N. digitata* are generally few in Biofacies 4 save in core 28B (Fig. 3) where the sample at 97cm is considered "early *C. reniforme*" on the basis of its abundance in *N. digitata*. In the late *C. reniforme* subfacies, the combined percentage of *Islandiella helenae* and *Euvigerina juncea* is usually greater than that of *N. labradorica*. These two species rarely exceed 10%

individually. From one core to the next, *E. excavatum* and *E. foraminosum* may vary from rare to abundant; we have found no clear trend in their distribution within Biofacies 3 and 4. *Q. stalkerii* may be present in the lowermost sample of Biofacies 4 but is otherwise absent.

Arenaceous species first appear in statistically significant numbers only in the *C. reniforme* biofacies. The species composition is the same as in Biofacies 5. They may appear early or late or at the end of the biofacies and rapidly grow in numbers until they account for 50% or more of the assemblage; this is the limit arbitrarily set between the *C. reniforme* and the *E. advena* biofacies. Most commonly, arenaceous forms develop in the late *C. reniforme* subfacies.

Three dates on the early *C. reniforme* subfacies range from 12,000 to 12,300 ¹⁴C yr BP, one "undifferentiated" *C. reniforme* date is 12,090 ± 100 ¹⁴C yr BP and one late *C. reniforme* date is 11,700 ± 80 ¹⁴C yr BP (Table 4).

- (5) *Eggerella advena*: The dominant species is *Eggerella advena* and it is accompanied by *Recurvoides turbinatus* and *Spiroplectammina biformis*. *Lepidodeuterammina ochracea* and *Trochammina* sp. 2 may occur in moderate numbers but their distribution is irregular and often they are absent. A sample is included in the *E. advena* biofacies if its arenaceous population is more than 50% of the total. Going up a given core, the arenaceous population may exceed 50%, then be less, then exceed 50% again. The calcareous species are often absent; when present, their numbers are often too small to give statistically significant percentages. When abundant, the major calcareous species is *C. reniforme*, followed by *E. excavatum*, *E. foraminosum*, *I. helenae*, *E. juncea* and *N. labradorica*, that is, by the major species of the late *C. reniforme* biofacies.

The high proportion of arenaceous forms coincides with the change in sediment colour and/or the passage from glacial clay to marine mud at the end

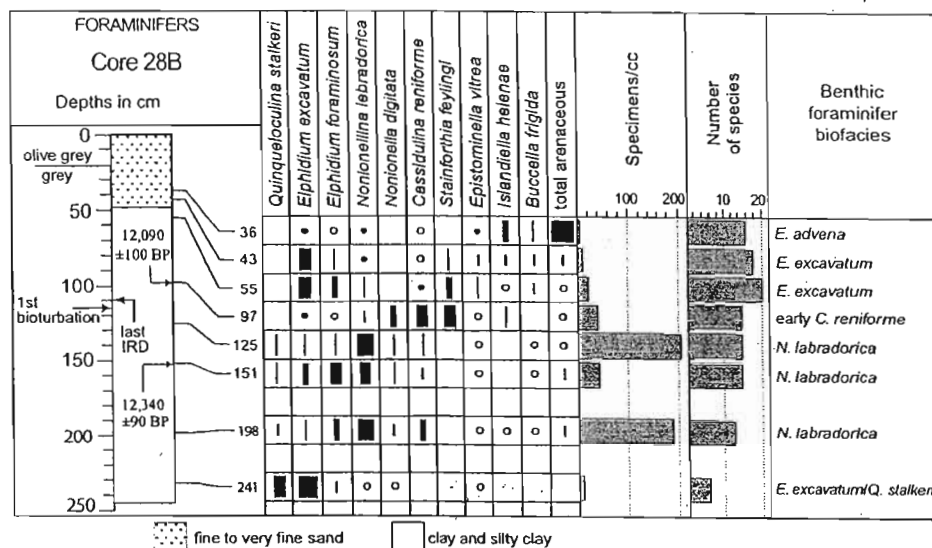


Fig. 3. Distribution of foraminifers in core 28B.

of the glacial marine phase. We have no radiocarbon date on this biofacies.

- (6) *E. excavatum*: This undated biofacies is present in only two samples in the upper part of core 28B (Fig. 3). The dominant species (no more than 50%) is *E. excavatum*; other major species are *E. foraminosum* and *Stainforthia feylingi* while *N. labradorica*, *Epistominella vitrea*, *Buccella frigida* and *I. helenae* occur in lesser numbers. The number of species in both samples is high, respectively 17 and 20. The foraminifers in these samples are poorly preserved, being encrusted by a powdery deposit that tends to conceal their features; therefore, an important proportion (20 and 30%) of the material is indeterminate. There is no suggestion of dissolution.

5.2. Diatoms

Twenty-four subsamples collected from Strait of Georgia cores 32, 35, 41, 58, 70 and 71 were selected for diatom analysis. A total of 56 taxa in 36 genera were identified (online appendix). Diatoms were generally well preserved and their concentrations commonly varied around 2 and 4×10^6 frustules/g dry sediment. We identified four diatom units that describe paleoenvironmental variations. The definition of these units is given here, starting with the oldest, along with a brief paleoecologic interpretation which will be referred to in the next section (Paleoecologic discussion):

- (1) *High-ice diatom concentrations (HID)*: This diatom unit was described in all cores except 32 and 70.

Mostly dominated by *Fragilariopsis cylindrus* and *Chaetoceros* spp., it is also characterized by *Thalassiosira antarctica* resting spores (in both cores 35 and 41), *Stephanodiscus* cf. *hantzschii* and *Cyclotella stelligerina* (in core 41, Fig. 4) and *Endocytia* spp. (in core 58). Predominance of the ice species *F. cylindrus* in this diatom assemblage indicates extended winter sea-ice conditions. The relative abundance in core 41 of the brackish, salty water tolerant *C. stelligerina* (Germain, 1981), could imply a short seasonal ice-free period, during which cold low-salinity surface waters would have supported a brief phytoplankton bloom. The same sort of phytoplankton bloom in cold waters and higher salinity is suggested by the presence of the marine species *Endocytia* spp. in core 58.

- (2) *Abundant marine planktonics with few ice diatoms (AMI)*: This diatom unit is observed in cores 32, 58, 70 (Fig. 5) and 71 (Fig. 6). The assemblage associated with this unit is defined by the abundance of the marine planktonic species *Chaetoceros* spp., *Thalassiosira eccentrica* and *Thalassiosira leptopus*, with fewer *Thalassionema nitzschioides*. It is also characterized by the presence of two important cold marine planktonic species: *Thalassiosira nordenskiöldii* and *Thalassiosira antarctica* resting spores (except for core 58). *Thalassiosira nordenskiöldii* is usually found in water temperature lower than 5°C , and together with *T. antarctica* resting spores, they were described in the Bering Sea as a typical cold water assemblage of an ice-margin productivity by Sancetta et al. (1985). The presence in this assemblage of the sea-ice

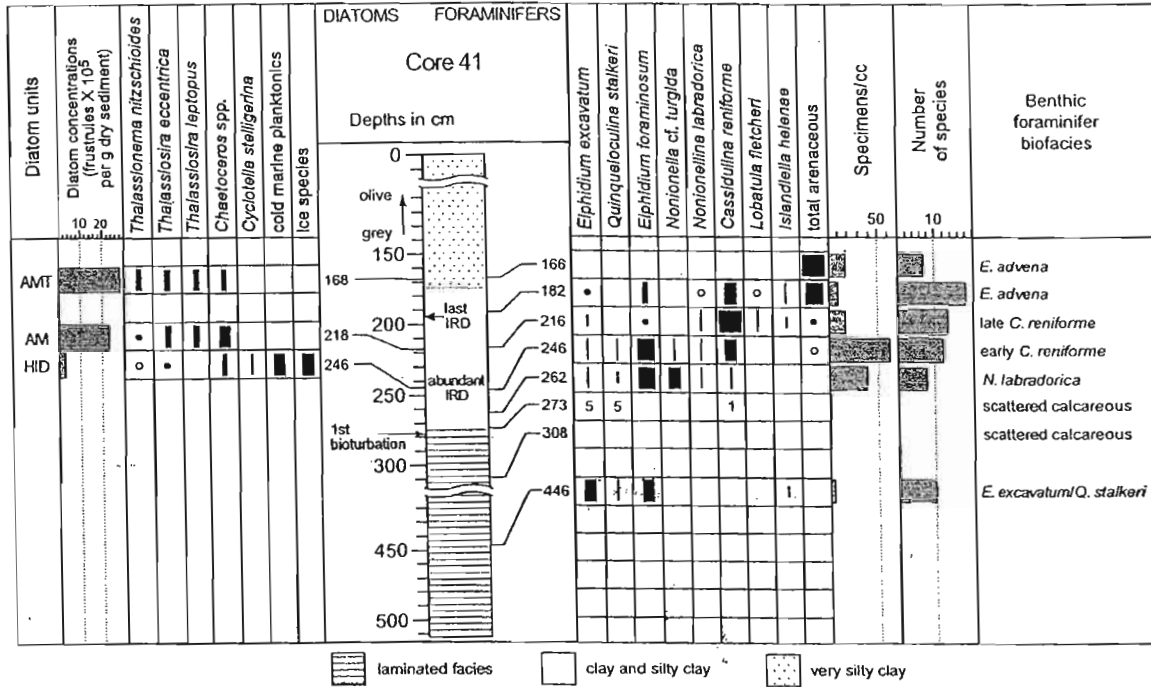


Fig. 4. Distribution of diatoms and foraminifers in core 41.

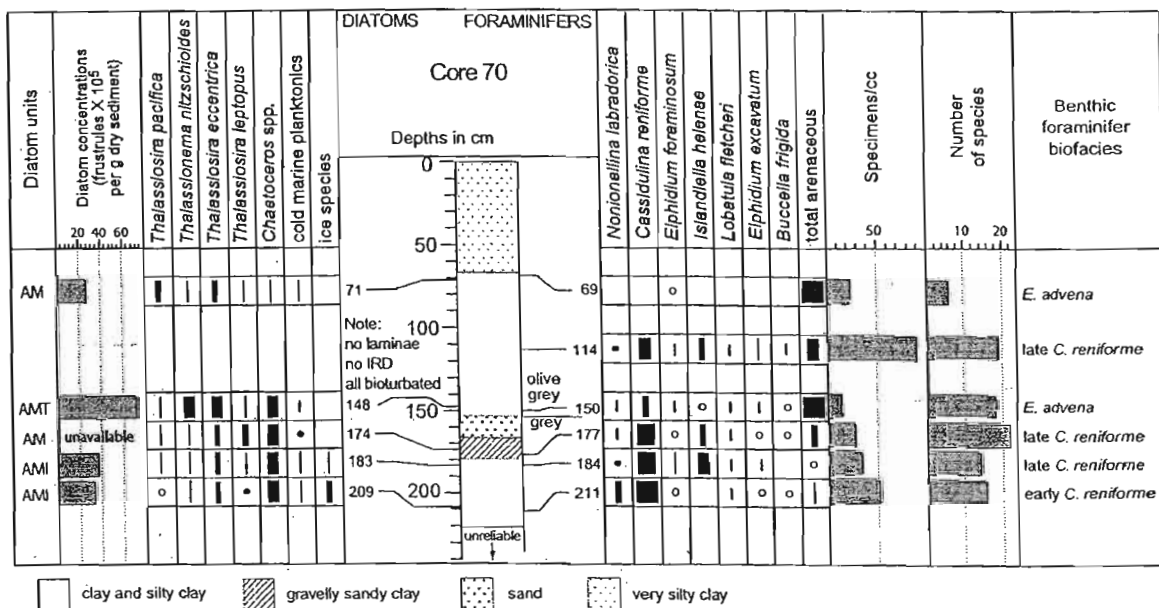


Fig. 5. Distribution of diatoms and foraminifers in core 70.

diatoms *F. cylindrus* and *Porosira glacialis* (except for core 71) also implies rather long winter sea-ice conditions. As a group, this assemblage suggests a

high seasonal variability with high productivity in relatively cold water with a limited sea-ice cover during the winter season.

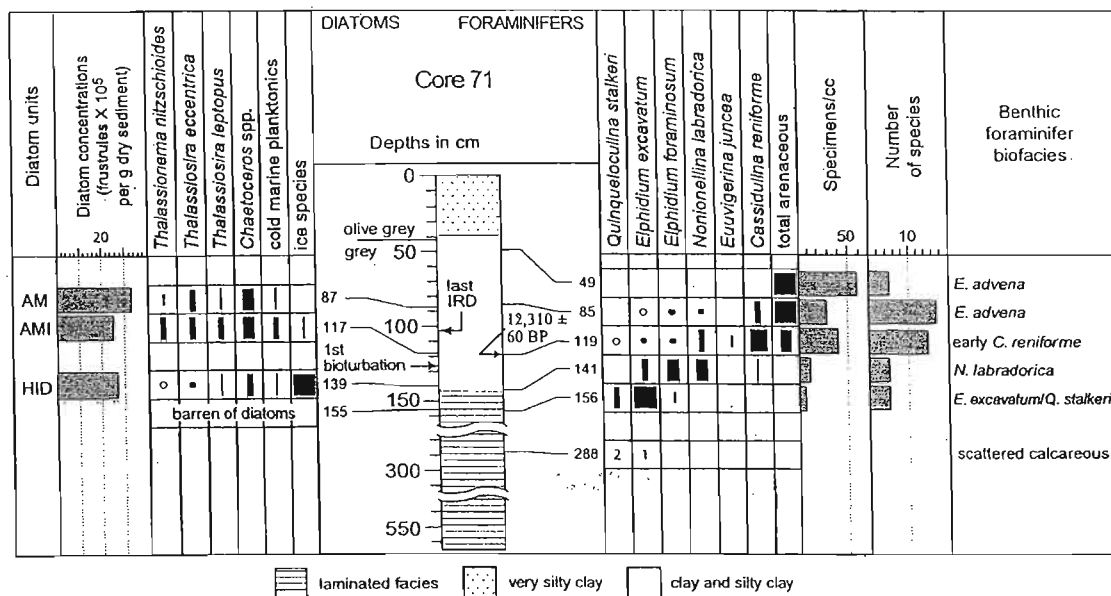


Fig. 6. Distribution of diatoms and foraminifers in core 71.

- (3) *Abundant marine planktonics (AM)*: This unit is present in all cores except 32. Characterized by the abundance of *Chaetoceros* spp., *T. eccentrica*, *Thalassiosira pacifica* and *T. leptopus*, it is also composed of minor amounts of *T. nitzschioides*, *Thalassiosira decipiens*, *Coscinodiscus* cf. *radiatus* and *Tabularia fasciculata* (except for cores 70 and 71, where *T. fasciculata* is absent). In core 41, *T. decipiens* and *T. fasciculata* are more abundant in this unit. Both *T. decipiens* (Sancetta, 1981) and *T. fasciculata* (Snoeijs, 1993) prefer to grow in rather lower salinities. This marine planktonic diatom assemblage suggests a warmer sea surface temperature than the previous AMI unit.
- (4) *Abundant marine planktonics with T. nitzschioides (AMT)*: This diatom unit is present in cores 41, 58 and 70. Mainly composed of *T. nitzschioides*, *T. eccentrica* and *Chaetoceros* spp, there are also some other characteristic marine planktonic species such as: *T. leptopus*, *Coscinodiscus asteromphalus*, *Coscinodiscus divisus*, *T. pacifica* and *Endyctia* spp. This diatom assemblage is similar to the preceding AM unit, but with a significantly increased number of *T. nitzschioides*. This last species is an indicator of late spring and summer productivity and prefers to grow in somewhat warmer and saline oceanic water (Sancetta, 1981). Diatom assemblage for this unit then defines warmer and saline surface water environment suggesting a warming gradient upcore.

5.3. Dinoflagellate cysts

The 11 dinocyst samples (Fig. 7) came from only two cores: 41 and 71 (online appendix). All the taxa encountered are listed in the text below. At the base of both cores, the dinocyst distribution shows low concentration and low species diversity. *Operculodinium centrocarpum* and *Brigantedinium* spp. constitute the dominant taxa. Pollen grains and foraminifer linings also record low concentrations. In both cores, the first sample at the base is marked by a very high autotroph/heterotroph ratio of about 2.5, *O. centrocarpum* being the autotrophic-related taxon, and in both cores also, the second sample is characterized by a very low (<0.5) value of the same ratio.

Higher in the sequence, there is a considerable increase in the dinocyst concentration and species diversity. The assemblages remain dominated by *O. centrocarpum* and *Brigantedinium* spp., but *Islandinium* spp., *Selenopemphix* spp., *Protoperidinium americanum*, *Quinquecupis concreta* and protoperidinoids record significant percentages. The other accompanying taxa which occur in low percentages are *Votadinium spinosum*, *Lejeunecysta* spp., the cyst of *Polykrikos kofoidii*, *Spiniferites elongatus*, *Spiniferites ramosus* and *Pentapharsodinium dalei*. The density of pollen grains (exclusive of reworked specimens) also increases in the upper part of the cores.

In core 71, the number of foraminifer linings, very low in the first two samples, increases gradually afterwards and peaks at the top of the sampled core. In core 41, the

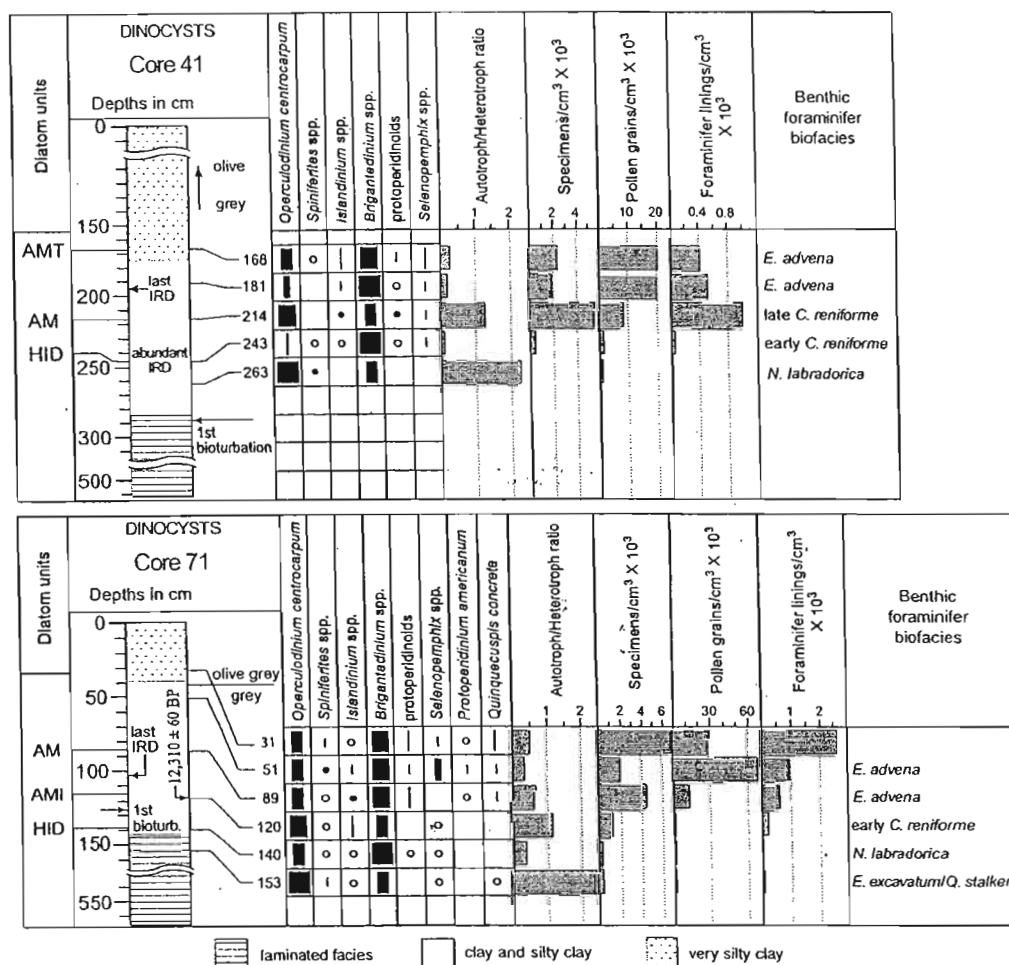


Fig. 7. Distribution of dinoflagellate cysts, total pollen grains (unworked) and organic foraminifer linings in cores 41 and 71. Diatom units and foraminifer biofacies are given for comparison.

number of linings increases abruptly at the third sample and stays high afterwards.

6. Paleocological discussion

We interpret the paleoenvironments represented by benthic foraminifers, and by (mostly) planktonic diatoms and dinocysts, and then relate these assemblages to the sedimentologic events. Since the biofacies boundaries do not necessarily coincide between each group, the interpretation will be centered on the foraminifer succession, whose sampling is the most extensive, and other evidence will be brought in to enrich the discussion.

6.1. "Scattered calcareous foraminifers"

The preservation of foraminifer tests does not clearly indicate reworking by ice transport and the virtual absence of species of temperate affinity does not allow the conclusion of resedimentation from pre-glacial marine deposits. There is no obvious trace of dissolution on the tests. Diatoms are absent except for a few indeterminate fragments, suggesting no productivity, which agrees with an origin underneath a meltwater plume. Korsun and Hald (1998, 2000) report a virtual absence of phytoplankton biomass close to "active" ice fronts. They also report reduced phytoplankton close to quieter ice fronts. Near active ice fronts, they observe a small number of living calcareous benthic foraminifers

in an Allogromiina-dominated assemblage; after post-mortem destruction of the latter, the leftover assemblage would be comparable to our “scattered calcareous” assemblages. In summary, the fossil evidence agrees with the sedimentology (Barrie and Conway, 2000) and is compatible with a near-ice, meltwater plume-influenced environment.

6.2. *E. excavatum*–*Q. stalker*i biofacies

This early biofacies occurs in the laminated clay or at the base of the massive clay, before the development of bioturbation (Table 3). It can be observed far below the top of the laminated clay, such as in core 41 (Fig. 4). It is the equivalent of the *E. excavatum*–*Q. stalker*i fauna that Korsun and Hald (1998, 2000; Fig. 8) report from under the meltwater plume in Novaya Zemlya and Svalbard, in salinities of 34‰. It is not a low-salinity indicator. Relative sea level must have been close to the maximum values given earlier, i.e., 120 m above present in the Gulf Islands, ocean water must have had comparatively easy access, and bottom salinity must have been higher than the present maximum of 31‰. Biofacies 2 indicates very low food supply, compatible with very low surface productivity due to high water turbidity. One major faunal difference between our assemblages and those of Korsun and Hald (1998, 2000) is the abundance of *E. foraminosum*: this species is absent from the modern Atlantic Ocean. In the absence of good modern evidence about its living requirements and based on its morphologic resemblance with *E. excavatum*, we will assume that it is as tolerant and undemanding as this last species. The most diagnostic species, despite its relatively low numbers, is *Q. stalker*i because, contrary to the immensely widespread *E. excavatum*, it tends to concentrate in the near-ice biofacies. Recent observations by Korsun and Hald (pers. comm., 2001) suggest that *Q. stalker*i lives on a non-algal diet, possibly bacteria. This makes it less dependent on local surface productivity. In the absence of modern data, and on the basis of its distribution, we will assume that the *Q. akneriana* in core 58 have the same ecology as *Q. stalker*i and that the above discussion applies to the sample at 666 cm.

The sand laminations are probably the result of turbidity currents. Their distribution does not necessarily coincide with that of the surface plume. The fact that in some cores the “scattered calcareous” and the *E. excavatum*–*Q. stalker*i facies extend above the laminations is not in contradiction with the above interpretation. Because of sampling methods, Korsun and Hald (1998, 2000) could not confirm whether or not their *E. excavatum*–*Q. stalker*i facies occurred in a laminated, non-bioturbated clay facies, but Korsun et al. (1995) did report the presence of the *E. excavatum*–

reniforme–*Q. stalker*i assemblage in a near-ice laminated facies in a Novaya Zemlya fjord.

Cores with early deglacial *E. excavatum*-dominated assemblages are reported on by Osterman (1984) from Frobisher Bay, Baffin Island, by Polyak and Mikhailov (1996) from the SE Barents Sea and by Scott et al. (1989) from the Atlantic coastal shelf of Canada. The last authors concluded to the high paleosalinity of these assemblages on the basis of stable isotopes.

We examined only one sample for diatoms from the *E. excavatum*–*Q. stalker*i biofacies (core 71, Fig. 6): it is barren of diatoms as other samples from the laminated clay. This is consistent with an origin from under the meltwater plume. It explains the dominance of trophically undemanding (or bacterivorous) foraminifer species. The same level in core 71 has been investigated for dinocysts: the number of specimens is very low and taxa related to autotrophic productivity (*O. centrocarpum*) largely dominate. Heterotrophs are known to consume diatoms and their low numbers are thus not surprising. Hamel et al., (2002) observe, in the northern Baffin Bay polynia, where diatom populations are abundant, dominant Protoperidinales in the dinocyst assemblages, whereas at the margin of the low diatom productivity zone, *O. centrocarpum* dominates.

6.3. *N. labradorica* biofacies

The *N. labradorica* biofacies occurs only after the end of the sand laminations, more often before than after the first bioturbation and always before the last IRD, when these are present (Table 3). Even though strongly influenced by melting ice, it must indicate a sudden increase in productivity because it usually contains a much larger number of foraminifers than the underlying levels. This is the first biofacies to give an indication of salinity: *N. labradorica* is known to live only at salinities greater than 30‰ (Cedhagen, 1991; Korsun and Hald, 2000; Polyak et al., 2002). In the deep waters of the deglacial Strait of Georgia, salinity probably remained high even close to the melting ice, the fresh meltwater remaining at the surface.

The *N. labradorica* biofacies is the first to contain diatoms. The first diatom population is largely comprised of ice-dwelling species (*F. cylindrus* and *P. glacialis*). Twenty-seven to 72% of the flora is accounted for by these two species, which suggests an extended sea-ice cover for most of the year. The low numbers of the cold-sensitive *T. nitzschioides* and the relatively high proportion of the specifically cold-water forms *T. antarctica* resting spores and *T. nordenskiöldii* agree with the ice diatoms in suggesting very cold conditions.

In core 71, the dinocysts assemblages of the *N. labradorica* biofacies are characterized by low diversity and the dominance of *Brigantedinium* spp., suggesting cold conditions. An increase in Protoperidinales cysts,

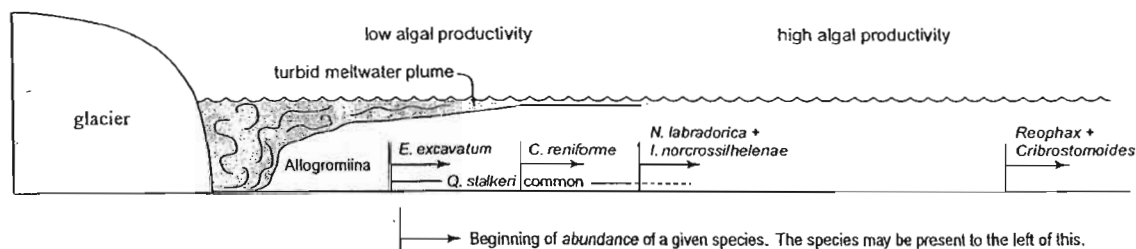
known to feed on diatoms, is expected at a level where there are abundant diatoms. In core 41 (at 262 cm; Fig. 4), the *N. labradorica* biofacies coincides with a dominance of *O. centrocarpum*. Diatoms were not sampled at this level but the ice-diatom flora usually associated with the *N. labradorica* biofacies occurs at 246 cm, with the early *C. reniforme* subfacies. Conditions at 262 cm may have been at the hinge between near-ice and ice-distal, and diatom numbers may have been small.

N. labradorica is known to sequester algal chloroplasts in its cytoplasm (Cedhagen, 1991; Bernhard and Bowser, 1999). This has been observed in specimens exposed to dysoxia/anoxia and appears to help survival under these conditions. It is not known what advantage the foraminifer gains from this association but at the depth where it lives, and because it is a burrower, photosynthesis is probably not a factor (Bernhard and Bowser, 1999; Bernhard, pers. comm., 2002). In the *N. labradorica* biofacies, we observe 200,000 to more than 2 million diatoms per cm³, which is considerable, whereas the underlying biofacies contained none. The sediment shows no clear mark of anoxia such as black sulfide specks, but there could have been anoxia below the sediment/water interface nonetheless, considering the still rather fast sedimentation and the frequent absence

of bioturbation. The *N. labradorica* peak could thus be a direct result of the sudden diatom bloom, although the more stable bottom conditions (no more turbidity currents) may have played a part. Observations by Korsun and Hald (2000) in a Svalbard fjord suggest a dependency of *N. labradorica* on early spring algal bloom. They found that *C. reniforme* thrived closer to the glacier than *N. labradorica*, under the more distal part of the meltwater plume (Fig. 8); this differs from our vertical succession where *C. reniforme* peaks in the ice-distal lithofacies, after *N. labradorica*. On the coast of British Columbia, with Ekman current-induced upwelling carrying nutrient-rich deep water up the Strait of Juan de Fuca and generating high productivity, conditions must have been created very early on that were favorable to any organism dependent on algal blooms. In addition, the presence of melting ice must have created locally an estuarine circulation that caused an upwelling of nutrient-rich saline waters. The subsequent upcore decline of *N. labradorica* while diatoms still increase and dinocysts begin to bloom could be explained by more intense bioturbation, hence better aeration, which would favor other species.

The late peaks of *N. labradorica* reported by Hald and Vorren (1987) off northern Norway and by Polyak and Mikhailov (1996) in the SE Barents Sea seem to

A) Novaya Zemlya and Svalbard fjords after Korsun and Hald (1999, 2000)



B) Strait of Georgia composite succession

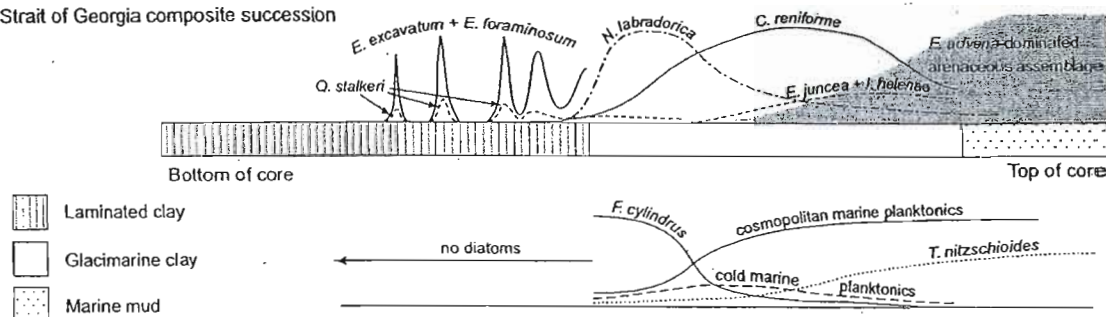


Fig. 8. (a) Distribution of major foraminifer species in front of active glacial fronts in Novaya Zemlya and Svalbard, summary of the findings of Korsun and Hald (1998, 2000). (b) Strait of Georgia's composite deglacial succession. The composite section is lying on its side to show the parallel we make with the Svalbard results above. Curves illustrate relative abundances of foraminifera (above) and diatoms (below).

correspond, at least following these last authors, to a productivity increase resulting from the start of normal marine conditions following invasion of Atlantic waters at the end of deglaciation. However, they result from a large-scale oceanic change, whereas our *N. labradorica* peak is likely due to strictly local estuarine circulation.

Although they contain fewer *N. labradorica*, the assemblages collected by Elverhøi et al. (1980) from as little as 500 m from a modern ice front in Svalbard are close to our *N. labradorica* facies. They report an average sedimentation rate of 10 cm per year and high summer turbidity. The sedimentation rate during the deposition of our turbidity-tolerant *E. excavatum*–*Q. stalkerii* biofacies was probably even higher.

The early deglacial *C. excavatum* biofacies reported by Patterson and Kumar (2002) from ODP cores in Saanich Inlet is probably intermediate between our *N. labradorica* and our *E. excavatum*–*Q. stalkerii* biofacies because of its species diversity and because it contains frequent *I. helenae* and *N. digitata*. Productivity may have been high but the sedimentation rate, due to the geometry of the basin which makes it a natural sediment trap, could have been such as to dilute the faunas and cause an additional stress favoring the more tolerant species *E. excavatum* and *Q. stalkerii*. The next deglacial biofacies of Patterson and Kumar (2002) is dominated by *Islandiella* spp. and is probably less stressed by turbidity; it may represent conditions closer to those in which our *N. labradorica* biofacies developed.

6.4. *C. reniforme* biofacies

The *C. reniforme* interval witnesses a gradual change from typical glacial marine with high influx of very fine grain sediment to non-glacial where “normal” marine mud is being deposited. This probably corresponds to the complete melting of the ice within the Strait of Georgia, any ice left being located either in the fjords or beyond, the fjords acting as sediment traps.

The early *C. reniforme* interval contains a large but declining proportion of *N. labradorica*, left over from the *N. labradorica* peak of the earlier biofacies. This decline is compensated by a dominance in *C. reniforme* and a greater number of species.

A recent study of Kara Sea living foraminifers by Polyak et al. (2002) shows that *I. norcrossi* (considered here as ecologically equivalent to *I. helenae*) and *N. labradorica* belong to two different groups in terms of resistance to river discharge, the first being less tolerant. Their distribution maps show the presence of *I. helenae* down to approx. 32.5‰ and *N. labradorica* to 31‰. Values recorded off Sweden by Cedhagen (1991) may differ somewhat because salinity is probably not the only factor affecting species distribution. Polyak et al. (2002) place *C. reniforme* in the same tolerance group as *N. labradorica* (“river intermediate”) but a close look at

the distribution maps shows that *C. reniforme* is recorded in salinities as low as 26‰.

Even though *C. reniforme* is more tolerant of hyposalinity than *N. labradorica*, higher diversities suggest environmental improvement, either higher salinity, or less stress by the presence of glacier ice. The fact that the early *C. reniforme* subfacies, contrary to the *N. labradorica* biofacies, usually occurs in bioturbated sediment (Table 3) means either environmental improvement or gradual colonization of the deglaciated seafloor, environmental parameters remaining the same. Given that the whole region was undergoing isostatic uplift, one should rather be on the lookout for a paleosalinity reduction. We will thus consider that salinities in the early *C. reniforme* subfacies remained about the same as in the earlier biofacies that is, higher than the modern 30–31‰.

There is no foraminiferal indication of an increase in bottom water temperature in the early *C. reniforme* subfacies, and not much either until the post-glacial marine sediments are reached, although there is diatom and dinocyst evidence of warmer surface waters at an earlier level. This may mean that bottom waters remained cold longer, but maybe also that temperature-sensitive species did not have yet the time to colonize the area. The paleosalinities proposed in the previous paragraph were sufficiently high so as to be no obstacle to colonization by most species.

The early *C. reniforme* subfacies in core 58 (Fig. 2) is split into two intervals by the presence of ca. 85 cm of laminated clay, itself surrounded by clay layers with only “scattered calcareous foraminifers”. This apparent return to more glacial conditions is difficult to reconcile with the absence of a mobile ice front, i.e., with only dead ice melting in situ. Since this site is located between Vancouver Island, Denman Island and Hornby Island (Fig. 1), it must have been, at least for a while, a bight surrounded by ice based on these islands and grounded on shallows SE of Hornby Island. Currents in this bight may have shifted as ice melted, and along with them the meltwater plumes and the laminated lithofacies. This implies that the various biofacies described herein were situated fairly close to one another on the floor of the deglaciating Strait of Georgia.

The early *C. reniforme* interval is marked by diatom populations with ice-dwelling species that vary from abundant to absent, generally less abundant however than in the *N. labradorica* biofacies and more than in the late *C. reniforme* interval. Typical cold water planktonics (*T. antarctica* resting spores and *T. nordenskiöldii*) remain frequent and the total population, mostly made of marine planktonics, is on the increase. Even though the temperatures are still cold, the reduction in sea-ice cover is such that a surface temperature increase is highly probable. The persistence of cold indicators at 246 cm in core 41 (Fig. 4) may be explained by one or

both of the following: first, this sample may have been collected close to the boundary with the *N. labradorica* biofacies and second, annual sea-ice cover may have been longer or shorter in various part of the basin due to wind and surface currents.

Dinocysts of the early *C. reniforme* subfacies in core 41 are still few in numbers and in diversity. They occur together with a high-ice-diatom flora. The autotroph/heterotroph ratio is very low: this is expected when there are abundant diatoms for the heterotrophs to consume (Hamel et al., 2002). At the same level in core 71, dinocysts are detectably more numerous and the autotroph/heterotroph ratio is about 1, but the diversities are still low. There are still some ice diatoms and typical cold marine planktonics. Dinocysts agree with diatoms to support the idea of a glaciomarine environment, though less harsh than in the *N. labradorica* biofacies.

The late *C. reniforme* subfacies is marked by a limited increase of *Euuvigerina juncea* and *Islandiella helenae*, and small numbers of *N. labradorica*. *Euuvigerina juncea* tolerates cold temperatures but is not reported living north of the Bering Strait and is not fully arctic. This is the only possible evidence in favor of bottom water warming. However, the deglaciating Strait of Georgia, even in its coldest phases, may never have been colder than the modern northern Bering Sea and thus the appearance of *E. juncea* may not indicate a warming trend. *Islandiella helenae* is one of the few species to live only in cold water, at least in the Atlantic (Guilbault, 1989). On the basis of the results of Polyak et al. (2002), we will assign to it a salinity tolerance of somewhat above 30‰, i.e. higher than *N. labradorica*.

Korsun and Hald (1998, 2000) report the first occurrence of *I. helenae* and *I. norcrossi* together with the first appearance of *N. labradorica*. They do not report *E. juncea* but this species is unknown from the North Atlantic and its absence is not diagnostic. The late appearance of *I. helenae* in our material, along with an increase in species diversity, could mean a slight increase in salinity, although it may just indicate that this species is a slow colonizer. Given the isostatic uplift context, we believe that gradual colonization and not higher salinity

caused the gradual increase in species number up to the point where the arenaceous dominate.

All the arenaceous species present in the late *C. reniforme* subfacies (see Section 5.1) except one form in open nomenclature have been recorded from the Arctic. Hence, they do not constitute evidence that it was less cold than the earlier intervals. Also, the occurrences of that subfacies are all situated below the increase in sediment grain size that marks the end of the glaciomarine influence in the strait (Table 3).

A reduction in bottom salinity can be expected sometime before 9000–10,000 ¹⁴C yr BP because isostatic uplift must have gradually impeded the influx of sea water through the Gulf/San Juan Islands. This is a corollary of the various post-glacial sea-level studies on the west coast (Mathews et al., 1970; Clague et al., 1982; Linden and Schurer, 1988; Dethier et al., 1995; Clague and James, 2002; James et al., 2002). The few radiocarbon ages we have indicate that the calcareous succession, from the base of the *E. excavatum*–*Q. stalker* to the top of the *C. reniforme* biofacies, was deposited within a few centuries at most (Table 5). If we assume that the near-ice laminated clay was deposited within decades, the sedimentation of the deglacial succession inclusive of the early *C. reniforme* subfacies was completed within five centuries. During that time span, the total isostatic rebound based on rates observed in the region (above-mentioned publications) must not have been more than 70 m. The marine limit at the northern edge of the Gulf/San Juan Islands can be estimated at 120–130 m based on Mathews et al. (1970), Clague et al., 1982; and Dethier et al. (1995). An uplift of less than 70 m would still leave plenty of space for ocean water to move in and allow bottom salinities greater than the present 30.5–31‰ (Table 2). If the results of Korsun and Hald (1998, 2000) can be applied here, salinities as high as 34‰ are thinkable for the *N. labradorica* biofacies. The composition of the early *C. reniforme* subfacies does not force us to conclude to any reduction in salinity. If we now consider the whole calcareous succession, up to the late *C. reniforme* subfacies (only one date: 11,700 ± 80 ¹⁴C yr BP, Table 5), then we can add 30 m of rebound and an effect on salinity

Table 5
Distribution of ¹⁴C ages in function of foraminifer biofacies and subfacies

Core time interval (kA BP)	North					South
	71	6	28	30	58	28B
11.50–12.00		Late <i>C. reniforme</i>				
12.00–12.25					Undiff. <i>C. reniforme</i>	Early <i>C. reniforme</i>
12.25–12.50	Early <i>C. reniforme</i>		Early <i>C. reniforme</i>	<i>N. labradorica</i>	? <i>E. excavatum</i> – <i>Q. stalker</i>	<i>N. labradorica</i>

is more likely. After 11,000 ^{14}C yr BP, relative sea level went through a minimum phase. In the Victoria area, Linden and Schurer (1988) report evidence of r.s.l. at 50 m below present. This probably had a clear and unmistakable effect on bottom microfaunas but its effect was felt later, probably in the *E. excavatum* assemblage.

Associated to the late *C. reniforme* subfacies are diatoms floras of the AM type, high in marine planktonics, with little or no ice-dwelling forms and a rather low percentage of typical cold water forms. Though the number of ice forms may be locally higher, as in core 70, this group suggests that glaci-marine influence diminished even more during deposition of the late *C. reniforme* subfacies. However, the rest of the flora does not give a clear signal. In cores 35 and 41, there are no typical cold forms in the upper *C. reniforme* level and the temperature-sensitive *Thalassionema nitzschioides* is increasing, whereas in cores 70 and 71, cold forms are still relatively abundant and *T. nitzschioides* is decreasing. Core 58 gives intermediate results. It is tempting to interpret this in terms of a N–S temperature gradient, but as these biofacies are probably time transgressive, additional dates would be needed to draw such a conclusion. Also, this distribution may be the result of unequal distribution of sea ice in the strait, due to winds and currents.

The increase in dinocyst diversity and numbers and the considerable increase in pollen grain numbers in the late *C. reniforme* subfacies indicates a change from a glaci-marine setting to warmer conditions, at least at the surface, and an increase in productivity. The pollen results imply the development of vegetation on the lands surrounding the Strait of Georgia and thus point in the direction of improved climate and glacier retreat.

The sudden increase in organic foraminifer linings in dinocyst preparations at the level where we see a decrease in the number of calcareous foraminifers retained by the 63 μm sieve is suggestive of dissolution of calcareous tests. This might be the explanation for the most obvious faunal change over this biofacies: the gradual invasion of arenaceous foraminifers to the point where, at the top, they completely replace the calcareous species.

6.5. *Eggerella advena* biofacies

The passage upward into arenaceous assemblages could be the result of postmortem dissolution of the calcareous species, as suggested by the organic foraminifer lining distribution which is essentially the same for the *E. advena* as for the late *C. reniforme* subfacies. Lowered salinity could have favoured dissolution of calcareous tests, but so could increased organic influx. The olive color, which is due partly to a change in clay content (Luternauer et al., 1989), partly to a higher organic content (Luternauer and Murray, 1983), occurs

from the late *C. reniforme* subfacies upwards (Table 3). Lower sedimentation rate due to disappearance of the ice and bioturbation could have favored oxidation of the organic matter, which would have generated acidity. In modern samples from Novaya Zemlya, Korsun and Hald (1998) report evidence of calcareous test dissolution (etch marks) in sediments where organic matter has been oxidized, causing a drop in pH. This takes place at ice-distal stations only; at ice-proximal stations rapid burial protects organic matter from oxidation.

E. advena is not a temperature indicator, being recorded from waters of widely different temperatures, including from the non-glaci-marine Arctic. However, its presence there is limited. Loeblich and Tappan (1953) report it at many stations but give no percentages; other authors report only small numbers (Phleger, 1952; Vilks, 1969; Vilks et al., 1979; Jennings and Helgadottir, 1994). By contrast, large concentrations can be found on the east coast of N. America in temperatures that vary from cold, in the Gulf of St. Lawrence, to temperate, on the New Jersey continental shelf (*E. advena* association of Murray, 1991). It is abundant to dominant in the modern Strait of Georgia (Cockbain, 1963). *Eggerella advena* may prefer locations far from the Arctic, but giving an interpretation to this biofacies remains hazardous because of the probable dissolution of the calcareous part of the assemblages. For the same reason, it is impossible to conclude on faunal grounds about the paleosalinity even though the arenaceous species are all hyposalinity tolerant. A reduction of salinity is probable, however, based on the known lowering of relative sea level in the region between 12,000 and 11,000 ^{14}C yr BP (Clague and James, 2002). If the number of organic foraminifer linings in dinocyst preparations is a guide, the original assemblage must have been much larger than what is left, and dominantly calcareous. A reasonable hypothesis would be that it was a continuation—at least at the beginning of the *E. advena* interval—of the *C. reniforme* biofacies because wherever there are calcareous forms leftover, they belong to the major *C. reniforme* biofacies species. Salinity was probably about the same, at the beginning, than in the late *C. reniforme* subfacies but could have decreased later. During deposition of the *E. advena* biofacies, the sedimentation rate was probably still higher than today, but since the ice had already melted away into the fjords or even further, the sediment was no longer glaci-marine (Table 3).

In the few instances where we have a diatom sample just above the last glaci-marine sediment (cores 41, 58 and 70), the assemblage (AM or AMT) suggests that earlier conditions persisted, with high-marine, low-brackish influences and no sea ice. The main difference is the significant increase in the temperature-sensitive marine planktonic *T. nitzschioides*, indicating increased surface temperatures. Dinocyst results show higher species diversities which also indicate warmer

temperatures. The increase in dinocyst and pollen numbers suggests the same. However, it is improbable that glacial meltwater stopped entering the basin after 12,000 ^{14}C yr BP. Stratification could have developed, with the meltwater spreading thinly at the surface and warming up quickly during the summer, while at depth, waters replenished by upwelling from Juan de Fuca Strait remained about as cold as before (R.E. Thomson, pers. comm., 2002).

6.6. *Elphidium excavatum* biofacies

This biofacies is observed only in core 28B (Fig. 3), which is the shallowest of the present series (71 m). It occurs both in the clay and in the muddy sand that cap the core. Whereas the assemblage from the sand (at 43 cm) could be interpreted as the result of downslope transport, the foraminifers from the clay (55 cm) are probably in situ. Such an *Elphidium*-dominated assemblage in a non-glacial setting is probably the result of hyposaline conditions. Salinity must not have been much less than 30‰ to accommodate the continued presence of small numbers of *N. labradorica* and *I. helenae*. Depth at this site was likely never less than 40–50 m and it was probably little affected by the seasonal brackish water. Hyposalinity is more probably indicative of changes at the scale of the basin. As discussed above, after 11,000 ^{14}C yr BP isostatic uplift must have reduced considerably the influx of ocean water at the southern end of the Strait; these undated *E. excavatum* assemblages could be of this age. The near absence of arenaceous forms in these samples (contrary to the modern Strait of Georgia faunas of Cockbain, 1963) is probably indicative of the influence of the geographic position, adjacent to small deltas. Core 28B was collected 1.2 km from shore just north of the Little Qualicum River. The submarine part of the modern Fraser delta contains essentially calcareous assemblages, the shallow species being mostly *E. excavatum*, *B. frigida* and *Elphidiella hannai* (Williams, 1989). Brackish elphidiids such as *Elphidium albiumbilicatum*, *Elphidium bartletti* or *Haynesina orbiculare* are not reported. Deeper than 50 m, the major species are *Nonionella stella*, *N. labradorica* and *Globobulimina pacifica*. Our *E. excavatum* biofacies is faunally closer to Williams's (1989) shallow samples. Patterson and Cameron (1991) and Patterson and Luternauer (1993) also report *E. excavatum*-dominated assemblages in Fraser delta cores dated at 11,000 ^{14}C yr BP and less. Like Williams's (1989) shallow samples, they are rich in *E. hannai*.

7. Summary and conclusion

In our Strait of Georgia cores, we have found evidence for the following upcore succession of

paleoenvironments, representing a gradual increase in distance from the ice:

- (1) A near-ice environment under the influence of the turbid meltwater plume. There is no bioturbation and phytoplankton productivity is minimal. Usually there are only a few calcareous foraminifers. Locally there are assemblages consisting essentially of *E. excavatum*, *E. foraminosum* and *Q. stalkerii*. Bottom salinity is unknown but could be close to normal (33–34‰). This stage may have lasted only a few decades.
- (2) An off-the-meltwater-plume environment with high diatoms and moderate dinocysts. Ice-dwelling diatoms indicate a very long sea-ice season. Foraminifers are abundant but assemblages have low diversities. *N. labradorica* peaks here, while the *C. reniforme* population gradually expands. Bottom salinity is above 31‰, maybe close to normal. The *N. labradorica* peak could be related to the sudden increase in algal productivity and to dysoxic conditions below the sediment/water interface. The low foraminifer diversity and the frequent lack of bioturbation suggest an area that is being colonized.
- (3) The sediment is now bioturbated and presents fewer signs of ice proximity. *Cassidulina reniforme* becomes the dominant foraminifer species while *N. labradorica* declines. Diatoms are very abundant and dinocysts are increasing. Ice diatoms and cold water indicator diatoms are still there but they are fewer and fewer. There are more foraminifer species, indicating continued colonization of the seafloor. There are still no signs of change in bottom temperature and salinity. Toward the end of the interval, arenaceous foraminifer percentages increase and dissolution of calcareous tests begins to be felt, while pollen becomes abundant indicating the development of land vegetation.
- (4) Gray silty clays are replaced by olive-gray marine muds. Glacial influence has disappeared altogether. Diatoms and dinocysts are very abundant and diverse. There are no more ice diatoms, few cold species and the temperature-sensitive *T. nitzschioides* is on the increase, indicating higher surface temperatures. Foraminifers are dominantly or totally arenaceous probably because of dissolution of calcareous tests, likely in connection with greater organic content of the sediment. We have no ^{14}C date from this phase.
- (5) There is one calcareous biofacies in one core that clearly indicates reduced salinity, probably 30‰ or slightly less. The core occurs in a deltaic setting. It is undated but may be of the same age or posterior to the restriction of the Strait of Georgia by isostatic rebound of the Gulf Island area (10,000–11,000 ^{14}C yr BP).

Table 5 shows that phases 1, 2 and early phase 3 took place everywhere within the same narrow time interval, whether north or south. This supports the idea of rapid deglaciation. The fact that the phases always come in the same order suggests that deglaciation happened in the same way everywhere. Phases 1 and 2 must have taken place very quickly so that 1, 2 and 3 probably existed side-by-side in the basin. The brief return to phase 1 in core 58 supports this. Phase 4 came later, at a time when there was no ice left in the basin, and any deglacial sedimentation from the mainland was trapped in the fjords.

Acknowledgements

We want to thank the officers and crew of CCGS *John P. Tully* for the field collection of the cores and geophysical data. Also B. Hill, I. Frydecky and G. Standen for technical support during data collection. Core location map was drafted by K. Iwanowska. For critical reading, useful discussions and help with the interpretation, we wish to thank (in alphabetical order): J. Bernhard, T. Cedhagen, J.J. Clague, A. de Vernal, M. Hald, T. James, A. Jennings, S. Korsun, R.T. Patterson, L. Polyak and R.E. Thomson.

References

- Barrie, J.V., Conway, K.W., 2000. A preliminary interpretation of surficial marine geology of central and northern Strait of Georgia, British Columbia. Geological Survey of Canada, Current Research 2000-A21, 1–7.
- Barrie, J.V., Conway, K.W., 2002. Sea level and glacial sedimentation on the Pacific margin of Canada. In: Dowdeswell, J., O'Cofoigh, C. (Eds.), *Glacier-influenced Sedimentation on High-latitude Continental Margins*. Geological Society Special Publication 203, 181–194.
- Bernhard, J.M., Bowser, S.S., 1999. Benthic foraminifera of dysoxic sediments: chloroplast sequestration and functional morphology. *Earth-Science Reviews* 46, 149–165.
- Cedhagen, T., 1991. Retention of chloroplasts and bathymetric distribution in the sublittoral foraminiferan *Nonionellina labradorica*. *Ophelia* 33, 17–30.
- Clague, J.J., 1994. Quaternary stratigraphy and history of south-coastal British Columbia. In: Monger, J.W.H. (Ed.), *Geology and Geological Hazards of the Vancouver Region, Southwestern British Columbia*. Geological Survey of Canada, Bulletin 481, 181–192.
- Clague, J.J., James, T.S., 2002. History and isostatic effects of the last ice sheet in southern British Columbia. *Quaternary Science Reviews* 21, 71–87.
- Clague, J.J., Harper, J.R., Hebda, R.J., Howes, D.E., 1982. Late Quaternary sea levels and crustal movements, coastal British Columbia. *Canadian Journal of Earth Sciences* 19, 597–618.
- Cockbain, A.E., 1963. Distribution of foraminifera in Juan de Fuca and Georgia straits, British Columbia, Canada. Cushman Foundation for Foraminiferal Research, Contributions 14 (Part 2), 37–57.
- Conway, K.W., Barrie, J.V., Hebda, R., 2001. Evidence for a Late Quaternary outburst flood event in the Georgia Basin, British Columbia. Geological Survey of Canada Current Research 2000-A13, 6pp.
- Crean, P.B., Ages, A., 1971. Oceanographic records from twelve cruises in the Strait of Georgia and Juan de Fuca Strait, 1968. Department of Energy, Mines and Resources, Canada, Vol. 1, 55pp.
- Dethier, D.P., Pessi, F., Keuler, R.F., Balzarini, M.A., Pevear, D.R., 1995. Late Wisconsinan glaciomarine deposition and isostatic rebound in the northern Puget Lowland, Washington. Geological Society of America Bulletin 107, 1288–1303.
- Elverhøi, A., Liestøl, O., Nagy, J., 1980. Glacial erosion, sedimentation and microfauna in the inner part of Kongsfjorden, Spitsbergen. *Norsk Polarinstittutt Skrifter* 172, 33–61.
- Fyles, J.G., 1963. In: *Surficial Geology of Horne Lake and Parksville map-areas, Vancouver Island, British Columbia*. Geological Survey of Canada, Memoir 318, 142pp.
- Germain, H., 1981. Flore des diatomées Diatomophycées eaux douces et saumâtres du Massif Armoricain et des contrées voisines d'Europe occidentale. Boubée, Paris, 444pp.
- Guilbault, J.-P., 1989. Foraminiferal distribution in the central and western parts of the late Pleistocene Champlain Sea basin, Eastern Canada. *Géographie physique et Quaternaire* 43, 3–26.
- Hald, M., Korsun, S., 1997. Distribution of modern Arctic benthic foraminifera from fjords of Svalbard, European arctic. *Journal of Foraminiferal Research* 27, 101–122.
- Hald, M., Vorren, T.O., 1987. Foraminifera stratigraphy and environment of late Weichselian deposits on the continental shelf off Troms, northern Norway. *Marine Micropaleontology* 12, 129–160.
- Hamel, D., de Vernal, A., Hillaire-Marcel, C., Gosselin, M., 2002. Organic-walled microfossils and geochemical tracers: sedimentary indicators of productivity changes in the North Water and northern Baffin Bay during the last centuries. *Deep-Sea Research II* 49, 5277–5295.
- James, T.S., Hutchinson, I., Clague, J.J., 2002. Improved relative sea-level histories for Victoria and Vancouver, British Columbia, from isolation-basin coring. Geological Survey of Canada Current Research 2002-A16, 7pp.
- Jennings, A.E., Helgadottir, G., 1994. Foraminiferal assemblages from the fjords and shelf of eastern Greenland. *Journal of Foraminiferal Research* 24, 124–144.
- Korsun, S., Hald, M., 1998. Modern benthic foraminifera off Novaya Zemlya tidewater glaciers, Russian Arctic. *Arctic and Alpine Research* 30, 61–77.
- Korsun, S., Hald, M., 2000. Seasonal dynamics of benthic foraminifera in a glacially fed fjord of Svalbard, European Arctic. *Journal of Foraminiferal Research* 30, 251–271.
- Korsun, S.A., Podogina, I.A., Forman, S.L., Lubinski, D.J., 1995. Recent foraminifera from three Arctic fjords of Novaya Zemlja and Svalbard. *Polar Research* 14, 15–31.
- LeBlond, P.H., 1983. The Strait of Georgia: functional anatomy of a coastal sea. *Canadian Journal of Fisheries and Aquatic Sciences* 40, 1033–1063.
- Linden, R.H., Schurer, P.J., 1988. Sediment characteristics and sea-level history of Royal Roads Anchorage, Victoria, British Columbia. *Canadian Journal of Earth Sciences* 25, 1800–1810.
- Loeblich, A.R., Tappan, H., 1953. Studies of Arctic foraminifera. Smithsonian Miscellaneous Collection, vol. 121, 150pp.
- Luternauer, J.L., Murray, J.W., 1983. Late Quaternary morphologic development and sedimentation, central British Columbia continental shelf. Geological Survey of Canada Paper 83–21, 38pp.
- Luternauer, J.L., Conway, K.W., Clague, J.J., Blaise, B., 1989. Late Quaternary geology and geochronology of the central continental shelf of western Canada. *Marine Geology* 89, 57–68.

- Mathews, W.H., Fyles, J.G., Nasmith, H.W., 1970. Postglacial crustal movements in southwestern British Columbia and adjacent Washington State. *Canadian Journal of Earth Sciences* 7, 690–702.
- Matthews, J., 1969. The assessment of a method for the determination of absolute pollen frequencies. *New Phytologist* 68, 161–166.
- Mosher, D.C., Thomson, R.E., 2002. The Foreslope Hills: large-scale, fine-grained sediment waves in the Strait of Georgia, British Columbia. *Marine Geology* 192, 275–295.
- Murray, J.W., 1991. Ecology and paleoecology of benthic foraminifera. Longman Scientific and Technical, Harlow, Essex, England, 416pp.
- Osterman, L.E., 1984. Benthic foraminiferal zonation of a glacial/interglacial transition from Frobisher Bay, Baffin Island, North West Territories, Canada. In: Oertli, H.J. (Ed.), *Benthos '83: Second International Symposium on Benthic Foraminifera* (Pau, April 1983), pp. 471–476. Pau and Bordeaux.
- Patterson, R.T., Cameron, B.E.B., 1991. Foraminiferal biofacies succession in the late Quaternary Fraser River Delta, British Columbia. *Journal of Foraminiferal Research* 21, 228–243.
- Patterson, R.T., Kumar, A., 2002. Post-glacial paleoceanographic history of Saanich Inlet, British Columbia, based on foraminiferal proxy data. *Journal of Foraminiferal Research* 32, 110–125.
- Patterson, R.T., Luternauer, J.L., 1993. Holocene foraminiferal faunas from cores collected on the Fraser River delta, British Columbia: a paleoecological interpretation. In: *Current Research, Part A. Geological Survey of Canada Paper 93-1A*, pp. 245–254.
- Phleger, F.B., 1952. Foraminifera distribution in some sediment samples from the Canadian and Greenland Arctic. *Contributions to the Cushman Foundation for Foraminiferal Research* 3 (Part 2), 80–89.
- Polyak, L., Mikhailov, V., 1996. Post-glacial environments of the southeastern Barents Sea: foraminiferal evidence. In: Andrews, J.T., Austin, W.E.N., Bergsten, H., Jennings, A.E. (Eds.), *Late Quaternary Palaeoceanography of the North Atlantic Margins*. Geological Society Special Publication 111, 323–337.
- Polyak, L., Korsun, S., Febo, L.A., Stanovoy, V., Khusid, T., Hald, M., Paulsen, B.E., Lubinski, D.J., 2002. Benthic foraminiferal assemblages from the southern Kara Sea, a river-influenced Arctic marine environment. *Journal of Foraminiferal Research* 32, 252–273.
- Porter, S.C., Swanson, T.W., 1998. Radiocarbon age constraints on rates of advance and retreat of the Puget lobe of the Cordilleran ice sheet during the last glaciation. *Quaternary Research* 50, 205–213.
- Radi, T., de Vernal, A., Peyron, O., 2001. Relationships between dinoflagellate cyst assemblages in surface sediment and hydrographic conditions in the Bering and Chukchi seas. *Journal of Quaternary Research* 16, 667–680.
- Sancetta, C., 1981. Diatoms as hydrographic tracers: example from Bering Sea sediments. *Science* 211 (16), 279–281.
- Sancetta, C., Heusser, L., Labeyrie, L., Naidu, A.S., Robinson, S.W., 1985. Wisconsin-Holocene Palaeoenvironment of the Bering Sea: evidence from diatoms, pollen, oxygen isotopes and clay minerals. *Marine Geology* 62, 55–68.
- Scott, D.B., Baki, V., Younger, C.D., 1989. Late Pleistocene-Holocene paleoceanographic changes on the eastern Canadian margin: stable isotopic evidence. *Palaeogeography, Palaeoclimatology, Palaeoecology* 74, 279–295.
- Snoeijs, P. (Ed.), 1993. Intercalibration and distribution of diatom species in the Baltic Sea. In: *The Baltic Marine Biologist*, Vol. 1, Publication No. 16a, Opulus Press, Uppsala, 130pp.
- Sóthón, J.R., Nelson, D.E., Vogel, J.S., 1990. A record of past ocean-atmosphere radiocarbon differences from the northeast Pacific. *Palaeoceanography* 5, 197–206.
- Thomson, R.E., 1981. Oceanography of the British Columbia coast. *Canadian Special Publication of Fisheries and Aquatic Sciences*, Vol. 56, 291pp.
- Thomson, R.R., 1994. Physical oceanography of the Strait of Georgia-Puget Sound-Juan de Fuca Strait system. In: Wilson, R.H., Beamish, R.J., Aitkens, F., Bell, J. (Eds.), *Review of the Marine Environment and Biota of Strait of Georgia, Puget Sound and Juan de Fuca Strait*. Canadian Technical Report of Fisheries and Aquatic Sciences 1948, pp. 36–100.
- Vilks, G., 1969. Recent foraminifera in the Canadian Arctic. *Micro-paleontology* 15, 35–60.
- Vilks, G., Wagner, F.J.E., Pelletier, B.R., 1979. The Holocene marine environment of the Beaufort shelf. *Geological Survey of Canada, Bulletin* 303, 1–43.
- Williams, H.F.L., 1989. Foraminiferal zonation on the Fraser River Delta and their application to paleoenvironmental interpretations. *Palaeogeography, Palaeoclimatology, Palaeoecology* 73, 39–50.

ANNEXE 2

Copie de l'article

RECONSTRUCTION OF SEA-SURFACE CONDITIONS AT MIDDLE TO HIGH
LATITUDES OF THE NORTHERN HEMISPHERE DURING THE LAST
GLACIAL MAXIMUM (LGM) BASED ON DINOFLAGELLATE CYST
ASSEMBLAGES

de Vernal, A., Eynaud, F., Henry, M., Hillaire-Marcel, C., Londeix, L., Mangin, S.,
Matthiessen, J., Marret, F., Radi, T., Rochon, A., Solignac, S., Turon, J.-L.

Quaternary Science Reviews (2005), vol. 24, 897-924



Reconstruction of sea-surface conditions at middle to high latitudes of the Northern Hemisphere during the Last Glacial Maximum (LGM) based on dinoflagellate cyst assemblages

A. de Vernal^{a,*}, F. Eynaud^b, M. Henry^a, C. Hillaire-Marcel^a, L. Londeix^b, S. Mangin^b, J. Matthiessen^c, F. Marret^d, T. Radi^a, A. Rochon^e, S. Solignac^a, J.-L. Turon^b

^aGEOTOP, Université du Québec à Montréal, P.O. Box 8888, Montréal, Qué., Canada H3C 3P8

^bDépartement de Géologie et Océanographie, UMR 5805 CNRS, Université Bordeaux I, Avenue des Facultés, 33405 Talence Cedex, France

^cAlfred Wegener Institute for Polar and Marine Research, P.O. Box 120161, D27515 Bremerhaven, Germany

^dSchool of Ocean Sciences, University of Wales Bangor, Menai Bridge LL59 5EY, UK

^eInstitut des Sciences de la mer de Rimouski (ISMER), Université du Québec à Rimouski, 310, allée des Ursulines, Rimouski, Qué., Canada G5L 3A1

Received 21 November 2003; accepted 30 June 2004

Abstract

A new calibration database of census counts of organic-walled dinoflagellate cyst (dinocyst) assemblages has been developed from the analyses of surface sediment samples collected at middle to high latitudes of the Northern Hemisphere after standardisation of taxonomy and laboratory procedures. The database comprises 940 reference data points from the North Atlantic, Arctic and North Pacific oceans and their adjacent seas, including the Mediterranean Sea, as well as epicontinental environments such as the Estuary and Gulf of St. Lawrence, the Bering Sea and the Hudson Bay. The relative abundance of taxa was analysed to describe the distribution of assemblages. The best analogue technique was used for the reconstruction of Last Glacial Maximum (LGM) sea-surface temperature and salinity during summer and winter, in addition to sea-ice cover extent, at sites from the North Atlantic ($n=63$), Mediterranean Sea ($n=1$) and eastern North Pacific ($n=1$). Three of the North Atlantic cores, from the continental margin of eastern Canada, revealed a barren LGM interval, probably because of quasi-permanent sea ice. Six other cores from the Greenland and Norwegian seas were excluded from the compilation because of too sparse assemblages and poor analogue situation. At the remaining sites ($n=54$), relatively close modern analogues were found for most LGM samples, which allowed reconstructions. The new LGM results are consistent with previous reconstructions based on dinocyst data, which show much cooler conditions than at present along the continental margins of Canada and Europe, but sharp gradients of increasing temperature offshore. The results also suggest low salinity and larger than present contrasts in seasonal temperatures with colder winters and more extensive sea-ice cover, whereas relatively warm conditions may have prevailed offshore in summer. From these data, we hypothesise low thermal inertia in a shallow and low-density surface water layer.

© 2004 Elsevier Ltd. All rights reserved.

1. Introduction

The earliest reconstructions of the Last Glacial Maximum (LGM) ocean published by CLIMAP (1981) constituted a major breakthrough in paleoceanography and paleoclimatology. These reconstructions of

summer and winter sea-surface temperatures (SSTs) were principally established from transfer functions based on multiple regression techniques and planktonic foraminifer data (Imbrie and Kipp, 1971). Since this pioneer work, many methodological approaches have been developed for the reconstruction of past climatic parameters based on an array of biological indicators, notably pollen grains, diatoms, dinoflagellate cysts, radiolarians, planktonic foraminifera, ostracods, and coccoliths. Various data treatment techniques were also

*Corresponding author. Tel.: +1-514-987-3000x8599; fax: +1-514-987-3635.

E-mail address: devernal.anne@uqam.ca (A. de Vernal).

developed or adapted to the analyses of the diverse micropaleontological populations. They mainly include techniques using the degree of similarity between fossil and modern assemblages (e.g., Guiot, 1990; Pflaumann et al., 1996; Waelbroeck et al., 1998), and the artificial neural network techniques (e.g., Malmgren and Nordlund, 1997; Weinelt et al., 2003). In addition to the above-mentioned approaches based on the analyses of microfossil populations, biogeochemical analyses of organic compounds, such as alkenones produced by coccolithophorids, or the measurement of trace elements, such as Mg/Ca or Sr/Ca in biogenic calcite, yielded insights into past temperatures in the water column (e.g., Rosell-Melé, 1998; Lea et al., 1999; Nürnberg et al., 2000).

Many of these recently developed methods have been applied to re-evaluate the sea-surface conditions which prevailed during the LGM. In addition to the CLIMAP (1981) scenario, there are now many LGM data sets available on regional scales. For example, at the scale of the northern North Atlantic, there are data sets based on planktonic foraminifera (Weinelt et al., 1996; Pflaumann et al., 2003; Saruweit et al., 2003), dinoflagellate cysts (de Vernal et al., 2000, 2002), and alkenone biomarkers (Rosell-Melé, 1997; Rosell-Melé and Comes, 1999; Rosell-Melé et al., 2004). Comparison of the paleoceanographical data sets has revealed significant discrepancies, notably in terms of paleotemperature estimates.

With the aim to compare and eventually to reconcile paleoceanographical reconstructions based on different proxies, an intercalibration exercise has been undertaken within the frame of the Multiproxy Approach for the Reconstruction of the Glacial Ocean (MARGO) Project. The first step was to adopt a common hydrography for the calibration of the temperature vs. proxy relationships, in order to avoid any bias that can be related to initial oceanographical data inputs. The “standardised” hydrography that has been selected for the present MARGO exercise is the 1998 version of the World Ocean Atlas produced by the National Oceanographic Data Center (NODC). In the present paper, we are thus reporting on (i) the updated modern database of dinoflagellate cyst assemblages, (ii) the results from calibration exercises with the standardised hydrography (summer and winter SSTs) and other key parameters such as salinity and sea-ice cover, (iii) the sea-surface condition reconstructions for the LGM interval defined by Environmental Processes of the Ice age: Land, Oceans, and Glaciers (EPILOG) criteria as the interval of maximum continental ice volume during the last glaciation, which spanned from ca. 23 to 19 kyr before present (Schneider et al., 2000; Mix et al., 2001).

Data presented here are representative of middle to high latitudes of the Northern Hemisphere. The reference dinocyst database for the hemisphere includes 940 sites from the North Atlantic, North Pacific and Arctic oceans,

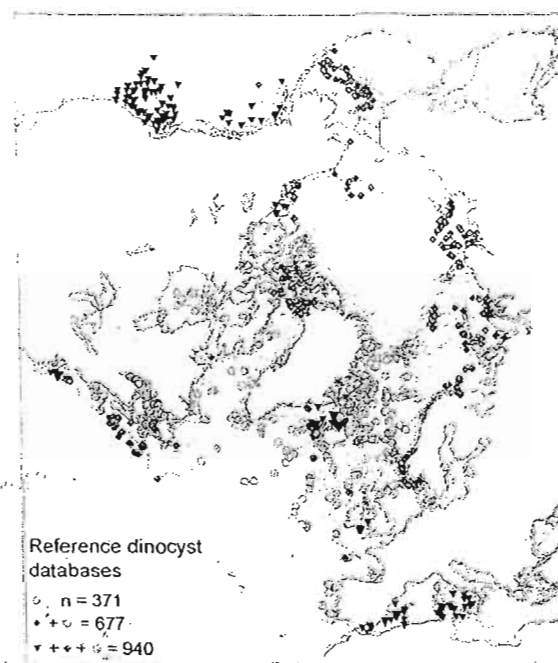


Fig. 1. Location of surface sediment samples used to establish the updated “ $n=940$ ” reference dinocyst database, which was developed after the “ $n=371$ ” database (de Vernal et al., 1997; Rochon et al., 1999) and the “ $n=677$ ” database (de Vernal et al., 2001), and includes the regional data sets from the northeastern North Pacific (Radi and de Vernal, 2004) and the Mediterranean Sea (Mangin, 2002), notably. The isobaths correspond to 1000 and 200 m of water depth.

and their adjacent seas (see Fig. 1). This database constitutes an update of the “ $n=371$ ” (cf. Rochon et al., 1999) and “ $n=677$ ” (cf. de Vernal et al., 2001) databases. The update notably includes additional sites from the North Atlantic (Marret and Scourse, 2003; Marret et al., 2004), the Mediterranean Sea (Mangin, 2002), and the North Pacific (Radi and de Vernal, 2004). This database was used here to produce an update of LGM reconstructions of SST, salinity and sea-ice cover, which were published previously for a number of sites from the northern North Atlantic (cf. de Vernal et al., 2000). Four additional LGM sites are included in the present compilation. Two are from the northern North Atlantic, one from the Mediterranean Sea, and one from the Gulf of Alaska in the northeastern Pacific.

2. Methodology for sea-surface reconstructions

2.1. Dinoflagellate cyst data

2.1.1. The ecology of dinoflagellates and their cysts

Dinoflagellates occur in most aquatic environments and constitute one of the main primary producers in

marine environments, together with diatoms and coccolithophorids. Living dinoflagellates are not fossilisable. However, during their life cycle, after the fusion of the gametes for sexual reproduction, some taxa produce highly resistant organic-walled cysts protecting the diploid cells for a dormancy period of variable length (e.g., Wall and Dale, 1968; Dale, 1983). The organic-walled cysts of dinoflagellates (or dinocysts) thus represent only a fragmentary picture of the original dinoflagellate populations (e.g., Dale, 1976; Head, 1996). Amongst dinoflagellates producing cysts currently recovered in geological samples, there are mainly species belonging to the orders of Gonyaulacales, Peridinales and Gymnodinales. Gonyaulacales are autotrophic whereas Peridinales and Gymnodinales may have heterotrophic or mixotrophic behaviour (e.g., Gaines and Elbrächer, 1987; Taylor and Pollinger, 1987). These taxa that belong to phytoplankton or microzooplankton develop and bloom in surface waters. They are usually recovered together, from plankton samples collected on a routine basis in the upper 50 m (e.g., Dodge and Harland, 1991) or 100 m (e.g., Raine et al., 2002) of the water column. Their living depth is relatively shallow since the autotrophic taxa are dependant upon light penetration, and because the habitat of the heterotrophic species appears to be closely coupled to diatoms on which they feed and/or to the maximum chlorophyll zone (e.g., Gaines and Elbrächer, 1987). Moreover, despite their ability to move vertically with their flagella, dinoflagellates generally inhabit a relatively thin and shallow surface layer, especially in stratified marine environments, because they cannot migrate across the pycnocline that constitutes an important physical barrier (cf. Levandowsky and Kaneta, 1987).

Planktonic dinoflagellates in the North Atlantic show distribution patterns of species in surface water closely related to salinity and temperature, which are controlled by current patterns (e.g., Dodge and Harland, 1991; Dodge, 1994; Raine et al., 2002). Nearshore assemblages can also be distinguished from oceanic assemblages, with regard to the species diversity and taxa dominance. The biogeographical distributions of cyst-forming dinoflagellates in surface waters and that of dinocysts in sediments are generally consistent with each other, notably with respect to their onshore–offshore patterns and latitudinal gradients (Dodge and Harland, 1991; Dodge, 1994). However, the correspondence between observations of motile and cyst assemblages is not perfect, probably due to the fact that the motile dinoflagellates in the plankton assemblages correspond to an instantaneous time interval, whereas the cysts in surface sediments may represent several years or decades of sedimentary fluxes.

The distribution of dinocysts in sediments has been relatively well documented and has contributed to our

understanding of the average sea-surface conditions that determine the distribution pattern and abundances of the taxa. Since the early works of Wall et al. (1977), Harland (1983), and Turon (1984), the relative abundance of dinocyst taxa is known to follow distribution patterns closely related to the temperature gradients and to show distinct neritic, outer neritic and oceanic assemblages. During the last two decades, many studies have contributed to the description of the dinocyst distribution on the sea floor. These illustrate qualitatively or quantitatively the relationships between dinocyst assemblages and sea-surface parameters including temperature and salinity, sea-ice cover, productivity, upwelling and eutrophication (for reviews, see e.g., Dale, 1996; Mudie et al., 2001; Marret and Zonneveld, 2003).

2.1.2. The establishment of the modern dinocyst database

To develop the reference database, we have analysed surface sediment samples that were mostly collected from box cores or gravity cores. Although samples were taken from the uppermost 1 or 2 cm in the sedimentary column, they may represent the last 10^1 – 10^3 years depending upon sediment accumulation rates, and biological mixing intensity and depth in sediment. More information on sampling or subsampling, laboratory procedures, the nature of palynological assemblages in general, and the abundance, preservation, and species diversity of dinocyst assemblages can be found in original publications of the regional data sets available for the northern Baffin Bay (Hamel et al., 2002), the Canadian Arctic (Mudie and Rochon, 2001), the Russian Arctic, including the Laptev Sea (Kunz-Pirring, 1998, 2001) and the Barents Sea (Voronina et al., 2001), the Arctic Ocean as a whole (de Vernal et al., 2001), the Labrador Sea (Rochon and de Vernal, 1994) and northwest North Atlantic (de Vernal et al., 1994), the northeast North Atlantic (Rochon et al., 1999), the Norwegian and Greenland Seas (Matthiessen, 1995), the Celtic Sea (Marret and Scourse, 2003), the Norwegian Coast (Grøsfjeld and Harland, 2001), the Icelandic Sea (Marret et al., 2004), the Estuary and Gulf of St. Lawrence in eastern Canada (de Vernal and Giroux, 1991), the Bering Sea (Radi et al., 2001), the north-eastern North Pacific (Radi and de Vernal, 2004), and the Mediterranean Sea (Mangin, 2002).

Although it is derived from a number of regional data sets, the $n=940$ database is internally consistent with respect to laboratory procedures and taxonomy. This database actually results from a collective endeavour that started about 15 years ago.

With regard to sample preparation, the standardised protocol consists of repeated HCl and HF treatments of the $>10\mu\text{m}$ fraction (for details, see de Vernal et al., 1999; Rochon et al., 1999). This protocol avoids treatment with oxidant agents because the organic cyst

Table 1
List of dinocyst taxa in the $n=940$ database

Taxa name	Code	Notes
Cyst of cf. <i>Scrippsiella trifida</i>	Alex	
<i>Achomosphaera</i> spp.	Acho	
<i>Ataxiodinium choane</i>	Atax	
<i>Bitectatodinium tepikiense</i>	Btep	
<i>Impagidinium aculeatum</i>	Iacu	
<i>Impagidinium pallidum</i>	Ipal	
<i>Impagidinium paradoxum</i>	Ipar	
<i>Impagidinium patulum</i>	Ipat	
<i>Impagidinium sphaericum</i>	Isph	
<i>Impagidinium striolatum</i>	Istr	
<i>Impagidinium plicatum</i>	Ipli	
<i>Impagidinium velorum</i>	Ivel	
<i>Impagidinium japonicum</i>	Ijap	
<i>Impagidinium</i> spp.	Ispp	
<i>Lingulodinium machaerophorum</i>	Lmac	
<i>Nematosphaeropsis labyrinthus</i>	Nlab	
<i>Operculodinium centrocarpum</i> sensu Wall & Dale 1966	Oced	
<i>O. centrocarpum</i> sensu Wall & Dale 1966—short processes	Ocss	Grouped with <i>O. centrocarpum</i> sensu Wall & Dale 1966
<i>Operculodinium centrocarpum</i> —Arctic morphotype	Oarc	Grouped with <i>O. centrocarpum</i> sensu Wall & Dale 1966
<i>Operculodinium israelianum</i>	Oisr	
<i>Operculodinium</i> cf. <i>janduchenei</i>	Ojan	
<i>Operculodinium centrocarpum</i> —morphotype <i>cezare</i>	Ocez	Grouped with <i>O. centrocarpum</i> sensu Wall & Dale 1966
<i>Polysphaeridium zoharyi</i>	Pzoh	
<i>Pyxidinospis reticulata</i>	Pret	
<i>Spiniferites septentrionalis</i>	Ssep	Grouped with <i>Achomosphaera</i> spp.
<i>Spiniferites alaskum</i>	Sala	
<i>Spiniferites membranaceus</i>	Smem	
<i>Spiniferites delicatus</i>	Sdel	
<i>Spiniferites elongatus</i>	Selo	
<i>Spiniferites ramosus</i>	Sram	
<i>Spiniferites beherius</i>	Sbel	Grouped with <i>S. membranaceus</i>
<i>Spiniferites bentorii</i>	Sben	
<i>Spiniferites bulloideus</i>	Sbul	Grouped with <i>S. ramosus</i>
<i>Spiniferites frigidus</i>	Sfri	Grouped with <i>S. elongatus</i>
<i>Spiniferites lazus</i>	Slaz	
<i>Spiniferites mirabilis-hyperucanthus</i>	Smir	
<i>Spiniferites ramosus</i> type <i>granosus</i>	Sgra	
<i>Spiniferites pachydermus</i>	Spac	
<i>Spiniferites</i> spp.	Sspp	
<i>Tectatodinium pellitum</i>	Tpel	
Cyst of <i>Pentapharsodinium dalei</i>	Pdal	
<i>Islandinium minutum</i>	Imin	
<i>Islandinium?</i> <i>cezare</i>	Imic	
<i>Echinidinium</i> cf. <i>karaense</i>	Espp	
<i>Brigantedinium</i> spp.	Bspp	
<i>Brigantedinium cariacense</i>	Bcar	Grouped with <i>Brigantedinium</i> spp.
<i>Brigantedinium simplex</i>	Bsim	Grouped with <i>Brigantedinium</i> spp.
<i>Dubridinium</i> spp.	Dubr	
Protoperidinioids	Peri	
<i>Lejeunecysta sabrina</i>	Lsab	
<i>Lejeunecysta oliva</i>	Loli	
<i>Lejeunecysta</i> spp.	Lspp	
<i>Selenopemphix nephroides</i>	Snep	
<i>Xandarodinium xanthum</i>	Xaid	
<i>Selenopemphix quanta</i>	Squa	
Cyst of <i>Protoperidinium nudum</i>	Pnud	
<i>Protoperidinium stellatum</i>	Pste	
<i>Trinovantedinium applanatum</i>	Tapp	
<i>Trinovantedinium variabile</i>	Tvar	
<i>Votadinium calvum</i>	Vcal	
<i>Votadinium spinosum</i>	Vspi	
Cyst of <i>Protoperidinium americanum</i>	Pame	

Table 1 (continued)

Taxa name	Code	Notes
<i>Quinquecuspis concreta</i>	Qcon	
Cyst of <i>Polykrikos schwartzii</i>	Psch	
Cyst of <i>Polykrikos</i> spp.—Arctic morphotype	Parc	
Cyst of <i>Polykrikos kofoidii</i>	Pkof	
Cyst of <i>Polykrikos</i> spp.—quadrangular morphotype	Pqua	Grouped with cyst of <i>Polykrikos</i> spp. Arctic morphotype
<i>Echinidinium granulatum</i>	Egra	
<i>Gymnodinium catenatum</i>	Gcat	
<i>Gymnodinium nolleri</i>	Gnol	

wall of some taxa can be altered by oxidation (cf. Marret, 1993). With the exception of a few studies suggesting in situ oxidation of the organic wall of protoperidinium cysts in sediment (cf. Zonneveld et al., 2001), dinoflagellate cysts are usually considered to be extremely resistant since they are composed of refractory organic matter called dinosporin (wax-like hydrocarbon; Kokinos et al., 1998). Their preservation is not affected by dissolution processes that result in alteration of siliceous or calcareous microfossils.

The taxonomy of dinoflagellates in the water column and that of their cysts preserved in sediment are mostly independent, because they reflect distinct stages in the dinoflagellate life cycle, i.e., a vegetative stage and a cyst stage following the sexual reproduction. The taxonomy of organic-walled dinoflagellate cysts is based on the morphology of the fossil remains. The taxonomy we are using for routine identification was developed after several workshops to ensure standardisation within the database. The nomenclature of dinocyst taxa used here conforms to Head (1996), Rochon et al. (1999), Head et al. (2001, 2005), Radi et al. (2001), de Vernal et al. (2001), Mangin (2002), and Radi and de Vernal (2004). A complete list of taxa used for statistical treatment and the application of the best analogue technique appears in Table 1. Counts of taxa in the 940 spectra of the reference database are reported following this taxa list (see GEOTOP site, www.geotop.uqam.ca/; see also MARGO data on the PANGAEA site, www.pangaea.de/).

2.1.3. The dinocyst distribution in the calibration database

The overall dinocyst database, including 940 spectra and 60 taxa, has been submitted to multivariate analyses. Canonical correspondence analyses were performed using the CANOCO software of Ter Braak and Smilauer (1998) after logarithmic transformation (\ln) of the relative frequency of taxa. Such a transformation is important to discriminate dinocyst assemblages in relation with environmental parameters because the dominant taxa are often opportunistic and ubiquitous, whereas accompanying taxa often show affinities for a narrow range of given hydrographical

parameters, such as salinity or temperature. The first and second axes, respectively, account for 14.9% and 12.2% of the total variance. Their geographical distribution and the weighting of the 60 taxa according to the two axes are shown in Fig. 2b. The spatial distribution of the values for the first axis reveals a latitudinal pattern, whereas the scores of the second axis show a nearshore to oceanic trend. Canonical correspondence analysis and cross-correlations of the axes with environmental parameters indicate that the assemblage distribution is predominantly controlled by SST and sea-ice cover extent, and that salinity also exerts a determinant role. The correspondence analysis results are consistent with those obtained from principal component analyses of samples from the North Atlantic and Arctic oceans (Rochon et al., 1999; de Vernal et al., 2001), which also demonstrated the dominant effect of the temperature and salinity on the dinocyst distribution. However, at regional scales, parameters other than temperature and salinity may determine dinocyst assemblages. Such is the case of the northeast Pacific margins, where productivity as estimated from satellite imagery (Antoine et al., 1996) seems to be the parameter that is most closely related to the spatial distribution of dinocysts in this area (cf. Radi and de Vernal, 2004).

2.2. Hydrographic data

Following the MARGO recommendation for hydrographical data standardisation, we have used the seasonal means of surface temperature at 10 m of water depth compiled from the 1998 version of the World Ocean Atlas (cf. National Oceanographic Data Center (NODC), 1994). However, at many stations, these data were not available. In such cases, we used seasonal means extracted from regional data sets, when possible. Alternatively, we have used the extrapolated fields of data available from the 1994 version of the World Ocean Atlas (cf. NODC, 1994), as developed for the $n=677$ database (cf. de Vernal et al., 2001). Fig. 3 illustrates the location of sites with available NODC (1998) data, and the location of the sites where we had to use other sources of hydrographic data. These sites are principally

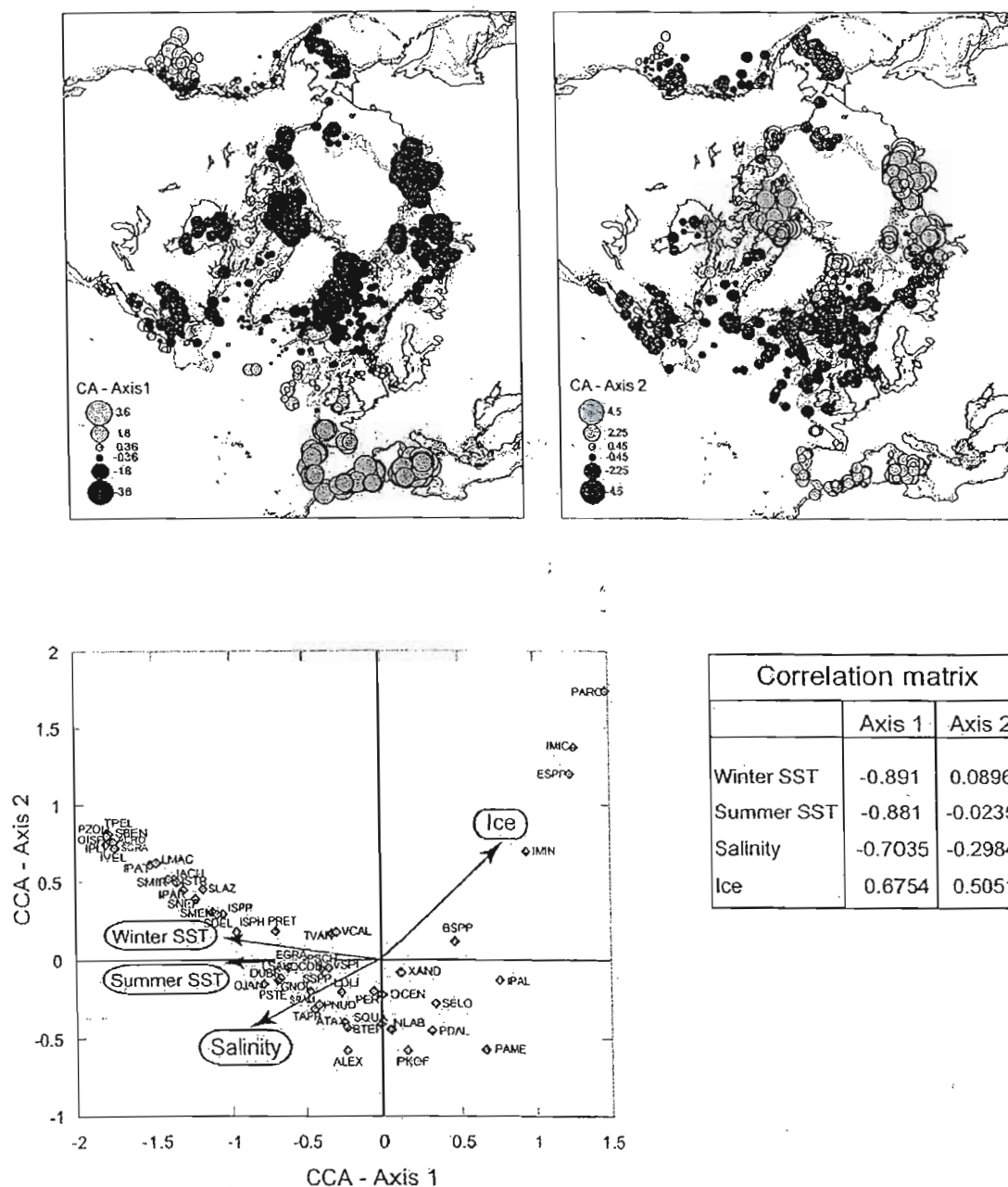


Fig. 2. Geographical distribution of the first two principal axes as defined from canonical correspondence analyses (axes 1 and 2 in the upper left and upper right diagrams, respectively), loading of the 60 dinocyst taxa in the 940 spectra of the reference database according to axes 1 and 2 (lower left diagram) and cross-correlation matrix between the axes and hydrographical parameters (lower right). Note that analyses were performed on logarithmic (ln) values of the relative frequency of taxa expressed in per mil, using the CANOCO software of Ter Braak and Smilauer (1998).

located in the Arctic or along continental margins, where instrumental data coverage is limited and where hydrographic conditions can be extremely variable from one year to another.

In addition to summer and winter mean SSTs, we have compiled the summer sea-surface salinity from NODC (1994). Note that salinity is reported as practical salinity units throughout the manuscript. We also

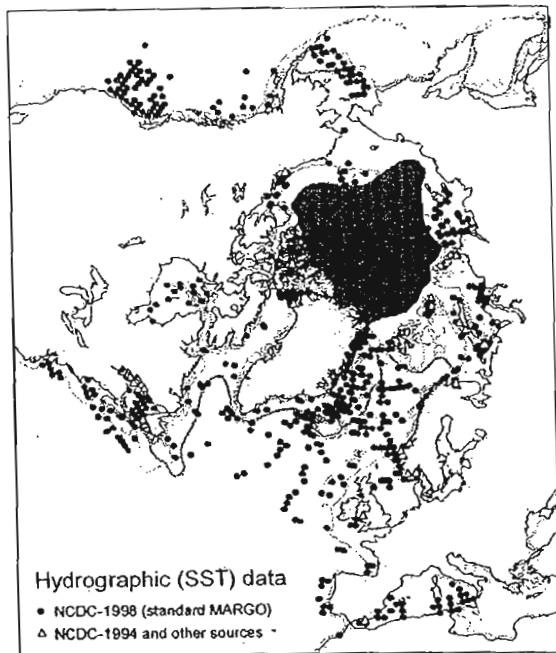


Fig. 3. Map showing the location of the 940 surface sediment samples in the calibration database. Different symbols illustrate the source of SST data. The black circles correspond to sites where hydrographic data from NODC (1998) following the standard defined for MARGO are available. The open triangles correspond to sites where NODC (1998) data were not available, and where compilations were made from the regional databases or from extrapolated values provided by NODC (1994). Details on the sources of these other data can be found in de Vernal et al. (2001). The minimum (grey zone) and maximum (grey line) limits of sea-ice cover are defined from a compilation of several sources.

compiled the seasonal duration of sea-ice cover with concentration greater than 50%, as expressed in number of months per year after the 1953–1990 data set provided by the National Climate Data Centre in Boulder. We have limited the database to areas with salinity higher than 17 because instrumental data are sparse and show very large dispersal of values at nearshore and estuarine sites of lower salinities. The summer and winter SSTs, the summer salinity and the sea-ice cover extent at each station of the $n=940$ database, which we use for the application of the best analogue technique, are archived on the websites of GEOTOP and PANGAEA.

The relationships between the summer and winter SSTs, the summer salinity and the sea-ice cover extent in the $n=940$ database are illustrated in Fig. 4. They show the combinations of summer temperature vs. winter temperature, or sea-ice cover or salinity, and illustrate the range of hydrographical conditions we may thus reconstruct from dinocyst assemblages. It is of note that the range of salinity covered by the dinocyst database is

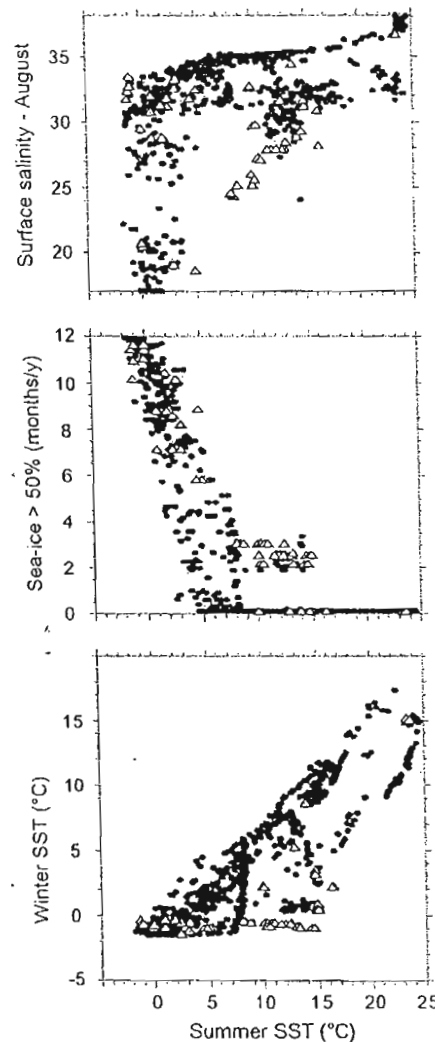


Fig. 4. Graph showing the relationships of summer temperature vs. winter temperature, sea-ice cover, and summer salinity in the $n=940$ database. As in Fig. 3, the black circles correspond to sites where seasonal temperature data from NODC (1998) are available, and the open triangles correspond to sites where other sources of data had to be used.

much larger than those of other micropaleontological tracers, notably planktonic foraminifera, which are much more stenohaline and representative of marine environments with salinity usually higher than 33 (Bé and Tolderlund, 1971). Diatoms that form assemblages characterised by large species diversity in a wide range of salinities and include sea-ice taxa would have been very useful as complementary indicators of sea-surface conditions. However, to date no attempt was made to set transfer functions for quantitative reconstruction of salinity and sea ice in the North Atlantic. Moreover, in

the sediments of the last glacial episode, diatoms are not abundant and their assemblages suffer from poor preservation of the opal silica (Koç et al., 1993; Lapointe, 2000).

The hydrographical parameters we have used for reconstructions based on dinocysts are considered to be the most important determinants of the distribution of assemblages. In temperate marine environments, dinoflagellates generally develop during the warmest part of the year, following the diatom bloom, and their maximum growth rate occurs when close to optimal temperature establishes (Taylor and Pollinger, 1987). The summer SST or the maximum SST is thus the parameter exerting the most influential role on the distribution of dinoflagellate population in the upper water column, as reflected by the cyst populations in sediment traps (cf. Godhe et al., 2001) or in sediments (see Fig. 2). Salinity is also a very important parameter controlling the distribution of assemblages since the range of salinity tolerance varies among species, with euryhaline taxa being abundant in nearshore and estuarine environments as seen in living populations (Taylor and Pollinger, 1987) and cyst assemblages in sediments (e.g., de Vernal and Giroux, 1991). In addition to temperature and salinity, the annual cycle of temperature or seasonality most probably exerts a determinant control on the life cycle of dinoflagellates, notably on the respective duration of vegetative vs. encysted stages. The seasonality can be expressed as the difference between the warmest and the coolest temperatures. It can also be expressed as the length of the season during which autotrophic or heterotrophic metabolic activities are interrupted, because of limited light due to sea-ice cover or to reduced primary production. This would explain how the seasonal duration of sea-ice cover is one of the parameters that can be reconstructed using dinoflagellate cyst assemblages.

2.3. The approach for quantitative reconstructions

Different approaches for estimating past sea-surface conditions based on dinocyst assemblages have been tested, including canonical regressions, several variants of the best analogue technique (de Vernal et al., 1994, 1997, 2001; Rochon et al., 1999), and the artificial neural network technique (Peyron and de Vernal, 2001). Validation tests revealed that the best analogue and the artificial neural network techniques may yield similarly accurate results (cf. Peyron and de Vernal, 2001). Nevertheless, we have decided to use here the best analogue technique because it requires the least manipulation and transformation of data. The database, which covers three oceans, several epicontinental seas, and includes 60 taxa, implies distinct strategies of preparation depending upon the technique to be

applied. In the case of the best analogue technique, we can use the entire database, without any discrimination of taxa and sites. In the case of the artificial neural network technique, however, the definition of regional calibration data sets with a reduced number of taxa would be a requirement. This is a step which may eventually help to constrain the accuracy of estimates, but which also relies on subjective decisions regarding the ultimate list of taxa and the geographical limits of the regional databases. Thus, we made the choice to be conservative by applying the best analogue technique, following the procedure adapted from the software of Guiot and Goeury (1996), which can be summarised as follows:

Prior to data analyses for the search of analogues, a few transformations are made. The abundance of taxa relative to the sum of dinocysts is calculated in per thousand instead of percentages in order to deal with whole numbers and to avoid decimals for further \ln -transformation. One (1) is added to the frequency of each taxon in order to deal with values greater than zero. Another minor transformation consists of adjusting the frequency data ranging between 2 and 5 to the value of 5 in order to make a better discrimination between absence (=1) and presence (>5). This transformation is further justified because of the count limit, which is as low as 100 or 200 specimens in some instances. The zero elements are thus replaced by a value lower than the precision with which data were produced (cf. Kucera and Malmgren, 1998). After these transformations, a distance (d) between the spectrum to be analysed (i) and the spectra in the reference database (j) is calculated based on the difference in relative frequency (f) for each taxon ($j=1-60$) as follows:

$$d = \sum_{j=1}^n [\ln f_{ij} - \ln f_{ij}]^2.$$

For estimating hydrographical conditions, we have used the five best analogues, which are the five modern samples with the lowest “ d ” values. The estimate for the “most probable” hydrographical values is obtained by calculating an average of the values for the five best analogues, weighted inversely by the distance. This most probable estimate is included within an interval corresponding to lower and upper limits, which are defined from the variances of the values below and above the most probable estimates, respectively. This technique leads to the calculation of a confidence interval that is not necessarily symmetric around the most probable estimate.

2.4. Validation of the approach

The degree of accuracy of reconstructions can be evaluated based on the estimations of the modern winter

and summer temperatures, sea-ice cover and summer sea-surface salinity, which were made based on the calibration data excluding the spectrum to analyse (leaving-one-out technique; see Fig. 5). The linearity of the relationship with a slope close to one, and the coefficients of correlation between estimates and observations provide a first indication of the reliability of the approach. The degree of accuracy of the reconstruction is constrained by the standard deviation of the difference between estimates and observations. Values of ± 1.2 and ± 1.7 °C have been calculated for the winter and summer SSTs, respectively, ± 1.7 for the salinity,

and ± 1.3 months/year for the sea-ice cover. On the whole, the degree of accuracy of estimates is of the same magnitude as the standard deviations around the mean for modern SST, salinity or sea-ice cover values collected instrumentally during the last decades (see also Rochon et al., 1999; de Vernal and Hillaire-Marcel, 2000). The degree of accuracy is better in open oceanic regions characterised by salinity higher than 33, and shows a larger spread of data in continental margin areas, estuaries, and ice marginal zones that are marked by highly variable hydrographical conditions on annual, decadal to centennial time scales. In the case of the

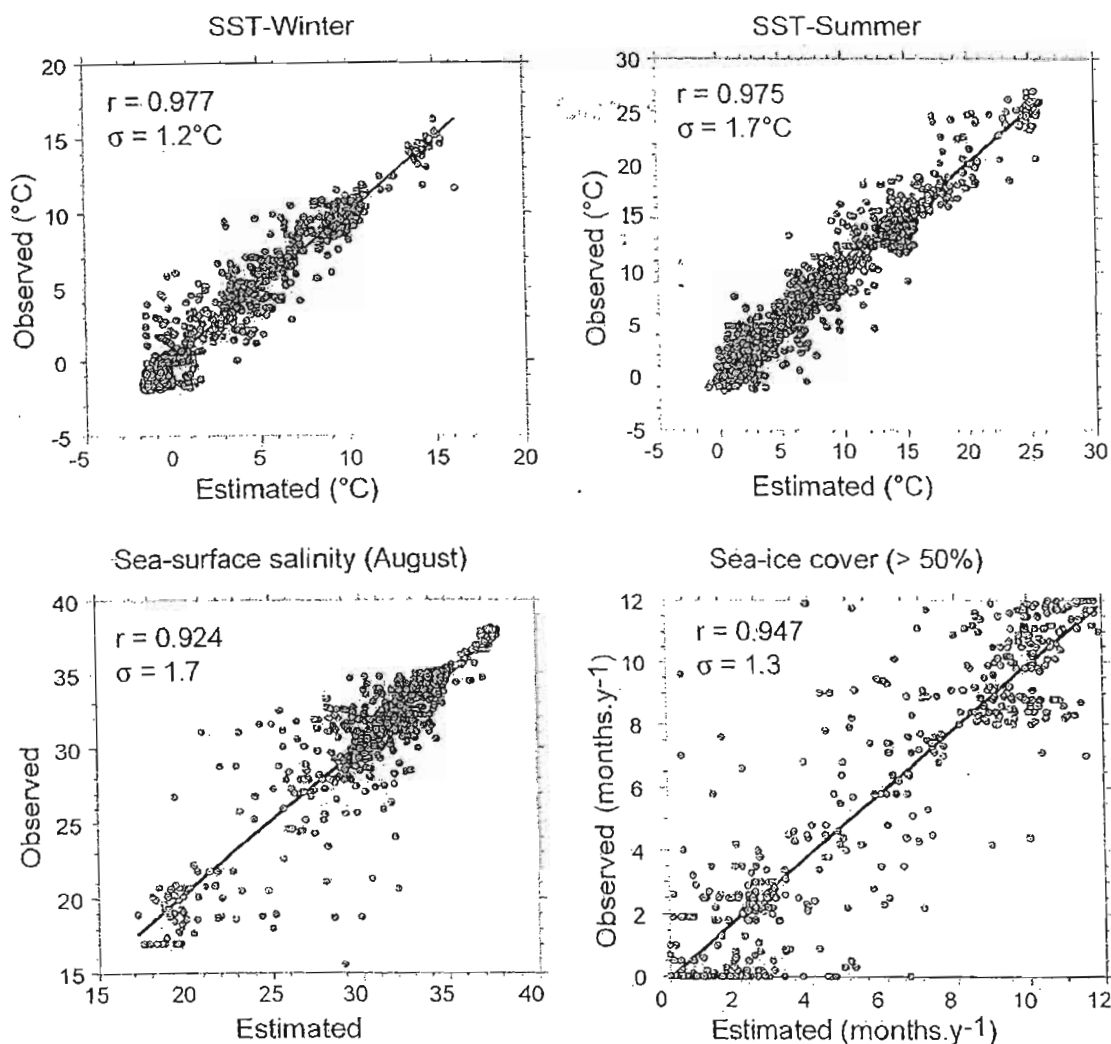


Fig. 5. Results of the validation test for the reconstruction of SST, salinity and sea-ice cover. The x-axis shows hydrographic averages resulting from instrumental observations, and y-axis shows estimates from the dinocyst data after the procedure described in the text. The coefficients of correlation (r) and the standard deviation (σ) of the difference between reconstruction and observation (i.e., the equivalent of the Root Mean Square Error of Prediction) provide the degree of accuracy of estimates. These accuracy indicators were calculated for all data points ($n=940$) although the prediction error clearly depends upon the geographical domain considered.

Canadian and Russian Arctic, there is a particularly large error for salinity, and to a lesser extent for temperature, which can be explained by the high variability of these parameters and by the lack of accuracy of instrumental data (e.g., Mudie and Rochon, 2001). We estimate that about half of the spread of estimated vs. observed values could be attributed to inaccurate hydrographical measurements.

2.5. Definition of reliability indices

All methods developed for quantitative reconstructions of hydrographic parameters based on microfossil assemblages have intrinsic uncertainties due to the accuracy of the calibration databases themselves. Another source of uncertainty derives from the assumption that the present relationships between hydrographical parameters and microfossil assemblages were identical in the past. When dealing with past intervals such as the LGM, this assumption is debatable because conditions of biological production were different than at present. Therefore, the reliability of reconstructions is a question that has to be addressed.

In order to define a reliability index, we have used the degree of similarity between microfossil spectra from LGM and modern based on the distance “*d*” as described above. From the calibration database, a threshold value of acceptable distance has been set on probabilistic grounds (i.e., a Monte-Carlo approach) for identification of a non-analogue or poor-analogue situation. In the case of the Northern Hemisphere $n=940$ database, the distance between pairs randomly taken in the database averages 130.87 with a standard deviation of 56.46. The average minus standard deviation gives a threshold distance (here, 74.39) below which we consider the similarity to be significant. On these grounds, we defined a reliability index according to three categories (cf. Fig. 8):

- (1) Good analogue situation when the distance is between 0 (perfect analogue) and half of the threshold value (37).
- (2) Acceptable analogue situation when the distance is between half of the threshold value and the threshold (37–74).
- (3) Poor analogue situation when the distance of the closest analogue is higher than the calculated threshold (>74).

The reliability index should be further constrained by the concentration of dinocysts, which depends on productivity and cyst fluxes, and sediment accumulation rates. When productivity and fluxes are low, reworking will have an increased influence on the assemblages and, therefore, on the reconstructed sea-surface conditions. Here, we have used a threshold value of 100 cysts/cm³ to

define critically low concentration. Taking into account sedimentation rates of 10 cm/kyr, this concentration value corresponds to a flux of the order of 1 cyst/cm²/year. For comparison, such a flux is lower than that of the modern Labrador Sea by one order of magnitude (Hillaire-Marcel et al., 1994), but is similar to the one presently recorded in the Baffin Bay basin (Rochon and de Vernal, 1994). In Table 2 and Fig. 8, “X” signs indicate which sites are characterised by critically low concentrations, below the threshold value of 100 cysts/cm³.

3. The LGM sea-surface conditions based on dinocyst data

3.1. The coring sites

A total of 65 cores have been analysed for their palynological content (see Fig. 6, Table 2) in order to reconstruct LGM conditions. Most of the cores are from the northern North Atlantic and adjacent subpolar seas: Labrador Sea and Baffin Bay, Irminger Basin, Norwegian and Greenland seas. One core from the Gulf of Alaska in northeastern North Pacific and one core from the western Mediterranean were also analysed.

The LGM time slice (~23,000–19,000 cal. years BP) has been defined following the recommendation made at the first EPILOG Workshop (cf. Schneider et al., 2000; Mix et al., 2001). In most of the cores, the LGM is defined with a good level of accuracy. It is based on radiocarbon dates, lithostratigraphical boundaries provided by the Heinrich layers H1 and H2, magnetic susceptibility or paleointensity correlations, and/or $\delta^{18}\text{O}$ stratigraphies. References about the stratigraphy of most cores we refer to can be found in de Vernal et al. (2000) or on the GEOTOP and PANGAEA websites. Additional information about the stratigraphy of the Mediterranean Sea core ODP161-976c is provided by von Grafenstein et al. (1999) and Combourieu-Nebout et al. (2002) and the stratigraphy of northeastern Pacific core PAR87-A10 can be found in de Vernal and Pedersen (1997). Stratigraphical data about the North Atlantic cores MD95-2002, MD95-2009 and MD95-2010 can be found in Zaragosi et al. (2001) and Eynaud et al. (2002), and about core MD99-2254 in Solignac et al. (2004).

3.2. The LGM dinocyst assemblages and their modern analogues

In many cores, the sediments of the LGM contain sparse palynological assemblages, with very low dinocyst concentrations. A few cores from Baffin Bay, and from the margins of Labrador and Greenland have revealed barren samples, with cyst concentration lower

Table 2
Summarised information about the cores analysed and the sea-surface conditions—estimates based on dinocyst data

Cores	Latitude	Longitude	n	nt	Annual SST		Summer SST		Winter SST		Salinity		Ice cover		d—first analogue		d—fifth analogue		Dinocyst concentration	Reliability index
					Mean	St. dev.	Mean	St. dev.	Mean	St. dev.	Mean	St. dev.	Mean	St. dev.	Mean	St. dev.	Mean	St. dev.		
HU-76-029-033	71.33	-64.27	2	5	-0.2	0.1	1.9	0.2	-1.9	0.1	29.7	3.6	9.3	0.9	27.0	31.9	34.0	22.2	28	1X
M17045	52.43	-16.39	2	2	7.1	1.1	10.7	0.8	4.5	1.0	34.2	0.1	0.2	0.3	40.3	1.8	51.9	3.5	1361	2
M17724	76.00	8.33	4	6	6.7	2.4	12.4	3.3	1.7	1.9	31.1	0.5	1.5	2.7	47.8	14.9	59.1	16.8	72	2X
M23041	68.68	0.23	0	1	—	—	—	—	—	—	—	—	—	—	—	—	—	—	21	—
M23071	67.08	2.90	4	4	7.9	1.4	13.3	0.4	4.1	2.1	33.0	1.0	0.4	0.5	52.6	11.1	65.1	10.4	155	2
M23074	66.66	4.91	5	5	4.5	4.1	9.7	4.6	0.2	1.6	31.5	0.7	3.7	3.3	35.4	10.6	44.9	13.8	354	1
M23259	72.03	9.27	11	11	6.8	1.5	13.0	1.1	1.8	1.7	31.5	0.7	1.3	1.1	35.5	12.6	43.4	14.1	270	1
M23294	72.36	-10.36	2	3	8.2	0.9	11.8	1.9	5.5	0.5	34.2	0.1	0.0	0.0	55.0	13.0	72.2	17.3	38	2X
M23519	64.83	-29.56	2	4	6.9	0.2	10.2	0.5	4.7	0.1	33.9	0.7	1.5	1.3	20.5	11.2	37.1	3.1	66	1X
*MD95-2002	47.45	-8.53	8	19	7.5	1.2	12.9	1.3	3.5	1.9	32.4	1.2	0.2	0.4	36.0	10.1	41.5	11.5	11068	1
MD95-2009	62.74	-4.00	5	8	6.7	3.0	12.4	4.1	1.5	2.9	31.4	1.4	1.3	2.5	33.8	8.2	41.8	9.0	162	1
MD95-2010	66.68	4.57	25	35	4.3	1.7	9.9	3.1	-0.2	0.8	31.6	0.7	3.0	1.9	27.1	9.5	34.8	10.6	1483	1
POS0006	69.20	-16.81	0	2	—	—	—	—	—	—	—	—	—	—	—	—	—	—	26	—
POS0020	67.98	-18.53	7	7	8.4	1.4	13.0	1.4	5.0	2.0	33.2	1.1	0.4	0.8	42.6	12.7	50.8	13.0	334	2
PS1842-6a	69.45	-16.52	8	11	7.4	1.5	12.9	1.0	3.3	2.2	31.7	1.3	1.0	0.9	49.0	22.9	58.0	21.3	142	2
PS1919-2	74.98	-11.92	0	10	—	—	—	—	—	—	—	—	—	—	—	—	—	—	56	—
PS1927-2	72.48	-17.12	0	7	—	—	—	—	—	—	—	—	—	—	—	—	—	—	38	—
PS1951-1	68.83	-20.81	0	7	—	—	—	—	—	—	—	—	—	—	—	—	—	—	26	—
SU8118	37.78	-10.19	9	13	10.7	7.3	13.0	8.5	8.9	6.2	34.6	1.8	2.8	4.8	86.7	20.7	110.9	23.7	169	3
SU9016	58.22	-45.16	7	7	4.4	3.2	7.7	4.6	2.2	2.6	33.2	1.4	3.0	3.9	55.5	30.7	66.2	27.5	92	2X
SU9019	59.53	-39.47	7	8	6.7	1.0	9.5	1.0	4.6	1.0	34.3	0.6	0.7	1.0	48.5	24.6	61.8	28.4	65	2X
SU9024	62.67	-37.38	4	7	6.7	1.0	10.1	1.0	4.3	1.1	34.0	1.2	0.3	0.4	51.6	27.1	64.0	30.6	140	2
SU9032	61.79	-22.43	7	7	6.0	1.2	10.2	1.9	3.1	1.5	33.3	1.3	1.0	1.0	41.3	19.0	50.8	22.8	230	1
SU9033	60.57	-22.08	5	5	7.0	1.6	11.9	2.3	3.6	2.1	33.0	1.8	0.9	1.0	32.0	13.6	44.5	12.6	1021	2
SU9044	50.02	-17.10	2	2	8.8	1.1	11.7	1.7	6.6	0.6	34.7	0.6	0.0	0.0	60.2	0.1	71.9	7.5	7092	1
MD95-2033	44.66	-55.62	22	22	7.1	1.7	13.1	1.4	2.3	1.7	31.4	0.5	0.7	1.0	23.0	4.6	30.1	4.9	1527	2
NA87-22	55.51	-14.71	6	6	6.0	1.2	8.9	2.1	3.7	0.8	34.3	0.7	1.7	1.6	40.9	9.9	57.5	4.9	<10	—
PS1730-2	70.12	-17.70	Barren	Barren	Barren	Barren	Barren	Barren	Barren	Barren	Barren	Barren	Barren	Barren	Barren	Barren	Barren	Barren	10555	2
SU8147	44.90	-3.31	17	17	7.6	1.5	13.3	1.5	3.2	2.1	32.2	1.0	0.6	0.9	48.0	11.1	57.7	10.0	43	2
SU9039	52.57	-21.94	1	1	6.0	—	8.8	—	4.0	—	35.0	—	0.0	—	68.6	—	80.7	—	162	2
*MD99-2254	56.80	-30.66	5	5	6.7	1.0	9.6	1.2	4.6	0.8	34.6	0.6	0.6	1.0	37.2	13.6	53.1	9.1	7041	2
*PAR87-A10	54.36	-148.47	3	3	3.3	3.1	9.6	1.2	4.6	0.8	32.2	2.1	0.6	1.0	37.2	13.6	53.1	9.1	7041	2
*ODP161-976c	36.21	-4.31	7	7	11.3	2.6	16.4	3.1	7.1	2.6	33.1	1.0	0.1	0.3	73.9	7.6	82.6	8.3	<10	—
HU-77-027-013	68.45	-63.53	Barren	Barren	Barren	Barren	Barren	Barren	Barren	Barren	Barren	Barren	Barren	Barren	Barren	Barren	Barren	Barren	37	—
HU-84-030-003	53.32	-45.26	0	3	—	—	—	—	—	—	—	—	—	—	—	—	—	—	241	1
HU-84-030-021	58.37	-57.50	13	13	-0.3	1.7	1.2	2.6	-1.2	1.0	31.1	1.7	9.1	2.9	25.6	17.8	33.2	19.1	<10	—
HU-85-027-016	70.51	-64.52	Barren	Barren	Barren	Barren	Barren	Barren	Barren	Barren	Barren	Barren	Barren	Barren	Barren	Barren	Barren	Barren	2580	1
HU-86-034-040	42.63	-63.10	5	5	6.4	1.1	12.6	0.5	1.7	1.7	31.6	0.7	1.7	0.6	20.5	7.2	27.2	5.8	19	1X
HU-87-033-007	65.40	-57.42	2	9	-0.7	1.1	0.1	1.3	-1.2	0.9	30.9	1.0	10.5	0.5	35.4	4.3	51.7	5.0	492	1
HU-87-033-008	62.64	-53.88	7	7	-0.0	2.4	1.6	4.1	-1.5	0.5	31.5	0.6	9.3	3.1	25.6	9.2	36.0	10.6	85	2X
HU-87-033-009	62.51	-59.44	6	8	0.1	1.2	1.4	1.6	-0.8	0.6	31.1	0.7	9.6	1.1	25.7	16.3	41.5	20.7	117	2
HU-90-013-012	58.92	-47.12	2	11	9.8	0.3	14.4	1.4	5.9	1.6	32.8	0.4	0.2	0.2	44.2	9.7	68.0	6.5	189	2
HU-90-013-013	58.21	-48.37	8	8	7.1	2.8	11.5	3.2	3.7	3.1	32.8	1.7	1.0	1.7	38.1	17.9	49.7	19.9	2277	1
HU-90-015-017	42.78	-61.65	7	7	5.4	2.5	10.7	3.5	1.4	1.9	31.5	0.6	2.6	2.0	31.7	8.9	38.1	12.1	1314	1
HU-91-020-013	41.83	-62.33	6	6	5.9	3.7	10.9	5.2	1.4	2.4	30.1	1.5	2.5	3.7	25.8	5.4	35.0	9.1	>10	—
HU-91-045-025	55.03	-52.13	0	8	—	—	—	—	—	—	—	—	—	—	—	—	—	—	34	1X
HU-91-045-044	59.36	-43.45	4	5	-1.5	0.1	-0.8	0.1	-1.7	0.2	31.4	0.4	11.2	0.1	34.4	4.1	56.5	9.9	55	2X
HU-91-045-052	59.49	-39.30	7	9	6.3	2.2	10.2	2.5	3.6	2.5	33.0	2.0	1.7	2.5	49.2	9.6	60.1	5.3	—	—

A. de Vernal et al. / Quaternary Science Reviews 24 (2005) 897–924

Table 2 (continued)

Cores	Latitude	Longitude	n	nt	Annual SST		Summer SST		Winter SST		Salinity		Ice cover		d—first analogue		d—fifth analogue		Dinocyst concentration	Reliability index
					Mean	St. dev.	Mean	St. dev.	Mean	St. dev.	Mean	St. dev.	Mean	St. dev.	Mean	St. dev.	Mean	St. dev.		
HU-91-045-058	59.84	-33.57	10	10	8.5	3.1	12.4	3.4	5.4	2.9	33.2	1.4	0.6	1.3	54.6	9.5	66.6	9.7	75	2X
HU-91-045-064	59.67	-30.57	6	6	7.7	1.8	11.1	2.4	5.3	1.2	34.0	0.6	0.4	0.7	56.6	11.0	68.7	10.9	65	2X
HU-91-045-072a	58.94	-28.74	9	9	5.2	2.8	7.9	3.8	3.4	2.2	33.6	1.0	2.9	2.9	49.4	20.9	66.1	22.7	70	2X
HU-91-045-074a	55.74	-30.22	5	5	7.8	2.4	11.7	2.7	4.9	1.8	34.2	0.6	0.2	0.3	60.2	9.3	71.1	10.0	76	2X
HU-91-045-080a	53.07	-33.52	10	10	8.5	2.3	12.9	2.8	5.2	2.5	33.2	1.4	0.5	0.9	65.5	16.8	75.3	20.6	104	2
HU-91-045-082a	52.86	-35.53	5	10	9.9	2.8	15.4	2.9	5.6	2.8	33.0	1.4	0.4	0.7	65.2	17.2	77.5	19.2	47	2X
HU-91-045-085	53.97	-38.64	3	3	11.0	3.0	14.8	2.9	8.1	2.8	33.5	0.7	0.2	0.3	62.5	8.9	81.5	4.1	134	2
HU-91-045-091a	53.33	-45.26	14	14	8.5	4.1	11.7	4.3	6.1	3.8	33.8	1.3	1.1	1.8	75.4	21.1	91.6	20.4	38	3X
HU-91-045-094a,c	50.20	-45.68	27	27	0.5	2.2	2.5	3.5	-0.7	1.2	31.0	1.8	8.4	3.1	30.3	19.2	39.6	20.5	1526	1
AII-94-PC3	62.09	-16.62	2	2	4.7	2.4	7.7	2.8	2.6	2.1	31.8	1.4	4.1	2.4	24.5	9.7	34.2	6.0	415	1
D89-BOFS-5K	50.69	-21.86	6	6	9.8	3.8	14.3	4.1	6.2	3.6	33.8	1.6	0.1	0.2	61.5	18.5	77.4	22.4	195	2
HM52-43	64.25	0.73	3	3	6.8	1.4	12.8	2.3	2.2	1.9	31.8	1.0	0.8	1.4	44.5	5.2	55.5	15.5	1143	2
HM71-19	69.49	-9.53	1	1	8.8	—	13.8	—	5.4	—	33.6	—	0.0	—	65.6	—	80.3	—	152	2
HM80-30	71.80	1.61	2	2	8.7	0.1	13.3	0.3	5.5	0.4	34.0	0.2	0.0	0.0	62.0	0.9	78.2	1.2	146	2
HM94-13	71.63	-1.63	1	1	3.3	—	6.4	—	1.1	—	31.9	—	5.3	—	63.6	—	69.3	—	238	2
HM94-25	75.60	1.30	1	1	7.1	—	10.9	—	4.1	—	33.0	—	2.2	—	63.3	—	76.7	—	37	2X
HM94-34	73.78	-2.54	3	3	8.7	1.6	13.0	1.7	5.5	1.7	33.6	1.2	0.7	1.2	71.8	22.0	88.8	30.6	202	2
M17730	72.05	7.31	1	1	9.2	—	13.6	—	5.8	—	33.9	—	0.0	—	89.1	—	101.4	—	—	3

All cores analysed for their LGM palynological content are listed in the table. The core location is also illustrated in Fig. 6. LGM data for the cores marked with an asterisk are reported in this manuscript for the first time. For all other cores, the reconstructions are updated from those published previously by de Vernal et al. (2000). The columns "n" and "nt" refer respectively to the number of spectra used for LGM reconstruction and to the total number of samples analysed in the LGM interval. The difference between the two numbers corresponds to the spectra discarded because of too low cyst counts, or no analogue situation. The mean and standard deviation (std. dev.) for each parameter are calculated on the basis of the most probable estimate of the "n" spectra retained for reconstructions. The mean distances of the first and fifth analogues also refer to the "n" spectra used for reconstructions. When available, the concentration of dinocysts is

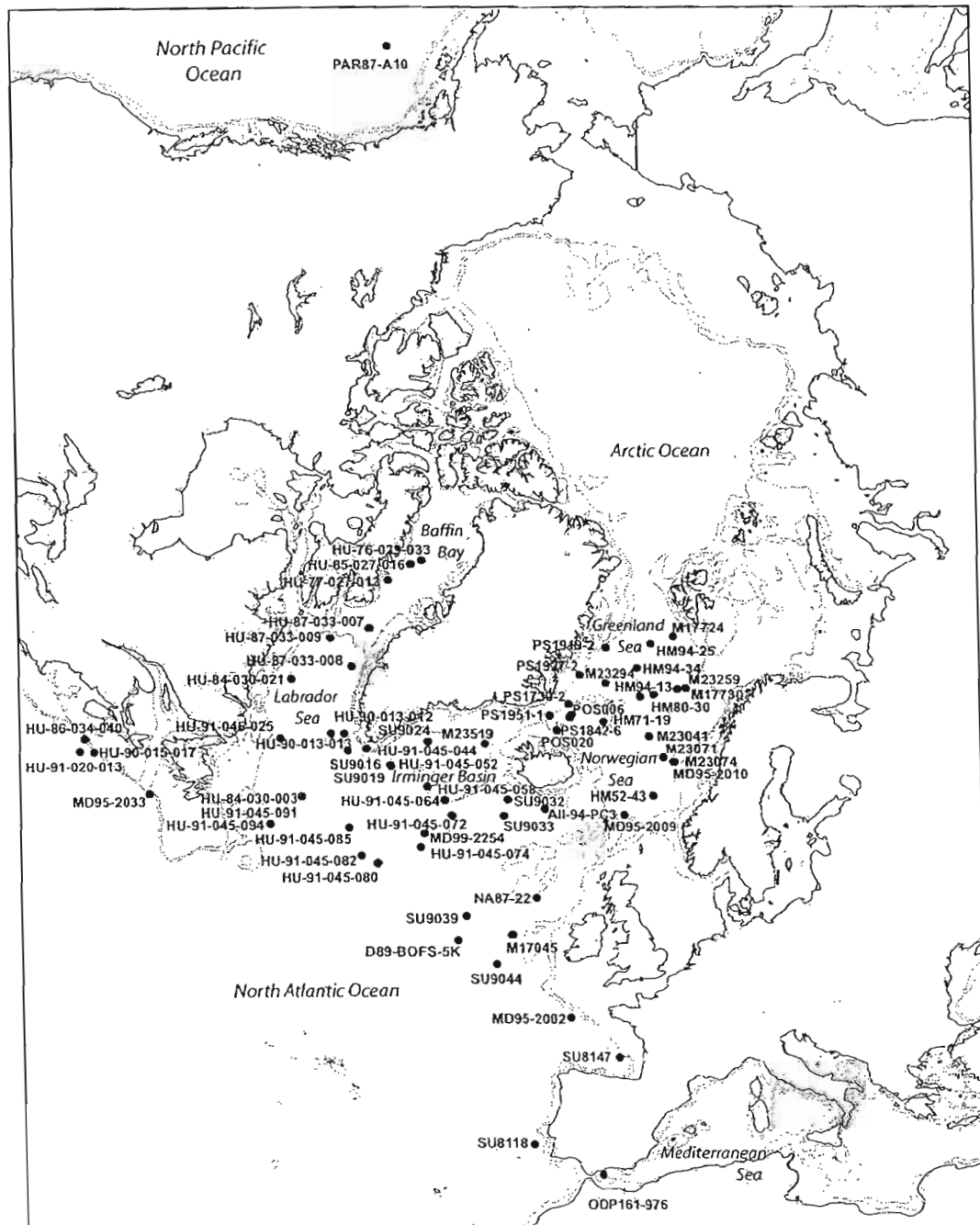


Fig. 6. Location map of the cores used to reconstruct sea-surface conditions during the LGM based on transfer functions using dinocyst assemblages (see Table 1 for core coordinates).

than 10 cysts/cm³ (see Table 2), which we have interpreted as the result of limited biogenic production because of permanent or quasi-permanent sea-ice cover (see also de Vernal et al., 2000). In other cores, some samples within the LGM interval yielded low dinocyst concentrations (<40 cysts/cm³), and their spectra were discarded (see Table 2 and Fig. 8; detailed counts and raw data tables are archived in the PANGAEA database and at GEOTOP).

As a general feature, the LGM samples from the northern North Atlantic contain dinocyst assemblages characterised by low concentrations, generally ranging between 10¹ and 10³ cysts/cm³, with higher values recorded along the margins of southeastern Canada and off western Europe and Scandinavia (Table 2). In the calibration database established from surface sediment samples (Rochon et al., 1999), the abundance of dinocysts is also at a maximum along the margins off southeastern Canada, Western Europe and Scandinavia. However, the concentrations are higher by one order of magnitude than those of the LGM samples. The low dinocyst concentrations in the LGM sediment samples indicate low productivity, due to low nutrient input and/or harsh conditions. Beyond these broad features, the dinocyst assemblages show some peculiarities in comparison with the modern ones:

- (1) The assemblages recovered along the continental margins of northeastern Canada and Scandinavia show a major southward shift of taxa usually associated with sea-ice cover, notably *Islandinium minutum* (Fig. 7a). Such assemblages have close modern analogues, and reveal more extensive seasonal sea ice, and much colder than present conditions especially in winter.
- (2) The offshore assemblages of the northern North Atlantic and adjacent subpolar seas are all characterised by high percentages of *Bitectatodinium tepikiense* (Fig. 7b), as already documented from many studies (e.g., Turon, 1984; Duane and Harland, 1990; Graham et al., 1990; Eynaud et al., 2002). In surface sediment samples, this taxon is common but rarely exceeds 10% of the assemblages. Its modern occurrence has been associated with the cool temperate domain (Turon, 1984) and with the subpolar–temperate boundary in the northern North Atlantic (Dale, 1996). High percentages (>10%) of *B. tepikiense* have been reported at middle latitudes, in the North Sea and along the margins of south eastern Canada (Rochon et al., 1999), with maximum abundances (up to 60–80%) in bays of Maine and Nova Scotia (Wall et al., 1977; Mudie, 1992). The modern distribution of *B. tepikiense* indicates a tolerance to a wide range of salinities and temperatures in winter, and a preference for summer temperatures greater than 10°C. Its maximum

occurrence in coastal bays of southern Nova Scotia (Mudie, 1992) suggests special affinities for stratified surface waters characterised by large seasonal amplitudes of temperature from winter to summer (up to 15°C) and low salinity (30–32‰). Therefore, the LGM dinocyst assemblages recovered offshore in the northern North Atlantic demonstrate very different conditions than at present. They show a relatively high degree of dissimilarity when compared to modern spectra, and the closest modern analogues for these assemblages are located in nearshore environments of the cool temperate domain.

3.3. The reliability of sea-surface condition estimates for the LGM

Beyond intrinsic limitations of any approaches based on the use of microfossil assemblages for quantitative paleoceanographical reconstructions, we have tried to clarify the reliability of estimates from dinocyst data using the indices defined in Section 2.5 (see Fig. 8 and Table 2). The reliability index based on the distance reveals good analogue situations for most sites located along the continental margins of eastern Canada and Scandinavia, in addition to a few offshore sites from the Iceland Basin, Irminger Sea, Baffin Bay, and Labrador Sea in the northern North Atlantic, and the Gulf of Alaska in the North Pacific (Fig. 8). At these sites, the LGM dinocyst concentrations are moderately high, with the exception of sites from the Irminger Basin and Baffin Bay. Therefore, despite some limitations, the reliability of LGM sea-surface condition estimates for the southeastern Canadian margins, Labrador Sea, Iceland Basin and eastern Norwegian Sea is reasonably high, within the range of accuracy defined by the validation exercise (Section 2.4).

The reliability index based on the distance shows acceptable but weak analogue situations in many cores of the northern North Atlantic, and the Greenland and Irminger seas. The weak analogue situation is notably due to the high frequency of *B. tepikiense* in LGM assemblages, which have no close equivalent in offshore areas of the modern database. At the sites from the Greenland and Irminger seas, the situation is particularly critical in view of the low dinocyst concentrations. In these areas, the confidence level of reconstructions is therefore lower.

3.4. Results

3.4.1. Sea-surface temperatures

The SST estimates based on dinocyst assemblages reveal LGM conditions that differ significantly from the modern situation with regard to the geographical distribution pattern of temperatures (Fig. 9). While

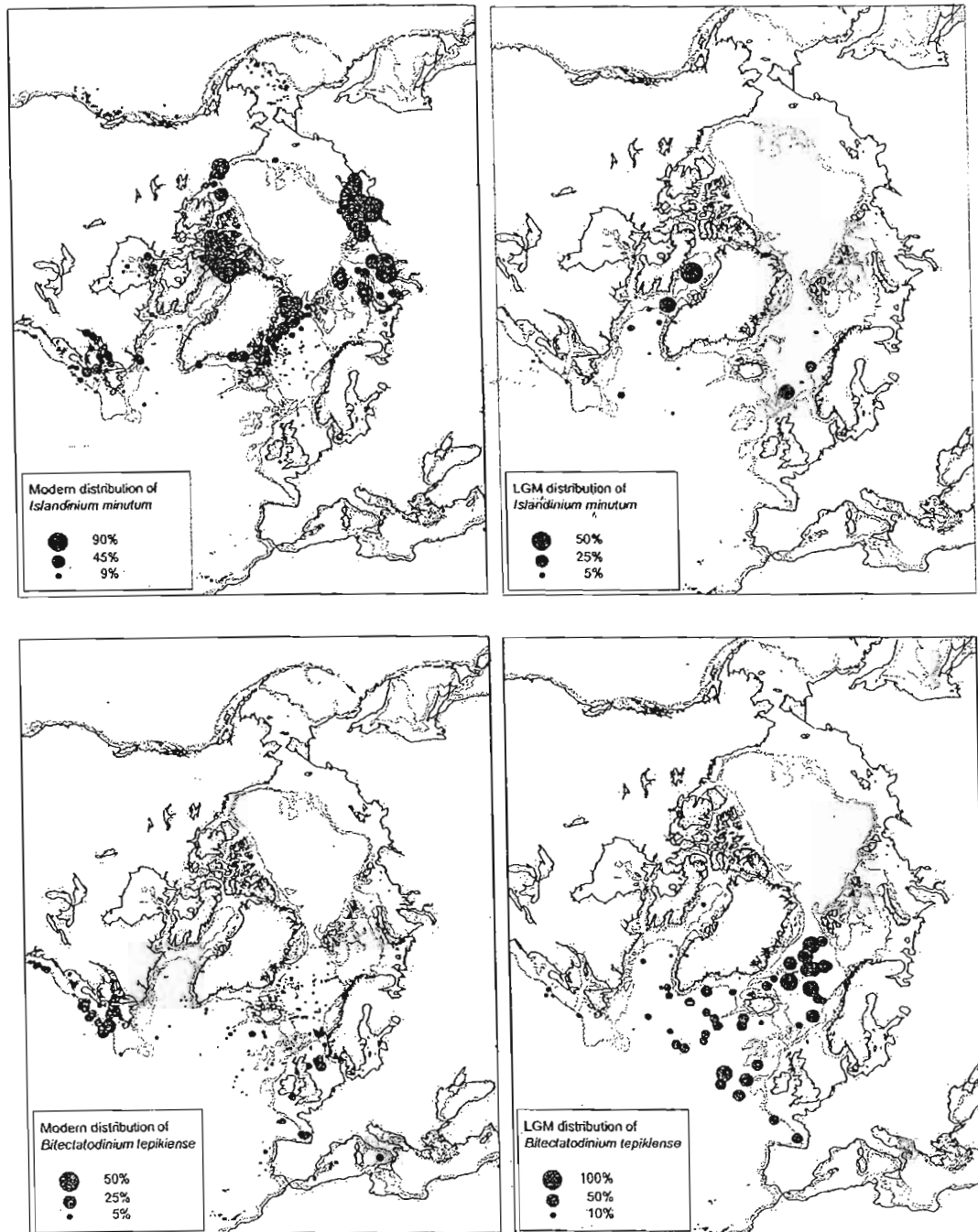


Fig. 7. Geographical distribution patterns of two characteristic dinocyst taxa in the modern (left diagrams) and LGM (right diagrams) databases. (a) Percentages of *I. minutum*; and (b) percentages of *B. tepikiense*.

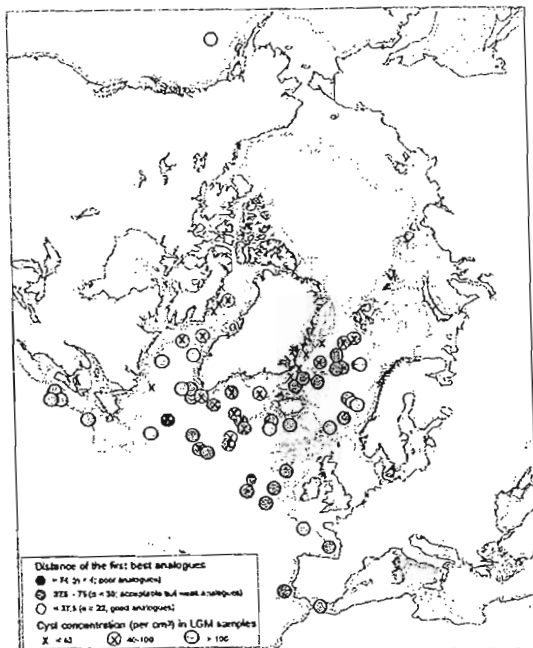


Fig. 8. Schematic illustration of the reliability of estimated sea-surface conditions for the LGM based on dinocyst data: the mean distance of the closest modern analogues permits the definition of a reliability index that is further constrained from the dinocyst concentrations (Table 2). Pale circles represent sites of relatively reliable LGM estimates and dark circles marked with "X" correspond to sites of less reliable LGM estimates (see text, Section 3.3).

some regions show negative anomalies (i.e., LGM minus present) as large as 10°C, others are characterised by insignificant difference or even positive anomalies (Fig. 9; Table 3).

In the northwest North Atlantic, off the eastern margin of Canada, very cold conditions are recorded, both in summer and winter. Offshore, a sharp gradient of increasing temperatures is reconstructed, especially for the summer (Fig. 9). Over mid-latitudes, summer SSTs ranging up to 19°C reveal relatively mild conditions, but still significantly cooler than the modern ones at most sites. In the subpolar basins of the Irminger, Greenland and Norwegian seas, however, LGM reconstructed summer SSTs are warmer than present (Fig. 9). The estimated SSTs in winter are less extreme, showing colder to cooler conditions than at present at most locations. The only exception concerns the Greenland Sea where warmer than present conditions are reconstructed. This is a peculiar, but apparently consistent feature.

On the whole, the anomalies in SSTs are more negative in winter than in summer (Fig. 9). Therefore,

the reconstructed LGM seasonal contrast of temperature in surface waters is larger than at present.

3.4.2. Sea-surface salinities

A particular feature of sea-surface condition estimates in the northern North Atlantic during the LGM is the low salinity, below 35, even at the most oceanic sites (see Fig. 10), which is much lower than at present. Very low salinities, ranging from 30 to 32, are reconstructed along the northeast margins of North America and off Scandinavia. The particularly low salinity recorded in surface waters of the Labrador Sea corresponds to areas also marked by extensive sea-ice cover. In such cases, the dilution in surface water can be associated with summer melting of sea ice. Such is not the case along the eastern Norwegian and southeastern Canadian margins, where the estimated average duration of seasonal sea ice during the LGM was restricted to a few weeks per year (cf. Fig. 10). The distribution pattern of sea-surface salinity estimates may indicate significant dilution resulting from meltwater discharges along the margins of the Laurentide and Fennoscandian ice sheets, which reached their maximum extent at that time.

In the offshore domain of the northern North Atlantic, the reconstructed sea-surface salinity ranges up to 35. This is lower by about one unit as compared to the present, suggesting that the dilution in surface waters was significant, beyond the degree of uncertainties of the reconstructions. The negative LGM anomaly of salinity in the northern North Atlantic is even more significant when taking into account that the salinity of the global LGM Ocean was higher than at present by approximately one (e.g., Broecker and Peng, 1982).

3.4.3. Sea-ice cover extent

In polar and subpolar environments, sea ice is a parameter closely interrelated with temperature and salinity. The freezing of sea water is accompanied by brine formation (e.g., Gascard et al., 2002), which usually sinks and may contribute to deep mixing, whereas the summer melt results in a low-salinity buoyant upper water layer. Thus, sea ice exerts a primary control on the thermohaline structure of the upper water mass and develops seasonally in areas that are often characterised by a strong stratification in the water column, at least during summer.

The LGM sea-ice distribution shows very important gradients in the northern North Atlantic, with an extensive cover in Baffin Bay and along the eastern continental margin of Canada and Greenland. At these locations, the proximity of the ice sheet margins, which were grounded on the shelves, may have fostered dense sea-ice formation: meltwater discharge from the base of the ice sheets together with iceberg flux no doubt resulted in the existence of a low saline and cold surface

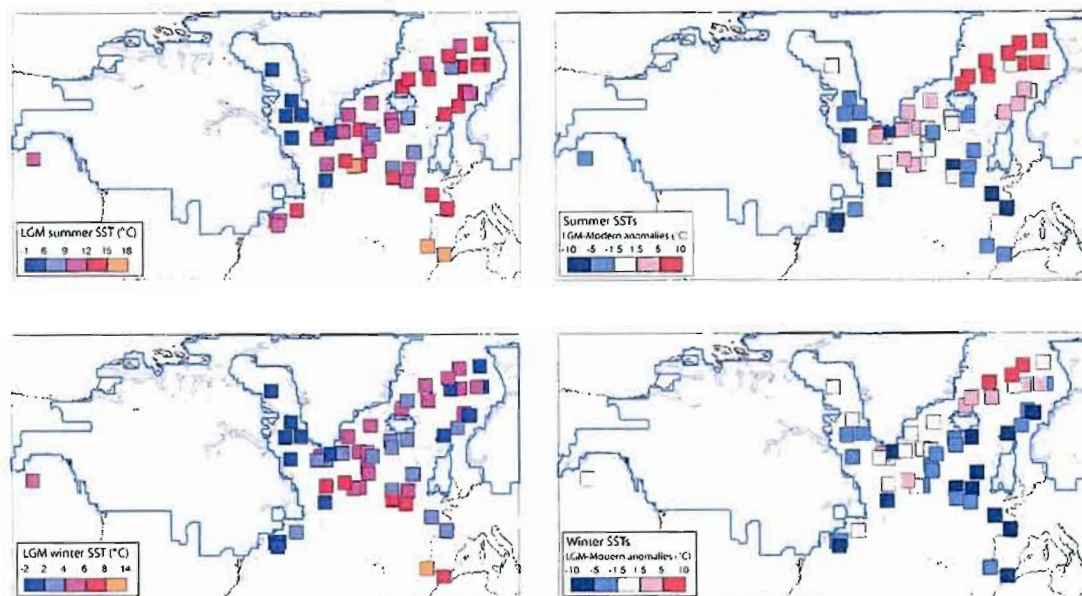


Fig. 9. Maps showing LGM SST estimates in summer (upper left diagram) and winter (bottom left diagram) and the LGM vs. modern SST anomalies in summer (upper right diagram) and winter (bottom right diagram). Note that anomalies within the $\pm 1.5^\circ\text{C}$ range are not considered to be significant taking into account the accuracy of reconstruction and that of modern hydrographical averages (see text, Section 3.4). The continental ice limits are delimited after Peltier (1994).

water layer leading to seasonal freezing and pack ice development as in modern circum-Antarctic seas.

In some of the cores, the palynological analyses reveal barren or close to barren assemblages, which we associate to a close to nil productivity due to permanent or quasi-permanent multiyear sea ice, as it is the case in areas of the Arctic Ocean with permanent pack ice (cf. Rochon et al., 1999). Close to barren assemblages are recorded in Baffin Bay, on the slope off Labrador, and along the eastern Greenland margins (see Fig. 8). Analyses of nearby sequences (from Baffin Bay, and Labrador Sea, notably) support an interpretation of quasi-perennial sea ice, with extensive cover of more than 9 months/year. On these grounds, we may tentatively draw the probable limit of quasi-permanent sea ice during the LGM (see dashed gray line in Fig. 10, upper left), which seems to have been close to the limit of the continental shelf off eastern Canada and Greenland.

LGM data also indicate that the North Atlantic was characterised by a zone with dense sea-ice cover that was relatively narrow and confined to the eastern continental margins. Offshore, in subpolar seas, seasonal sea ice spanning up to a few weeks or a few months per year is reconstructed. The heterogeneity in estimates from one site to another in the Irminger Basin or the Greenland-Norwegian seas can be attributed to the extreme variability of the sea-ice parameter both in time and space (Comiso, 2002). In the eastern sector of the North Atlantic south of about 50°N (see the dashed pink line in

Fig. 10, upper left), however, the data are not equivocal and show that ice-free conditions prevailed throughout the year on an average basis.

3.5. Comparison with previous LGM estimates based on dinocysts

As mentioned before, this manuscript presents an update of the LGM reconstructions published by de Vernal et al. in 2000. Most primary data are the same, with the exception of a few additional sites or additional spectra for some cores (Table 2). However, there are some differences in the databases used for reconstructions, as summarised below.

- (1) Here, we used seasonal averages of SSTs at 10 m depth from NODC (1998) as prescribed for the MARGO intercomparison exercise, instead of monthly averages compiled at 0 m depth, mainly on the basis of the data comprised in the 1994 version of the NODC Atlas. The differences from the temperatures compiled as described above are relatively low on the average but show a rather large dispersal as illustrated in Fig. 11. The August SSTs at 0 m in the NODC-1994 data set are slightly higher than the summer SSTs at 10 m in the NODC-1998 data set, with an average difference of $1.0 \pm 1.1^\circ\text{C}$. Inversely, the February SSTs at 0 m in the NODC-1994 data set are slightly lower than the winter

Table 3
Anomalies of sea-surface conditions between the LGM and the modern

Cores	Longitude	Latitude	Annual SSTs			Winter SSTs			Summer SSTs			Salinity			Sea ice (months/year)		
			LGM	Modern	Δ	LGM	Modern	Δ	LGM	Modern	Δ	LGM	Modern	Δ	LGM	Modern	Δ
HU-76-029-033	-64.27	71.33	-0.2	-0.2	0.0	-1.9	-1.6	-0.3	1.9	2.0	-0.2	29.7	29.0	0.6	9.3	9.3	0.0
M17045	-16.39	52.43	7.1	12.5	-5.4	4.5	10.6	-6.2	10.7	15.0	-4.4	34.3	35.5	-1.2	0.2	0	0.2
M17724	8.33	76	6.7	3.1	3.6	1.7	1.7	0.0	12.4	5.5	6.9	31.1	34.9	-3.8	1.5	0	1.5
M23071	2.9	67.08	7.9	7.9	0.0	4.1	6.2	-2.1	13.3	10.5	2.8	33.0	35.1	-2.1	0.4	0	0.4
M23074	4.91	66.66	4.5	8.2	-3.7	0.2	6.6	-6.5	9.7	10.9	-1.2	31.5	34.9	-3.4	3.7	0	3.7
M23259	9.27	72.03	6.8	5.6	1.1	1.8	4.2	-2.4	13.0	8.0	5.0	31.5	35.1	-3.7	1.3	0	1.3
M23294	-10.36	72.36	8.2	0.4	7.8	5.5	-0.9	6.3	11.8	3.1	8.8	34.2	32.1	2.1	0.0	4.5	-4.5
M23519	-29.56	64.83	6.9	5.7	1.2	4.7	4.7	0.0	10.2	7.2	3.0	33.9	35.1	-1.2	1.5	0	1.5
MD95-2002	-8.53	47.45	6.3	13.9	-7.5	2.1	11.4	-9.3	11.8	17.2	-5.4	32.5	35.5	-3.1	1.5	0	1.5
MD95-2009	-4	62.74	6.3	7.9	-1.6	0.9	6.1	-5.2	12.5	10.3	2.2	31.4	35.1	-3.8	1.5	0	1.5
MD95-2010	4.57	66.68	4.6	8.2	-3.6	0.0	6.6	-6.6	10.3	10.8	-0.5	31.6	35.1	-3.5	2.7	0	2.7
POS0020	-18.53	67.98	8.4	2.1	6.3	5.0	0.7	4.3	13.0	4.4	8.6	33.2	33.6	-0.4	0.4	0.8	-0.4
PS1842-6a	-16.52	69.45	7.4	1.1	6.4	3.3	0.0	3.3	12.9	3.3	9.6	31.7	33.7	-2.0	1.0	4.4	-3.4
SU8118	-10.19	37.78	10.7	17.7	-6.9	8.9	15.4	-6.5	13.0	20.0	-7.0	34.6	36.1	-1.5	2.8	0	2.8
SU9016	-45.16	58.22	4.4	4.8	-0.4	2.2	3.4	-1.2	7.7	7.2	0.5	33.2	34.6	-1.4	3.0	0	3.0
SU9019	-39.47	59.53	6.7	5.8	0.9	4.6	4.3	0.4	9.5	8.0	1.4	34.3	34.8	-0.5	0.7	0	0.7
SU9024	-37.38	62.67	6.7	5.6	1.1	4.3	4.4	-0.1	10.1	7.9	2.3	34.0	34.9	-0.9	0.3	0	0.3
SU9032	-22.43	61.79	6.0	9.1	-3.1	3.1	7.5	-4.4	10.2	11.3	-1.1	33.3	35.2	-1.9	1.0	0	1.0
SU9033	-22.08	60.57	7.0	9.4	-2.4	3.6	7.9	-4.4	11.9	11.5	0.5	33.0	35.1	-2.2	0.9	0	0.9
SU9044	-17.1	50.02	8.9	13.3	-4.5	6.6	11.2	-4.6	11.7	16.0	-4.4	34.7	35.5	-0.8	0.0	0	0.0
MD95-2033	-55.62	44.66	7.1	-1.4	8.6	2.3	-1.0	3.3	13.1	-1.5	14.6	31.4	32.1	-0.7	0.7	0	0.7
NA87-22	-14.71	55.51	6.0	11.4	-5.4	3.7	9.8	-6.1	8.9	13.8	-4.9	34.3	35.4	-1.1	1.7	0	1.7
SU8147	-3.31	44.9	7.6	15.2	-7.6	3.2	11.8	-8.5	13.3	19.4	-6.1	32.2	35.0	-2.9	0.6	0	0.6
SU9039	-21.94	52.57	6.0	12.0	-6.0	4.0	10.2	-6.2	8.8	14.5	-5.7	35.0	35.3	-0.4	0.0	0	0.0
MD99-2254	-30.66	56.8	6.7	8.6	-1.9	4.6	6.8	-2.2	9.6	10.9	-1.3	34.6	35.1	-0.5	0.6	0	0.6
PAR87-A10	-148.47	54.36	3.3	7.1	-3.8	4.6	4.2	0.5	9.6	11.3	-1.7	32.2	32.7	-0.4	0.6	0	0.6
ODP161-976	-4.31	36.21	11.3	18.0	-6.7	7.1	15.3	-8.3	16.4	21.4	-5.0	33.1	36.5	-3.4	0.1	0	0.1
HU-84-030-021	-57.5	58.37	-0.3	3.4	-3.7	-1.2	2.4	-3.6	1.2	6.2	-5.0	31.1	34.4	-3.3	9.1	0	9.1
HU-86-034-040	-63.1	42.63	6.4	10.5	-4.1	1.7	5.1	-3.4	12.7	17.0	-4.4	31.6	31.7	-0.1	1.7	0	1.7
HU-87-033-007	-57.42	65.4	-0.7	1.1	-1.8	-1.2	-0.1	-1.0	0.1	3.6	-3.5	30.9	32.6	-1.7	10.5	4	6.5
HU-87-033-008	-53.88	62.64	0.0	2.5	-2.6	-1.5	1.2	-2.7	1.6	5.2	-3.6	31.5	33.7	-2.2	9.3	0.5	8.8
HU-87-033-009	-59.44	62.51	0.1	2.1	-2.0	-0.8	1.7	-2.5	1.4	4.9	-3.5	31.1	33.8	-2.6	9.6	2.9	6.7
HU-90-013-012	-47.12	58.92	9.8	4.4	5.4	5.9	3.0	2.9	14.4	6.7	7.7	32.8	34.7	-1.8	0.2	0	0.2
HU-90-013-013	-48.37	58.21	7.1	4.7	2.4	3.7	3.2	0.6	11.5	7.3	4.2	32.9	34.6	-1.7	1.0	0	1.0
HU-90-015-017	-61.65	42.78	5.4	11.1	-5.7	1.4	5.8	-4.4	10.7	17.8	-7.1	31.5	32.0	-0.5	2.6	0	2.6
HU-91-020-013	-62.33	41.83	5.9	13.7	-7.8	1.4	8.8	-7.4	10.9	19.7	-8.8	30.1	33.7	-3.6	2.5	0	2.5
HU-91-045-044	-43.45	59.36	-1.5	4.9	-6.4	-1.7	3.4	-5.1	-0.8	6.9	-7.6	31.4	32.8	-1.4	11.2	2.5	8.7
HU-91-045-052	-39.3	59.49	6.4	5.9	0.5	3.6	4.3	-0.7	10.2	8.1	2.1	33.0	34.7	-1.7	1.7	0	1.7
HU-91-045-058	-33.57	59.84	8.5	7.3	1.2	5.4	5.7	-0.3	12.4	9.7	2.7	33.2	34.9	-1.7	0.7	0	0.7
HU-91-045-064	-30.57	59.67	7.8	8.0	-0.3	5.3	6.5	-1.2	11.1	10.2	0.9	34.0	35.0	-1.0	0.4	0	0.4
HU-91-045-072a	-28.74	58.94	5.2	8.6	-3.4	3.4	7.1	-3.7	7.9	10.6	-2.8	33.6	35.0	-1.4	2.9	0	2.9
HU-91-045-074a	-30.22	55.74	7.8	9.0	-1.2	4.9	7.2	-2.3	11.7	11.4	0.3	34.2	35.0	-0.8	0.2	0	0.2
HU-91-045-080a	-33.52	53.07	8.5	9.2	-0.6	5.2	7.0	-1.8	13.0	12.1	0.9	33.2	34.7	-1.5	0.5	0	0.5
HU-91-045-082a	-35.53	52.86	9.9	8.8	1.2	5.6	6.5	-0.9	15.4	11.7	3.7	33.0	34.6	-1.7	0.4	0	0.4
HU-91-045-085	-38.64	53.97	11.0	7.6	3.4	8.1	5.3	2.8	14.8	10.5	4.4	33.5	34.7	-1.1	0.2	0	0.2
HU-91-045-091a	-45.26	53.33	8.5	7.6	0.9	6.2	5.5	0.7	11.7	10.6	1.1	33.8	34.6	-0.8	1.1	0	1.1
HU-91-045-094a,c	-45.68	50.2	0.5	7.9	-7.5	-0.7	5.3	-6.0	2.5	11.5	-9.1	31.0	33.8	-2.9	8.4	0	8.4
AI1-94-PC3	-16.62	62.09	4.7	9.3	-4.6	2.6	7.8	-5.2	7.7	11.3	-3.7	31.8	35.2	-3.4	4.1	0	4.1
D89-BOFS-5K	-21.86	50.69	9.8	12.8	-3.0	6.2	10.9	-4.7	14.4	15.4	-1.0	33.8	35.4	-1.6	0.1	0	0.1
HM52-43	0.73	64.25	6.8	8.2	-1.4	2.2	6.3	-4.1	12.9	11.0	1.9	31.8	35.2	-3.4	0.8	0	0.8
HM71-19	-9.53	69.49	8.8	2.5	6.3	5.4	0.7	4.7	13.8	5.6	8.2	33.6	34.7	-1.1	0.0	0	0.0
HM80-30	1.61	71.8	8.7	3.9	4.8	5.5	2.1	3.5	13.3	6.9	6.4	34.0	35.0	-1.1	0.0	0	0.0
HM94-13	-1.63	71.63	3.3	3.2	0.1	1.1	1.4	-0.3	6.5	6.4	0.1	31.9	34.7	-2.8	5.3	0	5.3
HM94-25	1.3	75.6	7.1	0.8	6.4	4.1	-1.0	5.1	10.9	3.9	6.9	33.0	34.4	-1.3	2.2	0.9	1.3
HM94-34	-2.54	73.78	8.7	0.6	8.0	5.5	-1.3	6.8	13.0	4.1	8.9	33.6	33.8	-0.2	0.7	2.1	-1.4
M17730	7.31	72.05	9.2	5.2	4.1	5.8	3.6	2.2	13.6	7.7	5.9	33.9	35.1	-1.2	0.0	0	0.0

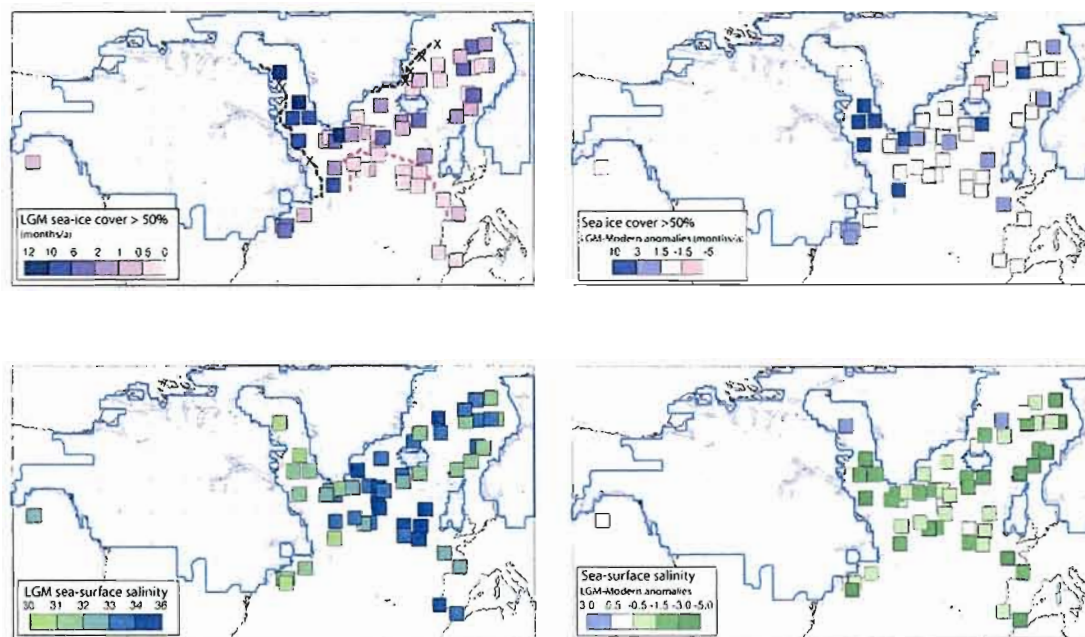


Fig. 10. Maps showing LGM sea-surface salinity estimates in summer (bottom left diagram), the seasonal extent in months per year of sea-ice cover with concentration greater than 50% (upper left diagram), the LGM vs. modern sea-surface salinity anomalies in summer (bottom right diagram) and the LGM vs. modern sea-ice cover extent (upper right diagram). The continental ice limits are delimited after Peltier (1994). In the upper left diagram, the dashed gray and pink lines would correspond to the southern limits of quasi-permanent pack-ice and extreme winter sea-ice cover, respectively.

SSTs at 10 m in the NODC-1998 data set, by -0.2 ± 0.9 °C. The largest differences concern the Arctic where there is limited information, and where the accuracy of hydrographic data is low.

- (2) The reference dinocyst database includes 940 stations from three oceans (Arctic, Pacific, Atlantic) and 60 taxa, instead of 371 stations from one ocean (Atlantic) and 25 taxa (cf. Rochon et al., 1999). The updated database is representative of a wider range of environmental and hydrographic conditions, in both the Arctic and temperate domains.
- (3) In addition to these differences with respect to databases used for the reconstructions, the procedures of data treatment were not exactly the same. In the case of the 2000 compilation, we have used the software provided by Guiot (1990) and we made estimates based on a set of 10 analogues, whereas we are now using the software 3PBase of Guiot and Goeury (1996) and we calculate them based on a set of five analogues. Tests of reproducibility have shown, however, that the two procedures yield almost identical results.

The LGM reconstructions of SSTs presented here (Table 2) are very similar to the ones which were published by de Vernal et al. in 2000 (see Table 4). On

average, for the 50 sites used in both LGM compilations, the difference between summer and August SST reconstruction is 0.61 ± 2.15 °C and the average difference between winter and February SSTs was 0.64 ± 1.1 °C. Such discrepancies are not significant given the differences in the two temperature databases and the calculated error of prediction. Similarly, the average differences in estimated salinity and sea ice are -0.23 ± 0.66 and -0.07 ± 1.14 months/year, respectively. Such differences are not significant either, given the range of accuracy of estimates. We are thus led to conclude that both sets of reconstruction are consistent and that the expansion of the reference database, from 371 to 940 stations, has a limited effect on estimating sea-surface conditions of the LGM in the northern North Atlantic.

4. Discussion

4.1. Uncertainties

4.1.1. Significance of anomalies

The reconstruction of hydrographical parameters based on microfossil assemblages implies a number of assumptions. One concerns the correspondence between

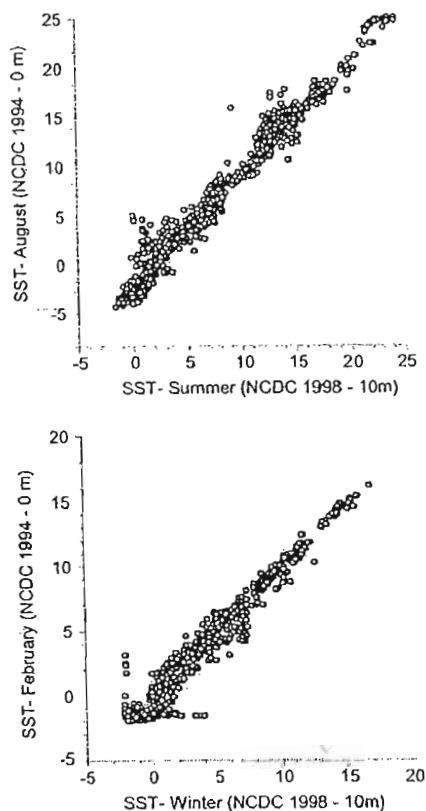


Fig. 11. Graphs showing the differences of SSTs in the two hydrographic databases (World Ocean Atlas versions of 1998 and 1994), which were used to estimate LGM sea-surface conditions in the present compilation and in the one published previously by de Vernal et al. (2000).

the “modern” assemblages recovered in surface sediment samples and the reference hydrographical data, which we assume to be contemporaneous. The interval represented by the microfossil assemblages may range from 10 to 1000 years, whereas mean value of hydrographic data collected over the last decades provide an average that is not necessarily accurate or representative of maximum productivity years. This is a problem especially when dealing with nearshore and circum-Arctic environments, where measurements are rare and where salinity, sea ice or temperature can be extremely variable in space and time. The degree of uncertainty or the inaccuracy of hydrographical averages can be illustrated by the comparison of salinity and temperature fields produced by NODC (1994) and Bedford Institute of Oceanography (BIO) (2003) following the method of analyses of Tang and Wang (1996). The comparison shows that there is a basic agreement in

open ocean, whereas significant differences are being recorded for the shelf and coastal ocean. As an example, the sharp front along the shelf edge of eastern Canada (Labrador Shelf and Grand Banks) clearly depicted in the gridded data from BIO (2003) is absent in the NODC Atlas. This is particularly critical in the case of the dinocyst database, which includes an important proportion of data points from epicontinental and nearshore areas. An illustration of the uncertainty concerning the hydrographical averages can also be found in the mapping of the standard deviations (one sigma) around the temperature average. The sigma value revealed to be very large, up to 4°C, along transitional zones such as those marked by sea-ice limits or the polar front in the North Atlantic (cf. e.g., Isemer and Hasse, 1985). Actually, the standard deviation around the average for instrumental data is comparable to the accuracy of reconstruction defined by validation exercises.

4.1.2. Weaknesses of the actualistic approach

Beyond the accuracy of reconstructions, an important source of uncertainty relies on the fact that the relationships between microfossil assemblages and SSTs are not unequivocal and may have changed through time, because of changes in the structure of water masses or productivity (cf. e.g., Fairbanks and Wiebe, 1980; Faul et al., 2000; de Vernal et al., 2002). In the case of dinocyst assemblages, there are clear relationships with the distribution of seasonal temperature, salinity and sea ice. However, the dinocyst distribution is also dependent upon other parameters, such as the trophic structure of planktonic populations (e.g., Devillers and de Vernal, 2000; Radi and de Vernal, 2004). During the LGM, lower dinocyst fluxes than at present characterised the northern North Atlantic. This suggests that nutrient distribution and productivity were different, which may introduce a bias when making quantitative reconstructions of SST or salinity.

Another source of uncertainty lies in the fact that the reconstructed LGM sea-surface conditions are not well represented in the modern hydrographic database. The dinocyst database is representative of a particularly wide range of sea-surface conditions as compared to other biogenic tracers, such as foraminifera, coccoliths or alkenones, which show relationships with temperature, but within a narrow salinity spectra and almost exclusively in ice-free areas. The LGM sea-surface conditions in most of the northern North Atlantic apparently belong to a domain characterised by seasonal sea-ice cover and relatively low salinity. In such a context, dinocysts appear to be much more sensitive indicators than many other microfossils that are rather representative of open ocean conditions. Therefore, dinocysts are likely to provide more adequate estimates than stenohaline micro-organisms. However,

Table 4
Difference between estimates of LGM sea-surface conditions presented here (black, normal characters) and those published in 2000 by de Vernal et al. (italic characters)

Cores	Latitude	Longitude	n	n	Annual SSTs		Δ -mean	Summer SSTs		August SSTs		Δ -mean	Winter SSTs		February SSTs		Δ -mean	Salinity		Salinity mean		Δ -mean	Sea ice		Sea ice		Δ -mean	Distance min mean		
					Mean	St. dev.		Mean	St. dev.	Mean	St. dev.		Mean	St. dev.	Mean	St. dev.		Mean	St. dev.	Mean	St. dev.		Mean	St. dev.	Mean	St. dev.			Mean	St. dev.
M17045	52.43	-16.39	2	2	7.1	1.1	6.2	0.9	10.7	0.8	9.2	0.3	1.5	4.5	1.0	3.2	0.8	1.3	34.2	0.1	<i>34.8</i>	0.1	-0.6	0.2	0.3	0.0	0.0	0.2	40.3	
M17724	76.00	8.33	4	5	6.7	2.4	7.4	-0.7	12.4	3.3	<i>13.3</i>	3.1	-0.9	1.7	1.9	<i>1.5</i>	1.0	0.2	31.1	0.5	<i>32.3</i>	0.8	-1.2	1.5	2.7	<i>1.1</i>	1.9	0.4	47.8	
M23071	67.08	2.90	4	4	7.9	1.4	7.6	0.3	13.3	0.4	<i>13.7</i>	1.3	-0.4	4.1	2.1	<i>1.4</i>	2.1	2.7	33.0	1.0	<i>32.1</i>	1.3	0.9	0.4	0.5	<i>0.8</i>	0.6	-0.4	52.6	
M23074	66.66	4.91	5	4	6.9	0.3	6.7	0.2	9.7	4.6	<i>13.8</i>	1.9	-4.1	0.2	1.6	-0.5	0.2	0.7	31.5	0.7	<i>30.8</i>	0.1	0.7	3.7	3.3	<i>1.8</i>	1.1	1.9	35.4	
M23259	72.03	9.27	11	13	6.8	1.5	7.5	-0.7	13.0	1.1	<i>13.8</i>	2.8	-0.8	1.8	1.7	<i>1.2</i>	1.4	0.6	31.5	0.7	<i>31.6</i>	0.7	-0.1	1.3	1.1	<i>1.6</i>	1.8	-0.3	35.5	
M23294	72.36	-10.36	2	3	8.2	0.9	6.6	1.6	11.8	1.9	9.3	1.3	2.5	5.5	0.5	3.8	0.6	1.7	34.2	0.1	<i>34.0</i>	0.7	0.2	0.0	0.0	2.2	2.0	-2.2	55.0	
M23519	64.83	-29.56	2	4	6.9	0.2	8.2	-1.3	10.2	0.5	<i>13.1</i>	1.8	-2.9	4.7	0.1	3.3	3.0	1.4	33.9	0.7	<i>33.3</i>	0.8	0.1	1.3	2.5	2.0	0.9	-0.7	33.8	
MD95-2009	62.74	-4.00	5	7	6.7	3.0	8.3	-1.6	12.4	4.1	<i>15.4</i>	1.0	-3.0	1.5	2.9	1.1	2.0	0.4	31.4	1.4	<i>31.3</i>	0.8	0.1	1.3	2.5	2.0	0.9	-0.7	33.8	
MD95-2010	66.68	4.57	25	4	3.7	6.2	-1.9	9.9	3.1	<i>13.4</i>	3.4	-3.5	-0.2	0.8	-1.0	0.2	0.8	31.6	0.7	<i>31.1</i>	0.6	0.5	3.0	1.9	2.5	1.6	0.5	27.1		
POS0020	67.98	-18.53	7	7	8.4	1.4	8.9	-0.5	13.0	1.4	<i>14.2</i>	1.4	-1.2	5.0	2.0	3.7	2.4	1.4	33.2	1.1	<i>32.9</i>	1.1	0.3	0.4	0.8	0.7	0.8	-0.3	42.6	
PS1842-6a	69.45	-16.52	8	12	7.4	1.5	8.9	-1.5	12.9	1.0	<i>14.1</i>	1.9	-1.2	3.3	2.2	3.7	2.6	-0.4	31.7	1.3	<i>33.1</i>	1.5	-1.4	1.0	0.9	0.8	0.6	0.2	49.0	
SU8118	37.78	-10.19	3	4	14.3	1.6	16.5	-2.2	17.1	2.5	<i>18.8</i>	1.0	-1.7	12.1	0.7	<i>14.2</i>	1.2	-2.1	35.5	0.8	<i>36.1</i>	0.2	-0.6	0.2	0.3	0.1	0.1	0.1	101.5	
SU9016	58.22	-45.16	7	6	4.4	3.2	5.2	-0.7	7.7	4.6	8.6	4.7	-0.9	2.2	2.6	1.7	2.0	0.5	33.2	1.4	<i>33.2</i>	1.7	0.0	3.0	3.9	2.8	3.3	0.2	55.5	
SU9019	59.53	-39.47	7	7	6.7	1.0	8.2	-1.5	9.5	1.0	<i>11.3</i>	1.6	-1.8	4.6	1.0	5.0	1.5	2.0	34.3	0.6	<i>34.3</i>	0.6	0.0	0.7	1.0	1.1	1.4	-0.4	48.5	
SU9024	62.67	-37.38	4	7	6.7	1.0	5.9	0.9	10.1	1.0	9.0	1.4	1.1	4.3	1.1	2.7	1.1	1.6	34.0	1.2	<i>33.7</i>	0.8	0.3	0.3	0.4	1.6	1.5	-1.3	51.6	
SU9032	61.79	-22.43	7	7	6.0	1.2	7.4	-1.4	10.2	1.9	<i>12.2</i>	1.8	-2.0	3.1	1.5	2.6	1.9	0.5	33.3	1.3	<i>33.2</i>	1.3	0.1	1.0	1.0	1.0	0.6	0.0	41.3	
SU9033	60.57	-22.08	5	5	7.0	1.6	8.7	-1.7	11.9	2.3	<i>14.0</i>	0.9	-2.1	3.6	2.1	3.4	1.8	0.2	33.0	1.8	<i>32.9</i>	0.6	0.1	0.9	1.0	0.9	0.6	0.0	32.0	
SU9033	60.57	-22.08	5	5	7.0	1.6	8.7	-1.7	11.9	2.3	<i>14.0</i>	0.9	-2.1	3.6	2.1	3.4	1.8	0.2	33.0	1.8	<i>32.9</i>	0.6	0.1	0.9	1.0	0.9	0.6	0.0	32.0	
SU9044	50.02	-17.10	2	2	8.8	1.1	7.7	1.2	11.7	1.7	<i>10.4</i>	0.0	1.3	6.6	0.6	4.9	0.1	1.7	34.7	0.6	<i>35.0</i>	0.1	-0.3	0.0	0.0	0.1	-0.1	60.2		
MD95-2033	44.66	-55.62	22	21	7.1	1.7	8.7	-1.6	13.1	1.4	<i>15.8</i>	0.6	-2.7	2.3	3.7	1.6	1.4	0.7	31.4	0.5	<i>31.4</i>	0.4	0.0	0.7	1.0	0.8	0.4	-0.1	23.0	
NA87-22	55.51	-14.71	6	6	6.0	1.2	6.1	-0.1	8.9	2.1	9.3	0.4	-0.4	3.7	0.8	2.9	0.4	0.8	34.3	0.7	<i>34.8</i>	0.4	-0.5	1.7	1.6	1.2	1.5	0.5	40.9	
SU8147	44.90	-3.31	17	8	7.6	1.5	7.8	-0.2	13.3	1.5	<i>14.5</i>	1.5	-1.2	3.2	2.1	1.0	0.6	32.2	1.3	<i>32.2</i>	0.8	0.2	0.6	0.9	0.2	0.1	0.4	48.0		
SU9039	52.57	-21.94	1	1	6.0	—	8.3	-2.3	8.8	—	<i>11.5</i>	—	-2.7	4.0	—	5.1	—	-1.1	35.0	—	<i>35.1</i>	—	-0.1	0.0	—	0.0	—	0.0	68.6	
HU-84-030-021	58.37	-57.50	13	14	-0.3	1.7	0.1	-0.4	1.2	2.6	1.5	2.0	-0.3	-1.2	1.0	-1.3	0.5	0.1	31.1	1.7	<i>31.3</i>	0.9	-0.2	9.1	2.9	9.2	2.1	-0.1	25.6	
HU-86-034-040	42.63	-63.10	5	5	6.4	1.1	8.4	-2.0	12.6	0.5	<i>15.7</i>	0.8	-3.1	1.7	1.7	1.0	1.6	0.7	31.6	0.7	<i>31.4</i>	0.7	0.2	1.7	0.6	1.0	0.6	0.7	20.5	
HU-87-033-007	65.40	-57.42	2	11	-0.7	1.1	0.4	-1.1	0.1	1.3	1.6	1.0	-1.5	-1.2	0.9	-0.8	0.5	-0.4	30.9	1.0	<i>31.8</i>	0.3	-0.9	10.5	0.5	9.3	1.2	1.2	35.4	
HU-87-033-008	62.64	-53.88	7	8	0.0	2.4	-1.3	1.3	1.6	4.1	-0.9	0.1	2.5	-1.5	0.5	-1.7	0.0	0.2	31.5	0.6	<i>30.6</i>	0.1	0.9	9.3	3.1	11.5	0.3	-2.2	25.6	
HU-87-033-009	62.51	-59.44	6	10	0.1	1.2	-1.3	1.4	1.4	1.6	-0.8	0.2	2.2	-0.8	0.6	-1.7	0.0	0.9	31.1	0.7	<i>30.7</i>	0.2	0.4	9.6	1.1	11.2	0.1	-1.6	25.7	
HU-90-013-012	58.92	-47.12	2	11	9.8	0.3	8.6	1.2	14.4	1.4	<i>11.6</i>	3.3	2.8	5.9	1.6	5.5	2.0	0.4	32.8	0.4	<i>33.8</i>	1.0	-1.0	0.2	0.2	1.8	1.9	-1.6	44.2	
HU-90-013-013	58.21	-48.37	8	9	7.1	2.8	4.7	2.4	11.5	3.2	8.4	1.2	3.1	3.7	3.1	0.9	1.2	2.8	32.8	1.7	<i>32.6</i>	0.9	0.2	1.0	1.7	2.9	1.3	-1.9	38.1	
HU-90-015-017	42.78	-61.65	7	7	5.4	2.5	8.3	-2.9	10.7	3.5	<i>14.7</i>	2.3	-4.0	1.4	1.9	1.9	0.7	-0.5	31.5	0.6	<i>31.7</i>	0.6	-0.2	2.6	2.0	2.0	1.2	0.6	31.7	
HU-91-020-013	41.83	-62.33	6	8	5.9	3.7	6.8	-0.9	10.9	5.2	<i>13.7</i>	2.7	-2.8	1.4	2.4	-0.1	0.8	1.5	30.1	1.5	<i>31.0</i>	0.4	-0.9	2.5	3.7	2.3	1.5	0.2	25.8	
HU-91-045-044	59.36	-43.45	4	4	-1.5	0.1	-0.6	-0.9	-0.8	0.1	0.2	1.1	-1.0	-1.7	0.2	-1.4	0.4	-0.3	31.4	0.4	<i>30.5</i>	0.9	0.9	11.2	0.1	9.7	1.1	1.5	34.4	
HU-91-045-052	59.49	-39.30	7	8	6.3	2.2	8.3	-1.9	10.2	2.5	<i>12.7</i>	1.1	-2.5	3.6	2.5	3.8	1.2	-0.2	33.0	2.0	<i>33.7</i>	0.8	-0.7	1.7	2.5	0.6	0.3	1.1	49.2	
HU-91-045-058	59.84	-33.57	10	9	8.5	3.1	9.5	-1.0	12.4	3.4	<i>13.3</i>	2.0	-0.9	5.4	2.9	5.7	1.5	-0.3	33.2	1.4	<i>34.2</i>	0.6	-1.0	0.6	1.3	0.3	0.2	0.3	54.6	
HU-91-045-064	59.67	-30.57	6	7	7.7	1.8	8.3	-0.5	11.1	2.4	<i>11.2</i>	1.0	-0.1	5.3	1.2	5.3	1.2	0.0	34.0	0.6	<i>34.5</i>	0.6	-0.5	0.4	0.7	0.6	1.5	-0.2	56.6	
HU-91-045-072a	58.94	-28.74	9	5	5.2	2.8	7.6	-2.4	7.9	3.8	<i>10.7</i>	1.6	-1.0	4.9	1.8	4.2	0.2	0.7	34.2	0.6	<i>33.7</i>	0.5	0.5	0.2	0.3	0.5	0.2	-0.3	60.2	
HU-91-045-074a	55.74	-30.22	5	4	7.8	2.4	8.5	-0.7	11.7	2.7	<i>12.7</i>	1.6	-1.0	4.9	1.8	4.2	0.2	0.7	34.2	0.6	<i>33.7</i>	0.5	0.5	0.2	0.3	0.5	0.2	-0.3	60.2	
HU-91-045-080a	53.07	-33.52	10	10	8.5	2.3	9.3	-0.8	12.9	2.8	<i>13.8</i>	1.1	-0.9	5.2	2.5	4.8	1.8	0.4	33.2	1.4	<i>33.6</i>	0.7	-0.4	0.5	0.9	0.5	0.1	0.0	65.5	
HU-91-045-082a	52.86	-35.53	5	5	9.9	2.8	8.5	1.4	15.4	2.9	<i>13.1</i>	2.0	2.3	5.6	2.8	3.9	1.5	1.7	33.0	1.4	<i>33.3</i>	1.1	-0.3	0.4	0.7	1.3	1.5	-0.9	65.2	
HU-91-045-085	53.97	-38.64	3	3	11.0	3.0	8.1	2.9	14.8	2.9	<i>11.7</i>	3.0	3.1	8.1	2.8	4.5	3.0	3.6	33.5	0.7	<i>33.8</i>	1.1	-0.3	0.2	0.3	1.6	2.0	-1.4	62.5	
HU-91-045-094a,c	50.20	-45.68	27	20	0.5	2.2	0.4	0.1	2.5	3.5	2.0	2.5	0.5	-0.7	1.2	-1.2	0.8	0.5	31.0	1.8	<i>31.2</i>	0.8	-0.2	8.4	3.1	9.6	1.7	-1.2	30.3	
AII-94-PC3	62.09	-16.62	2	3	4.7	2.4	7.9	-3.2	7.7	2.8	<i>12.8</i>	1.3	-5.1	2.6	2.1	3.0	0.7	-0.4	31.8	1.4	<i>32.8</i>	0.3	-1.0	4.1	2.4	0.7	0.5	3.4	24.5	
D89-BOFS-SK	50.69	-21.86	6	6	9.8	3.8	9.6	0.2	14.3	4.1	<i>13.5</i>	2.6	0.8	6.2	3.6	5.7	2.3	0.5	33.8	1.6	<i>34.1</i>	0.9	-1.0	0.1	0.2	0.1	0.3	0.0	61.5	
HM52-43	64.25	0.73	3	3	6.8	1.4	7.8	-1.0	12.8	2.3	<i>15.3</i>	0.2	-2.5	2.2	1.9	0.3	0.5	1.9	31											

the sea-surface reconstructions based on dinocysts are comprised in a domain of the reference database that is characterised by a low density of data points, with respect to summer SSTs vs. winter SSTs or salinity (Fig. 12). The dinocyst-based reconstructions of the LGM in the northern North Atlantic have no perfect analogue known from the modern hydrography of the high northern latitudes. Nevertheless, the LGM data points occur in a central area of the hydrographical domains represented by the modern database and likely occur within the range of values we may reconstruct based on dinocyst assemblages. In other words, the degree of accuracy of LGM reconstructions and estimated values may be discussed, but the hydrographical domains involved are probably correct.

4.2. The most salient features of the LGM based on dinocyst data

In spite of the uncertainties examined above, there are consistent features in the reconstructions of LGM sea-surface conditions based on dinocyst assemblages that appear as robust as possible given the context of weak analogue situation. These features are summarised below.

- (1) Sea-ice cover was much more extensive than at present, notably along the eastern Canadian margin. Offshore, in the subarctic basins of the North Atlantic, i.e., the Labrador Sea, the Irminger Basin, the Greenland and Norwegian seas, seasonal sea ice developed for a few weeks to a few months per year, whereas in the northeastern part of the North Atlantic, ice-free conditions prevailed throughout the year.
- (2) Relatively low sea-surface salinity during the LGM characterised the northern North Atlantic and adjacent basins (Fig. 13). In areas marked by extensive sea-ice cover, low sea-surface salinities may have been related to the summer melting of sea ice. However, the particularly low salinities recorded along the southern Canadian and Scandinavian margins (31–32) likely reflect mixing with large meltwater supplies from surrounding ice sheets, which resulted in the dilution of surface waters offshore. In the central part of the North Atlantic, a negative salinity anomaly of about one unit is recorded as compared with the modern situation. During the LGM, the buoyancy of the low-density surface water layer over the northern North Atlantic was responsible for reduced vertical convection from the surface and the absence of deep or intermediate water formation at the corresponding latitudes (cf. Hillaire-Marcel et al., 2001a,b; de Vernal et al., 2002).

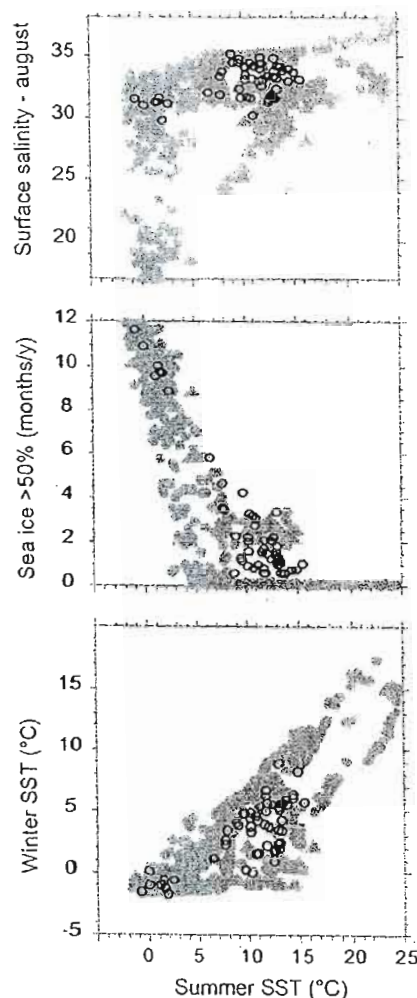


Fig. 12. Graph showing the hydrographical domains of the $n=940$ calibration database and that of the LGM reconstructions. The light gray circles illustrate the distribution of summer temperature vs. winter temperature, sea-ice cover, and summer salinity for the 940 modern samples (same as Fig. 4) and the open circles illustrate the same distribution for the LGM cores. Note that the LGM reconstructions are included in domains characterised by a low density of modern data points.

- (3) On the whole, winter conditions colder than at present and relatively mild summers resulted in significantly larger seasonal gradients of temperature in surface water masses (Fig. 13). The low thermal inertia of the shallow and buoyant upper water layer can be evoked to explain high energy uptake during the summer seasons, then characterised by an insolation roughly the same as at present, followed by rapid cooling during winters.

LGM vs. modern in mid-polar latitudes
of the Northern Hemisphere (n = 55)

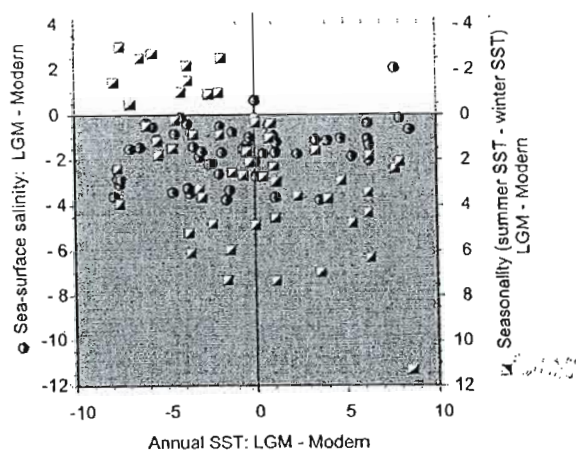


Fig. 13. Summary of the hydrographical anomalies between the LGM and the present.

- (4) Reconstruction of the mean annual temperature shows values colder, cooler or equivalent to present conditions on an average basis during the LGM, with some exceptions, notably in the Greenland and Norwegian seas (Fig. 13; Table 3). LGM data from the Greenland Sea are not very robust because of low dinocyst concentrations and weak analogue situations (Fig. 8), but data from the Norwegian Sea appear reliable and suggest the existence of mild conditions at least episodically.

4.3. The northern North Atlantic LGM SST: contrasting pictures depending on the choice of proxies?

4.3.1. Contribution of dinocyst data

In the northern North Atlantic, the LGM paleoceanographic data from dinocysts are complementary to those from planktonic foraminifer assemblages (Weinelt et al., 1996; Pflaumann et al., 2003) and alkenones (Rosell-Melé and Comes, 1999; Rosell-Melé et al., 2004). First, they improve the geographical coverage of LGM reconstructions along the margins of south eastern Canada, the Labrador Sea and Baffin Bay, where other data are very rare. Second, they help to constrain the limits of sea ice and also provide quantitative information on the seasonal extent of the ice coverage (Fig. 10). Third, dinocysts permit the estimation of sea-surface salinity, which is an important hydrographic parameter of the North Atlantic Ocean with respect to thermohaline circulation. Finally, the

calibration database of dinocysts includes large numbers of samples from the Arctic seas and subarctic basins, unlike other proxies. Therefore, dinocyst assemblages should permit identification of analogues from Arctic and subarctic environments for the LGM interval. One of the important findings from this study is the lack of perfect modern analogues for LGM North Atlantic Ocean, even in the Arctic and subarctic seas.

4.3.2. Consistent features and discrepancies from the comparison with other proxies

Despite discrepancies, there are converging features in the LGM reconstructions based on the different proxies. One of these features concerns sea ice. All proxies suggest seasonally ice-free conditions in the northern North Atlantic and the Nordic seas, and the maximum extent of LGM sea-ice cover shows similar limits in the central North Atlantic estimated from dinocysts (pink dashed line in upper left diagram of Fig. 10) and indirectly estimated from planktonic foraminifera (cf. Pflaumann et al., 2003). Another convergent feature between dinocyst and planktonic foraminifer data is the gradient of LGM-modern SST that shows similar patterns, although the absolute values differ significantly.

The reconstructions of LGM SSTs based on dinocysts are not in contradiction with temperatures derived from alkenone data (Rosell-Melé and Comes, 1999; Rosell-Melé et al., 2004), but they show discrepancies with data from planktonic foraminifera well beyond the degrees of uncertainty of the respective approaches. On the whole, dinocyst data yield much warmer estimates than planktonic foraminifera, whatever the type of transfer function used (cf. CLIMAP, 1981; Pflaumann et al., 1996, 2003; Weinelt et al., 1996, 2003; Waelbroeck et al., 1998), but are compatible with those obtained from alkenones (cf. Rosell-Melé and Comes, 1999) or coccoliths (de Vernal et al., 2000). Therefore, we are tempted to distinguish two types of tracers. The first category includes dinocysts as well as coccoliths and their alkenones. Worth of mention here is the fact that the LGM coccolith assemblages of the northern North Atlantic are mostly dominated by *Emiliania huxleyi* (cf. de Vernal et al., 2000), one of the rare euryhaline taxa amongst coccolithophorids (e.g., Winter et al., 1994) that is also responsible for alkenone production. The second category of tracers consists of planktonic foraminiferal assemblages that barely tolerate salinity below 32 or 33 (cf. Bé and Tolderlund, 1971). In the first case, i.e., that of coccoliths, alkenones and autotrophic dinocysts, the tracers relate to primary production in the photic zone of the upper surface water layer, whereas in the second case, they relate to heterotrophic production and characterise various depth habitats from the epipelagic to the mesopelagic domains. The two categories of tracers can thus be distinguished based on two patterns:

(1) their depth habitat and/or (2) their relative tolerance to low salinity. The discrepancy of temperature estimates obtained from the different types of proxies could thus simply reflect specificities in the vertical or temporal structure of the upper water masses.

Therefore, most LGM data from the various proxies, including microfossil assemblages, isotopic content of foraminifera or biomarkers, can be reconciled through an interpretation invoking either strong temperature-salinity gradients in the upper water column, with possible variations in the seasonal gradients of temperatures, or alternation of episodes of warm and dilute surface water with episodes of higher salinity but cold conditions. The existence of a sharp halo-thermocline separating a shallow and low saline mixed layer from a cold and dense mesopelagic water mass, could explain the co-occurrence of temperate autotrophic producers and polar zooplanktonic populations. As a matter of fact, sharp density gradients can be reconstructed for the LGM by combining information from dinocyst data and $\delta^{18}\text{O}$ in planktonic foraminifera (*Globigerina bulloides* and *Neogloboquadrina pachyderma* left coiled) recovered from different size fractions (Hillaire-Marcel et al., 2001a, b; de Vernal et al., 2002). The isotopic compositions of *N. pachyderma* shells of increasing size and density, which can be associated with gradational depths along the pycnocline, have been used to document the density gradient in the upper water column in the Labrador Sea (Hillaire-Marcel et al., 2001a) and the Arctic Ocean (Hillaire-Marcel et al., 2004). Using these data, together with $\delta^{18}\text{O}$ values in the epipelagic foraminifer *G. bulloides*, and estimated SSTs and salinities from dinocysts, it has been possible to propose the existence of vertical density gradients ranging from 1.5 to 3 density units (σ_θ) in the upper water masses of the northwestern North Atlantic during the LGM (de Vernal et al., 2002). However, it is not excluded that such gradients represent conditions occurring during distinct episodes.

4.3.3. The problem of the Nordic seas

Although the sea-surface conditions of the LGM reconstructed on the basis of dinocyst assemblages can be reconciled with other paleoceanographical data as outlined above, the case of the Nordic seas, and especially that of the Greenland Sea, remains problematic. The strongly positive LGM anomalies of temperatures obtained in the Greenland Sea based on dinocysts (de Vernal et al., 2000; this study) or alkenones (Rosell-Melé and Comes, 1999) are somewhat difficult to explain.

In the eastern part of the Nordic seas, along the Norwegian margins, the dinocyst assemblages are characterised by relatively high concentrations and large species diversity. The number of analysed samples, and the overall reliability of reconstructions based on

dinocysts (Fig. 8 and Table 2) in the eastern Norwegian Sea suggest that relatively warm conditions existed in the Nordic seas during the LGM, at least episodically and or seasonally. The dinocyst assemblages and other paleoceanographical tracers show large-amplitude changes in oceanographical conditions which can be linked with the high-frequency climate oscillations during the last ice age as recorded in the isotopic record of Greenland ice cores (e.g., Rasmussen et al., 1996).

The reconstructions from the central and western parts of the Nordic seas, however should be considered with caution. In general, this area is characterised by low biogenic productivity and low sedimentation rates (cf. Sarinthein et al., 1995; Hebbeln et al., 1998). As a consequence, the sedimentary interval representative of the LGM is relatively thin. Moreover, the interpretation of the sparse micropaleontological assemblages is equivocal also because of possible reworking and biological mixing.

Two hypothesis, not exclusive to each other, are tentatively proposed to explain the overall records of the Nordic seas:

Hypothesis 1. The sparse assemblages that are observed in the LGM interval of the central and western Nordic seas might reflect highly variable conditions, from generally cold and quasi-perennial sea-ice cover (nil productivity) to episodically mild conditions (with some productivity), e.g., when large anticyclonic gyre developed and sea ice broke due to strong storms. At present, sharp fronts and extremely high interannual-interdecadal variability in sea-surface conditions and sea-ice cover are recorded in the central part of the Nordic seas, and we may hypothesise that a similar variability existed during the LGM. The existence of fronts controlling pressure gradient and storm tracks may have played an important role in the moisture supply to feed the northern ice sheet.

Hypothesis 2. The assemblages might reflect nil regional productivity due to quasi-permanent sea ice in the eastern and northern parts of the Nordic seas. In such a case, the very sparse assemblages of the Greenland Sea might be due to lateral advection of fine material (dinocysts, alkenone, coccoliths) through a subsurface current flowing from the south and penetrating into the central Nordic seas by subduction. A modern equivalent for such a situation could be found in the northern Barents Sea where the North Atlantic Drift surface water mass is subducting below the low saline Arctic waters.

5. Conclusions

The dinocyst database that has been developed from the analyses of surface sediment samples collected in

middle- to high-latitude marine environments of the Northern Hemisphere covers a wide range of hydrographical conditions notably in the domain characterised by the presence of seasonal sea-ice cover. This database was used to reconstruct quantitatively the sea-surface conditions that prevailed during the LGM. It provides some clues about the paleoceanographical regime which prevailed over the northern North Atlantic when continental ice sheets reached their maximum extent over surrounding lands and continental shelves. The LGM reconstructions illustrate extensive sea-ice cover along the eastern Canadian margin, and some spreading of sea ice during winter, in subpolar basins and Nordic seas, whereas the northeast Atlantic south of 50°N remained free of sea ice. As a response to meltwater discharges from the surrounding ice sheets grounded on the shelves, relatively low salinity characterised surface waters, especially along the eastern Canadian and Scandinavian margins. A possible explanation would be the development of a buoyant and probably shallow mixed layer resulting in a low thermal inertia in the surface waters. This would explain the reconstructed large seasonal contrasts of temperatures with the cold winter and relatively mild summer. In this scenario, the sea-surface conditions reconstructed at the scale of the northern North Atlantic indicate strong stratification, unfavourable for vertical convection, and lead us to make a comparison with a large fjord-like system making the transition between the continental ice sheets and the ocean. In such a context, most bioindicators of “open ocean” conditions would have a limited sensitivity, which may explain the discrepancies between the different sets of LGM reconstructions based on different proxies. Another explanation would invoke alternation of episodes of low salinity and high summer SSTs in surface waters with episodes of higher salinity and lower temperature accounting for the reconstructed cold conditions based on foraminifera.

Acknowledgements

This study is a contribution to the Climate System, History and Dynamics (CSHD) project, supported by the National Science and Engineering Research Council (NSERC) of Canada, and to the international IMAGES program. Complementary support by the *Fonds québécois de Recherche sur la Nature et les Technologies* and by the Canadian Foundation for Climate and Atmospheric Sciences (project no. GR-240) is acknowledged. We are extremely grateful to many institutions for their most precious help in providing surface sediment samples, notably the Oregon State University, Lamont Doherty Earth Observatory, the Bedford Institute of Oceanography, the University of Kiel, GEOMAR, and the Alfred Wegener Institute. We also thank Karin

Zonneveld, Barrie Dale and Michal Kucera for their critical and constructive review of the manuscript.

References

- Antoine, D., André, J.M., Morel, A., 1996. Oceanic primary production. 2. Estimation at global scale from satellite (costal zone colour scanner) chlorophyll. *Global Biogeochemical Cycles* 10, 57–69.
- Bé, A.W.H., Tolderlund, D.S., 1971. Distribution and ecology of living planktonic foraminifera in surface waters of the Atlantic and Indian oceans. In: Funnel, B.M., Riedel, W.R. (Eds.), *The Micropaleontology of Oceans*. Cambridge University Press, Cambridge, pp. 105–149.
- Bedford Institute of Oceanography (BIO), 2003. A monthly gridded set of temperature and salinity for the northwest North Atlantic Ocean, CD-Rom data set.
- Broecker, W.S., Peng, T.-H., 1982. *Tracers in the Sea*. Lamont-Doherty Geological Observatory, Columbia University, New York.
- CLIMAP Project Members, 1981. Seasonal reconstructions of the earth's surface at the last glacial maximum. *Geological Society of America Map and Chart Series MC-56*.
- Combourieu-Nebout, N., Turon, J.L., Zaho, R., Capotondi, L., Londéix, L., Pahnke, K., 2002. Enhanced aridity and atmospheric high-pressure stability over the western Mediterranean during the North Atlantic cold events of the past 50kyrs. *Geology* 30, 863–866.
- Comiso, J.C., 2002. Correlation and trend studies of the sea-ice cover and surface temperatures in the Arctic. *Annals of Glaciology* 34, 420–428.
- Dale, B., 1976. Cyst formation, sedimentation, and preservation: factors affecting dinoflagellate assemblages in recent sediments from Trondheimsfjord, Norway: Review of Palaeobotany and Palynology 22, 39–60.
- Dale, B., 1983. Dinoflagellate resting cysts: benthic plankton. In: Fryxell, G.A. (Ed.), *Survival Strategies of Algae*. Cambridge University Press, Cambridge, pp. 69–136.
- Dale, B., 1996. Dinoflagellate cyst ecology: modeling and geological applications. In: Jansonius, J., McGregor, D.C. (Eds.), *Palynology: Principles and Applications*, vol. 3. American Association of Stratigraphic Palynologists Foundation, Dallas, TX, pp. 1249–1275.
- de Vernal, A., Giroux, L., 1991. Distribution of organic-walled microfossils in recent sediments from the Estuary and Gulf of St. Lawrence: some aspects of the organic matter fluxes. *Canadian Journal of Fisheries and Aquatic Sciences* 113, 189–199.
- de Vernal, A., Hillaire-Marcel, C., 2000. Sea-ice cover, sea-surface salinity and halo-thermocline structure of the northwest North Atlantic: modern versus full glacial conditions. *Quaternary Science Reviews* 19, 65–85.
- de Vernal, A., Pedersen, T., 1997. Micropaleontology and palynology of core PAR 87 A-10: a 30,000 years record of paleoenvironmental changes in the Gulf of Alaska, northeast North Pacific. *Paleoceanography* 12, 821–830.
- de Vernal, A., Turon, J.-L., Guiot, J., 1994. Dinoflagellate cyst distribution in high latitude environments and quantitative reconstruction of sea-surface temperature, salinity and seasonality. *Canadian Journal of Earth Sciences* 31, 48–62.
- de Vernal, A., Henry, M., Bilodeau, G., 1999. *Technique de préparation et d'analyse en micropaléontologie*. Les Cahiers du GEOTOP, Université du Québec à Montréal, 3. Unpublished report.
- de Vernal, A., Hillaire-Marcel, C., Turon, J.-L., Matthiessen, J., 2000. Reconstruction of sea-surface temperature, salinity, and sea-ice

- cover in the northern North Atlantic during the last glacial maximum based on dinocyst assemblages. *Canadian Journal of Earth Sciences* 37, 725–750.
- de Vernal, A., Rochon, A., Turon, J.-L., Matthiessen, J., 1997. Organic-walled dinoflagellate cysts: palynological tracers of sea-surface conditions in middle to high latitude marine environments. *GEOBIOS* 30, 905–920.
- de Vernal, A., Hillaire-Marcel, C., Peltier, W.R., Weaver, A.J., 2002. The structure of the upper water column in the northwest North Atlantic: modern vs. Last Glacial Maximum conditions. *Paleoceanography* 17, 1050.
- de Vernal, A., Henry, M., Matthiessen, J., Mudie, P.J., Rochon, A., Boessenkool, K., Eynaud, F., Grøsfjeld, K., Guiot, J., Hamel, D., Harland, R., Head, M.J., Kuuz-pirung, M., Levac, E., Loucheur, V., Peyron, O., Pospelova, V., Radi, T., Turon, J.-L., Voronina, E., 2001. dinoflagellate cyst assemblages as tracers of sea-surface conditions in the northern North Atlantic, Arctic and sub-arctic seas: the new “ $n=677$ ” database and application for quantitative paleoceanographical reconstruction. *Journal of Quaternary Science* 16, 681–699.
- Devillers, R., de Vernal, A., 2000. Distribution of dinocysts in surface sediments of the northern North Atlantic in relation with nutrients and productivity in surface waters. *Marine Geology* 166, 103–124.
- Dodge, J.D., 1994. Biogeography of marine armoured dinoflagellates and dinocysts in the NE Atlantic and North Sea. *Review of Palaeobotany and Palynology* 84, 169–180.
- Duane, A., Harland, R., 1990. Late Quaternary dinoflagellate cyst biostratigraphy for sediments of the Porcupine Basin, offshore western Ireland. *Review of Palaeobotany and Palynology* 63, 1–11.
- Dodge, J.D., Harland, R., 1991. The distribution of planktonic dinoflagellates and their cysts in the eastern and northeastern Atlantic Ocean. *New Phytologist* 118, 593–603.
- Eynaud, F., Turon, J.-L., Matthiessen, J., Kissel, C., Peypouquet, J.-P., de Vernal, A., Henry, M., 2002. Norwegian Sea surface palaeoenvironments of the Marine Isotopic Stage 3: the paradoxical response of dinoflagellate cysts. *Journal of Quaternary Science* 17, 349–359.
- Fairbanks, R.G., Wiebe, P.H., 1980. Foraminifera and chlorophyll maximum: vertical distribution, seasonal succession, and paleoceanographic significance. *Science* 209, 1524–1526.
- Faul, K., Ravelo, A.C., Delaney, M.L., 2000. Reconstructions of upwelling, productivity, and photic zone depth in the eastern equatorial Pacific ocean using planktonic foraminiferal stable isotopes and abundances. *Journal of Foraminiferal Research* 30, 110–125.
- Gaines, G., Elbrächer, M., 1987. Heterotrophic nutrition. In: Taylor, F.J.R. (Ed.), *The Biology of Dinoflagellates*, Botanical Monograph 21. Blackwell Scientific, Oxford, pp. 224–281.
- Gascard, J.-C., Watson, A.J., Messias, M.-J., Olsson, K.A., Johannessen, T., Simonsen, K., 2002. Long-lived vortices as a mode of deep ventilation in the Greenland Sea. *Nature* 416, 525–527.
- Godhe, A., Norén, F., Kuylenstierna, M., Ekberg, C., Karlson, B., 2001. Relationship between planktonic dinoflagellate abundance, cysts recovered in sediment traps and environmental factors in the Gullmar Fjord, Sweden. *Journal of Plankton Research* 23, 923–938.
- Graham, D.K., Harland, R., Gregory, D.M., Long, D., Morton, A.C., 1990. The biostratigraphy and chronostratigraphy of BGS Borehole 78/4, North Minch. *Scottish Journal of Geology* 26, 65–75.
- Grøsfjeld, K., Harland, R., 2001. Distribution of modern dinoflagellate cysts from inshore areas along the coast of southern Norway. *Journal of Quaternary Science* 16, 651–660.
- Guiot, J., 1990. Methods and programs of statistics for paleoclimatology and paleoecology. In: Guiot, J., Labeyrie, L. (Eds.), *Quantification des changements climatiques: méthode et programmes*. Institut National des Sciences de l’Univers (INSU-France), Monographie No 1. Paris.
- Guiot, J., Gocury, C., 1996. PPPbase, a software for statistical analysis of paleoecological data. *Dendrochronologia* 14, 295–300.
- Hamel, D., de Vernal, A., Gosselin, M., Hillaire-Marcel, C., 2002. Organic-walled microfossils and geochemical tracers: sedimentary indicators of productivity changes in the North Water and northern Baffin Bay (High Arctic) during the last centuries. *Deep-Sea Research II* 49, 5277–5295.
- Harland, R., 1983. Distribution maps of recent dinoflagellate cysts in bottom sediments from the North Atlantic Ocean and adjacent seas. *Palaeontology* 26, 321–387.
- Head, M.J., 1996. Modern dinoflagellate cysts and their biological affinities. In: Jansonius, J., McGregor, D.C. (Eds.), *Palynology: Principles and Applications*, vol. 3. American Association of Stratigraphic Palynologists Foundation, Dallas, TX, pp. 1197–1248.
- Head, M.J., Harland, R., Matthiessen, J., 2001. Cold marine indicators of the late Quaternary: the new dinoflagellate cyst genus *Islandinium* and related morphotypes. *Journal of Quaternary Science* 16, 621–636.
- Head, M.J., Lewis, J., de Vernal, A., The cyst of the calcareous dinoflagellate *Scrippsiella trifida*, and the fossil record of its organic wall. *Journal of Palaeontology*, in press.
- Hebbeln, D., Henrich, R., Baumann, K.-H., 1998. Paleocyanography of the last Interglacial/Glacial cycle in the polar North Atlantic. *Quaternary Science Reviews* 17, 125–153.
- Hillaire-Marcel, C., de Vernal, A., Lucotte, M., Mucci, A., Bilodeau, G., Rochon, A., Vallières, S., Wu, G., 1994. Productivité et flux de carbone dans la mer du Labrador au cours des derniers 40.000 ans. *Canadian Journal of Earth Sciences* 31, 139–158.
- Hillaire-Marcel, C., de Vernal, A., Candon, L., Bilodeau, G., Stoner, J., 2001a. Changes of potential density gradients in the northwestern North Atlantic during the last climatic cycle based on a multiproxy approach. In: Seidov, D., Maslin, M., Haupt, B. (Eds.), *The Oceans and Rapid Climate Changes: Past, Present and Future*. Geophysical Monograph Series, vol. 126. American Geophysical Union, Washington, DC, pp. 83–100.
- Hillaire-Marcel, C., de Vernal, A., Bilodeau, G., Weaver, A., 2001b. Absence of deep water formation in the Labrador Sea during the last interglacial. *Nature* 410, 1073–1077.
- Hillaire-Marcel, C., de Vernal, A., Polyak, L., Darby, D., 2004. Size dependent isotopic composition of planktic foraminifers from Chukchi Sea vs. NW Atlantic sediments—implications for the Holocene paleoceanography of the western Arctic. *Quaternary Science Reviews* 23, 245–260.
- Imbric, J., Kipp, N.G., 1971. A new micropaleontological method for quantitative paleoclimatology: application to a late Pleistocene Caribbean core. In: Turkian, K.K. (Ed.), *The Late Cenozoic Glacial Ages*. Yale University Press, New Haven, Conn., pp. 71–181.
- Isern, H.-J., Hasse, L., 1985. *The Bunker Climate Atlas of the North Atlantic Ocean*, vol. 1: Observations. Springer, Berlin, pp. 57–61.
- Koç, N., Jansen, E., Hafidason, H., 1993. Paleocyanographic reconstruction of surface ocean conditions in the Greenland, Iceland, and Norwegian seas through the last 14,000 years based on diatoms. *Quaternary Science Reviews* 12, 115–140.
- Kokinos, J.P., Eglinton, T.I., Goffi, M.A., Boon, J.J., Martoglio, P.A., Anderson, D.M., 1998. Characterisation of a highly resistant biomacromolecular material in the cell wall of a marine dinoflagellate resting cyst. *Organic Geochemistry* 28, 265–288.
- Kucera, M., Malmgren, B.A., 1998. Logratio transformation of compositional data—a resolution of the constant sum constraint. *Marine Micropaleontology* 34, 117–120.
- Kunz-Pirung, M., 1998. Rekonstruktion der Oberflächenwassermassen der östlichen Laptevsee im Holozän anhand von aquatischen Palynomorphen. *Berichte zur Polarforschung* 281, 117.

- Kunz-Pirrung, M., 2001. Dinoflagellate cyst assemblages in recent sediments of the Laptev Sea (Arctic Ocean) and their relation to hydrographic conditions. *Journal of Quaternary Science* 16, 637–650.
- Lapointe, M., 2000. Late Quaternary paleohydrology of the Gulf of St. Lawrence (Québec, Canada) based on diatom analysis. *Palaeogeography, Palaeoclimatology, and Palaeoecology* 156, 261–276.
- Lea, D.W., Mashiotta, T.A., Spero, H.J., 1999. Controls on magnesium and strontium uptake in planktonic foraminifera determined by live culturing. *Geochimica et Cosmochimica Acta* 63, 2369–2379.
- Lcvandowsky, M., Kaneta, P., 1987. Behaviour in dinoflagellates. In: Taylor, F.J.R. (Ed.), *The Biology of Dinoflagellates*. Botanical Monograph 21. Blackwell Scientific, Oxford, pp. 360–397.
- Malmgren, B., Nordlund, U., 1997. Application of artificial neural network to paleoceanographic data. *Palaeogeography, Palaeoclimatology, and Palaeoecology* 136, 359–373.
- Mangin, S., 2002. Distribution actuelle des kystes de dinoflagellés en Méditerranée occidentale et application aux fonctions de transfert, vol. 1. *Memoir of DEA, University of Bordeaux*, 34pp.
- Marret, F., 1993. Les effets de l'acétolyse sur les assemblages de kystes de dinoflagellés. *Palynosciences* 2, 267–272.
- Marret, F., Scourse, J., 2003. Control of modern dinoflagellate cyst distribution in the Irish and Celtic Seas by seasonal stratification dynamics. *Marine Micropaleontology* 47, 101–116.
- Marret, F., Zonneveld, K., 2003. Atlas of modern organic-walled dinoflagellate cyst distribution. *Review of Palaeobotany and Palynology* 125, 1–200.
- Marret, F., Eiriksson, J., Knudsen, K.-L., Turon, J.-L., Scourse, J., 2004. Distribution of dinoflagellate cyst assemblages in surface sediments from the northern and western shelf of Iceland. *Review of Palaeobotany and Palynology* 128, 35–53.
- Matthiessen, J., 1995. Distribution patterns of dinoflagellate cysts and other organic-walled microfossils in recent Norwegian–Greenland Sea sediments. *Marine Micropaleontology* 24, 307–334.
- Mix, A.E., Bard, E., Schneider, R., 2001. Environmental processes of the ice age: land, ocean, glaciers (EPILOG). *Quaternary Science Reviews* 20, 627–657.
- Mudie, P.J., 1992. Circum-arctic Quaternary and Neogene marine palynofloras: paleoecology and statistical analysis. In: Head, M.J., Wrenn, J.H. (Eds.), *Neogene and Quaternary Dinoflagellate Cysts and Acritarchs*. American Association of Stratigraphic Palynologists Foundation, College Station, TX, pp. 347–390.
- Mudie, P.J., Rochon, A., 2001. Distribution of dinoflagellate cysts in the Canadian Arctic marine region. *Journal of Quaternary Sciences* 16, 603–620.
- Mudie, P.J., Harland, R., Matthiessen, J., de Vernal, A., 2001. Dinoflagellate cysts and high latitude Quaternary paleoenvironmental reconstructions: an introduction. *Journal of Quaternary Science* 16, 595–602.
- National Oceanographic Data Center (NODC), 1994. *World Ocean Atlas*. National Oceanic and Atmospheric Administration, CD-Rom data sets.
- National Oceanographic Data Center (NODC), 1998. *World Ocean Atlas*. National Oceanic and Atmospheric Administration, http://www.nodc.noaa.gov/OC5/pr_woaf.html.
- Nürnberg, D., Müller, A., Schneider, R.R., 2000. Paleo-sea surface temperature calculations in the equatorial east Atlantic from Mg/Ca ratios in planktic foraminifera: A comparison to sea surface temperature estimates from U_{37}^K , oxygen isotopes, and foraminiferal transfer function. *Paleoceanography* 15, 124–134.
- Peltier, W.R., 1994. Ice age paleotopography. *Science* 265, 195–201.
- Peyron, O., de Vernal, A., 2001. Application of Artificial Neural Network (ANN) to high latitude dinocyst assemblages for the reconstruction of past sea-surface conditions in Arctic and sub-arctic seas. *Journal of Quaternary Science* 16, 699–711.
- Pflaumann, U., Duprat, J., Pujol, C., Labeyrie, L., 1996. SIMMAX: a modern analog technique to deduce Atlantic sea surface temperatures from planktonic foraminifera in deep-sea sediments. *Paleoceanography* 11, 15–35.
- Pflaumann, U., Sarnthein, M., Chapman, M., d'Abreu, L., Funnell, B., Huels, M., Kiefer, T., Maslin, M., Schulz, H., Swallow, J., van Kreveland, S., Vautravers, M., Vogelsang, E., Weinelt, M., 2003. Glacial North Atlantic: sea-surface conditions reconstructed by GLAMAP 2000. *Paleoceanography* 18, 1065.
- Radi, T., de Vernal, A., 2004. Dinocyst distribution in surface sediments from the northeastern Pacific margin (40–60°N) in relation to hydrographic conditions, productivity and upwelling. *Review of Palaeobotany and Palynology* 128, 169–193.
- Radi, T., de Vernal, A., Peyron, O., 2001. Relationships between dinocyst assemblages in surface sediment and hydrographic conditions in the Bering and Chukchi seas. *Journal of Quaternary Science* 16, 667–680.
- Raine, R., White, M., Dodge, J.D., 2002. The summer distribution of net plankton dinoflagellates and their relation to water movements in the NE Atlantic Ocean, west of Ireland. *Journal of Plankton Research* 24, 1131–1147.
- Rasmussen, T.L., Thomsen, E., van Weering, T.C.E., Labeyrie, L., 1996. Rapid changes in surface and deep water conditions at the Faeroe Margin during the last 58,000 years. *Paleoceanography* 11, 757–771.
- Rochon, A., de Vernal, A., 1994. Palynomorph distribution in recent sediments from the Labrador Sea. *Canadian Journal of Earth Sciences* 31, 115–127.
- Rochon, A., de Vernal, A., Turon, J.-L., Matthiessen, J., Head, M.J., 1999. Distribution of dinoflagellate cyst assemblages in surface sediments from the North Atlantic Ocean and adjacent basins and quantitative reconstruction of sea-surface parameters. *Special Contribution Series of the American Association of Stratigraphic Palynologists* 35.
- Rosell-Melé, A., 1997. Appraisal of CLIMAP temperature reconstruction in the NE Atlantic using alkenone proxies. *Eos* 78 (46), F28.
- Rosell-Melé, A., 1998. Interhemispheric appraisal of the value of alkenone indices as temperature and salinity proxies in high latitude locations. *Paleoceanography* 13, 694–703.
- Rosell-Melé, A., Comes, P., 1999. Evidence for a warm last glacial maximum in the Nordic Seas, or an example of shortcomings in U_{37}^K and U_{37}^H to estimate low sea surface temperature? *Paleoceanography* 13, 694–703.
- Rosell-Melé, A., Bard, E., Emeis, K.C., Grieger, B., Hewitt, C., Müller, P.J., Schneider, R., 2004. Sea surface temperature anomalies in the oceans at the LGM estimated from the alkenone- U_{37}^K index: comparison with GCMs. *Geophysical Research Letters* 31, L03208.
- Sarnthein, M., Gersonde, R., Niebler, S., Pflaumann, U., Spielhagen, R., Thiede, J., Wefer, G., Weinelt, M., 2003. Overview of Glacial Atlantic Ocean Mapping (GLAMAP 2000). *Paleoceanography* 18, 1071.
- Sarnthein, M., Jansen, E., Weinelt, M., Arnold, M., Duplessy, J.C., Erlenkeuser, H., Flåtøy, A., Johannessen, G., Johannessen, T., Jung, S., Koc, N., Labeyrie, L., Maslin, M., Pflaumann, U., Schulz, H., 1995. Variations in Atlantic surface ocean paleoceanography, 50°–80°N: A time-slice record of the last 30,000 years. *Paleoceanography* 10, 1063–1094.
- Schneider, R., Bard, E., Mix, A., 2000. Last Ice Age global ocean and land surface temperature: the EPILOG initiative. *PAGES Newsletter* 8, 19–21.
- Solignac, S., de Vernal, A., Hillaire-Marcel, C., 2004. Holocene sea-surface conditions in the North Atlantic—contrasted trends and regimes between the eastern and western sectors (Labrador Sea vs. Iceland Basin). *Quaternary Science Reviews* 23, 319–334.

- Tang, C.L., Wang, C.K., 1996. A gridded data set of temperature and salinity for the northwest Atlantic Ocean. Canadian Data Report of Hydrography and Ocean Sciences no. 148, 45pp.
- Taylor, F.J.R., Pollinger, U., 1987. Ecology of Dinoflagellates. In: Taylor, F.J.R. (Ed.), *The Biology of Dinoflagellates*. Botanical Monograph 21. Blackwell Scientific, Oxford, pp. 399–529.
- Ter Braak, C.J.F., Smilauer, P., 1998. CANOCO reference manual and user's guide to CANOCO for Windows software for canonical community ordination (Version 4). Centre for Biometry, Wageningen, 351pp.
- Turon, J.-L., 1984. Le palynoplankton dans l'environnement actuel de l'Atlantique nord-oriental. Évolution climatique et hydrologique depuis le dernier maximum glaciaire. Mémoire de L'Institut Géologique du Bassin d'Aquitaine 17, 1–313.
- von Grafenstein, R., Zahn, R., Tiedemann, R., Murat, A., 1999. Planktonic ^{18}O records at Sites 976 and 977, Alboran Sea: Stratigraphy, forcing, and paleoceanographic implications. In: Zahn, R., et al. (Eds.), *Proceedings of the Ocean Drilling Program, Scientific Results*, vol. 161. Ocean Drilling Program, College Station, TX, pp. 469–479.
- Voronina, E., Polyak, L., de Vernal, A., Peyron, O., 2001. Holocene variations of sea-surface conditions in the southeastern Barents Sea based on palynological data. *Journal of Quaternary Science* 16, 717–727.
- Waelbroeck, C., Labeyrie, L., Duplessy, J.-C., Guiot, J., Labracherie, M., Leclaire, H., Duprat, J., 1998. Improving paleo-SST estimates based on planktonic fossil faunas. *Paleoceanography* 12, 272–283.
- Wall, D., Dale, B., 1968. Modern dinoflagellate cysts and the evolution of the Peridiniales. *Micropaleontology* 14, 265–304.
- Wall, D., Dale, B., Lohman, G.P., Smith, W.K., 1977. The environmental and climatic distribution of dinoflagellate cysts in the North and South Atlantic Oceans and adjacent seas. *Marine Micropaleontology* 2, 121–200.
- Weinelt, M., Sarnthein, M., Pflaumann, U., Schulz, H., Jung, S., Erlenkeuser, H., 1996. Ice-free Nordic seas during the last glacial maximum? Potential sites of deep water formation. *Paleoclimates* 1, 283–309.
- Weinelt, M., Vogelsang, E., Kucera, M., Pflaumann, U., Sarnthein, M., Voelker, A., Erlenkeuser, H., Malmgren, B.A., 2003. Variability of North Atlantic heat transfer during MIS 2. *Paleoceanography* 18, 1071–10.
- Winter, A., Jordan, R.W., Roth, P.H., 1994. Biogeography of living coccolithophores in ocean waters. In: Winter, A., Siesser, W.G. (Eds.), *Coccolithophores*. Cambridge University Press, Cambridge, pp. 161–177.
- Zaragosi, S., Eynaud, F., Pujol, C., Auffret, G.A., Turon, J.-L., Garlan, T., 2001. Initiation of the European deglaciation as recorded in the northwestern Bay of Biscay slope environments (Meriadzek Terrace and Trevelyan Escarpment): a multi-proxy approach. *Earth and Planetary Science Letters* 188, 493–507.
- Zonneveld, K.A., Versteegh, G.H., de Lange, G.J., 2001. Palcoproductivity and postdepositional aerobic organic matter decay reflected by dinoflagellate cyst assemblages in Eastern Mediterranean S1 Sapropel. *Marine Geology* 172, 181–195.

ANNEXE 3

Copie de l'article

DINOFLAGELLATES

De Vernal, A., Rochon, A., Radi, T.

Encyclopedia of Quaternary Science (2007), Elsevier, 1652-1667

References

- Böhm, F., Joachimski, M. M., Dullo, W.-C., *et al.* (2000). Oxygen isotope fractionation in marine aragonite of coralline sponges. *Geochimica et Cosmochimica Acta* 64, 1695–1703.
- Clark, G. R., II (2005). Daily growth lines in some living *Pectens* (Mollusca: Bivalvia), and some applications in a fossil relative: Time and tide will tell. *Palaeogeography, Palaeoclimatology, Paleoecology* 228, 26–42.
- Druffel, E. R. M., and Benavides, L. M. (1986). Input of excess CO₂ to the surface ocean based on ¹³C/¹²C ratios in a banded Jamaican sclerosponge. *Nature* 321, 58.
- Druffel, E. R. M. (1997). Geochemistry of corals: Proxies of past ocean chemistry, ocean circulation, and climate. *Proceedings of the National Academy of Sciences* 94, 8354–8361.
- Felis, T., and Pätzold, J. (2004). Corals as Climate Archive. In *The Climate in Historical Times: Towards a Synthesis of Holocene Proxy Data and Climate Models* (H. Fischer, T. Kumke, G. Lohmann *et al.*, Eds.), pp. 91–108. Springer, Berlin.
- Gagan, M. K., Ayliff, L. K., Beck, J. W., *et al.* (2000). New views of tropical paleoclimate from corals. *Quaternary Science Reviews*, 19, 167–182.
- Jones, D. S. (1983). Sclerochronology: Reading the record of the molluscan shell. *American Scientist*, 71, 384–391.
- Lorrain, A., Gillikan, D. P., Pauler, Y.-M., *et al.* (2005). Strong kinetic effects on Sr/Ca ratios in the calcitic bivalve *Pecten maximus*. *Geology*, 33, 965–968.
- Rosenheim, B. E., Swart, P. K., Thorrold, S. R., Willenz, P., Berry, L., and Latkoczy, C. (2004). High-resolution Sr/Ca records in sclerosponges calibrated to temperature *in situ*. *Geology*, 32(2), 145–148.
- Schöne, B. R., Rodland, D. L., Fiebig, J., *et al.* (2006). Reliability of multi-taxon, multi-proxy reconstructions of environmental conditions from accretionary biogenic skeletons. *Journal of Geology*, 114, 267–285.
- Swart, P. K., Thorrold, S. R., Rosenheim, B. E., *et al.* (2002). Intra-annual variation in the stable oxygen and carbon and trace element composition of sclerosponges. *Paleoceanography*, 17, 1045, (doi:10.1029/2000PA000622).
- Tudhope, A. W., Chilcott, C. P., McCulloch, M. T., *et al.* (2001). Variability in the El Niño–Southern oscillation through a glacial–interglacial cycle. *Science*, 291, 1511–1517.

Dinoflagellates

A de Vernal, Université du Québec à Montréal, Montréal, Canada

A Rochon, Université du Québec à Rimouski, Québec, Canada

T Radi, Université du Québec à Montréal, Québec, Canada

© 2007 Elsevier B.V. All rights reserved.

Introduction

Dinoflagellates are microscopic unicellular organisms occupying most aquatic environments, from freshwater bodies to open ocean. Most dinoflagellates are planktonic and use their two flagella to swim in a spiral-like motion, which is the origin of

their name (from the Greek word *dinos* meaning whirling). In biological sciences, dinoflagellates receive special attention since they represent an important part of the net primary production in aquatic environments and because they are responsible for harmful algal blooms or red tides. In paleontology and Earth sciences, dinoflagellates merit particular interest since they yield microfossils, which constitute good biostratigraphical markers of the Mesozoic and Cenozoic and are useful paleoecological indicators of changes in sea-surface water masses.

The motile stage of dinoflagellates does not produce fossil remains, but about 10 to 20% of species go through a cyst stage that yields microfossils. These microfossils mostly consist of highly resistant organic-walled cysts, also called dinocysts, which can be routinely observed under optical microscope on palynological slides. Therefore, the fossil remains of dinoflagellates do not correspond to the vegetative stage of the cells, and the morphology of living and fossil forms may differ considerably (Figs. 1–2). Living dinoflagellates were described by naturalists in the eighteenth century, but the relationship between the microfossils and living dinoflagellates has only been known since the second half of the twentieth century. Most fossil dinoflagellate cysts

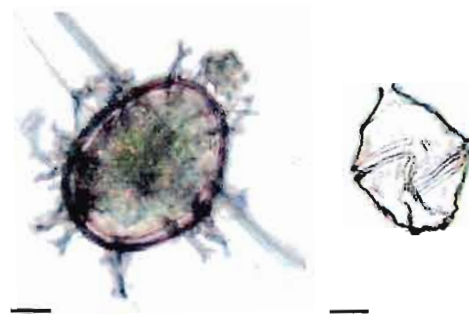


Figure 1 Photographs of *Gonyaulax* cyst and theca (scale bar = 10 μm).

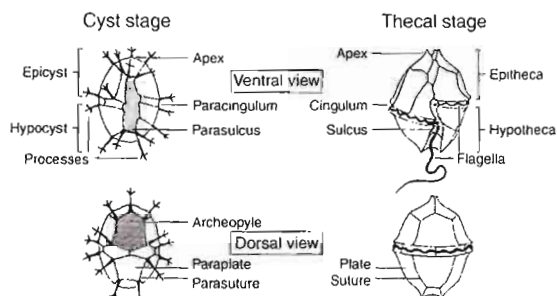


Figure 2 Scheme of dinoflagellate cyst and theca (*Gonyaulax*-type).

described from the beginning of nineteenth century until the end of the twentieth century were associated to 'hystrichospheres' and believed to be remineralized skeletons of algae. Important progress in the understanding of the status of dinoflagellate cysts in the living world has been made since the 1960s. The in-depth morphological observations of Evitt (1963) allowed the identification of structures relating the fossil organic-walled cysts with dinoflagellates. Moreover, the *in vitro* experiments by Wall and Dale (1966, 1968) demonstrated the biological affinities of dinocysts and contributed to the documentation of the life cycle and stages of many taxa.

Since the 1970s, many studies have been undertaken to document the distribution of dinocysts on the sea floor. About one hundred Quaternary dinocyst species have thus far been described. The dinocyst assemblages in surface sediment samples of the marine environment show a biogeographical distribution with distinct latitudinal gradients from Arctic seas to the circum-Antarctic Ocean, demonstrating a dependency upon temperature and sea ice (Rochon *et al.*, 1999, Mudie *et al.*, 2001). The dinocyst distribution also shows inshore to offshore gradients that have been linked to salinity, productivity, and eutrophication (Dale, 1996, Marret and Zonneveld, 2003). Based on these studies, it is possible to propose relationships between dinocyst assemblages and sea-surface conditions, including temperature, salinity, sea-ice cover, productivity, and trophic characteristics of waters, and therefore, to use dinocyst assemblages for qualitative or quantitative reconstruction of paleoceanographical conditions (de Vernal *et al.*, 2005).

In addition to organic-walled cysts or dinocysts, some dinoflagellate taxa yield calcareous microfossils generally associated with the cyst stage. Calcareous dinoflagellates appear to be abundant in oceanic sediments at middle to low latitudes, where they can be used as tracers of hydrographic conditions in the upper water column (Vink, 2004).

In this article, we principally summarize information on dinoflagellates and their organic-walled cysts, which are studied within the field of marine palynology and currently used for paleoenvironmental investigations in Quaternary science.

Ecology of Dinoflagellates

Dinoflagellates live in various types of aquatic environments, including lakes, estuaries, epicontinental seas, and the open ocean, from equatorial to polar latitudes (Taylor and Pollinger, 1987; Matthiessen *et al.*, 2005). However, most dinoflagellates are marine: a few thousand species are known from marine

waters, whereas only a few hundred species are known to live in fresh water.

In oceans, dinoflagellates seem to be particularly well adapted to neritic (shallow) environments, including the estuaries, epicontinental seas, and continental shelves. This is probably due to their tolerance to low salinity, in addition to nutrient availability and stratification of water masses. In general, the diversity of dinoflagellates in surface waters is larger at the Equator and decreases towards the poles.

The feeding strategy of dinoflagellates is variable. Many are autotrophic (photosynthetic) and form an important part of planktonic primary production in lakes and oceans. About half of dinoflagellate species are heterotrophic or mixotrophic (i.e., feeding on other organisms or on dissolved organic substances), and others are symbionts of marine invertebrates such as corals in which they are known as zooxanthellae. The autotrophic dinoflagellates depend upon light and nutrients (nitrogen and phosphorus, notably). They live in the photic zone at relatively shallow depths, usually within the upper 50 or 100 meters. The heterotrophic dinoflagellates depend upon the overall productivity and generally live in surface waters where their prey occurs.

Dinoflagellates are mobile in the water column. They have two flagella, one around the cingulum and the other longitudinal, which permit swimming with a spiral-like 'whirling' motion with a speed ranging from a few centimeters to a few meters per hour. They use their flagella together with physiologic adjustment of buoyancy to migrate vertically in the upper water in order to optimize their metabolic and feeding activities. During the day, dinoflagellates migrate to the surface for photosynthesis, and during the night, they migrate down, away from the nutrient-depleted surface waters. Despite their ability to move vertically, dinoflagellates generally inhabit a relatively thin and shallow surface layer, especially in stratified marine environments, because they cannot migrate across the pycnocline (vertical gradient of density) that constitutes an important physical barrier.

The reproduction of dinoflagellates is most commonly asexual by mitosis. In the blooming period, vegetative cell divisions occur at a rate of about one per day. Sexual reproduction is also observed for many species. When blooming, dinoflagellates can be responsible for 'red tides', so called because the large density of cells in the surface water induces a color change (green, brown, or red). Many dinoflagellates are bioluminescent and cause sparkling of the sea at night. A few dinoflagellate species produce neurotoxins that may be bioconcentrated by filtering organisms, notably shellfish, which then become poisonous and dangerous for the health of animals feeding on them.

In marine environments, dinoflagellates constitute one of the main primary producers, together with diatoms and coccolithophorids. Typically, dinoflagellates experience their blooms after diatoms.

The Life Cycle of Dinoflagellates and the Cyst Stage

Most dinoflagellates have a complex life cycle involving several stages, asexual and sexual, motile and non-motile (Pfiester and Anderson, 1987). In general, during the course of the sexual reproduction, the haploid vegetative cells (1-n chromosomes) become or produce haploid gametes that fuse to develop a zygote. The zygote rapidly enters into a dormant stage called 'hypnozygote', during which the diploid cell (with 2-n chromosomes) is protected in a cyst. After a dormancy period of variable length, the protoplasm excysts and meiosis occurs. The excystment of the cell occurs through an opening in the cyst called the archeopyle, which has a geometry determined by the morphology of the original theca (see below).

In the life strategy of dinoflagellates, the cyst has an extremely important function, since it constitutes a protective structure that fosters survival of the cell over long periods of time (several years to decades) and permits propagation and dispersal (Dale, 1983) (Fig. 3).

The cyst wall of many species is made of highly resistant organic matter called dinosporin that is similar in composition to the sporopollenin of pollen grains.

These organic-walled cysts called 'dinocysts' are typically 15 to 100 μm in diameter. They are observed on palynological slides prepared following standard laboratory procedures used for the study of pollen and spores, which involve chemical preparation with hydrofluoric and hydrochloric acids. The study of dinocysts is thus considered a sub-discipline of palynology.

Some dinoflagellates also produce cysts made of calcium carbonate, which fossilize in sediment. These are analyzed together with the calcareous nanoplankton. In addition to hypnozygotes, some dinoflagellates produce temporary cysts to survive adverse conditions. These types of cysts do not form fossils.

The life cycle of dinoflagellates is variable. Sexual reproduction has been observed only for a few taxa and more *in vitro* and *in vivo* studies are necessary for a comprehensive understanding of their life cycle. Only 10 to 20% of dinoflagellate taxa are known to produce durable cysts. The correspondence between the organic-walled or calcareous dinoflagellate cysts recovered in sediments and their motile stage in the water column is known for many species but still needs to be established for many others.

The Taxonomy and General Morphology of Dinoflagellates and Dinocysts

Dinoflagellates are unicellular eukaryotic organisms that belong to Protista, according to the classification system in five kingdoms. Because they include both autotrophic and heterotrophic species, dinoflagellates

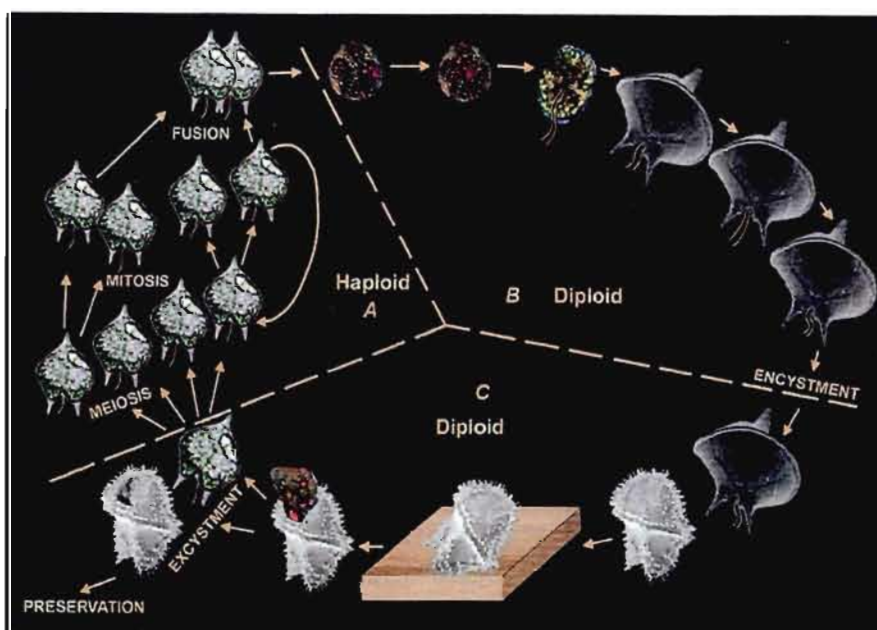


Figure 3 Schematic illustration of idealized dinoflagellate life cycle (adapted from Evitt, 1985).

can be classified both as plants and animals. Within the International Code of Zoological Nomenclature, they have been grouped under the phylum of Mastigophora. However, dinoflagellates and their cysts are more commonly treated as algae and are thus classified following the rules of the International Code of Botanical Nomenclature. For a long time, they have been placed in the division of Pyrrophyta named after the bioluminescent forms (from the Greek word *pyrros* meaning fire). Dinoflagellates are now grouped within the division of Dinoflagellata, which is distinguished on the bases of several criteria. A main one is the cell membrane that is characterized by a complex outer layer (the amphiesma) containing a single layer of flattened vesicles (the amphiesmal vesicle). In many dinoflagellates, the amphiesma vesicle contains thecal plates composed of cellulose. These dinoflagellates are described as thecate, whereas those lacking such plates of cellulose are termed 'naked' or 'unarmored'. Dinoflagellates also contain a unique type of nucleus, the dinokaryon, which is characterized by chromosomes remaining condensed between cell divisions and which lacks histones. Another peculiarity of dinoflagellates is their morphological asymmetry, and the possession of two dissimilar flagella (Fig. 2).

The classification of dinoflagellates and their cysts is principally based on the structure of the amphiesma and the organization of the thecal plates,

referred to as tabulation. Amongst dinoflagellates producing cysts currently recovered in Quaternary sediment samples, there are three principal groups represented: the Gymnodiniales that are unarmored and the Gonyaulacales and Peridinales that are thecate and show distinct types of tabulation (Fig. 4).

In the Peridinales and Gonyaulacales, the tabulation pattern is described according to the organization of the theca from the apex to the cingulum and antapex, and according to the ventral or dorsal orientation. The flagella are inserted on the ventral (or sulcal) side, whereas the archeopyle is often located on the dorsal side of the cysts. The types of tabulation include apical, precingular, cingular, postcingular, and antapical plates, which are labeled after different systems (Evvitt, 1985; Edwards, 1993). The most commonly used is Kofoid's system, describing the number of plates in each level of the theca. For the cyst stage, the prefix 'para' is used when referring to the outline of the plates on the cyst wall, and certain plates are called 'homologs' of their thecal counterpart. The tabulation system of Evvitt and Taylor, which provides indications on the interconnection between plates, is also often used for the description and classification of Gonyaulacales. The main morphological characteristic of Peridinales is the presence of intercalary plates between apical and precingular plate series on the dorsal side, which are lacking in Gonyaulacales (colored green in Fig. 5).

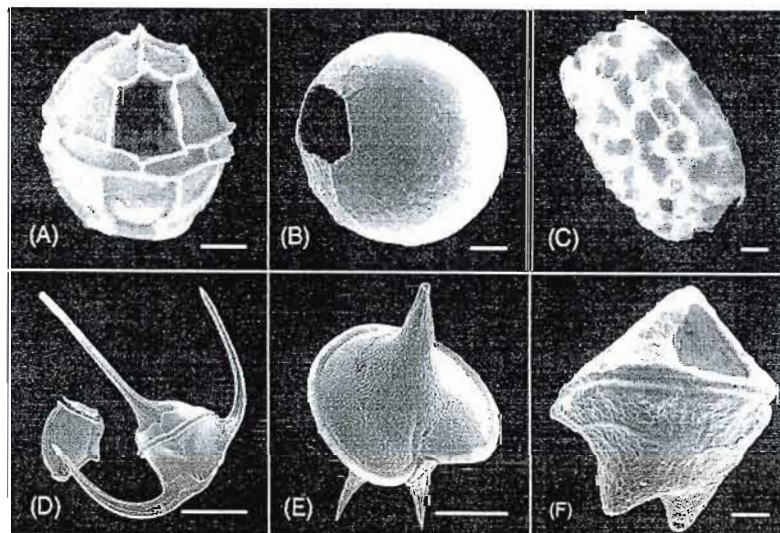


Figure 4 Scanning electron micrographs of dinoflagellates and dinocysts. Figures (A–C), (F) scale bar = 10 μm ; figures (D–E) scale bar = 50 μm . Figure (A) *Impagidinium paradoxum* (cyst of *Gonyaulax* sp., order Gonyaulacales) North Atlantic Ocean; Figure (B) *Brigantedinium cariacense* (cyst of *Protoperidinium avellanum*, order Peridinales), Bedford Basin, NS, Canada; Figure (C) Cyst of *Polykrikos schwartzii* (order Gymnodiniales), Lawrence Town, NS, Canada; Figure (D) *Ceratium tripos* and *Dinophysis acuminata* (theca; orders Ceratiales and Dinophysiales, respectively), Bedford Basin, NS, Canada; Figure (E) *Protoperidinium* cf. *depressum* (theca; order Peridinales) Bedford Basin, NS, Canada; Figure (F) *Quinquecuspsis concreta* (cyst of *Protoperidinium leone*, order Peridinales), Saanich Inlet, BC, Canada.

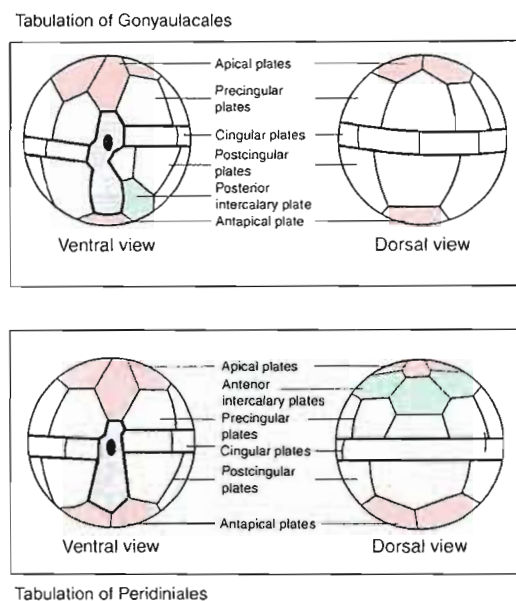


Figure 5 Simplified scheme showing the tabulation pattern of Peridinales and Gonyaulacales. The ventral view corresponds to where the flagellar pore is, on the surface of the sulcus (in gray). The dorsal view corresponds to the surface where the archeopyle is often located (often made of precingular plate or plates for Gonyaulacales and of intercalary plate or plates for Peridinales). The figure is adapted from Fensome *et al.* (1993).

Independent classifications of dinoflagellates have been proposed by biologists and paleontologists, and most of the literature of the nineteenth and twentieth centuries refers to distinct classification schemes for living and fossil dinoflagellates. Nevertheless, Fensome *et al.* (1993) made an attempt to reconcile the classification schemes by biologists and paleontologists using various criteria (nucleus type, structure of the amphiesma, tabulation) and proposed a common supra-generic classification for cyst and motile stages of dinoflagellates. At the generic and species levels, the motile stage name could be retained for both living and fossil forms for which the biological affinities of the cysts are known. However, these affinities are still uncertain for many Quaternary dinoflagellate cysts and for most pre-Quaternary ones. Therefore, the genera and species names given to the dinocysts often differ from the ones of their living counterparts (Head, 1996).

In the classification of living and fossil dinoflagellates, the tabulation constitutes an important diagnostic character. The tabulation pattern of the dinoflagellates can be reflected in various ways on the cysts. Some dinocysts may show sutures or septa defining the original pattern of thecal plates. Others possess extensions called processes that may have

their position determined by the original tabulation. Some do not show any evidence of tabular pattern, with the exception of the archeopyle that has a given position. Beyond the tabulation patterns, as reflected by sutures, processes or the archeopyle, there are many morphological criteria used to distinguish and identify dinocyst species. They include the structure of the layers of the wall (cavate or proximate), the overall shape of the cyst (elongate, round, or flattened), the presence of apical or antapical horns, the presence of processes and sutures, their respective positions (following tabulation or not), the ornamentation of the cyst wall, the size, the color (semi-transparent or brown), etc. Explicit descriptions on the morphological nomenclature of dinocysts have been published by the Dinoflagellate working group (1986), Head *et al.* (1989) and Edwards (1993).

The Organic-Walled Dinoflagellate Cysts or Dinocysts in the Marine Realm

Biostratigraphy of Dinocysts

Dinocysts are the most common organic-walled microfossils or palynomorphs in marine sediments. In the field of marine palynology, they have been intensively studied for biostratigraphical purposes, notably in aid of petroleum exploration. The oldest known dinocysts date from the Silurian, but they are more abundant from the Triassic to the modern, with maximum diversity of species recorded during the Cretaceous and Paleogene (Powell, 1992; Fensome and Williams, 2004). The diversity of species in Quaternary sediments is relatively low, with close to one hundred species formally described to date (Table 1). Although it still needs investigation, the Quaternary biostratigraphic record of dinocysts shows extinctions of a few species during the Pleistocene, and very rare first appearance of species (de Vernal *et al.*, 1992).

Biogeographical Distribution of Dinocysts

Since the early work of Wall *et al.* (1977), documenting the modern distribution of dinocysts in sediments, many palynological studies have described the distribution patterns of dinocysts on the sea floor. There are now regional data sets for the North Atlantic and the Arctic Ocean, the circum-Antarctic Ocean, the low latitudes of the Atlantic Ocean, the eastern and western Pacific margins (Rochon *et al.*, 1999; Marrer and Zonnevelt, 2003).

Studies of dinocyst abundance in sediments reveal high concentrations (up to 10^6 cysts cm^{-3}) along continental margins (shelves, inland seas, estuaries) and decreasing concentrations offshore, suggesting

Table 1 List of marine late Quaternary dinocyst taxa

Species – Dinocyst name	Motile affinity	Order
<i>Ataxiodinium choane</i>	<i>Gonyaulax</i> sp.	Gonyaulacales
<i>Bitectalodinium spongium</i>	Unknown	Gonyaulacales
<i>Bitectalodinium tepikiense</i>	<i>Gonyaulax</i> sp.	Gonyaulacales
<i>Brigantedinium cañacoense</i>	<i>Protooperidinium avellanum</i>	Peridinales
<i>Brigantedinium simplex</i>	<i>Protooperidinium conicooides</i>	Peridinales
<i>Dalella chathamensis</i>	<i>Gonyaulax</i> sp.	Gonyaulacales
<i>Dubridinium caperatum</i>	<i>Preperidinium meunien</i>	Peridinales
<i>Echinidinium aculeatum</i>	Unknown	Peridinales
<i>Echinidinium bispiniformum</i>	Unknown	Peridinales
<i>Echinidinium delicatum</i>	Unknown	Peridinales
<i>Echinidinium granulatum</i>	Unknown	Peridinales
<i>Echinidinium karaense</i>	Unknown	Peridinales
<i>Echinidinium transparentum</i>	Unknown	Peridinales
Cysts of <i>Gymnodinium catenatum</i>	<i>Gymnodinium catenatum</i>	Gymnodinales
<i>Impagidinium aculeatum</i>	<i>Gonyaulax</i> sp.	Gonyaulacales
<i>Impagidinium pacificum</i>	<i>Gonyaulax</i> sp.	Gonyaulacales
<i>Impagidinium pallidum</i>	<i>Gonyaulax</i> sp.	Gonyaulacales
<i>Impagidinium paradoxum</i>	<i>Gonyaulax</i> sp.	Gonyaulacales
<i>Impagidinium patulum</i>	<i>Gonyaulax</i> sp.	Gonyaulacales
<i>Impagidinium plicatum</i>	<i>Gonyaulax</i> sp.	Gonyaulacales
<i>Impagidinium sphaericum</i>	<i>Gonyaulax</i> sp.	Gonyaulacales
<i>Impagidinium striatum</i>	<i>Gonyaulax</i> sp.	Gonyaulacales
<i>Impagidinium variaseptum</i>	<i>Gonyaulax</i> sp.	Gonyaulacales
<i>Impagidinium velorum</i>	<i>Gonyaulax</i> sp.	Gonyaulacales
<i>Islandinium brevispinosum</i>	<i>Protooperidinium</i> sp.	Peridinales
<i>Islandinium? cezare</i>	<i>Protooperidinium</i> sp.	Peridinales
<i>Islandinium minutum</i>	<i>Protooperidinium</i> sp.	Peridinales
<i>Leipokatium invisitum</i>	Unknown	Peridinales
<i>Lejeunecysta otiva</i>	Unknown	Peridinales
<i>Lejeunecysta sabrina</i>	? <i>Protooperidinium leone</i>	Peridinales
<i>Lingulodinium machaerophorum</i>	<i>Lingulodinium polyedrum</i>	Gonyaulacales
<i>Nematosphaeropsis labyrinthus</i>	<i>Gonyaulax spinifera</i>	Gonyaulacales
<i>Nematosphaeropsis rigida</i>	<i>Gonyaulax</i> sp.	Gonyaulacales
<i>Operculodinium centrocarpum</i>	<i>Protoceratium reticulatum</i>	Gonyaulacales
<i>Operculodinium</i> short processes	? <i>Protoceratium reticulatum</i>	Gonyaulacales
<i>Operculodinium israelianum</i>	? <i>Protoceratium</i> sp.	Gonyaulacales
<i>Operculodinium janduchenei</i>	Unknown	Gonyaulacales
<i>Operculodinium longispinigerum</i>	Unknown	Gonyaulacales
Cysts of <i>Pentapharsodinium dalei</i>	<i>Pentapharsodinium dalei</i>	Peridinales
Cysts of <i>Pheopolykrikos hartmannii</i>	<i>Pheopolykrikos hartmannii</i>	Gymnodinales
Cyst of <i>Polykrikos</i> sp.-Arctic morphotype	<i>Polykrikos</i> sp.	Gymnodinales
Cysts of <i>Polykrikos kotoidii</i>	<i>Polykrikos kotoidii</i>	Gymnodinales
Cysts of <i>Polykrikos schwartzii</i>	<i>Polykrikos schwartzii</i>	Gymnodinales
<i>Polysphaeridium zoharyi</i>	<i>Pyrodinium bahamense</i>	Gonyaulacales
Cysts of <i>Protooperidinium americanum</i>	<i>Protooperidinium americanum</i>	Peridinales
Cysts of <i>Protooperidinium nudum</i>	<i>Protooperidinium nudum</i>	Peridinales
Cysts of <i>Protooperidinium stellatum</i>	<i>Protooperidinium stellatum</i>	Peridinales
<i>Pyxidinopsis psilata</i>	Unknown	Gonyaulacales
<i>Pyxidinopsis reticulata</i>	Unknown	Gonyaulacales
<i>Quinquecuspsis concreta</i>	? <i>Protooperidinium leone</i>	Peridinales
Cysts of cf. <i>Scrippsiella trifida</i>	<i>Scrippsiella trifida</i>	Gonyaulacales
<i>Selenopemphix antarctica</i>	Unknown	Peridinales
<i>Selenopemphix nephroides</i>	<i>Protooperidinium subinermis</i>	Peridinales
<i>Selenopemphix quanta</i>	<i>Protooperidinium conicum</i>	Peridinales
<i>Spiniferites alaskensis</i>	<i>Gonyaulax</i> sp.	Gonyaulacales
<i>Spiniferites belerius</i>	<i>Gonyaulax scrippsae</i>	Gonyaulacales
<i>Spiniferites bentoni</i>	<i>Gonyaulax digitale</i>	Gonyaulacales
<i>Spiniferites bulloideus</i>	<i>Gonyaulax scrippsae</i>	Gonyaulacales
<i>Spiniferites cruciformis</i>	<i>Gonyaulax</i> sp.	Gonyaulacales
<i>Spiniferites delicatus</i>	<i>Gonyaulax</i> sp.	Gonyaulacales

(Continued)

Table 1 (Continued)

Species – Dinocyst name	Motile affinity	Order
<i>Spiniferites elongatus</i>	<i>Gonyaulax elongata</i>	Gonyaulacales
<i>Spiniferites frigidus</i>	<i>Gonyaulax</i> sp.	Gonyaulacales
<i>Spiniferites hyperacanthus</i>	<i>Gonyaulax</i> sp.	Gonyaulacales
<i>Spiniferites lazus</i>	<i>Gonyaulax</i> sp.	Gonyaulacales
<i>Spiniferites membranaceus</i>	<i>Gonyaulax</i> sp.	Gonyaulacales
<i>Spiniferites mirabilis</i>	<i>Gonyaulax spinifera</i>	Gonyaulacales
<i>Spiniferites pachydermus</i>	<i>Gonyaulax</i> sp.	Gonyaulacales
<i>Spiniferites ramosus</i>	<i>Gonyaulax</i> sp.	Gonyaulacales
<i>Stelladinium reidii</i>	Unknown	Peridinales
<i>Stelladinium robustum</i>	Unknown	Peridinales
<i>Tectatodinium pellitum</i>	<i>Gonyaulax spinifera</i>	Gonyaulacales
<i>Trinovantedinium applanatum</i>	<i>Protoperidinium pentagonum</i>	Peridinales
<i>Trinovantedinium variabile</i>	Unknown	Peridinales
<i>Tuberculodinium vancampoe</i>	<i>Pyrophacus steinii</i>	Gonyaulacales
<i>Votadinium calvum</i>	<i>Protoperidinium oblongum</i>	Peridinales
<i>Votadinium spinosum</i>	<i>Protoperidinium claudicans</i>	Peridinales
<i>Xandarodinium xanthum</i>	<i>Protoperidinium divaricatum</i>	Peridinales

Gray zones: heterotrophic or mixotrophic taxa

White zones: autotrophic taxa

higher dinocyst fluxes in shallow seas, rather than in open oceans (Fig. 6).

The species assemblages show large variations from the Equator to the poles, with maximum species diversity at low latitudes. Many species appear ubiquitous or cosmopolitan and occur in wide latitudinal ranges of both hemispheres, but several appear to be restricted to equatorial-tropical environments. Only a few taxa seem to occur exclusively at polar and subpolar latitudes. Some species have been reported only from the Northern Hemisphere, whereas others only occur in the southern Ocean. Moreover, the species composition of assemblages apparently differs in the Atlantic and Pacific oceans. Thus, some regionalism seems to characterize dinocyst distribution (Figs. 7 and 8).

In general, the relative abundance of taxa in dinocyst assemblages follows distributional patterns closely related to the latitudinal and to nearshore to open ocean gradients. Multivariate analyses of assemblages clearly demonstrate relationships with sea-surface temperatures, whatever spatial scale is considered (Marret and Zonneveld, 2003). The analyses of assemblage distribution patterns at regional scales (e.g., sub-hemispheric ocean basins) also show relationships between cyst assemblages and sea-surface salinity, annual amplitude of sea-surface temperatures, sea-ice cover, primary productivity and upwelling intensity (Rochon *et al.*, 1999; de Vernal *et al.*, 2005; Radi and de Vernal, 2004). For example, as illustrated in Figure 8 summarizing data from the Northern Hemisphere, there are taxa occurring in high percentages in areas marked by extensive seasonal sea-ice cover and others tolerate some sea ice, whereas the

majority of species do not occur in polar and subpolar seas with freezing winter conditions (Figs. 9–13).

Several examples of the geographical distribution of dinocyst taxa in marine sediments of the Northern Hemisphere are illustrated in the maps of Figures 9 to 13. These maps show a clear latitudinal gradient in the occurrence and abundance of many autotrophic (Figs. 9, 11 and 12) and heterotrophic (Figs. 10 and 13) taxa, thus indicating close relationships with sea-surface temperature and sea-ice cover. The distribution patterns of some taxa also show nearshore to offshore gradients, which reflect some relationship with salinity gradients.

Beyond hemispheric patterns, at more local scales (estuarine systems, for example), the analyses of the dinocyst distribution suggest relationships with eutrophication (Dale and Dale, 2002). However, because the composition of assemblages may vary significantly between regions, the quantitative relationships between dinocyst assemblages and hydrographic or oceanic conditions at regional or local scales cannot be extrapolated on a global scale.

Ecological-Paleoecological Significance of Dinocysts in Sediment

The dinocysts represent only a fragmentary picture of the original dinoflagellate populations (Dale, 1976; Head, 1996; Matthiessen *et al.*, 2005). The ecological affinities of dinocyst taxa are actually known by default, more from distribution of the assemblages and species on the sea floor than from the ecology of their living counterparts. There are only a few studies documenting the ecology of non-toxic dinoflagellates and the works coupling

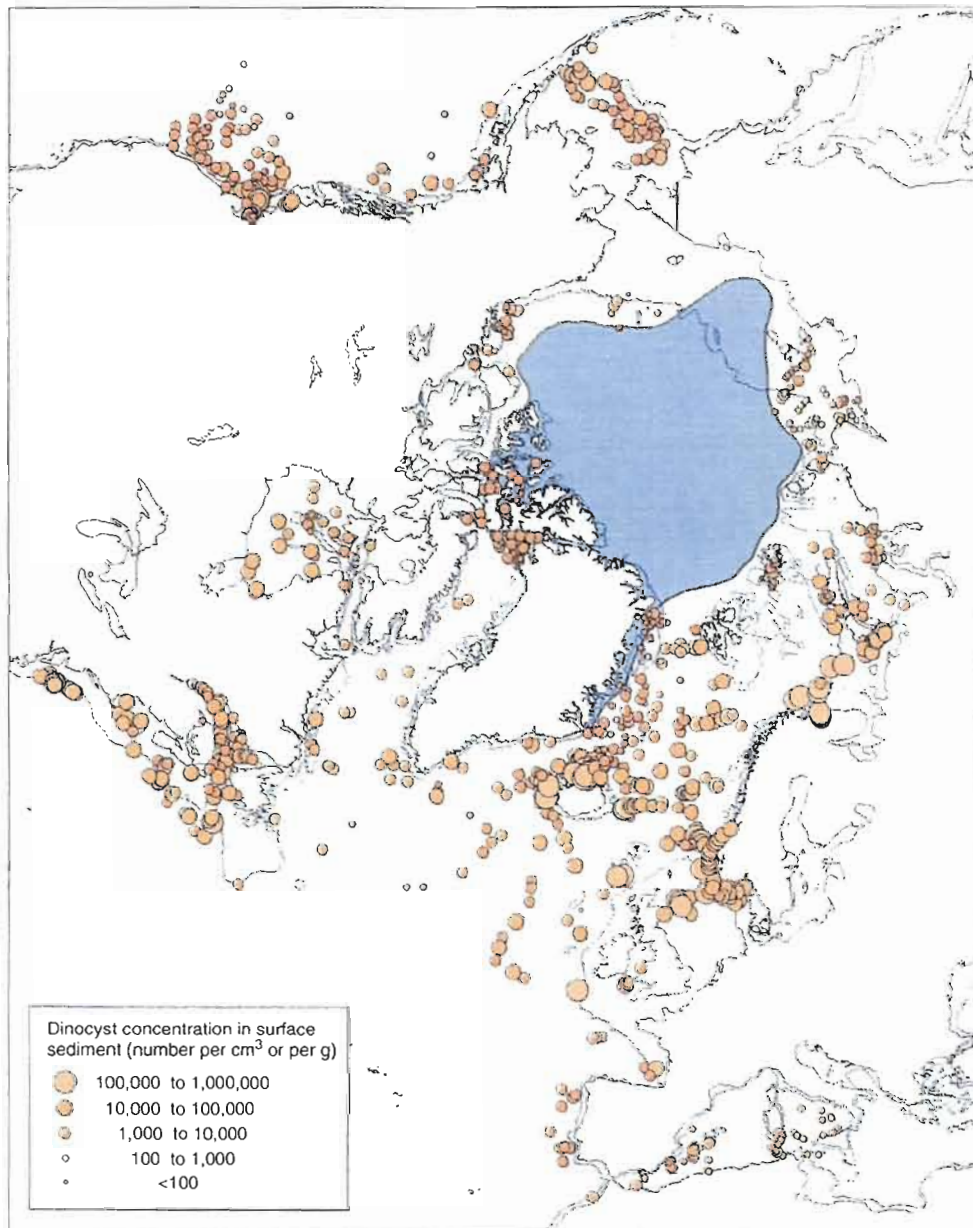


Figure 6 Dinocyst concentration in surface sediments of the Northern Hemisphere (data from de Vernal *et al.*, 2005).

information on planktonic dinoflagellates and fluxes of dinocysts to the sea floor are extremely rare. Nevertheless, it seems that the biogeographical distributions of cyst-forming dinoflagellates in surface waters and that of dinocysts in sediments are generally consistent with each other (Dodge, 1994). There is a general consistency with respect to onshore-offshore patterns and latitudinal gradients, which closely relate

to salinity and temperature controlled by current patterns. However, the correspondence between observations of motile and cyst assemblages is not perfect, due to the fact that the motile dinoflagellates in plankton assemblages represent an instantaneous time interval, whereas the cysts in the upper first centimeter of surface sediments may represent several years, decades, or centuries of sedimentary accumulation.

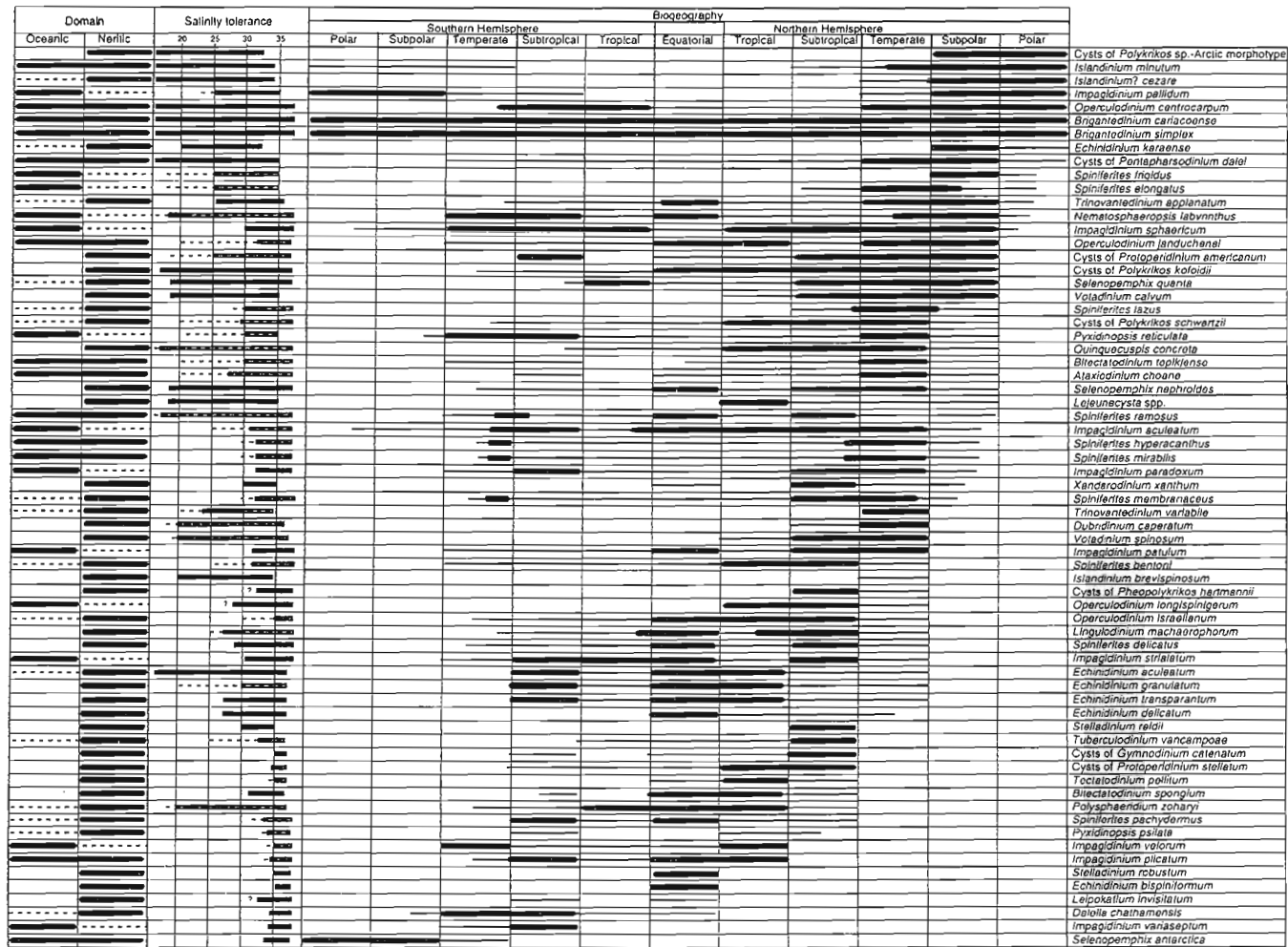


Figure 7 Latitudinal distribution of dinocysts in surface sediments, with salinity tolerance and shallow-water to oceanic occurrences (after Marret and Zonneveld 2003, Radi and de Vernal 2004, and de Vernal *et al.*, 2005). The thick lines correspond to common occurrence, whereas the thin and dashed lines correspond to occasional occurrences.

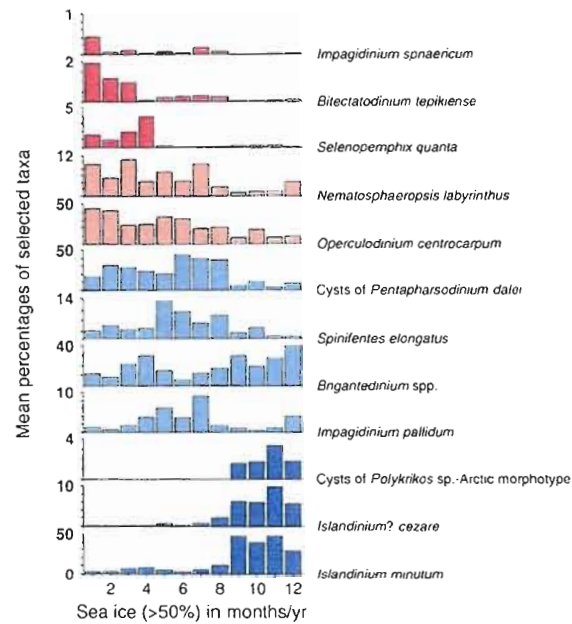


Figure 8 Mean percentage of selected dinocyst taxa vs. sea-ice extent in months per year with more than 50% of ice coverage. Note that most other taxa do not occur in areas characterized by seasonal sea ice (data from de Vernal *et al.*, 2005).

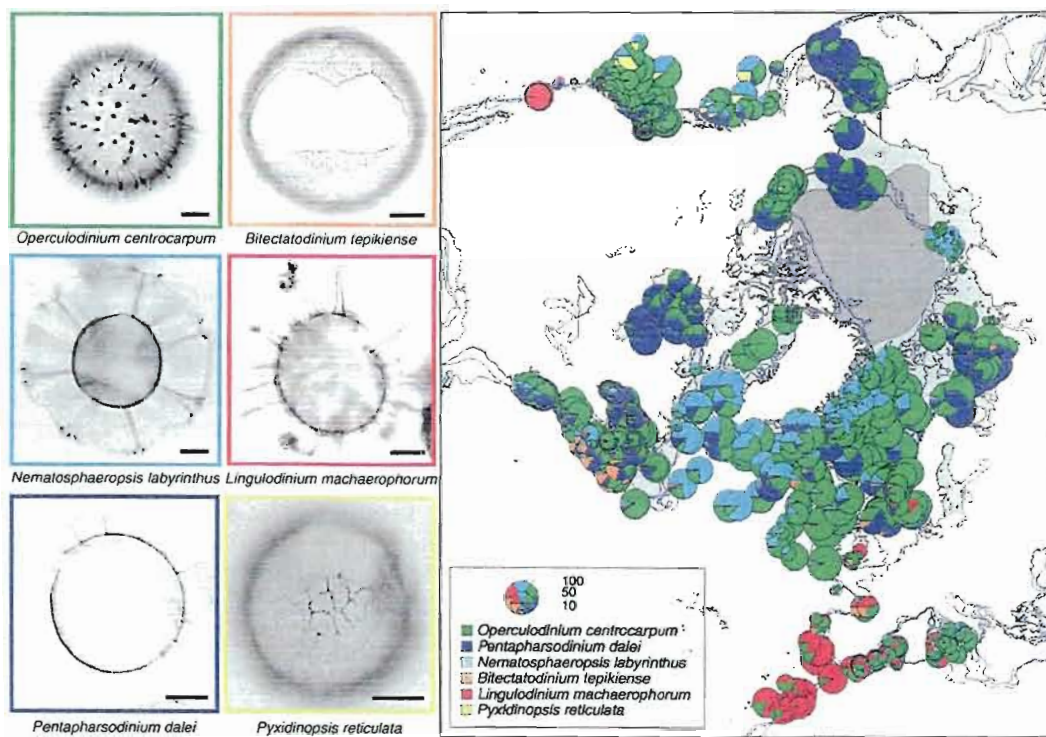


Figure 9 Photographs and distribution of selected dinocyst species belonging mostly to Gonyaulacales in surface sediment samples from the Northern Hemisphere (data from de Vernal *et al.*, 2005). The scale bars on the photographs correspond to 10 μ m. The circle diameter illustrates the cumulative percentage of the selected species in the dinocyst assemblages.

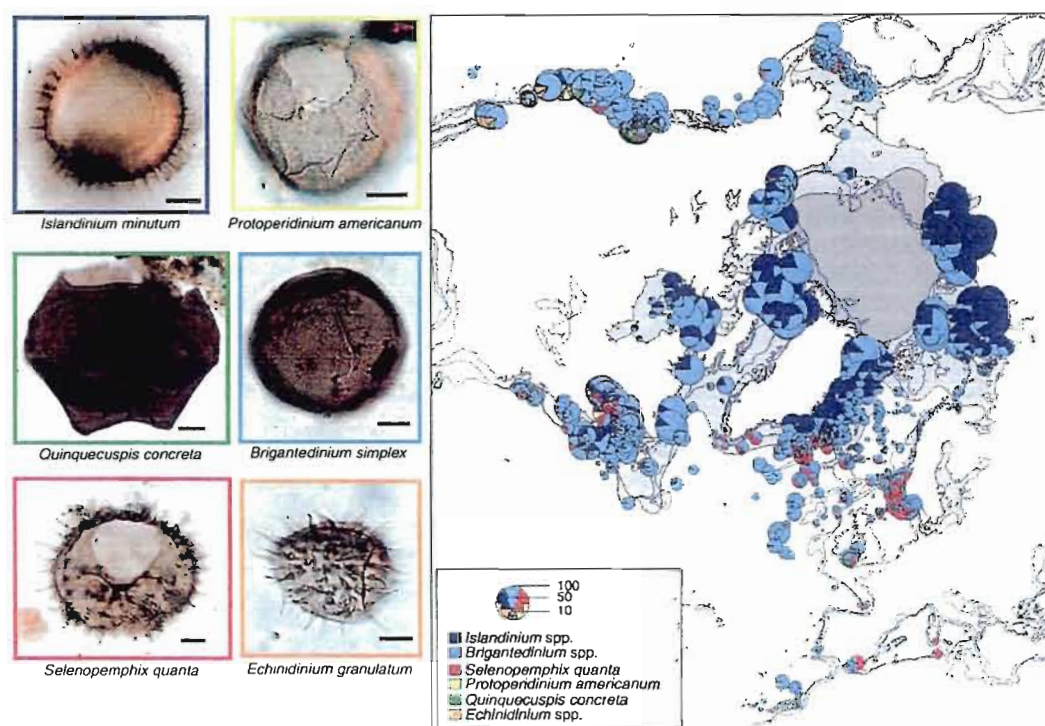


Figure 10 Photographs and distribution of selected dinocyst taxa belonging to Peridinales in surface sediment samples from the Northern Hemisphere (data from de Vernal *et al.*, 2005). The scale bars on the photographs correspond to 10 μm . The circle diameter illustrates the cumulative percentage of the selected species in the dinocyst assemblages.

In paleoceanographic studies, dinocysts are usually associated with production in the upper part of the water column at the site location. However, the sinking rate of individual cells or microscopic remains such as dinocysts is extremely slow (on the order of meters per day). Thus, incorporation within fecal pellets or marine snow (coherent aggregates of microscopic organic material having a sufficient density to sink in the water column) constitute mechanisms which likely explain the vertical fluxes of pelagic particles over hundreds or thousand of meters. Although the dinocyst assemblages on the sea floor probably relate to sedimentation within marine snow and fecal pellets, some lateral transport with surface, intermediate, or bottom currents, cannot be ruled out.

Dinocysts are made of refractory organic matter and usually preserve well in marine sediments, unlike diatoms or foraminifers that are subject to dissolution of opal silica or calcium carbonate, respectively. From this point of view, dinocysts constitute an extremely useful proxy of ocean changes in many shallow water environments and other regions of the world oceans, where calcium carbonate

dissolution occurs because of a shallow lysocline and/or oxidation of organic rich sediments that foster high pCO_2 . However, the cyst wall of some dinocyst taxa seems to be more susceptible to selective degradation when using strong oxidation techniques (e.g., acetolysis, KOH). Such techniques are used occasionally in palynology, but are avoided in the study of dinocysts. Good preservation of dinocyst taxa is generally assumed although it is possible that selective degradation occurs in sediment or at the water-sediment interface under extreme oxic conditions (Zonneveld *et al.*, 2001). The dinocyst taxa that are the most susceptible of degradation from oxidation are the cysts of *Protoperidinium* spp. and *Echinidinium* spp. (i.e., Peridinales taxa that are associated with heterotrophic productivity), which are usually characterized by a thin and brownish cyst wall.

Applications of Marine Dinocysts in Quaternary Sciences

Despite the caveats mentioned above, dinocysts constitute excellent tracers of sea-surface conditions.

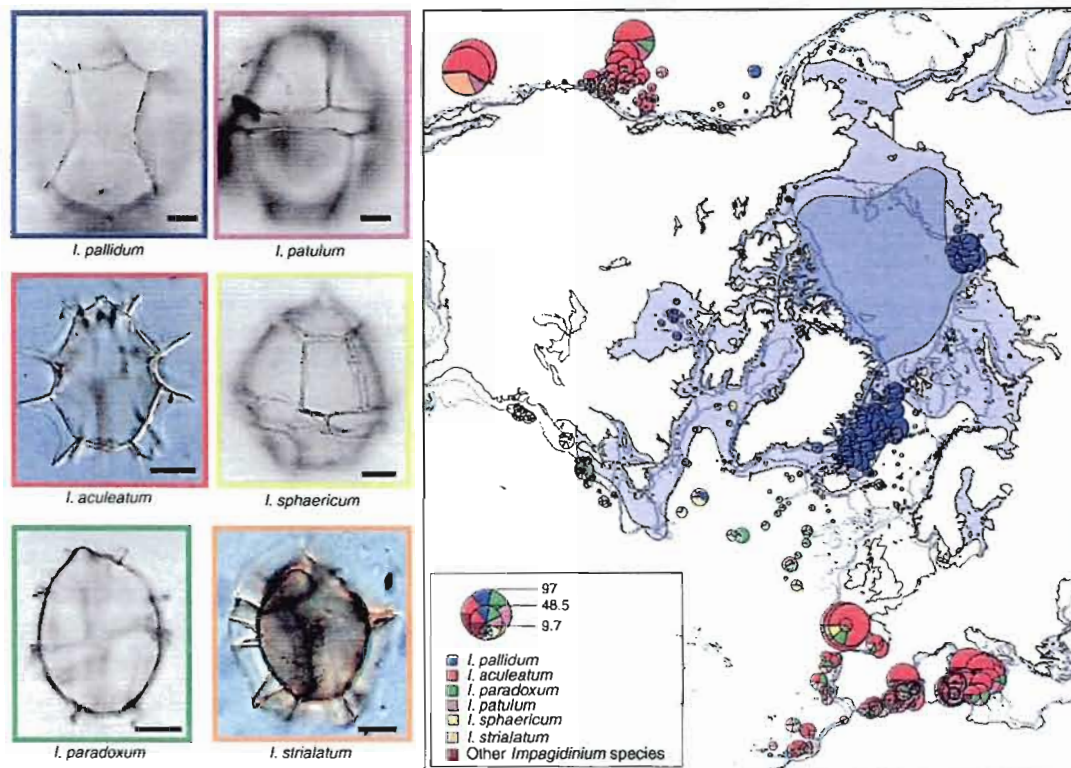


Figure 11 Photographs and distribution of selected dinocyst species of the genus *Impagidinium* (order Gonyaulales) in surface sediment samples from the Northern Hemisphere (data from de Vernal *et al.*, 2005). The scale bars on the photographs correspond to 10 µm. The circle diameter illustrates the cumulative percentage of the selected species in the dinocyst assemblages.

They usually are well preserved in sediments and the assemblages are characterized by relatively high species diversity, even in nearshore environments and in the Arctic and sub-Arctic domains. From these points of view, dinocysts are complementary to calcareous microfossils such as planktonic foraminifers, and coccoliths that are stenohaline (having narrow salinity tolerance) and used primarily in paleoceanography at low to middle latitudes. During recent decades, increasing numbers of dinocyst studies have been done as part of Quaternary science.

Hydrographical Reconstruction in Epicontinental Environments and Along the Continental Margin

In estuarine and marginal marine environments, dinocysts are a good proxy of changes in sea-surface conditions since they occur in a wide range of salinity and record both variations in salinity and temperature. Among dinocyst records from inland seas, the data from the Marmara and Black seas are particularly impressive (Mudie *et al.*, 2002) because the

assemblages reveal extremely large salinity changes and because some taxa show morphological variations reflecting endemism that is probably due to isolation and low salinity (Fig. 14).

In estuaries or deltaic environments, the various proportions of salinity-tolerant and stenohaline species have been used to estimate changes in salinity and freshwater discharge, for example off the coast of eastern Canada in the northwest North Atlantic or off the mouth of the Congo River in the Equatorial Atlantic.

Paleoceanographical Reconstruction

The development of reference dinocyst databases from studies of surface sediment samples has allowed the development of quantitative techniques for the reconstruction of sea-surface conditions such as the temperature and salinity. Various attempts have been made to adapt regression and multi-regression techniques (i.e., the conventional transfer functions), the best analog method, or neural network approaches. From the various trials, it seems that extrapolation

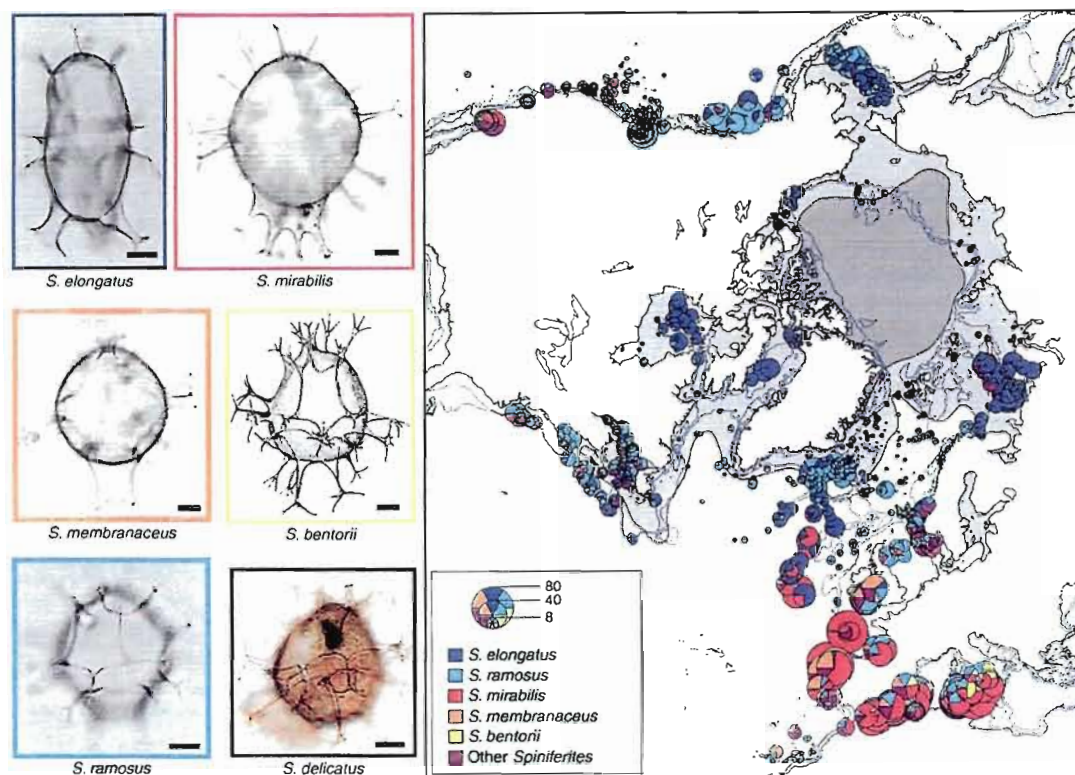


Figure 12 Photographs and distribution of selected dinocyst species of the genus *Spiniferites* (order Gonyaulacales) in surface sediment samples from the Northern Hemisphere (data from de Vernal *et al.*, 2005). The scale bars on the photographs correspond to 10 µm. The circle diameter illustrates the cumulative percentage of the selected species in the dinocyst assemblages.

approaches (neural networks and regressions) that rely on calibration between the assemblages and given oceanographical parameters strongly depend on the definition of the database. As a consequence, although the extrapolation techniques may yield very good validation results, the reconstructions can differ significantly, depending upon the calibration data set. Therefore, most paleoceanographic reconstructions from dinocyst data have been made on conservative grounds, using the modern analogue technique that does not involve any extrapolation but simply uses the similarity between the fossil spectrum and the modern assemblages to infer past sea-surface conditions (de Vernal *et al.*, 2001, 2005).

Quantitative reconstructions of sea-surface temperature, salinity, and sea-ice cover were made from many Quaternary sequences of the North Atlantic and compilations are available for the Last Glacial Maximum, 21,000 years ago (de Vernal *et al.*, 2005). In addition to significant changes in temperature, the dinocyst-based reconstructions point toward variations in the salinity and sea-ice cover. The example of

a record from the Labrador, in the Northwest North Atlantic, is presented in Figure 15. It shows extensive sea-ice cover and relatively low salinities off the east Canadian coasts during the Last Glacial Maximum.

Eutrophication, Productivity, and Upwelling

Dinocysts include fossil remains from both microzooplanktonic and phytoplanktonic communities. Thus, dinocyst assemblages, together with the overall fluxes, depend upon primary productivity and the structure of the planktonic population. Studies in fjords of northwest Europe, and along the coasts of Japan and America have shown increased fluxes of dinocysts with higher percentages of heterotrophic taxa (cysts of *Protoperdinium* sp., notably). These changes in assemblages appear related to recent eutrophication, due to human activities. Some attempts have been made to distinguish the effects of eutrophication from those of pollution in dinocyst assemblages, but the results are equivocal (Dale and Dale, 2002).

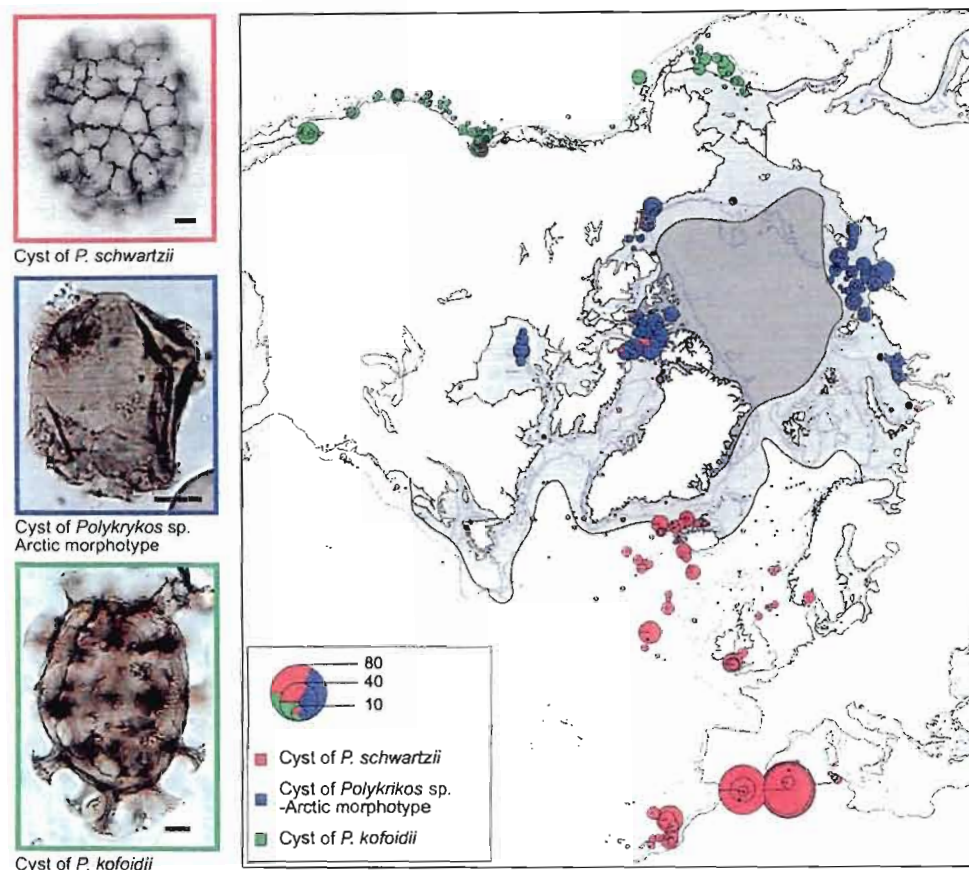


Figure 13 Photographs and distribution of selected dinocyst species of the genus *Polykrikos* (order Gymnodiniales) in surface sediment samples from the Northern Hemisphere (data from de Vernal *et al.*, 2005). The scale bars on the photographs correspond to 10 μm . The circle diameter illustrates the cumulative percentage of the selected species in the dinocyst assemblages.

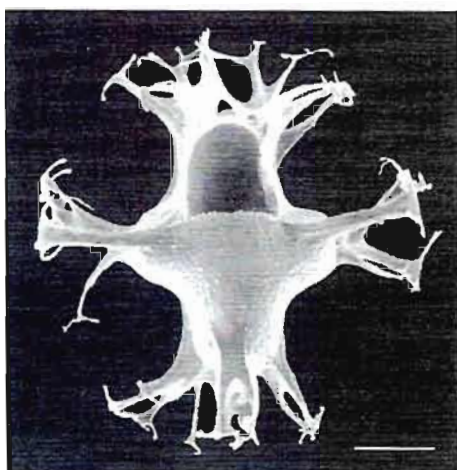


Figure 14 Scanning electron photograph of *Spiniferites cruciformis*. Specimen from sediment collected in the Black Sea. Scale bar = 20 μm .

In ocean environments, where upwelling results in high primary productivity and where the phytoplankton is dominated by diatoms, dinocyst fluxes are high and are characterized by the abundance of heterotrophic taxa over autotrophic ones (Radi and de Vernal, 2004). Downcore analyses performed on sediments taken off the African margin have shown variations in the abundance of Peridiniales over the last hundred thousand years, which indicate changes in productivity and upwelling strength in relation to orbital forcing (Höll *et al.*, 2000; Fig. 16).

Conclusion

Fossil dinocysts are mainly known from marine sediments, and appear to be particularly abundant along continental margins (estuaries, continental shelves and slopes, epicontinental seas). Dinocysts have been widely used in developing the biostratigraphy

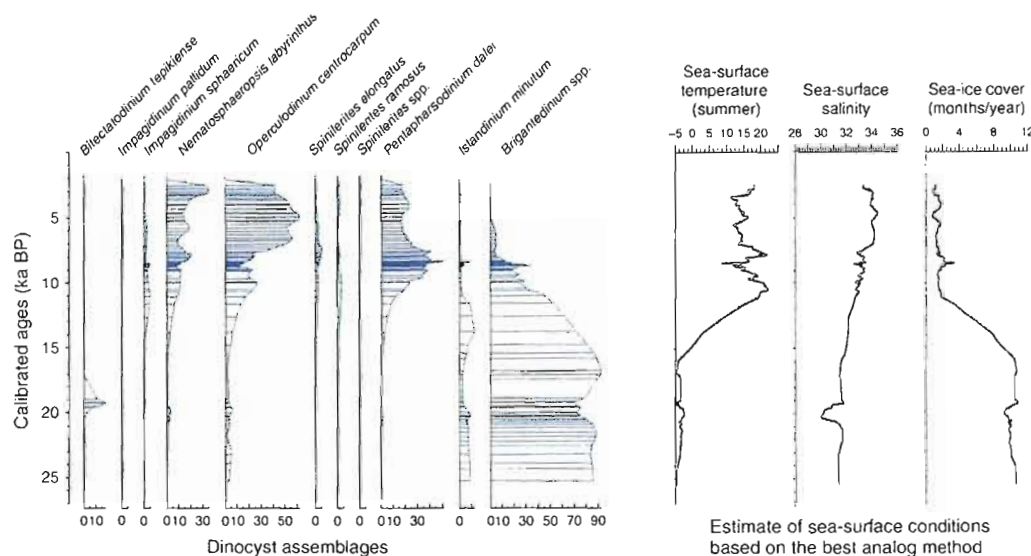


Figure 15 Example of late Quaternary dinocyst assemblages in the Labrador Sea, northwest North Atlantic, and corresponding reconstruction of sea-surface salinity, temperature and sea-ice cover based on the modern analog technique. The figure shows a smoothed record from core HU84-030-021 (58°22'W, 57°30'W; water depth = 2,853 meters). For more detail on the record, see de Vernal *et al.* (2001).

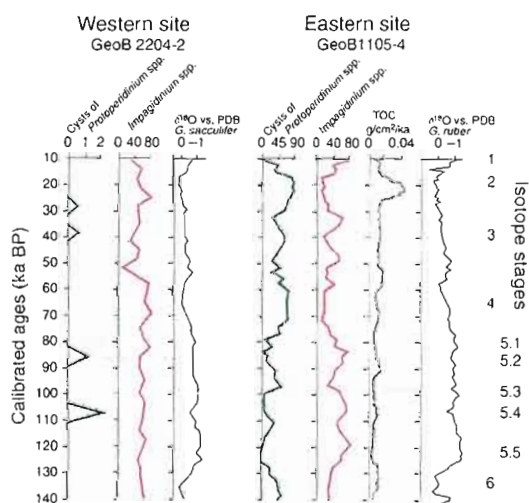


Figure 16 Example of dinocyst records representative of productivity and upwelling changes during the middle and late Pleistocene in the tropical Atlantic. The western site (core GeoB 2204-2, 8°32'S, 34°01'W; water depth = 2,072 m) is from a low productivity area and the eastern site (core GeoB 1105-4: 01°40'S, 12°26'W; water depth = 3,225 m) was collected in a productive upwelling region. In the sediments, the cysts of *Protopodidinium* spp. are associated with high productivity in surface waters whereas *Impagidinium* spp. are associated with oligotrophic conditions. The blue bands correspond to glacial episodes, which were marked by relatively high productivity in the eastern tropical Atlantic. Data redrafted from Höll *et al.* (2000).

and paleoecology of the Mesozoic and Tertiary. In the field of Quaternary paleoceanography and paleoecology, the study of dinocysts is of growing interest. Because they are very resistant, dinocysts are generally well preserved in sediment despite dissolution that may affect calcareous or siliceous biological remains. Moreover, the development of reference databases from surface sediment samples (Dale, 1996; Rochon *et al.*, 1999; de Vernal *et al.*, 2001, 2005; Zonneveld and Marret, 2003) has led to the documentation of relationships between the distribution of dinocyst assemblages and sea-surface parameters, including productivity and hydrographical conditions. Quantitative approaches, such as the best analogue method, have permitted the quantitative reconstruction of temperature, salinity, and sea-ice cover extent. For example, hydrographical maps of the northern North Atlantic during the Last Glacial Maximum were established using dinocyst data, and many regional reconstructions are currently being developed. Other applications of dinocysts in Quaternary sciences include the reconstruction of hydrological changes from the study of cores collected in epicontinental seas or deltaic environments. Dinocyst assemblages may also provide insights into variation of the trophic character of the upper water masses, leading to identify eutrophication in nearshore environments and to estimate changes of productivity in upwelling areas.

See also: **Paleoceanography.** **Paleoceanography, Biological Proxies:** Coccoliths; Marine Diatoms. **Quaternary Stratigraphy:** Biostratigraphy.

References

- Dale, B. (1976). Cyst formation, sedimentation, and preservation: factors affecting dinoflagellate assemblages in recent sediments from Trondheimsfjord, Norway. *Review of Palaeobotany and Palynology* 22, 39–60.
- Dale, B. (1983). Dinoflagellate resting cysts: 'benthic plankton'. In *Survival strategies of algae* (G. A. Fryxell, Ed.), pp. 69–136. Cambridge University Press, Cambridge.
- Dale, B. (1996). Dinoflagellate cyst ecology: modelling and geological applications. In *Palynology: Principles and Applications* (J. Jansonius and D. C. McGregor, Eds.), pp. 1249–1275. American Association of Stratigraphic Palynologists Foundation.
- Dale, B., and Dale, A. (2002). Environmental application of dinoflagellate cysts and acritarchs. In *Quaternary Environmental Micropaleontology* (S. K. Haslett, Ed.), pp. 207–240. Arnold.
- de Vernal, A., Eynaud, F., Henry, M., Hillaire-Marcel, C., Londeix, L., Mangin, S., Matthiessen, J., Marret, F., Radi, T., Rochon, A., Solignac, S., and Turon, J.-L. (2005). Reconstruction of sea-surface conditions at middle to high latitudes of the Northern Hemisphere during the Last Glacial Maximum (LGM) based on dinoflagellate cyst assemblages. *Quaternary Science Reviews* 24, 897–924.
- de Vernal, A., Henry, M., Matthiessen, J., Mudie, P. J., Rochon, A., Boessenkool, K., Eynaud, F., Grøsfjeld, K., Guior, J., Hamel, D., Harland, R., Head, M. J., Kunz-Pirrung, M., Levac, E., Loucheur, V., Peyron, O., Pospelova, V., Radi, T., Turon, J.-L., and Voronina, E. (2001). Dinoflagellate cyst assemblages as tracers of sea-surface conditions in the northern North Atlantic, Arctic and sub-Arctic seas: the new 'n = 677' database and application for quantitative paleoceanographical reconstruction. *Journal of Quaternary Science* 16, 681–699.
- de Vernal, A., Londeix, L., Harland, R., Morzadec-Kerfourn, M.-T., Mudie, P. J., Turon, J.-L., and Wrenn, J. (1992). The Quaternary organic walled dinoflagellate cyst of the North Atlantic Ocean and adjacent seas: eostratigraphic and biostratigraphic records. In *Neogene and Quaternary dinoflagellate cysts and acritarchs* (M. J. Head and J. H. Wrenn, Eds.), pp. 289–328. American Association of Stratigraphic palynologists Foundation.
- Dinoflagellate Working group (Groupe de travail 'Dinoflagellés') (1986). Guide pour la détermination de kystes de dinoflagellés fossiles, Le complexe Gonyaulacysta. *Mémoire Elf Aquitaine* 12, 478.
- Dodge, J. D. (1994). Biogeography of marine armoured dinoflagellates and dinocysts in the NE Atlantic and North Sea. *Review of Palaeobotany and Palynology* 84, 169–180.
- Edwards, L. (1993). Dinoflagellates. In *Fossil prokaryotes and protists* (J. H. Lipps, Ed.), pp. 105–129. Blackwell Scientific publication.
- Evitt, W. (1963). A discussion and proposals concerning fossil dinoflagellates, hystrichospheres and acritarchs. *Proceedings of the National Academy of Sciences* 49, 158–164.
- Evitt, W. R. (1985). Sporopollenin dinoflagellate cysts – Their morphology and Interpretation. *American Association of Stratigraphic Palynologists Foundation* 333.
- Fensome, R. A., Taylor, F. J. R., Norris, G., Sarjeant, W. A. S., Wharton, D. I., and Williams, G. L. (1993). A classification of living and fossil dinoflagellates. In *Micropaleontology special publication number 7*, p. 351. American Museum of Natural History.
- Fensome, R. A., and Williams, G. L. (2004). The Lentin and Williams Index of fossil dinoflagellate. American Association of Stratigraphic Palynologists Foundation. *Contribution Series* 42, 909.
- Head, M. J. (1996). Modern dinoflagellate cysts and their biological affinities. In *Palynology: principles and applications* (J. Jansonius and D. C. McGregor, Eds.), Vol. 3, pp. 1197–1248.
- Head, M. J., Edwards, L. E., and Steidinger, K. A., (1989) *Short Course on Neogene-Recent Dinoflagellates*. Course manual, American Association of Stratigraphic Palynologists Foundation.
- Höll, C., Zonneveld, K. A. F., and Willems, H. (2000). Organic-walled dinoflagellate cyst assemblages in the tropical Atlantic Ocean and oceanographical changes over the last 140 ka. *Palaeogeography, Palaeoclimatology, Palaeoecology* 160, 69–90.
- Marret, F., and Zonneveld, K. (2003). Atlas of modern global organic-walled dinoflagellate cyst distribution. *Review of Palaeobotany and Palynology* 125, 1–200.
- Matthiessen, J., de Vernal, A., Head, M., Okolodkov, Y., Zonneveld, K., and Harland, R. (2005). Modern organic-walled dinoflagellate cysts in Arctic marine environments and their (paleo-) environmental significance. *Paläontologische Zeitschrift* 79/1, 3–51.
- Mudie, P. J., Harland, R., Matthiessen, J., and de Vernal, A. (2001). Dinoflagellate cysts and high latitude Quaternary paleoenvironmental reconstructions: an introduction. *Journal of Quaternary Science* 16, 595–602.
- Mudie, P. J., Rochon, A., Aksu, A. E., and Gillespie, H. (2002). Dinoflagellate cysts, freshwater algae and fungal spores as salinity indicators in Late Quaternary cores from Marmara and Black seas. *Marine Geology* 190, 203–231.
- Pfiester, L. A., and Anderson, D. M. (1987). Dinoflagellate reproduction. In *The biology of Dinoflagellates* (F. J. R. Taylor, Ed.), pp. 611–648. Blackwell Scientific Publications.
- Powell, A. J. (ed.) (1992). *A stratigraphic Index of Dinoflagellate cysts*. British Micropaleontological society publication series, Chapman and Hall, p 290.
- Radi, T., and de Vernal, A. (2004). Dinocyst distribution in surface sediments from the northeastern Pacific margin (40–60°N) in relation to hydrographic conditions, productivity and upwelling. *Review of Palaeobotany and Palynology* 128, 163–193.
- Rochon, A., de Vernal, A., Turon, J.-L., Matthiessen, J., and Head, M. J. (1999). Distribution of dinoflagellate cysts in surface sediments from the North Atlantic Ocean and adjacent seas in relation to sea-surface parameters. Special Contribution Series. *American Association of Stratigraphic Palynologists Foundation* 35, 1–152.
- Taylor, F. J. R., and Pollinger, U. (1987). The ecology of Dinoflagellates. In *The biology of Dinoflagellates* (F. J. R. Taylor, Ed.), pp. 398–529. Blackwell Scientific Publications.
- Vink, A. (2004). Calcareous dinoflagellate cysts in South and equatorial Atlantic surface sediments: diversity, distribution, ecology and potential for palaeoenvironmental reconstruction. *Marine Micropaleontology* 50, 43–88.
- Wall, D., and Dale, B. (1968). Modern dinoflagellate cysts and evolution of the Peridinales. *Micropaleontology* 14, 265–304.
- Wall, D., and Dale, B. (1966). 'Living fossils' in western Atlantic plankton. *Nature* 211, 1025–1026.
- Zonneveld, K. A. F., Versteegh, G. J. M., and De Lange, G. J. (2001). Palaeoproductivity and post-depositional aerobic organic matter decay reflected by dinoflagellate cyst assemblages of the Eastern Mediterranean S1 sapropel. *Marine Geology* 172, 181–195.